A holistic framework of degradation modeling for reliability analysis and maintenance optimization of nuclear safety systems

Yanhui Lin

NNT : 2016SACLC002

THESE DE DOCTORAT
DE L'UNIVERSITE PARIS-SACLAY,
préparée à "CentraleSupélec"

ÉCOLE DOCTORALE N° 573
Interfaces : approches interdisciplinaires / fondements, applications et innovation

Spécialité de doctorat : Sciences et technologies industrielles

Par

M. Yanhui LIN

Un Cadre Holistique de la Modélisation de la Dégradation pour l'Analyse de Fiabilité et Optimisation de la Maintenance de Systèmes de Sécurité Nucléaires

A Holistic Framework of Degradation Modeling for Reliability Analysis and Maintenance Optimization of Nuclear Safety Systems

Thèse présentée et soutenue à Châtenay-Malabry, le 13 janvier 2016

Composition du Jury :

Mme. Sophie Mercier, Université de Pau et des Pays de l'Adour, Rapporteuse
Mme. Mitra Fouladirad, Université de technologie de Troyes, Rapporteuse
M. Oualid Jouini, CentraleSupélec, Examinateur
M. Piero Baraldi, Politecnico di Milano, Examinateur
M. Emmanuel Remy, Électricité de France R&D, Examinateur
M. Enrico Zio, CentraleSupélec, Directeur de thèse

ACKNOWLEDGEMENTS

I would like to express my profound gratitude and deep regards to my supervisor of this thesis, Professor Enrico Zio, for his exemplary guidance, monitoring and constant encouragement throughout the course of this thesis. The blessing, help and guidance given by him time to time shall carry me a long way in the journey of life on which I am about to embark. It was a pleasure and a great honor to pursue a Ph.D. degree under his supervision.

I would like to express my sincere appreciation and gratitude to my co-advisor, Dr. Yanfu LI, for his support, time and patience. This research work would have been much more difficult without his help.

My deepest appreciation goes to all the jury members that agreed to be part of the committee: Professor Sophie Mercier, Dr. Mitra Fouladirad, Dr. Oualid Jouini, Dr. Piero Baraldi and Dr. Emmanuel Remy. I am particularly grateful to the reviewers, Professor Sophie Mercier and Dr. Mitra Fouladirad, for their careful reading of the manuscript and all the constructive and helpful remarks, which helped to improve the quality of my thesis work.

I would like to offer my special thanks to my family for their love, support and constant encouragement. My parents are the meaning of my life, and I undoubtedly could not have done this without them.

I would like also to take this opportunity to thank all my friends/colleagues in SSEC and at Laboratory of Industrial Engineering, CentraleSupélec, University of Paris-Saclay. It has been a pleasure to work with them. I want to give them my great thanks for everything they have done, for their encouragement and their disposition to offer me a hand whenever I needed help.

ABSTRACT

Components of nuclear safety systems are in general highly reliable, which leads to a difficulty in modeling their degradation and failure behaviors due to the limited amount of data available. Besides, the complexity of such modeling task is increased by the fact that these systems are often subject to multiple competing degradation processes and that these can be dependent under certain circumstances, and influenced by a number of external factors (e.g. temperature, stress, mechanical shocks, etc.).

In this complicated problem setting, this PhD work aims to develop a holistic framework of models and computational methods for the reliability-based analysis and maintenance optimization of nuclear safety systems taking into account the available knowledge on the systems, degradation and failure behaviors, their dependencies, the external influencing factors and the associated uncertainties.

The original scientific contributions of the work are:

(1) For single components, we integrate random shocks into multi-state physics models for component reliability analysis, considering general dependencies between the degradation and two types of random shocks.

(2) For multi-component systems (with a limited number of components):

(a) a piecewise-deterministic Markov process modeling framework is developed to treat degradation dependency in a system whose degradation processes are modeled by physics-based models and multi-state models;

(b) epistemic uncertainty due to incomplete or imprecise knowledge is considered and a finite-volume scheme is extended to assess the (fuzzy) system reliability;

(c) the mean absolute deviation importance measures are extended for components with multiple dependent competing degradation processes and subject to maintenance;

(d) the optimal maintenance policy considering epistemic uncertainty and degradation dependency is derived by combining finite-volume scheme, differential evolution and non-dominated sorting differential evolution;

(e) the modeling framework of (a) is extended by including the impacts of random shocks on the dependent degradation processes.

(3) For multi-component systems (with a large number of components), a reliability assessment

method is proposed considering degradation dependency, by combining binary decision diagrams and Monte Carlo simulation to reduce computational costs.

Key words: Reliability analysis, multiple competing degradation processes, degradation dependency, piecewise-deterministic Markov processes, multi-state models, physics-based models, random shocks, epistemic uncertainty, Monte Carlo simulation, finite-volume method, importance measures, maintenance optimization, binary decision diagrams

RESUME

Composants de systèmes de sûreté nucléaire sont en général très fiable, ce qui conduit à une difficulté de modéliser leurs comportements de dégradation et d'échec en raison de la quantité limitée de données disponibles. Par ailleurs, la complexité de cette tâche de modélisation est augmentée par le fait que ces systèmes sont souvent l'objet de multiples processus concurrents de dégradation et que ceux-ci peut être dépendants dans certaines circonstances, et influencé par un certain nombre de facteurs externes (par exemple la température, le stress, les chocs mécaniques, etc.).

Dans ce cadre de problème compliqué, ce travail de thèse vise à développer un cadre holistique de modèles et de méthodes de calcul pour l'analyse basée sur la fiabilité et la maintenance d'optimisation des systèmes de sûreté nucléaire en tenant compte des connaissances disponibles sur les systèmes, les comportements de dégradation et de défaillance, de leurs dépendances, les facteurs influençant externes et les incertitudes associées.

Les contributions scientifiques originales dans la thèse sont:

(1) Pour les composants simples, nous intégrons des chocs aléatoires dans les modèles de physique multi-états pour l'analyse de la fiabilité des composants qui envisagent dépendances générales entre la dégradation et de deux types de chocs aléatoires.

(2) Pour les systèmes multi-composants (avec un nombre limité de composants):

(a) un cadre de modélisation de processus de Markov déterministes par morceaux est développé pour traiter la dépendance de dégradation dans un système dont les processus de dégradation sont modélisées par des modèles basés sur la physique et des modèles multi-états;

(b) l'incertitude épistémique à cause de la connaissance incomplète ou imprécise est considéré et une méthode volumes finis est prolongée pour évaluer la fiabilité (floue) du système;

(c) les mesures d'importance de l'écart moyen absolu sont étendues pour les composants avec multiples processus concurrents dépendants de dégradation et soumis à l'entretien;

(d) la politique optimale de maintenance compte tenu de l'incertitude épistémique et la dépendance de dégradation est dérivé en combinant schéma volumes finis, évolution différentielle et non-dominée de tri évolution différentielle;

(e) le cadre de la modélisation de (a) est étendu en incluant les impacts des chocs aléatoires sur les processus dépendants de dégradation.

(3) Pour les systèmes multi-composants (avec un grand nombre de composants), une méthode d'évaluation de la fiabilité est proposé considérant la dépendance dégradation en combinant des diagrammes de décision binaires et simulation de Monte Carlo pour réduire le coût de calcul.

Mots Clés: Analyse de fiabilité, multiples processus concurrents de dégradation, dépendance de dégradation, processus de Markov déterministe par morceaux, modèles multi-états, modèles basés sur la physique, chocs aléatoires, incertitude épistémique, simulation de Monte Carlo, méthode volumes finis, mesures d'importance, optimisation de la maintenance, diagrammes de décision binaires

TABLE OF CONTENTS

LIST OF TABLES

LIST OF FIGURES

1. INTRODUCTION

The focus of the present PhD thesis is on the development of a holistic framework of models and computational methods for the reliability-based analysis and maintenance optimization of nuclear safety systems, taking into account the available knowledge about the component degradation and failure behaviors, their dependencies, the external influencing factors and the associated uncertainties. This introductory chapter is organized as follows. Section 1.1 describes the background of the work and discusses the importance of degradation modeling. Section 1.2 reviews different types of degradation models. Section 1.3 presents the issues to be addressed in degradation modeling. Section 1.4 states the research motivations and objectives. Section 1.5 presents the structure of the thesis.

1.1 Background

Safety-critical plants, like the nuclear power plants, are designed not to fail, i.e. with very high reliability, because of the potentially catastrophic consequences of their failures. Traditional data-based reliability analysis, based on failure data, is, then, unsuitable. On the other hand, most failure mechanisms can be traced to underlying degradation processes (e.g. wear, stress corrosion, shocks, cracking, fatigue, etc.) [1], for which models exist.

In general, the reliability of a system decreases as the degradation processes develop, eventually leading to failure [2]. In reliability engineering, degradation processes have been widely studied and different degradation models have been developed. A review of degradation models is given in the following chapter.

1.2 Degradation modeling

The existing degradation models can mainly be classified into the following categories:

- statistical models of time to failure, based on degradation data (e.g. Bernstein distribution [3], Weibull distribution [4]).
- stochastic process models (e.g. Gamma processes [5], inverse Gaussian process [6]) describing the evolution of one or more degradation parameters by gradual degradation

increments over time, and the failure occurs when the degradation parameter values reach predefined thresholds.

- physics-based models (PBMs), based on the knowledge of the physics of degradation, which is translated into equations to give a quantitative description (e.g. the physics functions based on critical environmental stresses, e.g. amplitude and frequency of mechanical loads, used to model the pitting and corrosion-fatigue degradation mechanisms [7]).
- multi-state models (MSMs) describing by finite degradation states of the underlying degradation process (e.g. semi-Markov models for the deterioration of infrastructure systems [8]).

The recent literature on degradation modeling can be organized under the above taxonomy. For statistical models, Lu *et al.* [9] have combined random regression coefficients and a standard deviation function for analyzing linear degradation data for statistical inference of a time-to-failure distribution. Lu and Meeker [4] have developed methods using degradation measures to estimate a time-to-failure distribution for a broad class of degradation models and demonstrated some special cases for which it is possible to obtain closed-form expressions of the distributions. Yang and Yang [10] have estimated the parameters of lifetime distributions using a random-coefficient-based approach that uses the lifetimes of failed devices, combined with degradation information from operating devices.

For stochastic models, Whitmore [11] has estimated the degradation process by a Wiener diffusion process subject to measurement errors due to imperfect instruments, procedures and environments. Lawless and Crowder [5] have constructed a tractable Gamma-process model incorporating a random effect for taking into account different degradation rates of the individual components. Chen *et al.* [6] have employed the inverse Gaussian process with random-drift mode, in which the random drifts are used to represent heterogeneities commonly observed across the product population. Note that the aforementioned degradation models are always built on sufficient degradation/failure data.

PBMs [12-14] and MSMs [15-17] can be used to describe the evolution of degradation in structures, systems and components, for which statistical degradation/failure data are insufficient, e.g. the highly reliable devices in the nuclear and aerospace industries. For PBMs, Daigle and Goebel [12] have developed a physics model of a pneumatic valve, based on mass

and energy balances in which the damages depend on sliding velocity. Reggiani *et al.* [13] have developed a physics-based analytical expression of the linear drain current for hot-carrier stress degradation in transistors. Keedy and Feng [14] have proposed a probabilistic reliability and maintenance modeling framework for stent deployment and operation, based on physics-of-failure mechanisms, e.g. delayed failure due to fatigue crack and instantaneous failure due to overload fracture.

For MSMs, Moghaddass and Zuo [15] have employed the nonhomogeneous continuous-time hidden semi-Markov process to model the degradation and observation processes associated with the device. Giorgio *et al.* [18] have developed an age- and state-dependent Markov model for the wear process of cylinder liners of identical heavy-duty diesel engines for marine propulsion. Unwin *et al.* [19] have proposed a multi-state physics model (MSPM) for the cracking process in an dissimilar metal weld in a primary coolant system of a nuclear power plant.

1.3 Factors considered in degradation modeling

There are several factors, which can influence degradation evolution and, thus, need to be accounted for in degradation modeling.

1.3.1 Degradation dependency

In reality, components and systems are often subject to multiple competing degradation processes and any of them may cause failure [20]. The dependencies among these processes within one component (e.g. the wear of rubbing surfaces influenced by the environmental stress shock within a micro-engine [21]), or/and among different components (e.g. the degradation of the pre-filtrations stations leading to a lower performance level of the sand filter in a water treatment plant [22]) need to be considered, under certain circumstances. Components can be dependent due to functional dependence, where the failure of a trigger component causes other components to become inaccessible or unusable [23, 24]. Failure isolation effects can induce degradation dependency among different components, since failure of one component may cause other components within the same system to become isolated from the system due to the failure isolation actions [25, 26]. This renders challenging the analysis and prediction of the

components and systems reliability [27]. Wang and Pham [20] applied time-varying copulas for describing the dependencies between the degradation processes modeled by statistical distributions. Straub [28] used a dynamic Bayesian network to represent the dependencies between degradation processes modeled by multi-state models. However, no studies have considered degradation dependency in a system whose degradation processes are modeled by PBMs and MSMs.

1.3.2 Random shocks

Components may also suddenly fail due to randomly occurring events of excessive loading or temperature [29]. For example, thermal and mechanical shocks (e.g. internal thermal shocks and water hammers) [30, 31] onto power plant components can lead to intense increases in temperatures and stresses, respectively. These events, referred to as random shocks, need to be accounted for on top of the underlying degradation processes, because they can contribute to accelerating the degradation processes. In the literature, random shocks are typically modeled by Poisson processes [17], distinguishing two main types, extreme shock and cumulative shock processes [32], according to the severity of the damage. The former could directly lead the component to immediate failure [33], whereas the latter increases the degree of damage in a cumulative way [34]. Esary *et al.* [35] have considered extreme shocks in a component reliability model, whereas Wang *et al.* [29], Klutke and Yang [36] and Wortman *et al.* [37] have modeled the influences of cumulative shocks on a degradation process. Both extreme and cumulative random shocks have been considered by Li and Pham [17], and Wang and Pham [20]. Additionally, Ye *et al.* [38] and Fan *et al.* [39] have considered that a high severity of degradation can lead to a high probability that a random shock causes extreme damage. However, the fact that the effects of cumulative shocks can vary according to the severity of degradation has also to be considered.

Besides, previous research has focused on the dependency between continuous/multi-state degradation processes and random shocks. For continuous degradation processes, Peng *et al.* [27] considered systems with one linear degradation path where shocks can bring additional abrupt degradation damage if the shock loads do not exceed the maximum strength of the material. Multi-component systems subject to multiple linear degradation paths have been further considered by Song *et al.* [40]. Jiang *et al.* [21] studied changes in the maximal strength of the material when systems are deteriorating under different situations. Becker *et al.* [41]

extended the theory of dynamic reliability to incorporate random changes of the degradation variables due to random shocks. Rafiee *et al.* [42] proposed reliability models for systems for which the degradation path has a changing degradation rate according to particular random shock patterns. Song *et al.* [43] studied random shocks with specific sizes or functions, which can selectively affect the degradation processes of one or more components (not necessarily all components) in one system. For multi-state degradation processes, Yang *et al*. [44] combined random shocks with Markov degradation models where shocks can lead the systems to further degraded states. However, few studies have explicitly considered both the dependencies between degradation processes and the random shocks, and among the degradation processes themselves.

1.3.3 Maintenance policy

Maintenance contributes to ensuring the safe and efficient operation of industrial systems [45]. The degradation processes can be interrupted by maintenance tasks (e.g. one component can be restored to its initial state by preventive maintenance if any of its degradations exceed the respective critical level [46] and by corrective maintenance upon its failure [21]). The interactions among components complicate the modeling for maintenance planning, which becomes a big challenge [47]. Thomas [48] has categorized these interactions in the maintenance modeling into three groups: economic, structural and stochastic dependences. Economic dependence exists when the maintenance cost of several components is not equal to the sum of their individual maintenance costs. For example, Castanier *et al.* [49] have considered a condition-based maintenance policy for a two-unit deteriorating system, where the set-up cost of inspection is charged only once if the actions on the two components are combined. Van Dijkhuizen [50] has investigated the long-term grouping of preventive maintenance jobs in a multi-setup, multi-component production system where the set-up activities can be combined when several components are maintained at the same time. Structural dependence occurs if some working components need to be replaced or dismantled in order to execute the maintenance of the failed ones. For example, Dekker *et al.* [51] have studied the maintenance policy for asphalt roads, where the number of maintenance services is limited by integrating neighboring segments into a homogeneous section which is completely repaired. Stochastic dependence, also referred to as probabilistic dependence, applies when the state of one component can affect those of other components or their failure rates. Failure interactions

have been the most discussed cases for stochastic dependence [22] and imply that the failure of one component may lead to the failure of other components with certain probabilities, and/or influence their failure rates [52]. For example, Lai and Chen [53] have presented an economic periodic replacement model for a two-unit system where the failure of unit 1 can increase the failure rate of unit 2, while the failure of unit 2 induces unit 1 into instantaneous failure. Zequeira and Bérenguer [54] have studied the inspection policies for a two-component standby system, where the failure of one component can modify the conditional failure probability of the component still in operation with probability p and does not modify it with probability $1-p$. Barros *et al.* [55] have optimized the maintenance policy for a two-unit parallel system where the failure of a component increases the failure rate of the surviving one.

Dependency among degradation mechanisms or processes has received less attention within the framework of maintenance modeling and optimization of multi-component systems, although they are of real concern in practice (e.g. the failure of a pump due to oxidation of contacts and bear wearing). Peng *et al.* [27] have developed a maintenance policy with periodic inspections when two dependent or correlated failure processes are considered. Jiang *et al.* [21] have further compared two preventive maintenance (PM) policies, age replacement policy and block replacement policy, combining immediate corrective replacement in consideration of shifting failure thresholds. Özekici [56] has considered interdependent aging processes between components due to continuous wear and shocks, and proposed an optimal periodic replacement policy. Rasmekomen and Parlikad [22] have considered degradation dependency in terms of output performance between one critical component and other parallel components based on aging processes, and the optimal age-based maintenance policy for this case was also studied. Yang *et al.* [57] have proposed a general statistical reliability model for repairable multi-component systems considering dependent competing risks, under a partially perfect repair assumption which considers that only the failed component, rather than the whole system, is replaced. Hong *et al.* [58] have used copulas to model degradation dependency among all the components of a system and obtained the optimal maintenance policy including condition-based maintenance with periodic inspections and instantaneous corrective maintenance (CM). Van Horenbeek and Pintelon [59] have proposed a dynamic predictive maintenance policy that minimizes the long-term mean maintenance cost per unit time while considering different component dependencies (i.e. economic, structural and stochastic dependence). Song *et al.* [40] have applied age replacement policy and inspection-based maintenance policy for systems whose components have *s*-dependent failure times, and the optimal replacement interval or

inspection times are determined. Note that maintenance optimization for multi-component systems with multiple dependent competing degradation processes within individual components has not been considered and only the pre-scheduled periods for inspection or maintenance are considered as the decision variables of the optimization problem.

1.4 Research objectives

This PhD work aims to develop a holistic framework of models and computational methods for the reliability analysis and maintenance optimization of nuclear safety components and systems, taking into account the available knowledge on the degradation and failure behaviors, their dependencies, the external influencing factors and the associated uncertainties.

The availability of such modeling framework would be strongly beneficial for the asset management of nuclear power plants, because it would enable to successfully predict component and degradation behaviors and optimally plan the necessary maintenance activities.

The research objectives, which also derive the main contributions of this PhD work, addressing the challenging issues presented in Chapter 1.3, are divided into the following three groups:

- For single components:
  - Degradation dependency: to study the dependency between random shock and degradation processes, both can lead components to failure.
  - Random shocks: to establish a general random shock model, where the impacts of a random shock are dependent on the current component degradation condition (the component degradation state and residence time in the state).
  - Maintenance policy: to extend the MSPM framework to include semi-Markov modeling, where the time of transition to a state can depend on the residence time in the current state, and hence is more suitable for including maintenance.
- For multi-component systems (with a limited number of components):
  - Degradation dependency: to develop a modeling framework for systems whose degradation processes are modeled by PBMs and MSMs to treat degradation dependencies between the degradation processes within one component or/and among components; to account for epistemic uncertainty due to incomplete or imprecise knowledge on dependent degradation processes and assess the (fuzzy)

system reliability; to evaluate the dynamic criticality of components over time.

- Random shocks: to consider the impacts of random shocks on PBMs and MSMs at the same time, which have to be characterized in different ways due to the different nature of the two types of degradation models.
- Maintenance policy: to derive the optimal maintenance policy considering degradation dependency and epistemic uncertainty, and design an efficient optimization method.

- For multi-component systems (with a large number of components):
  - To develop an efficient reliability assessment method considering degradation dependency.

1.5 Structure of the thesis

The thesis is composed of two parts. Part I, made of ten Chapters, presents, in synthesis, the motivations, contents and conclusions of the PhD work. Part II, contains a collection of seven journal papers, reporting each research work performed during the PhD. The readers may refer to them for detailed information about the research.

The Chapters in Part I are summarized as follows.

Chapter I (current Chapter) introduces the issues and challenges in reliability analysis and maintenance optimization of nuclear safety components and systems, taking into account the available knowledge on the system functionalities, degradation and failure behaviors, dependencies, external influencing factors and associated uncertainties. It also describes the research objectives of the work.

Chapter 2 (Paper I) first includes semi-Markov models in the original MSPM framework for component reliability assessment and, then, incorporates the generalized random shock models where the probability of a random shock resulting in extreme or cumulative damage, and the cumulative damages, are both *s*-dependent on the current component degradation condition.

Chapter 3 (Paper II) firstly introduces PBMs and MSMs for degradation processes. The piecewise-deterministic Markov processes (PDMPs) are then employed to handle the dependencies between PBMs, between MSMs and between these two types of models.

Chapter 4 (Paper III) deals with the epistemic uncertainty in the degradation processes. To account for this, the parameters of the PDMP model are described by fuzzy numbers. The extension of the finite-volume (FV) method to quantify the (fuzzy) reliability of the systems is proposed.

Chapter 5 (Paper IV) focuses on the component importance measures (IMs). The extended mean absolute deviation (MAD) IMs for components with degradation dependency and subject to maintenance are proposed. The quantification of the extended component IM is developed based on the FV method.

Chapter 6 (Paper V) focuses on the maintenance optimization for systems considering epistemic uncertainty and degradation dependency. The pre-scheduled period for inspection tasks and the thresholds for PM are considered as the decision variables in the optimization problem formulation. A new optimization method integrating non-dominated sorting differential evolution (NSDE) [60], differential evolution (DE) [61] and the FV method for solving PDMP [62] is proposed to derive the optimal maintenance policy.

Chapter 7 (Paper VI) extends the modeling framework presented in Chapter 2 by including the impacts of random shocks on the dependent degradation processes. The dependencies between degradation processes and random shocks, and among degradation processes are explicitly modelled.

Chapter 8 (Paper VII) proposes a reliability assessment method for multi-component systems (with a large number of components) considering degradation dependency. Binary decision diagrams (BDDs) and MC simulation are combined to reduce computational cost.

Chapter 9 summarizes the applications of the proposed models and methodologies to real cases related to nuclear safety components and systems.

Chapter 10 draws the conclusions of this PhD work and presents relevant open issues and perspectives for future research.

Fig. 1-1 provides a pictorial view of the issues addressed in the PhD work.

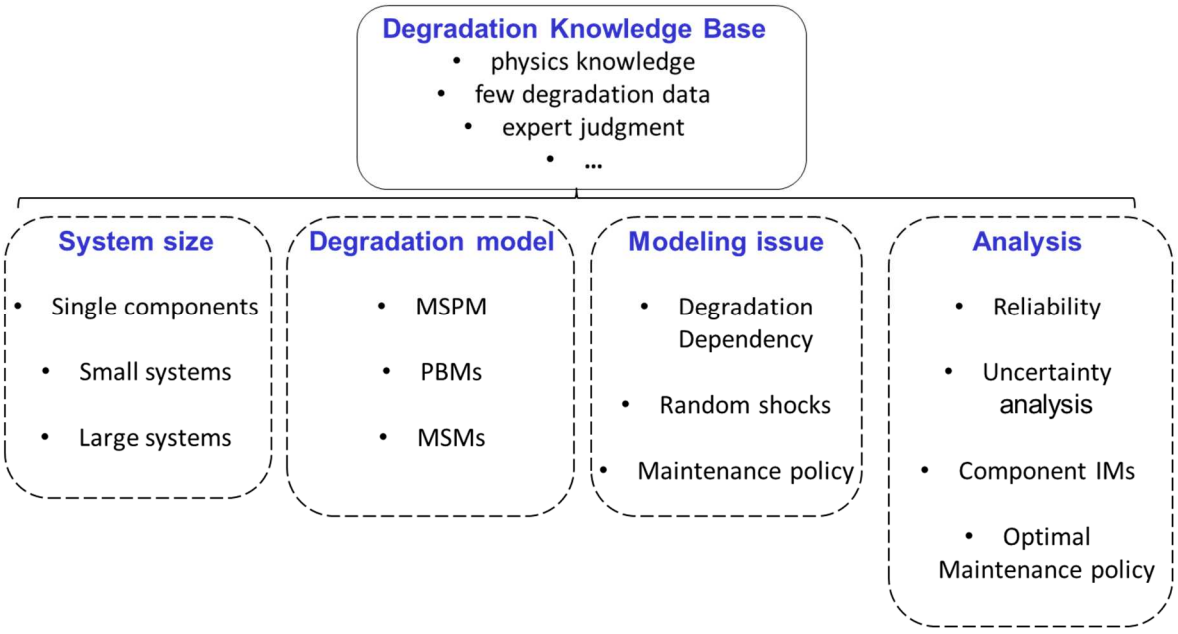

Fig. 1-1. A pictorial view of the issues addressed in the PhD work.

2. MULTI-STATE PHYSICS MODEL (MSPM) FRAMEWORK FOR COMPONENT RELIAIBLITY ASSESSMENT INCLUDING SEMI-MARKOV AND RANDOM SHOCK PROCESSES

MSPM framework is proposed by Unwin *et al.* [19] for modeling nuclear component degradation, also accounting for the effects of environmental factors (e.g. temperature and stress) within certain predetermined ranges [63]. Random shocks need to be accounted for on top of the underlying degradation processes because they can bring variations to influencing environmental factors, even outside their predetermined boundaries [64] that can accelerate the degradation processes. For example, thermal, and mechanical shocks (e.g. internal thermal shocks and water hammers) [30, 31] onto power plant components can lead to intense increases in temperatures, and stresses, respectively; under these extreme conditions, the original physics functions in MSPM might be insufficient to characterize the influences of random shocks onto the degradation processes, and must, therefore, be modified. In this Chapter, we extend the MSPM framework for component reliability assessment by including semi-Markov and random shock processes, where the probability of a random shock resulting in extreme or cumulative shock, and the cumulative damages, are both *s*-dependent on the current component degradation condition.

2.1 Extended MSPM framework

A continuous-time stochastic process is called a semi-Markov process if the embedded jump chain is a Markov Chain and the times between transitions may be random variables with any distribution [65]. It more generally describes the fact that the time of transition to a state can depend on the residence time in the current state, and hence is more suitable for including maintenance [66]. The following assumptions are made for the extended MSPM framework based on semi-Markov processes:

- The degradation process has a finite number of states $\boldsymbol{S} = \{0,1, \dots, M\}$ where states *0,* and *M* represent the complete failure state, and perfect functioning state, respectively. The generic intermediate degradation states i ($0<i<M$) are established according to the degradation development and condition, wherein the component is functioning or partially functioning.

- The degradation follows a continuous-time semi-Markov process; the transition rate between state *i* and state *j*, denoted by $\lambda_{i,j}(\tau_i, \boldsymbol{\theta})$, is a function of τ_i which is the residence time of the component being in the current state *i* since the last transition, and $\boldsymbol{\theta}$ which represents the external influencing factors (including physical factors).
- The initial state (at time $t = 0$) of the component is *M*.
- Maintenance can be carried out from any degradation state, except for the complete failure state (in other words, there is no repair from failure).

Fig. 2-1 presents the diagram of the semi-Markov component degradation process.

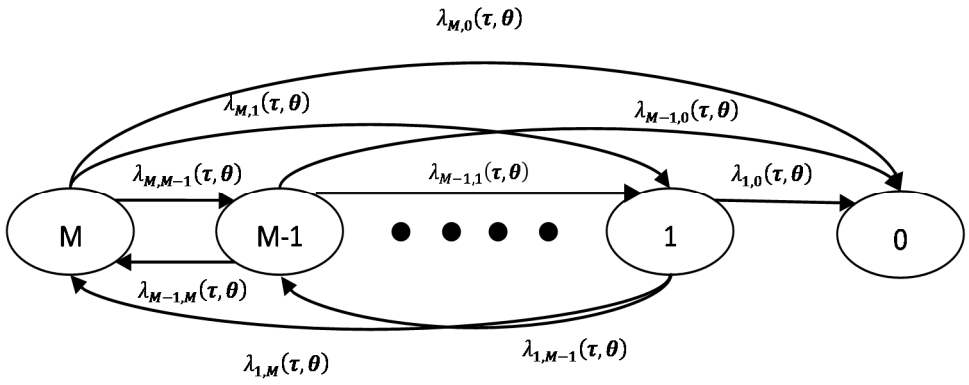

Fig. 2-1. The diagram of the semi-Markov process.

The probability that the continuous time semi-Markov process will step to state *j* in the next infinitesimal time interval $(t, t + \Delta t)$, given that it has arrived at state *i* at time T_n after *n* transitions and remained stable in *i* from T_n until time *t* , is defined as

$$P[X_{n+1} = j, T_{n+1} \in [t, t + \Delta t] \mid \{X_{k,}\, T_k\}_{k=0}^{n-1}, (X_n = i, T_n), T_n \le t \le T_{n+1}, \boldsymbol{\theta}]$$
$$= P[X_{n+1} = j, T_{n+1} \in [t, t + \Delta t] \mid (X_n = i, T_n)\,, T_n \le t \le T_{n+1}, \boldsymbol{\theta}]$$
$$= \lambda_{i,j}(\tau_i = t - T_n, \boldsymbol{\theta})\Delta t,\ \forall\, i, j\ \in\ \boldsymbol{S}, i \ne j. \qquad (2.1)$$

where X_k denotes the state of the component after *k* transitions. The degradation transition rates can be obtained from the structural reliability analysis of the degradation processes (e.g. the crack propagation process [67], whereas the transition rates related to maintenance tasks can be estimated from the frequencies of maintenance activities). For example, the authors of [63]

divided the degradation process of the alloy metal weld into six states dependent on the underlying physics phenomenon, and some degradation transition rates are represented by corresponding physics equations.

The solution to the semi-Markov process model is the state probability vector $P(t) = \{p_M(t), p_{M-1}(t), \dots, p_0(t)\}$. Because no maintenance is carried out from the component failure state, and the component is regarded as functioning in all other intermediate alternative states, its reliability can be expressed as

$$R(t) = 1 - p_0(t). \tag{2.2}$$

Analytically solving the continuous time semi-Markov model with state residence time-dependent transition rates is a difficult or sometimes impossible task, and the Monte Carlo simulation method is usually applied to obtain $P(t)$ [68, 69].

2.2 Generalized random shock models

The following assumptions are made on the random shock process.

- The arrivals of random shocks follow a homogeneous Poisson process $\{N(t), t \geq 0\}$ [32] with constant arrival rate μ. The random shocks are *s*-independent of the degradation process, but they can influence the degradation process (see Fig. 2-2).
- The damages of random shocks are divided into two types: extreme, and cumulative.
- Extreme shock and cumulative shock are mutually exclusive.
- The component fails immediately upon occurrence of extreme shocks.
- The probability of a random shock resulting in extreme or cumulative damage is *s*-dependent on the current component degradation.
- The damage of cumulative shocks can only influence the degradation transition departing from the current state, and its impact on the degradation process is *s*-dependent on the current component degradation.

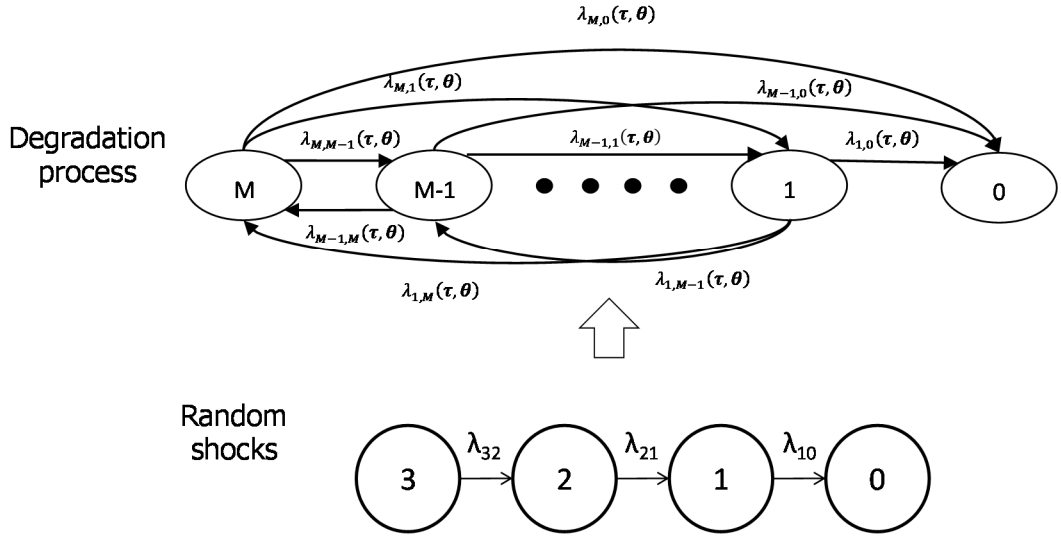

Fig. 2-2. Degradation and random shock processes.

The first five assumptions are taken from [20]. The sixth assumption reflects the aging effects addressed in Fan *et al.*'s shock model [39], where the random shocks are more fatal to the component (i.e. more likely lead to extreme damages) when the component is in severe degradation states. However, the influences of cumulative shocks under aging effects have not been considered in Fan *et al.*'s model. In addition, the random shock damage is assumed to depend on the current degradation, characterized by three parameters: 1) the current degradation state *i*, 2) the number of cumulative shocks *m* that occurred while in the current degradation state since the last degradation state transition, and 3) the residence time $\tau'_{i,m}$ of the component in the current degradation state *i* after *m* cumulative shocks $\tau'_{i,m}\geq 0$.

Let $p_{i,m}(\tau'_{i,m})$ denote the probability that one shock results in extreme damage (the cumulative damage probability is then $1-p_{i,m}(\tau'_{i,m})$). In the case of cumulative shock, the degradation transition rates for the current state change at the moment of the occurrence of the shock, whereas the other transition rates are not affected. Let $\lambda_{i,j}^{(m)}(\tau'_{i,m},\boldsymbol{\theta})$ denote the transition rates after *m* cumulative random shocks, where $\lambda_{i,j}^{(0)}(\tau'_{i,0},\boldsymbol{\theta})$ holds the same expression as the transition rate $\lambda_{i,j}(\tau'_{i,0},\boldsymbol{\theta})$ in the pure degradation model, and the other transition rates (i.e. $m>0$) depend on the degradation and the external influencing factors. Because the influences of random shocks can render invalid the original physics functions, we propose a general model which allows the formulation of physics functions dependent on the effects of shocks. The

modified transition rates can be obtained by material science knowledge, and data from shock tests [70]. These quantities will be used as the key linking elements in the integration work of the next section.

2.3 Proposed modeling framework

Based on the first and second assumptions on random shocks, the new model that integrates random shocks into MSPM is shown in Fig 2-3. In the model, the states of the component are represented by pair (*i*,*m*), where *i* is the degradation state, and *m* is the number of cumulative shocks that occurred during the residence time in the current state. For all the degradation states of the component except for state *0*, the number of cumulative shocks could range from *0* to positive infinity. If the transition to a new degradation state occurs, the number of cumulative shocks is set to *0*, coherently with the last assumption on random shocks. The state space of the new integrated model is denoted by $\boldsymbol{S}' = \{(M,0),(M,1),(M,2),\dots,(M-1,0),(M-1,1),\dots,(0,0)\}$. The component is failed whenever the model reaches (*0*,*0*). The transition rate denoted by $\lambda_{(i,m),(j,n)}(\tau'_{i,m},\boldsymbol{\theta})$ is residence time-dependent, thus rendering the process a continuous time semi-Markov process.

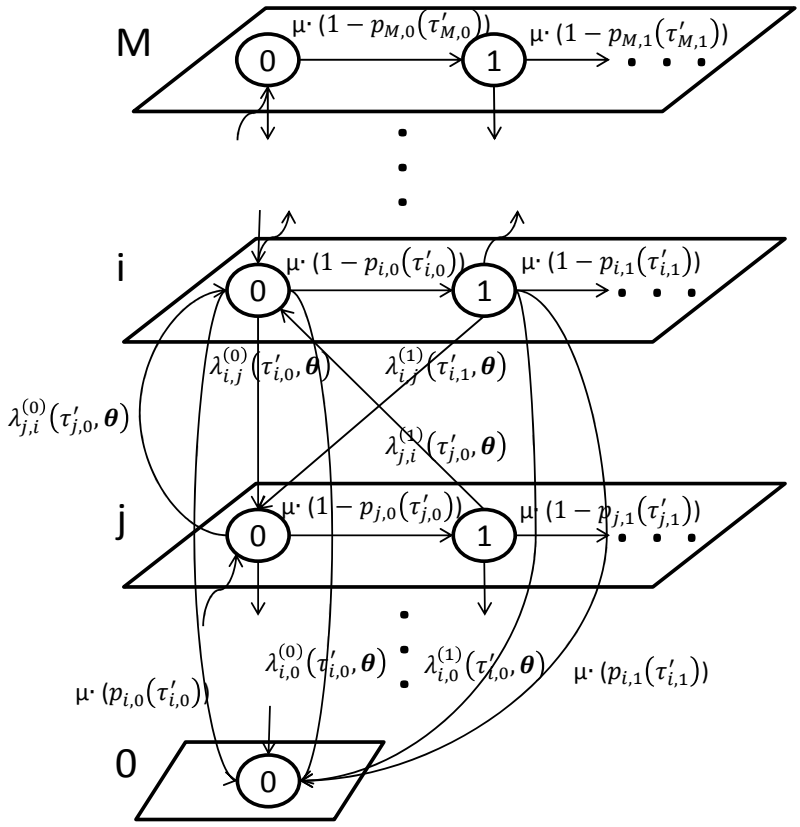

Fig. 2-3. Degradation and random shock processes.

Suppose that the component is in a non-failure state (*i*,*m*); then, we have three types of outgoing transition rates:

$$\lambda_{(i,m),(0,0)}(\tau'_{i,m},\boldsymbol{\theta}) = \mu\cdot(p_{i,m}(\tau'_{i,m})), \tag{2.3}$$

the rate of occurrence of an extreme shock which will cause the component to go to state (*0*,*0*);

$$\lambda_{(i,m),(i,m+1)}(\tau'_{i,m},\boldsymbol{\theta}) = \mu\cdot(1-p_{i,m}(\tau'_{i,m})), \tag{2.4}$$

the rate of occurrence of a cumulative shock which will cause the component to go to state (*i*,*m+1*); and

$$\lambda_{(i,m),(j,0)}(\tau'_{i,m},\boldsymbol{\theta}) = \lambda_{i,j}^{(m)}(\tau'_{i,j},\boldsymbol{\theta}), \tag{2.5}$$

the rate of transition (i.e. degradation or maintenance) which will cause the component to make the transition to state (*j*,*0*).

The effect of random shocks on the degradation processes is shown in eq. (2.5) by using the

superscript (m), where m is the number of cumulative shocks occurring during the residence time in the current state. It means that the transition rate functions depend on the number of cumulative shocks. This is a general formulation.

The first two types eqs. (2.3) and (2.4) depend on the probability of a random shock resulting in extreme damage, and in cumulative damage, respectively; the last type of transition rates eq. (2.5) depends on the cumulative damage of random shocks. In this model, we do not directly associate a failure threshold to the cumulative shocks, because the damage of cumulative shocks can only influence the degradation transition departing from the current state, and its impact on the degradation process is *s*-dependent on the current component degradation. The cumulative shocks can only aggravate the degradation condition of the component instead of leading it suddenly to failure (which is the role of extreme shocks). The effect of the cumulative shocks is reflected in the change of transition rates. The probability of a shock becoming an extreme one depends on the degradation condition of the component. The extreme shocks immediately lead the component to failure, whereas the damage of cumulative shocks accelerates the degradation processes of the component.

The proposed model is based on a semi-Markov process and random shocks. Under this general structure, as explained in the paragraph above, the physics lies in the transition rates of the semi-Markov process. We refer to it as a physics model because the stressors (e.g. the crack in the case study) that cause the component degradation are explicitly modeled, differently from the conventional way of estimating the transition rates from historical failure and degradation data, which are relatively rare for the critical components. More information about MSPM can be found in [9]. In addition, the random shocks are integrated into the MSPM in a way that they may change the physics functions of the transition rates, within a general formulation.

Similarly to what was said for the semi-Markov process presented in Section 2.2, the state probabilities of the new integrated model can be obtained by MC simulation, and the expression of component reliability is

$$R(t) = 1 - p_{(0,0)}(t). \tag{2.6}$$

2.4 Component reliability estimation method

2.4.1 Basics of Monte Carlo simulation

The key theoretical construct upon which MC simulation is based is the transition probability density function $f_{(i,m),(j,n)}(\tau'_{i,m} \mid t, \boldsymbol{\theta})$, defined as

$$f_{(i,m),(j,n)}(\tau'_{i,m} \mid t, \boldsymbol{\theta})d\tau'_{i,m} \equiv \text{the probability that, given that the system arrives at the state } (i,m) \text{ at time } t\text{, with physical factors } \boldsymbol{\theta}\text{, the next transition will occur in the infinitesimal time interval } (t+\tau'_{i,m}, t+\tau'_{i,m}+d\tau'_{i,m})\text{, and will be to the state } (j,n) \text{ [68]} \tag{2.7}$$

By using the previously introduced transition rates, eq. (2.7) can be expressed as

$$f_{(i,m),(j,n)}(\tau'_{i,m} \mid t, \boldsymbol{\theta})d\tau'_{i,m} = P_{(i,m)}(\tau'_{i,m} \mid t, \boldsymbol{\theta})\lambda_{(i,m),(j,n)}\left(\tau'_{i,m}, \boldsymbol{\theta}\right)d\tau'_{i,m} \tag{2.8}$$

$P_{(i,m)}(\tau'_{i,m} \mid t, \boldsymbol{\theta})$ is the probability that, given that the component arrives at the state (i,m) at time t with physical factors $\boldsymbol{\theta}$, no transition will occur in the time interval $(t, t+\tau'_{i,m})$. It satisfies

$$\frac{dP_{(i,m)}(\tau'_{i,m} \mid t,\boldsymbol{\theta})}{P_{(i,m)}(\tau'_{i,m} \mid t,\boldsymbol{\theta})} = -\lambda_{(i,m)}\left(\tau'_{i,m}, \boldsymbol{\theta}\right)d\tau'_{i,m} \tag{2.9}$$

$\lambda_{(i,m)}\left(\tau'_{i,m}, \boldsymbol{\theta}\right)d\tau'_{i,m}$ is the conditional probability that, given that the component is in the state (i,m) at time t, having arrived there at time $t-\tau'_{i,m}$, with physical factors $\boldsymbol{\theta}$, it will depart from (i,m) during $(t, t+d\tau'_{i,m})$. $\lambda_{(i,m)}\left(\tau'_{i,m}, \boldsymbol{\theta}\right)$ is obtained as

$$\lambda_{(i,m)}\left(\tau'_{i,m}, \boldsymbol{\theta}\right) = \sum_{(i',m')} \lambda_{(i,m),(i',m')}\left(\tau'_{i,m}, \boldsymbol{\theta}\right) \tag{2.10}$$

Taking the integral of both sides of eq. (2.9) with the initial condition $P_{(i,m)}(0 \mid t, \boldsymbol{\theta}) = 1$, we obtain

$$P_{(i,m)}(\tau'_{i,m} \mid t, \boldsymbol{\theta}) = exp[-\int_0^{\tau'_{i,m}} \lambda_{(i,m)}(s, \boldsymbol{\theta})ds] \tag{2.11}$$

Substituting eq. (2.11) into eq. (2.8), we obtain

$$f_{(i,m),(j,n)}(\tau'_{i,m} \mid t, \boldsymbol{\theta}) = \lambda_{(i,m),(j,n)}\left(\tau'_{i,m}, \boldsymbol{\theta}\right)exp[-\int_0^{\tau'_{i,m}} \lambda_{(i,m)}(s, \boldsymbol{\theta})ds] \tag{2.12}$$

To derive a Monte Carlo simulation procedure, eq. (2.12) is rewritten as

$$f_{(i,m),(j,n)}(\tau'_{i,m} \mid t, \boldsymbol{\theta}) = \frac{\lambda_{(i,m),(j,n)}(\tau'_{i,m}, \boldsymbol{\theta})}{\lambda_{(i,m)}(\tau'_{i,m}, \boldsymbol{\theta})} \cdot \lambda_{(i,m)}(\tau'_{i,m}, \boldsymbol{\theta}) exp[-\int_0^{\tau'_{i,m}} \lambda_{(i,m)}(s, \boldsymbol{\theta}) ds]$$

$$= \pi_{(i,m),(j,n)}(\tau'_{i,m} \mid \boldsymbol{\theta}) \cdot \psi_{(i,m)}(\tau'_{i,m} \mid \boldsymbol{\theta}). \quad (13)$$

$\psi_{(i,m)}(\tau'_{i,m} \mid \boldsymbol{\theta})$ is the probability density function for the holding time $\tau'_{i,m}$ in the state (i,m), given the physical factors $\boldsymbol{\theta}$. It satisfies

$$\psi_{(i,m)}(\tau'_{i,m} \mid \boldsymbol{\theta}) = \lambda_{(i,m)}(\tau'_{i,m}, \boldsymbol{\theta}) exp[-\int_0^{\tau'_{i,m}} \lambda_{(i,m)}(s, \boldsymbol{\theta}) ds]. \quad (2.14)$$

$$\pi_{(i,m),(j,n)}(\tau'_{i,m} \mid \boldsymbol{\theta}) = \frac{\lambda_{(i,m),(j,n)}(\tau'_{i,m}, \boldsymbol{\theta})}{\lambda_{(i,m)}(\tau'_{i,m}, \boldsymbol{\theta})}, \quad (2.15)$$

is regarded as the conditional probability that, for the transition out of state (i,m) after holding time $\tau'_{i,m}$, with the physical factors $\boldsymbol{\theta}$, the transition arrival state will be (j,n).

In the Monte Carlo simulation, for the component arriving at any non-failure state (i,m) at any time *t*, the process at first samples the holding time at state (i,m) corresponding to eq. (2.14), and then determines the transition arrival state (j,n) from state (i,m) according to eq. (2.15). This procedure is repeated until the accumulated holding time reaches the predefined time horizon, or the component reaches the failure state $(0,0)$.

2.4.2 The simulation procedure

To generate the holding time $\tau'_{i,m}$ and the next state (j,n) for the component arriving in any non-failure state (i,m) at any time *t*, one proceeds as follows. Two uniformly distributed random numbers u_1 and u_2 are sampled in the interval [0, 1]; then, $\tau'_{i,m}$ is chosen so that

$$\int_0^{\tau'_{i,m}} \lambda_{(i,m)}(s, \boldsymbol{\theta})\, ds = \ln(1/u_1)\,, \quad (2.16)$$

and $(j,n) = a^*$ that satisfies

$$\sum_{k=0}^{a^*-1} \lambda_{(i,m),k}(\tau'_{i,m}, \boldsymbol{\theta}) < u_2 \lambda_{(i,m)}(\tau'_{i,m}, \boldsymbol{\theta}) \leq \sum_{k=0}^{a^*} \lambda_{(i,m),k}(\tau'_{i,m}, \boldsymbol{\theta}) \quad (2.17)$$

where a^* represents one state in the ordered sequence of all possible outgoing states of state (i,m). The state a^* is determined by going through the ordered sequence of all possible outgoing states of state (i,m) until eq. (2.17) is satisfied. The algorithm of Monte Carlo simulation for solving the integrated MSPM on a time horizon $[0, t_{max}]$ is presented as follows.

Set N_{max} (the maximum number of replications), and $k = 0$.

While $k < N_{max}$, do the following.

Initialize the system by setting $s = (M, 0)$ (initial state of perfect performance), setting the time $t = 0$ (initial time).

Set $t' = 0$ (state holding time).

While $t < t_{max}$, do the following.

Calculate (10).

Sample a t' by using eq. (2.16).

Sample an arrival state (j, n) by using eq. (2.17).

Set $t = t + t'$.

Set $s = (j, n)$.

If $s = (0,0)$,

then break.

End if.

End While.

Set $k = k + 1$.

End While. □

The estimation of the state probability vector $\widehat{\boldsymbol{P}}(t) = \{\widehat{p_M}(t), \widehat{p_{M-1}}(t), \dots, \widehat{p_0}(t)\}$ at time t is

$$\widehat{\boldsymbol{P}}(t) = \frac{1}{N_{max}}\{n_M(t), n_{M-1}(t), \dots, n_0(t)\} \tag{2.18}$$

where $\{n_i(t)|i = M, \dots, 0, t \leq t_{max}\}$ is the total number of visits to state *i* at time *t*, with sample variance [71] defined as

$$var_{\widehat{p_i}(t)} = \widehat{p_i}(t)(1 - \widehat{p_i}(t))/(N_{max} - 1) \tag{2.19}$$

3. DYNAMIC RELIABILITY MODELS FOR SYSTEMS WITH DEGRADATION DEPENDENCY

For highly reliable systems, such as nuclear safety systems, it is relatively difficult to model their degradation and failure behaviors due to the limited amount of data available. In these cases, PBMs and MSMs are two modeling frameworks that can be used for describing the evolution of degradation in systems. Systems are often subject to multiple competing degradation processes and any of them may cause failure. The dependences among these processes need to be considered under certain circumstances. In this chapter, a PDMP modeling framework is developed to treat degradation dependency in a system whose degradation processes are modeled by PBMs and MSMs.

3.1 Degradation models

We consider a multi-component system made of Q components denoted by $O = \{O_1, O_2, \dots, O_Q\}$. Each component may be affected by multiple degradation mechanisms or processes, possibly dependent. The degradation processes can be separated into two groups: (1) $\boldsymbol{L} = \{L_1, L_2, \dots, L_M\}$ modeled by M PBMs; (2) $\boldsymbol{K} = \{K_1, K_2, \dots, K_N\}$ modeled by N MSMs, where $L_m, m = 1, 2, \dots, M$ and $K_n, n = 1, 2, \dots, N$ are the indexes of the degradation processes.

3.1.1 Physics-based models (PBMs)

The following assumptions on PBMs are made:

- A degradation process $\boldsymbol{X}_{L_m}(t), L_m \in \boldsymbol{L}$ in the first group, has d_{L_m} time-dependent continuous variables $\boldsymbol{X}_{L_m}(t) = \left(x_{L_m}^1(t), x_{L_m}^2(t), \dots, x_{L_m}^{d_{L_m}}(t)\right) \in \mathbb{R}^{d_{L_m}}$. A system of first-order differential equations (i.e. physics equations) $\dot{\boldsymbol{X}_{L_m}}(t) = \boldsymbol{f}_{L_m}\left(\boldsymbol{X}_{L_m}(t), t \mid \boldsymbol{\theta}_{L_m}\right)$, are used to characterize its evolution, where $\boldsymbol{\theta}_{L_m}$ are the environmental factors influential to L_m (e.g. temperature and pressure) and the parameters used in $\boldsymbol{f}_{L_m}$. This assumption is made in [72] and widely used in practice [12, 73]. Note that higher-order differential equations can be converted into a system of a large number of first-order differential equations by introducing extra variables [74].

- $\boldsymbol{X}_{L_m}(t)$ can be divided into two groups of varaibles $\boldsymbol{X}_{L_m}(t) = (\boldsymbol{X}_{L_m}^{\boldsymbol{D}}(t), \boldsymbol{X}_{L_m}^{\boldsymbol{P}}(t))$: (1) $\boldsymbol{X}_{L_m}^{\boldsymbol{D}}(t)$ are the non-decreasing degradation variables describing the degradation process (e.g. leak area of the piston of the valve [12]]), where $\boldsymbol{D}$ is the set of degradation variables indices; (2) $\boldsymbol{X}_{L_m}^{\boldsymbol{P}}(t)$ are the physical variables influencing $\boldsymbol{X}_{L_m}^{\boldsymbol{D}}(t)$ (e.g. velocity and force [73]), where $\boldsymbol{P}$ is the set of physical variable indices. For example, the friction-induced wear of the bearings is considered as one degradation process in [73]. It is represented by the increase in friction coefficients. The two friction coefficients associated with sliding and rolling friction are considered as the degradation variables. The rotational velocity of the pump is considered as the physical variable since it influences the increase in the coefficients of friction. The evolution of physical variables can be characterized by physics equations. If the variables can be modeled by physics equations and influence certain degradation variables, then, they are considered as physical variables. As long as one $x_{L_m}^i(t) \in \boldsymbol{X}_{L_m}^{\boldsymbol{D}}(t)$ reaches or exceeds its corresponding failure threshold $x_{L_m}^{i\ *}$, the generic degradation process L_m fails. Let $\boldsymbol{\mathcal{F}}_{L_m}$ denote the failure state set of L_m and $\boldsymbol{x}_{L_m}^*$ denote the set of all the failure thresholds of $\boldsymbol{X}_{L_m}^{\boldsymbol{D}}(t)$. An example of L_1 is shown in Fig. 3-1.

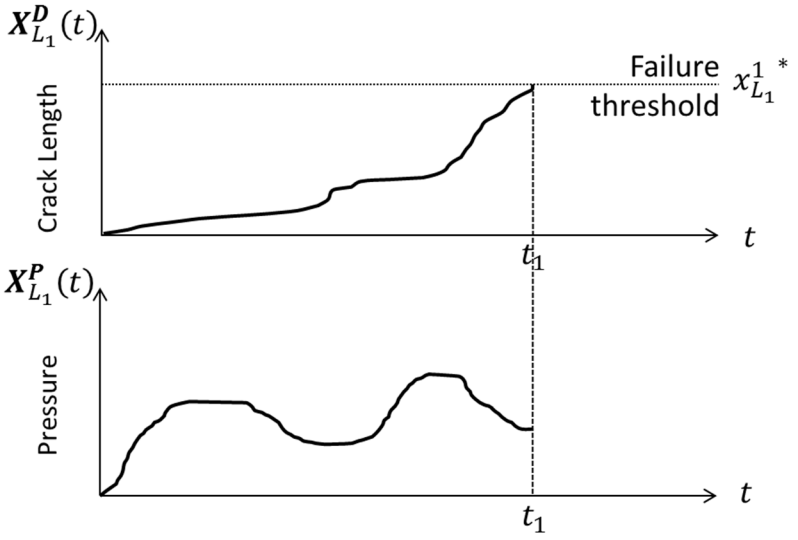

Fig. 3-1. An illustration of L_1.

3.1.2 Multi-state models (MSMs)

The following assumptions on MSMs are made:

- A degradation process, $Y_{K_n}(t)$, $K_n \in K$ in the second group, takes values from a finite state set denoted by $S_{K_n} = \{0, 1, \dots, d_{K_n}\}$, where '$d_{K_n}$' is the perfect functioning state and '0' is the complete failure state. The transition rates $\lambda_i(j \mid \boldsymbol{\theta}_{K_n}), \forall\, i, j \in \boldsymbol{S}_{K_n}, i > j$ characterize the degradation transition probabilities from state i to state j, where $\boldsymbol{\theta}_{K_n}$ is the set of the environmental factors to K_n and the related parameters used in λ_i. We follow the assumption of Markov property which is widely used in practice to describe components degradation processes [18]. The transition rates between different degradation states are estimated from the degradation and/or failure data from historical field collection. Let $\boldsymbol{\mathcal{F}}_{K_n} = \{0\}$ denote the failure state set of K_n. An example of K_1 is shown in Fig. 3-2.

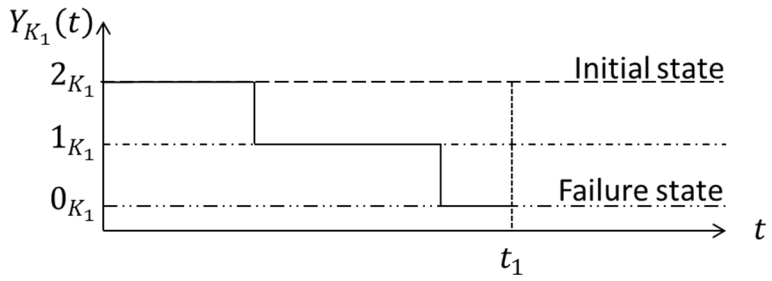

Fig. 3-2. An illustration of K_1.

3.2 Degradation model of the system considering dependency

The dependencies between degradation mechanisms or processes may exist within each group and between the two groups. The evolution trajectories of the continuous variables in the first group may be influenced by the degradation states of the second group. The transition times and transition directions of the degradation processes of the second group may depend on the degradation levels of the components in the first group [75]. PDMPs [76], which are a family of Markov processes involving deterministic evolution punctuated by random jumps, can be employed to model this type of dependency (the detailed formulations are shown in eqs. (3.2)

and (3.3)). Let $\boldsymbol{X}(t) = \begin{pmatrix} \boldsymbol{X}_{L_1}(t) \\ \vdots \\ \boldsymbol{X}_{L_M}(t) \end{pmatrix}$ denote the degradation processes of the first group and $\boldsymbol{Y}(t) = \begin{pmatrix} Y_{K_1}(t) \\ \vdots \\ Y_{K_N}(t) \end{pmatrix}$ denote the degradation processes of the second group. The overall degradation process of the system is presented as

$$\boldsymbol{Z}(t) = \begin{pmatrix} \boldsymbol{X}(t) \\ \boldsymbol{Y}(t) \end{pmatrix} \in \boldsymbol{E} = \mathbb{R}^{d_L} \times \boldsymbol{S} \tag{3.1}$$

where $\boldsymbol{E}$ is a space combining $\mathbb{R}^{d_L}$ $(d_L = \sum_{m=1}^{M} d_{L_m})$ and $\boldsymbol{S} = \{0, 1, \dots, d_{\boldsymbol{S}}\}$ denotes the state set of process $\boldsymbol{Y}(t)$. The evolution of $\boldsymbol{Z}(t)$ has two parts: (1) the stochastic behavior of $\boldsymbol{Y}(t)$ and (2) the deterministic behavior of $\boldsymbol{X}(t)$ between two consecutive jumps of $\boldsymbol{Y}(t)$, given $\boldsymbol{Y}(t)$. The former is governed by the transition rates of $\boldsymbol{Y}(t)$, which depend on the states of the degradation processes in $\boldsymbol{X}(t)$ and also in $\boldsymbol{Y}(t)$, as follows:

$$\begin{aligned} &\lim_{\Delta t \to 0} P\left(\boldsymbol{Y}(t + \Delta t) = j \mid \boldsymbol{X}(t), \boldsymbol{Y}(t) = i, \boldsymbol{\theta}_{\boldsymbol{K}} = \cup_{n=1}^{N} \boldsymbol{\theta}_{K_n}\right) / \Delta t \\ &= \lambda_i(j \mid \boldsymbol{X}(t), \boldsymbol{\theta}_{\boldsymbol{K}}), \forall\, t \geq 0, i, j \in \boldsymbol{S}, i \neq j \end{aligned} \tag{3.2}$$

The latter is described by the deterministic physics, which depends on the states of the degradation processes in $\boldsymbol{Y}(t)$ and also in $\boldsymbol{X}(t)$, as follows:

$$\begin{aligned} \dot{\boldsymbol{X}}(t) &= \begin{pmatrix} \dot{\boldsymbol{X}}_{L_1}(t) \\ \vdots \\ \dot{\boldsymbol{X}}_{L_M}(t) \end{pmatrix} = \begin{pmatrix} \boldsymbol{f}_{L_1}^{\boldsymbol{Y}(t)}(\boldsymbol{X}(t), t \mid \boldsymbol{\theta}_{L_1}) \\ \vdots \\ \boldsymbol{f}_{L_M}^{\boldsymbol{Y}(t)}(\boldsymbol{X}(t), t \mid \boldsymbol{\theta}_{L_M}) \end{pmatrix} \\ &= \boldsymbol{f}_{L}^{\boldsymbol{Y}(t)}(\boldsymbol{X}(t), t \mid \boldsymbol{\theta}_{\boldsymbol{L}} = \cup_{m=1}^{M} \boldsymbol{\theta}_{L_m}) \end{aligned} \tag{3.3}$$

Let $\boldsymbol{\mathcal{F}}$ denote the system failure state set, which depends on the structure of the system: then, the system reliability at mission time T_{miss} can be obtained as follows:

$$R(T_{miss}) = P[\boldsymbol{Z}(s) \notin \boldsymbol{\mathcal{F}}, \forall s \leq T_{miss}] \tag{3.4}$$

The system failure state set is dependent on system structure. To determine this set, reliability analysis tools such as fault tree [77] can be used to identify the combination of primary failure events leading to system failure.

3.3 System reliability estimation method

Analytically solving the PDMP is a difficult task due to the complex behavior of the system [78], which contains the stochasticities in the components modeled by MSMs and the time-dependent evolutions of the components modeled by PBMs. On the other hand, MC simulation methods are suited for the reliability estimation of the system.

Refer to the system presented in Section 3.2. Let $\boldsymbol{Z}_k = \boldsymbol{Z}(T_k) = \begin{pmatrix} \boldsymbol{X}(T_k) \\ \boldsymbol{Y}(T_k) \end{pmatrix} \in \boldsymbol{E}, k \in \mathbb{N}$, where T_k denotes the time of the k-th transition of $\boldsymbol{Y}(t)$ from the beginning. Then, $\{\boldsymbol{Z}_k, T_k\}_{k\geq 0}$ is a Markov renewal process defined on the space $\boldsymbol{E} \times \mathbb{R}^+$ [76], which is characterized as follows:

$$\begin{aligned} &P[\boldsymbol{Z}_{k+1} \in \boldsymbol{B}, T_{k+1} \in [T_k, T_k + \Delta t] | \boldsymbol{Z}_k = i, \boldsymbol{\theta} = \boldsymbol{\theta_K} \cup \boldsymbol{\theta_L}] \\ &= \iint_{\boldsymbol{B}*[0,\Delta t]} N(i, d\boldsymbol{z}, ds|\boldsymbol{\theta}), \forall\, k \geq 0, \Delta t \geq 0, i \in \boldsymbol{E}, \boldsymbol{B} \in \varepsilon \end{aligned} \tag{3.5}$$

where ε is a σ-algebra of $\boldsymbol{E}$ and $N(i, d\boldsymbol{z}, ds|\boldsymbol{\theta})$ is a semi-Markov kernel on $\boldsymbol{E}$, which verifies that $\iint_{\boldsymbol{E}*[0,\Delta\, t]} N(i, d\boldsymbol{z}, ds|\boldsymbol{\theta}) \leq 1, \forall\, \Delta t \geq 0, i \in \boldsymbol{E}$. It can be further developed as:

$$N(i, d\boldsymbol{z}, ds|\boldsymbol{\theta}) = dF_i(s|\boldsymbol{\theta})\beta(i, d\boldsymbol{z}|s, \boldsymbol{\theta}) \tag{3.6}$$

where

$$dF_i(s|\boldsymbol{\theta}) \tag{3.7}$$

is the probability density function of $T_{k+1} - T_k$ given $\boldsymbol{Z}_k = i$ and

$$\beta(i, d\boldsymbol{z}|s, \boldsymbol{\theta}) \tag{3.8}$$

is the conditional probability distribution of state $\boldsymbol{Z}_{k+1}$ starting from $\boldsymbol{Z}_k = i$ given $T_{k+1} - T_k = s$.

The simulation procedure consists of sampling the transition time from (3.7) and the arrival state from (3.8) for $\boldsymbol{Y}(t)$, then, calculating $\boldsymbol{X}(t)$ within the transition times, by using the physics equation eq. (3.3) until the time of system evolution reaches a certain mission time T_{miss} or the system enters the failure space $\boldsymbol{\mathcal{F}}$.

To calculate the system reliability, the procedure of the MC simulation is presented as follows:

Set N_{max} (the maximum number of replications) and $k = 0$ (index of replication)

Set $k' = 0$ (number of trials that end in the failure state)

While $k < N_{max}$

Initialize the system by setting $\boldsymbol{Z}' = \begin{pmatrix} \boldsymbol{X}(0) \\ \boldsymbol{Y}(0) \end{pmatrix}$ (initial state), and the time $T = 0$ (initial system time)

Set $t' = 0$ (state holding time)

While $T < T_{miss}$

Sample a t' by using the probability density function (3.7)

Sample an arrival state $\boldsymbol{Y}'$ for stochastic process $\boldsymbol{Y}(t)$ from all the possible states by using the conditional probability distribution (3.8)

Set $T = T + t'$

Calculate $\boldsymbol{X}(T)$ by using the physics eq. (3.3)

Set $\boldsymbol{Z}' = \begin{pmatrix} \boldsymbol{X}(T) \\ \boldsymbol{Y}' \end{pmatrix}$

If $T \leq T_{miss}$

If $\boldsymbol{Z}' \in \boldsymbol{\mathcal{F}}$

Set $k' = k' + 1$

Break

End if

Else (when $T > T_{miss}$)

Calculate $\boldsymbol{Z}(T_{miss})$

If $\boldsymbol{Z}(T_{miss}) \in \boldsymbol{\mathcal{F}}$

Set $k' = k' + 1$

Break

End if

End if

End While

Set $k = k + 1$

End While □

The estimated probability of occurrence of one path at time T_{miss} can be obtained by

$$\hat{R}(T_{miss}) = 1 - k'/N_{max} \tag{3.9}$$

with the sample variance [71] as follows:

$$var_{\hat{P}(T_{miss})} = \hat{R}(T_{miss})(1 - \hat{R}(T_{miss}))/(N_{max} - 1) \tag{3.10}$$

4. SYSTEMS RELIABILITY ASSESSMENT CONSIDERING DEGRADATION DEPENDENCY AND EPISTEMIC UNCERTAINTY

Epistemic (subjective) uncertainty [79] can affect the system reliability assessment due to the incomplete or imprecise knowledge about the degradation processes of the components [80, 81]. For PBMs, the parameters (e.g. wear coefficient) and influencing factors (e.g. temperature and pressure) may be unknown [82] and elicited from expert judgment [83]; for MSMs, the state performances may be poorly defined due to the imprecise discretization of the underlying continuous degradation processes [84] and the transition rates between states may be difficult to estimate statistically due to insufficient data, especially for those highly reliable critical components (e.g. valves and pumps in nuclear power plants or aircrafts, etc.) [85].

4.1 State of the art

In literature, fuzzy reliability has been studied by many researchers to account for imprecision and uncertainty in the system model parameters. Tanaka *et al.* [86] have proposed the fuzzy fault tree for the fuzzy reliability assessment of binary-state systems and Singer [87] has assigned fuzzy probabilities to the basic events. Dunyak *et al.* [88] have proposed another fuzzy extension to assign fuzzy probability to all events, which is consistent with the calculations from fuzzy fault trees. Ding et *al.* [80] have developed fuzzy multi-state systems (FMSS) models by considering the steady state probabilities, or/and steady state performance levels of a component as fuzzy numbers. Ding and Lisnianski [89] have proposed the fuzzy universal generating function (FUGF) for the quantification of the fuzzy reliability of FMSS. Later, Li *et al.* [90] have developed a random fuzzy extension of the universal generating function and Sallak et al. [91] have employed Dempster–Shafer theory to quantify the fuzzy reliability of MSS. Liu *et al.* [84] have proposed a fuzzy Markov model with fuzzy transition rates for FMSS when the steady fuzzy state probabilities are not available.

In this Chapter, the influence of epistemic uncertainty to PDMP system degradation models proposed in Chapter 3 is analyzed.

4.2 Piecewise-deterministic Markov process (PDMP) modeling framework under epistemic uncertainty

Fuzzy set theories and techniques introduced by Zadeh [92, 93] have been employed in reliability models under epistemic uncertainty when the crisp values are insufficient to capture the actual behavior of components. In this section, the following assumptions are made to extend the previous PDMP model presented in Section 3.2 with the consideration of epistemic uncertainty:

- The values of $\boldsymbol{\theta_L}$, the environmental factors and the parameters used in ${\boldsymbol{f}_L}^{\boldsymbol{Y}(t)}(\boldsymbol{X}(t), t \mid \boldsymbol{\theta_L})$ for degradation processes $\boldsymbol{X}(t)$, can be fuzzy numbers, denoted by $\widetilde{\boldsymbol{\theta_L}}$.
- The values of $\boldsymbol{\theta_K}$, the environmental factors and the parameters used in the transition rates $\lambda_i(j \mid \boldsymbol{X}(t), \boldsymbol{\theta_K})$ for the degradation processes $\boldsymbol{Y}(t)$, can be fuzzy numbers, denoted by $\widetilde{\boldsymbol{\theta_K}}$.

Let $p_t(d\boldsymbol{z} = (d\boldsymbol{x}, \boldsymbol{y}) \mid \boldsymbol{\theta})$ denote the probability distribution of $\boldsymbol{Z}(t)$, the system reliability at time t can be defined as follows:

$$R(t) = P[\boldsymbol{Z}(s) \notin \boldsymbol{\mathcal{F}}, \forall s \leq t] = \int_{\boldsymbol{z} \notin \boldsymbol{\mathcal{F}}} p_t(d\boldsymbol{z} \mid \boldsymbol{\theta}) \tag{4.1}$$

Due to the epistemic uncertainty $p_t(d\boldsymbol{z} \mid \boldsymbol{\theta})$ and reliability function $R(t)$ have, therefore, changed from crisp values to fuzzy numbers, denoted by $\widetilde{p_t}(d\boldsymbol{z} \mid \widetilde{\boldsymbol{\theta}} = \widetilde{\boldsymbol{\theta_L}} \cup \widetilde{\boldsymbol{\theta_K}})$ and $\tilde{R}(t)$ respectively.

4.3 Solution methodology

In this section, we extend a FV method to assess the (fuzzy) system reliability. Analytical solution of $p_t(d\boldsymbol{z} \mid \boldsymbol{\theta})$ is difficult to to obtain due to the complex behavior of the processes [78, 94]. MC simulation methods can be applied for such numerical computations, but the major shortcoming is that they are typically time-consuming [95]. FV methods is an alternative that can lead to comparable results as MC simulation, but within a more acceptable computing time [95].

4.3.1 Finite-volume (FV) for solving PDMP

Here, we employ an explicit FV method to PDMP, developed by Cocozza-Thivent *et al.* [62].

This approach can be applied under the following assumptions:

- The transition rates $\lambda_i(j \mid \cdot, \boldsymbol{\theta_K}), \forall i, j \in \boldsymbol{S}$ are continuous and bounded functions from $\mathbb{R}^{d_L}$ to $\mathbb{R}^+$.
- The physics equations ${\boldsymbol{f}_L}^i(\cdot,\cdot \mid \boldsymbol{\theta}_L), \forall i \in \boldsymbol{S}$ are continuous functions from $\mathbb{R}^{d_L} \times \mathbb{R}^+$ to $\mathbb{R}^{d_L}$ and locally Lipschitz continuous.
- The physics equations ${\boldsymbol{f}_L}^i(\cdot, t \mid \boldsymbol{\theta}_L), \forall i \in \boldsymbol{S}$ are sub-linear, i.e. there are some $V_1 > 0$ and $V_2 > 0$ such that

$$\forall \boldsymbol{x} \in \mathbb{R}^{d_L}, t \in \mathbb{R}^+ \left|{\boldsymbol{f}_L}^i(\boldsymbol{x}, t \mid \boldsymbol{\theta}_L)\right| \leq V_1(\|\boldsymbol{x}\| + |t|) + V_2$$

- The functions $div({\boldsymbol{f}_L}^i(\cdot,\cdot \mid \boldsymbol{\theta}_L)), \forall i \in \boldsymbol{S}$ are almost everywhere bounded in absolute value by some real value $D > 0$ (independent of i).

For the ease of notation, first we let $\boldsymbol{g}^i(\cdot,\cdot)$: $\mathbb{R}^{d_L} \times \mathbb{R} \to \mathbb{R}^{d_L}$ denote the solution of

$$\frac{\partial}{\partial t}\boldsymbol{g}^i(\boldsymbol{x}, t \mid \boldsymbol{\theta}_L) = {\boldsymbol{f}_L}^i\left(\boldsymbol{g}^i(\boldsymbol{x}, t \mid \boldsymbol{\theta}_L), t \,\middle|\, \boldsymbol{\theta}_L\right), \forall i \in \boldsymbol{S}, \boldsymbol{x} \in \mathbb{R}^{d_L}, t \in \mathbb{R} \tag{4.2}$$

with

$$\boldsymbol{g}^i(\boldsymbol{x}, 0 \mid \boldsymbol{\theta}_L) = \boldsymbol{x}, \forall i \in \boldsymbol{S}, \boldsymbol{x} \in \mathbb{R}^{d_L} \tag{4.3}$$

and $\boldsymbol{g}^i(\boldsymbol{x}, t \mid \boldsymbol{\theta}_L)$ is the result of the deterministic behavior of $\boldsymbol{X}(t)$ after time *t*, starting from the point $\boldsymbol{x}$ and while the processes $\boldsymbol{Y}(t)$ hold on state i.

The state space $\mathbb{R}^{d_L}$ of continuous variables $\boldsymbol{X}(t)$ is divided into an admissible mesh $\mathcal{M}$, which is a family of measurable subsets of $\mathbb{R}^{d_L}$ ($\mathcal{M}$ is a partition of $\mathbb{R}^{d_L}$) such that:

(1) $\bigcup_{A \in \mathcal{M}} A = \mathbb{R}^{d_L}$.

(2) $\forall A, B \in \mathcal{M},\ A \neq B \Rightarrow A \cap B = \emptyset$.

(3) $m_A = \int_A d\boldsymbol{x} > 0, \forall A \in \mathcal{M}$, where m_A is the volume of grid A.

(4) $sup_{A \in \mathcal{M}} diam(A) < +\infty$ where $diam(A) = sup_{\forall \boldsymbol{x}, \boldsymbol{y} \in A}|\boldsymbol{x} - \boldsymbol{y}|$.

Additionally, the time space $\mathbb{R}^+$ is divided into small intervals $\mathbb{R}^+ = \bigcup_{n=0,1,2,\ldots} [n\Delta t, (n+1)\Delta t[$, by setting the time step $\Delta t > 0$ (the length of each interval).

The numerical scheme aims at constructing an approximate value $\rho_t(\boldsymbol{x}, i \mid \boldsymbol{\theta})d\boldsymbol{x}$ for

$p_t(d\boldsymbol{x}, i \mid \boldsymbol{\theta})$, such that $p_t(\boldsymbol{x}, i \mid \boldsymbol{\theta})$ is constant for $\forall \boldsymbol{x} \in A, t \in [n\Delta t, (n+1)\Delta t[, \forall A \in \mathcal{M}$:

$$\rho_t(\boldsymbol{x}, i \mid \boldsymbol{\theta}) = P_n(A, i \mid \boldsymbol{\theta}), \forall i \in \boldsymbol{S}, \boldsymbol{x} \in A, t \in [n\Delta t, (n+1)\Delta t[\tag{4.4}$$

$P_0(A, i \mid \boldsymbol{\theta}), \forall i \in \boldsymbol{S}, A \in \mathcal{M}$ is defined as follows:

$$P_0(A, i \mid \boldsymbol{\theta}) = \int_A p_0(d\boldsymbol{x}, i \mid \boldsymbol{\theta}) / m_A \tag{4.5}$$

Then, $P_{n+1}(A, i \mid \boldsymbol{\theta}), \forall i \in \boldsymbol{S}, A \in \mathcal{M}, n \in \mathbb{N}$ can be calculated considering the deterministic evaluation of $\boldsymbol{X}(t)$ and the stochastic evolution of $\boldsymbol{Y}(t)$ based on $P_n(\mathcal{M}, i \mid \boldsymbol{\theta})$ by the Chapman-Kolmogorov forward equation, as follows:

$$P_{n+1}(A, i \mid \boldsymbol{\theta}) = \frac{1}{1+\Delta t b_A^i} \widehat{P_{n+1}}(A, i \mid \boldsymbol{\theta}) + \Delta t \sum_{j \in \boldsymbol{S}} \frac{a_A^{ji}}{1+\Delta t b_A^j} \widehat{P_{n+1}}(A, j \mid \boldsymbol{\theta}) \tag{4.6}$$

where

$$a_A^{ji} = \int_A \lambda_j(i, \boldsymbol{x} \mid \boldsymbol{\theta}_K) d\boldsymbol{x} / m_A, \forall i \in \boldsymbol{S}, A \in \mathcal{M} \tag{4.7}$$

is the average transition rate from state j to state i for grid A,

$$b_A^i = \sum_{j \neq i} a_A^{ij}, \forall i \in \boldsymbol{S}, A \in \mathcal{M} \tag{4.8}$$

is the average transition rate out of state i for grid A,

$$\widehat{P_{n+1}}(A, i \mid \boldsymbol{\theta}) = \sum_{B \in \mathcal{M}} m_{BA}^i P_n(B, i \mid \boldsymbol{\theta}) / m_A, \ \forall i \in \boldsymbol{S}, A \in \mathcal{M} \tag{4.9}$$

is the approximate value of probability density function on $A \times \{i\} \times [(n+1)\Delta t, (n+2)\Delta t[$ according to the deterministic evaluation of $\boldsymbol{X}(t)$,

$$m_{BA}^i = \int_{\{\boldsymbol{y} \in B \mid \boldsymbol{g}^i(\boldsymbol{y}, \Delta t \mid \boldsymbol{\theta}_L) \in A\}} d\boldsymbol{y}, \forall i \in \boldsymbol{S}, A, B \in \mathcal{M} \tag{4.10}$$

is the volume of the part of grid B which will enter grid A after time Δt according to the deterministic evaluation of $\boldsymbol{X}(t)$.

The first term of the right-hand parts of eq. (4.6) accounts for the situation that processes $\boldsymbol{Y}(t)$ hold on state i during time $[n\Delta t, (n+1)\Delta t]$, represented by "1" in an illustrated example in $\mathbb{R}^2$ (Fig. 4-1), where $\frac{1}{1+\Delta t b_A^i}, \forall i \in S, A \in \mathcal{M}$ is the approximated probability that no transition happens from state i for grid A and the second term of the right-hand parts of eq. (4.6) accounts for the situation that processes $\boldsymbol{Y}(t)$ step to state i from another state j at time $(n+1)\Delta t$, represented by "2" in an illustrated example in $\mathbb{R}^2$ (Fig. 4-1), where $a_A^{ji}\Delta t, \forall i, j \in S, A \in \mathcal{M}$ is the transition probability from state j to state i for grid A (B_1, B_2, B_3 and B_4

are the grids of which some parts will enter grid A according to the deterministic evaluation of $\boldsymbol{X}(t)$ at time $(n+1)\Delta t)$.

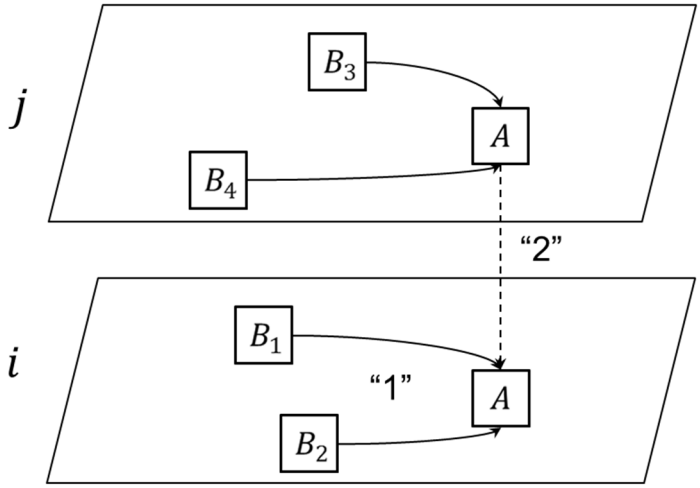

Fig. 4-1. The evolution of degradation processes during $[n\Delta t, (n+1)\Delta t]$.

The approximated solution $\rho_t(\boldsymbol{x},\cdot \mid \boldsymbol{\theta})d\boldsymbol{x}$ weakly converges towards $p_t(d\boldsymbol{x},\cdot \mid \boldsymbol{\theta})$ when $\Delta t \to 0$ and $|\mathcal{M}|/\Delta t \to 0$ where $|\mathcal{M}| = sup_{A\in\mathcal{M}} diam(A)$ [62].

4.3.2 Quantification of fuzzy system reliability

Let $[\tilde{a}]_\alpha = [\underline{a}_\alpha, \overline{a}_\alpha]$ denote the α-cut of a fuzzy number $\tilde{a}$, where $\underline{a}_\alpha$ and $\overline{a}_\alpha$ are the bounds; then, the α-cut of $\widetilde{p_t}\left(d\boldsymbol{x}, i \mid \widetilde{\boldsymbol{\theta}}\right), \forall \vec{\imath} \in S, \vec{x} \in \mathbb{R}^{d_L}, t \in \mathbb{R}$ can be obtained based on the extension principle [93] as follows:

$$\left[\widetilde{p_t}\left(d\boldsymbol{x}, i \mid \widetilde{\boldsymbol{\theta}}\right)\right]_\alpha = \left[min_{\theta\in[\widetilde{\boldsymbol{\theta}}]_\alpha} p_t(d\boldsymbol{x}, i \mid \theta), max_{\theta\in[\widetilde{\boldsymbol{\theta}}]_\alpha} p_t(d\boldsymbol{x}, i \mid \theta)\right] \tag{4.11}$$

The approximate solution for $\left[\widetilde{p_t}\left(d\boldsymbol{x}, i \mid \widetilde{\boldsymbol{\theta}}\right)\right]_\alpha, \forall i \in S, \boldsymbol{x} \in A, t \in [n\Delta t, (n+1)\Delta t[$ denoted by $\widetilde{P_n}\left(A, i \mid \widetilde{\boldsymbol{\theta}}\right)$ can be obtained by varying θ in $\widetilde{\boldsymbol{\theta}}$ as follows:

$$\left[\widetilde{P_n}\left(A, i \mid \widetilde{\boldsymbol{\theta}}\right)\right]_\alpha = \left[min_{\theta\in[\widetilde{\boldsymbol{\theta}}]_\alpha} P_n(A, i \mid \boldsymbol{\theta}'), max_{\theta\in[\widetilde{\boldsymbol{\theta}}]_\alpha} P_n(A, i \mid \boldsymbol{\theta}')\right] \tag{4.12}$$

where $P_n(A, i \mid \boldsymbol{\theta}')$ is obtained by using eq. (4.6) through the FV method. Then, the parametric programming algorithms [84] can be applied to find the fuzzy probability in eq. (4.12).

The approximate solution for the α-cut of fuzzy reliability $\tilde{R}(t)$ of the system at time $t \in [n\Delta t, (n+1)\Delta t[$ can, then, be obtained as follows:

$$[\tilde{R}(t)]_\alpha = \sum_{(A,i)\subseteq \boldsymbol{\mathcal{F}}} [\widetilde{P_n}(A, i \mid \tilde{\boldsymbol{\theta}})]_\alpha \int_{\{x\in A \mid (x,i)\notin \boldsymbol{\mathcal{F}}\}} dx \tag{4.13}$$

In many cases, the original $R(t)$ is monotonic with $\boldsymbol{\theta}$; then, we can directly obtain that instead of using eq. (4.13):

$$[\tilde{R}(t)]_\alpha = \left[\sum_{(A,i)\subseteq \boldsymbol{\mathcal{F}}} P_n(A, i \mid \underline{\boldsymbol{\theta}}_\alpha) \int_{\{x\in A \mid (x,i)\notin \boldsymbol{\mathcal{F}}\}} dx \, , \sum_{(A,i)\subseteq \boldsymbol{\mathcal{F}}} P_n(A, i \mid \overline{\boldsymbol{\theta}}_\alpha) \int_{\{x\in A \mid (x,i)\notin \boldsymbol{\mathcal{F}}\}} dx\right] \tag{4.14}$$

5. IMPORTANCE MEASURES (IMS) FOR COMPONENTS WITH DEGRADATION DEPENDENCY AND SUBJECT TO MAINTENANCE

In reliability engineering, component IMs are used to quantify and rank the importance of different components within a system. By determining the criticalities of the components, limited resources can be allocated according to components prioritization for reliability improvement during the system design and maintenance planning phases [96].

The criticality of a component changes over time, due to the evolution of its underlying degradation processes [97]. The dependency among the degradation processes within one component and of different components have to be considered in the calculation of component IMs. Moreover, the degradation processes can be interrupted by maintenance tasks (e.g. one component can be restored to its initial state by preventive maintenance if any of its degradations exceed the respective critical level [46] and by corrective maintenance upon its failure [21]).

Neglecting the factors that influence the state of being of components can result in inaccurate estimation of component IMs and, thus, mislead the system designers, operators and managers in the assignment of priorities to component criticalities. In this Chapter, we investigate the criticality of components taking into account the degradation dependency and maintenance tasks.

5.1 State of the art

A literature review on component IMs is presented below, to position our contribution within the existing works. Component IMs were first introduced mathematically by Birnbaum [98] in 1969, in a binary setting (i.e. the system and its components are either functioning or faulty). The Birnbaum IM (BIM) allows ranking components by looking at what happens to the system reliability when the reliabilities of the components are changed, one at a time. Afterwards, various IMs have been developed for binary components, including reliability achievement worth (RAW), reliability reduction worth (RRW), Fussel-Vesely and Barlow-Proschan IMs [99-101]. Other concepts of IMs have been proposed with focus to different aspects of the system, such as structure IMs, lifetime IMs, differential IMs and joint IMs [102].

For components whose description requires more than two states, e.g. to describe different degrees of functionalities or levels of degradation, definition of the component IMs have been extended in two directions: (1) metrics for components modeled by MSMs; (2) metrics for components modeled by continuous processes.

For the first type, Armstrong [103] proposed IMs for multi-state systems (MSSs) with dual-mode failure components. For MSSs with multi-state components, Griffith [104] formalized the concept of system performance based on expected utility and generalized the BIM to evaluate the effect of component improvement onto system performance. Wu and Chan [105] improved the Griffith IM by proposing a new utility importance of a state of a component to measure which component or which state of a certain component contributes the most to system performance. Si *et al.* [106] proposed the integrated IM, based on Griffith IM, to incorporate the probability distributions and transition rates of the component states, and the changes in system performance. Integrated IM can be used to evaluate how the transition of component states affects the system performance from unit time to different life stages, to system lifetime, and provide useful information for preventive actions (such as monitoring enhancement, construction improvement etc.) [107, 108]. The multi-state generalized forms of classically binary IMs have been proposed by Zio and Podofillini [109] and Levitin *et al.* [110]: these IMs quantify the importance of a multi-state component for achieving a given level of performance. Ramirez-Marquez and Coit [111] developed two types of composite IMs: (1) the general composite IMs considering only the possible component states; (2) the alternative composite IMs considering both the possible component states and the associated probabilities.

For the second type, Gebraeel [112] proposed a prognostics-based ranking algorithm to rank the identical components based on their residual lives. Liu *et al.* [113] extended the BIM for components with multi-dimensional degradation processes under dynamic environments. Note that no IM has been developed for components whose (degradation) states are determined by both discrete and continuous processes, and are dependent upon other components, as it is often the case in practice [114].

To include dependency, Iyer [115] extended the Barlow-Proschan IM for components whose lifetimes are jointly absolutely continuous and possibly dependent, and Peng *et al.* [97] adapted the mean absolute deviation (MAD) IM (one of the alternative composite IMs) for statistically correlated (s-correlated) components subject to a one-dimension continuous degradation process; this enables to measure the expected absolute deviation in the reliability of a system

with s-correlated degrading components, caused by different degrading performance levels of a particular component and the associated probabilities. To the knowledge of the authors, component IMs taking into account the dependency of multiple degradation processes within one component and among different components, with the inclusion of maintenance activities, have not been investigated in the literature (studies of IMs for repairable systems with *s*-independent components can be found in [108, 116]).

5.2 PDMP modeling framework considering maintenance

In this section, the following assumptions are made to extend the previous PDMP model presented in Section 3.2 with the consideration of condition-based preventive maintenance (PM) via periodic inspections and corrective maintenance (CM):

- For degradation process $i \in \boldsymbol{L} \cup \boldsymbol{K}$, the inspection task I_i of PM is performed with fixed period T_i and brings the related component back to its initial state when i is found in the predefined state set $\boldsymbol{H}_i$.
- The degradation state of a component $O_q \in \boldsymbol{O}, q = 1, 2, \dots, Q$, is determined by its degradation processes $\boldsymbol{D}_{O_q} \subseteq \boldsymbol{L} \cup \boldsymbol{K}$ and the component fails either when one of the degradation processes evolves beyond a threshold of failure in PBMs or reaches the discrete failure state in MSMs .
- The component is restored to its initial state by CM, as soon as it fails.
- The inspection tasks and all maintenance actions are done instantaneously and without errors.

An illustration of two components O_1 and O_2 is shown in Fig. 5-1, where $\boldsymbol{D}_{O_1} = \{L_1\}$ and $\boldsymbol{D}_{O_2} = \{K_1\}$. PM is performed for L_1 if $\boldsymbol{X}_{L_1}^{\boldsymbol{D}}(t)$ exceeds its threshold $x_{L_1}{}^{p}$ at the time of inspection and for K_1 if $Y_{K_1}(t)$ is in state 1 at the time of inspection.

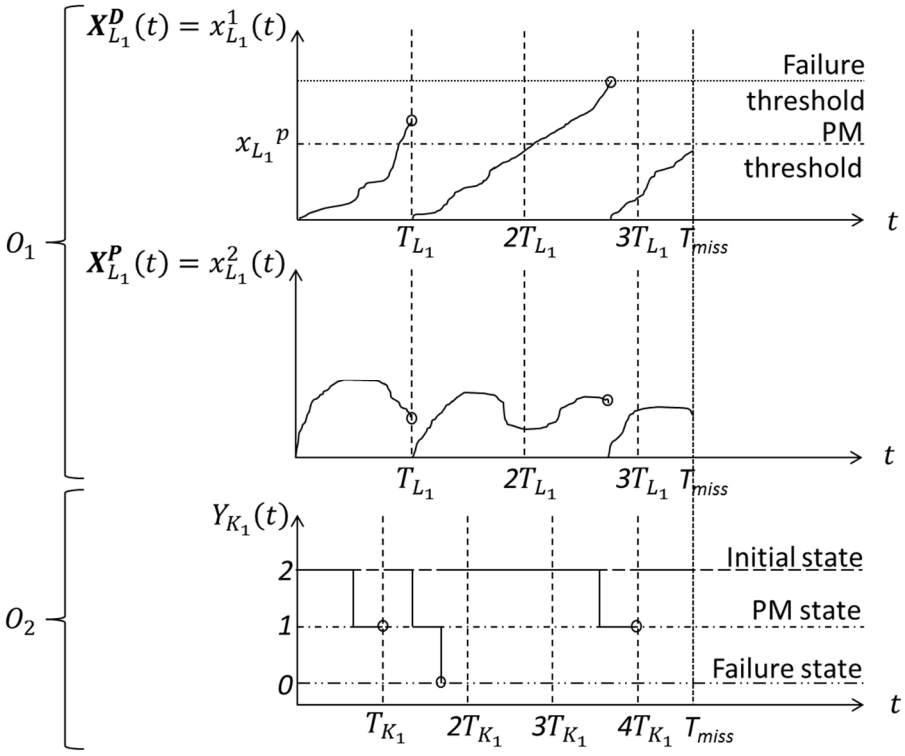

Fig. 5-1. An illustration of two components.

To extend the previous PDMP modeling framework by including the maintenance policy, the difficulty is the discontinuity of $\boldsymbol{X}(t)$ due to the instantaneous change caused by the maintenance task. To solve this problem, a set of PDMPs $\boldsymbol{Z}_k(t), k = 1,2, \ldots$ is employed to model the system degradation processes, where a new PDMP is established once a maintenance task is performed. Let N_m denote the total number of maintenance tasks (PM and CM) the system has experienced till the mission time T_{miss}, then, $\boldsymbol{Z}_k(t), k = 1,2, \ldots, N_m$ is defined on $[T_m^{k-1}, T_m^k]$, where $T_m^k, k = 1,2, \ldots, N_m$ denotes the execution time of the *k*-th maintenance task and $T_m^0 = 0$. $\boldsymbol{Z}_{N_m+1}(t)$ is defined on $\left[T_m^{N_m}, T_{miss}\right]$. This treatment is only for formulating the problem within the settings of PDMP and it does not impact the computational complexity. Fig. 5-2 shows this for the degradation processes in Fig. 5-1.

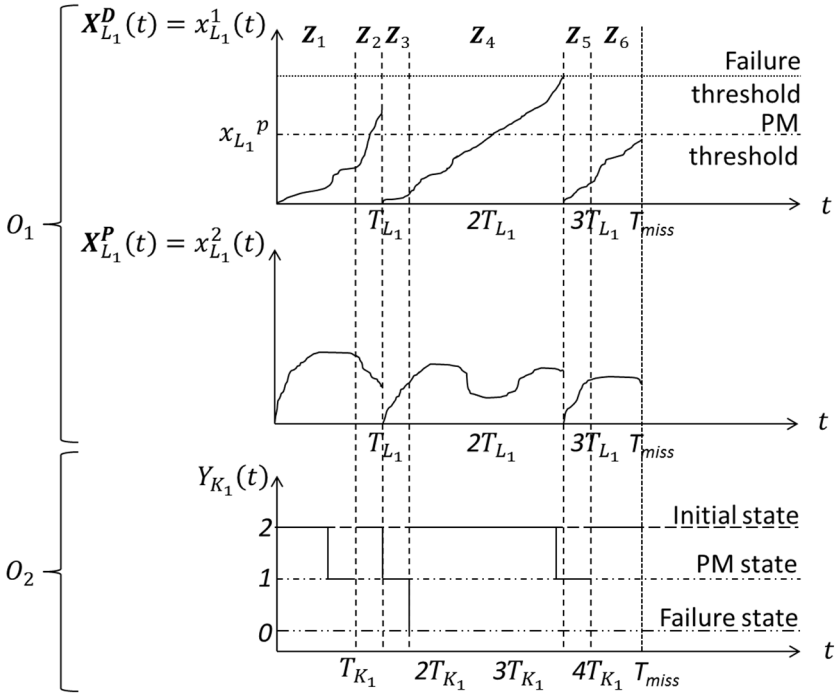

Fig. 5-2. An illustration of two components, modeled by a set of PDMPs.

$\boldsymbol{Z}_k(T_m^{k-1})$ (the initial states of $\boldsymbol{Z}_k(t), k = 2, \dots, N_m + 1$) can be obtained according to $\boldsymbol{Z}_{k-1}(T_m^{k-1})$ and the (k-1)-th maintenance task. The degradation states of the system till T_{miss} can be represented by

$$\boldsymbol{Z}(t) = \sum_{k=1}^{N_m} \mathbf{1}_{[T_m^{k-1}, T_m^k[}(t) \cdot \boldsymbol{Z}_k(t) + \mathbf{1}_{\left[T_m^{N_m}, T_{miss}\right]}(t) \cdot \boldsymbol{Z}_{N_m+1}(t) \tag{5.1}$$

Since maintenance is performed instantaneously, the failure states of the system are infinitely approachable by $\boldsymbol{Z}(t)$, instead of being truly reached. We, then, use another stochastic process $\boldsymbol{Z}'(t)$, which can record the failure of the system as follows:

$$\boldsymbol{Z}'(t) = \mathbf{1}_{[0, T_m^1]}(t) \cdot \boldsymbol{Z}_1(t) + \sum_{k=2}^{N_m} \mathbf{1}_{]T_m^{k-1}, T_m^k]} \cdot \boldsymbol{Z}_k(t) + \mathbf{1}_{\left]T_m^{N_m}, T_{miss}\right]}(t) \cdot \boldsymbol{Z}_{N_m+1}(t) \tag{5.2}$$

Let $\boldsymbol{\mathcal{F}}$ denote the system failure state set: then, the system reliability at T_{miss} can be defined as follows:

$$R(T_{miss}) = P[\boldsymbol{Z}'(s) \notin \boldsymbol{\mathcal{F}}, \forall s \le T_{miss}] = P\left[\cap_{k=1}^{N_m} (\boldsymbol{Z}_k(T_m^k) \notin \boldsymbol{\mathcal{F}}) \cap \left(\boldsymbol{Z}_{N_m+1}(T_{miss}) \notin \boldsymbol{\mathcal{F}}\right)\right] \tag{5.3}$$

Since the component is restored to its initial state by corrective maintenance as soon as it fails,

the failure states of the system can only be reached by $\boldsymbol{Z}'(t)$ at the execution time of the maintenance tasks $T_m^k, k = 1,2,\dots,N_m$ or at the mission time T_{miss}. Therefore, the event $\boldsymbol{Z}'(s) \notin \boldsymbol{\mathcal{F}}, \forall s \leq T_{miss}$ can be represented by $\bigcap_{k=1}^{N_m}(\boldsymbol{Z}_k(T_m^k) \notin \boldsymbol{\mathcal{F}}) \cap \left(\boldsymbol{Z}_{N_m+1}(T_{miss}) \notin \boldsymbol{\mathcal{F}}\right)$.

5.3 Component IMs

Ramirez-Marquez and Coit [111] proposed the MAD IM for MSSs with multi-state components, which evaluates the components criticality taking into account all the possible states and associated probabilities. Peng *et al.* [97] adapted it for binary systems with *s*-correlated components subject to one continuous degradation process.

For components whose (degradation) states are determined by both discrete and continuous processes, we propose an extension of MAD to provide timely feedbacks of the criticality of component O_q with multiple dependent competing degradation processes modeled by MSMs and PBMs, and giving consideration to PM and CM. The formulation is presented as follows:

$$CI_{O_q}(t) = E\left[\left|P\left(\boldsymbol{Z}'(s) \notin \boldsymbol{\mathcal{F}}, \forall s \leq t | \boldsymbol{D}_{O_q}(t)\right) - R(t)\right|\right] \tag{5.4}$$

where $\boldsymbol{D}_{O_q}(t) = (\boldsymbol{X}_{\boldsymbol{L}_p}(t) = (\boldsymbol{X}_{L_{p_1}}(t), \dots, \boldsymbol{X}_{L_{p_n}}(t)), \boldsymbol{Y}_{\boldsymbol{K}_q}(t) = (Y_{K_{q_1}}(t), \dots, Y_{K_{q_m}}(t)))$ and $\boldsymbol{D}_{O_q} = \{\boldsymbol{L}_p = \{L_{p_1}, \dots, L_{p_n}\}, \boldsymbol{K}_q = \{K_{q_1}, \dots, K_{q_m}\}\}$. It accounts for the expected absolute deviation in the system reliability caused by changes of all degradation processes of component O_q. Let $\mathbb{R}^{d_{\boldsymbol{L}p}} = \mathbb{R}^{\sum_{i=1}^{n} d_{L_{p_i}}}$ and $\boldsymbol{S}_{\boldsymbol{K}_q}$ denote the state space of $\boldsymbol{X}_{\boldsymbol{L}_p}(t)$ and $\boldsymbol{Y}_{\boldsymbol{K}_q}(t)$, respectively; eq. (5.4) can, then, be expressed as

$$CI_{O_q}(t) = \sum_{y_{\boldsymbol{K}_q} \in \boldsymbol{S}_{\boldsymbol{K}_q}} \int_{x_{\boldsymbol{L}_p} \in \mathbb{R}^{d_{\boldsymbol{L}p}}} f_{\boldsymbol{D}_{O_q}(t)}\left(dx_{\boldsymbol{L}_p}, y_{\boldsymbol{K}_q}\right)$$

$$\left|P(\boldsymbol{Z}'(s) \notin \boldsymbol{\mathcal{F}}, \forall s \leq t \mid \boldsymbol{X}_{\boldsymbol{L}_p}(t) = x_{\boldsymbol{L}_p}, \boldsymbol{Y}_{\boldsymbol{K}_q}(t) = y_{\boldsymbol{K}_q}) - R(t)\right| \tag{5.5}$$

where $f_{\boldsymbol{D}_{O_q}(t)}\left(dx_{\boldsymbol{L}_p}, y_{\boldsymbol{K}_q}\right)$ is the probability distribution of $\boldsymbol{D}_{O_q}(t)$.

Let $N_m^t \geq 1$ denote the number of maintenance tasks that the system has experienced till t. According to eq. (5.3), we can obtain that:

$$R(T_{miss}) = P\left[\left(\bigcap_{k=1}^{N_m^t}(\boldsymbol{Z}_k(T_m^k) \notin \boldsymbol{\mathcal{F}})\right) \cap \left(\boldsymbol{Z}_{N_m^t+1}(t) \notin \boldsymbol{\mathcal{F}}\right)\right] \tag{5.6}$$

and

$$P(\boldsymbol{Z}'(s) \notin \boldsymbol{\mathcal{F}}, \forall s \le t | \boldsymbol{X}_{\boldsymbol{L}_p}(t) = x_{\boldsymbol{L}_p}, \boldsymbol{Y}_{\boldsymbol{K}_q}(t) = y_{\boldsymbol{K}_q}) =$$

$$\begin{cases} \frac{dx_{\boldsymbol{L}_p}}{f_{\boldsymbol{D}_{Oq}(t)}\left(dx_{\boldsymbol{L}_p}, y_{\boldsymbol{K}_q}\right)} P\left[\left(\bigcap_{k=1}^{N_m^t}(\boldsymbol{Z}_k(T_m^k) \notin \boldsymbol{\mathcal{F}})\right) \cap \right. \\ \left. (\boldsymbol{Z}_{N_m^t+1}^{\boldsymbol{D}_{Oq}}\left(t | \boldsymbol{X}_{\boldsymbol{L}_p}(t) = x_{\boldsymbol{L}_p}, \boldsymbol{Y}_{\boldsymbol{K}_q}(t) = y_{\boldsymbol{K}_q}\right) \notin \boldsymbol{\mathcal{F}})\right], if\ f_{\boldsymbol{D}_{Oq}(t)}\left(dx_{\boldsymbol{L}_p}, y_{\boldsymbol{K}_q}\right) \neq 0 \\ 0, if\ f_{\boldsymbol{D}_{Oq}(t)}\left(dx_{\boldsymbol{L}_p}, y_{\boldsymbol{K}_q}\right) = 0 \end{cases} \quad (5.7)$$

where $\boldsymbol{Z}_{N_m^t+1}^{\boldsymbol{D}_{Oq}}\left(t | \boldsymbol{X}_{\boldsymbol{L}_p}(t) = x_{\boldsymbol{L}_p}, \boldsymbol{Y}_{\boldsymbol{K}_q}(t) = y_{\boldsymbol{K}_q}\right) = (\boldsymbol{X}_{L_1}(t), \dots, \boldsymbol{X}_{\boldsymbol{L}_p}(t) = x_{\boldsymbol{L}_p}, \dots, \boldsymbol{X}_{L_M}(t), Y_{K_1}(t), \dots, \boldsymbol{Y}_{\boldsymbol{K}_q}(t) = y_{\boldsymbol{K}_q}, \dots, Y_{K_N}(t))^T$.

5.4 Quantification of Component IMs

Let $p_t^{\boldsymbol{Z}_k}(d\boldsymbol{z} = (d\boldsymbol{x}, \boldsymbol{i}) \mid \boldsymbol{\theta})$ denote the probability distribution of $\boldsymbol{Z}_k(t)$, it can be approximated by $P_n^{\boldsymbol{Z}_k}(A, i \mid \boldsymbol{\theta})d\boldsymbol{x},\ \boldsymbol{x} \in A, t \in [n\Delta t, (n+1)\Delta t[$ by using the explicit FV method, developed by Cocozza-Thivent *et al.* [62], presented in Section 4.2.1.

Given the initial probability distribution $p_0^{\boldsymbol{Z}_1}(d\boldsymbol{x}, i \mid \boldsymbol{\theta})$ of the system, $P_0^{\boldsymbol{Z}_1}(A, i \mid \boldsymbol{\theta}), \forall i \in \boldsymbol{S}, A \in \mathcal{M}$, can be obtained as:

$$P_0^{\boldsymbol{Z}_1}(A, i \mid \boldsymbol{\theta}) = \int_A p_0^{\boldsymbol{Z}_1}(d\boldsymbol{x}, i \mid \boldsymbol{\theta}) / m_A \quad (5.8)$$

$P_{\lceil T_m^1/\Delta t \rceil}^{\boldsymbol{Z}_1}(A,\ i \mid \boldsymbol{\theta}), \forall i \in \boldsymbol{S}, A \in \mathcal{M}$ can, then, be calculated through the FV method.

To calculate eq. (5.6) and $P[\left(\bigcap_{k=1}^{N_m^t}(\boldsymbol{Z}_k(T_m^k) \notin \boldsymbol{\mathcal{F}})\right) \cap (\boldsymbol{Z}_{N_m^t+1}^{\boldsymbol{D}_{Oq}}\left(t | \boldsymbol{X}_{\boldsymbol{L}_p}(t) = x_{\boldsymbol{L}_p}, \boldsymbol{Y}_{\boldsymbol{K}_q}(t) = y_{\boldsymbol{K}_q}\right) \notin \boldsymbol{\mathcal{F}})]$ in eq. (5.7), we are only interested in the situation that the system is functioning till t; thus, $P_{\lceil T_m^{k-1}/\Delta t \rceil}^{\boldsymbol{Z}_k}(A, i \mid \boldsymbol{\theta}), \forall i \in \boldsymbol{S}, A \in \mathcal{M}, k = 2, 3, \dots N_m^t + 1$ is initiated as follows:

$$P_{\left\lceil \frac{T_m^{k-1}}{\Delta t} \right\rceil}^{\boldsymbol{Z}_k}(A, i \mid \boldsymbol{\theta}) = \begin{cases} P_{\left\lceil \frac{T_m^{k-1}}{\Delta t} \right\rceil}^{\boldsymbol{Z}_{k-1}}(A, i \mid \boldsymbol{\theta}) + \sum_{\substack{(A', i') \in \{(A^{k-1}, i^{k-1})\} \\ (A', i') \notin \boldsymbol{\mathcal{F}}}} P_{\left\lceil \frac{T_m^{k-1}}{\Delta t} \right\rceil}^{\boldsymbol{Z}_{k-1}}(A', i' \mid \boldsymbol{\theta}), \\ if\ \left((A, i) \notin \boldsymbol{\mathcal{F}}\right)\ and\ (\nexists B \in \mathcal{M}, j \in \boldsymbol{S}: (A, i) \in \{(B^{k-1}, j^{k-1})\}) \\ 0, \\ if\ \left((A, i) \in \boldsymbol{\mathcal{F}}\right)\ or\ (\exists B \in \mathcal{M}, j \in \boldsymbol{S}: (A, i) \in \{(B^{k-1}, j^{k-1})\}) \end{cases} \quad (5.9)$$

where $\{(A^{k-1}, i^{k-1})\}$, is the set containing all the states that step to the state (A, i) caused by the $(k-1)$-th maintenance task. Then, we can obtain that

$$P\left[\left(\cap_{k=1}^{N_m^t}(\boldsymbol{Z}_k(T_m^k)\notin\boldsymbol{\mathcal{F}})\right)\cap\left(\boldsymbol{Z}_{N_m^t+1}(t)\notin\boldsymbol{\mathcal{F}}\right)\right]=\sum_{(A,i)\notin\boldsymbol{\mathcal{F}}} m_A P_{\left\lfloor\frac{t}{\Delta t}\right\rfloor}^{\boldsymbol{Z}_{N_m^t+1}}(A,i\mid\boldsymbol{\theta}) \quad (5.10)$$

$$P\left[\left(\cap_{k=1}^{N_m^t}(\boldsymbol{Z}_k(T_m^k)\notin\boldsymbol{\mathcal{F}})\right)\cap\left(\boldsymbol{Z}_{N_m^t+1}^{\boldsymbol{D}_{O_q}}\left(t\mid\boldsymbol{X}_{\boldsymbol{L}_p}(t)=x_{\boldsymbol{L}_p},\boldsymbol{Y}_{\boldsymbol{K}_q}(t)=y_{\boldsymbol{K}_q}\right)\notin\boldsymbol{\mathcal{F}}\right)\right]=$$

$$\sum_{\substack{(A,i)\notin\boldsymbol{\mathcal{F}}\\ \left(x_{\boldsymbol{L}_p},y_{\boldsymbol{K}_q}\right)\subseteq(A,i)}} P_{\left\lfloor\frac{t}{\Delta t}\right\rfloor}^{\boldsymbol{Z}_{N_m^t+1}}(A,i\mid\boldsymbol{\theta})\int_{A/\left(x_{\boldsymbol{L}_p},y_{\boldsymbol{K}_q}\right)}dx \quad (5.11)$$

where $A/\left(x_{\boldsymbol{L}_p},y_{\boldsymbol{K}_q}\right)$ is the mesh by fixing $\boldsymbol{D}_{O_q}(t)$ to $(x_{\boldsymbol{L}_p},y_{\boldsymbol{K}_q})$.

To calculate $f_{\boldsymbol{D}_{O_q}(t)}\left(dx_{\boldsymbol{L}_p},y_{\boldsymbol{K}_q}\right)$ in eqs. (5.5) and (5.7), we are interested in the state of the system at t no matter whether the system is functioning till t or not; thus, $P_{\left\lfloor\frac{T_m^{k-1}}{\Delta t}\right\rfloor}^{\boldsymbol{Z}_k}(A,i\mid\boldsymbol{\theta}),\forall i\in\boldsymbol{S},A\in\mathcal{M},k=2,3,\dots N_m^t+1$ is initiated as follows:

$$P_{\left\lfloor\frac{T_m^{k-1}}{\Delta t}\right\rfloor}^{\boldsymbol{Z}_k}(A,i\mid\boldsymbol{\theta})=\begin{cases}P_{\left\lfloor\frac{T_m^{k-1}}{\Delta t}\right\rfloor}^{\boldsymbol{Z}_{k-1}}(A,i\mid\boldsymbol{\theta})+\sum_{(A',i')\in\{(A^{k-1},i^{k-1})\}}P_{\left\lfloor\frac{T_m^{k-1}}{\Delta t}\right\rfloor}^{\boldsymbol{Z}_{k-1}}(A',i'\mid\boldsymbol{\theta}), & \\ \quad if\ \nexists B\in\mathcal{M},j\in\boldsymbol{S}\colon(A,i)\in\{(B^{k-1},j^{k-1})\} & \\ 0, & \\ \quad if\ \exists B\in\mathcal{M},j\in\boldsymbol{S}\colon(A,i)\in\{(B^{k-1},j^{k-1})\} & \end{cases} \quad (5.12)$$

We can obtain that

$$f_{\boldsymbol{D}_{O_q}(t)}\left(dx_{\boldsymbol{L}_p},y_{\boldsymbol{K}_q}\right)=dx_{\boldsymbol{L}_p}\sum_{\substack{A\in\mathcal{M},i\in\boldsymbol{S}\\ \left(x_{\boldsymbol{L}_p},y_{\boldsymbol{K}_q}\right)\subseteq(A,i)}} P_{\left\lfloor\frac{t}{\Delta t}\right\rfloor}^{\boldsymbol{Z}_{N_m^t+1}}(A,\ i\mid\boldsymbol{\theta})\int_{A/\left(x_{\boldsymbol{L}_p},y_{\boldsymbol{K}_q}\right)}dx \quad (5.13)$$

$CI_{O_q}(t)$ can, then, be obtained by using eqs. (5.5)-(5.13).

The pseudo-code for the quantification of component IM $CI_{O_q}(t)$ is presented as follows:

Set time t, length of each interval Δt and admissible mesh $\mathcal{M}$

Set the initial probability distribution $p_0^{\boldsymbol{Z}_1}(d\boldsymbol{x},i\mid\boldsymbol{\theta})$

Initialize the probability distribution of $\boldsymbol{Z}_1(0)$ by using eq. (5.8)

For $j=1$ to N_m^t **do**

Calculate the probability distribution of $\boldsymbol{Z}_j(T_m^j)$ by using FV method

Calculate the initial probability distribution of $\boldsymbol{Z}_{j+1}(T_m^j)$ by using eq. (5.9)

End

Calculate the probability distribution of $\boldsymbol{Z}_{N_m^t+1}(t)$ by using FV method

Calculate the system reliability at time t by using eq. (5.10)

Calculate the conditional system reliability at time t by using eq. (5.11)

For $j = 1$ to N_m^t **do**

Calculate the probability distribution of $\boldsymbol{Z}_j(T_m^j)$ by using FV method

Calculate the initial probability distribution of $\boldsymbol{Z}_{j+1}(T_m^j)$ by using eq. (5.12)

End

Calculate the probability distribution of $\boldsymbol{Z}_{N_m^t+1}(t)$ by using FV method

Calculate the probability distribution of $\boldsymbol{D}_{O_q}(t)$ by using eq. (5.13)

Calculate the component IM $CI_{O_q}(t)$ by using eqs. (5.5)-(5.7)

□

6. MAINTENANCE OPTIMIZATION FOR SYSTEMS CONSDERING EPISTEMIC UNCERTAINTY AND DEGRADATION DEPENDENCY

Maintenance contributes to the safe and efficient operation of industrial systems [45]. The contribution to safety especially is in highly hazardous industries, such as the nuclear and aerospace ones. In this Chapter, a modeling and optimization framework for the maintenance of systems considering epistemic uncertainty and degradation dependency is proposed.

6.1 Maintenance policy

We refer to the system presented in Section 3.2, and follow the assumptions on actual maintenance activities performed in industrial practice made in Section 3.2, the associated costs are further considered as follows:

- The PM involves condition-based maintenance tasks, which recommend maintenance actions according to the information collected through condition inspections [117]. The inspection task $I_i, \forall\, i \in \boldsymbol{L} \cup \boldsymbol{K}$ related to one degradation process i is carried out with fixed period and a cost is associated with each inspection.
- If the state of one degradation process $i \in \boldsymbol{L} \cup \boldsymbol{K}$, reported by condition inspection, enters the predefined state set for PM denoted by $\boldsymbol{H}_i$, then the component containing this degradation process is restored to its initial state and a PM cost is incurred depending on the component type. Otherwise, no maintenance action is performed.
- Component failure can be detected immediately and the failed component is restored to its initial state by the CM [21], and a CM cost is incurred depending on the component type.
- The duration of inspection tasks is negligible and all maintenance actions are done instantaneously, compared with the lifetime of the components [27].

The PDMP modeling framework including maintenance policy presented in Section 5.2 can be employed to model degradation processes of systems considering degradation dependency and subject to maintenance.

In reality, the two major issues for the maintenance policy are to determine (1) the period $T_i, \forall\, i \in \boldsymbol{L} \cup \boldsymbol{K}$ for each inspection task I_i and (2) the state set for PM $\boldsymbol{H}_i, \forall\, i \in \boldsymbol{L} \cup \boldsymbol{K}$ for

each degradation process i.

6.2 Maintenance optimization under uncertainty

6.2.1 Maintenance optimization objective function

In order to optimize the maintenance policy, the criterion considered is the expected maintenance cost over the system mission time. Let $C(t)$ denote the maintenance cost, $\boldsymbol{H} = \bigcup_{\forall\, i\in \boldsymbol{L}\cup \boldsymbol{K}} \boldsymbol{H}_i$ and $\boldsymbol{T} = \bigcup_{\forall\, i\in \boldsymbol{L}\cup \boldsymbol{K}} \boldsymbol{T}_i$, $\boldsymbol{\theta} = \boldsymbol{\theta_L} \cup \boldsymbol{\theta_K}$, $\boldsymbol{x_L^*} = \bigcup_{m=1}^{M} \boldsymbol{x}_{L_m}^*$ for the system functioning until time t, we can write:

$$\mathbb{E}\big(C(t, \boldsymbol{H}, \boldsymbol{T} \mid \boldsymbol{\theta}, \boldsymbol{x_L^*})\big) = \sum_{i\in \boldsymbol{L}\cup \boldsymbol{K}} C_{I_i} \cdot \left\lfloor \frac{t}{T_i} \right\rfloor + \sum_{O_q\in \boldsymbol{O}} C_P^{O_q} \cdot \mathbb{E}(N_P^{O_q}(t, \boldsymbol{H}, \boldsymbol{T} \mid \boldsymbol{\theta}))$$

$$+ \sum_{O_q\in \boldsymbol{O}} C_D^{O_q} \cdot \mathbb{E}(N_D^{O_q}(t, \boldsymbol{H}, \boldsymbol{T} \mid \boldsymbol{\theta}, \boldsymbol{x_L^*})) + C_F \cdot \mathbb{E}(N_F(t, \boldsymbol{H}, \boldsymbol{T} \mid \boldsymbol{\theta}, \boldsymbol{x_L^*})) \tag{6.1}$$

where C_{I_i} is the cost of the inspection task I_i, $\left\lfloor \frac{t}{T_i} \right\rfloor$ is the number of times the inspection task I_i has been performed until time t, $C_P^{O_q}$ is the cost of PM to component O_q, $N_P^{O_q}(t, \boldsymbol{H}, \boldsymbol{T} \mid \boldsymbol{\theta})$ is the number of PM tasks to component O_q until time t, $N_D^{O_q}(t, \boldsymbol{H}, \boldsymbol{T} \mid \boldsymbol{\theta}, \boldsymbol{x_L^*})$ is the number of CM tasks to component O_q until time t, C_F is the penalty cost of experiencing a system failure and $N_F(t, \boldsymbol{H}, \boldsymbol{T} \mid \boldsymbol{\theta}, \boldsymbol{x_L^*})$ is the number of system failures until time t.

Let $p_t^{\boldsymbol{Z}_k}(d\boldsymbol{z} \mid \boldsymbol{\theta})$ denote the probability distribution of $\boldsymbol{Z}_k(t)$; we, then, obtain that

$$\mathbb{E}(N_P^{O_q}(t, \boldsymbol{H}, \boldsymbol{T} \mid \boldsymbol{\theta})) = \sum_{k\in\mathbb{N}^*} \sum_{T^{\boldsymbol{i}}\in \boldsymbol{T}^{O_q}} \int_{\boldsymbol{z}_{O_q}\in \boldsymbol{H}_{O_q}} p_{T^{\boldsymbol{i}}}^{\boldsymbol{Z}_k}(d\boldsymbol{z} \mid \boldsymbol{\theta}) \tag{6.2}$$

where $\boldsymbol{z}_{O_q}$ denotes the degradation state of the component O_q in $\boldsymbol{z}$, $\boldsymbol{H}_{O_q} = \bigcup_{i\in \boldsymbol{D}_{O_q}} \boldsymbol{H}_i$ denotes the state set for PM of the component O_q and $\boldsymbol{T}^{O_q}$ denotes the set of inspection time of the component O_q. The function $p_{T^{\boldsymbol{i}}}^{\boldsymbol{Z}_k}(d\boldsymbol{z} \mid \boldsymbol{\theta})$ is the probability distribution of $\boldsymbol{Z}_k(t)$ at the inspection time $T^{\boldsymbol{i}}$,

$$\mathbb{E}(N_D^{O_q}(t, \boldsymbol{H}, \boldsymbol{T} \mid \boldsymbol{\theta}, \boldsymbol{x_L^*})) = \sum_{k\in\mathbb{N}^*} \int_0^t \int_{\boldsymbol{z}_{O_q}\in \boldsymbol{\mathcal{F}}_{O_q}} p_s^{\boldsymbol{Z}_k}(d\boldsymbol{z} \mid \boldsymbol{\theta}) ds \tag{6.3}$$

where $\boldsymbol{\mathcal{F}}_{O_q} = \bigcup_{i\in \boldsymbol{D}_{O_q}} \boldsymbol{\mathcal{F}}_i$ denotes the failure state set of the component O_q,

$$\mathbb{E}(N_F(t, \boldsymbol{H}, \boldsymbol{T} \mid \boldsymbol{\theta}, \boldsymbol{x_L^*})) = \sum_{k\in\mathbb{N}^*} \int_0^t \int_{\boldsymbol{z}\in\boldsymbol{\mathcal{F}}} p_s^{\boldsymbol{Z}_k}(d\boldsymbol{z} \mid \boldsymbol{\theta}) ds \quad (6.4)$$

6.2.2 Epistemic uncertainty

Due to the incomplete or imprecise knowledge about the degradation processes, epistemic uncertainty may exist:

- For PBMs: (1) the parameters (e.g. wear coefficient) and influencing factors (e.g. temperature and pressure) $\boldsymbol{\theta}_L$ may be poorly known and elicited from expert judgment [82]; (2) the failure thresholds $\boldsymbol{x_L^*}$ may be uncertain due to imperfect information [118].
- For MSMs: (1) the state performances may be vaguely defined due to the imprecise discretization of the underlying continuous degradation processes [119]; (2) the transition rates between states may be difficult to estimate statistically due to insufficient data, especially for highly reliable components (e.g. valves and pumps in nuclear power plants, etc.) [120].

This uncertainty must be reflected in the modeling and accounted for in the maintenance optimization that rests on it. Fuzzy sets have been employed to mathematically represent epistemic uncertainty in some works [87, 121, 122] related to degradation modeling and maintenance. However, determining appropriate membership functions may be a difficult task in practice. The experts in many cases can only confirm an interval of the possible minimum and maximum values of the uncertain transition rate. One practical way of dealing with epistemic uncertainty is to use intervals of values for the uncertain parameters [123]. In this respect, the following assumptions are made (a symbol with an underbar indicates the left limit of that interval, while a symbol with an overbar indicates the right limit of that interval):

- The value of $\forall \theta_i \in \boldsymbol{\theta}$, is represented by an interval $[\theta_i] = \left[\underline{\theta_i}, \overline{\theta_i}\right]$. Let $[\boldsymbol{\theta}] = \bigcup_{\theta_i\in\boldsymbol{\theta}}[\theta_i]$.
- The value of $\forall {x_{L_m}^i}^* \in \boldsymbol{x_{L_m}^*}, \forall\, L_m \in \boldsymbol{L}$, is represented by an interval $\left[{x_{L_m}^i}^*\right] = \left[\underline{{x_{L_m}^i}^*}, \overline{{x_{L_m}^i}^*}\right]$. Let $\left[\boldsymbol{x_{L_m}^*}\right] = \bigcup_{{x_{L_m}^i}^*\in\boldsymbol{x_{L_m}^*}} \left[{x_{L_m}^i}^*\right]$ and $[\boldsymbol{x_L^*}] = \bigcup_{m=1}^{M} \left[\boldsymbol{x_{L_m}^*}\right]$.

$\mathbb{E}\left(C(t, \boldsymbol{H}, \boldsymbol{T} \mid \boldsymbol{\theta}, \boldsymbol{x_L^*})\right)$, then, is also an interval, denoted by

$$\left[\mathbb{E}\left(C(t, \boldsymbol{H}, \boldsymbol{T} \mid [\boldsymbol{\theta}], [\boldsymbol{x_L^*}])\right)\right] =$$

$$\left[\min_{\substack{\boldsymbol{\theta}\in[\boldsymbol{\theta}]\\ \boldsymbol{x_L^*}\in[\boldsymbol{x_L^*}]}} \mathbb{E}\left(C(t,\boldsymbol{H},\boldsymbol{T}\mid\boldsymbol{\theta},\boldsymbol{x_L^*})\right), \max_{\substack{\boldsymbol{\theta}\in[\boldsymbol{\theta}]\\ \boldsymbol{x_L^*}\in[\boldsymbol{x_L^*}]}} \mathbb{E}\left(C(t,\boldsymbol{H},\boldsymbol{T}\mid\boldsymbol{\theta},\boldsymbol{x_L^*})\right)\right]$$

$$= \left[\underline{\mathbb{E}\left(C(t,\boldsymbol{H},\boldsymbol{T}\mid[\boldsymbol{\theta}],[\boldsymbol{x_L^*}])\right)},\ \overline{\mathbb{E}\left(C(t,\boldsymbol{H},\boldsymbol{T}\mid[\boldsymbol{\theta}],[\boldsymbol{x_L^*}])\right)}\right] \tag{6.5}$$

6.2.3 Optimization problem definition

Based on the models presented above, the problem of maintenance optimization under uncertainty, on a mission time horizon T_{miss}, can be defined as:

$$\begin{gathered}\text{Min } \left[\mathbb{E}\left(C(T_{miss},\boldsymbol{H},\boldsymbol{T}\mid[\boldsymbol{\theta}],[\boldsymbol{x_L^*}])\right)\right]\\ \text{Subject to } \boldsymbol{H}_i \subseteq W_i,\ \forall\, i\in\boldsymbol{L}\cup\boldsymbol{K}\\ 0\le T_i\le T_{miss},\ \forall\, i\in\boldsymbol{L}\cup\boldsymbol{K}\end{gathered} \tag{6.6}$$

where $W_i = \begin{cases}\mathbb{R}^{d_i}, if & i\in\boldsymbol{L}\\ \boldsymbol{S}_i, if & i\in\boldsymbol{K}\end{cases}$.

For its solution, it can be reformulated as a multi-objective optimization problem:

$$\begin{gathered}\text{Min } \underline{\mathbb{E}\left(C(T_{miss},\boldsymbol{H},\boldsymbol{T}\mid[\boldsymbol{\theta}],[\boldsymbol{x_L^*}])\right)}\\ \text{Min } \overline{\mathbb{E}\left(C(T_{miss},\boldsymbol{H},\boldsymbol{T}\mid[\boldsymbol{\theta}],[\boldsymbol{x_L^*}])\right)}\\ \text{Subject to } \boldsymbol{H}_i \subseteq W_i,\ \forall\, i\in\boldsymbol{L}\cup\boldsymbol{K}\\ 0\le T_i\le T_{miss},\ \forall\, i\in\boldsymbol{L}\cup\boldsymbol{K}\end{gathered} \tag{6.7}$$

where $W_i = \begin{cases}\mathbb{R}^{d_i}, if & i\in\boldsymbol{L}\\ \boldsymbol{S}_i, if & i\in\boldsymbol{K}\end{cases}$.

This formulation optimizes the lower and upper bounds of interval simultaneously. Due to the limit of data, no probability distribution or membership function is assumed on the interval. The order relation between intervals which requires no information about distribution or membership function [124] (Definitions 3.1 and 3.3) can be used in this situation (let $A = [a_L, a_R]$ and $B = [b_L, b_R]$ denote two intervals, according to these definitions, $A \le B\ iff\ a_L \le b_L\ and\ a_R \le b_R$). This leads to the definition of a multi-objective optimization problem with respect to the lower and upper bounds of the expected maintenance cost

($\underline{\mathbb{E}\big(C(T_{miss}, \boldsymbol{H}, \boldsymbol{T} \mid [\boldsymbol{\theta}], [\boldsymbol{x}_L^*])\big)}$ and $\overline{\mathbb{E}\big(C(T_{miss}, \boldsymbol{H}, \boldsymbol{T} \mid [\boldsymbol{\theta}], [\boldsymbol{x}_L^*])\big)}$). It also covers the minimax type of robust optimization based on worst-case analysis, which may generate conservative decisions under some situations [125]. Note that this order relation is a partial order so that the solutions of eq. (6.7) obtained are Pareto optimal solutions.

Finding the Pareto optimal maintenance policy is a challenging problem, due to the complex behavior of the system involving the stochasticities of MSMs, time-dependent evolutions of PBMs and effects of the two types of maintenance.

6.3 Solution methodology

In order to solve the multi-objective optimization problem defined in eq. (6.7), we employ (1) FV method to calculate $\mathbb{E}\big(C(T_{miss}, \boldsymbol{H}, \boldsymbol{T} \mid \boldsymbol{\theta}, \boldsymbol{x}_L^*)\big)$; (2) two DEs to compute the upper and lower bounds of the interval $\left[\mathbb{E}\big(C(T_{miss}, \boldsymbol{H}, \boldsymbol{T} \mid [\boldsymbol{\theta}], [\boldsymbol{x}_L^*])\big)\right]$, using the FV method for fitness evaluation; (3) NSDE to find the Pareto-optimal maintenance policy for $\boldsymbol{H}$ and $\boldsymbol{T}$, aiming at optimizing the interval produced by the two DEs. The meta-heuristic algorithm DE is chosen as the solution approach because 1) PDMP model is highly complex and non-linear and 2) DE is fit to optimizing continuous decision variables.

6.3.1 FV method

To obtain $\mathbb{E}\big(C(t, \boldsymbol{H}, \boldsymbol{T} \mid \boldsymbol{\theta}, \boldsymbol{x}_L^*)\big)$, the probability distribution of PDMPs $p_t^{\boldsymbol{Z}_k}(d\boldsymbol{z} = (d\boldsymbol{x}, i) \mid \boldsymbol{\theta})$ need to be calculated at first. We employ the explicit FV method to estimate it, developed by Cocozza-Thivent *et al.* [62], presented in Section 4.2.1.

6.3.2 DE approach

DE is a simple and efficient heuristic approach for single-objective global optimization, originally developed by Store and Price [61] for continuous problems. It often shows better performance than alternative optimization algorithms, e.g. genetic algorithms. The procedure of DE is briefly presented as follows:

Step 1: Initialize randomly the population P of $N_c \geq 4$ target individuals over the variables space.

Step 2: Generate the mutant individuals through the following mutation equation:

$$v_{i,G+1} = x_{r1,G} + F \cdot \left(x_{r2,G} - x_{r3,G}\right), \forall i \in \{1,2,\dots,N_c\} \tag{21}$$

where G is the current iteration number, $r_1, r_2, r_3 \in \{1,2,\dots,N_c\}$ are random indices satisfying $r_1 \neq r_2 \neq r_3 \neq i$ and $F \in [0,2]$, determined by the user, is a constant factor controlling the amplification of $\left(x_{r2,G} - x_{r3,G}\right)$.

Step 3: Generate each trial individual through the following crossover equation:

$$u_{i,G+1}^{j} = \begin{cases} v_{i,G+1}^{j}, if\ (rand \leq CR)\ or\ j = irand(D) \\ x_{i,G}^{j}, if\ (rand > CR)\ and\ j \neq irand(D) \end{cases}, j = 1,2,\dots,D \tag{22}$$

where $u_{i,G+1}^{j}$, $v_{i,G+1}^{j}$ and $x_{i,G}^{j}$ are the j-th parameters of the vectors $u_{i,G+1}$, $v_{i,G+1}$ and $x_{i,G}$, respectively; $rand \in [0,1]$ is a uniform random number; $CR \in [0,1]$ is the crossover constant, determined by the user; D is the dimension of the individual vector; $irand(i)$ is a uniform discrete random number in the set $\{1,2,\dots,D\}$.

Step 4: Evaluate the target individual and its trial individual; select the best one as the target individual for the next generation.

Step 5: Go back to step 2, if the termination criterion is not met; otherwise, stop the algorithm.

The maximum iteration number (N_{max}), maximum fitness evaluation number (T_{max}) and minimum fitness error (eps) are typically employed individually or jointly as the termination criterion.

We use two DE algorithms (DE1 and DE2) using the FV scheme for the fitness function evaluation to obtain $\underline{\mathbb{E}\left(C(T_{miss}, \boldsymbol{H}, \boldsymbol{T} \mid [\boldsymbol{\theta}], [\boldsymbol{x}_{\boldsymbol{L}}^{*}])\right)}$ and $\overline{\mathbb{E}\left(C(T_{miss}, \boldsymbol{H}, \boldsymbol{T} \mid [\boldsymbol{\theta}], [\boldsymbol{x}_{\boldsymbol{L}}^{*}])\right)}$, respectively: DE1 selects the one with smallest value as the target individual for the next generation at step 4 whereas DE2 selects the one with largest value.

6.3.3 NSDE

For solving the multi-objective problem formulated in eq. (11), the non-dominated sorting mechanisms are incorporated into the single objective DE, similar to the work [60] where the non-dominated sorting mechanisms are combined with a modified binary DE (MBDE). For the details about this approach, please kindly refer to [60].

6.3.4 Integration of methods

These methods are integrated by using (1) FV scheme for the fitness evaluation in DE and (2) DE for the fitness evaluation in NSDE; the solution methods are integrated, for the first time, for maintenance optimization. The flowchart of the entire optimization methodology that integrates the methods mentioned above is shown in Fig. 6-1.

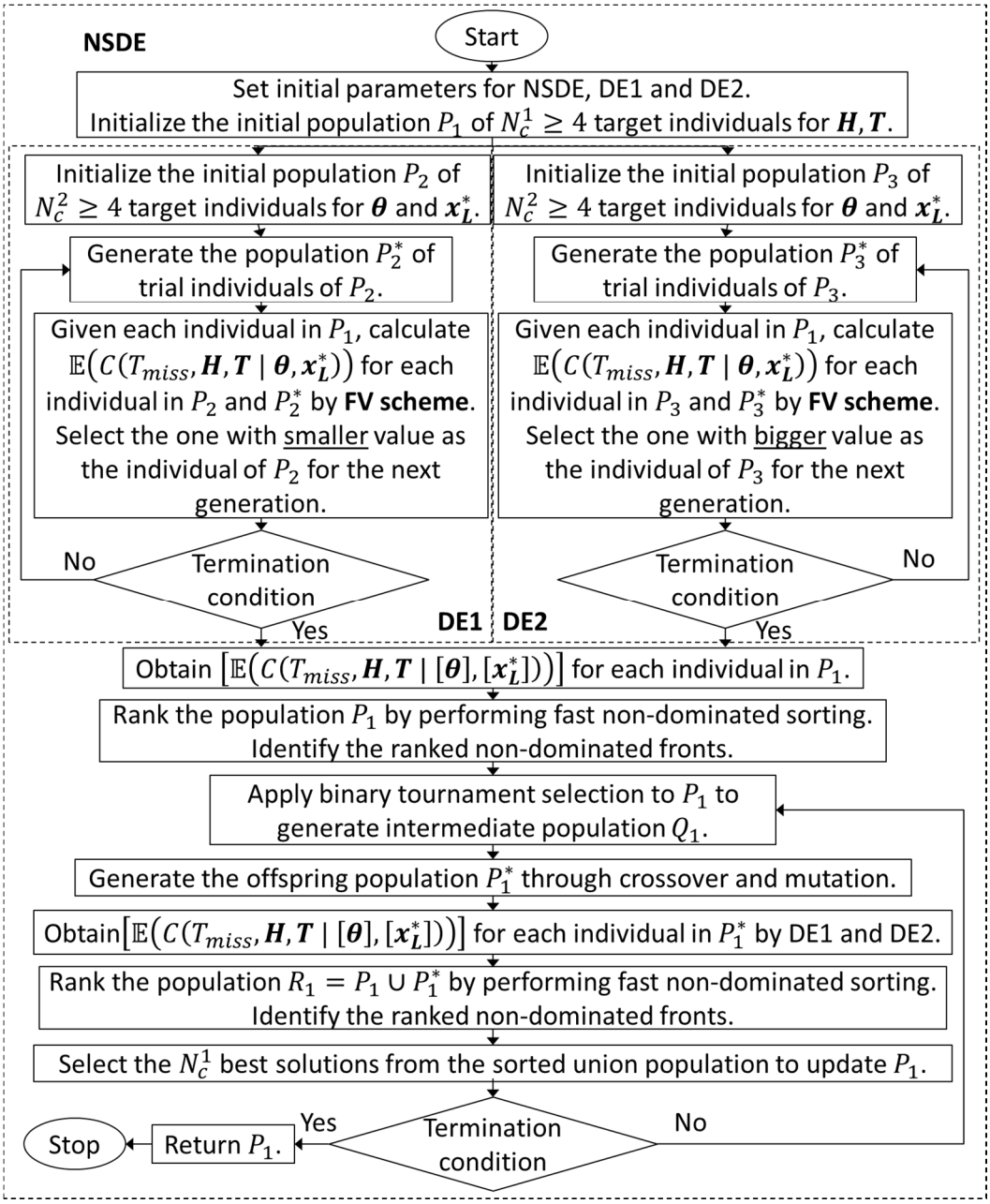

Fig. 6-1. Flowchart of the proposed optimization methodology.

In Fig. 6-1, N_c^1 is the size of the population P_1 of NSDE, which contains the target individuals for $\boldsymbol{H}$ and $\boldsymbol{T}$; N_c^2 and N_c^3 are respectively the sizes of population P_2 of DE1 and population P_3 of DE2, which contain the target individuals for $\boldsymbol{\theta}$; $P_i^*, i = 1, 2, 3$ is the population generated from P_i. The method starts with the random generation of N_c^1 individuals (i.e. candidate solutions) of $\boldsymbol{H}$ and $\boldsymbol{T}$ in the initial population P_1 in NSDE. Then, DE1 and DE2 are executed in parallel to calculate $\left[\mathbb{E}\left(C(T_{miss}, \boldsymbol{H}, \boldsymbol{T} \mid [\boldsymbol{\theta}], [\boldsymbol{x}_L^*])\right)\right]$ for each individual in P_1

as follows: (1) randomly generate N_c^2/N_c^3 individuals of $\boldsymbol{\theta}$ and $\boldsymbol{x}_{\boldsymbol{L}}^*$, as the initial population P_2/P_3 in DE1/DE2; (2) generate the trial populations P_2^*/P_3^* for P_2/P_3 through mutation and crossover; (3) given the individual in P_1, use FV scheme to calculate $\mathbb{E}\left(C\left(T_{miss}, \boldsymbol{H}, \boldsymbol{T} \mid \boldsymbol{\theta}, \boldsymbol{x}_{\boldsymbol{L}}^*\right)\right)$ for the paired individuals in P_2 and P_2^*/(P_3 and P_3^*), and select the one with smaller/bigger value as the individual of P_2/P_3 for the next generation; (4) go back to step (2), if the termination criterion is not met; otherwise, $\left[\mathbb{E}\left(C\left(T_{miss}, \boldsymbol{H}, \boldsymbol{T} \mid [\boldsymbol{\theta}], [\boldsymbol{x}_{\boldsymbol{L}}^*]\right)\right)\right]$ is obtained for each individual in P_1. Afterwards, the method returns to NSDE: (5) rank population P_1 by performing fast non-dominated sorting on $\left[\mathbb{E}\left(C\left(T_{miss}, \boldsymbol{H}, \boldsymbol{T} \mid [\boldsymbol{\theta}], [\boldsymbol{x}_{\boldsymbol{L}}^*]\right)\right)\right]$ and the ranked non-dominated fronts are, then, identified; (6) select the offspring population P_1^* based on the intermediate population Q_1, generated by crossover and mutation; (7) use DE1 and DE2 to obtain $\left[\mathbb{E}\left(C\left(T_{miss}, \boldsymbol{H}, \boldsymbol{T} \mid [\boldsymbol{\theta}], [\boldsymbol{x}_{\boldsymbol{L}}^*]\right)\right)\right]$ for each individual in P_1^*; (8) identify the ranked non-dominated fronts by performing fast non-dominated sorting on the population union $R_1 = P_1 \cup P_1^*$; (9) select the best N_c^1 solutions from the sorted union as the updated P_1; (10) go back to the step (6), if the termination criterion is not met; otherwise, the Pareto optimal maintenance policies are obtained.

7. RELIABILITY ASSESSMENT OF SYSTEMS SUBJECT TO DEPENDENT DEGRADATION PROCESSESA DN RANDOM SHOCKS

System failures can be induced by internal degradation mechanisms (e.g. wear, fatigue and erosion) or by external causes (e.g. thermal and mechanical shocks) [126]. The reliability of systems experiencing both degradation and random shocks is a problem that has been widely studied [20, 21, 27, 40-44, 127]. The dependency among these processes leading to failure has posed some challenges to reliability modeling. Previous research has focused on the dependency between continuous/multi-state degradation processes and random shocks. However, few studies have explicitly considered both the dependencies between degradation processes and random shocks, and among the degradation processes themselves. In this Chapter, we extend the PDMP modeling framework for system reliability assessment by these two types of dependencies.

7.1 Dependency between degradation processes and random shocks

We refer to the system presented in Section 3.2, and the following assumptions on random shocks are made, similarly to various previous works [21, 27, 42-44]:

- Random shocks occur in time according to a homogeneous Poisson process $\{N(t), t \geq 0\}$ with constant arrival rate μ, where the random variable $N(t)$ denotes the number of random shocks occurred until time t.
- The damages of random shocks are divided into two types: extreme and cumulative.
- Extreme and cumulative shocks are mutually exclusive.
- Extreme shocks immediately lead the components to failure, whereas cumulative shocks gradually deteriorate the components.

Due to the different nature of PBMs and MSMs, the impacts of random shocks on the two groups of components are characterized in different ways.

7.1.1 Impacts on MSMs

In the generic degradation process $K_n \in \boldsymbol{K}$, random shocks can cause the process variable $Y_{K_n}(t)$ to step from state i to a further degraded state j with probability $p_{ij}, i > j$ [44], with p_{i0} denoting the probability that the random shock is extreme, i.e. leading to failure state 0 upon occurrence from state $Y_{K_n}(t) = i$. By combining the original degradation and the random shock processes, the resulting process is a homogeneous continuous-time Markov chain of the kind depicted in Fig. 7-1. The state of the process is represented by $\boldsymbol{Y}'_{K_n}(t) = \left(Y_{K_n}(t), k\right)$, where $k \in \mathbb{N}$ is the number of shocks experienced up to time t in the process K_n. The state space of the new process is denoted by $\boldsymbol{S}'_{K_n} = \{(a, b), \forall a \in \boldsymbol{S}_{K_n}, b \in \mathbb{N}\}$ and the space of the failure states of K_n is denoted by $\boldsymbol{\mathcal{F}}'_{K_n} = \{(0, b), \forall b \in \mathbb{N}\}$. Note that the component fails when it reaches the degradation state 0, no matter how many shocks it has experienced.

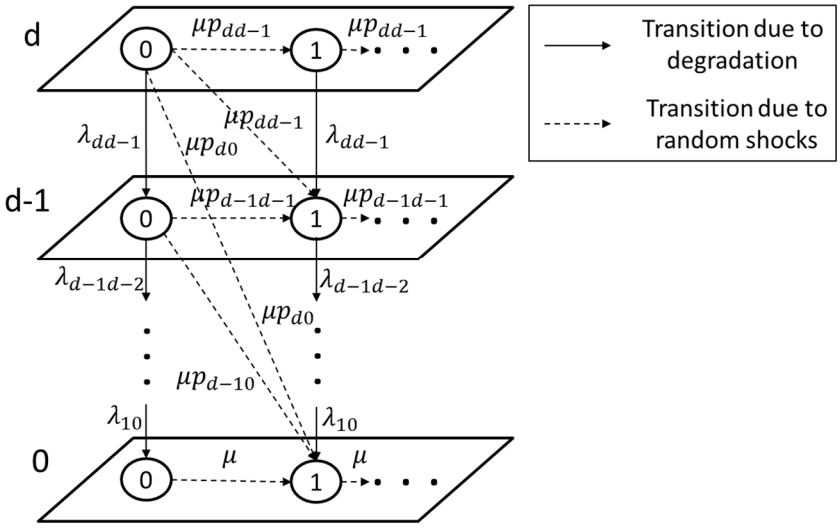

Fig. 7-1. Degradation process K_n and random shocks.

7.1.2 Impacts on PBMs

In the generic degradation process $L_m \in \boldsymbol{L}$, the i-th shock becomes extreme if the shock load W_i exceeds the maximal material strength D, otherwise, it can bring an instantaneous random

increase $\boldsymbol{H}_i$ to $\boldsymbol{X}_{L_m}(t)$ [40]. Let $\boldsymbol{X}_{L_m}^S(t)$ denote the cumulative change to $\boldsymbol{X}_{L_m}(t)$ caused by random shocks until time t as follows:

$$\boldsymbol{X}_{L_m}^S(t) = \begin{cases} \sum_{i=1}^{N'(t)} \boldsymbol{H}_i, & if\ N'(t) \neq 0 \\ 0, & if\ N'(t) = 0 \end{cases} \tag{7.1}$$

where $N'(t)$ is the number of cumulative shocks occurred in the developing L_m process before the extreme shock occurs. The overall degradation level of L_m is expressed as $\boldsymbol{D}_{L_m}(t) = \boldsymbol{X}_{L_m}(t) + \boldsymbol{X}_{L_m}^S(t)$. The process L_m leads to failure if $\boldsymbol{D}_{L_m}(t)$ reaches the predefined failure state set $\boldsymbol{\mathcal{F}}_{L_m}$ or a shock with load larger than D occurs. An example of degradation process L_m considering random shocks is shown in Fig. 7-2, where W_i is the shock load of the i-th shock occurred at time t_i, $i = 1,2,3$. The first two shocks are cumulative which cause instantaneous random changes on $\boldsymbol{D}_{L_m}(t)$, the last shock is extreme which lead $\boldsymbol{D}_{L_m}(t)$ to failure.

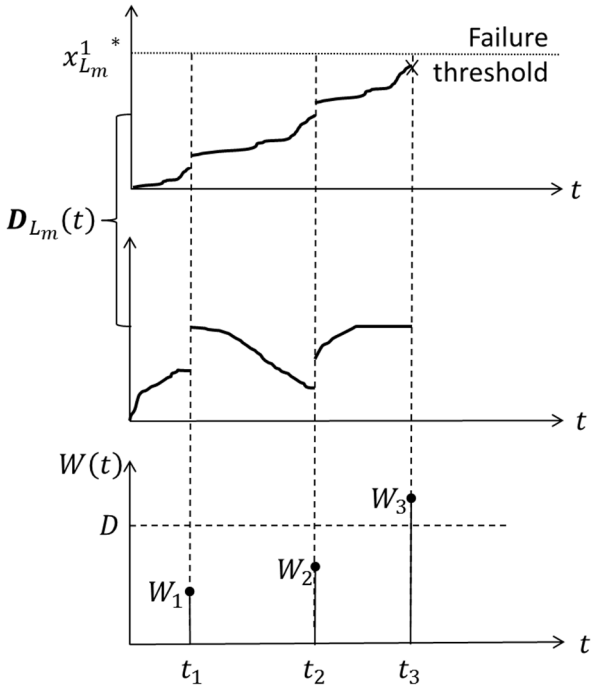

Fig. 7-2. An example of degradation process L_m with random shocks. Top Figure: degradation variable; Center Figure: physical variable; Bottom Figure: random shock process.

7.2 PDMP modeling framework for systems subject to degradation dependency and random shocks

Let $\boldsymbol{Z}(t)$denote the overall degradation process of the system:

$$\boldsymbol{Z}(t) = \left(\boldsymbol{X}'(t) = \left(\boldsymbol{D}_{L_1}(t), \dots, \boldsymbol{D}_{L_M}(t)\right), \boldsymbol{Y}'(t) = (\boldsymbol{Y}(t), N(t))\right) \in \boldsymbol{E} = \mathbb{R}^{d_L} \times \boldsymbol{S}' \quad (7.2)$$

where $\boldsymbol{E}$ is a space combining $\mathbb{R}^{d_L}$ and $\boldsymbol{S}' = \boldsymbol{S} \times \mathbb{N}$. Let $T_k, k \in \mathbb{N}$ denote the k-th jump time in $\boldsymbol{Y}'(t)$ and $\boldsymbol{Z}_k = \boldsymbol{Z}(T_k) = \left(\boldsymbol{X}'(T_k), \boldsymbol{Y}'(T_k)\right) = (\boldsymbol{X}'_k, \boldsymbol{Y}'_k)$. The evolution of $\boldsymbol{Z}(t)$ between two consecutive jumps of $\boldsymbol{Y}'(t)$, between which no shock occurs to the system and the degradation state does not change, can be written as follows:

$$\dot{\boldsymbol{Z}}(t) = (\dot{\boldsymbol{X}}'(t), \dot{\boldsymbol{Y}}'(t)) = \left(\boldsymbol{f_L}^{\boldsymbol{Y}'(t)}(\boldsymbol{X}(t) \mid \boldsymbol{\theta_L}), (\boldsymbol{0}, 0)\right), for\ t \in [T_k, T_{k+1}[\quad (7.3)$$

According to the definition in [128], $\boldsymbol{Z}(t)$ is a PDMP since (1) it can be written as $\boldsymbol{Z}(t) = \varphi(\boldsymbol{Z}_k, t - T_k), for\ t \in [T_k, T_{k+1}[$ and φ satisfies $\varphi(\boldsymbol{y}, t + s) = \varphi(\varphi(\boldsymbol{y}, t), s),\ \forall t, s \geq 0, \boldsymbol{y} \in \boldsymbol{E}$, and $t \to \varphi(\boldsymbol{y}, t), \forall t \geq 0, \boldsymbol{y} \in \boldsymbol{E}$ is right continuous with left limits and (2) $\{\boldsymbol{Z}_n, T_n\}_{n \geq 0}$is a Markov renewal process defined on the space $\boldsymbol{E} \times \mathbb{R}^+$. The probability that $\boldsymbol{Z}(t)$ will step to state $\boldsymbol{j}$ from state $\boldsymbol{Z}_k$ in the time interval $[T_k, T_k + t]$, given $\{\boldsymbol{Z}_i, T_i\}_{i \leq k}$ is as follows:

$$P[\boldsymbol{Z}_{k+1} = \boldsymbol{j}, T_{k+1} \in [T_k, T_k + t] \mid \{\boldsymbol{Z}_i,\ T_i\}_{i \leq k}] = P[\boldsymbol{Z}_{k+1} = \boldsymbol{j}, T_{k+1} \in [T_k, T_k + t] \mid \boldsymbol{Z}_k],$$
$$\forall k \in \mathbb{N}, \boldsymbol{j} \in \boldsymbol{E}, \boldsymbol{j} \neq \boldsymbol{Z}_k \quad (7.4)$$

$\{\boldsymbol{Z}_n, T_n\}_{n \geq 0}$ is characterized by the semi-Markov kernel $N\left(\boldsymbol{i} = (\boldsymbol{x}_i, \boldsymbol{y}_i), (d\boldsymbol{x}, \boldsymbol{y}_j), dt\right) = P\left[\boldsymbol{X}'_{k+1} \in [\boldsymbol{x}, \boldsymbol{x} + d\boldsymbol{x}], \boldsymbol{Y}'_{k+1} = \boldsymbol{y}_j, T_{k+1} - T_k \in [t, t + dt] \mid \boldsymbol{Z}_k = \boldsymbol{i}\right], \forall k \in \mathbb{N}, \boldsymbol{y}_i, \boldsymbol{y}_j \in \boldsymbol{S}', \boldsymbol{x}_i, d\boldsymbol{x} \in \mathbb{R}^{d_L}, d\boldsymbol{x} \to \boldsymbol{0}, dt \to 0$, which can be reformulated as follows:

$$N\left(\boldsymbol{i} = (\boldsymbol{x}_i, \boldsymbol{y}_i), (d\boldsymbol{x}, \boldsymbol{y}_j), dt\right)$$
$$= P\left[\boldsymbol{X}'_{k+1} \in [\boldsymbol{x}, \boldsymbol{x} + d\boldsymbol{x}], \boldsymbol{Y}'_{k+1} = \boldsymbol{y}_j \mid T_{k+1} - T_k \in [t, t + dt], \boldsymbol{Z}_k = \boldsymbol{i}\right]$$
$$\cdot P[T_{k+1} - T_k \in [t, t + dt] \mid \boldsymbol{Z}_k = \boldsymbol{i}]$$
$$= Q\left(\varphi(\boldsymbol{i}, t), (d\boldsymbol{x}, \boldsymbol{y}_j)\right) dF_{\boldsymbol{i}}(t) \quad (7.5)$$

where $Q\left(\varphi(\boldsymbol{i}, t), (d\boldsymbol{x}, \boldsymbol{y}_j)\right)$ is the probability distribution of state $\boldsymbol{Z}_{k+1}$ given $T_{k+1} - T_k = t$ and $\boldsymbol{Z}_k = \boldsymbol{i}$ and $dF_{\boldsymbol{i}}(t)$ is the probability distribution of $T_{k+1} - T_k$ given $\boldsymbol{Z}_k = \boldsymbol{i}$. $Q\left(\varphi(\boldsymbol{i}, t), (d\boldsymbol{x}, \boldsymbol{y}_j)\right)$ can be reformulated as follows:

$$Q\big(\varphi(\boldsymbol{i}=(\boldsymbol{x}_i,\boldsymbol{y}_i),t),(d\boldsymbol{x},\boldsymbol{y}_j)\big)$$

$$= P\big[\boldsymbol{X}'_{k+1}\in[\boldsymbol{x},\boldsymbol{x}+d\boldsymbol{x}],\boldsymbol{Y}'_{k+1}=\boldsymbol{y}_j \mid T_{k+1}-T_k\in[t,t+dt],\boldsymbol{Z}_k=\boldsymbol{i}\big]$$

$$= P\big[\boldsymbol{X}'_{k+1}\in[\boldsymbol{x},\boldsymbol{x}+d\boldsymbol{x}] \mid \boldsymbol{Y}'_{k+1}=\boldsymbol{y}_j, T_{k+1}-T_k\in[t,t+dt],\boldsymbol{Z}_k=\boldsymbol{i}\big]$$

$$\cdot P\big[\boldsymbol{Y}'_{k+1}=\boldsymbol{y}_j \mid T_{k+1}-T_k\in[t,t+dt],\boldsymbol{Z}_k=\boldsymbol{i}\big] \tag{7.6}$$

Let $p_t(d\boldsymbol{z}=(d\boldsymbol{x},\boldsymbol{y}_i))$ denote the probability distribution of $\boldsymbol{Z}(t)$, which obeys the Chapman-Kolmogorov equation [129] as follows:

$$\int_0^t \sum_{\boldsymbol{y}_i\in\boldsymbol{S}'}\int_{\mathbb{R}^{d_L}}\sum_{\boldsymbol{y}_j\in\boldsymbol{S}'}\lambda_{\boldsymbol{y}_i,\boldsymbol{y}_j}(\boldsymbol{x}\mid\boldsymbol{\theta}_{\boldsymbol{K}})\Big(\int_{\mathbb{R}^{d_L}}\psi(\boldsymbol{y}_j,y)\mu(\boldsymbol{y}_i,\boldsymbol{y}_j,\boldsymbol{x})(d\boldsymbol{y})-$$
$$\psi(\boldsymbol{y}_i,\boldsymbol{x})\Big)p_s(d\boldsymbol{x},\boldsymbol{y}_i)ds+$$

$$\int_0^t\sum_{\boldsymbol{y}_i\in\boldsymbol{S}'}\int_{\mathbb{R}^{d_L}}\boldsymbol{f}_{\boldsymbol{L}}^{\boldsymbol{y}_i}(\boldsymbol{x}\mid\boldsymbol{\theta}_{\boldsymbol{L}})div\big(\psi(\boldsymbol{y}_i,\boldsymbol{x})\big)p_s(d\boldsymbol{x},\boldsymbol{y}_i)ds-$$

$$\sum_{\boldsymbol{y}_i\in\boldsymbol{S}'}\int_{\mathbb{R}^{d_L}}\psi(\boldsymbol{y}_i,\boldsymbol{x})\,p_t(d\boldsymbol{x},\boldsymbol{y}_i)+\sum_{\boldsymbol{y}'_i\in\boldsymbol{S}'}\int_{\mathbb{R}^{d_L}}\psi(\boldsymbol{y}_i,\boldsymbol{x})\,p_0(d\boldsymbol{x},\boldsymbol{y}_i)=0 \tag{7.7}$$

where $\lambda_{\boldsymbol{y}_i,\boldsymbol{y}_j}(\boldsymbol{x}\mid\boldsymbol{\theta}_{\boldsymbol{K}})$ is the transition rate of $\boldsymbol{Y}'(t)$ from state $\boldsymbol{y}_i$ to $\boldsymbol{y}_j$, $\psi(\cdot,\cdot)$ is any continuously differentiable function from $\boldsymbol{S}'\times\mathbb{R}^{d_L}$ to $\mathbb{R}$ with a compact support and $\mu(\boldsymbol{y}_i,\boldsymbol{y}_j,\boldsymbol{x})(d\boldsymbol{y})$ is the probability of $\boldsymbol{X}'(t)\in[\boldsymbol{y},\boldsymbol{y}+d\boldsymbol{y}]$ after jumping from $\boldsymbol{x}$ when $\boldsymbol{Y}'(t)$ steps to state $\boldsymbol{y}_j$ from state $\boldsymbol{y}_i$.

The reliability of the system at time t is defined as follows:

$$R(t)=P[\boldsymbol{Z}(s)\notin\boldsymbol{\mathcal{F}},\forall s\le t]=\int_{\boldsymbol{z}\notin\boldsymbol{\mathcal{F}}}p_t(d\boldsymbol{z}) \tag{7.8}$$

where $\boldsymbol{\mathcal{F}}$ is the space of the failure states of the system.

The parameters in the proposed model can be mainly separated into three groups: (1) transition rates in multi-state models; (2) parameters in physics equations of physics-based models and (3) parameters charactering random shock processes. The first group can be estimated, by using degradation and/or failure data from historical field collection or degradation tests, trough maximum likelihood estimation for complete or incomplete data [130, 131], it can also be estimated by using material science knowledge (e.g. multi-state physics model [127]) instead of degradation and/or failure data. The values of the second group are given by the existing physics knowledge on the underlying degradation mechanisms (e.g. fatigue, wear, corrosion, etc.) [12]. The third group can be estimated by using material science knowledge on the influence of random shocks and related information obtained from historical field collection or shock tests [70].

7.3 Solution methodology

The analytical solution of $R(t)$ is difficult to obtain due to the complex behavior of the dependent degradation and random shock processes affecting the system [94]. The MC simulation method [78] based on the semi-Markov kernel of $\{\boldsymbol{Z}_n, T_n\}_{n\geq 0}$ (eq. (7.5)) and the FV method [62] based on the Chapman-Kolmogorov equation (eq. (7.7)) can be used to solve PDMPs like the ones describing the dependent processes of interest here.

7.3.1 MC simulation method

The MC simulation method to compute the system reliability at time t consists of replicating several times the life process of the system by repeatedly sampling its holding time and arrival state from the corresponding probability distributions. Each replication continues until the time of system evolution reaches t or until the system enters a state in the failure set $\boldsymbol{\mathcal{F}}$. The procedure of the MC simulation method is as follows:

Set N_{max} (the maximum number of replications) and $k = 0$ (index of replication)

Set $k' = 0$ (number of replications that end in a system failure state)

While $k < N_{max}$

Initialize the system by setting $\boldsymbol{Z} = (\boldsymbol{X}'(0), \boldsymbol{Y}'(0))$ (initial system state), and the time $T = 0$ (initial system time)

Set $t' = 0$ (state holding time)

While $T < t$

Sample a t' by using the probability distribution $dF_{\boldsymbol{Z}}(t)$

Sample an arrival state $\boldsymbol{y}$ for stochastic process $\boldsymbol{Y}'(t)$ and an arrival state $\boldsymbol{x}$ for process $\boldsymbol{X}'(t)$ by using eq. (7.6)

Set $T = T + t'$

If $T \leq t$

Set $\boldsymbol{Z} = (\boldsymbol{x}, \boldsymbol{y})$

If $\boldsymbol{Z} \in \boldsymbol{\mathcal{F}}$

Set $k' = k' + 1$

Break

End if

Else (when $T > t$)

If $\varphi(\boldsymbol{Z}, t + t' - T) \in \boldsymbol{\mathcal{F}}$

Set $k' = k' + 1$

Break

End if

End if

End While

Set $k = k + 1$

End While □

The estimated system reliability at time t can be obtained by

$$\widehat{R_{MC}}(t) = 1 - k'/N_{max} \tag{7.9}$$

where *k*' represents the number of trials that end in the failure state of the system, and the sample variance [71] is:

$$var_{\widehat{R_{MC}}(t)} = \widehat{R_{MC}}(t)(1 - \widehat{R_{MC}}(t))/(N_{max} - 1) \tag{7.10}$$

7.3.2 FV method

We employ the explicit FV method, developed by Cocozza-Thivent *et al.* [62], presented in Section 4.2.1. It approximates $p_t^{\boldsymbol{Z}_k}(d\boldsymbol{z} = (d\boldsymbol{x}, \boldsymbol{i}) \mid \boldsymbol{\theta})$, the probability distribution of $\boldsymbol{Z}_k(t)$, by $P_n^{\boldsymbol{Z}_k}(A, i \mid \boldsymbol{\theta})d\boldsymbol{x},\ \boldsymbol{x} \in A, t \in [n\Delta t, (n+1)\Delta t[$. $P_{n+1}(A, \boldsymbol{y}_i)$ can be calculated considering the deterministic evaluation of $\boldsymbol{X}(t)$ and the stochastic evolution of $\boldsymbol{Y}'(t)$ based on $P_n(\mathcal{M}, \boldsymbol{y}_i)$ by the Chapman-Kolmogorov forward equation, as follows:

$$P_{n+1}(A, \boldsymbol{y}_i)$$

$$= \frac{1}{1+\Delta t b_A^{\boldsymbol{y}_i}} \widehat{P_{n+1}}(A, \boldsymbol{y}_i) + \Delta t \sum_{B \in \mathcal{M}} \sum_{\boldsymbol{y}_j \in \boldsymbol{S}'} \frac{a_{B,A}^{\boldsymbol{y}_j, \boldsymbol{y}_i}}{1+\Delta t b_A^{\boldsymbol{y}_j}} \widehat{P_{n+1}}(B, \boldsymbol{y}_j) \tag{7.11}$$

where

$$a_{B,A}^{\boldsymbol{y}_j, \boldsymbol{y}_i} = \int_A \lambda_{\boldsymbol{y}_j, \boldsymbol{y}_i}(\boldsymbol{x} \mid \boldsymbol{\theta_K}) \int_B \mu(\boldsymbol{y}_j, \boldsymbol{y}_i, \boldsymbol{x})(d\boldsymbol{y})\boldsymbol{x}/m_A \tag{7.12}$$

is the average transition rate from state $\boldsymbol{y}_j$ and grid B to state $\boldsymbol{y}_i$ and grid A,

$$b_A^{\boldsymbol{y}_i} = \int_A \sum_{\boldsymbol{y}_j \in \boldsymbol{S}'} \lambda_{\boldsymbol{y}_i, \boldsymbol{y}_j}(\boldsymbol{x} \mid \boldsymbol{\theta_K}) d\boldsymbol{x} / m_A \tag{7.13}$$

is the average transition rate out of state $\boldsymbol{y}_i$ for grid A,

$$\widehat{P_{n+1}}(A, \boldsymbol{y}_i) = \sum_{B \in \mathcal{M}} m_{BA}^{\boldsymbol{y}_i} P_n(B, \boldsymbol{y}_i)/m_A \tag{7.14}$$

is the approximate value of probability density function on $[(n+1)\Delta t, (n+2)\Delta t[\times A \times \{\boldsymbol{y}_i\}$ according to the deterministic evolution of $\boldsymbol{X}(t)$,

$$m_{BA}^{\boldsymbol{y}_i} = \int_{\{\boldsymbol{y} \in B \mid \boldsymbol{g}^{\boldsymbol{y}_i}(\boldsymbol{y}, \Delta t \mid \boldsymbol{\theta_L}) \in A\}} d\boldsymbol{y} \tag{7.15}$$

is the volume of the part of grid B which will enter grid A after time Δt, according to the deterministic evolution of $\boldsymbol{X}(t)$.

The approximated solution $\rho_t(\boldsymbol{x}, \cdot)d\boldsymbol{x}$ weakly converges towards $p_t(d\boldsymbol{x}, \cdot)$ when $\Delta t \to 0$ and $|\mathcal{M}|/\Delta t \to 0$ where $|\mathcal{M}| = sup_{A \in \mathcal{M}} diam(A)$.

The estimated system reliability at time t, then, can be calculated as follows:

$$\widehat{R_{FV}}(t) = \int_{\boldsymbol{z} \notin \boldsymbol{\mathcal{F}}} \rho_t(\boldsymbol{z}) d\boldsymbol{z} \tag{7.16}$$

8. RELIABILITY ASSESSMENT METHOD FOR SYSTEMS WITH A LARGE NUMBER OF COMPONENTS CONSIDERING DEGRADATION DEPENDENCY

In previous Chapters, we have employed the PDMP modeling framework to integrate PBMs and MSMs for treating the dependencies among degradation processes [75] for a system with a small number of components, where the whole system is modeled by one PDMP. For systems of larger size, the high dimension of its PDMP can lead to very heavy computational burdens, because solving the PDMP of a small system is already time consuming due to the combinatorial nature of MSMs and the need to simulate the trajectory between any two system states [75]. In addition, the dependencies may only exist within certain groups of components and leave different groups being independent [43], and the causes to systems failure are not easy to be identified. Fault tree analysis (FTA) [132] is typically used to identify the combinations of events leading to system failure and compute its probability by using minimal cut sets found from the fault tree structure. For real systems, this can be computationally intensive, when the tree structure is large and, especially, if it contains repeated basic events [133]. In addition, all basic events are usually assumed statistically independent. The dependencies of the degradation processes leading to failure of different components need to be considered which render certain basic events under different gates being dependent. In this Chapter, a system reliability assessment method is proposed considering degradation dependency by combining BDDs and MC simulation method to reduce computational cost.

8.1 Methodology

We refer to the system presented in Section 3.2. The fault tree of the system is available and contains Q basic events denoted by $\boldsymbol{e} = \{e_1, e_2, \dots, e_Q\}$ which include the failures of components and other events such as erroneous operation caused by human errors. The component-failure type of events are determined by their underlying degradation processes.

8.1.1 Binary decision diagrams (BDDs)

A BDD is a directed acyclic graph encoding Shannon's decomposition of a formula. A BDD has two terminal vertices labeled 1 and 0 to indicate the failure and operation of the system, respectively. Each non-terminal vertex is labeled with a variable and has two outgoing edges: 1-edge and 0-edge which indicate the occurrence and non-occurrence of the corresponding basic event, respectively.

A BDD is employed to encode the fault tree of the system according to the given ordering of the indicator variable X_i used to denote the occurrence or non-occurrence of the basic event i ($X_i = 1$ indicating the occurrence of the basic event i and $X_i = 0$ indicating the opposite). The size of the BDD largely depends on the given ordering and the problem of finding the global optimal ordering is an intractable task [134, 135]. Several ordering heuristics have been developed, whose performances may vary on different problems. In this work, we employ the weighting depth-first left-most (WDFLM) ordering technique proposed in [136], which leads to satisfactory results according to the tests in [137, 138]. WDFLM first assigns weight 1 to each basic event. Then, it traverses the fault tree bottom-up to calculate the weight of each gate by adding the weights of all its inputs, i.e. gates and basic events. Fig. 8-1 shows an example of a fault tree where the weights of the gates are obtained through WDFLM.

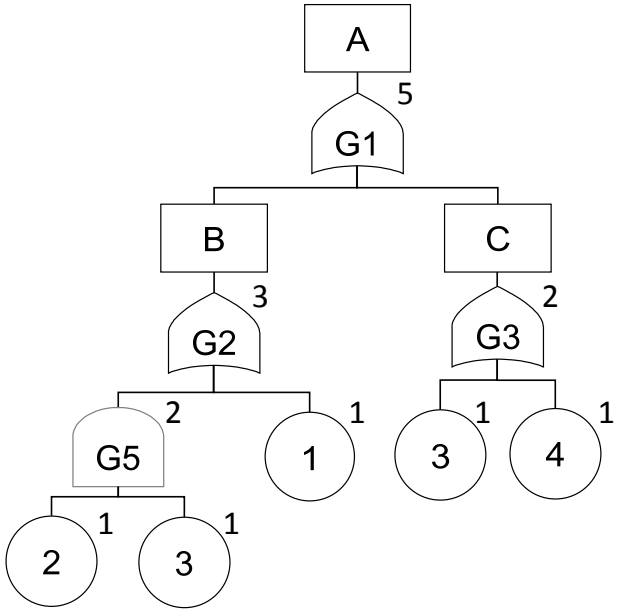

Fig. 8-1. An illustration of fault tree labeled with weights.

Then, the inputs of a gate are rearranged in the order of increasing weights as shown in Fig. 8-2.

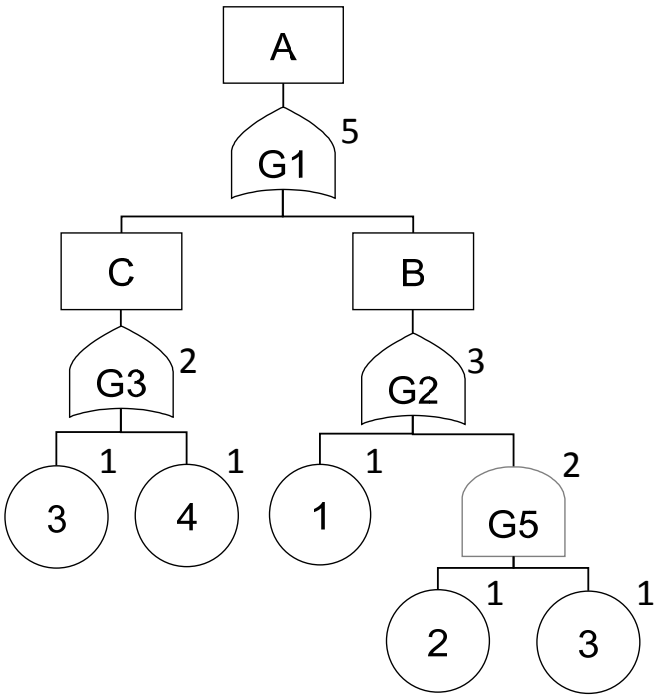

Fig. 8-2. An illustration of fault tree with rearranged inputs of gates.

Finally, the depth-first left-most (DFLM) ordering technique [139] is applied to the fault tree to get the variable ordering. In this technique, the basic events are placed in the ordered list as soon as they are encountered during the DFLM traversal of the fault tree. Let $<$ be a total ordering of variables, for the fault tree in Fig. 8-1 it is $X_3 < X_4 < X_1 < X_2$.

Based on the variable ordering, the related BDD can be constructed using the bottom-up procedure. Firstly, all basic events $i, i \in \boldsymbol{e}$ are associated with the if-then-else (ite) structure [140] $ite(X_i, 1, 0)$, where $ite(X_i, f_1, f_2) = (X_i \wedge f_1) \vee (\neg X_i \wedge f_2)$, which means if the basic event i occurs then consider function f_1 else consider function f_2. Then, work from the bottom to the top of the fault tree and obtain the ite structure for each gate by using the following principle: let us consider two variables $X_a < X_b$ and four functions f_1, f_2, f_3, f_4, let $<>$ be any logic operation AND or OR, then:

$$ite(X_a, f_1, f_2) <> ite(X_a, f_3, f_4) = ite(X_a, f_1 <> f_3, f_2 <> f_4) \qquad (8.1)$$

and

$$ite(X_a, f_1, f_2) <> ite(X_b, f_3, f_4) = ite\big(X_a, f_1 <> ite(X_b, f_3, f_4), f_2 <> ite(X_b, f_3, f_4)\big) \quad (8.2)$$

The ite structure of the top event of the fault tree in Fig. 8-1 can be obtained as $ite(X_3, 1, ite(X_4, 1, ite(X_1, 1, 0)))$. The associated BDD shown in Fig. 8-3 can be constructed by breaking down each ite structure into its left and right branches, and eliminating the vertexes that are not useful (a vertex is not useful when its two outgoing edges point to the same vertex or it is equivalent to another vertex) [141].

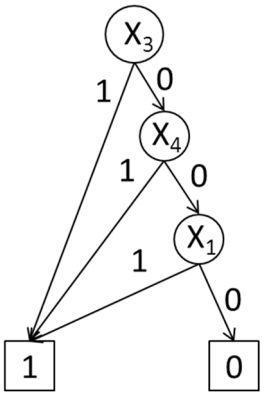

Fig. 8-3. BDD for fault tree in Fig. 8-1.

Finally, all the paths leading to system failure can be obtained as $(1)X_3 = 1, (2)X_3 = 0, X_4 = 1, (3)X_3 = 0, X_4 = 0, X_1 = 1$ and the path leading to system operation is $X_3 = 0, X_4 = 0, X_1 = 0$. The exact system reliability is equal to the sum of the probability of occurrence of the paths leading to system operation or $1 -$ the sum of the probability of occurrence of the paths leading to system failure.

8.1.2 MC simulation method

To derive the probability of occurrence of one path, all the PDMPs containing the variables involved in that path need to be solved. Since the PDMPs are independent from each other, the product of the probabilities of PDMPs being in the states indicated by the path equals the

probability of occurrence of that path. Analytically solving the PDMPs is a difficult task, whereas MC simulation method is well suited.

We employ the MC simulation method for solving the PDMPs developed in Chapter 3.3. It consists of sampling the transition time and the arrival state for the MSMs and, then, calculating the behavior of the PBMs within the transition times using the physics equation.

Let us consider one group of interdependent degradation processes $\boldsymbol{L}_p = \{L_{p_1}, \dots, L_{p_n}\}$ and $\boldsymbol{K}_q = \{K_{q_1}, \dots, K_{q_m}\}$, which have no dependencies with the other degradation processes. Their degradation states are represented by

$$\boldsymbol{Z}_{p,q}(t) = \begin{pmatrix} \begin{pmatrix} \boldsymbol{X}_{L_{p_1}}(t) \\ \vdots \\ \boldsymbol{X}_{L_{p_n}}(t) \end{pmatrix} = \boldsymbol{X}_p(t) \\ \begin{pmatrix} Y_{q_1}(t) \\ \vdots \\ Y_{q_m}(t) \end{pmatrix} = \boldsymbol{Y}_q(t) \end{pmatrix} \in \boldsymbol{E}_{p,q} = \mathbb{R}^{d_{\boldsymbol{L}_p}} \times \boldsymbol{S}_{\boldsymbol{K}_q}, \forall t \geq 0 \qquad (8.3)$$

where $\boldsymbol{E}_{p,q}$ is the space combining $\mathbb{R}^{d_{\boldsymbol{L}_p}}$ ($d_{\boldsymbol{L}_p} = \sum_{k=1}^{n} d_{L_{p_k}}$) and $\boldsymbol{S}_{\boldsymbol{K}_q} = \{0, 1, \dots, d_{\boldsymbol{K}_q}\}$ denotes the state set of process $\boldsymbol{Y}_q(t)$.

To calculate the probability of occurrence of one path (let $\boldsymbol{Z}^*_{p,q}$ indicate the state space, which contains all the states of $\boldsymbol{Z}_{p,q}(t)$ that are consistent with the state of the path), the procedure of the MCS is presented as follows.

Set N_{max} (the maximum number of replications) and $k = 0$ (index of replication)

Set $k' = 0$ (number of trials that end in the state indicated by the path)

While $k < N_{max}$

Initialize the system by setting $\boldsymbol{Z}'_{p,q}(0) = \begin{pmatrix} \boldsymbol{X}_p(0) \\ \boldsymbol{Y}'_q \end{pmatrix}$ (initial state), and the time $T = 0$ (initial system time)

Set $t' = 0$ (state holding time)

While $T \leq T_{miss}$

Sample a holding time t' for current degradation state

Sample an arrival state $\boldsymbol{Y}''_q$ for stochastic process $\boldsymbol{Y}_q(t)$ from all the possible states

Calculate $\boldsymbol{X}_p(s), \forall s \in [T, T+t']$

Set $\boldsymbol{Z}'_{p,q}(s) = \begin{pmatrix} \boldsymbol{X}_p(s) \\ \boldsymbol{Y}'_q \end{pmatrix}, \forall s \in [T, T+t'[$

Set $T = T + t'$, $\boldsymbol{Z}'_{p,q}(T) = \begin{pmatrix} \boldsymbol{X}_p(T) \\ \boldsymbol{Y}''_q \end{pmatrix}$ and $\boldsymbol{Y}'_q = \boldsymbol{Y}''_q$

End While

If $\boldsymbol{Z}'_{p,q}(T_{miss}) \in \boldsymbol{Z}^*_{p,q}$

Set $k' = k' + 1$

End if

Set $k = k + 1$

End While □

The estimated probability of occurrence of one path at time T_{miss} can be obtained by

$$\hat{P}(T_{miss}) = 1 - k'/N_{max} \tag{8.4}$$

with the sample variance [71] as follows:

$$var_{\hat{P}(T_{miss})} = \hat{P}(T_{miss})(1 - \hat{P}(T_{miss}))/(N_{max} - 1) \tag{8.5}$$

8.1.3 Flowchart of the proposed method

The flowchart of the whole proposed computational method combining BDDs and MC simulation method is shown in Fig. 8-4.

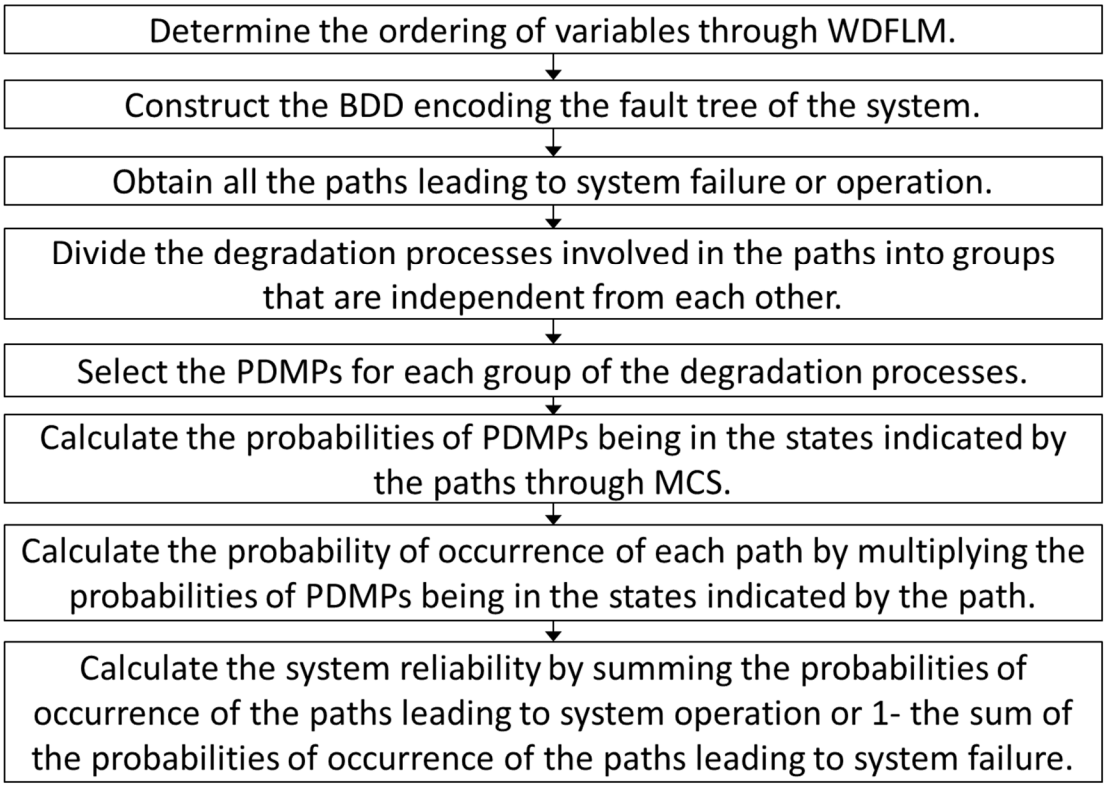

Fig. 8-4. The flowchart of the computational method.

9. APPLICATIONS

This Chapter reports the results of the applications of the developed models and proposed methodologies within the holistic framework for the reliability-based analysis and maintenance optimization of nuclear safety systems. Case studies on nuclear safety systems related to single components, multi-components systems (with a limited number of components) and multi-components systems (with a large number of components) are illustrated. For further details the interested reader is referred to the corresponding Papers (I)-(VII) of Part II.

9.1 Single components

9.1.1 Reliability assessment of a dissimilar metal weld in a primary coolant system

In this Section, we illustrate the MSPM framework for component reliability assessment by including semi-Markov and random shock processes, proposed in Chapter 2, on a case study slightly modified from an Alloy 82/182 dissimilar metal weld in a primary coolant system of a nuclear power plant in [63]. The MSPM of the original crack growth is shown in Fig. 9-1.

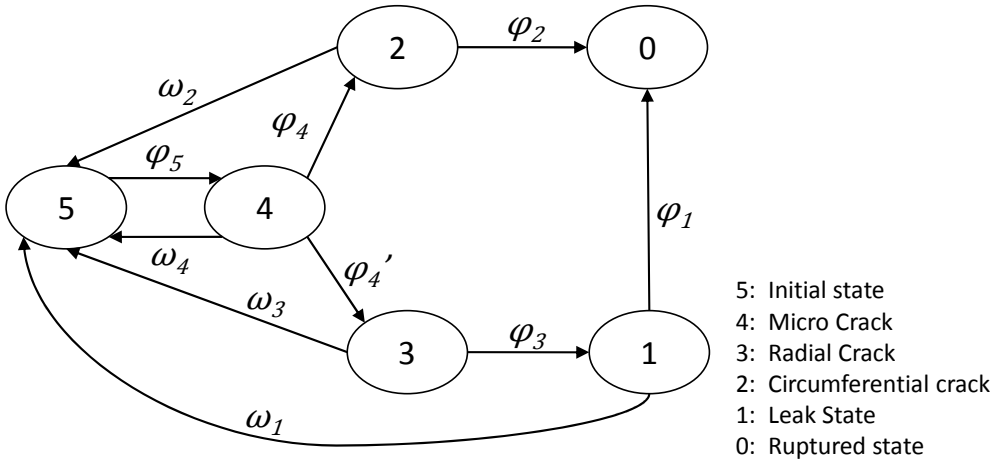

Fig. 9-1. MSPM of crack development in Alloy 82/182 dissimilar metal welds.

where φ_i, and ω_i represent the degradation transition rate, and maintenance transition rate,

respectively. Except for φ_5,φ_4, $\varphi_{4'}$ and φ_3, all the other transition rates are assumed to be constant. The expressions of the variable transition rates are

$$\varphi_5 = \left(\frac{b}{\tau}\right) \cdot \left(\frac{\tau_5}{\tau}\right)^{b-1}; \tag{9.1}$$

$$\varphi_4 = \begin{cases} \frac{a_C P_C}{\dot{a}_M {\tau_4}^2 (1 - P_C(1 - a_C/(u\dot{a}_M)))}, & if\ \tau_4 > a_C/\dot{a}_M \\ 0, & else; \end{cases} \tag{9.2}$$

$$\varphi_4{}' = \begin{cases} \frac{a_D P_D}{\dot{a}_M {\tau_4}^2 (1 - P_D(1 - a_D/(u\dot{a}_M)))}, & if\ \tau_4 > a_D/\dot{a}_M \\ 0, & else; \end{cases} \tag{9.3}$$

$$\varphi_3 = \begin{cases} \frac{1}{\tau_3}, & if\ \tau_3 > (a_L - a_D)/\dot{a}_M \\ 0, & else. \end{cases} \tag{9.4}$$

The random shocks correspond to the thermal and mechanical shocks (e.g. internal thermal shocks and water hammers) [30, 31] applied to the dissimilar metal welds. The damage of random shocks can accelerate the degradation processes, and hence increase the rate of component degradation. We set the probability of a random shock becoming an extreme shock as $p_{i,m}(\tau'_{i,m}) = 1 - exp\left[-\delta m(6-i)\left(2 - e^{-\tau'_{i,m}}\right)\right]$, taking the exponential formulation from Fan *et al.*'s work [39]. In this formula, we use $m(6-i)(2-e^{-\tau'_{i,m}})$ to quantify the component degradation. It is noted that the quantity $2 - e^{-\tau'_{i,m}}$ ranges from *1* to *2*, representing the relatively small effect of $\tau'_{i,m}$ onto the degradation situation in comparison with the other two parameters m and *i*, and δ is a predetermined constant which controls the influence of the degradation onto the probability $p_{i,m}(\tau'_{i,m})$. In addition, we assume the corresponding degradation transition rates after m cumulative shocks to be $\lambda_{i,j}^{(m)}(\tau'_{i,m}, \boldsymbol{\theta}) = (1 + \varepsilon)^m \lambda_{i,j}(\tau'_{i,m}, \boldsymbol{\theta})$, where ε is the relative increment of transition rates after one cumulative shock happens, and the formulation $(1+\varepsilon)^m$ is used to characterize the accumulated effect of such shocks. To characterize the increase of the transition rates, in the case study we have used the parameter ε to represent the relative increment of degradation transition rate after one cumulative shock occurs. For the sake of simplicity, but without loss of generality in the framework for integration, we assume that the values of ε for each cumulative shock are equal. But the model can handle different ε for different stages of the crack process.

The Monte Carlo simulation over a time horizon of $t_{max} = 80$ years is run $N_{max} = 10^6$

times. The results are collected and analyzed in the following sections.

The estimated state probabilities without, and with random shocks throughout the time horizon are shown in Figs. 9-2, and 9-3, respectively.

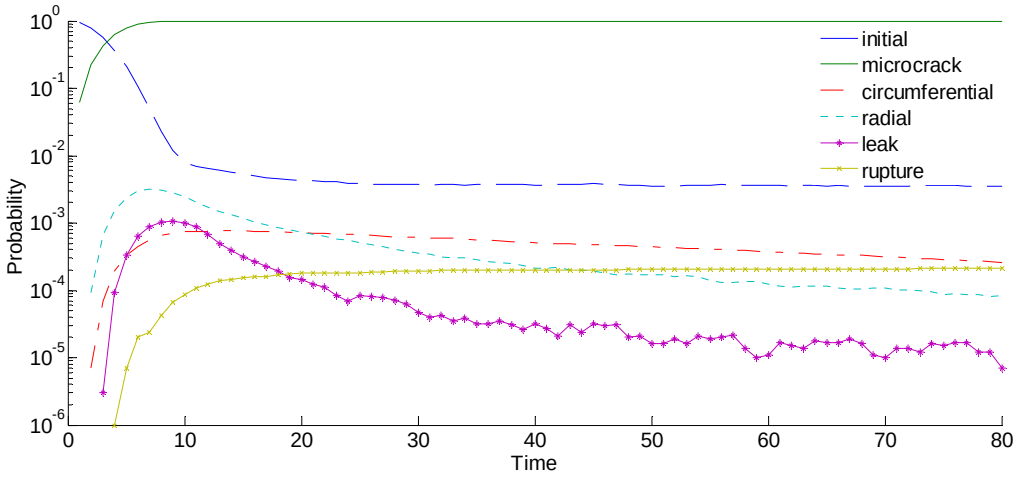

Fig. 9-2. State probabilities obtained without random shocks.

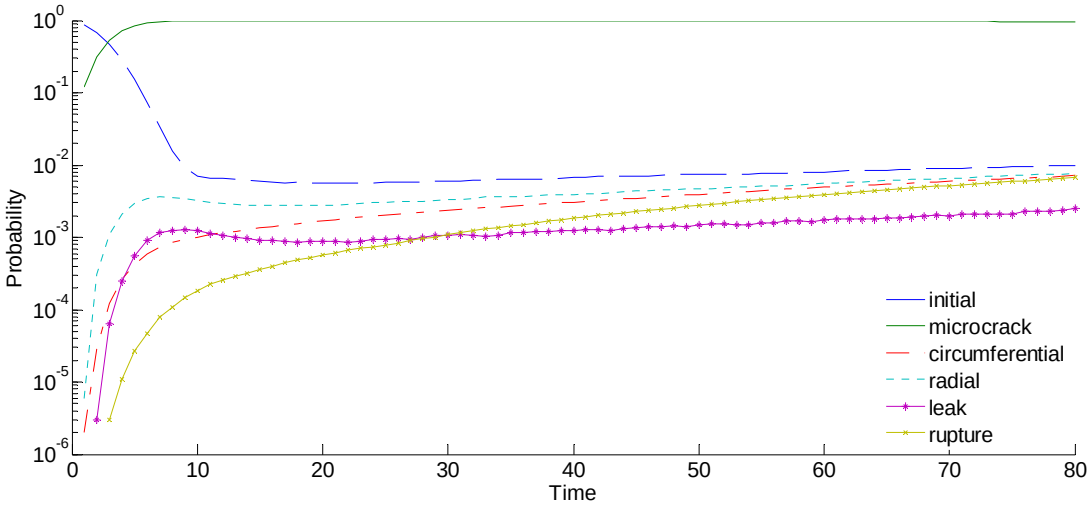

Fig. 9-3. State probabilities obtained with random shocks.

Comparing the above two figures, it can be observed that as expected the random shocks drive the component to higher degradation states than the micro-crack state. The numerical

comparisons on the state probabilities with/without random shocks at year 80 are reported in Table 9-1. It is seen that, except for the micro-crack state probability, all the other state probabilities at year 80 have increased due to the random shocks, with the increase in leak probability being the most significant.

Table 9-1 Comparison of state probabilities with/without random shocks (at year 80).

State	Probability without random shocks	Probability with random shocks	Relative difference
Initial	3.52e-3	9.82e-3	180.00%
Micro-crack	0.9959	0.9661	-2.99%
Circumferential crack	3.05e-4	7.28e-3	2286.89%
Radial crack	1.00e-4	7.75e-3	7650.00%
Leak	1.30e-5	2.59e-3	19823.08%
Rupture state	2.06e-4	7.00e-3	3298.06%

The fact that the probability of the initial state (compared with no random shocks) at 80 years has increased is attributed to the maintenance tasks. All the maintenance tasks lead the component to the initial state, and the repair rates from radial macro-crack state, circumferential macro-crack state, and leak state are higher than that from the micro-crack state. The shocks generally increase the component degradation speed, i.e. render the component step to further degradation states (other than micro-crack state) faster than the case without shocks. The transitions to initial state occur more frequently from further degradation states (other than from the micro-crack state) due to their higher maintenance rates. In summary, this phenomenon is due to the combined effects of shocks.

The estimated component reliabilities with/without random shocks and with only cumulative shocks throughout the time horizon are shown in Fig. 9-4. At year 80, the estimated component reliability with random shocks is 0.9930, with sample variance equal to 6.95e-9. Compared with the case without random shocks (reliability equals to 0.9998, with sample variance 2.00e-10), the component reliability has decreased by 0.68%. The estimated component reliability with only cumulative shocks is 0.9973, and the sample variance equals 2.69e-9. Compared with the case without random shocks, the component reliability has decreased by 0.26%.

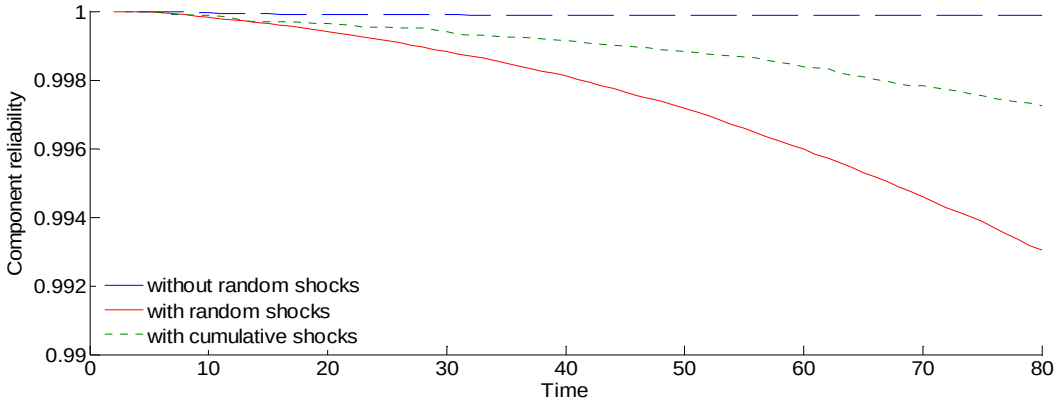

Fig. 9-4. Component reliability with/without random shocks, and with only cumulative shocks.

9.2 Multi-component systems (with a limited number of components)

9.2.1 Subsystem of the residual heat removal system (RHRS)

In this Section, we illustrate the models and methodologies for multi-component systems (with a limited number of components), proposed in Chapters 3-7, on a case study of one subsystem of the RHRS of a nuclear power plant of Électricité de France (EDF). The system consists of a centrifugal pump and a pneumatic valve in series. Given the series configuration, the failure of anyone of the two components can lead the subsystem to failure. Dependency in the degradation processes of the two components has been indicated by the experts: the pump vibrates due to degradation [142] which, in turn, leads the valve to vibrate, aggravating its own degradation processes [143].

The pump is modeled by a MSM, modified from the one originally supplied by EDF upon

discussion with the experts. It is a continuous-time homogeneous Markov chain as shown in Fig. 9-5:

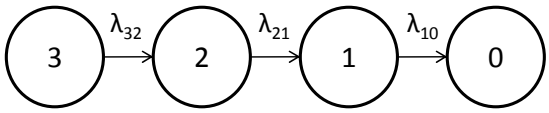

Fig. 9-5. Degradation process of the pump.

$S_p = \{0, 1, 2, 3\}$ denotes its degradation states set, where 3 is the perfect functioning state and 0 is the complete failure state. The parameters λ_{32}, λ_{21} and λ_{10} are the transition rates between the degradation states. Due to degradation, the pump vibrates when it reaches the degradation states 2 and 1. The intensity of the vibration of the pump on states 2 and 1 is evaluated as by the experts 'smooth' and 'rough', respectively.

The simplified scheme of the pneumatic valve is shown in Fig. 9-6. It is a normally-closed, gas-actuated valve with a linear cylinder actuator.

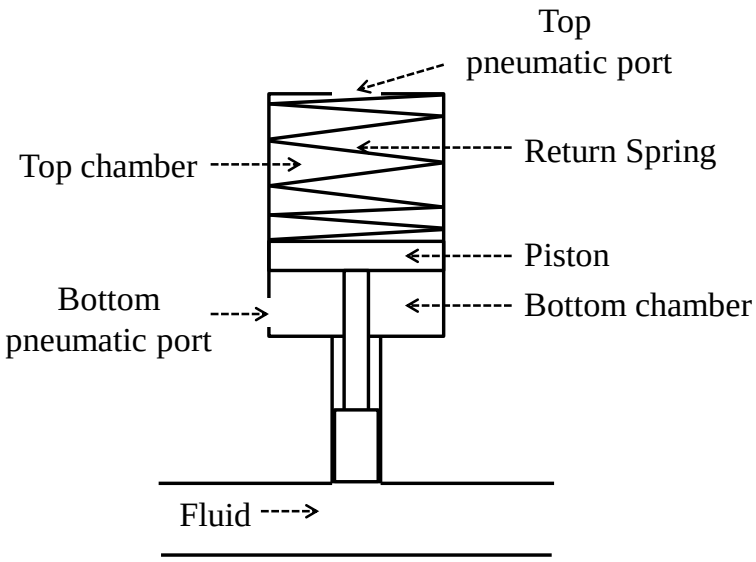

Fig. 9-6. Simplified scheme of the pneumatic valve [12].

By regulating the pressure of the pneumatic ports to fill or evacuate the top and bottom

chambers, the position of the piston can be controlled. A return spring is linked with the piston to ensure the closure of the valve, when pressure is lost. The external leak at the actuator connections to the bottom pneumatic port due to corrosion and other environmental factors is chosen as the degradation mechanism of the valve, which is much more significant than the other degradation mechanisms according to the results shown in [12].

Let $D_b(t)$ denote the area of the leak hole at the bottom pneumatic port at time t, the development of the leak size is described by:

$$\dot{D_b}(t) = \omega_b(1 + \beta_{Y_p(t)}) \tag{9.5}$$

where ω_b is the original wear coefficient and where $\beta_{Y_p(t)}$ is the relative increment of the developing rate of the external leak at the bottom pneumatic port caused by the vibration of the pump at degradation state '2' or '1'.

The leak will lead the valve to be more difficult to open but easier to close. The threshold of the area of leak hole D_b^* is defined as the value above which ($D_b(t) > D_b^*$) the valve cannot reach the fully open position within the 15s time limit from the fully closed position, after an opening command is executed.

9.2.1.1 Reliability assessment under degradation dependency

The degradation of the valve $\boldsymbol{L} = \{L_1\}$ is described by PBM and the degradation of the pump $\boldsymbol{K} = \{K_1\}$ is described by MSM. The degradation processes of the whole system are modeled by PDMP as follows:

$$\boldsymbol{Z}(t) = \begin{pmatrix} D_b(t) \\ Y_p(t) \end{pmatrix} \in \mathbb{R}^+ \times S_p \tag{9.6}$$

where $Y_p(t)$ denotes the degradation state of the pump at time t and $D_b(t)$ denotes the area of the leak hole at the bottom pneumatic port of the valve at time t. The space of the failure states of $\vec{Z}(t)$ is $\boldsymbol{\mathcal{F}} = [0, +\infty) \times \{\text{'0'}\} \cup [D_b^*, +\infty) \times \{1, 2, 3\}$. The development of the leak size is described by:

$$\dot{D_b}(t) = \omega_b(1 + \beta_{Y_p(t)}) \tag{9.7}$$

where ω_b is the original wear coefficient and where $\beta_{Y_p(t)}$ is the relative increment of the developing rate of the external leak caused by the vibration of the pump at the degradation state $Y_p = 2$ or 1.

The initial state of the system is assumed as follows:

$$\boldsymbol{Z}_0 = \begin{pmatrix} D_b(0) \\ Y_p(0) \end{pmatrix} = \begin{pmatrix} 0 \\ 3 \end{pmatrix} \tag{9.8}$$

which means that the two components are both in their perfect state. The initial probability distribution of the processes $(D_b(t), Y_p(t))_{t\geq 0}$, $p_0(d\boldsymbol{z} \mid \boldsymbol{\theta})$, hence, equals to $\delta_{\boldsymbol{Z}_0}(d\boldsymbol{z})$, where δ is the Dirac delta function.

The system reliability at time t can be calculated as follows:

$$R(t) = P\left[(D_b(s) < D_b^*) \cap (Y_p(s) \neq 0), \forall s \leq t\right] \tag{9.9}$$

We consider MC simulations with 10^6 trials for the estimation of the system reliability over a time horizon of $T_{miss} = 1000\ s$. The results are shown in Fig. 9-7.

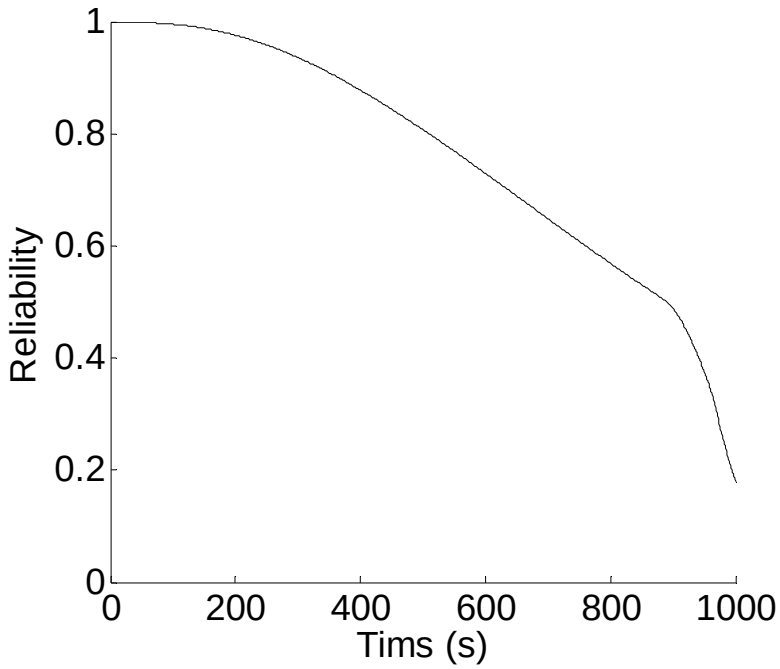

Fig. 9-7. Estimated system reliability.

The system reliability decreases more rapidly after around 885 s, because at that time the valve could fail, corresponding to the situation when the pump steps to the state ‘1’ very quickly and stays there until the valve fails.

9.2.1.2 Fuzzy reliability assessment

We have $\boldsymbol{\theta}_L = (\omega_b, \beta_{Y_p(t)})$ and $\boldsymbol{\theta}_K = (\lambda_{32}, \lambda_{21}, \lambda_{10})$ which are the uncertain parameters due to the fact that their values are estimated from insufficient degradation data or elicited from expert judgment. Epistemic uncertainty associated to them, hence, needs to be taken into account and a proper mathematical representation of uncertainty of this nature is by fuzzy numbers. We choose triangular fuzzy numbers [144] to represent the uncertain parameters because their boundary values and most probable or most advisable values are considered easier to be elicited from experts than other FN types and they are widely used to represent uncertain parameters in reliability engineering [80, 84, 89, 144]. The fuzzy numbers are assigned by considering a relative uncertainty of $\pm 10\%$ of the original parameters values. However, the proposed framework is generally suitable for fuzzy numbers with other types of membership functions.

The results of the fuzzy reliability of the system at cut levels $\alpha = 0$ and $\alpha = 1$ over a time horizon 1000 s obtained by MC simulation with 10^6 trials and FV method are shown in Fig 9-8. The lower bound of the fuzzy reliability of the system at cut level $\alpha = 0$ decreases more sharply after around 790 s, earlier than the fuzzy reliability at $\alpha = 1$. It is seen that the system fails after around 964 s, because at that time the valve is completely failed. The upper bound of the fuzzy reliability at $\alpha = 0$ does not experience a rapid decrease because the valve is mostly functioning over the time horizon.

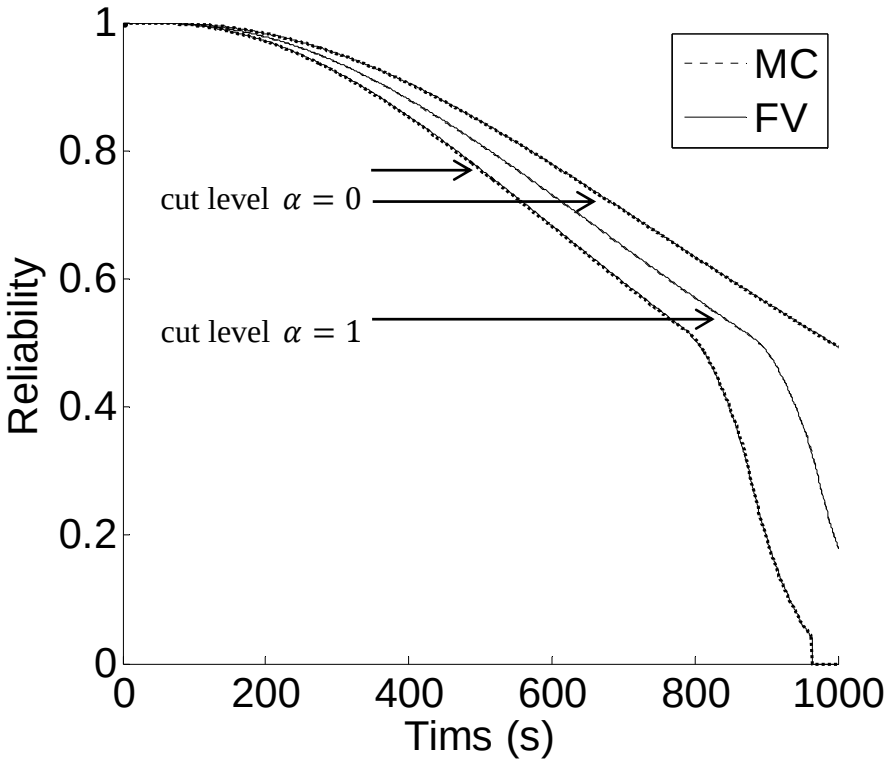

Fig 9-8. Fuzzy reliability at cut levels $\alpha = 0$ and $\alpha = 1$ obtained by MC and FV.

The membership function of fuzzy reliability $\tilde{R}(t)$ at mission time $t = 800$ s at different cut levels $\alpha \in [0, 1]$ obtained by MC simulation and FV method are illustrated in Fig. 9-9 (we have uniformly chosen 51 points in $[0, 1]$ with a step equal to 0.02 assigned to α). The average computation time of MC simulation is 201.94 s, while that of FV scheme is 15.91 s. The results show that the FV method achieves comparable results as MC simulation, with less computational burden.

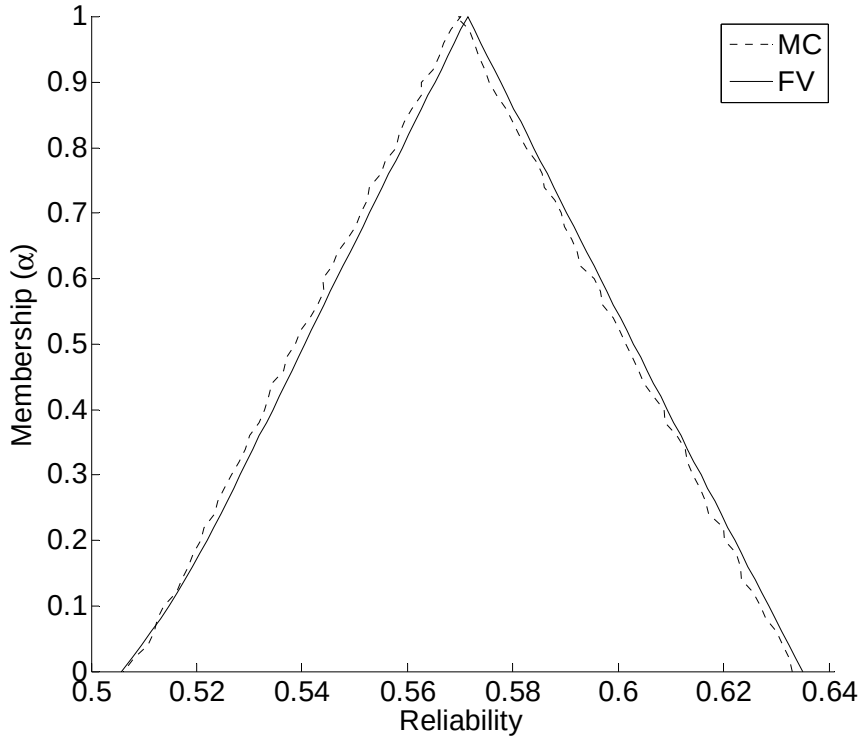

Fig. 9-9. Membership function of fuzzy reliability $\tilde{R}(t)$ at mission time $t = 800$ s obtained by MC simulation and FV method.

9.2.1.3 Computation of component IMs

The component IMs for the valve and the pump with condition-based preventive maintenance by periodic inspections and corrective maintenance are given in the following equations, respectively, as follows:

$$CI_V(t) = \int_{\mathbb{R}^+} f_{\boldsymbol{D}_V(t)}(x) \left| P[(D_b(s) < D_b^*) \cap (Y_p(s) \neq 0), \forall s \leq t \middle| D_b(t) = x)] - R(t) \right| dx \tag{9.10}$$

$$CI_P(t) = \sum_{i=0}^{3} P[Y_p(t) = i] \left| P[(D_b(s) < D_b^*) \cap (Y_p(s) \neq 0), \forall s \leq t \middle| Y_p(t) = i)] - R(t) \right| \tag{9.11}$$

Then, by using the proposed numerical method introduced in Chapter 5.4, the values of the above equations can be calculated.

The reliabilities of the whole system and of the two components over a time horizon of T_{miss} =2000s, regarded as the mission time under accelerated conditions, are shown in Fig. 9-

10. We can see from the figure that before around 870s (point A), the system reliability is basically determined by the pump reliability, since the valve is highly reliable. After that, the sharp decrease of the reliability of the valve due to degradation drives that of the system reliability, until the execution of the inspection tasks for the two components at 1000s. Because of the preventive maintenance, the failures of the system, the valve and the pump are mitigated.

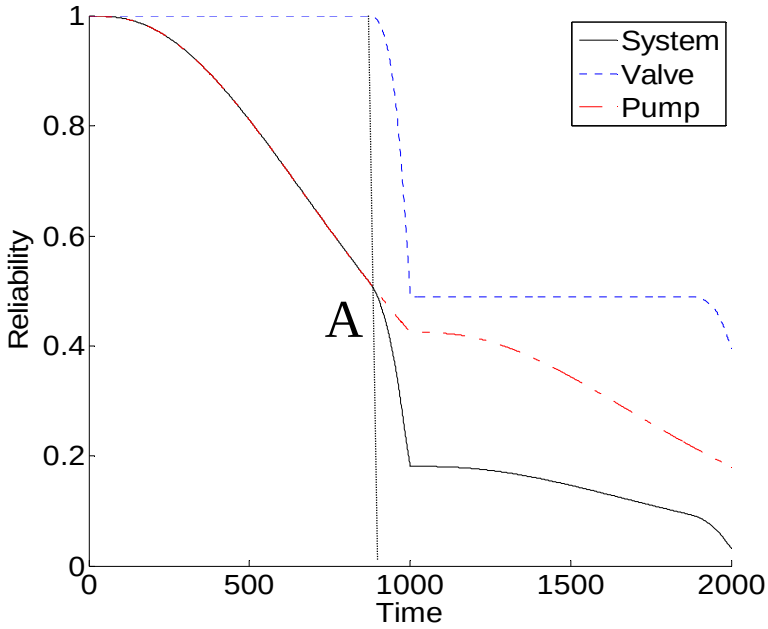

Fig. 9-10. The reliabilities of the system, the valve and the pump.

The components IMs are shown in Fig. 9-11. Before around 400s (point B), the IMs of the two components are relatively close. Although the system reliability is dominated by the reliability of the pump, the probability of the pump at state 0 over the time horizon is limited to a very small value due to the corrective maintenance shown in Fig. 9-12, which can limit the component IM. After around 870s (point C), the pump IM experiences a sharp decrease while that of the valve experiences a sharp increase until 1000s, due to the evolution shown in Fig. 9-10. After the preventive maintenance is implemented, the difference between the components IMs begins to reduce. Then, one can conclude that attention should be focused on the pump before 1000s and on the valve afterwards, to achieve higher levels of system reliability.

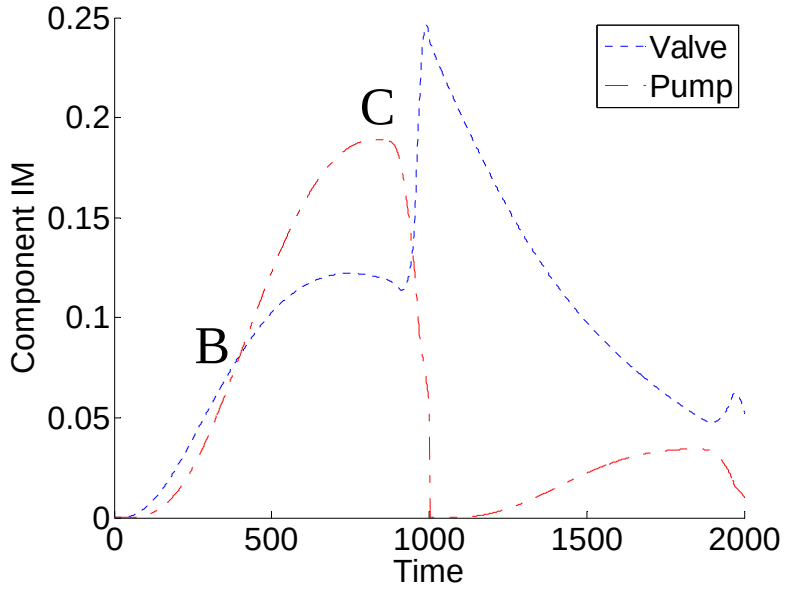

Fig. 9-11. The valve and pump IMs.

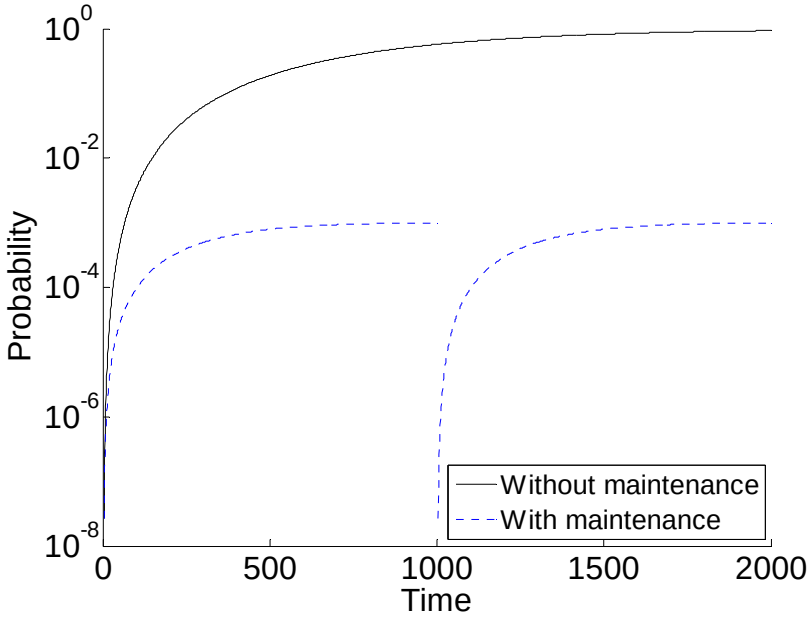

Fig. 9-12. The probability of the pump at state 0 (failure).

9.2.1.4 Maintenance optimization

The proposed method has been run 150 generations to obtain the Pareto optimal maintenance

policies. The obtained Pareto front in the plane of the two objective functions, i.e. lower and upper bounds of the maintenance cost, is shown in Fig. 9-13.

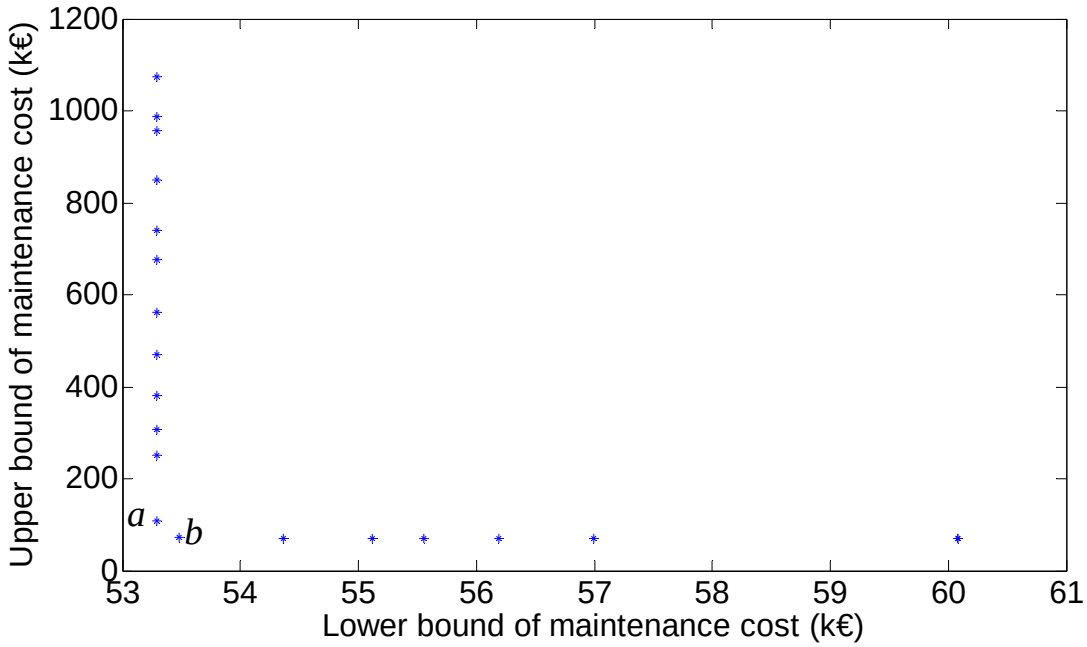

Fig. 9-13. The obtained Pareto front.

It is observed that the upper bounds cover a wide range whereas the lower bounds show much less variability. The solutions above a = (53.30, 108.45) k€ have big increments with respect to the upper bound, but they have nearly no difference in the lower bound compared with those of a. The solutions to the right of b = (53.49, 72.75) k€ show nearly no difference in the upper bound value, compared with that of b. The small differences between lower bounds are due to the fact that the failure of the components or of the system rarely occurs under these situations, so that the total cost is mainly composed of the PM costs and the inspections costs; on the contrary, the big differences between upper bounds are mainly due to the failures of components, which lead to the system failure and, thus, carry a high penalty cost. It also implies the fact that if the frequencies of inspections and PM exceed some value, then, the high penalty cost may be largely avoided. In practice, the solutions with very high upper bounds might not be appropriate for decision makers (DMs).

In case that the DMs intend to conduct a search within a certain budget, the method proposed is also capable of dealing with this situation. For instance, we can focus on the solutions within

the region $[0, 100]$ k€ $\times$ $[0, 100]$ k€. The proposed method is run with the previous configurations plus a penalty of 100 k€ to be added to one objective of a solution, whenever the other objective exceeds 100 k€. The newly obtained Pareto front is shown in Fig. 9-14.

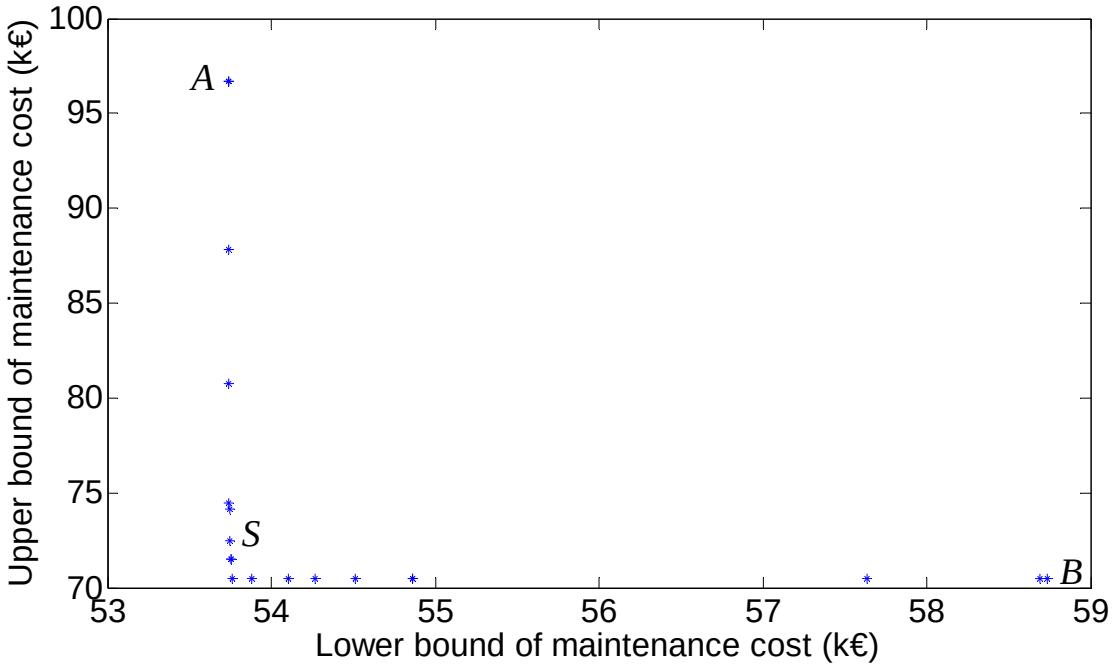

Fig. 9-14. The Pareto front obtained within the region $[0, 100]$ k€ $\times$ $[0, 100]$ k€.

Given the Pareto front, the DMs need eventually choose the maintenance policy according to their preferences since the solutions do not dominate each other. To simulate those common preferences of the DMs, we choose three solutions: *S*, the solution selected by the 'Min-Max' method, which selects the representative center of the Pareto front, and is among the most used ones [145]; *A* (corresponding to a selection by decision makers who are optimistic and pay more attention to the lower bound of the cost objective factor) and *B* (corresponding to a selection by decision makers who are conservative and pay more attention to the upper bound of the cost objective factor), the solutions with the minimum lower bound and minimum upper bound values, respectively. Solutions *A*, *B* and *S* represent three different preferences of the DMs. Detailed information on *S*, *A* and *B* is reported in Table 9-2.

Table 9-2 Solutions S, A and B.

Solution	*S*	*A*	*B*
Lower bound	53.74 k€	53.73 k€	58.69 k€
Upper bound	74.17 k€	96.69 k€	70.46 k€
T_{L_1}	773.47 s	808.55 s	563.00 s
T_{K_1}	66.77 s	66.77 s	66.77 s
H_{L_1}	[7.28 e-6, D_b^*) m^2	[7.66 e-6, D_b^*) m^2	[4.91 e-6, D_b^*) m^2
H_{K_1}	{'1', '2'}	{'1', '2'}	{'1', '2'}

It can be observed that *S* and *A* have nearly the same lower bound value, whereas *A* has a much higher upper bound. For the DMs, *S* might be more appropriate than *A* if the small difference 0.01 can be considered negligible. *S* and *A* both contain *B*: the DMs may choose *B* as the result of minimax robust optimization, whereas if they pay more attention to the lower bound, *A* can be the choice.

9.2.1.5 Reliability assessment under degradation dependency and random shocks

According to the experts of EDF, random shocks like water hammers and internal thermal shocks [31] can worsen the degradation condition of both components of the subsystem considered or even immediately lead them to failures.

Random shocks can deteriorate the pump from its current state i to a degraded state j, as $p_{ij} = \frac{9\times(0.1)^{(i-j+1)}}{1-(0.1)^{(i+1)}}, i \geq j$, where p_{i0} denotes the probability of an extreme random shock leading the pump from state i directly to failure state 0. The formulation is taken from Yang *et al.*'s work [44], which satisfies that $\sum_{j=i}^{0} p_{ij} = 1$. By combining the degradation process of the pump with the random shock process, the resulting process takes the form shown in Fig. 9-15. The state of the process is represented by $Y(t) = \big(Y_p(t), m\big), m \in \mathbb{N}$, where m is the number of shocks experienced by the pump. The state space of the new process is denoted by $\boldsymbol{S} = \{(a, b), \forall a \in \boldsymbol{S_p}, b \in \mathbb{N}\}$ and the set of failure states of the pump is $\boldsymbol{\mathcal{F}_p'} = \{(0, b), \forall b \in \mathbb{N}\}$.

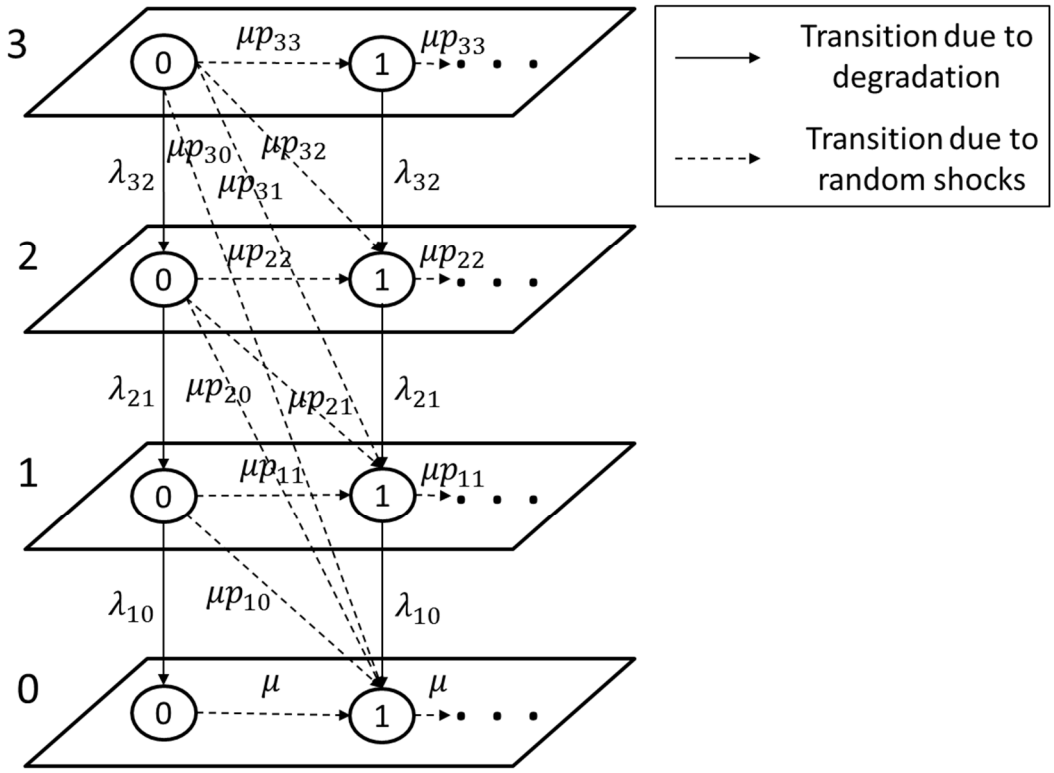

Fig. 9-15. Degradation and random shock processes of the pump.

For the valve, the i-th shock becomes extreme if the shock load W_i exceeds the maximal material strength D, otherwise, it can bring an instantaneous random increase H_i to the total external leak size [40]. W_i and H_i are assumed to be i.i.d. random variables following folded normal distributions, $W_i = |a|$ and $H_i = |b|$, where $a \sim N(\mu_h, \sigma_h^2)$ and $b \sim N(\mu_w, \sigma_w^2)$.

An illustration of the composite degradation process of the valve considering random shocks and the degradation state of the pump is shown in Fig. 9-16, where the system experienced a random shock at time t_i, with the shock load W_i, $i = 1,3,4$. The first two shocks cause instantaneous random increases on $D(t)$, the last shock lead the valve to failure. The vibration of the pump accelerates the degradation process of the valve at time t_2 and t_3, when the pump stepped to a further degraded state.

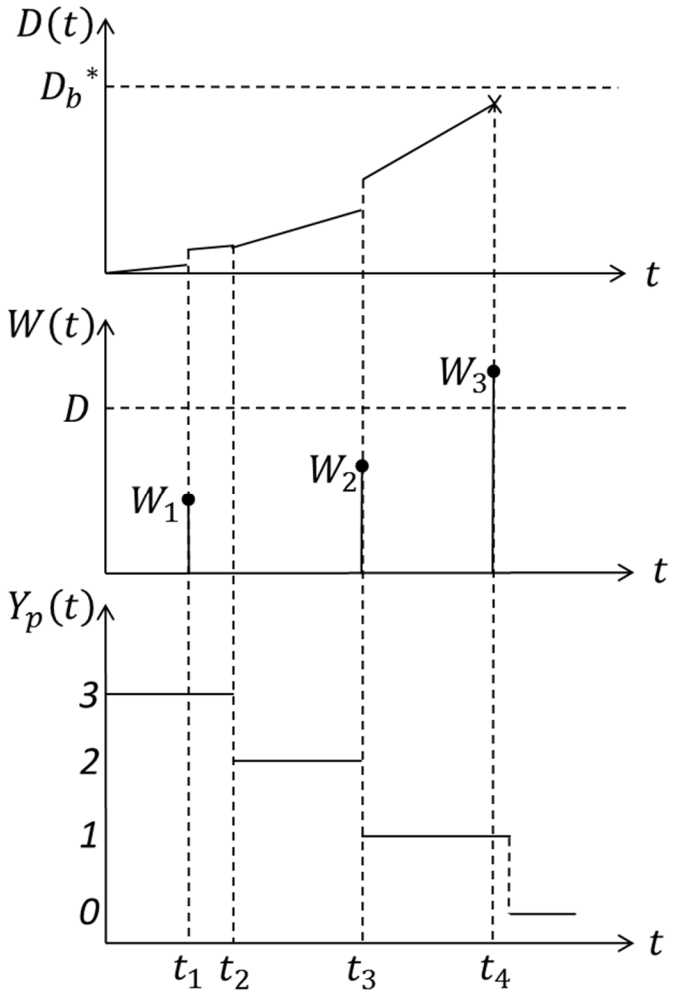

Fig. 9-16. An illustration of the degradation of the valve considering random shocks and the degradation state of the pump. (Top Figure: degradation process of the valve; Center Figure: random shock processes; Bottom Figure: degradation process of the pump.)

The reliability values of the valve, the pump and the system with/without random shocks, obtained by MC3, are shown in Fig. 9-17. The numerical comparisons on the reliability of the system, the valve and the pump with/without random shocks at the final time of 1000 s are presented in Table 9-3.

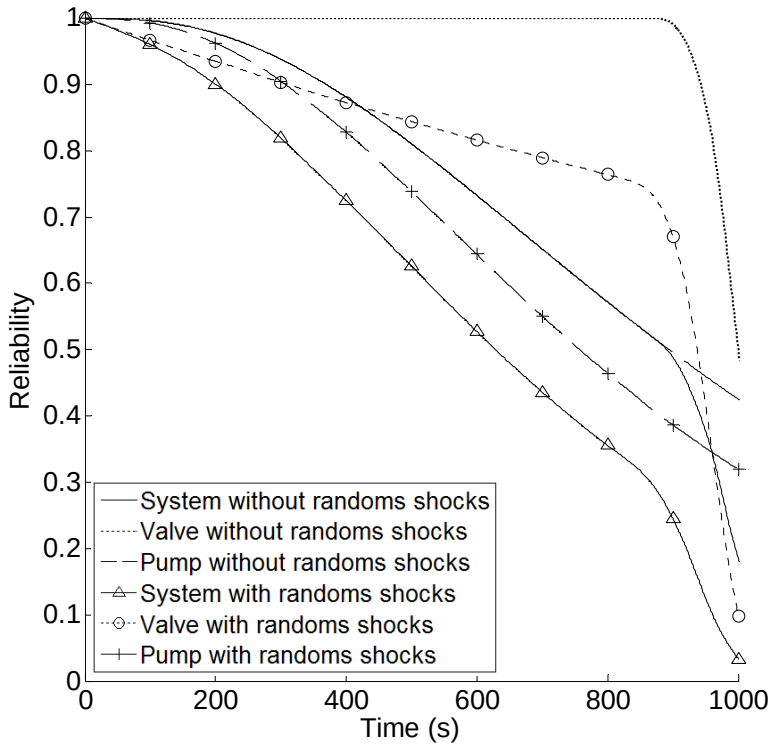

Fig. 9-17. The reliability of the system, the valve and the pump with/without random shocks.

When random shocks are ignored, the system reliability is basically determined by the pump before around 870 s, since the valve is highly reliable. After that, the sharp decrease of the valve reliability due to degradation leads to the same behavior in the system reliability. When random shocks are considered, the system reliability is determined by both the pump reliability and the valve reliability from the beginning until around 850 s, since the valve is no longer as highly reliable as before. Then, the valve reliability decreases sharply due to the joint effects of random shocks and degradation, and this drives also the sharp decrease of the system reliability. We can see from the results that neglecting random shocks can result in an underestimation of the reliability of the system and of the components.

Table 9-3 Comparison of reliability with/without random shocks at 1000 s.

	Reliability without	Reliability with	Relative

	random shocks	random shocks	change
System	0.18	0.033	81.67%
Valve	0.50	0.099	80.20%
Pump	0.43	0.32	25.58%

9.3 Multi-component systems (with a large number of components)

9.3.1 Reliability assessment of one branch of the residual heat removal system

In this Section, we illustrate the reliability assessment method for multi-component systems (with a large number of components) with degradation dependency, proposed in Chapter 2, on a illustrative case refers to one branch of the RHRS [146] of a nuclear power plant shown in Fig. 9-18. The fault tree is shown in Fig. 9-19.

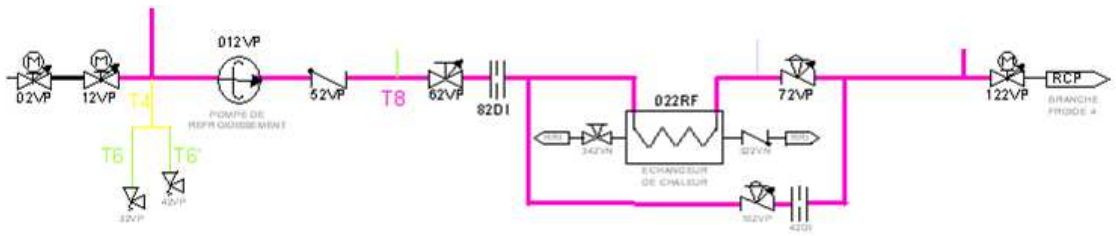

Fig. 9-18. The diagram of one branch of the RHRS.

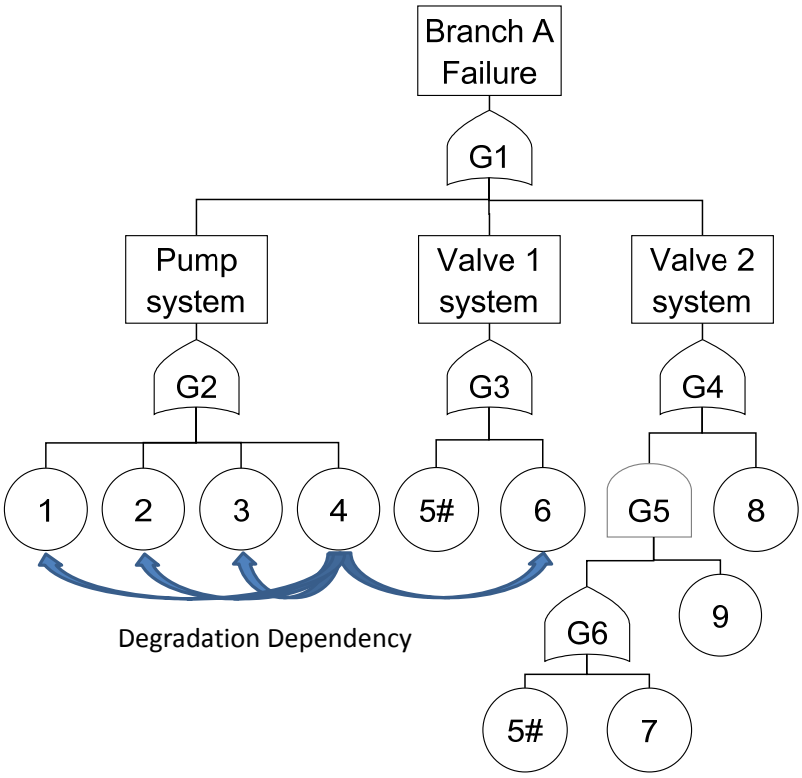

Fig. 9-19. The fault tree of one branch of the RHRS.

By knowledge and experience of the field experts, the degradation dependency is described as follows: the degradation of the pump can lead it to vibrate [142], which will, in turn, cause the vibration of the other neighboring components (e.g. the valve) and therefore aggravate the degradation process of the latters [143]. The dependency exists between basic events 1,2,3,4 and 6, as indicated in Fig. 9-19.

Applying the WDFLM ordering heuristic [136], the variable ordering obtained is $X_{5\#} < X_6 < X_1 < X_2 < X_3 < X_4 < X_8 < X_9 < X_7$. The corresponding BDD is shown in Fig. 9-20. There are two paths leading to system operation: (1) $X_{5\#} = 0, X_6 = 0, X_1 = 0, X_2 = 0, X_3 = 0, X_4 = 0, X_8 = 0, X_9 = 0$ and (2) $X_{5\#} = 0, X_6 = 0, X_1 = 0, X_2 = 0, X_3 = 0, X_4 = 0, X_8 = 0, X_9 = 1, X_7 = 0$.

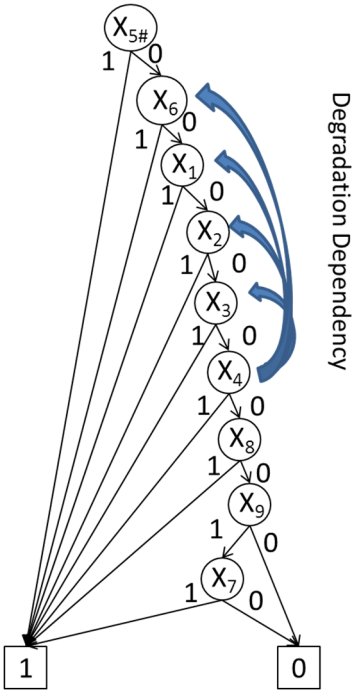

Fig. 9-20. The BDD corresponding to the fault tree shown in Fig. 9-19.

The degradation processes are divided into five groups: $\{K_6\}, \{L_2\}, \{K_7\}, \{K_8\}$ and $\{K_1, K_2, K_3, K_4, K_5, L_1\}$. Each of the first four groups has only one degradation model. The last group is modeled by one PDMP.

MCS over a time horizon of 8 years has been run 10^6 times to solve the PDMPs and, then, estimate the probability of occurrence of each path. The estimated system reliability with and without dependency throughout the time horizon, under accelerated conditions, is shown in Fig. 9-21. The average computation time is 34.3 s. We can see from the Figure that neglecting dependency can lead to overestimation of the system reliability. The system reliability with dependency has experienced one rapid decrease after around 6.2 year (point A), which is due to the valve failure in some simulation trials caused by the vibration of the pump. This sharp decrease in system reliability relates to the sharp increase in the system failure time density function, as shown in Fig. 9-22.

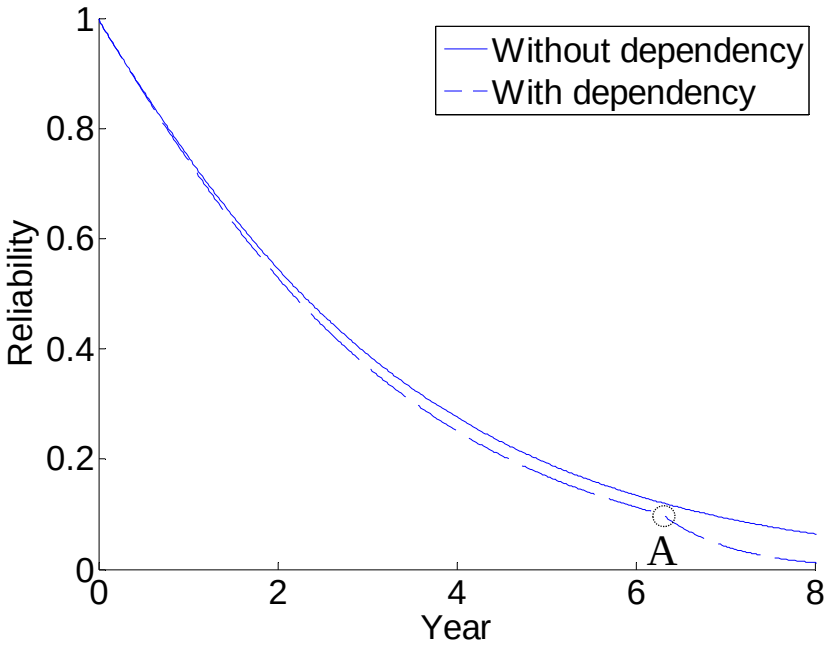

Fig. 9-21. The estimated system reliability with/without dependency.

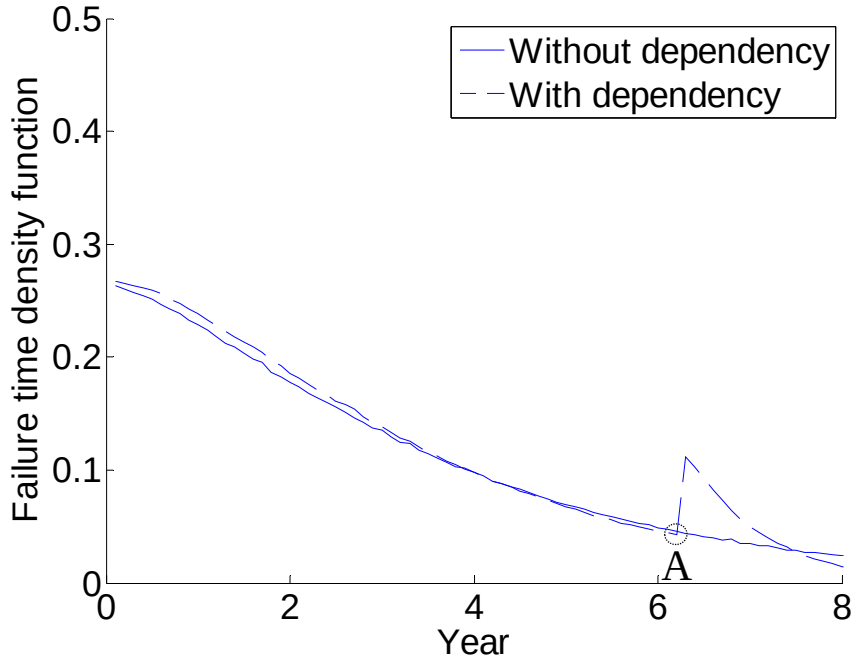

Fig. 9-22. The system failure time density function with/without dependency.

10. CONCLUSIONS

This dissertation aims to develop a holistic framework of models and computational methods for the reliability analysis and maintenance optimization of nuclear safety components and systems, taking into account the available knowledge on the system functionalities, degradation and failure behaviors, their dependencies, the external influencing factors and the associated uncertainties.

10.1 Original contributions

The original contributions of the PhD work are:

- For single components:

  Firstly, the MSPM framework is extended to semi-Markov modeling to describe the fact that the time of transition to a state can depend on the residence time in the current state; this makes the framework more suitable to considering maintenance. Then, a general random shock model is proposed, where the probability of a random shock resulting in extreme or cumulative damage, and the cumulative damages, are both s-dependent on the current component degradation condition (the component degradation state and residence time in that state). Finally, the random shock model is integrated into the MSPM framework to describe the influence of the shocks on the degradation processes. The results show that the proposed model is able to characterize the influences of different types of random shocks onto the component state probabilities and the reliability estimates.

- For multi-component systems (with a limited number of components):

  a. A PDMP modeling framework is proposed to model multiple dependent competing degradation processes. The significance of the proposed method lies in its capability to describe the degradation dependency between PBMs, between MSMs and between the two types of models.

  b. Epistemic uncertainty due to the incomplete or imprecise knowledge about the degradation processes is included in the PDMP modeling framework by describing the model parameters as fuzzy numbers and the FV method is extended to calculate the system (fuzzy) reliability. The results show that the FV method can lead to comparable results as MC simulation, but with reduced

computation time.

c. MAD IM is extended to provide timely feedback on the criticality of a component in the PDMP modeling framework. The extended IM can effectively estimate the criticality of different components subject to multiple dependent discrete and continuous degradation processes, condition-based PM via periodic inspections and CM.

d. The Pareto optimal maintenance policies considering epistemic uncertainty and degradation dependency are derived by combining NSDE, DE and FV. Epistemic uncertainty in the parameters of the model is taken into account by interval values, this leads to the formulation of a multi-objective optimization problem whose objectives are the lower and upper bounds of the expected maintenance cost. Given the Pareto front, the DMs can eventually choose the maintenance policy according to their preferences.

e. The PDMP modeling framework of (a) is extended for system reliability assessment, by considering the impacts of random shocks. The impacts of random shocks on the PBMs and MSMs at the same time can be characterized in different ways, due to the different nature of two types of degradation models. The dependencies between degradation processes and random shocks, and among degradation processes are addressed.

- For multi-component systems (with a large number of components):

  A computational method combining BDDs and MCS is developed for the reliability assessment of systems with degradation dependency, to reduce computational costs. Firstly, a fault tree is transformed to a BDD from which all paths leading to the system failure or operation can be efficiently obtained. Secondly, MCS is used to estimate the probability of each path to compute the system reliability taking into account the dependencies between basic events. The results show that instead of modeling the degradation of the whole system by one PDMP, the proposed method can identify the groups of components being dependent and decompose the original PDMP into a group of smaller ones, which are independent from each other and easier to be solved. Besides, the states of these PDMPs leading to system failure can be easily obtained.

10.2 Future research

Further developments can be sought in the following directions:

- For single components: the extended MSPM framework considers only one type of random shock models. The other types of random shock models can be studied, such as (a) run shock models, where failure of one component occurs when there is a run of k shocks exceeding a critical magnitude and (b) δ-shock models, where failure of one component occurs when the time lag between two successive shocks is shorter than a threshold δ [21].
- For multi-component systems (with a limited number of components): firstly, only the influence of epistemic (subjective) uncertainty to PDMP system degradation models is investigated. The aleatory uncertainty associated with the parameters, such as the friction coefficients in physics equations of PBMs, in the PDMP system degradation models have to be studied. Additionally, the uncertain parameters in PDMP system degradation models can also influence the proposed component IMs. Global Sensitivity Analysis (GSA) has been employed to produce indices that assess the importance of the uncertain factors in the models, taking into account interactions among them [147]. It would be interesting to study how the sensitivity indices of the parameters of a component relate to the importance indices of that component, within a GSA framework. Moreover, the limitations of the proposed optimization method lie in the computational burden and the memory requirements, when applied to high-dimensional problems, due to the FV method which discretizes the state space of the continuous variables of PDMP. The computational expenses and memory requirement of the FV method increase almost linearly as the number of meshes partitioning the state space increases, which is a choice of the analysts. For high-dimensional problems, the optimal number of meshes has to be found to compromise the computational burden. Besides, sparse matrices can be employed to reduce the amount of memory required. Finally, the proposed PDMP models for systems subject to degradation dependency and random shocks consider only constant thresholds of shock loads, for shocks becoming extreme. In some cases, the components are deteriorating when withstanding shocks, and their resistance to failure is weakening [21]. In this case, they become more sensitive to shock loads. The changes in thresholds for shock loads have to be considered in the models.
- For multi-component systems (with a large number of components): the proposed

system reliability assessment methods are solved by MC simulation, which is relatively time consuming. MC simulation acceleration techniques need to be developed to improve computation efficiency, thus, enabling to extend the applications to systems of larger sizes.

REFERENCES

[1] G. Yang, "Environmental-stress-screening using degradation measurements," *Reliability, IEEE Transactions on,* vol. 51, no. 3, pp. 288-293, 2002.

[2] Z.-S. Ye and M. Xie, "Stochastic modelling and analysis of degradation for highly reliable products," *Applied Stochastic Models in Business and Industry,* vol. 31, no. 1, pp. 16-32, 20145.

[3] N. Gebraeel, A. Elwany, and J. Pan, "Residual life predictions in the absence of prior degradation knowledge," *Reliability, IEEE Transactions on,* vol. 58, no. 1, pp. 106-117, 2009.

[4] C. J. Lu and W. O. Meeker, "Using degradation measures to estimate a time-to-failure distribution," *Technometrics,* vol. 35, no. 2, pp. 161-174, 1993.

[5] J. Lawless and M. Crowder, "Covariates and random effects in a gamma process model with application to degradation and failure," *Lifetime Data Analysis,* vol. 10, no. 3, pp. 213-227, 2004.

[6] N. Chen, Z.-S. Ye, Y. Xiang, and L. Zhang, "Condition-based maintenance using the inverse Gaussian degradation model," *European Journal of Operational Research,* vol. 243, no. 1, pp. 190-199, 2015.

[7] M. Chookah, M. Nuhi, and M. Modarres, "A probabilistic physics-of-failure model for prognostic health management of structures subject to pitting and corrosion-fatigue," *Reliability Engineering & System Safety,* vol. 96, no. 12, pp. 1601-1610.

[8] M. Black, A. Brint, and J. Brailsford, "A semi-Markov approach for modelling asset deterioration," *Journal of the Operational Research Society,* vol. 56, no. 11, pp. 1241-1249, 2005.

[9] J.-C. Lu, J. Park, and Q. Yang, "Statistical inference of a time-to-failure distribution derived from linear degradation data," *Technometrics,* vol. 39, no. 4, pp. 391-400, 1997.

[10] K. Yang and G. Yang, "Degradation reliability assessment using severe critical values," *International Journal of Reliability, Quality and Safety Engineering,* vol. 5, no. 01, pp. 85-95, 1998.

[11] G. Whitmore, "Estimating degradation by a Wiener diffusion process subject to measurement error," *Lifetime Data Analysis,* vol. 1, no. 3, pp. 307-319, 1995.

[12] M. Daigle and K. Goebel, "A model-based prognostics approach applied to pneumatic valves," *International journal of prognostics and health management,* vol. 2, no. 2, p. 008, 2011.

[13] S. Reggiani, S. Poli, M. Denison, E. Gnani, A. Gnudi, G. Baccarani, S. Pendharkar, and R. Wise, "Physics-Based Analytical Model for HCS Degradation in STI-LDMOS Transistors," *Electron Devices, IEEE Transactions on,* vol. 58, no. 9, pp. 3072-3080, 2011.

[14] E. Keedy and Q. Feng, "A physics-of-failure based reliability and maintenance modeling framework for stent deployment and operation," *Reliability Engineering & System Safety,* vol. 103, no. pp. 94-101, 2012.

[15] R. Moghaddass and M. J. Zuo, "Multistate degradation and supervised estimation methods for a condition-monitored device," *IIE Transactions,* vol. 46, no. 2, pp. 131-148, 2014.

[16] A. Lisnianski and G. Levitin, *Multi-state system reliability: assessment, optimization and applications*: World scientific, 2003.

[17] W. Li and H. Pham, "Reliability modeling of multi-state degraded systems with multi-competing failures and random shocks," *Reliability, IEEE Transactions on,* vol. 54, no. 2, pp. 297-303, 2005.

[18] M. Giorgio, M. Guida, and G. Pulcini, "An age-and state-dependent Markov model for degradation processes," *IIE Transactions,* vol. 43, no. 9, pp. 621-632, 2011.

[19] S. D. Unwin, P. P. Lowry, R. F. Layton, P. G. Heasler, and M. B. Toloczko, "Multi-state physics models of aging passive components in probabilistic risk assessment," in *International Topical Meeting on Probabilistic Safety Assessment and Analysis (PSA 2011).* vol. 1 Wilmington, North Carolina, 2011, pp. 161-172.

[20] Y. Wang and H. Pham, "Modeling the dependent competing risks with multiple degradation processes and random shock using time-varying copulas," *Reliability, IEEE Transactions on,* vol. 61, no. 1, pp. 13-22, 2012.

[21] L. Jiang, Q. Feng, and D. W. Coit, "Reliability and maintenance modeling for dependent competing failure processes with shifting failure thresholds," *Reliability, IEEE Transactions on,* vol. 61, no. 4, pp. 932-948, 2012.

[22] N. Rasmekomen and A. K. Parlikad, "Maintenance Optimization for Asset Systems With Dependent Performance Degradation," *Reliability, IEEE Transactions on,* vol. 62, no. 2, pp. 362-367, 2013.

[23] L. Xing, C. Wang, and G. Levitin, "Competing failure analysis in non-repairable binary systems subject to functional dependence," *Proceedings of the Institution of Mechanical Engineers, Part O: Journal of Risk and Reliability,* vol. 226, no. 4, pp. 406-416, 2012.

[24] C. Wang, L. Xing, and G. Levitin, "Competing failure analysis in phased-mission systems with functional dependence in one of phases," *Reliability Engineering & System Safety,* vol. 108, no. pp. 90-99, 2012.

[25] L. Xing and G. Levitin, "Combinatorial analysis of systems with competing failures subject to failure isolation and propagation effects," *Reliability Engineering & System Safety,* vol. 95, no. 11, pp. 1210-1215, 2010.

[26] C. Wang, L. Xing, and G. Levitin, "Reliability analysis of multi-trigger binary systems subject to competing failures," *Reliability Engineering & System Safety,* vol. 111, no. pp. 9-17, 2013.

[27] H. Peng, Q. Feng, and D. W. Coit, "Reliability and maintenance modeling for systems subject to multiple dependent competing failure processes," *IIE transactions*, vol. 43, no. 1, pp. 12-22, 2010.
[28] D. Straub, "Stochastic modeling of deterioration processes through dynamic Bayesian networks," *Journal of Engineering Mechanics*, vol. 135, no. 10, pp. 1089-1099, 2009.
[29] Z. Wang, H.-Z. Huang, Y. Li, and N.-C. Xiao, "An approach to reliability assessment under degradation and shock process," *Reliability, IEEE Transactions on*, vol. 60, no. 4, pp. 852-863, 2011.
[30] B. Lydell, "Pipe failure probability—the Thomas paper revisited," *Reliability Engineering & System Safety*, vol. 68, no. 3, pp. 207-217, 2000.
[31] J. Salonen, P. Auerkari, O. Lehtinen, and M. Pihkakoski, "Experience on in-service damage in power plant components," *Engineering Failure Analysis*, vol. 14, no. 6, pp. 970-977, 2007.
[32] J.-M. Bai, Z.-H. Li, and X.-B. Kong, "Generalized shock models based on a cluster point process," *Reliability, IEEE Transactions on*, vol. 55, no. 3, pp. 542-550, 2006.
[33] K. K. Anderson, "Limit theorems for general shock models with infinite mean intershock times," *Journal of applied probability*, no. pp. 449-456, 1987.
[34] G. Agrafiotis and M. Tsoukalas, "On excess-time correlated cumulative processes," *Journal of the Operational Research Society*, no. pp. 1269-1280, 1995.
[35] J. Esary and A. Marshall, "Shock models and wear processes," *The annals of probability*, no. pp. 627-649, 1973.
[36] G.-A. Klutke and Y. Yang, "The availability of inspected systems subject to shocks and graceful degradation," *Reliability, IEEE Transactions on*, vol. 51, no. 3, pp. 371-374, 2002.
[37] M. Wortman, G.-A. Klutke, and H. Ayhan, "A maintenance strategy for systems subjected to deterioration governed by random shocks," *Reliability, IEEE Transactions on*, vol. 43, no. 3, pp. 439-445, 1994.
[38] Z. S. Ye, L. C. Tang, and H. Y. Xu, "A distribution-based systems reliability model under extreme shocks and natural degradation," *Reliability, IEEE Transactions on*, vol. 60, no. 1, pp. 246-256, 2011.
[39] J. Fan, S. Ghurye, and R. A. Levine, "Multicomponent lifetime distributions in the presence of ageing," *Journal of applied probability*, vol. 37, no. 2, pp. 521-533, 2000.
[40] S. Song, D. W. Coit, Q. Feng, and H. Peng, "Reliability analysis for multi-component systems subject to multiple dependent competing failure processes," *Reliability, IEEE Transactions on*, vol. 63, no. 1, pp. 331-345, 2014.
[41] G. Becker, L. Camarinopoulos, and D. Kabranis, "Dynamic reliability under random shocks," *Reliability Engineering & System Safety*, vol. 77, no. 3, pp. 239-251, 2002.
[42] K. Rafiee, Q. Feng, and D. W. Coit, "Reliability modeling for dependent competing failure processes with changing degradation rate," *IIE Transactions*, vol. 46, no. 5, pp. 483-496, 2014.
[43] S. Song, D. W. Coit, and Q. Feng, "Reliability for systems of degrading components with distinct component shock sets," *Reliability Engineering & System Safety*, vol. 132, no. pp. 115-124, 2014.
[44] W. S. Yang, D. E. Lim, and K. C. Chae, "Maintenance of multi-state production systems deteriorated by random shocks and production," *Journal of Systems Science and Systems Engineering*, vol. 20, no. 1, pp. 110-118, 2011.
[45] G. Susto, A. Schirru, S. Pampuri, S. McLoone, and A. Beghi, "Machine Learning for Predictive Maintenance: a Multiple Classifiers Approach," *Industrial Informatics, IEEE Transactions on*, no. 2015.
[46] S. Albin and S. Chao, "Preventive replacement in systems with dependent components," *Reliability, IEEE Transactions on*, vol. 41, no. 2, pp. 230-238, 1992.
[47] R. P. Nicolai and R. Dekker, *Optimal maintenance of multi-component systems: a review*: Springer, 2008.
[48] L. Thomas, "A survey of maintenance and replacement models for maintainability and reliability of multi-item systems," *Reliability Engineering*, vol. 16, no. 4, pp. 297-309, 1986.
[49] B. Castanier, A. Grall, and C. Bérenguer, "A condition-based maintenance policy with non-periodic inspections for a two-unit series system," *Reliability Engineering & System Safety*, vol. 87, no. 1, pp. 109-120, 2005.
[50] G. van Dijkhuizen, "Maintenance grouping in multi-step multi-component production systems," in *Maintenance, Modeling and Optimization*: Springer, 2000, pp. 283-306.
[51] R. Dekker, R. P. PLASMEIJER, and J. H. SWART, "Evaluation of a new maintenance concept for the preservation of highways," *IMA Journal of Management Mathematics*, vol. 9, no. 2, pp. 109-156, 1998.
[52] D. Murthy and D. Nguyen, "Study of a multi-component system with failure interaction," *European Journal of Operational Research*, vol. 21, no. 3, pp. 330-338, 1985.
[53] M.-T. Lai and Y.-C. Chen, "Optimal periodic replacement policy for a two-unit system with failure rate interaction," *The international journal of advanced manufacturing technology*, vol. 29, no. 3-4, pp. 367-371, 2006.
[54] R. I. Zequeira and C. Bérenguer, "On the inspection policy of a two-component parallel system with failure interaction," *Reliability Engineering & System Safety*, vol. 88, no. 1, pp. 99-107, 2005.
[55] A. Barros, C. Berenguer, and A. Grall, "A maintenance policy for two-unit parallel systems based on

imperfect monitoring information," *Reliability Engineering & System Safety,* vol. 91, no. 2, pp. 131-136, 2006.
[56] S. Özekici, "Optimal periodic replacement of multicomponent reliability systems," *Operations Research,* vol. 36, no. 4, pp. 542-552, 1988.
[57] Q. Yang, N. Zhang, and Y. Hong, "Reliability analysis of repairable systems with dependent component failures under partially perfect repair," *Reliability, IEEE Transactions on,* vol. 62, no. 2, pp. 490-498, 2013.
[58] H. Hong, W. Zhou, S. Zhang, and W. Ye, "Optimal condition-based maintenance decisions for systems with dependent stochastic degradation of components," *Reliability Engineering & System Safety,* vol. 121, no. pp. 276-288, 2014.
[59] A. Van Horenbeek and L. Pintelon, "A dynamic predictive maintenance policy for complex multi-component systems," *Reliability Engineering & System Safety,* vol. 120, no. pp. 39-50, 2013.
[60] Y.-F. Li, G. Sansavini, and E. Zio, "Non-dominated sorting binary differential evolution for the multi-objective optimization of cascading failures protection in complex networks," *Reliability Engineering & System Safety,* vol. 111, no. pp. 195-205, 2013.
[61] R. Storn and K. Price, "Differential evolution–a simple and efficient heuristic for global optimization over continuous spaces," *Journal of global optimization,* vol. 11, no. 4, pp. 341-359, 1997.
[62] C. Cocozza-Thivent, R. Eymard, and S. Mercier, "A finite-volume scheme for dynamic reliability models," *IMA journal of numerical analysis,* vol. 26, no. 3, pp. 446-471, 2006.
[63] K. N. Fleming, S. D. Unwin, D. Kelly, P. P. Lowry, M. B. Toloczko, R. F. Layton, R. Youngblood, D. Collins, A. V. Huzurbazar, and B. Williams, "Treatment of Passive Component Reliability in Risk-Informed Safety Margin Characterization," 2010.
[64] T. Nakagawa, *Shock and damage models in reliability theory*: Springer, 2007.
[65] Z. Schuss, *Theory and applications of stochastic processes: an analytical approach* vol. 170: Springer Science & Business Media, 2009.
[66] A. V. Huzurbazar and B. Williams, "Flowgraph models for complex multistate system reliability," *Modern statistical and mathematical methods in reliability,* vol. 10, no. pp. 247-262, 2005.
[67] E. E. Kostandyan and J. D. Sørensen, "Physics of failure as a basis for solder elements reliability assessment in wind turbines," *Reliability Engineering & System Safety,* no. 2012.
[68] D. T. Gillespie, "Monte Carlo simulation of random walks with residence time dependent transition probability rates," *Journal of Computational Physics,* vol. 28, no. 3, pp. 395-407, 1978.
[69] E. Rachelson, G. Quesnel, F. Garcia, and P. Fabiani, "A simulation-based approach for solving generalized semi-markov decision processes," in *European Conference on Artificial Intelligence*, 2008.
[70] H. A. Chan and P. J. Englert, *Accelerated stress testing handbook: Guide for achieving quality products*: Wiley-IEEE Press, 2001.
[71] E. Lewis and F. Böhm, "Monte Carlo simulation of Markov unreliability models," *Nuclear Engineering and Design,* vol. 77, no. 1, pp. 49-62, 1984.
[72] A. Lorton, M. Fouladirad, and A. Grall, "A methodology for probabilistic model-based prognosis," *European Journal of Operational Research,* vol. 225, no. 3, pp. 443-454, 2013.
[73] M. Daigle and K. Goebel, "Multiple damage progression paths in model-based prognostics," in *Aerospace Conference, 2011 IEEE*, 2011, pp. 1-10.
[74] D. Zwillinger, *Handbook of differential equations*: Gulf Professional Publishing, 1998.
[75] Y.-H. Lin, Y. Li, and E. Zio, "Dynamic Reliability Models for Multiple Dependent Competing Degradation Processes," in *ESREL 2014*.
[76] C. Cocozza-Thivent, "Processus de renouvellement markovien, Processus de Markov déterministes par morceaux," *Online book available on the webpage: http://perso-math. univ-mlv. fr/users/cocozza. christiane/recherche-pageperso/PresentationRMetPDMP. html,* no. 2011.
[77] W.-S. Lee, D. L. Grosh, F. A. Tillman, and C. H. Lie, "Fault Tree Analysis, Methods, and Applications ß A Review," *Reliability, IEEE Transactions on,* vol. 34, no. 3, pp. 194-203, 1985.
[78] M. Marseguerra and E. Zio, "Monte Carlo approach to PSA for dynamic process systems," *Reliability Engineering & System Safety,* vol. 52, no. 3, pp. 227-241, 1996.
[79] M. Laviolette and J. W. Seaman Jr, "The efficacy of fuzzy representations of uncertainty," *Fuzzy Systems, IEEE Transactions on,* vol. 2, no. 1, pp. 4-15, 1994.
[80] Y. Ding, M. J. Zuo, A. Lisnianski, and Z. Tian, "Fuzzy multi-state systems: general definitions, and performance assessment," *Reliability, IEEE Transactions on,* vol. 57, no. 4, pp. 589-594, 2008.
[81] Y. Liu, W. Tang, and R. Zhao, "Reliability and mean time to failure of unrepairable systems with fuzzy random lifetimes," *Fuzzy Systems, IEEE Transactions on,* vol. 15, no. 5, pp. 1009-1026, 2007.
[82] M. Bazu, "A combined fuzzy-logic and physics-of-failure approach to reliability prediction," *Reliability, IEEE Transactions on,* vol. 44, no. 2, pp. 237-242, 1995.
[83] S. A. Sandri, D. Dubois, and H. W. Kalfsbeek, "Elicitation, assessment, and pooling of expert judgments using possibility theory," *Fuzzy Systems, IEEE Transactions on,* vol. 3, no. 3, pp. 313-335, 1995.
[84] Y. Liu, H. Huang, and G. Levitin, "Reliability and performance assessment for fuzzy multi-state elements,"

Proceedings of the Institution of Mechanical Engineers, Part O: Journal of Risk and Reliability, vol. 222, no. 4, pp. 675-686, 2008.
[85] Y. Li, E. Zio, and Y.-H. Lin, "A Multistate Physics Model of Component Degradation Based on Stochastic Petri Nets and Simulation," *Reliability, IEEE Transactions on,* vol. 61, no. 4, pp. 921-931, 2012.
[86] H. Tanaka, L. Fan, F. Lai, and K. Toguchi, "Fault-tree analysis by fuzzy probability," *Reliability, IEEE Transactions on,* vol. 32, no. 5, pp. 453-457, 1983.
[87] D. Singer, "A fuzzy set approach to fault tree and reliability analysis," *Fuzzy sets and systems,* vol. 34, no. 2, pp. 145-155, 1990.
[88] J. Dunyak, I. W. Saad, and D. Wunsch, "A theory of independent fuzzy probability for system reliability," *Fuzzy Systems, IEEE Transactions on,* vol. 7, no. 3, pp. 286-294, 1999.
[89] Y. Ding and A. Lisnianski, "Fuzzy universal generating functions for multi-state system reliability assessment," *Fuzzy Sets and Systems,* vol. 159, no. 3, pp. 307-324, 2008.
[90] Y. F. Li, Y. Ding, and E. Zio, "Random Fuzzy Extension of the Universal Generating Function Approach for the Reliability Assessment of Multi-State Systems Under Aleatory and Epistemic Uncertainties," *Reliability, IEEE Transactions on,* vol. PP, no. 99, pp. 1-1, 2014.
[91] M. Sallak, W. Schön, and F. Aguirre, "Reliability assessment for multi-state systems under uncertainties based on the Dempster–Shafer theory," *IIE Transactions,* vol. 45, no. 9, pp. 995-1007, 2013/09/01 2012.
[92] L. A. Zadeh, "Fuzzy sets," *Information and control,* vol. 8, no. 3, pp. 338-353, 1965.
[93] L. A. Zadeh, "Fuzzy sets as a basis for a theory of possibility," *Fuzzy sets and systems,* vol. 100, no. pp. 9-34, 1999.
[94] P.-E. Labeau, "A Monte Carlo estimation of the marginal distributions in a problem of probabilistic dynamics," *Reliability Engineering & System Safety,* vol. 52, no. 1, pp. 65-75, 1996.
[95] R. Eymard and S. Mercier, "Comparison of numerical methods for the assessment of production availability of a hybrid system," *Reliability Engineering & System Safety,* vol. 93, no. 1, pp. 168-177, 2008.
[96] W. Kuo and X. Zhu, "Some recent advances on importance measures in reliability," *Reliability, IEEE Transactions on,* vol. 61, no. 2, pp. 344-360, 2012.
[97] H. Peng, D. W. Coit, and Q. Feng, "Component reliability criticality or importance measures for systems with degrading components," *Reliability, IEEE Transactions on,* vol. 61, no. 1, pp. 4-12, 2012.
[98] Z. W. Birnbaum, "On the importance of different components in a multicomponent system," *Multivariable analysis 2, New York: Academic Press,* no. pp. 581-592, 1969.
[99] W. Kuo and X. Zhu, "Relations and generalizations of importance measures in reliability," *Reliability, IEEE Transactions on,* vol. 61, no. 3, pp. 659-674, 2012.
[100] R. E. Barlow and F. Proschan, "Importance of system components and fault tree events," *Stochastic Processes and their Applications,* vol. 3, no. 2, pp. 153-173, 1975.
[101] D. Vasseur and M. Llory, "International survey on PSA figures of merit," *Reliability Engineering & System Safety,* vol. 66, no. 3, pp. 261-274, 1999.
[102] W. Kuo and X. Zhu, *Importance measures in reliability, risk, and optimization: principles and applications*: John Wiley & Sons, 2012.
[103] M. J. Armstrong, "Reliability-importance and dual failure-mode components," *Reliability, IEEE Transactions on,* vol. 46, no. 2, pp. 212-221, 1997.
[104] W. S. Griffith, "Multistate reliability models," *Journal of Applied Probability,* no. pp. 735-744, 1980.
[105] S. Wu and L.-Y. Chan, "Performance utility-analysis of multi-state systems," *Reliability, IEEE Transactions on,* vol. 52, no. 1, pp. 14-21, 2003.
[106] S. Si, H. Dui, X. Zhao, S. Zhang, and S. Sun, "Integrated importance measure of component states based on loss of system performance," *Reliability, IEEE Transactions on,* vol. 61, no. 1, pp. 192-202, 2012.
[107] S. Si, G. Levitin, H. Dui, and S. Sun, "Component state-based integrated importance measure for multi-state systems," *Reliability Engineering & System Safety,* vol. 116, no. pp. 75-83, 2013.
[108] H. Dui, S. Si, L. Cui, Z. Cai, and S. Sun, "Component Importance for Multi-State System Lifetimes With Renewal Functions," *Reliability, IEEE Transactions on,* vol. 63, no. 1, pp. 105-117, 2014.
[109] E. Zio and L. Podofillini, "Monte Carlo simulation analysis of the effects of different system performance levels on the importance of multi-state components," *Reliability Engineering & System Safety,* vol. 82, no. 1, pp. 63-73, 2003.
[110] G. Levitin, L. Podofillini, and E. Zio, "Generalised importance measures for multi-state elements based on performance level restrictions," *Reliability Engineering & System Safety,* vol. 82, no. 3, pp. 287-298, 2003.
[111]J. E. Ramirez-Marquez and D. W. Coit, "Composite importance measures for multi-state systems with multi-state components," *Reliability, IEEE Transactions on,* vol. 54, no. 3, pp. 517-529, 2005.
[112] N. Gebraeel, "Prognostics-Based Identification of the Top-Units in a Fleet," *Automation Science and Engineering, IEEE Transactions on,* vol. 7, no. 1, pp. 37-48, 2010.
[113] X. Liu, K. N. Al-Khalifa, E. A. Elsayed, D. W. Coit, and A. S. Hamouda, "Criticality measures for components with multi-dimensional degradation," *IIE Transactions,* no. just-accepted, 2013.

[114] S. Song, D. W. Coit, Q. Feng, and H. Peng, "Reliability Analysis for Multi-Component Systems Subject to Multiple Dependent Competing Failure Processes," no. 2014.
[115] S. Iyer, "The Barlow–Proschan importance and its generalizations with dependent components," *Stochastic processes and their applications*, vol. 42, no. 2, pp. 353-359, 1992.
[116] B. Natvig, "Measures of component importance in nonrepairable and repairable multistate strongly coherent systems," *Methodology and Computing in Applied Probability*, vol. 13, no. 3, pp. 523-547, 2011.
[117] H. R. Golmakani, "Optimal age-based inspection scheme for condition-based maintenance using A* search algorithm," *International Journal of Production Research*, vol. 50, no. 23, pp. 7068-7080, 2012.
[118] A. Usynin, J. W. Hines, and A. Urmanov, "Uncertain failure thresholds in cumulative damage models," in *Reliability and Maintainability Symposium, 2008. RAMS 2008. Annual*, 2008, pp. 334-340.
[119] Y. Liu, H.-Z. Huang, and G. Levitin, "Reliability and performance assessment for fuzzy multi-state elements," *Proceedings of the Institution of Mechanical Engineers, Part O: Journal of Risk and Reliability*, vol. 222, no. 4, pp. 675-686, 2008.
[120] Y.-F. Li, E. Zio, and Y.-H. Lin, "A Multistate Physics Model of Component Degradation Based on Stochastic Petri Nets and Simulation," *Reliability, IEEE Transactions on*, vol. 61, no. 4, pp. 921-931, 2012.
[121] P.-T. Chang, "Fuzzy strategic replacement analysis," *European Journal of Operational Research*, vol. 160, no. 2, pp. 532-559, 2005.
[122] O. Linda and M. Manic, "Uncertainty-robust design of interval type-2 fuzzy logic controller for delta parallel robot," *Industrial Informatics, IEEE Transactions on*, vol. 7, no. 4, pp. 661-670, 2011.
[123] Z. Chaoyue, W. Jianhui, J. P. Watson, and G. Yongpei, "Multi-Stage Robust Unit Commitment Considering Wind and Demand Response Uncertainties," *Power Systems, IEEE Transactions on*, vol. 28, no. 3, pp. 2708-2717, 2013.
[124] H. Ishibuchi and H. Tanaka, "Multiobjective programming in optimization of the interval objective function," *European Journal of Operational Research*, vol. 48, no. 2, pp. 219-225, 1990.
[125] D. Bertsimas and M. Sim, "The price of robustness," *Operations research*, vol. 52, no. 1, pp. 35-53, 2004.
[126] L. Jiang, Q. Feng, and D. W. Coit, "Modeling zoned shock effects on stochastic degradation in dependent failure processes," *IIE Transactions*, vol. 47, no. 5, pp. 460-470, 2015.
[127] Y.-H. Lin, Y.-F. Li, and E. Zio, "Integrating Random Shocks Into Multi-State Physics Models of Degradation Processes for Component Reliability Assessment," *Reliability, IEEE Transactions on*, vol. 64, no. 1, pp. 154-166, 2015.
[128] C. Cocozza-Thivent, "Processus de renouvellement markovien, Processus de Markov déterministes par morceaux," *Online book available on the webpage: http://perso-math.univ-mlv.fr/users/cocozza.christiane/recherche-page-perso/PresentationRMetPDMP.html*, no.
[129] M. H. Davis, *Markov Models & Optimization* vol. 49: CRC Press, 1993.
[130] A. Lisnianski, I. Frenkel, and Y. Ding, "Statistical Analysis of Reliability Data for Multi-state Systems," *Multi-state System Reliability Analysis and Optimization for Engineers and Industrial Managers*, no. pp. 117-142, 2010.
[131] E. Ogurtsova, "Estimating transition rates for multistate models from panel data and repeated cross-sections," *University of Groningen*, no. 2014.
[132] W.-S. Lee, D. L. Grosh, F. A. Tillman, and C. H. Lie, "Fault Tree Analysis, Methods, and Applications ✍ A Review," *Reliability, IEEE Transactions on*, vol. 34, no. 3, pp. 194-203, 1985.
[133] R. M. Sinnamon and J. Andrews, "New approaches to evaluating fault trees," *Reliability Engineering & System Safety*, vol. 58, no. 2, pp. 89-96, 1997.
[134] B. Bollig and I. Wegener, "Improving the variable ordering of OBDDs is NP-complete," *Computers, IEEE Transactions on*, vol. 45, no. 9, pp. 993-1002, 1996.
[135] S. J. Friedman and K. J. Supowit, "Finding the optimal variable ordering for binary decision diagrams," in *Proceedings of the 24th ACM/IEEE Design Automation Conference*, 1987, pp. 348-356.
[136] S.-i. Minato, N. Ishiura, and S. Yajima, "Shared binary decision diagram with attributed edges for efficient Boolean function manipulation," in *Design Automation Conference, 1990. Proceedings., 27th ACM/IEEE*, 1990, pp. 52-57.
[137] M. Bouissou, F. Bruyere, and A. Rauzy, "BDD based fault-tree processing: A comparison of variable ordering heuristics," in *Proceedings of European Safety and Reliability Association Conference, ESREL'97*, 1997.
[138] Y. Mo, F. Zhong, H. Liu, Q. Yang, and G. Cui, "Efficient Ordering Heuristics in Binary Decision Diagram–based Fault Tree Analysis," *Quality and Reliability Engineering International*, vol. 29, no. 3, pp. 307-315, 2013.
[139] R. Tarjan, "Depth-first search and linear graph algorithms," *SIAM journal on computing*, vol. 1, no. 2, pp. 146-160, 1972.
[140] K. S. Brace, R. L. Rudell, and R. E. Bryant, "Efficient implementation of a BDD package," in

Proceedings of the 27th ACM/IEEE design automation conference, 1991, pp. 40-45.
[141] N. Limnios, *Fault trees* vol. 675: John Wiley & Sons, 2010.
[142] S. Zhang, M. Hodkiewicz, L. Ma, and J. Mathew, "Machinery condition prognosis using multivariate analysis," in *Engineering asset management*: Springer, 2006, pp. 847-854.
[143] P. Moussou, S. Cambier, D. Lachene, S. Longarini, L. Paulhiac, and V. Villouvier, "Vibration investigation of a French PWR power plant piping system caused by cavitating butterfly valves," *ASME-PUBLICATIONS-PVP*, vol. 420, no. pp. 99-106, 2001.
[144] M. Sallak, C. Simon, and J.-F. Aubry, "A fuzzy probabilistic approach for determining safety integrity level," *Fuzzy Systems, IEEE Transactions on*, vol. 16, no. 1, pp. 239-248, 2008.
[145] A. D. Belegundu and T. R. Chandrupatla, *Optimization concepts and applications in engineering*: Cambridge University Press, 2011.
[146] R. Coudray and J. Mattei, "System reliability: An example of nuclear reactor system analysis," *Reliability Engineering*, vol. 7, no. 2, pp. 89-121, 1984.
[147] C. M. Rocco and E. Zio, "Global sensitivity analysis in a Multi-state Physics Model of Component Degradation based on a hybrid State-Space Enrichment and Polynomial Chaos Expansion approach," *Reliability, IEEE Transactions on*, vol. 62, no. 4, pp. 781-788.

APPENDED PAPERS

This part lists all the papers published or submitted to international journals.

PAPER I: Y.-H. Lin, Y.-F. Li, E. Zio. Integrating Random Shocks into Multi-State Physics Models of Degradation Processes for Component Reliability Assessment. *Reliability, IEEE Transactions on*, VOL.64, NO.1, PP.154-166, 2015.

Integrating Random Shocks into Multi-State Physics Models of Degradation Processes for Component Reliability Assessment

Yan-Hui Lin, Yan-Fu Li, *member IEEE*, Enrico Zio, *senior member IEEE*

Index Terms – Component Degradation, Random shocks, Multi-state physics model, Semi-Markov process, Monte Carlo simulation.

Abstract - We extend a multi-state physics model (MSPM) framework for component reliability assessment by including semi-Markov and random shock processes. Two mutually exclusive types of random shocks are considered: extreme and cumulative. The former leads the component to immediate failure, whereas the latter influences the component degradation rates. General dependences between the degradation and the two types of random shocks are considered. A Monte Carlo simulation algorithm is implemented to compute component state probabilities. An illustrative example is presented and a sensitivity analysis is conducted on the model parameters. The results show that our extended model is able to characterize the influences of different types of random shocks onto the component state probabilities and the reliability estimates.

Acronyms

MSPM	Multi-state physics model

Notations

$\boldsymbol{S}$	The states set of component degradation processes
τ_i	The residence time of component being in the state i since the last transition
$\boldsymbol{\theta}$	The external influencing factors
$\lambda_{i,j}(\tau_i, \boldsymbol{\theta})$	The transition rate between state *i* and state *j*
t	Time
$(t, t+\Delta t)$	Infinitesimal time interval
X_k	The state of the component after *k* transitions
T_k	The time of arrival at X_k of component
$P(t)$	The state probability vector
$p_i(t)$	The probability of component being in state *i* at time *t*
$R(t)$	The component reliability

$N(t)$	The number of random shocks occurred until time t
μ	The constant Arrival rate of random shocks
$\tau'_{i,m}$	The residence time of the component in the current degradation state *i* after *m* cumulative shocks
$p_{i,m}(\tau'_{i,m})$	The probability that one shock results in extreme damage
$\lambda_{i,j}^{(m)}(\tau'_{i,m}, \boldsymbol{\theta})$	The transition rates after *m* cumulative random shocks
$\boldsymbol{S}'$	The state space of the integrated model
$\lambda_{(i,m),(j,n)}(\tau'_{i,m}, \boldsymbol{\theta})$	The transition rate between state (i,m) and state (j,n)
$f_{(i,m),(j,n)}(\tau'_{i,m} \mid t, \boldsymbol{\theta})$	The transition probability density function
$P_{(i,m)}(\tau'_{i,m} \mid t, \boldsymbol{\theta})$	The probability that, given that the component arrives at the state (i,m) at *t* and $\boldsymbol{\theta}$, no transition will occur in $(t, t+\tau'_{i,m})$
$\lambda_{(i,m)}(\tau'_{i,m}, \boldsymbol{\theta})$	The conditional probability that, given that the component is in the state (i,m) at time *t*, having arrived there at time $t-\tau'_{i,m}$, and $\boldsymbol{\theta}$, it will depart from (i,m) during $(t, t+d\tau'_{i,m})$
$\psi_{(i,m)}(\tau'_{i,m} \mid \theta)$	The probability density function for $\tau'_{\mathrm{i,m}}$ in the state $(\mathrm{i,m})$, given $\boldsymbol{\theta}$
$\pi_{(i,m),(j,n)}(\tau'_{i,m} \mid \boldsymbol{\theta})$	The conditional probability that, for the transition out of state (i,m) after holding time $\tau'_{i,m}$ and $\boldsymbol{\theta}$, the transition arrival state will be (j,n)
N_{max}	The maximum number of replications
$\widehat{\boldsymbol{P}}(t) = \{\widehat{p_M}(t), \widehat{p_{M-1}}(t), \dots, \widehat{p_0}(t)\}$	The estimation of the state probability vector
$var_{\widehat{p_i}(t)}$	The sample variance of estimated state probability $\widehat{p_i}(t)$
δ	The predetermined constant which controls the influence of the degradation onto the probability $p_{i,m}(\tau'_{i,m})$
ε	The relative increment of transition rates after one cumulative shock happens

1. INTRODUCTION

Failures of components generally occur in two modes: degradation failures due to physical deterioration in the form of wear, erosion, fatigue, etc, and catastrophic failures due to damages caused by sudden shocks in the form of jolts, blows, etc [1]-[2].

In the past decades, a number of degradation models have been proposed in the field of reliability engineering [3]-[9]. They can be grouped into the following categories [9]: statistical distributions (e.g. Bernstein distribution [3]), stochastic processes (e.g. Gamma process and Wiener process) [4]-[5], and multi-state models [6]-[8].

Most of the existing models are typically built on degradation data from historical collection [3], [5]-[7] or degradation tests [4], which however are suited for components of relatively low cost or/and high failure rates (e.g. electronic devices and vehicle components) [10]-[12]. In industrial systems, there are a number of critical components (e.g. valves and pumps in nuclear power plants or aircraft [13]-[14], engines of airplanes, etc.) designed to be highly reliable to ensure system operation and safety, but for which degradation experiments are costly. In practice, it is then often difficult to collect sufficient degradation/failure samples to calibrate the degradation models mentioned above.

An alternative is to resort to failure physics and structural reliability, to incorporate knowledge on the physics of failure of the particular component (passive and active) [13-17]. Recently, Unwin *et al.* [16] have proposed a multi-state physics model (MSPM) for modeling nuclear component degradation, also accounting for the effects of environmental factors (e.g. temperature and stress) within certain predetermined ranges [17]. In a previous work by the authors [9], the model has been formulated under the framework of inhomogeneous continuous time Markov chain and solved by Monte Carlo simulation.

Random shocks need to be accounted for on top of the underlying degradation processes, because they can bring variations to influencing environmental factors, even outside their predetermined boundaries [18], that can accelerate the degradation processes. For example, thermal and mechanical shocks (e.g. internal thermal shocks and water hammers) [17], [19]-[20] onto power plant components can lead to intense increases in temperatures and stresses, respectively; under these extreme conditions, the original physics functions in MSPM might be insufficient to characterize the influences of random shocks onto the degradation processes and must, therefore, be modified. In the literature, random shocks are typically modeled by Poisson processes [1], [18], [21]-[23], distinguishing two main types, extreme shock and cumulative shock processes [21], according to the severity of the damage. The former could directly lead the component to immediate failure [24]-[25], whereas the latter increases the degree of damage in a cumulative way [26]-[27].

Random shocks have been intensively studied [1]-[2], [22]-[23], [28]-[33]. Esary *et al.* [23] have considered extreme shocks in a component reliability model, whereas Wang *et al.* [2], Klutke and Yang [30], and Wortman *et al.* [31] have modeled the influences of cumulative shocks onto a degradation process. Both extreme and cumulative random shocks have been considered by Li and Pham [1], Wang and Pham [22]. Additionally, Ye *et al.* [28] and Fan *et al.* [29] have considered that high severity of degradation can lead to high probability that a random shock causes extreme damage. However, the fact that the effects of cumulative shocks can vary according to the severity of degradation has also to be considered.

Among the models mixing the multi-state degradation models and random shocks, Li and Pham [1] divided the underlining continuous and monotonically increasing degradation processes into a finite number of states and combined them with independent random shocks. Wang and Pham [22], further considered the dependences among the continuous and monotone (increasing or decreasing) degradation processes and between degradation processes and random shocks. Yang et al. [33] integrated random shocks into a Markov degradation model. Becker et al. [32] combined semi-Markov degradation model, which is more general than Markov model, with random shocks in a dynamic reliability formulation, where the influence

of random shocks is characterized by the change of continuous degradation variables (e.g. structure strength). To the best knowledge of the authors, this is the first work of semi-Markov degradation modeling that represents the influence of random shocks by changing the transition rates, which might also be physics functions.

The contribution of the paper is that it generalizes the MSPM framework to handle both degradation and random shocks, which have not been previously considered by the existing MSPMs. More specifically: first, we extend our previous MSPM framework [9] to semi-Markov modeling, which more generally describes the fact that the time of transition to a state can depend on the residence time in the current state, and hence is more suitable for including maintenance [34]; then, we propose a general random shock model, where the probability of a random shock resulting in extreme or cumulative damage, and the cumulative damages, are both dependent on the current component degradation condition (the component degradation state and residence time in the state); finally, we integrate the random shock model into the MSPM framework to describe the influence of random shocks on the degradation processes. The rest of this paper is organized as follows. Section 2 introduces the semi-Markov scheme into the MSPM framework. Section 3 presents the random shock model; in Section 4, its integration into MSPM is presented. Monte Carlo simulation procedures to solve the integrated model are presented in Section 5. Section 6 uses a numerical example regarding a case study of literature, to illustrate the proposed model. Section 7 concludes the work.

2. MSPM OF COMPONENT DEGRADATION PROCESSES

A continuous-time stochastic process is called a semi-Markov process if the embedded jump chain is a Markov Chain and the times between transitions may be random variables with any distribution [35]. The following assumptions are made for the extended MSPM framework [9] based on semi-Markov processes:

- The degradation process has a finite number of states $\boldsymbol{S} = \{0,1,\dots,M\}$ where states '*0*' and '*M*' represent the complete failure state and perfect functioning state, respectively; The generic intermediate degradation states *i* ($0<i<M$) are established according to the degradation development and condition, wherein the component is functioning or partially functioning.
- The degradation follows a continuous-time semi-Markov process; the transition rate between state *i* and state *j*, denoted by $\lambda_{i,j}(\tau_i, \boldsymbol{\theta})$, is a function of τ_i, which is the residence time of the component being in the current state *i* since the last transition, and $\boldsymbol{\theta}$, which represents the external influencing factors (including physical factors).
- The initial state (at time $t = 0$) of the component is *M*.
- Maintenance can be carried out from any degradation state, except the complete failure state (in other words, there is no repair from failure).

Fig. 1 presents the diagram of the semi-Markov component degradation process.

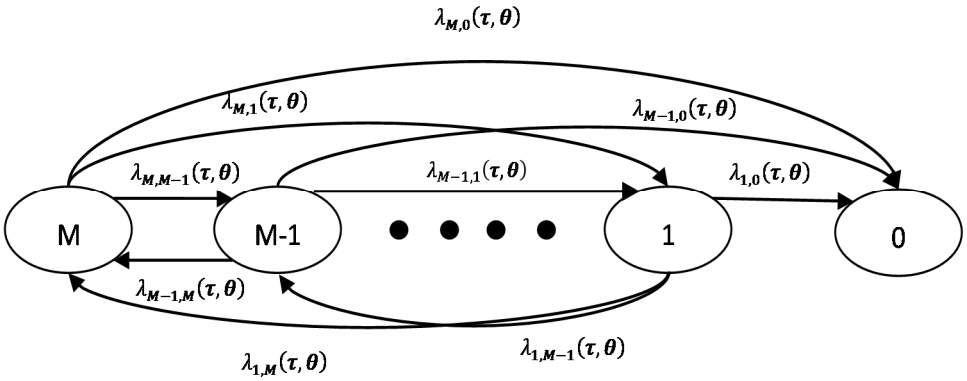

Fig 1. The diagram of the semi-Markov process

The probability that the continuous time semi-Markov process will step to state *j* in the next infinitesimal time interval $(t, t+\Delta t)$, given that it has arrived at state *i* at time T_n after *n* transitions and remained stable in *i* from T_n until time *t* , is defined as follows,

$$P[X_{n+1}=j, T_{n+1}\in[t,t+\Delta t] \mid \{X_k, T_k\}_{k=0}^{n-1}, (X_n=i,T_n), T_n\le t\le T_{n+1}, \boldsymbol{\theta}]$$
$$= P[X_{n+1}=j, T_{n+1}\in[t,t+\Delta t] \mid (X_n=i,T_n), T_n\le t\le T_{n+1}, \boldsymbol{\theta}]$$
$$= \lambda_{i,j}(\tau_i = t-T_n, \boldsymbol{\theta})\Delta t,\ \forall\, i,j\in \boldsymbol{S}, i\neq j \quad (1)$$

where X_k denotes the state of the component after *k* transitions and T_k denotes the time of arrival at X_k. The degradation transition rates can be obtained from the structural reliability analysis of the degradation processes (e.g. the crack propagation process ([15], [17]), whereas the transition rates related to maintenance tasks can be estimated from the frequencies of maintenance activities). For example, the authors of [17] divided the degradation process of the alloy metal weld into six states dependent on the underlying physics phenomenon, and some degradation transition rates are represented by corresponding physics equations.

The solution to the semi-Markov process model is the state probability vector $P(t) = \{p_M(t), p_{M-1}(t), \dots, p_0(t)\}$, where $p_i(t)$ is the probability of the component being in state *i* at time *t*. Since no maintenance is carried out from the component failure state and the component is regarded as functioning in all other intermediate alternative states, its reliability can be expressed as

$$R(t) = 1 - p_0(t) \quad (2)$$

where $p_0(t)$ is the probability of the complete failure state at time t. Analytically solving the continuous time semi-Markov model with state residence time-dependent transition rates is a difficult or sometimes impossible task, and the Monte Carlo simulation method is usually applied to obtain $P(t)$ [36]-[37].

3. RANDOM SHOCKS

The following assumptions are made on the random shock process:

- The arrivals of random shocks follow a homogeneous Poisson process $\{N(t), t \geq 0\}$ [21] with constant arrival rate μ, where the random variable $N(t)$ denotes the number of random shocks occurred until time *t*. The random shocks are independent of the degradation process, but they can influence the degradation process (see Fig. 2).
- The damages of random shocks are divided into two types: extreme and cumulative.
- Extreme shock and cumulative shock are mutually exclusive.
- The component fails immediately upon occurrence of extreme shocks.
- The probability of a random shock resulting in extreme or cumulative damage is dependent on the current component degradation.
- The damage of cumulative shocks can only influence the degradation transition departing from the current state and its impact on the degradation process is dependent on the current component degradation.

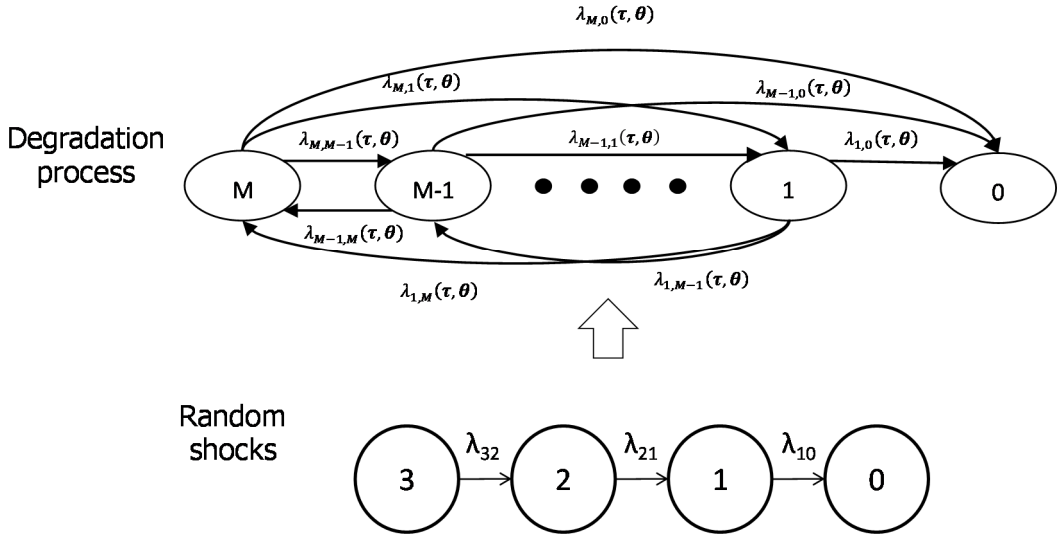

Fig 2. Degradation and random shock processes

The first five assumptions are taken from [22]. The sixth assumption reflects the aging effects addressed in Fan *et al.*'s shock model [29], where the random shocks are more fatal to the component (i.e. more likely lead to extreme damages) when the component is in severe degradation states. However, the influences of cumulative shocks under aging effects have not been considered in Fan *et al.*'s model, as in the last assumption. In addition, the random shock damage is assumed to depend on the current degradation, characterized by three parameters: 1) the current degradation state *i*, 2) the number of cumulative shocks *m* occurred while in the current degradation state since the last degradation state transition, 3) the residence time $\tau'_{i,m}$ of the component in the current degradation state *i* after *m* cumulative shocks $\tau'_{i,m} \geq 0$.

Let $p_{i,m}(\tau'_{i,m})$ denote the probability that one shock results in extreme damage (the cumulative damage probability is then $1 - p_{i,m}(\tau'_{i,m})$). In case of cumulative shock, the degradation transition rates for the current state change at the moment of occurrence of the shock, whereas the other transition rates are not affected. Let $\lambda_{i,j}^{(m)}(\tau'_{i,m}, \boldsymbol{\theta})$ denote the

transition rates after m cumulative random shocks, where $\lambda_{i,j}^{(0)}(\tau'_{i,0},\boldsymbol{\theta})$ holds the same expression as the transition rate $\lambda_{i,j}(\tau'_{i,0},\boldsymbol{\theta})$ in the pure degradation model, and the other transition rates (i.e. m>0) depend on the degradation and the external influencing factors. Because the influences of random shocks can render invalid the original physics functions, we propose a general model which allows the formulation of 'physics' functions dependent on the effects of shocks. The modified transition rates can be obtained by material science knowledge and/or data from shock tests [38]. These quantities will be used as the key linking elements in the integration work of next section.

4. INTEGRATION OF RANDOM SHOCKS IN THE MSPM

Based on the first and second assumptions on random shocks, the new model that integrates random shocks into MSPM is shown in Fig 3. In the model, the states of the component are represented by pair (i,m), where i is the degradation state and m is the number of cumulative shocks occurred during the residence time in the current state. For all the degradation states of component except for the state '*0*', the number of cumulative shocks could range from *0* to positive infinity. If the transition to a new degradation state occurs, the number of cumulative shocks is set to *0*, coherently with the last assumption on random shocks. The state space of the new integrated model is denoted by $\boldsymbol{S}' = \{(M,0),(M,1),(M,2),\dots,(M-1,0),(M-1,1),\dots,(0,0)\}$. The component is failed whenever it reaches (*0*,*0*). The transition rate denoted by $\lambda_{(i,m),(j,n)}(\tau'_{i,m},\boldsymbol{\theta})$ is residence time-dependent, thus rendering the process a continuous time semi-Markov process.

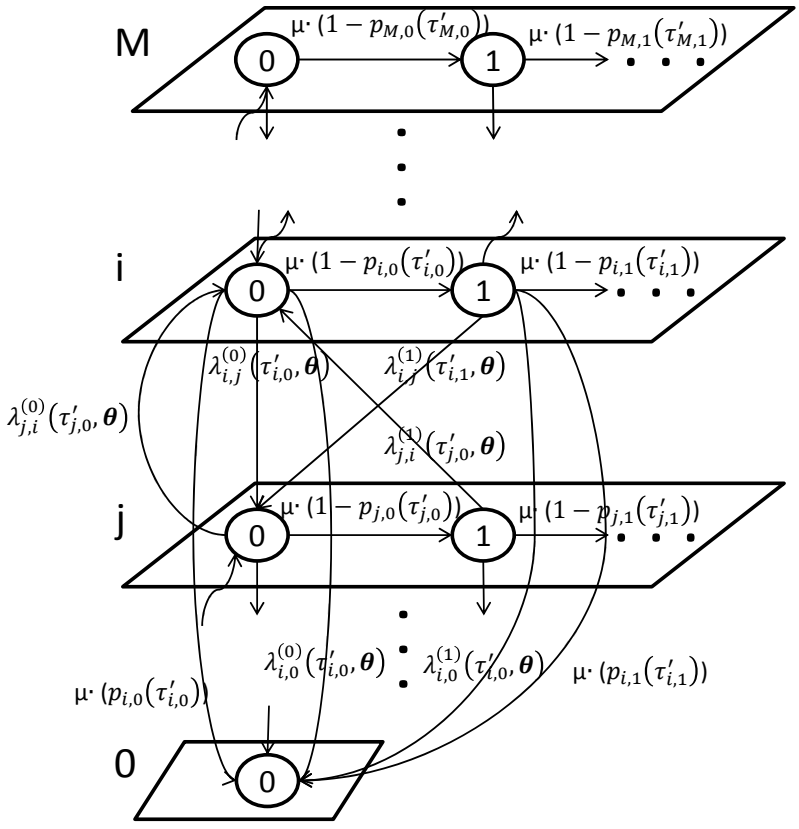

Fig 3. Degradation and random shock processes

Suppose that the component is in a non-failure state (*i*,*m*); then, we have three types of outgoing transition rates:

$$\lambda_{(i,m),(0,0)}(\tau'_{i,m}, \boldsymbol{\theta}) = \mu \cdot (p_{i,m}(\tau'_{i,m})) \quad (3)$$

the rate of occurrence of an extreme shock which will cause the component to go to state (*0,0*),

$$\lambda_{(i,m),(i,m+1)}(\tau'_{i,m}, \boldsymbol{\theta}) = \mu \cdot (1 - p_{i,m}(\tau'_{i,m})) \quad (4)$$

the rate of occurrence of a cumulative shock which will cause the component to go to state (*i*,*m+1*) and

$$\lambda_{(i,m),(j,0)}(\tau'_{i,m}, \boldsymbol{\theta}) = \lambda_{i,j}^{(m)}(\tau'_{i,j}, \boldsymbol{\theta}) \quad (5)$$

the rate of transition (i.e. degradation or maintenance) which will cause the component to make the transition to state (j,0).

The effect of random shocks on the degradation processes is shown in equation (5) by using the superscript (m) where m is the number of cumulative shocks occurred during the residence time in the current state. It means that the transition rate functions depend on the number of cumulative shocks. This is a general formulation.

The first two types (equation (3) and equation (4)) depend on the probability of a random shock resulting in extreme damage and in cumulative damage, respectively; the last type of transition rates (equation (5)) depends on the cumulative damage of random shocks. In this model, we do not directly associate a failure threshold to the cumulative shocks, since the damage of cumulative shocks can only influence the degradation transition departing from the current state and its impact on the degradation process is dependent on the current component degradation. The cumulative shocks can only aggravate the degradation condition of the component instead of leading it suddenly to failure (which is the role of extreme shocks). The effect of the cumulative shocks is reflected in the change of transition rates. The probability of a shock becoming an extreme one depends on the degradation condition of the component. The extreme shocks immediately lead the component to failure, whereas the damage of cumulative shocks aggravates the degradation processes of the component.

The proposed model is based on semi-Markov process and random shocks. Under this general structure, as explained in the paragraph above, the physics lies in the transition rates of the semi-Markov process. We name it a ‘physics’ model because the stressors (e.g. the crack in the case study) that cause the component degradation are explicitly modeled, differently from the conventional way of estimating the transition rates from historical failure/degradation data, which are relatively rare for the critical components. More information about MSPM can be found in [9]. In addition, the random shocks are integrated into the MSPM in a way that they may change the ‘physics’ functions of the transition rates, within a general formulation.

Similarly to what was said for the semi-Markov process presented in Section 2, the state probabilities of the new integrated model can be obtained by Monte Carlo simulation and the expression of component reliability is:

$$R(t) = 1 - p_{(0,0)}(t) \quad (6)$$

5. RELIABILITY ESTIMATION

5.1 Basics of Monte Carlo simulation

The key theoretical construct upon which Monte Carlo simulation is based is the transition probability density function $f_{(i,m),(j,n)}(\tau'_{i,m} \mid t, \boldsymbol{\theta})$, defined as follows

$$f_{(i,m),(j,n)}(\tau'_{i,m} \mid t, \boldsymbol{\theta})d\tau'_{i,m} \equiv \text{probability that, given that the system arrives at the state } (i,m) \text{ at time } t \text{ and physical factors } \boldsymbol{\theta}, \text{ the next transition will occur in the infinitesimal time interval } (t+\tau'_{i,m}, t+\tau'_{i,m}+d\tau'_{i,m}) \text{ and will be to the state } (j,n) \text{ [36].} \quad (7)$$

By using the previously introduced transition rates, equation (7) can be expressed as

$$f_{(i,m),(j,n)}(\tau'_{i,m} \mid t, \boldsymbol{\theta})d\tau'_{i,m} = P_{(i,m)}(\tau'_{i,m} \mid t, \boldsymbol{\theta})\lambda_{(i,m),(j,n)}(\tau'_{i,m}, \boldsymbol{\theta})d\tau'_{i,m} \quad (8)$$

where $P_{(i,m)}(\tau'_{i,m} \mid t, \boldsymbol{\theta})$ is the probability that, given that the component arrives at the state (i,m) at time t and physical factors $\boldsymbol{\theta}$, no transition will occur in the time interval $(t, t+\tau'_{i,m})$ and it satisfies:

$$\frac{dP_{(i,m)}(\tau'_{i,m} \mid t,\boldsymbol{\theta})}{P_{(i,m)}(\tau'_{i,m} \mid t,\boldsymbol{\theta})} = -\lambda_{(i,m)}(\tau'_{i,m}, \boldsymbol{\theta})d\tau'_{i,m} \quad (9)$$

where

$$\lambda_{(i,m)}(\tau'_{i,m}, \boldsymbol{\theta}) = \sum_{(i',m')} \lambda_{(i,m),(i',m')}(\tau'_{i,m}, \boldsymbol{\theta}) \quad (10)$$

and $\lambda_{(i,m)}(\tau'_{i,m}, \boldsymbol{\theta})d\tau'_{i,m}$ is the conditional probability that, given that the component is in the state (i,m) at time t, having arrived there at time $t-\tau'_{i,m}$, and physical factors $\boldsymbol{\theta}$, it will depart from (i,m) during $(t, t+d\tau'_{i,m})$.

Taking the integral at both sides of equation (9) with the initial condition $P_{(i,m)}(0 \mid t, \boldsymbol{\theta}) = 1$, we obtain

$$P_{(i,m)}(\tau'_{i,m} \mid t, \boldsymbol{\theta}) = exp[-\int_0^{\tau'_{i,m}} \lambda_{(i,m)}(s, \boldsymbol{\theta})ds] \quad (11)$$

Substituting equation (11) into equation (8), we obtain

$$f_{(i,m),(j,n)}(\tau'_{i,m} \mid t, \boldsymbol{\theta}) = \lambda_{(i,m),(j,n)}(\tau'_{i,m}, \boldsymbol{\theta})exp[-\int_0^{\tau'_{i,m}} \lambda_{(i,m)}(s, \boldsymbol{\theta})ds] \quad (12)$$

To derive a Monte Carlo simulation procedure, equation (12) is rewritten as

$$f_{(i,m),(j,n)}(\tau'_{i,m} \mid t, \boldsymbol{\theta}) = \frac{\lambda_{(i,m),(j,n)}(\tau'_{i,m},\boldsymbol{\theta})}{\lambda_{(i,m)}(\tau'_{i,m},\boldsymbol{\theta})} \cdot \lambda_{(i,m)}(\tau'_{i,m}, \boldsymbol{\theta})exp[-\int_0^{\tau'_{i,m}} \lambda_{(i,m)}(s, \boldsymbol{\theta})ds]$$
$$= \pi_{(i,m),(j,n)}(\tau'_{i,m} \mid \boldsymbol{\theta}) \cdot \psi_{(i,m)}(\tau'_{i,m} \mid \boldsymbol{\theta}) \quad (13)$$

where

$$\psi_{(i,m)}(\tau'_{i,m} \mid \boldsymbol{\theta}) = \lambda_{(i,m)}(\tau'_{i,m}, \boldsymbol{\theta})exp[-\int_0^{\tau'_{i,m}} \lambda_{(i,m)}(s, \boldsymbol{\theta})ds] \quad (14)$$

is the probability density function for the holding time $\tau'_{i,m}$ in the state (i,m), given the physical factors $\boldsymbol{\theta}$, and

$$\pi_{(i,m),(j,n)}(\tau'_{i,m} \mid \boldsymbol{\theta}) = \frac{\lambda_{(i,m),(j,n)}(\tau'_{i,m},\boldsymbol{\theta})}{\lambda_{(i,m)}(\tau'_{i,m},\boldsymbol{\theta})} \quad (15)$$

is regarded as the conditional probability that, for the transition out of state (i,m) after holding time $\tau'_{i,m}$ and the physical factors $\boldsymbol{\theta}$, the transition arrival state will be (j,n).

In the Monte Carlo simulation, for the component arriving at any non-failure state (i,m) at any time *t*, the process at first samples the holding time at state (i,m) corresponding to equation (14), and then determines the transition arrival state (j,n) from state (i,m) according to equation (15). This procedure is repeated until the accumulated holding time reaches the predefined time horizon or the component reaches the failure state $(0,0)$.

5.2 The simulation procedure

To generate the holding time $\tau'_{i,m}$ and the next state (j,n) for the component arriving in any non-failure state (i,m) at any time *t*, one proceeds as follows: two uniformly distributed random numbers u_1 and u_2 are sampled in the interval [0, 1]; then, $\tau'_{i,m}$ is chosen so that

$$\int_0^{\tau'_{i,m}} \lambda_{(i,m)}(s,\boldsymbol{\theta})\, ds = \ln(1/u_1) \tag{16}$$

and $(j,n) = a^*$ that satisfies

$$\sum_{k=0}^{a^*-1} \lambda_{(i,m),k}\left(\tau'_{i,m},\boldsymbol{\theta}\right) < u_2 \lambda_{(i,m)}\left(\tau'_{i,m},\boldsymbol{\theta}\right) \le \sum_{k=0}^{a^*} \lambda_{(i,m),k}\left(\tau'_{i,m},\boldsymbol{\theta}\right) \tag{17}$$

where a^* represents one state in the ordered sequence of all possible outgoing states of state (i,m).The state a^* is determined by going through the ordered sequence of all possible outgoing states of state (i,m) until the equation (17) is satisfied. The algorithm of Monte Carlo simulation for solving the integrated MSPM on a time horizon $[0, t_{max}]$ is presented as follows:

Set N_{max} (the maximum number of replications) and $k = 0$

While $k < N_{max}$

Initialize the system by setting $s = (M,0)$ (initial state of perfect performance), setting the time $t = 0$ (initial time)

Set $t' = 0$ (state holding time)

While $t < t_{max}$

Calculate the equation (10)

Sample a t' by using equation (16)

Sample an arrival state (j,n) by using equation (17)

Set $t = t + t'$

Set $s = (j,n)$

If $s = (0,0)$

then break

End if

End While

Set $k = k + 1$

End While □

The estimation of the state probability vector $\widehat{\boldsymbol{P}}(t) = \{\widehat{p_M}(t), \widehat{p_{M-1}}(t), \dots, \widehat{p_0}(t)\}$ at time t is done as,

$$\widehat{\boldsymbol{P}}(t) = \frac{1}{N_{max}}\{n_M(t), n_{M-1}(t), \dots, n_0(t)\} \tag{18}$$

where $\{n_i(t)|i = M, \dots, 0, t \le t_{max}\}$ is the total number of visits to state *i* at time *t*, with sample variance [39] defined as follows

$$var_{\widehat{p_i}(t)} = \widehat{p_i}(t)(1 - \widehat{p_i}(t))/(N_{max} - 1) \tag{19}$$

6. CASE STUDY AND RESULTS

6.1 Case study

We illustrate the proposed modeling framework on a case study slightly modified from an Alloy 82/182 dissimilar metal weld in a primary coolant system of a nuclear power plant in [17]. The MSPM of the original crack growth is shown in Fig. 4.

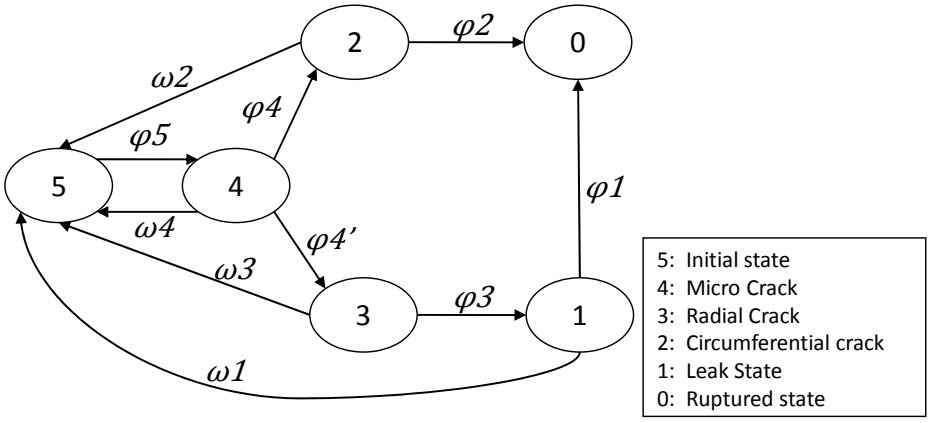

Fig 4. MSPM of crack development in Alloy 82/182 dissimilar metal welds

where φ_i and ω_i represent the degradation transition rate and maintenance transition rate, respectively. Except for φ_5,φ_4, $\varphi_{4'}$ and φ_3, all the other transition rates are assumed to be constant. The expressions of the variable transition rates are as follows:

$$\varphi_5 = \left(\frac{b}{\tau}\right) \cdot \left(\frac{\tau_5}{\tau}\right)^{b-1} \tag{20}$$

$$\varphi_4 = \begin{cases} \frac{a_C P_C}{\dot{a}_M {\tau_4}^2 (1 - P_C(1 - a_C/(u\dot{a}_M)))}, & if\ \tau_4 > a_C/\dot{a}_M \\ 0, & else \end{cases} \tag{21}$$

$$\varphi_4{}' = \begin{cases} \frac{a_D P_D}{\dot{a}_M {\tau_4}^2 (1 - P_D(1 - a_D/(u\dot{a}_M)))}, & if\ \tau_4 > a_D/\dot{a}_M \\ 0, & else \end{cases} \tag{22}$$

$$\varphi_3 = \begin{cases} \frac{1}{\tau_3}, & if\ \tau_3 > (a_L - a_D)/\dot{a}_M \\ 0, & else. \end{cases} \tag{23}$$

The other transition rates and the parameters values are presented in Table I below.

Table I Parameters and constant transition rates [17]

b –Weibull shape parameter for crack initiation model	2.0
τ – Weibull scale parameter for crack initiation model	4 years
a_D – Crack length threshold for radial macro-crack	10 mm
P_D – Probability that micro-crack evolves as radial crack	0.009
$\dot{a}_M$ – Maximum credible crack growth rate	9.46 mm/yr
a_C – Crack length threshold for circumferential macro-crack	10 mm
P_C – Probability that micro-crack evolves as circumferential crack	0.001
a_L – Crack length threshold for leak	20 mm
ω_4 – Repair transition rate from micro-crack	1 x10-3 /yr
ω_3 – Repair transition rate from radial macro-crack	2 x10-2 /yr
ω_2 – Repair transition rate from circumferential macro-crack	2 x10-2 /yr
ω_1 – Repair transition rate from leak	8 x10-1 /yr
φ_1 – Leak to rupture transition rate	2x10-2 /yr
φ_2 – Macro-crack to rupture transition rate	1x10-5 /yr

The random shocks correspond to the thermal and mechanical shocks (e.g. internal thermal shocks and water hammers) [17], [19]-[20] to the dissimilar metal welds. The damage of random shocks can accelerate the degradation processes, and hence, increase the rate of component degradation. Note that Yang *et al* [33] have related random shocks to the degradation rates in their work. To assess the degree of impact of shocks, we may use 1) physics functions for the influence of random shocks through material science knowledge; 2) transition times, speed of cracking development and other related information obtained from shock tests [38]. We set the occurrence rate $\mu = 1/15\, y^{-1}$ and the probability of a random shock becoming extreme shock $p_{i,m}(\tau'_{i,m}) = 1 - exp\left[-\delta m(6-i)\left(2 - e^{-\tau'_{i,m}}\right)\right]$, taking the exponential formulation from Fan *et al.*'s work [29]. In this formula, we use $m(6-i)(2 - e^{-\tau'_{i,m}})$ to quantify the component degradation. It is noted that the quantity $2 - e^{-\tau'_{i,m}}$ ranges from *1* to *2*, representing the relatively small effect of $\tau'_{i,m}$ onto the degradation situation in comparison with the other two parameters m and *i*, and δ is a predetermined constant which controls the influence of the degradation onto the probability $p_{i,m}(\tau'_{i,m})$. In this study, we set

$\delta = 0.0001$. The value of δ was set considering the balance between showing the impact of extreme shocks and reflecting the high reliability of the critical component. In addition, we assume the corresponding degradation transition rates after m cumulative shocks to be $\lambda_{i,j}^{(m)}(\tau'_{i,m}, \boldsymbol{\theta}) = (1+\varepsilon)^m \lambda_{i,j}(\tau'_{i,m}, \boldsymbol{\theta})$, where $\varepsilon = 0.3$ is the relative increment of transition rates after one cumulative shock happens, and the formulation $(1+\varepsilon)^m$ is used to characterize the accumulated effect of such shocks. In order to characterize the increase of the transition rates, in the case study we have used the parameter ε to represent the relative increment of degradation transition rate after one cumulative shock occurs. For the sake of simplicity, but without loss of generality in the framework for integration, we assume that the values of ε for each cumulative shock are equal. But the model can handle different εs for different stages of the crack process.

6.2 Results and analysis

The Monte Carlo simulation over a time horizon of $t_{max} = 80$ years is run $N_{max} = 10^6$ times. The results are collected and analyzed in the following sections.

6.2.1 Results of state probabilities

The estimated state probabilities without and with random shocks throughout the time horizon are shown in Figs. 5 and 6, respectively.

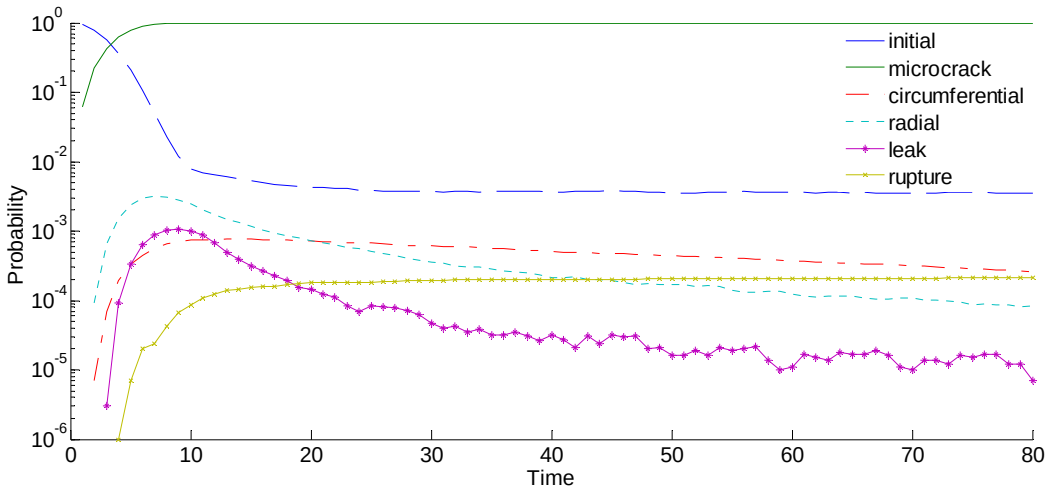

Fig 5. State probabilities obtained without random shocks

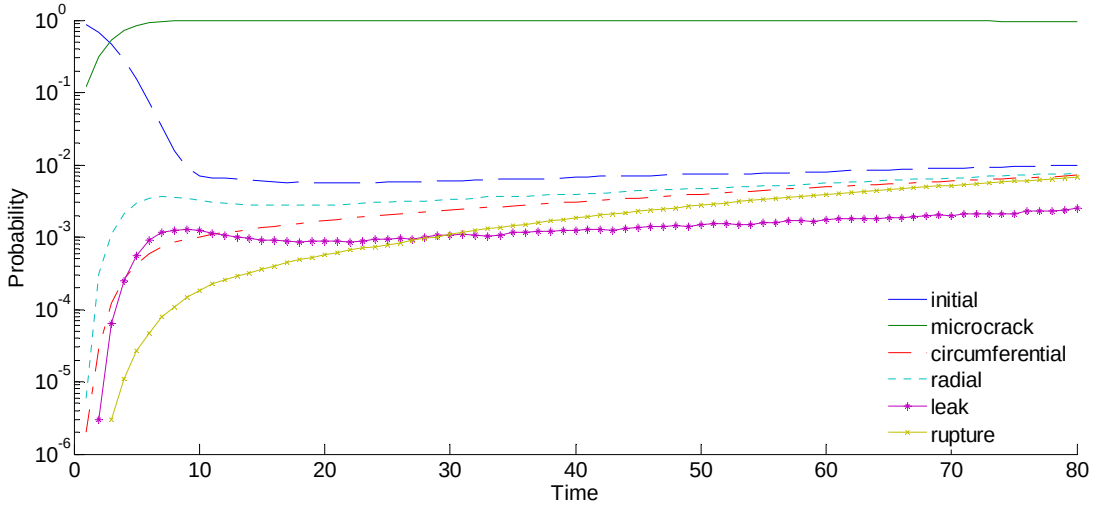

Fig 6. State probabilities obtained with random shocks

Comparing the above two Figures, it can be observed that as expected the random shocks drive the component to higher degradation states than the micro-crack state. The numerical comparisons on the state probabilities w/o random shocks at year 80 are reported in Table II. It is seen that except for the micro-crack state probability, all the other state probabilities at year 80 have increased due to the random shocks, with the increase in leak probability being the most significant.

Table II Comparison of state probabilities w/o random shocks (at year 80)

State	Probability without random shocks	Probability with random shocks	Relative difference
Initial	3.52e-3	9.82e-3	180.00%
Micro-crack	0.9959	0.9661	-2.99%
Circumferential crack	3.05e-4	7.28e-3	2286.89%
Radial crack	1.00e-4	7.75e-3	7650.00%
Leak	1.30e-5	2.59e-3	19823.08%
Rupture state	2.06e-4	7.00e-3	3298.06%

The fact that the probability of the initial state (compared with no random shocks) at 80 years has increased is attributed to the maintenance tasks. All the maintenance tasks lead the

component to the initial state and the repair rates from radial macro-crack state, circumferential macro-crack state and leak state are higher than that from micro-crack state. The shocks generally increase the speed of the component to step back to further degradation states from where it steps to the initial state more quickly. In summary, this phenomenon is due to the combined effects of shocks.

6.2.2 Results of component reliability

The estimated component reliabilities with and without random shocks throughout the time horizon are shown in Fig. 7, respectively. At year 80, the estimated component reliability with random shocks is 0.9930, with sample variance equal to 6.95e-9. Compared with the case without random shocks (reliability equals to 0.9998, with sample variance 2.00e-10), the component reliability has decreased by 0.68%.

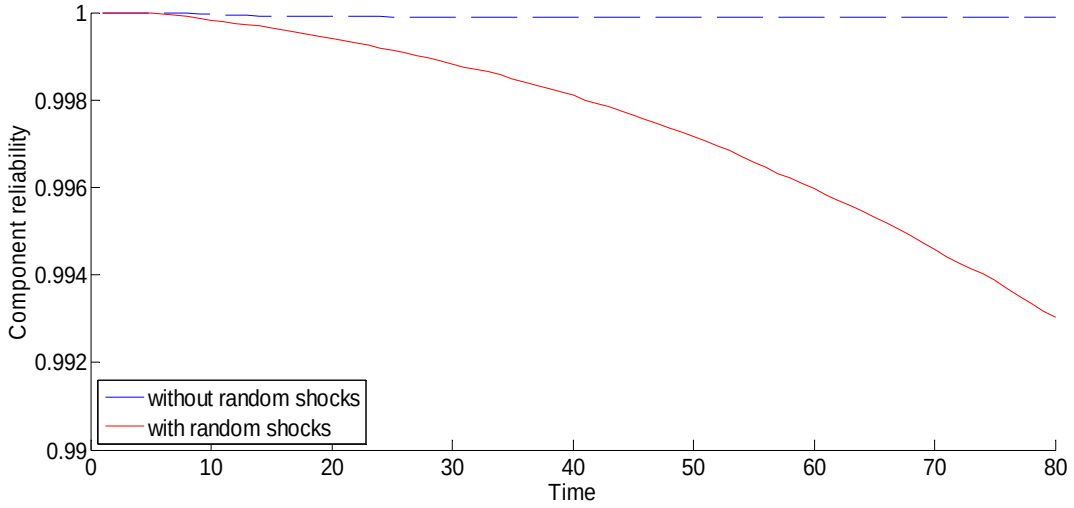

Fig 7. Component reliability estimation w/o random shocks.

6.2.3 Analysis of the extreme shocks

Table III presents the frequencies of different numbers of random shocks occurred per simulation trial. The most likely number is around 5, which is consistent with our assumption on the value of the occurrence rate ($\mu = 1/15y^{-1}$) of random shocks.

Table III Frequency of the number of random shocks occurred per trial

(mission time t = 80 years)

Nb of random shocks/trial	0	1	2	3	4	5	6	7	8	9	>9
Percentage (%)	0.63	3.14	8.00	13.55	17.15	17.56	14.91	10.83	6.87	3.90	3.45

In total, 6973 trials ended in failure, among which 4531 trials (64.98%) are caused by extreme shocks. Table IV reports the number of trials ending with extreme shocks, for different numbers of cumulative shocks occurred per trial.

Table IV Number of trials ended with extreme shocks for different numbers of cumulative shocks (mission time t = 80 years)

Nb of cumulative shocks per trial	Nb of trials	Nb of trials ending with extreme shock
0	6345	0
1	31739	367
2	80292	633
3	135676	812
4	171526	809
5	175569	743
6	148844	500
7	108101	332
8	68579	172
9	38964	90
10	19569	43
11	8998	19
>11	5798	11

The influence of the number of cumulative shocks occurred per trial on the probability of the next random shock being extreme is shown in Fig. 8: as expected, the larger the number of cumulative shocks the higher the probability of extreme shock.

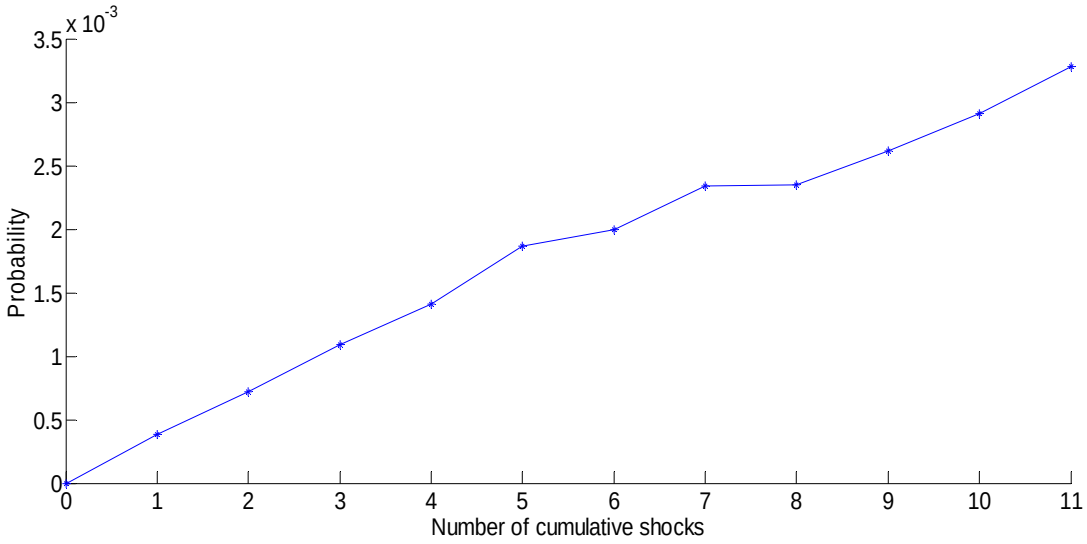

Fig 8. Probability of the next random shock being extreme as a function of the number of cumulative shocks occurred per trial.

The influence of the degradation state on the probability of the next random shock being extreme is shown in Fig. 9: as expected, the likelihood of extreme shocks is higher when the component degradation state is closer to the failure state.

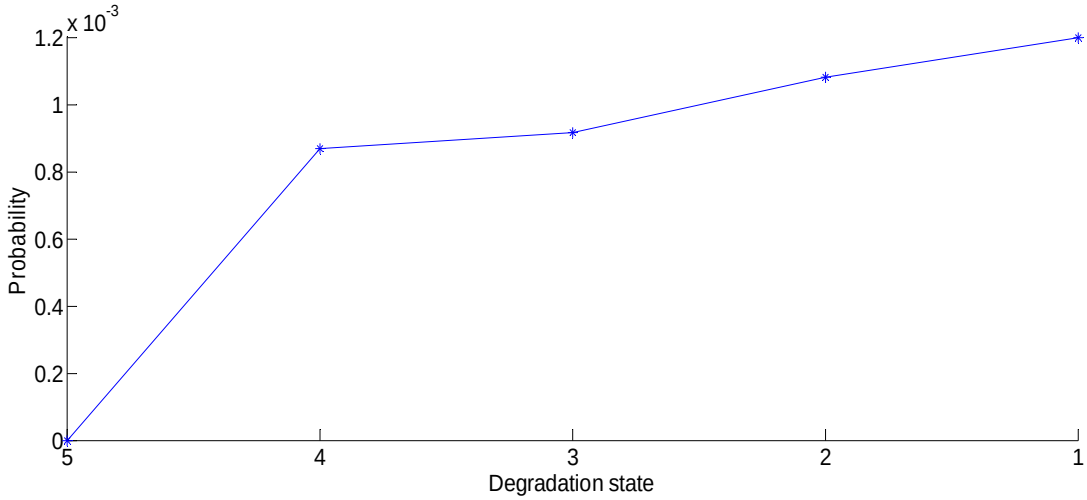

Fig 9. Probability of the next random shock being extreme as a function of the degradation state of the component.

6.2.4 Influence of cumulative shocks on degradation

In order to characterize the influence of cumulative shocks on the degradation processes, we set to *0* the probability of a random shock being extreme, so that all random shocks will be

cumulative. The estimated state probabilities are shown in Fig. 10.

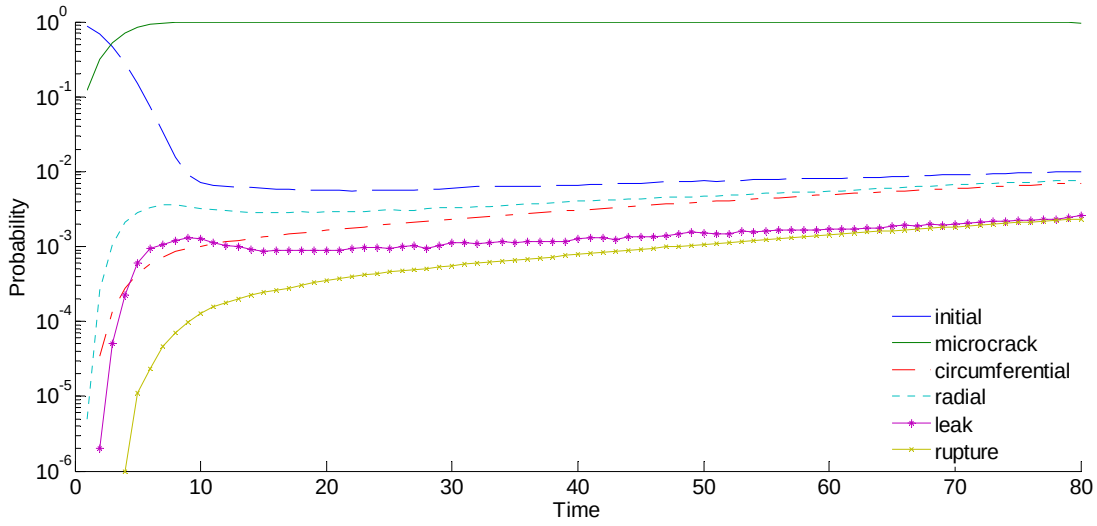

Fig 10. State probabilities obtained with cumulative shocks only.

The state probabilities with cumulative shocks exhibit similar patterns as those in Fig. 6; only the rupture state probability has decreased due to the lack of extreme shocks. The numerical comparisons on the state probabilities without random shocks and with cumulative shocks at year 80 are reported in Table V.

Table V Comparison of state probabilities without random shocks and with cumulative shocks

(at year 80)

State	Probability without random shocks	Probability with cumulative shocks	Relative difference
Initial	3.52e-3	9.94e-3	184.11%
Micro-crack	0.9959	0.9704	-2.56%
Circumferential crack	3.05e-4	7.05e-3	2210.16%
Radial crack	1.00e-4	7.52e-3	7419.00%
Leak	1.30e-5	2.76e-3	21161.54%
Rupture	2.06e-4	2.70e-3	1212.62%

As for the case with random shocks, cumulative shocks have a similar influence on the state probabilities. In Fig. 11, we compare the estimated component reliability with cumulative shocks with the other two estimated probabilities of Fig. 7. At year 80, the estimated component reliability with cumulative shocks is 0.9973 and the sample variance equals to 2.69e-9. Considering cumulative shocks only, the component reliability has decreased by 0.26%.

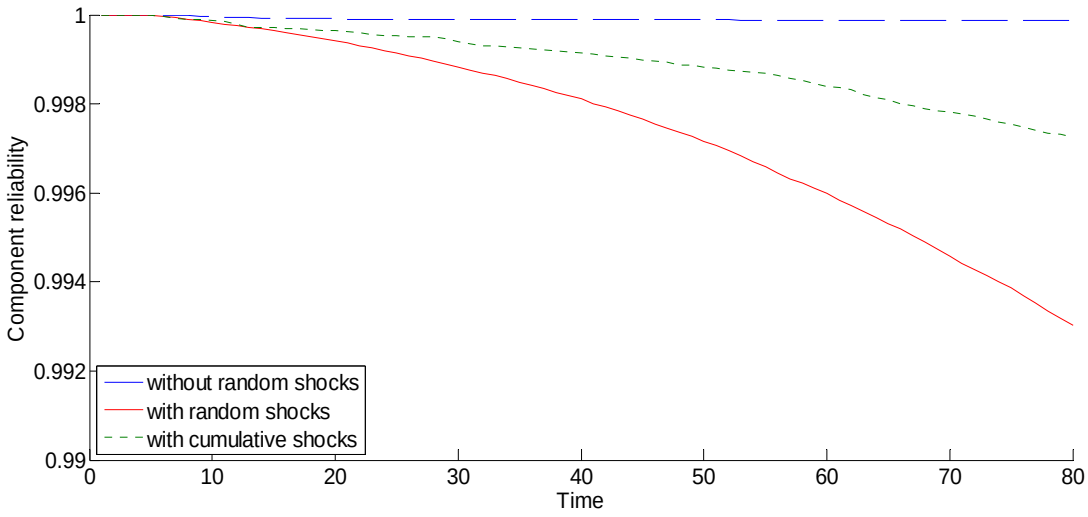

Fig 11. Component reliability w/o random shocks and with only cumulative shocks.

6.3 Sensitivity analysis

With the model specifications of Section 6.1, two important parameters are: the constant δ in $p_{\mathrm{i,m}}(\tau'_{\mathrm{i,m}})$ and the relative increment ε in $\lambda_{i,j}^{(m)}(\tau'_{i,m}, \boldsymbol{\theta})$. To analyze the sensitivity of the component reliability estimates to these two parameters, we take values of δ within the range [0.0001, 0.0002] and ε within the range [0.2, 0.4].

Fig. 12 shows the estimated component reliabilities with different combinations of the two parameters. In general, the component reliability decreases when any of the parameters increases. In fact, higher δ in $p_{\mathrm{i,m}}(\tau'_{\mathrm{i,m}})$ leads to higher probability of the random shock being extreme, which is more critical to the component, and higher relative increment ε in $\lambda_{i,j}^{(m)}(\tau'_{i,m}, \boldsymbol{\theta})$ results in larger degradation transition rates. We can also see from the Figure that in this situation, when the same percentage of variation applies to the two parameters, ε is more influential than δ on the component reliability. The corresponding variances of the estimated component reliability computed using equation (19) are shown in Fig. 13, where it is seen that the high reliability estimates have low variance levels.

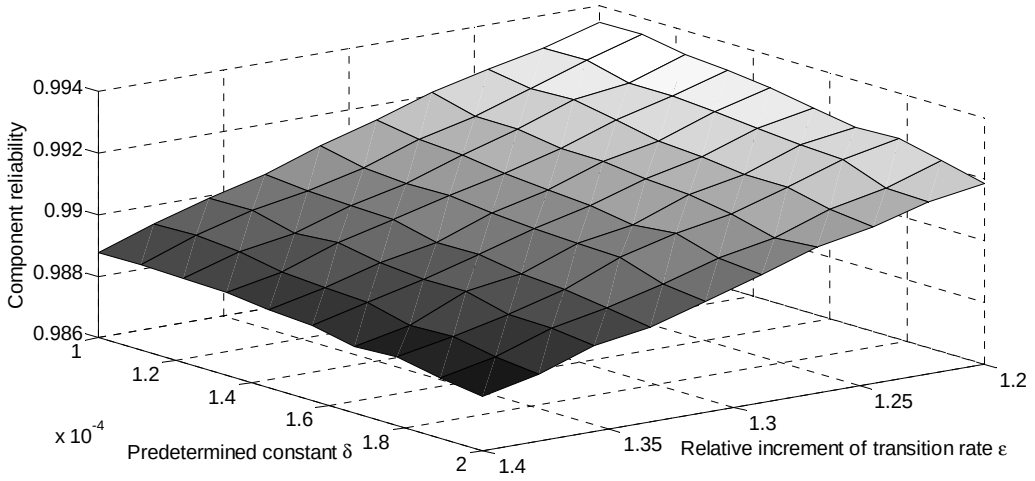

Fig 12. Component reliability estimate as a function of ε and δ (at year 80).

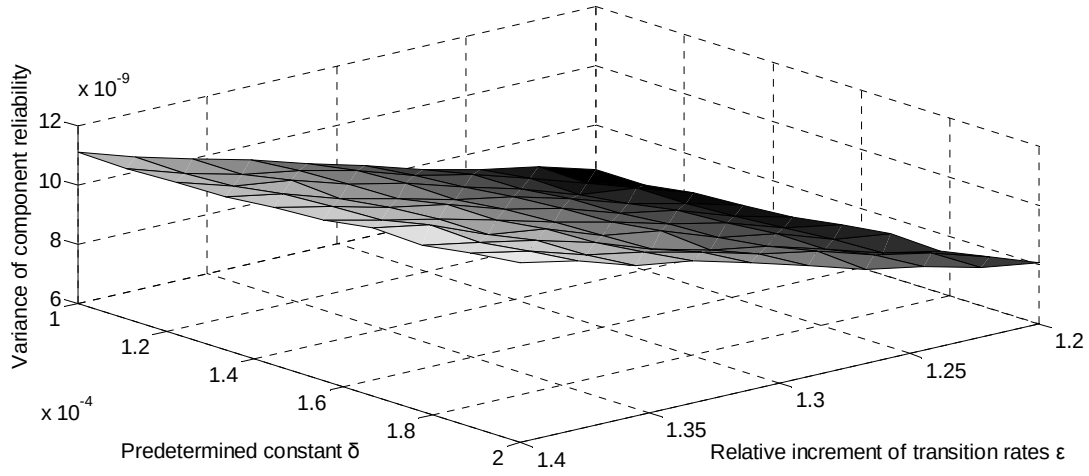

Fig 13.Variance of component reliability estimate as a function of ε and δ (at year 80).

7. CONCLUSIONS

An original, general model of a degradation process dependent on random shocks has been proposed and integrated into a MSPM framework with semi-Markov processes, which also considers two types of random shocks: extreme and cumulative. General dependences between the degradation and the effects of shocks can be considered.

A literature case study has been illustrated to show the effectiveness and modeling capabilities of the proposal, and a crude sensitivity analysis has been applied to a pair of characteristic parameters newly introduced. The significance of the findings in the case study considered is that our extended model is able to characterize the influences of different types of random shocks onto the component state probabilities and the reliability estimates.

REFERENCES

[1] W. Li and H. Pham, "Reliability modeling of multi-state degraded systems with multi-competing failures and random shocks," Reliability, IEEE Transactions on, vol. 54, pp. 297-303, 2005.
[2] Z. Wang, H.-Z. Huang, Y. Li, and N.-C. Xiao, "An approach to reliability assessment under degradation and shock process," Reliability, IEEE Transactions on, vol. 60, pp. 852-863, 2011.
[3] N. Gebraeel, A. Elwany, and J. Pan, "Residual life predictions in the absence of prior degradation knowledge," Reliability, IEEE Transactions on, vol. 58, pp. 106-117, 2009.
[4] J. Lawless and M. Crowder, "Covariates and random effects in a gamma process model with application to degradation and failure," Lifetime Data Analysis, vol. 10, pp. 213-227, 2004.
[5] C. Guo, W. Wang, B. Guo, and X. Si, "A Maintenance optimization model for mission-oriented systems based on wiener degradation," Reliability Engineering & System Safety, vol. 111, pp. 183–194, 2013.
[6] A. Lisnianski and G. Levitin, Multi-state system reliability: assessment, optimization and applications vol. 6: World Scientific Publishing Company, 2003.
[7] M. Giorgio, M. Guida, and G. Pulcini, "An age-and state-dependent Markov model for degradation processes," IIE Transactions, vol. 43, pp. 621-632, 2011.
[8] M. J. Kim and V. Makis, "Optimal maintenance policy for a multi-state deteriorating system with two types of failures under general repair," Computers & Industrial Engineering, vol. 57, pp. 298-303, 2009.
[9] Y.-F. Li, E. Zio, and Y.-H. Lin, "A Multistate Physics Model of Component Degradation Based on Stochastic Petri Nets and Simulation," Reliability, IEEE Transactions on, vol. 61, pp. 921-931, 2012.
[10] G. Yang, Life cycle reliability engineering: Wiley, 2007.
[11] M.-W. Lu and R. J. Rudy, "Laboratory reliability demonstration test considerations," Reliability, IEEE Transactions on, vol. 50, pp. 12-16, 2001.
[12] J. I. Park and S. J. Bae, "Direct prediction methods on lifetime distribution of organic light-emitting diodes from accelerated degradation tests," Reliability, IEEE Transactions on, vol. 59, pp. 74-90, 2010.
[13] M. Daigle and K. Goebel, "A model-based prognostics approach applied to pneumatic valves," International Journal of Prognostics and Health Management, vol. 2, pp. 1-16, 2011.
[14] M. Daigle and K. Goebel, "Multiple damage progression paths in model-based prognostics," in Aerospace Conference, 2011 IEEE, March 5-12, 2011, pp. 1-10.
[15] E. E. Kostandyan and J. D. Sørensen, "Physics of failure as a basis for solder elements reliability assessment in wind turbines," Reliability Engineering & System Safety, 2012.
[16] S. D. Unwin, P. P. Lowry, R. F. Layton, P. G. Heasler, and M. B. Toloczko, "Multi-state physics models of aging passive components in probabilistic risk assessment," in International Topical Meeting on Probabilistic Safety Assessment and Analysis (PSA 2011), March 13-17, 2011, Wilmington, North Carolina, vol. 1, pp. 161-172.
[17] K. N. Fleming, S. D. Unwin, D. Kelly, P. P. Lowry, M. B. Toloczko, R. F. Layton, et al., "Treatment of Passive Component Reliability in Risk-Informed Safety Margin Characterization," Idaho National Laboratory, INL/EXT-10-20013, Idaho Falls, Idaho2010, pp. 1-210.
[18] T. Nakagawa, Shock and damage models in reliability theory: Springer, 2007.
[19] B. O. Y. Lydell, "Pipe failure probability—the Thomas paper revisited," Reliability Engineering & System Safety, vol. 68, no 3, p. 207-217, 2000.
[20] J. Salonen, P. Auerkari, O. Lehtinen, and M. Pihkakoski, "Experience on in-service damage in power plant components," Engineering Failure Analysis, vol. 14, no 6, pp. 970-977, 2007.
[21] J.-M. Bai, Z.-H. Li, and X.-B. Kong, "Generalized shock models based on a cluster point process," Reliability, IEEE Transactions on, vol. 55, pp. 542-550, 2006.
[22] Y. Wang and H. Pham, "Modeling the dependent competing risks with multiple degradation processes and random shock using time-varying copulas," Reliability, IEEE Transactions on, vol. 61, pp. 13-22, 2012.
[23] J. Esary and A. Marshall, "Shock models and wear processes," The annals of probability, pp. 627-649, 1973.
[24] A. Gut, "Extreme shock models," Extremes, vol. 2, pp. 295-307, 1999.
[25] K. K. Anderson, "Limit theorems for general shock models with infinite mean intershock times," Journal of applied probability, pp. 449-456, 1987.
[26] G. Agrafiotis and M. Tsoukalas, "On excess-time correlated cumulative processes," Journal of the Operational Research Society, pp. 1269-1280, 1995.
[27] T. Nakagawa and M. Kijima, "Replacement policies for a cumulative damage model with minimal repair at failure," Reliability, IEEE Transactions on, vol. 38, pp. 581-584, 1989.
[28] Z. S. Ye, L. C. Tang, and H. Y. Xu, "A distribution-based systems reliability model under extreme shocks and natural degradation," Reliability, IEEE Transactions on, vol. 60, pp. 246-256, 2011.

[29] J. Fan, S. Ghurye, and R. A. Levine, "Multicomponent lifetime distributions in the presence of ageing," Journal of applied probability, vol. 37, pp. 521-533, 2000.
[30] G.-A. Klutke and Y. Yang, "The availability of inspected systems subject to shocks and graceful degradation," Reliability, IEEE Transactions on, vol. 51, pp. 371-374, 2002.
[31] M. Wortman, G.-A. Klutke, and H. Ayhan, "A maintenance strategy for systems subjected to deterioration governed by random shocks," Reliability, IEEE Transactions on, vol. 43, pp. 439-445, 1994.
[32] G. Becker, L. Camarinopoulos, and D. Kabranis, “Dynamic reliability under random shocks,” Reliability Engineering & System Safety, vol. 77, no 3, pp. 239-251, 2002.
[33] W. S. Yang, D. E. Lim, and K. C. Chae, “Maintenance of multi-state production systems deteriorated by random shocks and production,” Journal of Systems Science and Systems Engineering, vol. 20, pp. 110-118, 2011.
[34] A. V. Huzurbazar and B. Williams, "Flowgraph models for complex multistate system reliability," Modern statistical and mathematical methods in reliability, vol. 10, pp. 247-262, 2005.
[35] Z. Schuss, Theory and applications of stochastic processes: Springer, 2010.
[36] D. T. Gillespie, "Monte Carlo simulation of random walks with residence time dependent transition probability rates," Journal of Computational Physics, vol. 28, pp. 395-407, 1978.
[37] E. Rachelson, G. Quesnel, F. Garcia, and P. Fabiani, "A simulation-based approach for solving generalized semi-markov decision processes," in European Conference on Artificial Intelligence, 2008.
[38] H. A. Chan and P. J. Englert, Accelerated stress testing handbook: JW, 2001.
[39] E. Lewis and F. Böhm, "Monte Carlo simulation of Markov unreliability models," Nuclear Engineering and Design, vol. 77, pp. 49-62, 1984.

PAPER II: Y.-H. Lin, Y.-F. Li, E. Zio. Reliability Assessment of Systems Subject to Dependent Degradation Processes: A Comparison between Monte Carlo Simulation and Finite-Volume Scheme. Reliability Engineering & System Safety. (Under review)

Reliability Assessment of Systems Subject to Dependent Degradation Processes: A Comparison between Monte Carlo Simulation and Finite-Volume Scheme

Yan-Hui Lin[1], Yan-Fu Li[1,*] and Enrico Zio[1,2]

[1] *Chair on Systems Science and the Energetic Challenge, Foundation EDF, at CentraleSupelec, France*

[2]*Politecnico di Milano, Italy*

Email address: yanfu.li@ecp.fr

Abstract –A modeling framework for the treatment of systems subject to dependent degradation processes is adopted, based on piecewise-deterministic Markov process (PDMP). Due to the complexity of PDMP, analytical solutions are difficult to obtain. In this paper, we, then, consider the Monte Carlo simulation method and finite-volume scheme for system reliability assessment, and provide the guidelines for their implementation. To examine their properties, a comparative study of the two approaches is conducted on two case studies regarding a subsystem of the residual heat removal system of a nuclear power plant.

Keywords: dependent degradation processes, piecewise-deterministic Markov process, multi-state model, physics-based model, Monte Carlo simulation method, finite-volume scheme.

1. INTRODUCTION

In the field of reliability engineering, a number of degradation models have been proposed, which can mainly be classified into the following categories: statistical distributions (e.g. Bernstein distribution [1]), stochastic processes (e.g. Gamma process [2]), multi-state models (e.g. semi-Markov models [3]) and physics-based models (e.g. probabilistic superposition model [4]). In practice, appropriate degradation models have to be chosen based on the available information/data. For some highly reliable components/systems (e.g. pumps and valves in nuclear power plants), their degradation and/or failure data are often limited and do not allow building their lifetime distributions or assigning the values to the parameters of the stochastic degradation processes. Physics-based models (PBMs) [5-8] and multi-state models (MSMs) [9-14] are two widely used modeling frameworks. A PBM aims at developing an integrated mechanistic description of the component/system life consistent with the underlying real degradation mechanisms (e.g. wear, corrosion, cracking, etc.) by using physics knowledge and equations [4], whereas a MSM describes the degradation process in a discrete way, supported by material science knowledge [15], degradation and/or failure data [10] from historical field collection or degradation tests.

In reality, systems are often subject to multiple degradation processes. These degradation processes can be dependent under certain circumstances, e.g. when the degradation dynamics of some components depend on the degradation state of other components [16], or the various degradation processes share the same influencing factors [17]. This renders the system reliability analysis and prediction a challenging problem.

Peng *et al.* [18] considered two dependent failure processes modeled as stochastic processes. Wang and Pham [19] applied time-varying copulas for describing the dependence between the degradation processes modeled by statistical distributions. Yang *et al.* [20] modeled the components dependence through the joint distribution of failure time. Straub [21] used a dynamic Bayesian network to represent the dependence between degradation processes modeled by multi-state models. The dependence is handled in different ways according to the types of degradation models involved.

Piecewise-deterministic Markov process (PDMP) can be employed to integrate PBMs and MSMs for dealing with the degradation dependence among different components, as shown in our previous preliminary study [22]. The PDMP, firstly introduced by Davis in [23, 24], and further studied by Jacobsen [25] and Cocozza-Thivent [26] is a general model that includes many other models (e.g. semi-Markov process, Markov process, etc.) as special cases. Marseguerra and Zio [27] have applied the PDMP approach to the dynamic reliability assessment of a heated hold-up tank system, whereas Chiquet *et al.* [28] used PDMP to model fatigue crack in a structural component. However, due to the complex behavior of PDMP, analytical solutions are difficult to obtain [27].

The Monte Carlo (MC) simulation method and finite-volume (FV) approach are two widely used approaches for solving PDMP models to evaluate reliability quantities. Zhang *et al.* [29] have used the MC simulation method to assess the safety and production availability of an offshore oil production system. Lair *et al.* [30] have developed a FV scheme to optimize the preventive maintenance of air-conditioning systems used in trains. Cocozza-Thivent *et al.* [31] have proposed an explicit FV scheme for dynamic reliability assessment. An implicit FV scheme has been proposed by Eymard *et al.* [32] to assess the marginal distribution of a process describing the time evolution of a hybrid system.

In this paper, we develop the MC simulation method and the FV scheme to solve a model for system reliability analysis considering degradation dependence, proposed in our previous study [22]. A comparative analysis of the two methods is offered, considering the following evaluation criteria: accuracy, computation time, memory consumption, efficiency, scope of application and ease of implementation. Guidelines for implementing the two methods are developed, based upon the findings of the comparative study.

The reminder of this article is organized as follows. Section 2 introduces the PDMP for systems with degradation dependence. The procedures of MC simulation method and FV scheme to solve the model are presented in Section 3. Section 4 presents the evaluation criteria, the case study and the comparison of the two methods. Section 5 concludes the work.

2. PDMP MODELING OF DEGRADATION WITH DEPENDENCE

Based on the available information/data, two main types of models can be used to represent the degradation processes of components: PBMs and MSMs. We consider a multi-component system consisting of two groups of components. There are M components in the first group $\boldsymbol{L} = \{L_1, L_2, \dots, L_M\}$, whose degradation processes are described PBMs (one for each

component) and N components in the second group $\boldsymbol{K} = \{K_1, K_2, \dots, K_M\}$, whose degradation processes are described by MSMs (one for each component).

2.1 PBMs

For component $L_m \in \boldsymbol{L}$, the vector $\overrightarrow{X_{L_m}}(t)$ containing d_{L_m} time-dependent continuous variables is used to describe its degradation level, whose evolution in time is characterized by a system of first-order differential equations $\dot{\overrightarrow{X_{L_m}}}(t) = \overrightarrow{f_{L_m}}\left(\overrightarrow{X_{L_m}}(t), t \mid \theta_{L_m}\right)$, i.e. physics equations, where θ_{L_m} are the parameters in $\overrightarrow{f_{L_m}}$ representing the environmental influencing factors. $\overrightarrow{X_{L_m}}(t)$ contains degradation variables such as crack length [7] and wear area [6], and physical variables such as velocity and force [5], which influence the evolution of the degradation variables. The generic component L_m fails when $\overrightarrow{X_{L_m}}(t)$ exceeds the degradation threshold $\overrightarrow{x_{L_m}}^* = \left(x_{L_m}^{1\ *}, x_{L_m}^{2\ *}, \dots, x_{L_m}^{d_{L_m}\ *}\right)$.

2.2 MSMs

For component $K_n \in \boldsymbol{K}$, the vector $Y_{K_n}(t)$ is used to describe its degradation level, taking values from a finite state set denoted by $S_{K_n} = \{0, 1, \dots, d_{K_n}\}$, where d_{K_n} is the perfect functioning state and 0 is the complete failure state. The component is partially functioning in all generic intermediate states. Markov processes [10] and semi-Markov processes [9, 33] are widely used in practice as MSMs. The transition rates $\lambda_i\left(j \mid \theta_{K_n}\right), \forall\, i, j \in S_{K_n}, i > j$ are used to describe the speed of degradation from state i to state j, where θ_{K_n} represents the environmental influencing factors and the related coefficients. The generic component K_n fails when $Y_{K_n}(t)$ reaches the state 0.

2.3 PDMP for systems with dependence

The degradation levels of one component may influence the degradation dynamics of the others (e,g, the degradation levels of the components in the first group may influence the transition rates of the degradation processes of the second group, and the degradation states of the second group may influence the evolution trajectories of the continuous degradation variables in the first group). PDMP can be employed to model this type of interdependence [22]. The overall degradation processes of the system are presented as

$$\vec{Z}(t) = \begin{pmatrix} \begin{pmatrix} \overrightarrow{X_{L_1}}(t) \\ \vdots \\ \overrightarrow{X_{L_M}}(t) \end{pmatrix} = \overrightarrow{X}(t) \\ \begin{pmatrix} Y_{K_1}(t) \\ \vdots \\ Y_{K_N}(t) \end{pmatrix} = \overrightarrow{Y}(t) \end{pmatrix} \in \boldsymbol{E} = \mathbb{R}^{d_L} \times \boldsymbol{S} \tag{1}$$

where $\boldsymbol{E}$ is the space combining $\mathbb{R}^{d_L}$ ($d_L = \sum_{m=1}^{M} d_{L_m}$) and $\boldsymbol{S} = \{0, 1, \dots, d_S\}$ ($\boldsymbol{S} = \prod_{n=1}^{N} \boldsymbol{S}_{K_n}$). The evolution of $\vec{Z}(t)$ has two parts: (1) the stochastic behavior of $\vec{Y}(t)$ and (2) the deterministic behavior of $\overrightarrow{X}(t)$ between two consecutive jumps of $\vec{Y}(t)$, given $\vec{Y}(t)$. The

first process is governed by the transition rates of $\vec{Y}(t)$, which depend on the degradation states of all the components as follows:

$$\lim_{\Delta t \to 0} P\left(\vec{Y}(t+\Delta t) = \vec{j} \,\middle|\, \overrightarrow{X}(t), \vec{Y}(t) = \vec{\imath}, \boldsymbol{\theta_K} = \prod_{n=1}^{N} \boldsymbol{\theta}_{K_n}\right)/\Delta t$$
$$= \lambda_{\vec{\imath}}\left(\vec{j} \mid \overrightarrow{X}(t), \boldsymbol{\theta_K}\right), \forall\, t \geq 0, \vec{\imath}, \vec{j} \in \boldsymbol{S}, \vec{\imath} \neq \vec{j} \tag{2}$$

The second process is described by the deterministic physic equations, which depend on the degradation states of all the components as follows:

$$\dot{\vec{X}}(t) = \begin{pmatrix} \overrightarrow{\dot{X}_{L_1}}(t) \\ \vdots \\ \overrightarrow{\dot{X}_{L_M}}(t) \end{pmatrix} = \begin{pmatrix} \overrightarrow{f_{L_1}^{\vec{Y}(t)}}\left(\overrightarrow{X}(t), t \mid \boldsymbol{\theta}_{L_1}\right) \\ \vdots \\ \overrightarrow{f_{L_M}^{\vec{Y}(t)}}\left(\overrightarrow{X}(t), t \mid \boldsymbol{\theta}_{L_M}\right) \end{pmatrix}$$
$$= \overrightarrow{f_L^{\vec{Y}(t)}}\left(\overrightarrow{X}(t), t \mid \boldsymbol{\theta_L} = \prod_{m=1}^{M} \boldsymbol{\theta}_{L_m}\right) \tag{3}$$

Let T_k denote the k-th transition time of the process $\vec{Y}(t)$. $\left\{\overrightarrow{Z_k}, T_k\right\}_{k\geq 0}$ is, then, a Markov renewal process [26] defined on the space $E \times \mathbb{R}^+$, since the probability that the whole system will step to state $\vec{j}$ from state $\vec{\imath}$ in the time interval $[T_n, T_n + \Delta t]$, given $\left\{\overrightarrow{Z_k}, T_k\right\}_{k\leq n}$ is:

$$P\left[\overrightarrow{Z_{n+1}} = \vec{j}, T_{n+1} \in [T_n, T_n + \Delta t] \mid \left\{\overrightarrow{Z_k},\ T_k\right\}_{k\leq n-1}, \left\{\overrightarrow{Z_n} = \vec{\imath},\ T_n\right\}\right]$$
$$= P\left[\overrightarrow{Z_{n+1}} = \vec{j}, T_{n+1} \in [T_n, T_n + \Delta t] \mid \overrightarrow{Z_n} = \vec{\imath}\right]$$
$$\forall\, n \geq 0, \vec{\imath}, \vec{j} \in \boldsymbol{E}, \vec{\imath} \neq \vec{j} \tag{4}$$

The process $\vec{Z}(t)$ that takes values in $\boldsymbol{E}$ is a Piecewise-Deterministic Process (PDP), since it can be written as follows [26]:

$$\vec{Z}(t) = \varphi\left(\overrightarrow{Z_k}, t - T_k\right),\ for\ t \in [T_k, T_{k+1}[,\ \forall\, k \in \mathbb{N} \tag{5}$$

and $\vec{Z}(t)$ is a PDMP on the condition that φ satisfies the following [26]:

$$\varphi(\vec{y}, t+s) = \varphi(\varphi(\vec{y}, t), s),\ \forall t, s \geq 0, \vec{y} \in \boldsymbol{E} \tag{6}$$

This is especially true in our case, as φ is the solution of a first-order ordinary differential equations system [34].

Let $\boldsymbol{\mathcal{F}}$ denote the space of the failure states of $\vec{Z}(t)$: then, the reliability of the system at time t is defined as follows:

$$R(t) = P[\vec{Z}(s) \notin \boldsymbol{\mathcal{F}}, \forall s \leq t] \tag{7}$$

3. METHODS FOR RELIABILITY ASSESSMENT

Analytically solving the PDMP is a difficult task due to the complexity in the system behavior[27], with stochastic state transitions occurring in the components modeled by MSMs and time-dependent evolutions of the characteristic variables in the components modeled by PBMs. In this section, the procedures of the MC simulation method and FV scheme to solve the model are presented.

3.1 MC simulation method for solving PDMP

To apply the MC simulation method, eq. (4) is written as follows:

$$P\left[\overrightarrow{Z_{n+1}} \in B, T_{n+1} \in [T_n, T_n + \Delta t] \mid \overrightarrow{Z_n} = \vec{\imath}, \boldsymbol{\theta_K}\right] = \iint_{B*[0,\Delta t]} N\left(\vec{\imath}, \overrightarrow{dz}, ds \mid \boldsymbol{\theta_K}\right) \quad \forall\, n \geq 0, \Delta t \geq 0, \vec{\imath} \in \boldsymbol{E}, B \in \varepsilon \tag{8}$$

where ε is a σ-algebra of $\boldsymbol{E}$ [26] and $N\left(\vec{\imath}, \overrightarrow{dz}, ds \mid \boldsymbol{\theta_K}\right)$ is a semi-Markov kernel on $\boldsymbol{E}$, which verifies that $\iint_{\boldsymbol{E}*[0,\Delta\, t]} N(\vec{\imath}, \overrightarrow{dz}, ds \mid \boldsymbol{\theta_K}) \leq 1, \forall\, \Delta t \geq 0, \vec{\imath} \in \boldsymbol{E}$. It can be further developed as:

$$N\left(\vec{\imath}, \overrightarrow{dz}, ds \mid \boldsymbol{\theta_K}\right) = dF_{\vec{\imath}}(s \mid \boldsymbol{\theta_K})\beta\left(\vec{\imath}, s, \overrightarrow{dz} \mid \boldsymbol{\theta_K}\right) \tag{9}$$

where

$$dF_{\vec{\imath}}(s \mid \boldsymbol{\theta_K}) \tag{10}$$

is the probability density function of $T_{n+1} - T_n$ given $\overrightarrow{Z_n} = \vec{\imath}$ and

$$\beta\left(\vec{\imath}, s, \overrightarrow{dz} \mid \boldsymbol{\theta_K}\right) \tag{11}$$

is the conditional probability of state $\overrightarrow{Z_{n+1}}$ given $T_{n+1} - T_n = s$.

Then, the MC simulation method can be used to estimate the reliability of the system within a certain mission time T_{miss}, given the initial system state $\overrightarrow{Z_0}$ at time $T_0 = 0$. The method to simulate the behavior of the system consists in sampling the transition time from eq. (10) and the arrival state from eq. (11) for the components in the second group and, then, using the physics eq. (3) to calculate the evolution of the components in the first group within the transition times. Each simulation trial continues until the time of system evolution reaches T_{miss} or until the system enters the failure space $\boldsymbol{\mathcal{F}}$, event whose occurrence is recorded for the statistical estimation of the system reliability.

3.1.1 The simulation procedure

The procedure of the MC simulation method is as follows:

Set N_{max} (the maximum number of replications) and $k = 0$ (index of MC trials)

Set $k' = 0$ (number of MC trials that end in failure state)

While $k < N_{max}$

Initialize the system by setting $\overrightarrow{Z'} = \begin{pmatrix} \vec{X}(0) \\ \vec{Y} \end{pmatrix}$ (initial system state) and the time $T = 0$ (initial system time)

Set $t' = 0$ (state holding time)

While $T < T_{miss}$

Sample a t' by using the probability density function (10)

Sample an arrival state $\overrightarrow{Y'}$ for stochastic process $\vec{Y}(t)$ from all possible states, by using the conditional probability function (11)

Set $T = T + t'$

Calculate $\overrightarrow{X}(t)$ in the interval $[T - t', T]$ by using the physics equations eq. (3)

Set $\overrightarrow{Z'} = \begin{pmatrix} \overrightarrow{X}(T) \\ \overrightarrow{Y'} \end{pmatrix}$

If $T \leq T_{miss}$

If $\exists t \in [T - t', T], \vec{Z}(t) = \begin{pmatrix} \overrightarrow{X}(t) \\ \vec{Y} \end{pmatrix} \in \boldsymbol{\mathcal{F}}$

Set $k' = k' + 1$

Break

End if

Else (when $T > T_{miss}$)

If $\exists t \in [T - t', T_{miss}], \vec{Z}(t) = \begin{pmatrix} \overrightarrow{X}(t) \\ \vec{Y} \end{pmatrix} \in \boldsymbol{\mathcal{F}}$

Set $k' = k' + 1$

Break

End if

End if

Set $\vec{Y} = \overrightarrow{Y'}$

End While

Set $k = k + 1$

End While □

To calculate the value of $\overrightarrow{X}(t)$, Runge-Kutta methods can be applied for the numerical solution of the ordinary differential equations [35, 36]. The estimated component reliability at time T_{miss} can be obtained by

$$\hat{R}(T_{miss}) = 1 - k'/N_{max} \tag{12}$$

where *k*' represents the number of trials that end in the failure state of the system and the sample variance is [37]:

$$var_{\hat{R}(T_{miss})} = \hat{R}(T_{miss})(1 - \hat{R}(T_{miss}))/(N_{max} - 1) \tag{13}$$

3.2 FV scheme for solving PDMP

The MC simulation method is conceptually easy to apply and without particular restrictions on the dimension of PDMP. On the contrary, it can be quiet time-consuming because of the

repetition of many trials in order to get a satisfactory accuracy in the system reliability estimate.

An FV scheme discretizing the state space of the continuous variables and the time space of PDMP is an alternative that in certain cases can lead to results comparable to the MC simulation method, but in significantly shorter computing times. Here, we employ an explicit FV scheme for system reliability estimation [31].

3.2.1 Assumptions

This approach can be applied under the following assumptions:

- The transition rates $\lambda_{\vec{i}}(\vec{j} \mid \cdot, \boldsymbol{\theta_K}), \forall \vec{i}, \vec{j} \in \boldsymbol{S}$ are continuous and bounded functions from $\mathbb{R}^{d_L}$ to $\mathbb{R}^+$.
- The physic equations $\overrightarrow{f_L^{\vec{i}}}(\cdot,\cdot \mid \boldsymbol{\theta}_L), \forall \vec{i} \in \boldsymbol{S}$ are continuous functions from $\mathbb{R}^{d_L} \times \mathbb{R}^+$ to $\mathbb{R}^{d_L}$ and locally Lipschitz continuous.
- The physic equations $\overrightarrow{f_L^{\vec{i}}}(\cdot, t \mid \boldsymbol{\theta}_L), \forall \vec{i} \in \boldsymbol{S}$ are sub-linear, i.e. there are some $V_1 > 0$ and $V_2 > 0$ such that
$$\forall \vec{x} \in \mathbb{R}^{d_L}, t \in \mathbb{R}^+ \left| \overrightarrow{f_L^{\vec{i}}}(\vec{x}, t \mid \boldsymbol{\theta}_L) \right| \leq V_1(\|\vec{x}\| + |t|) + V_2$$
- The functions $div(\overrightarrow{f_L^{\vec{i}}}(\cdot,\cdot \mid \boldsymbol{\theta}_L)), \forall \vec{i} \in \boldsymbol{S}$ are almost everywhere bounded in absolute value by some real value $D > 0$ (independent of $\vec{i}$).

3.2.2 Solution approach

For ease of notation, first we let $\overrightarrow{g^{\vec{i}}}(\cdot,\cdot)$: $\mathbb{R}^{d_L} \times \mathbb{R} \to \mathbb{R}^{d_L}$ denote the solution of

$$\frac{\partial}{\partial t}\overrightarrow{g^{\vec{i}}}(\vec{x}, t \mid \boldsymbol{\theta}_L) = \overrightarrow{f_L^{\vec{i}}}\left(\overrightarrow{g^{\vec{i}}}(\vec{x}, t \mid \boldsymbol{\theta}_L), t \,\middle|\, \boldsymbol{\theta}_L\right), \forall \vec{i} \in \boldsymbol{S}, \vec{x} \in \mathbb{R}^{d_L}, t \in \mathbb{R} \quad (14)$$

with

$$\overrightarrow{g^{\vec{i}}}(\vec{x}, 0 \mid \boldsymbol{\theta}_L) = \vec{x}, \forall \vec{i} \in \boldsymbol{S}, \vec{\mathrm{x}} \in \mathbb{R}^{\mathrm{d_L}} \quad (15)$$

and $\overrightarrow{g^{\vec{i}}}(\vec{x}, t \mid \boldsymbol{\theta}_L)$ represents the deterministic evolution of $\overrightarrow{X}(t)$ at time *t*, starting from the condition $\vec{x}$ and while the processes $\vec{Y}(t)$ hold in state $\vec{i}$.

The state space $\mathbb{R}^{d_L}$ of continuous variables $\overrightarrow{X}(t)$ is divided into an admissible mesh $\mathcal{M}$, which is a family of measurable subsets of $\mathbb{R}^{d_L}$ ($\mathcal{M}$ is a partition of $\mathbb{R}^{d_L}$) such that:

(5) $\bigcup_{A\in\mathcal{M}} A = \mathbb{R}^{d_L}$.
(6) $\forall A, B \in \mathcal{M},\ A \neq B \Rightarrow A \cap B = \emptyset$.
(7) $m_A = \int_A \overrightarrow{dx} > 0, \forall A \in \mathcal{M}$, where m_A is the volume of grid A.
(8) $sup_{A\in\mathcal{M}} diam(A) < +\infty$ where $diam(A) = sup_{\forall \vec{x},\vec{y}\in A}|\vec{x} - \vec{y}|$.

Additionally, the time space $\mathbb{R}^+$ is divided into small intervals $\mathbb{R}^+ = \bigcup_{n=0,1,2,\ldots} [n\Delta t, (n+1)\Delta t[$, by setting the time step $\Delta t > 0$ (the length of each interval).

Let $p_t(d\vec{z} \mid \boldsymbol{\theta} = \boldsymbol{\theta}_L \cup \boldsymbol{\theta}_K)$ denote the probability distribution of $\vec{Z}(t)$. The numerical scheme aims at constructing an approximate value $\rho_t(\overrightarrow{x},\cdot \mid \boldsymbol{\theta})d\overrightarrow{x}$ for $p_t(d\overrightarrow{x},\cdot \mid \boldsymbol{\theta})$, such that

$\rho_t(\overrightarrow{x},\cdot \mid \boldsymbol{\theta})$ is constant on each $A \times \{\vec{\imath}\} \times [n\Delta t, (n+1)\Delta t[, \forall A \in \mathcal{M}, \vec{\imath} \in \boldsymbol{S}$:

$$\rho_t(\overrightarrow{x},\vec{\imath} \mid \boldsymbol{\theta}) = P_n(A,\vec{\imath} \mid \boldsymbol{\theta}), \forall \vec{\imath} \in \boldsymbol{S}, \vec{x} \in A, t \in [n\Delta t, (n+1)\Delta t[\quad (16)$$

$P_0(A,\vec{\imath} \mid \boldsymbol{\theta}), \forall \vec{\imath} \in \boldsymbol{S}, A \in \mathcal{M}$ is defined as follows:

$$P_0(A,\vec{\imath} \mid \boldsymbol{\theta}) = \int_A p_0(d\overrightarrow{x},\vec{\imath} \mid \boldsymbol{\theta}) / m_A \quad (17)$$

Then, $P_{n+1}(A,\vec{\imath} \mid \boldsymbol{\theta}), \forall \vec{\imath} \in \boldsymbol{S}, A \in \mathcal{M}, n \in \mathbb{N}$ can be calculated considering the deterministic evaluation of $\overrightarrow{X}(t)$ and the stochastic evolution of $\overrightarrow{Y}(t)$ based on $P_n(\mathcal{M},\vec{\imath} \mid \boldsymbol{\theta})$ by the Chapman-Kolmogorov forward equation, as follows:

$$P_{n+1}(A,\vec{\imath} \mid \boldsymbol{\theta}) = \frac{1}{1+\Delta t b_A^{\vec{\imath}}} \widehat{P_{n+1}}(A,\vec{\imath} \mid \boldsymbol{\theta}) + \Delta t \sum_{\vec{\jmath} \in \boldsymbol{S}} \frac{a_A^{\vec{\jmath}\vec{\imath}}}{1+\Delta t b_A^{\vec{\jmath}}} \widehat{P_{n+1}}(A,\vec{\jmath} \mid \boldsymbol{\theta}) \quad (18)$$

where

$$a_A^{\vec{\jmath}\vec{\imath}} = \int_A \lambda_{\vec{\jmath}}(\vec{\imath},\vec{x} \mid \boldsymbol{\theta}_K) \overrightarrow{dx} / m_A, \forall \vec{\imath} \in \boldsymbol{S}, A \in \mathcal{M} \quad (19)$$

is the average transition rate from state $\vec{\jmath}$ to state $\vec{\imath}$ for grid A,

$$b_A^{\vec{\imath}} = \sum_{\vec{\jmath} \neq \vec{\imath}} a_A^{\vec{\imath}\vec{\jmath}}, \forall \vec{\imath} \in \boldsymbol{S}, A \in \mathcal{M} \quad (20)$$

is the average transition rate out of state $\vec{\imath}$ for grid A,

$$\widehat{P_{n+1}}(A,\vec{\imath} \mid \boldsymbol{\theta}) = \sum_{B \in \mathcal{M}} m_{BA}^{\vec{\imath}} P_n(B,\vec{\imath} \mid \boldsymbol{\theta}) / m_A, \ \forall \vec{\imath} \in \boldsymbol{S}, A \in \mathcal{M} \quad (21)$$

is the approximate value of probability density function on $\{\vec{\imath}\} \times [(n+1)\Delta t, (n+2)\Delta t[\times A$ according to the deterministic evolution of $\overrightarrow{X}(t)$,

$$m_{BA}^{\vec{\imath}} = \int_{\{\vec{y} \in B \mid \overrightarrow{g^{\vec{\imath}}}(\vec{y},\Delta t \mid \boldsymbol{\theta}_L) \in A\}} \overrightarrow{dy}, \forall \vec{\imath} \in \boldsymbol{S}, A, B \in \mathcal{M} \quad (22)$$

is the volume of the part of grid B which will enter grid A after time Δt, according to the deterministic evolution of $\overrightarrow{X}(t)$.

The approximated solution $\rho_t(\overrightarrow{x},\cdot \mid \boldsymbol{\theta})d\overrightarrow{x}$ weakly converges towards $p_t(d\overrightarrow{x},\cdot \mid \boldsymbol{\theta})$ when $\Delta t \to 0$ and $|\mathcal{M}|/\Delta t \to 0$ where $|\mathcal{M}| = sup_{A \in \mathcal{M}} diam(A)$.

The reliability of the system can, then, be calculated as follows:

$$R(t) = \int_{\vec{z} \notin \boldsymbol{F}} p_t(d\vec{z} \mid \boldsymbol{\theta}) \quad (23)$$

The shortcomings of the FV scheme is that it suffers for high dimensional problems and it is relatively more difficult to develop than the MC simulation method.

4. Comparative Study

4.1. Evaluation criteria

The evaluation criteria for the comparative study are accuracy, computation time, memory consumption, scope of application and ease of implementation. The first three attributes are quantitative and the rests are qualitative.

To compute accuracy, we use the results obtained by the MC simulation with 10^5 trials as reference values $x_{reference}$ and compute the relative change of the results x obtained by

another method: $Relative\ change(x, x_{reference}) = (x - x_{reference})/x_{reference}$, where x is the obtained system reliability.

The efficiency is also an important measure of performance. A method is more efficient if it can produce results comparable with the other, but with less computation time (here measured in seconds).

The memory consumption refers to the amount of digital information stored in the computer during the calculation and is measured in kilobytes (KB).

For the scope of application, we consider two case studies: one with high dimension and the other with low dimension, since the two methods mainly differ in their capacity of treating different dimensions of the problem.

The ease of implementation describes how easy it is to implement a method in practice.

4.2. Numerica experiment design

All the numerical experiments are carried out in MATLAB on a PC with an Intel Core 2 Duo CPU at 3.06 GHz and a RAM of 3.07 GB.

We consider MC simulations with 10^3, 10^4 and 10^5 trials (for ease of reference, hereafter named MC1, MC2 and MC3, respectively). The parameters of the FV scheme are problem-dependent. Their tuning can be achieved by gradually decreasing the space step and the time step. To compare the two methods, the parameter setting of FV scheme is first assigned such that it can lead to similar results as MC3, which gives the most accurate results that are used for reference. Then, we consider several parameter settings around it.

4.3. Test cases and results

We consider an important subsystem of a residual heat removal system of a nuclear power plant [38], consisting of a pneumatic valve and a centrifugal pump, which are used in conjunction in a variety of domains for fluid delivery [5, 39]. The degradation model of the pump is the one originally considered in [22] while that of the valve is the physics-based model presented in [5]. Dependence is considered, as a result of discussions with experts: the degradation of the pump can lead it to vibrate [39], which will, in turn, cause the vibration of the valve and, therefore, aggravate the degradation process of the latter [40].

The degradation process of the centrifugal pump is modeled by a continuous-time homogeneous Markov chain with constant transition rates as shown in Fig. 1:

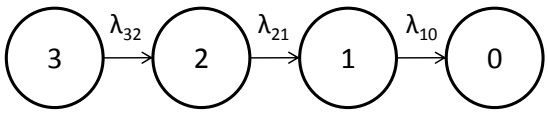

Fig. 1. Degradation process of the pump [22].

The perfect functioning state is denoted with the label ‘3’ and ‘0’ is the label of the complete

failure state. The vibration of the pump caused by degradation is classified into two levels: 'smooth' and 'rough' [41], corresponding to the degradation states '2' and '1', respectively. Let $Y_p(t)$ denote the degradation state of the pump at time t and $\boldsymbol{S}_p = \{0, 1, 2, 3\}$ denote the degradation states set. The values of the degradation transition rates are presented in Table I.

Table I Values of the degradation transition rates of the pump

Parameter	Value
λ_{32}	6.00e-3 /s
λ_{21}	6.00e-3 /s
λ_{10}	6.00e-3 /s

The pneumatic valve refers to a normally-closed and gas-actuated valve with a linear cylinder actuator, which has been studied in [5, 42] and [34] by physics-based modeling. A simplified scheme of the valve is shown in Fig. 2.

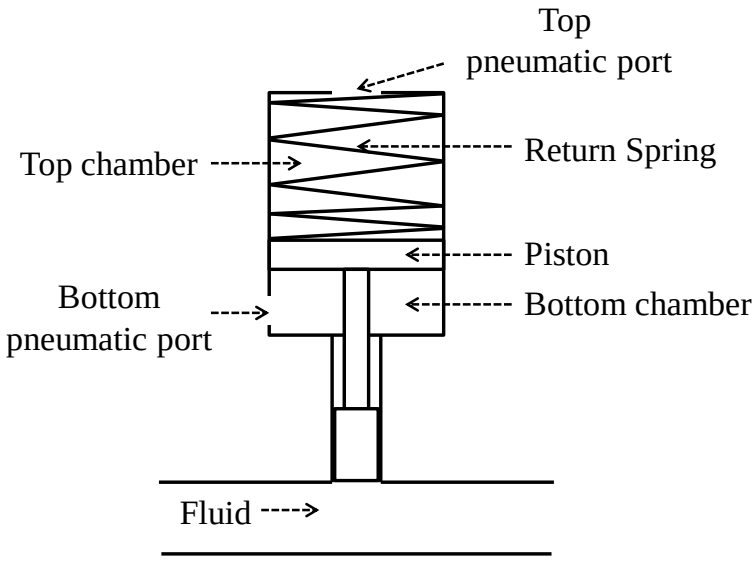

Fig. 2. Simplified scheme of the pneumatic valve [42].

Two case studies considering two different degradation mechanisms of the valve will be carried out in the following section.

4.3.1. Case 1

A common degradation mechanism of the valve is the internal leakage from the seal surrounding the piston [34]. Owing to this, the pneumatic gas can flow between the two chambers therefore influencing the response time and behavior of the valve. The degradation variable of the valve is the equivalent orifice area of the internal leakage of the piston, denoted by $L(t)$, and the degradation process of the valve at time t is described by the following vector:

$$\overrightarrow{X_v}(t) = \begin{pmatrix} L(t) \\ x(t) \\ v(t) \\ m_t(t) \\ m_b(t) \\ t \end{pmatrix} \tag{24}$$

where $x(t)$ is the position of the valve, $v(t)$ is the velocity of the valve, $m_t(t)$ is the mass of the gas in the top chamber, $m_b(t)$ is the mass of the gas in the bottom chamber and t is the running time of the valve. The derivatives of these variables are represented by:

$$\overrightarrow{\dot{X}_v}(t) = \begin{pmatrix} \dot{L}(t) \\ v(t) \\ a(t) \\ f_t(t) \\ f_b(t) \\ 1 \end{pmatrix} \tag{25}$$

where $a(t)$ is the valve acceleration, $f_t(t)$ and $f_b(t)$ are the mass flows going into the top and bottom chambers, respectively. The details of the physic functions governing the evolutions of the above variables are as follows:

$$\dot{L}(t) = wrv(t)^2 \tag{26}$$

where w is the wear coefficient,

$$a(t) = \frac{1}{m}[\big(p_b(t) - p_t(t)\big)\Big(A_p - L(t)\Big) - mg + \\ -k(x(t) + x_0) - rv(t) + F_c\big(x(t)\big)] \tag{27}$$

where

$$p_b(t) = \frac{m_b(t)R_gT}{V_{b0} + A_p x(t)} \tag{28}$$

is the gas pressure on the bottom of the piston,

$$p_t(t) = \frac{m_t(t)R_gT}{V_{t0} + A_p(L_s - x(t))} \tag{29}$$

is the gas pressure on the top of the piston,

$$F_c\big(x(t)\big) = \begin{cases} k_c(-x(t)), & if\ x(t) < 0 \\ 0, & if\ 0 \le x(t) \le L_s \\ -k_c(x(t) - L_s), & if\ x(t) > L_s \end{cases} \tag{30}$$

is the contact force,

$$f_t(t) = f_g(u_t(t), p_t(t), A_s) + f_g(p_b(t), p_t(t), L(t)) \tag{31}$$

$$f_b(t) = f_g(u_b(t), p_b(t), A_s) + f_g(p_t(t), p_b(t), L(t)) \tag{32}$$

where $u_t(t)$ and $u_b(t)$ are the pressures on the top and bottom pneumatic ports, respectively, alternating between P_{sup} and P_{atm} depending on the command (opening command: $u_t(t) = P_{atm}$ and $u_b(t) = P_{sup}$; closing command: $u_t(t) = P_{sup}$ and $u_b(t) = P_{atm}$), and f_g defines the gas flow through an orifice as follows:

$$f_g(p_1, p_2, A) = \begin{cases} \varepsilon P C_s A \sqrt{\frac{\gamma}{zR_gT}\left(\frac{2}{\gamma+1}\right)^{\frac{\gamma+1}{\gamma-1}}}, & if\ \delta \le \left(\frac{2}{\gamma+1}\right)^{\frac{\gamma}{\gamma-1}} \\ \varepsilon P C_s A \sqrt{\frac{\gamma}{zR_gT}\left(\frac{2}{\gamma-1}\right)\left(\delta^{\frac{2}{\gamma}} - \delta^{\frac{\gamma+1}{\gamma}}\right)}, & if\ \delta > \left(\frac{2}{\gamma+1}\right)^{\frac{\gamma}{\gamma-1}} \end{cases} \tag{33}$$

where $\begin{cases} P = \max(p_1, p_2) \\ \delta = \frac{\min(p_1, p_2)}{\max(p_1, p_2)} \\ \varepsilon = sgn(p_1 - p_2) \end{cases}$.

The parameters definitions and numerical values related to the internal leakage degradation are presented in Table II below.

Table II Parameter Definitions and Values of Internal Leakage variables [5]

Parameter – Definition	Value
g – acceleration due to gravity	9.8 m/s
P_{sup} – supply pressure	5.27e6 Pa
P_{atm} – atmospheric pressure	1.01e5 Pa
m – mass of the moving parts of the valve	50 kg
r – coefficient of kinetic friction	6.00e3 Ns/m
k – spring constant	4.80e4 N/s
k_c – large spring constant associated with the flexible seals	1.00e8 N/s
x_0 – amount of spring compression when the valve is closed	0.254 m
L_s – fully open position of the valve	0.1 m
A_p – surface area of the piston	8.10e-3 m^2
V_{t0} – minimum gas volume of the top chamber	8.11e-4 m^3
V_{b0} – minimum gas volume of the bottom chamber	8.11e-4 m^3

R_g – gas constant for the pneumatic gas	296 J/K/kg
T – ideal gas temperature	293 K
γ – ration of specific heats	1.4
z – gas compressibility factor	1
A_s – orifice area of the pneumatic port	1.00e-5 m^2
w – wear coefficient	6e-9 m/N
C_s – flow coefficient	0.1

At the initial stage, the valve is set to the fully closed position with the values:

$$\overrightarrow{X_v}(0) = \begin{pmatrix} L(0) \\ 0 \\ 0 \\ \frac{P_{sup}(L_s A_p + V_{t0})}{R_g T} \\ \frac{P_{atm} V_{b0}}{R_g T} \\ 0 \end{pmatrix} \tag{34}$$

The threshold L^* for the internal leakage of the piston $L(t)$ is defined as the value above which ($L(0) > L^*$) the valve cannot reach the fully open position within the 15s time limit after an opening command is executed at time $t = 0s$. The size of the internal leakage is assumed to be constant during the opening procedure ($\dot{L}(t) = 0,\ 0 \le t \le 15$) [34] to obtain a conservative threshold of $L^* = 3.20e-6\ m^2$ in this case. The behavior of the valve within 15s with different values of $L(0)$ is shown in Fig. 3.

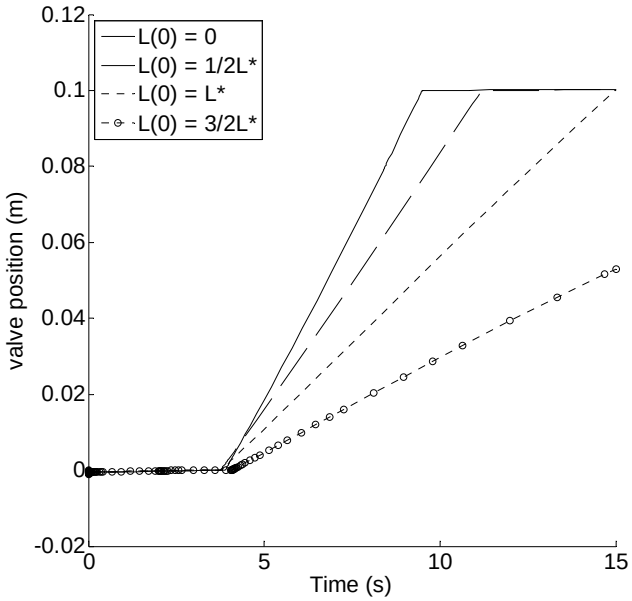

Fig. 3. Valve position for different sizes of the internal leakage.

4.3.1.1.PDMP for the degradation processes of the system considering dependence

The degradation processes of the whole system are modeled by PDMP as follows:

$$\vec{Z}(t) = \begin{pmatrix} \overrightarrow{X_v}(t) \\ Y_p(t) \end{pmatrix} = \begin{pmatrix} L(t) \\ x(t) \\ v(t) \\ m_t(t) \\ m_b(t) \\ t \\ Y_p(t) \end{pmatrix} \in \mathbb{R}^6 \times \boldsymbol{S}_p \tag{35}$$

and

$$\dot{\vec{Z}}(t) = \begin{pmatrix} \overrightarrow{\dot{X}_v}(t) \\ 0 \end{pmatrix} = \begin{pmatrix} \dot{L}'(t, Y_p(t)) \\ v(t) \\ a(t) \\ f_t(t) \\ f_b(t) \\ 1 \\ 0 \end{pmatrix} \tag{36}$$

where $\dot{L}'(t, Y_p(t))$ is the derivative of the internal leakage of the valve, with consideration of the degradation dependence between the valve and the pump whereas the development of the internal leakage of the valve is dependent on the degradation state of the pump,

$$\dot{L}'\left(t, Y_p(t)\right) = w(1 + \beta_{Y_p(t)}) r v(t)^2 \tag{37}$$

where $\beta_{Y_p(t)}$ is the relative increment of the developing rate of the internal leakage caused by the vibration of the pump (if we ignore the degradation dependence, then $\beta_{Y_p(t)} = 0$). For illustrative purposes, we assume that $\beta_3 = \beta_0 = 0$, $\beta_2 = 10\%$ and $\beta_1 = 20\%$. The times between two consequent jumps of PDMP follow the exponential distribution with constant degradation transition rates of the pump. The space of the failure states of $\vec{Z}(t)$ is $\boldsymbol{\mathcal{F}} = \mathbb{R}^6 \times \{0\} \cup [L^*, +\infty) \times \mathbb{R}^5 \times \boldsymbol{S}_p$.

4.3.1.2. Results and analysis

Due to the large dimension of the PDMP and the complex formulation of the physic equations, the MC simulation method is adopted to solve the model.

The initial state of the system is as follows:

$$\overrightarrow{Z'} = \begin{pmatrix} \overrightarrow{X_v}(0) \\ Y_p(0) \end{pmatrix} = \begin{pmatrix} L(0) = 0 \\ 0 \\ 0 \\ \frac{P_{sup}(L_s A_p + V_{t0})}{R_g T} \\ \frac{P_{atm} V_{b0}}{R_g T} \\ 0 \\ 3 \end{pmatrix} \tag{38}$$

which means that the two components are both in perfect state and the valve is in the fully closed position. The command of the valve is a 30s-periodic-signal and the valve is commanded to open in the first half-period and to close in the second half. The pump is functioning until it reaches the failure state ‘0’.

MC1, MC2 and MC3 are applied for the system reliability estimation over a time horizon of $T_{miss} = 700\ s$. The results are shown in Fig. 4. In order to appreciate the differences in the curves plotted in Fig. 4, the results between 460 s and 560 s are presented in Fig. 5.

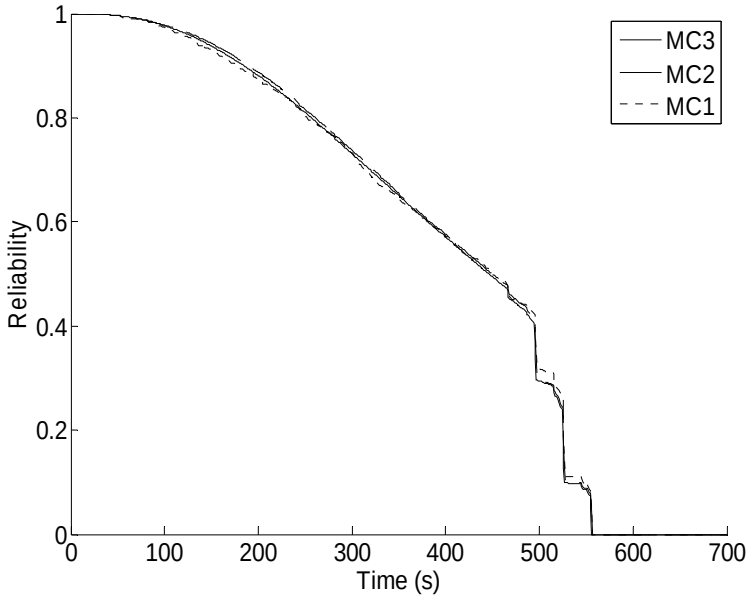

Fig. 4. System reliability obtained by MC1, MC2 and MC3.

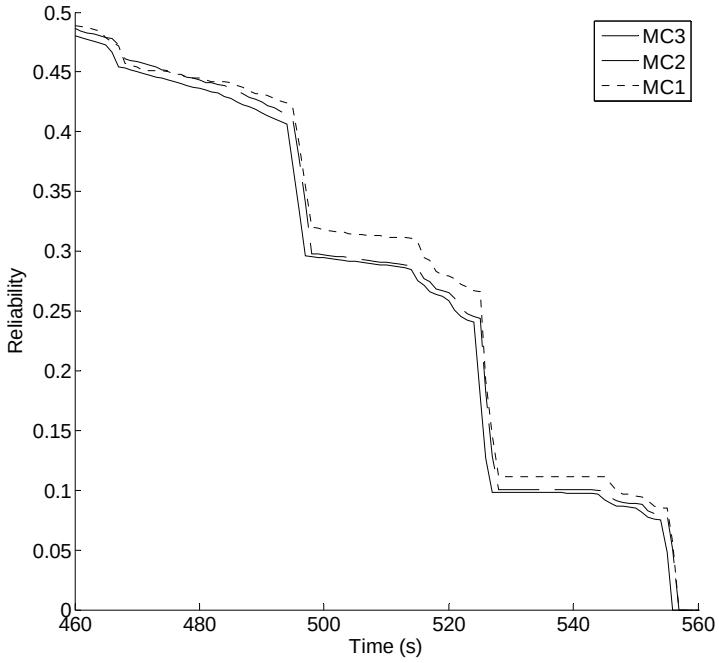

Fig. 5. System reliability with common degradation cause and degradation dependence obtained by MC1, MC2 and MC3 between 460 s and 560 s.

In Fig. 6, we compare the system reliability with/without dependence, obtained by MC3. From the Figure, we can see that before 465.67 s (point A) the two curves coincide and the

system reliability is equal to the reliability of the pump. After that time, valve failures begin to occur in some simulation trials, corresponding to realizations in which the pump jumps to state '1' very soon and stays there until the valve fails. The system reliability, then, experiences three sharp decreases at around 497.39 s (point B), 526.77 s (point C) and 556.45 s (point D) respectively, and the system is definitely failed afterwards. The longest failure time of the valve is at point D, corresponding to the situation when the pump stays in the initial state '3' from the beginning until the failure of the valve. It is seen that neglecting degradation dependence might underestimate the system reliability.

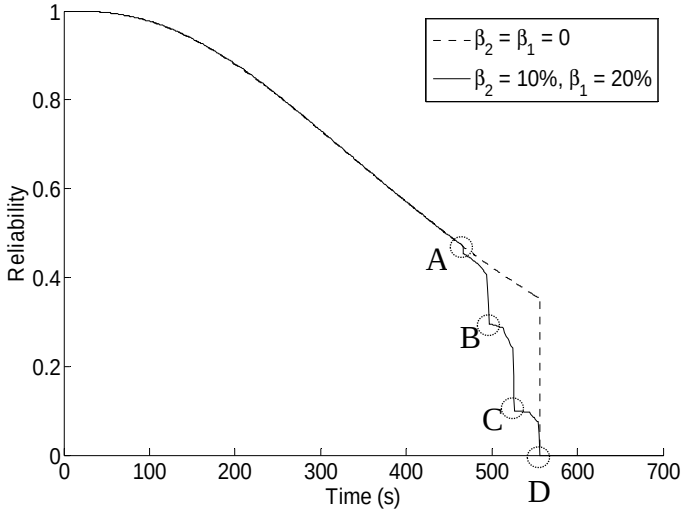

Fig. 6. System reliability with/without dependence.

4.3.2. Case 2

In this case study, the external leakage at the actuator connections to the bottom pneumatic port due to corrosion and other environmental factors is considered as relevant degradation mechanism, [5].

Let $D_b(t)$ denote the area of the leakage hole at the bottom pneumatic port at time *t*; the development of the leakage size is described by:

$$\dot{D_b}(t) = \omega_b \tag{39}$$

where $\omega_b = 1e-8\, m2/s$ is the original wear coefficient. The threshold of the area of the leakage hole can be calculated as $D_b^* = 1.06\text{e}-5\, m^2$ by using the same criteria given in Section 4.1.

4.3.2.1. PDMP for the degradation processes of the system considering dependence

The degradation processes of the whole system are modeled by PDMP as follows:

$$\vec{Z}(t) = \begin{pmatrix} D_b(t) \\ Y_p(t) \end{pmatrix} \in \mathbb{R}^+ \times \boldsymbol{S}_p \tag{40}$$

and

$$\dot{\vec{Z}}(t) = \begin{pmatrix} \dot{D}_b'(t) \\ 0 \end{pmatrix} = \begin{pmatrix} \omega_b(1 + \alpha_{Y_p(t)}) \\ 0 \end{pmatrix} \tag{41}$$

where $\alpha_{Y_p(t)}$ is the relative increment of the developing rate of the external leakage at the bottom pneumatic port caused by the vibration of the pump at the degradation state '2' or '1' (if we ignore the degradation dependence, then $\alpha_{Y_p(t)} = 0$). We assume that $\alpha_3 = \alpha_0 = 0$, $\alpha_2 = 10\%$ and $\alpha_1 = 20\%$. The times between two consequent jumps of PDMP follow the exponential distribution with constant degradation transition rates of the pump. The space of the failure states of $\vec{Z}(t)$ is $\boldsymbol{\mathcal{F}} = \mathbb{R}^+ \times \{0\} \cup [D_b^*, +\infty) \times \boldsymbol{S}_p$.

The initial state of the system is assumed as follows:

$$\overrightarrow{Z_0} = \begin{pmatrix} D_b(0) \\ Y_p(0) \end{pmatrix} = \begin{pmatrix} 0 \\ 3 \end{pmatrix} \tag{42}$$

which means that the two components are both in their perfect state.

4.3.2.2.Results and analysis

MC simulation method and FV scheme are applied for the estimation of the system reliability over a time horizon of $T_{miss} = 1000\ s$. The results obtained by MC1, MC2 and MC3 are shown in Fig. 7.

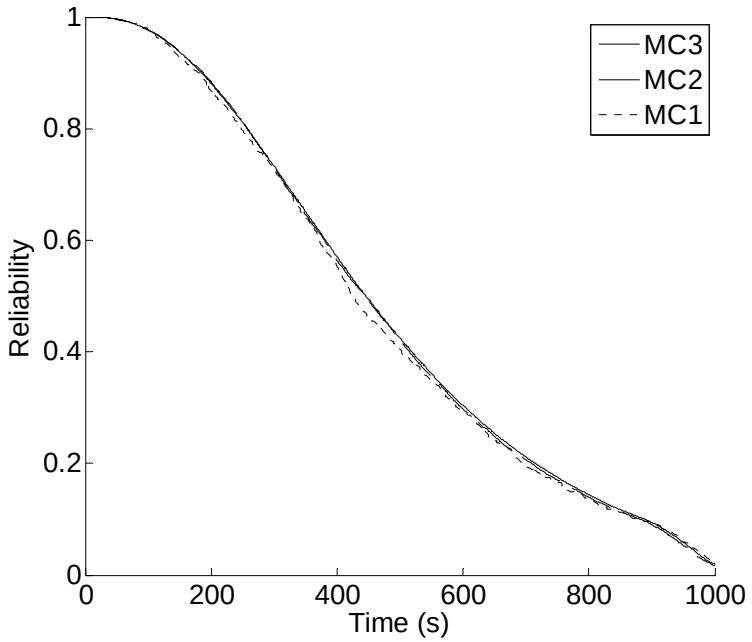

Fig. 7. System reliability obtained by MC1, MC2 and MC3.

For the FV scheme, the state space $\mathbb{R}^+$ of $D_b(t)$ has been divided into an admissible mesh $\mathcal{M} = \bigcup_{n=0,1,2,\dots} [n\Delta x, (n+1)\Delta x[$ and the time space $\mathbb{R}^+$ has been divided into small intervals $\mathbb{R}^+ = \bigcup_{n=0,1,2,\dots} [n\Delta t, (n+1)\Delta t[$. The values of space step Δx and time step Δt can influence the accuracy of the results. We have considered 7 different parameter settings: (1) FV1: $\Delta x = 1e-8, \Delta t = 1$; (2) FV2: $\Delta x = 5e-8, \Delta t = 1$; (3) FV2a: $\Delta x = 10e-8, \Delta t = 1$; (4) FV3: $\Delta x = 1e-8, \Delta t = 5$, (5) FV3a: $\Delta x = 1e-8, \Delta t = 10$, (6) FV4: $\Delta x = 5e-8, \Delta t = 5$ and (7) FV5: $\Delta x = 10e-8, \Delta t = 10$. Their results are shown in Fig. 8-11.

We compare the results obtained by FV1 and MC3 in Fig. 8, where it is shown that FV scheme can lead to results comparable to those of the MC simulation method. The effect of variations in Δx is studied in Fig. 9, where it can be seen that before around 730 s (point A) the three curves match. Up to that time, the system reliability is equal to the reliability of the pump. After that time, $D_b(t)$ approaches the threshold D_b^* and valve failure begins to occur, so that the effect of variations in Δx becomes more distinct since smaller Δx leads to more accurate estimation of $D_b(t)$ and, thus, more accurate estimation of the system reliability. The effect of variation in Δt is studied in Fig. 10, where we can see that the effect of variations in Δt is visible from the beginning, since Δt can influence the estimation of both $D_b(t)$ and $Y_p(t)$ and, thus, influence the estimation of the system reliability from the beginning. The joint effect of variations in Δx and Δt is shown in Fig. 11.

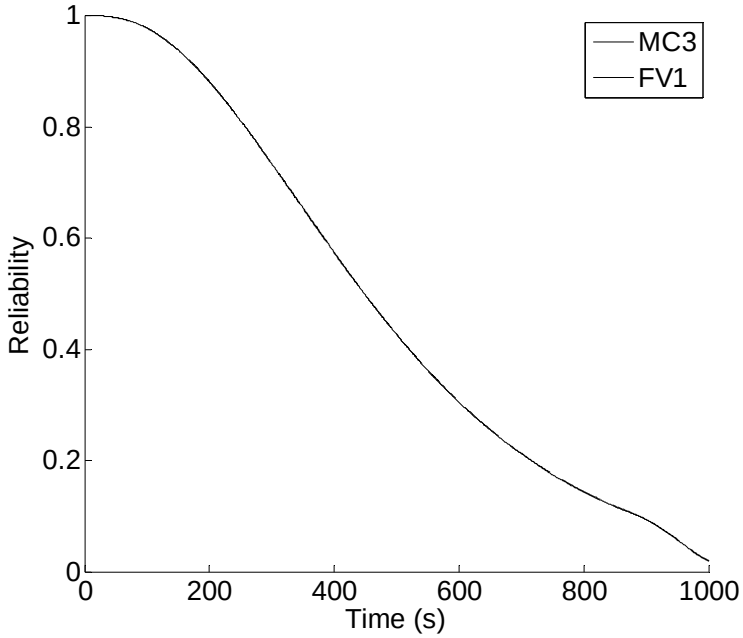

Fig. 8. System reliability obtained by FV1 and MC3.

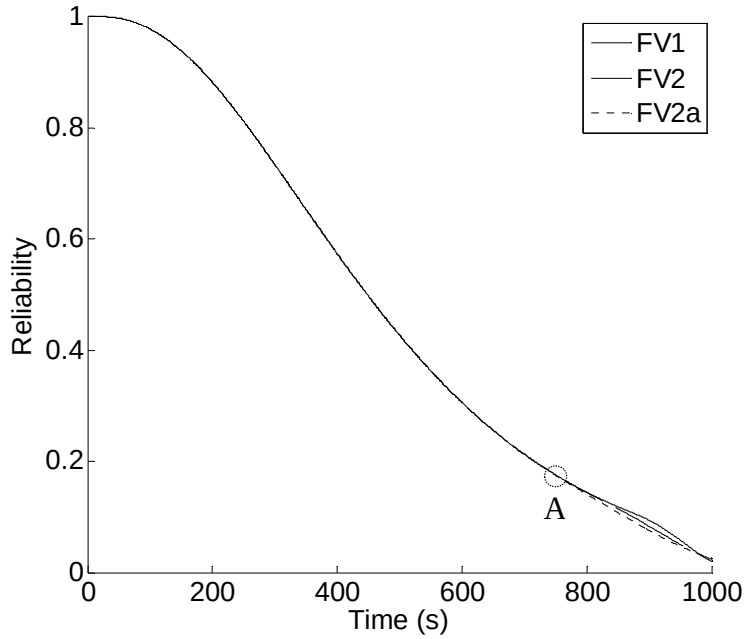

Fig. 9. System reliability obtained by FV1, FV2 and FV2a.

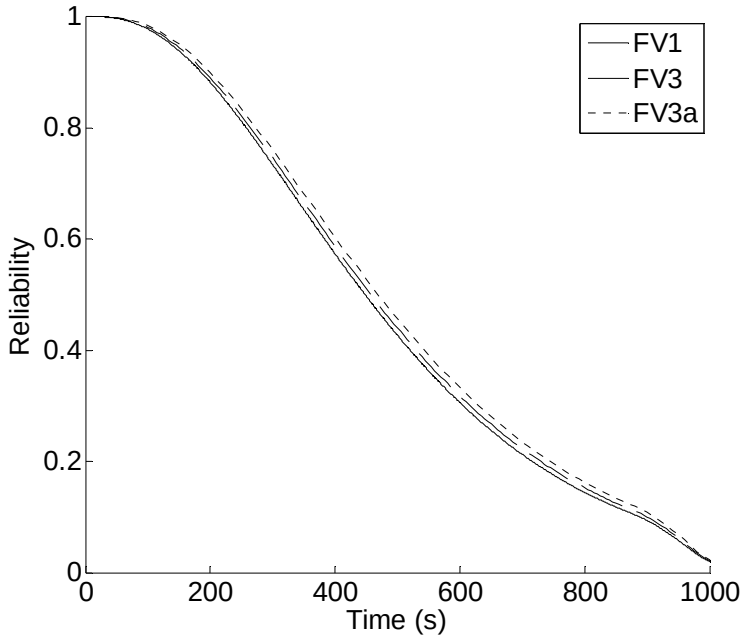

Fig. 10. System reliability obtained by FV1, FV3 and FV3a.

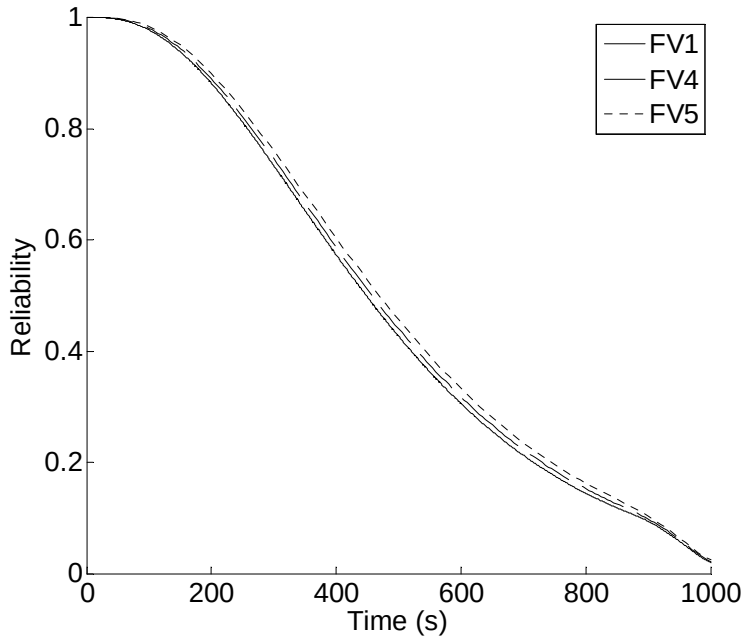

Fig. 11. System reliability obtained by FV1, FV4 and FV5.

4.4. Comparisons

The numerical comparisons of the two methods are reported in Table III. With reference to the results obtained by MC3, as expected that the relative change of the other MC simulation settings decrease as the number of replications is increased and that of FV scheme decreases as the space step Δx and/or the time step Δt is reduced. The average computation time of the two methods shows that the FV scheme is more efficient and less memory demanding than MC simulation for simple and low dimensional problems. However, it should be noted that the memory requirement of the FV scheme is much higher than that of MC simulation method and the FV scheme is sensitive to the space step and time step. The computational expenses of the MC simulation method increase linearly as the number of replications increases and that of FV scheme is almost linear with $\Delta x \cdot \Delta t$.

Table III Comparisons of the system reliability results obtained by MC simulation method and FV scheme

Methods		System reliability at 1000 s	Relative change with respect to MC3	Average computation time (s)	Memory consumption (KB)
MC	MC3	**0.0197**		1.41	8.17

simulation method	MC2	0.0175	11.17%	0.14	8.17
	MC1	0.023	16.75%	0.014	8.17
FV scheme	FV1	0.0199	1.02%	0.17	33.62
	FV2	0.0237	20.30%	0.042	13.26
	FV2a	0.0253	28.43%	0.021	10.72
	FV3	0.0212	7.61%	0.033	27.22
	FV3a	0.0231	17.26%	0.017	26.41
	FV4	0.0218	10.66%	0.0058	6.86
	FV5	0.0241	22.34%	0.00027	3.51

4.5. Guidelines for the use of the MC simulation method and FV scheme

Table IV summarizes the qualitative insights drawn from the comparative studies of the two numerical approaches.

Table IV Comparisons of the two numerical approaches

	MC simulation method	FV scheme
Parameters	Number of replications	Space step, Time step
Accuracy	Medium	High
Computation time	Long	Short
Memory consumption	Low	High
Efficiency	Low	High
Scope of application	Large	Small
Ease of Implementation	Yes	Generally no

The MC simulation method requires a number of replications to achieve a desired level of accuracy, whereas the FV scheme needs to discretize the time space and state space by properly choosing the corresponding step sizes. Due to the discretization, the memory consumption of FV scheme is typically larger than that of the MC simulation method. The MC simulation method is easy to be implemented by the practitioners without restrictions on the dimension of the problem, like for PDMP. In reverse, the price to pay is that the MC simulation method can

be quiet time-consuming. The FV scheme is an alternative that appears to be efficient and lead to results comparable to those of the MC simulation method with acceptable computing time. However, it is unsuited for high-dimensional problems or problems with complex equations describing the deterministic evolution, and it is also relatively difficult to implement and deploy.

Given the above observations, the following guidelines for utilization may be helpful:

- For high dimensional problems or problems with complex equations describing the deterministic evolution, the MC simulation method is preferred.
- For low dimensional problems or problems with simple equations describing the deterministic evolution, the FV scheme is preferred. Note that in some cases the high dimensional problem can be decomposed into several low dimensional ones mutually independent on each other. Then, the FV schemes can be run on low dimensional problems in parallel.

5. CONCLUSIONS

We employ the PDMP approach to model degradation processes of systems subject to degradation dependence. The significance of the method lies in the possibility that it offers to describe the degradation dependence between PBMs, between MSMs and between the two types of models. The MC simulation method and FV scheme have been designed for the system reliability assessment based on the PDMP. Two case studies based on a real industrial system have been solved to illustrate the advantages and limitations of the two numerical approaches. A comparative study has been carried out to study their accuracy, efficiency, memory requirement, scope of application and ease of implementation. Results show that the MC simulation method is easy to be implemented and has wide applicability, since it has no restriction on the dimension of the underlying PDMP modeling the degradation processes. The FV scheme, although relatively difficult to handle and more demanding in terms of computer memory, is computationally more efficient and can lead to results comparable to those of the MC simulation method for simple and low dimensional problems.

As future research, we plan to study acceleration techniques for the MC simulation method, to relieve the computational burden.

References

[1] N. Gebraeel, A. Elwany, and J. Pan, "Residual life predictions in the absence of prior degradation knowledge," *Reliability, IEEE Transactions on,* vol. 58, pp. 106-117, 2009.

[2] J. Lawless and M. Crowder, "Covariates and random effects in a gamma process model with application to degradation and failure," *Lifetime Data Analysis,* vol. 10, pp. 213-227, 2004.

[3] M. Black, A. Brint, and J. Brailsford, "A semi-Markov approach for modelling asset deterioration," *Journal of the Operational Research Society,* vol. 56, pp. 1241-1249, 2005.

[4] M. Chookah, M. Nuhi, and M. Modarres, "A probabilistic physics-of-failure model for prognostic health management of structures subject to pitting and corrosion-fatigue," *Reliability Engineering & System Safety,* vol. 96, pp. 1601-1610, 2011.

[5] M. Daigle and K. Goebel, "A model-based prognostics approach applied to pneumatic valves," *International Journal of Prognostics and Health Management,* vol. 2, pp. 1-16, 2011.

[6] M. Daigle and K. Goebel, "Multiple damage progression paths in model-based prognostics," in *Aerospace Conference, 2011 IEEE*, 2011, pp. 1-10.

[7] E. Keedy and Q. Feng, "A physics-of-failure based reliability and maintenance modeling framework for stent deployment and operation," *Reliability Engineering & System Safety,* vol. 103, pp. 94-101, 2012.

[8] S. Reggiani, S. Poli, M. Denison, E. Gnani, A. Gnudi, G. Baccarani, S. Pendharkar, and R. Wise, "Physics-Based Analytical Model for HCS Degradation in STI-LDMOS Transistors," *Electron Devices, IEEE Transactions on,* vol. 58, pp. 3072-3080, 2011.

[9] O. Chryssaphinou, N. Limnios, and S. Malefaki, "Multi-state reliability systems under discrete time semi-Markovian hypothesis," *Reliability, IEEE Transactions on,* vol. 60, pp. 80-87, 2011.

[10] M. Giorgio, M. Guida, and G. Pulcini, "An age-and state-dependent Markov model for degradation processes," *IIE Transactions,* vol. 43, pp. 621-632, 2011.

[11] W. Li and H. Pham, "Reliability modeling of multi-state degraded systems with multi-competing failures and random shocks," *Reliability, IEEE Transactions on,* vol. 54, pp. 297-303, 2005.

[12] A. Lisnianski and G. Levitin, *Multi-state system reliability: assessment, optimization and applications*: World scientific, 2003.

[13] Y. Ding, M. J. Zuo, A. Lisnianski, and Z. Tian, "Fuzzy multi-state systems: general definitions, and performance assessment," *Reliability, IEEE Transactions on,* vol. 57, pp. 589-594, 2008.

[14] R. Moghaddass and M. J. Zuo, "Multistate Degradation and Supervised Estimation Methods for a Condition-Monitored Device," *IIE Transactions,* vol. 46, pp. 131-148, 2014.

[15] Y.-F. Li, E. Zio, and Y.-H. Lin, "A Multistate Physics Model of Component Degradation Based on Stochastic Petri Nets and Simulation," *Reliability, IEEE Transactions on,* vol. 61, pp. 921 - 931, 2012.

[16] N. Rasmekomen and A. K. Parlikad, "Maintenance Optimization for Asset Systems With Dependent Performance Degradation," *Reliability, IEEE Transactions on,* vol. 62, pp. 362 - 367, 2013.

[17] S. Song, D. W. Coit, Q. Feng, and H. Peng, "Reliability analysis for multi-component systems subject to multiple dependent competing failure processes," *Reliability, IEEE Transactions on,* vol. 63, pp. 331-345.

[18] H. Peng, Q. Feng, and D. W. Coit, "Reliability and maintenance modeling for systems subject to multiple dependent competing failure processes," *IIE transactions,* vol. 43, pp. 12-22, 2010.

[19] Y. Wang and H. Pham, "Modeling the dependent competing risks with multiple degradation processes and random shock using time-varying copulas," *Reliability, IEEE Transactions on,* vol. 61, pp. 13-22, 2012.

[20] Q. Yang, N. Zhang, and Y. Hong, "Reliability Analysis of Repairable Systems With Dependent Component Failures Under Partially Perfect Repair," *Reliability, IEEE Transactions on,* vol. 62, pp. 490-498, 2013.

[21] D. Straub, "Stochastic modeling of deterioration processes through dynamic Bayesian networks," *Journal of Engineering Mechanics,* vol. 135, pp. 1089-1099, 2009.

[22] Y.-H. Lin, Y. Li, and E. Zio, "Dynamic Reliability Models for Multiple Dependent Competing Degradation Processes," *Proceedings of ESREL 2014,* pp. 775–782, 2014.

[23] M. H. Davis, *Markov models and optimization* vol. 49: CRC Press, 1993.

[24] M. H. Davis, "Piecewise-deterministic Markov processes: A general class of non-diffusion stochastic models," *Journal of the Royal Statistical Society. Series B (Methodological),* pp. 353-388, 1984.

[25] M. Jacobsen, *Point process theory and applications: marked point and piecewise deterministic processes*: Springer, 2006.

[26] C. Cocozza-Thivent, "Processus de renouvellement markovien, Processus de Markov déterministes par morceaux," *Online book available on the webpage: http://perso-math. univ-mlv. fr/users/cocozza. christiane/recherche-pageperso/PresentationRMetPDMP. html,* 2011.

[27] M. Marseguerra and E. Zio, "Monte Carlo approach to PSA for dynamic process systems," *Reliability Engineering & System Safety,* vol. 52, pp. 227-241, 1996.

[28] J. Chiquet, N. Limnios, and M. Eid, "Piecewise deterministic Markov processes applied to fatigue crack growth modelling," *Journal of Statistical Planning and Inference,* vol. 139, pp. 1657-1667, 2009.

[29] H. Zhang, F. Innal, F. o. Dufour, and Y. Dutuit, "Piecewise Deterministic Markov Processes based approach applied to an offshore oil production system," *Reliability Engineering & System Safety,* vol. 126, pp. 126-134.

[30] W. Lair, S. Mercier, M. Roussignol, and R. Ziani, "Piecewise deterministic Markov processes and maintenance modeling: application to maintenance of a train air-conditioning system," *Proceedings of the Institution of Mechanical Engineers, Part O: Journal of Risk and Reliability,* vol. 225, pp. 199-209, 2011.

[31] C. Cocozza-Thivent, R. Eymard, and S. Mercier, "A finite-volume scheme for dynamic reliability models,"

IMA journal of numerical analysis, vol. 26, pp. 446-471, 2006.

[32] R. Eymard, S. Mercier, and A. Prignet, "An implicit finite volume scheme for a scalar hyperbolic problem with measure data related to piecewise deterministic Markov processes," *journal of Computational and Applied Mathematics,* vol. 222, pp. 293-323, 2008.

[33] M. L. Gamiz, "Smoothed Estimation of a 3-State Semi-Markov Reliability Model," *Reliability, IEEE Transactions on,* vol. 61, pp. 336-343, 2012.

[34] A. Lorton, M. Fouladirad, and A. Grall, "Computation of remaining useful life on a physic-based model and impact of a prognosis on the maintenance process," *Proceedings of the Institution of Mechanical Engineers, Part O: Journal of Risk and Reliability,* 2013.

[35] E. Hairer, S. P. Nørsett, and G. Wanner, *Solving Ordinary Differential Equations I: Nonstiff Problems*: Springer, 1993.

[36] E. Hairer, S. P. Nørsett, and G. Wanner, *Solving Ordinary Differential Equations II: Stiff and Differential-Algebraic Problems*: Springer, 1996.

[37] E. Lewis and F. Böhm, "Monte Carlo simulation of Markov unreliability models," *Nuclear Engineering and Design,* vol. 77, pp. 49-62, 1984.

[38] R. Coudray and J. Mattei, "System reliability: An example of nuclear reactor system analysis," *Reliability Engineering,* vol. 7, pp. 89-121, 1984.

[39] S. Zhang, M. Hodkiewicz, L. Ma, and J. Mathew, "Machinery condition prognosis using multivariate analysis," in *Engineering Asset Management*: Springer, 2006, pp. 847-854.

[40] P. Moussou, S. Cambier, D. Lachene, S. Longarini, L. Paulhiac, and V. Villouvier, "Vibration investigation of a French PWR power plant piping system caused by cavitating butterfly valves," *ASME-PUBLICATIONS-PVP,* vol. 420, pp. 99-106, 2001.

[41] P. Vlok, J. Coetzee, D. Banjevic, A. Jardine, and V. Makis, "Optimal component replacement decisions using vibration monitoring and the proportional-hazards model," *Journal of the operational research society,* pp. 193-202, 2002.

[42] M. Daigle and K. Goebel, "Model-based prognostics under limited sensing," in *Aerospace Conference, 2010 IEEE*, 2010, pp. 1-12.

PAPER III: Y.-H. Lin, Y.-F. Li, E. Zio. Fuzzy Reliability Assessment of Systems with Multiple Dependent Competing Degradation Processes. *Fuzzy Systems, IEEE Transactions on*, vol.23, no.5, pp.1428-1438, 2015.

PAPER III: Y.-H. Lin, Y.-F. Li, E. Zio. Fuzzy Reliability Assessment of Systems with Multiple Dependent Competing Degradation Processes. Fuzzy Systems, IEEE Transactions on, vol.23, no.5, pp.1428-1438, 2015.

Fuzzy Reliability Assessment of Systems with Multiple Dependent Competing Degradation Processes

Y.H. Lin[1], Y.F. Li[1] member IEEE, E. Zio[1,2] senior member IEEE

[1] *Chair on Systems Science and the Energetic Challenge, European Foundation for New Energy-Electricite' de France, at Ecole Centrale Paris- Supelec, France*

[2]*Politecnico di Milano, Italy*

Abstract – Components are often subject to multiple competing degradation processes. For multi-component systems, the degradation dependency within one component or/and among components need to be considered. Physics-based models (PBMs) and multi-state models (MSMs) are often used for component degradation processes, particularly when statistical data are limited. In this paper, we treat dependencies between degradation processes within a piecewise-deterministic Markov process (PDMP) modeling framework. Epistemic (subjective) uncertainty can arise due to the incomplete or imprecise knowledge about the degradation processes and the governing parameters: to take into account this, we describe the parameters of the PDMP model as fuzzy numbers. Then, we extend the finite-volume (FV) method to quantify the (fuzzy) reliability of the system. The proposed method is tested on one subsystem of the residual heat removal system (RHRS) of a nuclear power plant, and a comparison is offered with a Monte Carlo (MC) simulation solution: the results show that our method can be most efficient.

Keywords – Multiple dependent competing degradation processes, piecewise-deterministic Markov process (PDMP), epistemic uncertainty, fuzzy set theory, fuzzy reliability, finite-volume (FV) method.

1. INTRODUCTION

Industrial components are often subject to multiple competing degradation processes, whereby any of them may cause failure [1]. For multi-component systems, the dependency between degradation processes within one component (e.g. the wear of rubbing surfaces influenced by the environmental stress shock within a micro-engine [2]), or/and the degradation dependency among components (e.g. the degradation of the pre-filtrations stations leading to a lower performance level of the sand filter in a water treatment plant [3]) need to be considered.

Physics-based models (PBMs) [4-7] and multi-state models (MSMs) [8-11] are two modeling frameworks that can be used for describing the evolution of degradation in structures and components. The former uses physics knowledge that is implemented into mathematical equations for an integrated mechanistic description of the component behavior given the underlying degradation mechanisms (e.g. shocks, fatigue, wear, corrosion, etc.). The latter generally uses degradation and/or failure data from historical field collection or degradation tests, or material science knowledge (e.g. multi-state physics model [12]) to describe the degradation processes by a finite number of states of degradation severity and a set of transition rates (estimated from historical data) between the different degradation states.

To treat degradation dependencies in a system whose components are modeled by these two types of models, a piecewise-deterministic Markov process (PDMP) approach was employed in our previous work [13]. Monte Carlo (MC) simulation methods [14, 15] can be used to solve PDMP, since the analytical solution is difficult to obtain due to the complex behavior of the system, resulting in the stochasticities of MSMs and time-dependent evolutions of PBMs. However, the major shortcoming is that MC can be quiet time-consuming [16]. The finite-volume (FV) scheme studied by Cocozza-Thivent *et al.* [17] and Eymard *et al.* [18] appears to be more efficient, leading to comparable results as MC simulation with acceptable computing time [16].

Epistemic (subjective) uncertainty [19] can affect the analysis due to the incomplete or imprecise knowledge about the degradation processes of the components [20, 21]. For PBMs, the parameters (e.g. wear coefficient) and influencing factors (e.g. temperature and pressure) may be unknown [22] and elicited from expert judgment [23]; for MSMs, the state performances may be poorly defined due to the imprecise discretization of the underlying continuous degradation processes [24] and the transition rates between states may be difficult to estimate statistically due to insufficient data, especially for those highly reliable critical components (e.g. valves and pumps in nuclear power plants or aircrafts, etc.) [25].

In literature, fuzzy reliability has been studied by many researchers to account for imprecision and uncertainty in the system model parameters. Tanaka *et al.* [26] have proposed the fuzzy fault tree for the fuzzy reliability assessment of binary-state systems and Singer [27] has assigned fuzzy probabilities to the basic events. Dunyak *et al.* [28] have proposed another fuzzy extension to assign fuzzy probability to all events, which is consistent with the calculations from fuzzy fault trees. Ding *et al.* [20] have developed fuzzy multi-state systems (FMSS) models by considering the steady state probabilities, or/and steady state performance levels of a component as fuzzy numbers. Ding and Lisnianski [29] have proposed the fuzzy universal generating function (FUGF) for the quantification of the fuzzy reliability of FMSS. Later, Li *et al.* [30] have developed a random fuzzy extension of the universal generating function and Sallak *et al.* [31] have employed Dempster–Shafer theory to quantify the fuzzy reliability of MSS. Liu *et al.* [24] have proposed a fuzzy Markov model with fuzzy transition rates for FMSS when the steady fuzzy state probabilities are not available. To the knowledge of the authors, none of the previous studies has considered epistemic uncertainty in PDMP system models.

The contributions of the paper are twofold. First, we employ fuzzy numbers to represent various epistemic uncertainties in multiple dependent competing degradation processes modeled by PDMP. Second, we extend the FV scheme for the quantification of PDMP under epistemic uncertainty instead of using time-consuming MC simulation methods [32, 33]. The reminder of the paper is structured as follows. Section 2 introduces the PDMP for multiple dependent competing degradation processes. Section 3 presents the FV scheme for PDMP. Section 4 presents the PDMP under uncertainty and the extended FV scheme for system reliability quantification. Section 5 presents a case study on one subsystem of the residual heat removal system (RHRS) [34] of a nuclear power plant. Section 6 presents numerical results and analysis. Section 7 concludes the work.

2. PDMP FOR SYSTEMS DEGRADATION CONSIDERING DEPENDENCY

The following assumptions are made on the multiple dependent competing degradation processes of a system [13]:

- The system consists of two groups of components: the first group contains M components, $\vec{L} = (L_1, L_2, \dots, L_M)$, whose degradation processes are modeled by PBMs; the second group contains N components, $\vec{K} = (K_1, K_2, \dots, K_N)$, whose degradation processes are modeled by MSMs including MSPM.
- All degradation processes of the system follow the PDMP, taking into account the degradation dependency of components within each group and between the groups.
- For a generic component $L_m, m = 1, 2, \dots, M$, of the first group, d_{L_m} time-dependent continuous variables are used to describe the degradation process; the variables vector $\overrightarrow{X_{L_m}}(t) = (\overrightarrow{X_{L_m}^D}(t), \overrightarrow{X_{L_m}^P}(t))$ contains (1) non-decreasing degradation variables $\overrightarrow{X_{L_m}^D}(t)$ (e.g. crack length) and (2) physical variables $\overrightarrow{X_{L_m}^P}(t)$ (e.g. velocity and force), whose evolution in time is described by a set of first-order differential equations mathematically representing the underlying physical processes. The component L_m fails when one variable of the first type $x_{L_m}^i(t) \in \overrightarrow{X_{L_m}^D}(t)$ reaches or exceeds its corresponding failure threshold, denoted by ${x_{L_m}^i}^*$; the set of failure states of L_m is denoted by $\mathcal{F}_{L_m}$.
- For a generic component $K_n, n = 1, 2, \dots, N$, in the second group, its discrete degradation state space is denoted by $S_{K_n} = \{0_{K_n}, 1_{K_n}, \dots, d_{K_n}\}$, ranging from perfect functioning state 'd_{K_n}' to complete failure state '0'. The component is functioning or partially functioning in all generic intermediate states. The transition rates between two different degradation states are used to describe the speed of reaching another degradation state. The performance level of one component (e.g. vibration of the valve due to degradation) at each degradation state and the impact on the other components are considered as deterministic. The failure state set of K_n is denoted by $\boldsymbol{\mathcal{F}}_{K_n} = \{0_{K_n}\}$.

The degradation condition of the whole system is, then, represented as follows:

$$\vec{Z}(t) = \begin{pmatrix} \begin{pmatrix} \overrightarrow{X_{L_1}}(t) \\ \overrightarrow{X_{L_2}}(t) \\ \vdots \\ \overrightarrow{X_{L_M}}(t) \end{pmatrix} = \overrightarrow{X}(t) \\ \left(Y_{K_1}(t), Y_{K_2}(t), \dots, Y_{K_N}(t)\right) = \vec{Y}(t) \end{pmatrix} \in E = \mathbb{R}^{d_L} \times S \tag{1}$$

where $Y_{K_n}(t), n = 1, 2, \dots, N$ denotes the degradation state of component K_n at time t, E is a hybrid space of $\mathbb{R}^{d_L}$ ($d_L = d_{L_1} + d_{L_2} + \dots + d_{L_M}$) and S ($S = S_{K_1} \times S_{K_2} \dots \times S_{K_N}$).

The evolution of the degradation processes $\vec{Z}(t)$ involves the stochastic behavior of $\vec{Y}(t)$ and the deterministic behavior of $\overrightarrow{X}(t)$, between two consecutive jumps of $\vec{Y}(t)$, given $\vec{Y}(t)$. Let $\overrightarrow{Y_k} \in S, k \in \mathbb{N}$ denote the state of the N components in the second group after k transitions (a transition occurs as long as any one of the N components changes its state) and $T_k \in \mathbb{R}^+, k \in \mathbb{N}$ denote the time of arrival at state $\overrightarrow{Y_k}$. $\vec{Y}(t)$ is written as follows:

$$\vec{Y}(t) = \overrightarrow{Y_k}, \forall t \in [T_k, T_{k+1}[\tag{2}$$

The probability that $\vec{Y}(t)$ will step to state $\vec{j}$ from state $\vec{\imath}$ in the next infinitesimal time interval $[T_n, T_n + \Delta t]$, given $(\overrightarrow{Z}(t))_{0 \le t \le T_n}$, is as follows:

$$P\left[\overrightarrow{Y_{n+1}} = \vec{j}, T_{n+1} \in [T_n, T_n + \Delta t] \,\middle|\, (\overrightarrow{Z}(t))_{0 \le t \le T_n}, \overrightarrow{\theta_K}\right]$$

$$= P\left[\overrightarrow{Y_{n+1}} = \vec{j}, T_{n+1} \in [T_n, T_n + \Delta t] \,\middle|\, \overrightarrow{Z}(T_n) = (\overrightarrow{X}(T_n), \vec{\imath}), \overrightarrow{\theta_K}\right]$$

$$= \lambda_{\vec{\imath}}\left(\vec{j}, \overrightarrow{X}(T_n) \mid \overrightarrow{\theta_K}\right)\Delta t$$

$$\forall\, n \geq 0, \vec{\imath}, \vec{j} \in S, \vec{\imath} \neq \vec{j} \tag{3}$$

where $\overrightarrow{\theta_K}$ represents the external influencing factors of the components in the second group and the related coefficients to the transition rates, $\lambda_{\vec{\imath}}\left(\vec{j}, \overrightarrow{X}(T_n) \mid \overrightarrow{\theta_K}\right)$ represents the corresponding transition rate. The evolution of $\overrightarrow{X}(t)$, when $t \in [T_k, T_{k+1}[, k \in \mathbb{N}$, is deterministically described by a set of differential equations as follows:

$$\dot{\vec{X}}(t) = \begin{pmatrix} \overrightarrow{\dot{X}_{L_1}}(t) \\ \overrightarrow{\dot{X}_{L_2}}(t) \\ \vdots \\ \overrightarrow{\dot{X}_{L_M}}(t) \end{pmatrix} = \begin{pmatrix} \overrightarrow{f_{L_1}^{\overrightarrow{Y_k}}}\left(\overrightarrow{X}(t), t \mid \overrightarrow{\theta_{L_1}}\right) \\ \overrightarrow{f_{L_2}^{\overrightarrow{Y_k}}}\left(\overrightarrow{X}(t), t \mid \overrightarrow{\theta_{L_2}}\right) \\ \vdots \\ \overrightarrow{f_{L_M}^{\overrightarrow{Y_k}}}\left(\overrightarrow{X}(t), t \mid \overrightarrow{\theta_{L_M}}\right) \end{pmatrix} = \overrightarrow{f_L^{\overrightarrow{Y_k}}}\left(\overrightarrow{X}(t), t \mid \overrightarrow{\theta_L}\right) \tag{4}$$

where $\overrightarrow{f_{L_m}^{Y_k}}, m = 1, 2, \ldots, M$ are the set of physics equations, given the influence of the degradation state $\overrightarrow{Y_k}$ of the second group components, $\overrightarrow{\theta_{L_m}}, m = 1, 2, \ldots, M$ represents the external influencing factors of the component L_n and the physical parameters used in the physics equations. Mathematically, the dependency within each group and between two groups is treated in the framework of a piecewise-deterministic Markov process (PDMP) modeling, where the physics equations in the first group, denoted by $\overrightarrow{f_L^{\overrightarrow{Y_k}}}\left(\overrightarrow{X}(t), t \mid \overrightarrow{\theta_L}\right)$, are dependent on the states ($\overrightarrow{Y_k}$) of the components in the second group and the transition rates in the second group, denoted by $\lambda_{\vec{\imath}}\left(\vec{j}, \overrightarrow{X}(t) \mid \overrightarrow{\theta_K}\right)$, are dependent on the evolution of the variables ($\overrightarrow{X}(t)$) in the first group.

The reliability of the system at time *t* is defined as follows:

$$R(t) = P[\vec{Z}(s) \notin \mathcal{F}, \forall s \leq t] \tag{5}$$

where $\mathcal{F} = \mathcal{F}_{\vec{X}} \times \mathcal{F}_{\vec{Y}} \subsetneq E$ denotes the space of the failure states of $\vec{Z}(t)$, where $\mathcal{F}_{\vec{X}}$ denotes the sub-space of the states of $\vec{X}(t)$ and $\mathcal{F}_{\vec{Y}}$ denotes the sub-space of the states of $\vec{Y}(t)$. Let $p_t\left(\vec{x}, \vec{\imath} \mid \overrightarrow{\theta_L}, \overrightarrow{\theta_K}\right), \vec{x} \in \mathbb{R}^{d_L}, \vec{\imath} \in S$ denote the probability density function (PDF) of processes $\left(\overrightarrow{X}(t), \overrightarrow{Y}(t)\right)_{t \geq 0}$ being in state $(\vec{x}, \vec{\imath})$ at time *t*, which satisfies:

$$\int_{\mathbb{R}^{d_L}} \sum_{\vec{\imath} \in S} p_t\left(\vec{x}, \vec{\imath} \mid \overrightarrow{\theta_L}, \overrightarrow{\theta_K}\right) d\vec{x} = 1 \tag{6}$$

The reliability of the system can be calculated as:

$$R(t) = \int_{\vec{x} \notin \mathcal{F}_{\overrightarrow{X}}} \sum_{\vec{\imath} \notin \mathcal{F}_{\overrightarrow{Y}}} p_t\left(\vec{x}, \vec{\imath} \mid \overrightarrow{\theta_L}, \overrightarrow{\theta_K}\right) d\vec{x} \tag{7}$$

The PDF $p_t\left(\vec{x}, \vec{\imath} \mid \overrightarrow{\theta_L}, \overrightarrow{\theta_K}\right)$ obeys the Chapman-Kolmogorov equation [35] as follows:

$$\frac{\partial}{\partial t} p_t\left(\vec{x}, \vec{\imath} \mid \overrightarrow{\theta_L}, \overrightarrow{\theta_K}\right) =$$

$$\sum_{\vec{\jmath} \neq \vec{\imath}} \lambda_{\vec{\jmath}}\left(\vec{\imath}, \vec{x} \mid \overrightarrow{\theta_K}\right) p_t\left(\vec{x}, \vec{\jmath} \mid \overrightarrow{\theta_L}, \overrightarrow{\theta_K}\right)$$

$$-\lambda_{\vec{\imath}}\left(\vec{x} \mid \overrightarrow{\theta_K}\right) p_t\left(\vec{x}, \vec{\imath} \mid \overrightarrow{\theta_L}, \overrightarrow{\theta_K}\right) - \operatorname{div}\left(\overrightarrow{f_L^{\vec{\imath}}}(\vec{x}, t \mid \overrightarrow{\theta_L}) p_t\left(\vec{x}, \vec{\imath} \mid \overrightarrow{\theta_L}, \overrightarrow{\theta_K}\right)\right) \tag{8}$$

where $\lambda_{\vec{\imath}}(\vec{x} \mid \overrightarrow{\theta_K}) = \sum_{\vec{\jmath} \neq \vec{\imath}} \lambda_{\vec{\imath}}(\vec{\jmath}, \vec{x} \mid \overrightarrow{\theta_K})$ is the transition rate departing from the state $\vec{\imath}$. Among the right-hand parts of equation (8), the first two terms are due to the stochastic behavior of processes $\vec{Y}(t)$: the first term accounts for the transition of processes $\vec{Z}(t)$ into state $(\vec{\imath}, \vec{x})$, the second term accounts for the transition of processes $\vec{Z}(t)$ out of state $(\vec{\imath}, \vec{x})$; the last term is due to the deterministic behavior of processes $\vec{X}(t)$, which represents the volume density of the outward flux of the probability field around the point $(\vec{\imath}, \vec{x})$. Given the initial probability distribution of the system $p_0(\vec{x}, \vec{\imath} \mid \overrightarrow{\theta_L}, \overrightarrow{\theta_K})$, its evolution in time and that of the system reliability can be obtained solving equations (8) and (7), respectively.

A challenging problem is to calculate the probability density function $p_t(\vec{x}, \vec{\imath} \mid \overrightarrow{\theta_L}, \overrightarrow{\theta_K})$, because the analytical solution is difficult to obtain due to the complex behavior of the processes [14, 15]. MC simulation methods can be applied for such numerical computations, but the major shortcoming is that they are typically time-consuming [16]. FV methods is an alternative that can lead to comparable results as MC simulation, but within a more acceptable computing time [16].

3. FINITE-VOLUME SCHEME FOR PDMP

Instead of directly solving the probability density function $p_t(\vec{x}, \vec{\imath} \mid \overrightarrow{\theta_L}, \overrightarrow{\theta_K})$ through the Chapman-Kolmogorov equation (8), an approximate solution can be obtained by the FV scheme by discretizing the state space of the continuous variables and the time space of PDMP. The approximated solution converges towards the accurate solution under certain conditions. Here, we employ an explicit FV scheme to PDMP, developed by Cocozza-Thivent *et al.* [17].

3.1 Assumptions

This approach can be applied under the following assumptions [17]:

- The transition rates $\lambda_{\vec{\imath}}(\vec{\jmath}, \cdot \mid \overrightarrow{\theta_K}), \forall \vec{\imath}, \vec{\jmath} \in S$ are continuous and bounded functions from $\mathbb{R}^{d_L}$ to $\mathbb{R}^+$.
- The physics equations $\overrightarrow{f_L^{\vec{\imath}}}(\cdot, \cdot \mid \overrightarrow{\theta_L}), \forall \vec{\imath} \in S$ are continuous functions from $\mathbb{R}^{d_L} \times \mathbb{R}^+$ to $\mathbb{R}^{d_L}$ and locally Lipschitz continuous.
- The physics equations $\overrightarrow{f_L^{\vec{\imath}}}(\cdot, t \mid \overrightarrow{\theta_L}), \forall \vec{\imath} \in S$ are sub-linear, i.e. there are some $V_1 > 0$ and $V_2 > 0$ such that
$$\forall \vec{x} \in \mathbb{R}^{d_L}, t \in \mathbb{R}^+ \left| \overrightarrow{f_L^{\vec{\imath}}}(\vec{x}, t \mid \overrightarrow{\theta_L}) \right| \leq V_1(\|\vec{x}\| + |t|) + V_2$$
- The functions $div(\overrightarrow{f_L^{\vec{\imath}}}(\cdot, \cdot \mid \overrightarrow{\theta_L})), \forall \vec{\imath} \in S$ are almost everywhere bounded in absolute value by some real value $D > 0$ (independent of *i*).

3.2 Numerical scheme

For the ease of notation, first we let $\overrightarrow{g^{\vec{\imath}}}(\cdot, \cdot)$: $\mathbb{R}^{d_L} \times \mathbb{R} \to \mathbb{R}^{d_L}$ denote the solution of

$$\frac{\partial}{\partial t} \overrightarrow{g^{\vec{\imath}}}(\vec{x}, t \mid \overrightarrow{\theta_L}) = \overrightarrow{f_L^{\vec{\imath}}}\left(\overrightarrow{g^{\vec{\imath}}}(\vec{x}, t \mid \overrightarrow{\theta_L}), t \,\middle|\, \overrightarrow{\theta_L}\right), \forall \vec{\imath} \in S, \vec{x} \in \mathbb{R}^{d_L}, t \in \mathbb{R} \qquad (9)$$

with

$$\overrightarrow{g^{\vec{\imath}}}\left(\vec{x}, 0 \mid \overrightarrow{\theta_L}\right) = \vec{x}, \forall \vec{\imath} \in S, \vec{x} \in \mathbb{R}^{d_L} \tag{10}$$

and $\overrightarrow{g^{\vec{\imath}}}\left(\vec{x}, t \mid \overrightarrow{\theta_L}\right)$ is the result of the deterministic behavior of $\overrightarrow{X}(t)$ after time *t*, starting from the point $\vec{x}$ while the processes $\vec{Y}(t)$ hold on state $\vec{\imath}$.

The state space $\mathbb{R}^{d_L}$ of continuous variables $\overrightarrow{X}(t)$ is divided into an admissible mesh $\mathcal{M}$, which is a family of measurable subsets of $\mathbb{R}^{d_L}$ ($\mathcal{M}$ is a partition of $\mathbb{R}^{d_L}$) such that [17]:

(9) $\bigcup_{A\in\mathcal{M}} A = \mathbb{R}^{d_L}$.
(10) $\forall A, B \in \mathcal{M},\ A \neq B \Rightarrow A \cap B = \emptyset$.
(11) $m_A = \int_A \overrightarrow{dx} > 0, \forall A \in \mathcal{M}$, where m_A is the volume of grid A.
(12) $sup_{A\in\mathcal{M}} diam(A) < +\infty$ where $diam(A) = sup_{\forall \vec{x},\vec{y}\in A}|\vec{x} - \vec{y}|$.

Additionally, the time space $\mathbb{R}^+$is divided into small intervals $\mathbb{R}^+ = \bigcup_{n=0,1,2,\dots}[n\Delta t, (n+1)\Delta t[$ by setting the time step $\Delta t > 0$ (the length of each interval).

The numerical scheme aims at giving an approximate value for the probability density function $p_t\left(\vec{x}, \vec{\imath} \mid \overrightarrow{\theta_L}, \overrightarrow{\theta_K}\right)$ on each $\{i\} \times [n\Delta t, (n+1)\Delta t[\times A, \forall \vec{\imath} \in S, n \in \mathbb{N}, A \in \mathcal{M}$ denoted by $p_n\left(A, \vec{\imath} \mid \overrightarrow{\theta_L}, \overrightarrow{\theta_K}\right)$, by assuming that:

$$p_t\left(\vec{x}, \vec{\imath} \mid \overrightarrow{\theta_L}, \overrightarrow{\theta_K}\right) = p_n\left(A, \vec{\imath} \mid \overrightarrow{\theta_L}, \overrightarrow{\theta_K}\right), \forall \vec{\imath} \in S, \vec{x} \in A, t \in [n\Delta t, (n+1)\Delta t[\tag{11}$$

Given the initial probability density function $p_0\left(\vec{x}, \vec{\imath} \mid \overrightarrow{\theta_L}, \overrightarrow{\theta_K}\right)$ of the system at time $t = 0$, $p_0\left(A, \vec{\imath} \mid \overrightarrow{\theta_L}, \overrightarrow{\theta_K}\right), \forall \vec{\imath} \in S, A \in \mathcal{M}$ can be obtained as:

$$p_0\left(A, \vec{\imath} \mid \overrightarrow{\theta_L}, \overrightarrow{\theta_K}\right) = \int_A p_0\left(\vec{x}, \vec{\imath} \mid \overrightarrow{\theta_L}, \overrightarrow{\theta_K}\right)\overrightarrow{dx}\,/m_A \tag{12}$$

Then, $p_{n+1}\left(A, \vec{\imath} \mid \overrightarrow{\theta_L}, \overrightarrow{\theta_K}\right), \forall \vec{\imath} \in S, A \in \mathcal{M}, n \in \mathbb{N}$ can be calculated considering the deterministic evaluation of $\overrightarrow{X}(t)$ and the stochastic evolution of $\overrightarrow{Y}(t)$ based on $p_n\left(\mathcal{M}, \vec{\imath} \mid \overrightarrow{\theta_L}, \overrightarrow{\theta_K}\right)$ by the Chapman-Kolmogorov forward equation [36], as follows:

$$\begin{aligned} &p_{n+1}\left(A, \vec{\imath} \mid \overrightarrow{\theta_L}, \overrightarrow{\theta_K}\right) \\ &= \frac{1}{1+\Delta t b_A^{\vec{\imath}}}\widehat{p_{n+1}}\left(A, \vec{\imath} \mid \overrightarrow{\theta_L}, \overrightarrow{\theta_K}\right) + \Delta t \sum_{\substack{\vec{\jmath}\in S \\ \vec{\jmath} \neq \vec{\imath}}} \frac{a_A^{\vec{\jmath}\vec{\imath}}}{1+\Delta t b_A^{\vec{\jmath}}}\widehat{p_{n+1}}\left(A, \vec{\jmath} \mid \overrightarrow{\theta_L}, \overrightarrow{\theta_K}\right) \end{aligned} \tag{13}$$

where

$$a_A^{\vec{\jmath}\vec{\imath}} = \int_A \lambda_{\vec{\jmath}}\left(\vec{\imath}, \vec{x} \mid \overrightarrow{\theta_K}\right)\overrightarrow{dx}/m_A\,, \forall \vec{\imath} \in S, A \in \mathcal{M} \tag{14}$$

is the average transition rate from state $\vec{\jmath}$ to state $\vec{\imath}$ for grid A,

$$b_A^{\vec{\jmath}} = \sum_{\vec{\imath} \neq \vec{\jmath}} a_A^{\vec{\jmath}\vec{\imath}}\,, \forall \vec{\jmath} \in S, A \in \mathcal{M} \tag{15}$$

is the average transition rate out of state $\vec{\imath}$ for grid A,

$$\widehat{p_{n+1}}\left(A, \vec{\imath} \mid \overrightarrow{\theta_L}, \overrightarrow{\theta_K}\right) = \sum_{B\in\mathcal{M}} m_{BA}^{\vec{\imath}}\, p_n\left(B, \vec{\imath} \mid \overrightarrow{\theta_L}, \overrightarrow{\theta_K}\right)/m_A,\ \forall \vec{\imath} \in S, A \in \mathcal{M} \tag{16}$$

is the approximate value for probability density function on $\{i\} \times [(n+1)\Delta t, (n+2)\Delta t[\times A$ according to the deterministic evaluation of $\overrightarrow{X}(t)$,

$$m_{BA}^{\vec{\imath}} = \int_{\{\vec{y}\in B \mid \overrightarrow{g^{\vec{\imath}}}(\vec{y}, \Delta t \mid \overrightarrow{\theta_L})\in A\}} \overrightarrow{dy}\,, \forall \vec{\imath} \in S, A, B \in \mathcal{M} \tag{17}$$

is the volume of the part of grid B, which will enter grid A after time Δt according to the deterministic evaluation of $\overrightarrow{X}(t)$.

The first term of the right-hand parts of equation (13) accounts for the situation that processes $\vec{Y}(t)$ hold on state $\vec{\imath}$ during time $[n\Delta t,(n+1)\Delta t]$, represented by "1" in an illustrated example in $\mathbb{R}^2$ (Fig 1), where $\frac{1}{1+\Delta t b_A^{\vec{\imath}}}, \forall \vec{\imath} \in S, A \in \mathcal{M}$ is the approximated probability that no transition happens from state $\vec{\imath}$ for grid A and the second term of the right-hand parts of equation (13) accounts for the situation that processes $\vec{Y}(t)$ step to state $\vec{\imath}$ from another state $\vec{\jmath}$ at time $(n+1)\Delta t$, represented by "2" in an illustrated example in $\mathbb{R}^2$ (Fig 1), where $a_A^{\vec{\jmath}\vec{\imath}}\Delta t, \forall \vec{\imath}, \vec{\jmath} \in S, A \in \mathcal{M}$ is the transition probability from state $\vec{\jmath}$ to state $\vec{\imath}$ for grid A (B_1, B_2, B_3 and B_4 are the grids of which some parts will enter grid A according to the deterministic evaluation of $\overrightarrow{X}(t)$ at time $(n+1)\Delta t$).

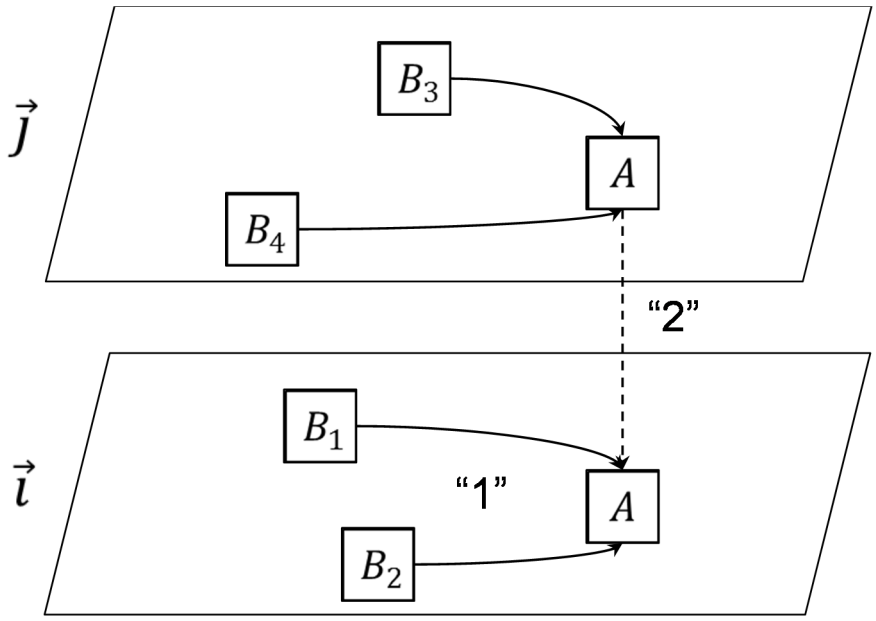

Fig 1. The evolution of degradation processes during $[n\Delta t,(n+1)\Delta t]$.

The approximated solution $p_n\left(A,\vec{\imath} \mid \overrightarrow{\theta_L},\overrightarrow{\theta_K}\right)$ weakly converges towards the unique solution of equation (8) when $\Delta t \to 0$ and $|\mathcal{M}|/\Delta t \to 0$ where $|\mathcal{M}| = sup_{A\in\mathcal{M}} diam(A)$ [17].

4. PDMP UNDER UNCERTAINTY

Fuzzy set theories and techniques introduced by Zadeh [37, 38] have been employed in reliability models under epistemic uncertainty when the crisp values are insufficient to capture the actual behavior of components. In this work, the following assumptions are made to extend the previous PDMP model with the consideration of epistemic uncertainty:

- The values of the external influencing factors and physical parameters $\overrightarrow{\theta_L}$ in the physics equations $\overrightarrow{f_L^{\vec{\imath}}}(\vec{x}, t \mid \overrightarrow{\theta_L}), \forall \vec{\imath} \in S, \vec{x} \in \mathbb{R}^{d_L}$ and equations $\overrightarrow{g^{\vec{\imath}}}(\vec{x}, t \mid \overrightarrow{\theta_L}), \forall \vec{\imath} \in S, \vec{x} \in \mathbb{R}^{d_L}, t \in \mathbb{R}$ for the deterministic processes $\vec{X}(t)$ can be fuzzy numbers, denoted by $\widetilde{\overrightarrow{\theta_L}}$.
- The values of the external influencing factors and the related coefficients $\overrightarrow{\theta_K}$ in the transition rates for the stochastic processes $\vec{Y}(t)$ between two different states $\lambda_{\vec{\imath}}(\vec{\jmath}, \vec{x} \mid \overrightarrow{\theta_K}), \forall\, t \in \mathbb{R}^+, \vec{x} \in \mathbb{R}^{d_L}, \vec{\imath}, \vec{\jmath} \in S, \vec{\imath} \neq \vec{\jmath}$ can be fuzzy numbers, denoted by $\widetilde{\overrightarrow{\theta_K}}$.

The values of the probability density function $p(t, \vec{x}, \vec{\imath} \mid \overrightarrow{\theta_L}, \overrightarrow{\theta_K})$ and reliability function $R(t)$ have, therefore, changed from crisp values to fuzzy numbers, denoted by $\tilde{p}\left(t, \vec{x}, \vec{\imath} \mid \widetilde{\overrightarrow{\theta_L}}, \widetilde{\overrightarrow{\theta_K}}\right)$ and $\tilde{R}(t)$ respectively. In the next section, we extend the approach presented in Section 2 to quantify the dependent degradation processes modeled by PDMP under uncertainty.

4.1 Quantification of PDMP under uncertainty

Let $[\tilde{a}]_\alpha = [\underline{a}_\alpha, \overline{a}_\alpha\,]$ denote the α-cut of a fuzzy number $\tilde{a}$, where $\underline{a}_\alpha$ and $\overline{a}_\alpha$ are the bounds; then, the α-cut of $\tilde{p}\left(t, \vec{x}, \vec{\imath} \mid \widetilde{\overrightarrow{\theta_L}}, \widetilde{\overrightarrow{\theta_K}}\right), \forall \vec{\imath} \in S, \vec{x} \in \mathbb{R}^{d_L}, t \in \mathbb{R}$ can be obtained based on the extension principle [38] as:

$$\left[\tilde{p}\left(t, \vec{x}, \vec{\imath} \mid \widetilde{\overrightarrow{\theta_L}}, \widetilde{\overrightarrow{\theta_K}}\right)\right]_\alpha =$$

$$\begin{bmatrix} min_{\substack{\overrightarrow{\theta_L} \in \left[\widetilde{\overrightarrow{\theta_L}}\right]_\alpha \\ \overrightarrow{\theta_K} \in \left[\widetilde{\overrightarrow{\theta_K}}\right]_\alpha}} p(t, \vec{x}, \vec{\imath} \mid \overrightarrow{\theta_L}, \overrightarrow{\theta_K}), max_{\substack{\overrightarrow{\theta_L} \in \left[\widetilde{\overrightarrow{\theta_L}}\right]_\alpha \\ \overrightarrow{\theta_K} \in \left[\widetilde{\overrightarrow{\theta_K}}\right]_\alpha}} p(t, \vec{x}, \vec{\imath} \mid \overrightarrow{\theta_L}, \overrightarrow{\theta_K}) \end{bmatrix} \tag{18}$$

The approximate solution for $\left[\tilde{p}\left(t, \vec{x}, \vec{\imath} \mid \widetilde{\overrightarrow{\theta_L}}, \widetilde{\overrightarrow{\theta_K}}\right)\right]_\alpha, \forall \vec{\imath} \in S, \vec{x} \in A, t \in [n\Delta t, (n+1)\Delta t[$ denoted by $\widetilde{p_n}\left(A, \vec{\imath} \mid \widetilde{\overrightarrow{\theta_L}}, \widetilde{\overrightarrow{\theta_K}}\right)$ can be obtained by varying $\overrightarrow{\theta_L}$ in $\left[\widetilde{\overrightarrow{\theta_L}}\right]_\alpha$ and $\overrightarrow{\theta_K}$ in $\left[\widetilde{\overrightarrow{\theta_K}}\right]_\alpha$ as follows

$$\left[\widetilde{p_n}\left(A, \vec{\imath} \mid \widetilde{\overrightarrow{\theta_L}}, \widetilde{\overrightarrow{\theta_K}}\right)\right]_\alpha =$$

$$\begin{bmatrix} min_{\substack{\overrightarrow{\theta_L} \in \left[\widetilde{\overrightarrow{\theta_L}}\right]_\alpha \\ \overrightarrow{\theta_K} \in \left[\widetilde{\overrightarrow{\theta_K}}\right]_\alpha}} p_n(A, \vec{\imath} \mid \overrightarrow{\theta_L}, \overrightarrow{\theta_K}), max_{\substack{\overrightarrow{\theta_L} \in \left[\widetilde{\overrightarrow{\theta_L}}\right]_\alpha \\ \overrightarrow{\theta_K} \in \left[\widetilde{\overrightarrow{\theta_K}}\right]_\alpha}} p_n(A, \vec{\imath} \mid \overrightarrow{\theta_L}, \overrightarrow{\theta_K}) \end{bmatrix} \tag{19}$$

where $p_n(A, \vec{\imath} \mid \overrightarrow{\theta_L}, \overrightarrow{\theta_K})$ is obtained by eq. (13) through the FV scheme. Then, the parametric programming algorithms [24] can be applied to find the fuzzy probability in eq. (19).

The approximate solution for the α-cut of fuzzy reliability $\tilde{R}(t)$ of the system at time $t \in [n\Delta t, (n+1)\Delta t[$ can, then, be obtained as follows:

$$[\tilde{R}(t)]_\alpha = \sum_{A\in\mathcal{M}} \sum_{\vec{\imath}\notin\mathcal{F}_{\overline{Y}}} [\widetilde{p_n}\left(A, \vec{\imath} \mid \widetilde{\overrightarrow{\theta_L}}, \widetilde{\overrightarrow{\theta_K}}\right)]_\alpha \int_{\{\vec{x}\in A \mid \vec{x}\notin\mathcal{F}_{\overline{X}}\}} \overrightarrow{dx} \tag{20}$$

In most cases, the original $R(t)$ is monotonic with $\overrightarrow{\theta_L}$ and $\overrightarrow{\theta_k}$; then, we can directly obtain that instead of using eq. (19):

$$[\tilde{R}(t)]_\alpha = \left[\sum_{A\in\mathcal{M}} \sum_{\vec{\imath}\notin\mathcal{F}_{\overline{Y}}} p_n\left(A, \vec{\imath} \mid \underline{\overrightarrow{\theta_L}}_\alpha, \underline{\overrightarrow{\theta_K}}_\alpha\right) \int_{\{\vec{x}\in A \mid \vec{x}\notin\mathcal{F}_{\overline{X}}\}} \overrightarrow{dx}, \right.$$
$$\left. \sum_{A\in\mathcal{M}} \sum_{\vec{\imath}\notin\mathcal{F}_{\overline{Y}}} p_n\left(A, \vec{\imath} \mid \overline{\overrightarrow{\theta_L}}_\alpha, \overline{\overrightarrow{\theta_K}}_\alpha\right) \int_{\{\vec{x}\in A \mid \vec{x}\notin\mathcal{F}_{\overline{X}}\}} \overrightarrow{dx}\right] \tag{21}$$

5. ILLUSTRATIVE CASE

The illustrative case refers to one important subsystem of a residual heat removal system (RHRS) consisting of a centrifugal pump and a pneumatic valve. The definition of the system has been provided by Électricité de France (EDF). The degradation model of the pump is a modified MSM from the one originally supplied by EDF, while that of the valve is a PBM developed by Daigle and Goebel [4]. Upon discussion with the experts, a degradation dependency between the two components has been considered, as follows: the degradation of the pump will cause it to vibrate [39] which, in turn, will lead the valve to vibrate and therefore aggravate the degradation processes of the latter [40].

Given its series logic structure, the subsystem is considered failed when one of the two components is failed.

5.1 Centrifugal pump

The multi-state model of the degradation processes of the centrifugal pump is a continuous-time homogeneous Markov chain with constant transition rates as shown in Fig 2:

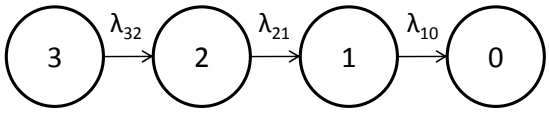

Fig 2. Degradation processes of the pump.

There are four degradation states for the pump, from the perfect functioning state ‘3’ to the complete failure state ‘0’. Due to the degradation, the pump can vibrate when it reaches the degradation states ‘2’ and ‘1’. The intensity of the vibration of the state ‘2’ is assigned as ‘smooth’ and that of the state ‘1’ is assigned as ‘rough’ by the experts. Let $Y_p(t)$ denote the degradation state of the pump at time t and $S_p = \{‘0’, ‘1’, ‘2’, ‘3’\}$ denote the degradation states set. The pump is functioning until it reaches the complete failure state ‘0’; λ_{32}, λ_{21} and λ_{10} are the transition rates of the degradation process.

5.2 Pneumatic valve

The simplified scheme of the pneumatic valve is shown in Fig 3.

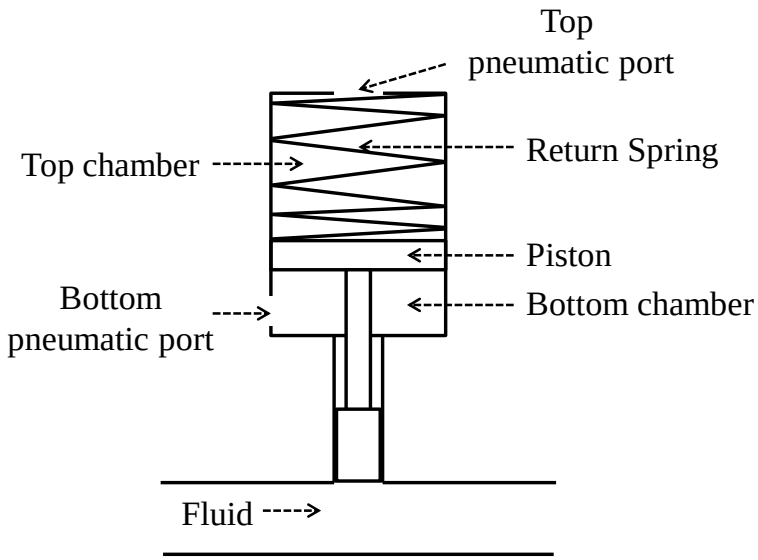

Fig 3. Simplified scheme of the pneumatic valve [4].

The pneumatic valve is a normally-closed and gas-actuated valve with a linear cylinder actuator. Top chamber and bottom chamber are separated by the piston, and are connected to a top pneumatic port and a bottom pneumatic port, respectively. The position of the piston between fully closed position '*0*' and fully open position 'x_s' can be controlled by regulating the pressure of the pneumatic ports to fill or evacuate the two chambers. A return spring is linked with the piston to ensure that the valve will close when pressure is lost, due to the spring force.

There are several common degradation mechanisms of the valve (e.g. sliding wear, internal leaks, external leaks, etc.). In this case study, as degradation mechanism we have chosen the external leak at the actuator connections to the bottom pneumatic port due to corrosion and other environmental factors, for two reasons: 1) it is more significant than the other degradation mechanisms according to the results shown in [4]; 2) the uncertainty associated with the wear coefficient estimated from a limited amount of data should be taken into account. The leak will lead the valve to be more difficult to open but easier to close. The threshold of the area of leak hole D_b^* is defined as the value above which ($D_b(t) > D_b^*$) the valve cannot reach the fully open position within the 15s time limit from the fully closed position, after an opening command is executed.

Let $D_b(t)$ denote the area of the leak hole at the bottom pneumatic port at time *t*, the development of the leak size is described by:

$$\dot{D}_b(t) = \omega_b(1 + \beta_{Y_p(t)}) \tag{22}$$

where ω_b is the original wear coefficient and where $\beta_{Y_p(t)}$ is the relative increment of the developing rate of the external leak at the bottom pneumatic port caused by the vibration of the pump at the degradation state '2' or '1' (if we ignore the degradation dependency, then $\beta_{Y_p(t)} = 0$).

The function command of the valve cycle is a 30s-periodic-signal and the valve is

commanded to open in the first half-period and to close in the second half by changing the pressure of the top bottom pneumatic port $u_t(t)$ and that of the bottom pneumatic port $u_b(t)$ (opening command: $u_t(t) = P_{atm}$ and $u_b(t) = P_{sup}$; closing command: $u_t(t) = P_{sup}$ and $u_b(t) = P_{atm}$). At the beginning, the valve is set to the fully closed position.

Let $x(t)$ denote the position of the valve at time t, whose evolution in time is described by the following equations:

$$\ddot{x}(t) = a(t) \tag{23}$$

where

$$a(t) = \frac{1}{m}[\big(p_b(t) - p_t(t)\big)A_p - mg + \\ -k(x(t) + x_0) - rv(t) + F_c\big(x(t)\big)] \tag{24}$$

is the valve acceleration, where

$$p_b(t) = \frac{m_b(t)R_gT}{V_{b0}+A_px(t)} \tag{25}$$

is the gas pressure of the bottom of the piston,

$$p_t(t) = \frac{m_t(t)R_gT}{V_{t0}+A_p(x_s-x(t))} \tag{26}$$

is the gas pressure of the top of the piston and where

$$m_t(t) = m_t(0) + \int_0^t f_g(u_t(t), p_t(t), A_s)dt \\ \text{with } m_t(0) = \frac{P_{sup}(L_sA_p+V_{t0})}{R_gT} \tag{27}$$

and

$$m_b(t) = m_b(0) + \int_0^t f_g(u_b(t), p_b(t), A_s) + f_g(P_{atm}, p_b(t), D_b(t))dt \\ \text{with } \mathrm{m_b(0)} = \frac{\mathrm{P_{atm}V_{b0}}}{\mathrm{R_gT}} \tag{28}$$

are respectively the masses of the gas in the top chamber and bottom chamber at time t, and where

$$f_g(p_1, p_2, A) = \begin{cases} \varepsilon PC_sA\sqrt{\frac{\gamma}{zR_gT}(\frac{2}{\gamma+1})^{\frac{\gamma+1}{\gamma-1}}}, & if\ \delta \le (\frac{2}{\gamma+1})^{\frac{\gamma}{\gamma-1}} \\ \varepsilon PC_sA\sqrt{\frac{\gamma}{zR_gT}(\frac{2}{\gamma-1})(\delta^{\frac{2}{\gamma}} - \delta^{\frac{\gamma+1}{\gamma}})}, & if\ \delta > (\frac{2}{\gamma+1})^{\frac{\gamma}{\gamma-1}} \end{cases} \\ \text{with } \begin{cases} P = \max(p_1, p_2) \\ \delta = \frac{\min(p_1,p_2)}{\max(p_1,p_2)} \\ \varepsilon = sgn(p_1 - p_2) \end{cases} \tag{29}$$

defines the gas flow through an orifice, and

$$F_c\big(x(t)\big) = \begin{cases} k_c(-x(t)), & if\ x(t) < 0 \\ 0, & if\ 0 \le x(t) \le L_s \\ -k_c(x(t) - x_s), & if\ x(t) > L_s \end{cases} \quad (30)$$

is the contact force exerted on the piston by the flexible seals.

The parameters definitions and values (except for ω_b and $\beta_{Y_p(t)}$) of the valve are presented in Table I below.

Table I Valve Parameter Definitions and Values

Parameter – Definition	Value
g – acceleration due to gravity	9.8 m/s
P_{sup} – supply pressure	5.27e6 Pa
P_{atm} – atmospheric pressure	1.01e5 Pa
m – mass of the moving parts of the valve	50 kg
r – coefficient of kinetic friction	6.00e3 Ns/m
k – spring constant	4.80e4 N/s
k_c – large spring constant associated with the flexible seals	1.00e8 N/s
x_0 – amount of spring compression when the valve is closed	0.254 m
x_s – fully open position of the valve	0.1 m
A_p – surface area of the piston	8.10e-3 m^2
V_{t0} – minimum gas volume of the top chamber	8.11e-4 m^3
V_{b0} – minimum gas volume of the bottom chamber	8.11e-4 m^3
R_g – gas constant for the pneumatic gas	296 J/K/kg
T – ideal gas temperature	293 K
γ – ratio of specific heats	1.4
z – gas compressibility factor	1
A_s – orifice area of the pneumatic port	1.00e-5 m^2
C_s – flow coefficient	0.1

With the given values, the threshold of the area of leak hole $D_b^* = 1.06\text{e}-5\ m^2$ (maximum damage) can be calculated: once exceeded, the valve will not reach the fully open position within the 15s limit, as shown in Fig 4.

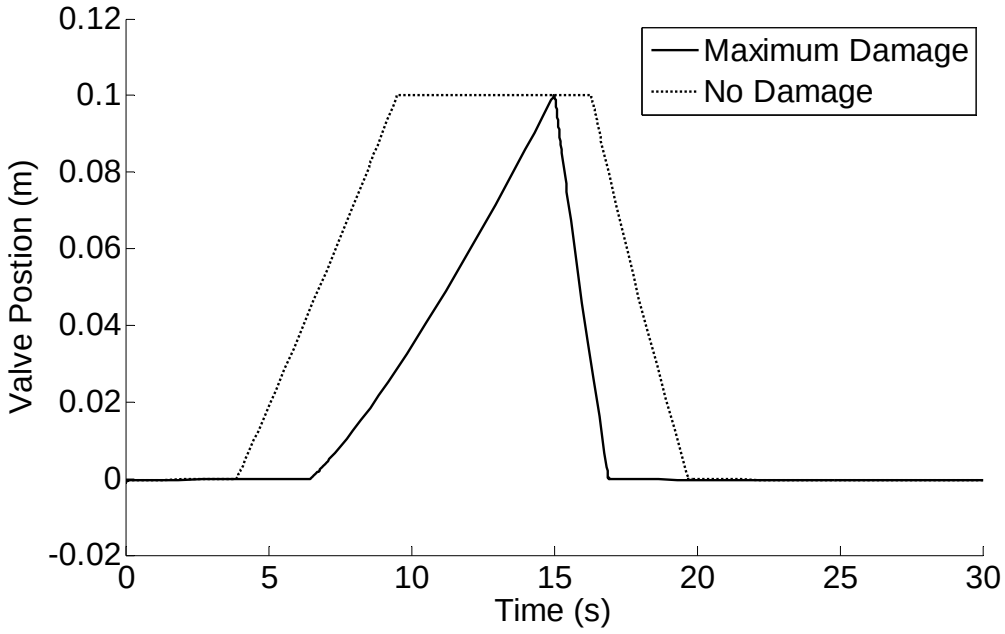

Fig 4. Valve behavior with different sizes of the external leak.

5.3 PDMP for the system under uncertainty

The degradation processes of the whole system are modeled by PDMP as follows:

$$\vec{Z}(t) = \begin{pmatrix} D_b(t) \\ Y_p(t) \end{pmatrix} \in \mathbb{R}^+ \times S_p \tag{31}$$

The space of the failure states of $\vec{Z}(t)$ is $\mathcal{F} = \mathcal{F}_{D_b} \times \mathcal{F}_{Y_p} = [D_b^*, +\infty) \times \{\text{'0'}\}$. We have $\overrightarrow{\theta_L} = (\omega_b, \beta_{Y_p(t)})$ and $\overrightarrow{\theta_K} = (\lambda_{32}, \lambda_{21}, \lambda_{10})$ which are the uncertain parameters due to the fact that their values are estimated from insufficient degradation data or elicited from expert judgment. Epistemic uncertainty associated to them, hence, needs to be taken into account and a proper mathematical representation of uncertainty of this nature is by fuzzy numbers (FNs). We choose triangular fuzzy numbers (TFNs) [41] to represent the uncertain parameters because their boundary values and most probable or most advisable values are considered easier to be elicited from experts than other FN types and they are widely used to represent uncertain parameters in reliability engineering [20, 24, 29, 41]. However, the proposed framework is generally suitable for fuzzy numbers with other types of membership functions. The values of $\widetilde{\omega_b}$, $\widetilde{\beta_{Y_p(t)}}$, $\widetilde{\lambda_{32}}$, $\widetilde{\lambda_{21}}$ and $\widetilde{\lambda_{10}}$ are shown in Table II. The fuzzy numbers are assigned by considering a relative uncertainty of $\pm$10% of the original parameters values.

Table II The values of the fuzzy parameters in PDMP

Parameter	Value
$\widetilde{\omega_b}$	(9e-9, 1e-8, 1.1e-8) m^2/s
$\widetilde{\beta_2}$	(9%, 10%, 11%)
$\widetilde{\beta_1}$	(18%, 20%, 22%)
$\widetilde{\lambda_{32}}$	(2.7e-3, 3e-3, 3.3e-3) s^{-1}
$\widetilde{\lambda_{21}}$	(2.7e-3, 3e-3, 3.3e-3) s^{-1}
$\widetilde{\lambda_{10}}$	(2.7e-3, 3e-3, 3.3e-3) s^{-1}

The initial state of the system is assumed as follows:

$$\overrightarrow{Z_0} = \begin{pmatrix} D_b(0) \\ Y_p(0) \end{pmatrix} = \begin{pmatrix} 0 \\ \text{'3'} \end{pmatrix}$$

which means that the two components are both in their perfect state. The initial PDF of the processes $(D_b(t), Y_p(t))_{t\geq 0}$, $p_0\left(x, i \mid \overrightarrow{\widetilde{\theta_L}}, \overrightarrow{\widetilde{\theta_K}}\right)$, hence equals to 1 if $(x, i) = (0, \text{'3'})$ and to 0 otherwise.

6. RESULTS

A MC-based approach [33] can also be used to quantify the epistemic uncertainty, in alternative to the fuzzy arithmetic operations and fuzzy parameter programming procedure. The comparisons between the results of the reliability of the system at cut level $\alpha = 1$, i.e. without fuzziness in the parameters values, over a time horizon 1000s calculated by MC simulation and the FV scheme are shown in Fig 5 and Fig 6. In order to better understand the differences presented in Fig 5 and Fig 6, we have added below each original Figure one extra Figure, zooming on the time horizon between 800 s and 900 s to illustrate the results obtained by different methods. For the FV scheme, the state space $\mathbb{R}^+$ of $D_b(t)$ has been divided into an admissible mesh $\mathcal{M} = \bigcup_{n=0,1,2,\dots} [n\Delta x, (n+1)\Delta x[$ where $\Delta x = 1\text{e}-8\ \text{m}^2/\text{s}$ and the time space $\mathbb{R}^+$ into small intervals $\mathbb{R}^+ = \bigcup_{n=0,1,2,\dots} [n\Delta t, (n+1)\Delta t[$ by setting the time step $\Delta t = 1$ s. All the experiments were carried out in MATLAB on a PC with an Intel Core 2 Duo CPU at 1.97 GHz and a RAM of 1.95 GB. The MC simulation method with 10^5 and 10^6 replications (named MC1 and MC2, respectively), and the proposed FV scheme are applied for the fuzzy reliability assessment of the system. The average computation time of MC1 and MC2 is respectively 0.94 s and 9.40 s, while that of the FV scheme is 0.20 s. The system reliability decreases more rapidly after around 885 s, because at that time the valve could fail, corresponding to the situation when the pump steps to the state '1' very quickly and stays there until the valve fails.

The quantitative comparison of the results over a time horizon 1000 s is shown in Table III. Compared with the results of MC2, the mean absolute relative difference (MARD) of the results of MC1 is 0.40%, while that of the results of the FV scheme is 0.17%. It is observed that the results of the FV scheme are closer to those of MC2, which is more accurate than that of MC1

because of the larger number of simulations.

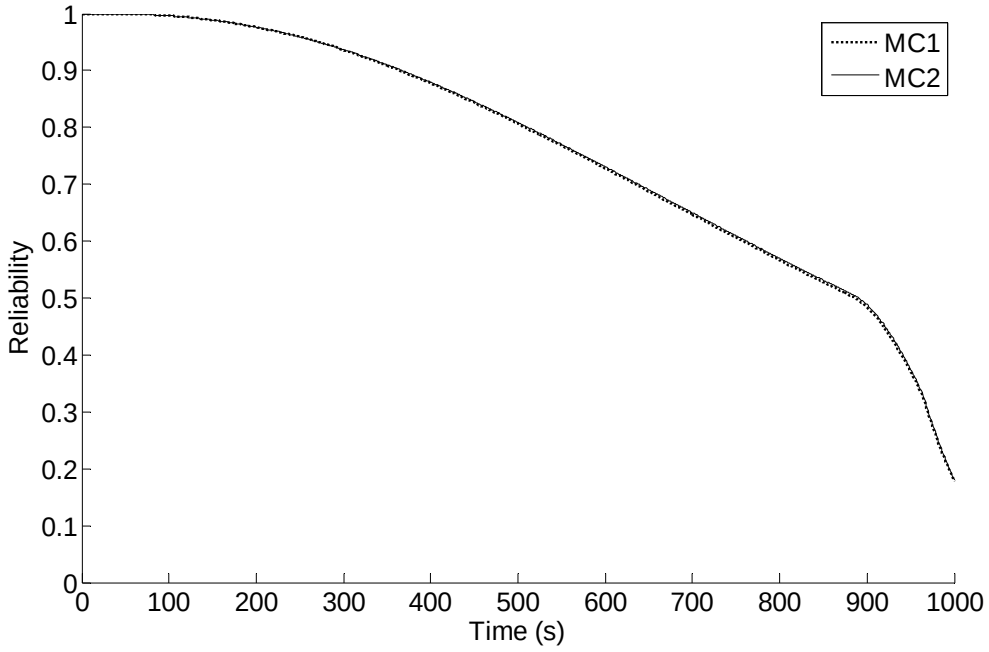

Fig 5. Fuzzy reliability at cut level $\alpha = 1$ (no fuzziness) obtained by MC1 and MC2.

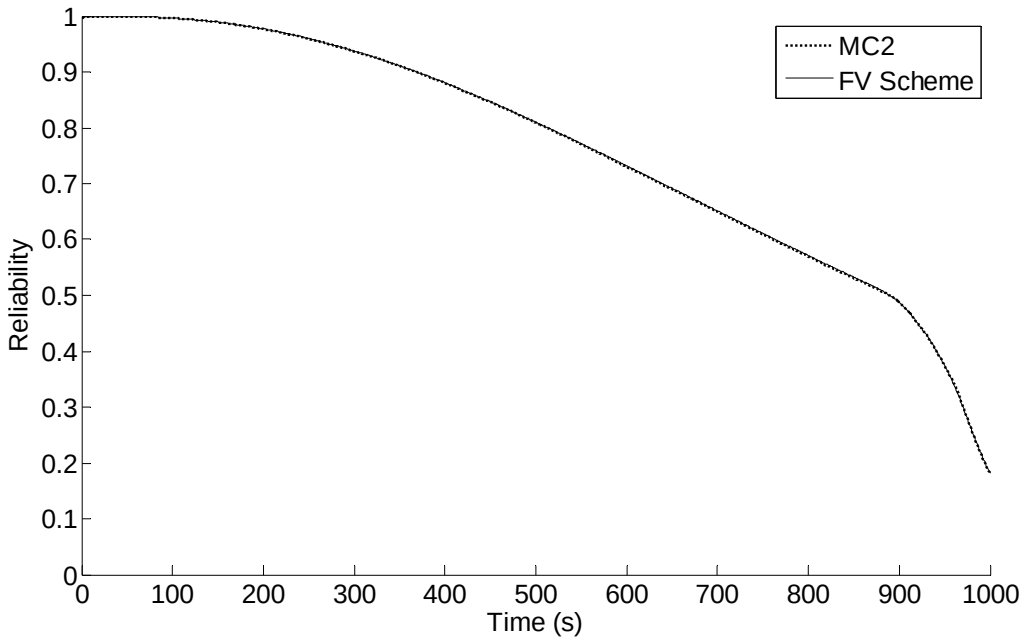

Fig 6. Fuzzy reliability at cut level $\alpha = 1$ (no fuzziness) obtained by MC2 and FV scheme.

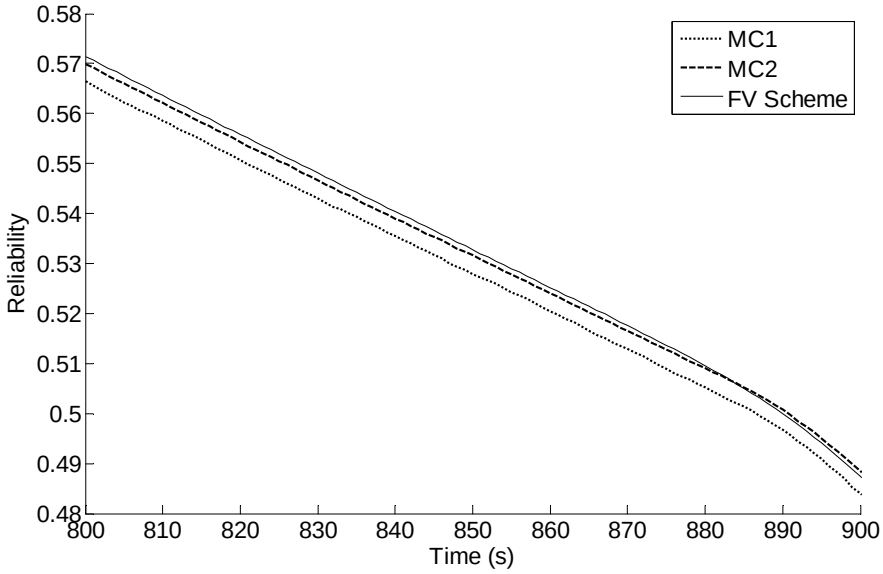

Fig 7. Fuzzy reliability at cut level $\alpha = 1$ (no fuzziness) obtained by MC1, MC2 and FV scheme of time horizon between 800 s and 900 s.

Table III Comparison of the fuzzy reliability of the system at cut level $\alpha = 1$ (no fuzziness) between MC simulation methods and FV scheme at different times

Method / Time	MC2	MC1	Relative difference	FV scheme	Relative difference
100s	**0.9965**	0.9966	0.01%	0.9964	-0.01%
200s	**0.9769**	0.9766	-0.03%	0.9773	0.04%
300s	**0.9372**	0.9364	-0.09%	0.9379	0.07%
400s	**0.8799**	0.8780	-0.22%	0.8805	0.07%
500s	**0.8094**	0.8063	-0.38%	0.8102	0.10%
600s	**0.7305**	0.7283	-0.30%	0.7321	0.22%
700s	**0.6496**	0.6469	-0.42%	0.6513	0.26%
800s	**0.5696**	0.5664	-0.56%	0.5714	0.32%
900s	**0.4873**	0.4839	-0.70%	0.4874	0.02%
1000s	**0.1801**	0.1778	-1.28%	0.1811	0.56%

The results of the fuzzy reliability of the system at cut levels $\alpha = 0$ and $\alpha = 1$ over a time horizon 1000 s obtained by MC2 and FV scheme are shown in Fig 8. The lower bound of the fuzzy reliability of the system at cut level $\alpha = 0$ decreases more sharply after around 790 s, earlier than the fuzzy reliability at $\alpha = 1$. It is seen that the system fails after around 964 s, because at that time the valve is completely failed. The upper bound of the fuzzy reliability at $\alpha = 0$ does not experience a rapid decrease because the valve is mostly functioning over the time horizon.

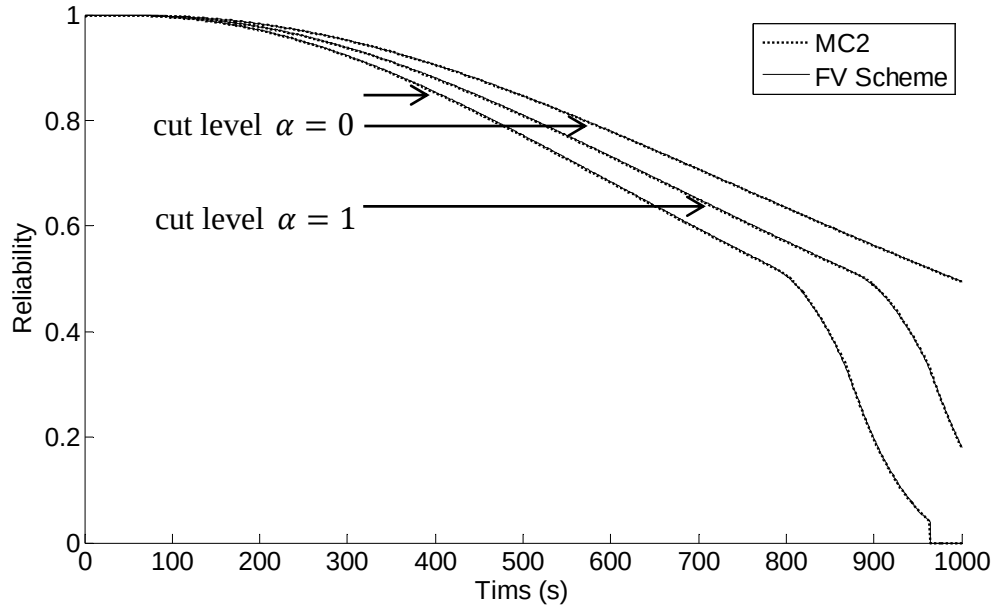

Fig 8. Fuzzy reliability at cut levels $\alpha = 0$ and $\alpha = 1$ obtained by MC2 and FV scheme.

The membership function of fuzzy reliability $\tilde{R}(t)$ at mission time $t = 800$ s at different cut levels $\alpha \in [0, 1]$ obtained by MC simulation methods and FV scheme are illustrated in Fig 9 and Fig 10 (we have uniformly chosen 51 points in $[0, 1]$ with a step equal to 0.02 assigned to α). The average computation times of MC1 and MC2 are 20.19 s and 201.94 s respectively, while that of FV scheme is 15.91 s.

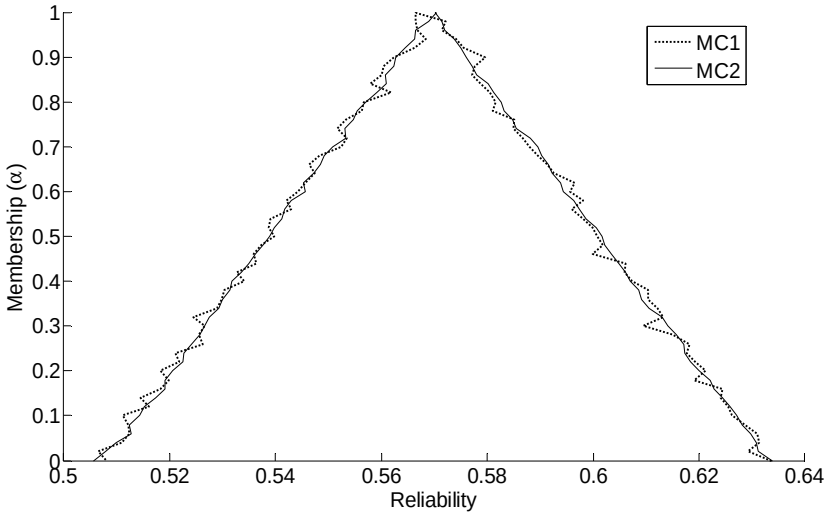

Fig 9. Membership function of fuzzy reliability $\tilde{R}(t)$ at mission time $t = 800$ s obtained by MC1 and MC2.

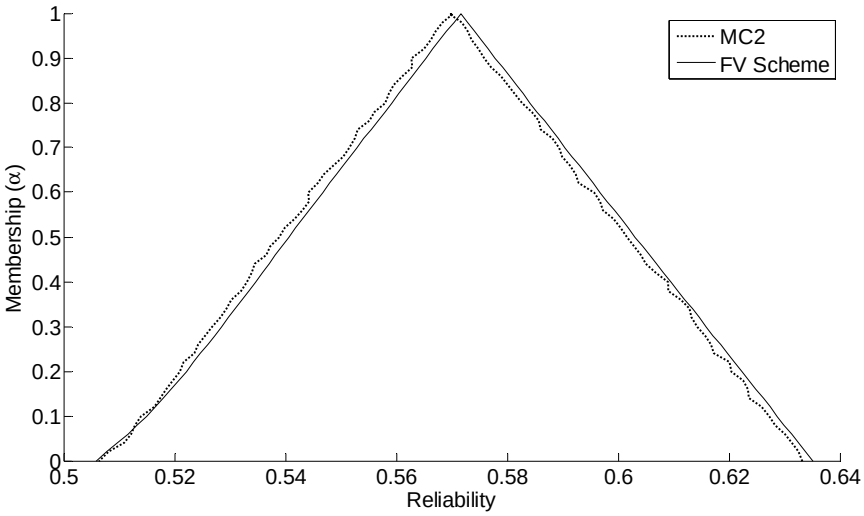

Fig 10. Membership function of fuzzy reliability $\tilde{R}(t)$ at mission time $t = 800$ s obtained by MC2 and FV scheme.

The quantitative comparison of the results of the membership functions obtained by the MC simulation methods and FV scheme is shown in Table IV. Compared with the results of MC2, the MARD of the results of MC1 is 0.38% while that of the FV scheme is 0.27%.

Table IV Comparison of the results of the membership function obtained by MC simulation methods and FV scheme

Method / Cut level	MC2	MC1	Relative difference (Minimum/Maximum)	FV scheme	Relative difference (Minimum/Maximum)
$\alpha = 0$	**[0.5062, 0.6330]**	[0.5086, 0.6340]	0.47% / 0.16%	[0.5057, 0.6350]	-0.10% / 0.32%
$\alpha = 0.1$	**[0.5137, 0.6271]**	[0.5111, 0.6260]	-0.51% / 0.18%	[0.5148, 0.6285]	0.21% / 0.22%
$\alpha = 0.2$	**[0.5209, 0.6203]**	[0.5181, 0.6218]	-0.54% / 0.24%	[0.5220, 0.6221]	0.21% / 0.29%
$\alpha = 0.3$	**[0.5266, 0.6141]**	[0.5249, 0.6095]	-0.32% / -0.75%	[0.5283, 0.6157]	0.32% / 0.26%
$\alpha = 0.4$	**[0.5329, 0.6088]**	[0.5348, 0.6071]	0.36% / -0.28%	[0.5344, 0.6093]	0.28% / 0.08%
$\alpha = 0.5$	**[0.5386, 0.6015]**	[0.5413, 0.6001]	0.50% / -0.23%	[0.5405, 0.6030]	0.35% / 0.25%
$\alpha = 0.6$	**[0.5440, 0.5955]**	[0.5476, 0.5976]	0.66% / 0.35%	[0.5466, 0.5966]	0.48% / 0.18%
$\alpha = 0.7$	**[0.5513, 0.5892]**	[0.5529, 0.5880]	0.29% / -0.20%	[0.5528, 0.5903]	0.27% / 0.19%
$\alpha = 0.8$	**[0.5577, 0.5825]**	[0.5559, 0.5808]	-0.32% / -0.29%	[0.5590, 0.5840]	0.23% / 0.26%
$\alpha = 0.9$	**[0.5626, 0.5756]**	[0.5643, 0.5797]	0.30%/ 0.71%	[0.5652, 0.5777]	0.46% / 0.36%

The above results show that the FV scheme achieves comparable results as MC2, with less computational burden.

7. CONCLUSIONS

In system reliability modeling, it is important to be able to describe multiple dependent degradation processes, while including the uncertainty in their quantitative evaluation. In this work, we have considered the degradation dependencies among different system components and within one component in the framework of PDMP modeling. Both PBMs and MSMs are used to describe the components degradation behavior. Epistemic Uncertainty due to the incomplete or imprecise knowledge about the degradation processes and the governing parameters is included by describing the model parameters as fuzzy numbers. For the calculation of the system (fuzzy) reliability, the FV method has been extended and shown to lead to comparable results as MC simulation, but with reduced computing time.

In future research, it will be interesting to consider the situation when aleatory uncertainty is associated with the parameters in the PDMP model.

Acknowledgement

The authors would like to thank Mrs. Dominique VASSEUR, Mr. Antoine DESPUJOLS and Mr. Emmanuel ARDILLON from the Department Industrial Risks Management (MRI),

Electricité de France R&D for their insightful comments. The work was supported by Electricité de France Contract No.8610-5910112096.

References

[1] Y. Wang and H. Pham, "Modeling the dependent competing risks with multiple degradation processes and random shock using time-varying copulas," *Reliability, IEEE Transactions on,* vol. 61, pp. 13-22, 2012.

[2] J. Lei, F. Qianmei, and D. W. Coit, "Reliability and Maintenance Modeling for Dependent Competing Failure Processes With Shifting Failure Thresholds," *Reliability, IEEE Transactions on,* vol. 61, pp. 932-948, 2012.

[3] N. Rasmekomen and A. K. Parlikad, "Maintenance Optimization for Asset Systems With Dependent Performance Degradation," *Reliability, IEEE Transactions on,* vol. 62, pp. 362 - 367, 2013.

[4] M. Daigle and K. Goebel, "A model-based prognostics approach applied to pneumatic valves," *International Journal of Prognostics and Health Management,* vol. 2, p. 008, 2011.

[5] M. Daigle and K. Goebel, "Multiple damage progression paths in model-based prognostics," in *Aerospace Conference, 2011 IEEE*, 2011, pp. 1-10.

[6] E. Keedy and Q. Feng, "A physics-of-failure based reliability and maintenance modeling framework for stent deployment and operation," *Reliability Engineering & System Safety,* vol. 103, pp. 94-101, 2012.

[7] S. Reggiani, S. Poli, M. Denison, E. Gnani, A. Gnudi, G. Baccarani*, et al.*, "Physics-Based Analytical Model for HCS Degradation in STI-LDMOS Transistors," *Electron Devices, IEEE Transactions on,* vol. 58, pp. 3072-3080, 2011.

[8] O. Chryssaphinou, N. Limnios, and S. Malefaki, "Multi-state reliability systems under discrete time semi-Markovian hypothesis," *Reliability, IEEE Transactions on,* vol. 60, pp. 80-87, 2011.

[9] M. Giorgio, M. Guida, and G. Pulcini, "An age-and state-dependent Markov model for degradation processes," *IIE Transactions,* vol. 43, pp. 621-632, 2011.

[10] W. Li and H. Pham, "Reliability modeling of multi-state degraded systems with multi-competing failures and random shocks," *Reliability, IEEE Transactions on,* vol. 54, pp. 297-303, 2005.

[11] A. Lisnianski and G. Levitin, *Multi-state system reliability: assessment, optimization and applications*: World scientific, 2003.

[12] Y.-F. Li, E. Zio, and Y.-H. Lin, "A Multistate Physics Model of Component Degradation Based on Stochastic Petri Nets and Simulation," *Reliability, IEEE Transactions on,* vol. 61, pp. 921-931, 2012.

[13] Y.-H. Lin, Y.-F. Li, and E. Zio, "Modeling Multiple Dependent Competing Degradation via Piecewise Deterministic Markov Process," *Manuscript sumbitted for publication*.

[14] P.-E. Labeau, "A Monte Carlo estimation of the marginal distributions in a problem of probabilistic dynamics," *Reliability Engineering & System Safety,* vol. 52, pp. 65-75, 1996.

[15] M. Marseguerra and E. Zio, "Monte Carlo approach to PSA for dynamic process systems," *Reliability Engineering & System Safety,* vol. 52, pp. 227-241, 1996.

[16] R. Eymard and S. Mercier, "Comparison of numerical methods for the assessment of production availability of a hybrid system," *Reliability Engineering & System Safety,* vol. 93, pp. 168-177, 2008.

[17] C. Cocozza-Thivent, R. Eymard, and S. Mercier, "A finite-volume scheme for dynamic reliability models," *IMA journal of numerical analysis,* vol. 26, pp. 446-471, 2006.

[18] R. Eymard, S. Mercier, and A. Prignet, "An implicit finite volume scheme for a scalar hyperbolic problem with measure data related to piecewise deterministic Markov processes," *journal of Computational and Applied Mathematics,* vol. 222, pp. 293-323, 2008.

[19] M. Laviolette and J. W. Seaman Jr, "The efficacy of fuzzy representations of uncertainty," *Fuzzy Systems, IEEE Transactions on,* vol. 2, pp. 4-15, 1994.

[20] Y. Ding, M. J. Zuo, A. Lisnianski, and Z. Tian, "Fuzzy multi-state systems: general definitions, and performance assessment," *Reliability, IEEE Transactions on,* vol. 57, pp. 589-594, 2008.

[21] Y. Liu, W. Tang, and R. Zhao, "Reliability and mean time to failure of unrepairable systems with fuzzy random lifetimes," *Fuzzy Systems, IEEE Transactions on,* vol. 15, pp. 1009-1026, 2007.

[22] M. Bazu, "A combined fuzzy-logic and physics-of-failure approach to reliability prediction," *Reliability, IEEE Transactions on,* vol. 44, pp. 237-242, 1995.

[23] S. A. Sandri, D. Dubois, and H. W. Kalfsbeek, "Elicitation, assessment, and pooling of expert judgments using possibility theory," *Fuzzy Systems, IEEE Transactions on,* vol. 3, pp. 313-335, 1995.

[24] Y. Liu, H. Huang, and G. Levitin, "Reliability and performance assessment for fuzzy multi-state elements," *Proceedings of the Institution of Mechanical Engineers, Part O: Journal of Risk and Reliability,* vol. 222, pp. 675-686, 2008.

[25] Y. Li, E. Zio, and Y.-H. Lin, "A Multistate Physics Model of Component Degradation Based on Stochastic Petri Nets and Simulation," *Reliability, IEEE Transactions on,* vol. 61, pp. 921-931, 2012.

[26] H. Tanaka, L. Fan, F. Lai, and K. Toguchi, "Fault-tree analysis by fuzzy probability," *Reliability, IEEE Transactions on,* vol. 32, pp. 453-457, 1983.

[27] D. Singer, "A fuzzy set approach to fault tree and reliability analysis," *Fuzzy Sets and Systems,* vol. 34, pp. 145-155, 1990.

[28] J. Dunyak, I. W. Saad, and D. Wunsch, "A theory of independent fuzzy probability for system reliability," *Fuzzy Systems, IEEE Transactions on,* vol. 7, pp. 286-294, 1999.

[29] Y. Ding and A. Lisnianski, "Fuzzy universal generating functions for multi-state system reliability assessment," *Fuzzy Sets and Systems,* vol. 159, pp. 307-324, 2008.

[30] Y. F. Li, Y. Ding, and E. Zio, "Random Fuzzy Extension of the Universal Generating Function Approach for the Reliability Assessment of Multi-State Systems Under Aleatory and Epistemic Uncertainties," *Reliability, IEEE Transactions on,* vol. PP, pp. 1-1, 2014.

[31] M. Sallak, W. Schön, and F. Aguirre, "Reliability assessment for multi-state systems under uncertainties based on the Dempster–Shafer theory," *IIE Transactions,* vol. 45, pp. 995-1007, 2013/09/01 2012.

[32] C. Baudrit, D. Dubois, and D. Guyonnet, "Joint propagation and exploitation of probabilistic and possibilistic information in risk assessment," *Fuzzy Systems, IEEE Transactions on,* vol. 14, pp. 593-608, 2006.

[33] C. Baudrit, D. Dubois, and N. Perrot, "Representing parametric probabilistic models tainted with imprecision," *Fuzzy sets and systems,* vol. 159, pp. 1913-1928, 2008.

[34] R. Coudray and J. Mattei, "System reliability: An example of nuclear reactor system analysis," *Reliability Engineering,* vol. 7, pp. 89-121, 1984.

[35] J. Devooght and C. Smidts, "Probabilistic dynamics as a tool for dynamic PSA," *Reliability Engineering & System Safety,* vol. 52, pp. 185-196, 1996.

[36] M. H. Davis, *Markov models and optimization* vol. 49: CRC Press, 1993.

[37] L. A. Zadeh, "Fuzzy sets," *Information and control,* vol. 8, pp. 338-353, 1965.

[38] L. A. Zadeh, "Fuzzy sets as a basis for a theory of possibility," *Fuzzy sets and systems,* vol. 100, pp. 9-34, 1999.

[39] S. Zhang, M. Hodkiewicz, L. Ma, and J. Mathew, "Machinery condition prognosis using multivariate analysis," in *Engineering Asset Management*, ed: Springer, 2006, pp. 847-854.

[40] P. Moussou, S. Cambier, D. Lachene, S. Longarini, L. Paulhiac, and V. Villouvier, "Vibration investigation of a French PWR power plant piping system caused by cavitating butterfly valves," *ASME-PUBLICATIONS-PVP,* vol. 420, pp. 99-106, 2001.

[41] M. Sallak, C. Simon, and J.-F. Aubry, "A fuzzy probabilistic approach for determining safety integrity level," *Fuzzy Systems, IEEE Transactions on,* vol. 16, pp. 239-248, 2008.

PAPER IV: Y.-H. Lin, Y.-F. Li, E. Zio. Component Importance Measures for Components with Multiple Dependent Competing Degradation Processes and Subject to Maintenance. *Reliability, IEEE Transactions on*. (Accepted)

Component Importance Measures for Components with Multiple Dependent Competing Degradation Processes and Subject to Maintenance

Yan-Hui Lin, Yan-Fu Li, *senior member IEEE*, Enrico Zio, *senior member IEEE*

Index Terms – Degradation dependency, importance measures, multiple dependent competing degradation processes, piecewise-deterministic Markov process (PDMP), finite-volume approach, residual heat removal system, nuclear power plant.

Abstract - Component importance measures (IMs) are widely used to rank the importance of different component within a system and guide allocation of resources. The criticality of a component may vary over time, under the influence of multiple dependent competing degradation processes and maintenance tasks. Neglecting this may lead to inaccurate estimation of the component IMs and inefficient related decisions (e.g. maintenance, replacement, etc.). The work presented in this paper addresses the issue by extending the mean absolute deviation IM by taking into account: (1) the dependency of multiple degradation processes within one component and among different components; (2) discrete and continuous degradation processes; (3) two types of maintenance tasks: condition-based preventive maintenance via periodic inspections and corrective maintenance. Piecewise-deterministic Markov processes are employed to describe the stochastic process of degradation of the component under these factors. A method for the quantification of the component IM is developed based on the finite-volume approach. A case study on one section of the residual heat removal system of a nuclear power plant is considered as an example for numerical quantification.

Acronyms

IMs	Importance measures
PBMs	Physics-based models
MSMs	Multi-state models
GSA	Global sensitivity analysis
BIM	Birnbaum IM
MAD	Mean absolute deviation
MSSs	Multi-state systems
PM	Preventive maintenance
CM	Corrective maintenance
FV	Finite-volume
RHRS	Residual heat removal system

Notations

Q	Number of components in the system
$\boldsymbol{L}$	Group of degradation processes modeled by PBMs
$\boldsymbol{K}$	Group of degradation processes modeled by MSMs
$\boldsymbol{D}_{O_q}$	Degradation state of component O_q
$\overrightarrow{X_{L_m}}(t)$	Time-dependent continuous variables of degradation process L_m
$\overrightarrow{X_{L_m}^{\boldsymbol{D}}}(t)$	Non-decreasing degradation variables vector
$\overrightarrow{X_{L_m}^{\boldsymbol{P}}}(t)$	Physical variables vector
$\boldsymbol{\mathcal{F}}_{L_m}$	Set of failure states of degradation process L_m
$Y_{K_n}(t)$	State variable of degradation process K_n
$\boldsymbol{S}_{K_n}$	Finite state set of degradation process K_n
$\boldsymbol{\mathcal{F}}_{K_n}$	Set of failure states of degradation process K_n
$\boldsymbol{H}_i$	Predefined state set of PM for degradation process i
T_i	Fixed period of PM for degradation process i
$\vec{Z}(t)$	Degradation state of the system
N_m	Number of maintenance tasks experienced by the system
T_{miss}	System mission time
T_m^k	Execution time of the *k*-th maintenance task
$\overrightarrow{Z_k}(t)$	Degradation state of the system defined on $[T_m^{k-1}, T_m^k]$
$\boldsymbol{\theta_K}$	Environmental and operational factors in $\boldsymbol{K}$
$\lambda_{\vec{\imath}}\left(\vec{\jmath}\middle\|\overrightarrow{X}(t), \boldsymbol{\theta_K}\right)$	Transition rate from state $\vec{\imath}$ to $\vec{\jmath}$
$\boldsymbol{\theta_L}$	Environmental and operational factors in $\boldsymbol{L}$
$\overrightarrow{f_{\boldsymbol{L}}}\left(\overrightarrow{Z_k}(t), t\middle\|\boldsymbol{\theta_L}\right)$	Deterministic physics equations in $\boldsymbol{L}$
$\overrightarrow{Z'}(t)$	Stochastic process recording the failure of the system
$\boldsymbol{\mathcal{F}}$	System failure state set
$CI_{O_q}(t)$	Component IM of component O_q at time t
$f_{\overrightarrow{\boldsymbol{D}_{O_q}}(t)}\left(d\overrightarrow{x_{\boldsymbol{L}_p}}, \overrightarrow{y_{\boldsymbol{K}_q}}\right)$	Probability distribution of $\overrightarrow{\boldsymbol{D}_{O_q}}(t)$
$p_t^{\overrightarrow{Z_k}}(d\vec{x}, \vec{\imath} \mid \boldsymbol{\theta})$	Probability distribution of processes $\overrightarrow{Z_k}(t)$
$P_n^{\overrightarrow{Z_k}}(A, \vec{\imath}\|\boldsymbol{\theta})$	Approximate value for $\rho_t^{\overrightarrow{Z_k}}(\cdot,\cdot\|\boldsymbol{\theta})$ on $\{\vec{\imath}\} \times [(n+1)\Delta t, (n+2)\Delta t[\times A$
$\left\{\left(A^{k-1}, \overrightarrow{\imath^{k-1}}\right)\right\}$	Set containing all the states that step to the state $(A, \vec{\imath})$ after the $(k-1)$-th maintenance task

$A/\left(\overrightarrow{x_{L_p}}, \overrightarrow{y_{K_q}}\right)$ Mesh by fixing $\overrightarrow{\boldsymbol{D}_{O_q}}(t)$ to $(\overrightarrow{x_{L_p}}, \overrightarrow{y_{K_q}})$.

1. INTRODUCTION

In reliability engineering, component importance measures (IMs) are used to quantify and rank the importance of different components within a system. By determining the criticalities of the components, limited resources can be allocated according to components prioritization for reliability improvement during the system design and maintenance planning phases [1].

The criticality of a component changes over time, due to the evolution of its underlying degradation processes [2]. Also, in practice, components are often subject to multiple competing degradation processes and any of them may individually lead to component failure [3]. The dependency among the degradation processes within one component (e.g. in a micro-engine, the shock process can enhance the wear process of rubbing surfaces and each process can lead to failure [4]) and of different components (e.g. in a water treatment plant, the decaying pre-filtrations often lower the performance of sand filter [5]) have to be considered in the calculation of component IMs. Moreover, the degradation processes can be interrupted by maintenance tasks (e.g. one component can be restored to its initial state by preventive maintenance if any of its degradations exceed the respective critical level [6] and by corrective maintenance upon its failure [7]).

Neglecting the factors that influence the state of being of components can result in inaccurate estimation of component IMs and, thus, mislead the system designers, operators and managers in the assignment of priorities to component criticalities. In this paper, we investigate the criticality of components taking into account the influence of multiple dependent competing degradation processes and maintenance tasks.

Physics-based models (PBMs) [8] and multi-state models (MSMs) [9] are used to describe the component degradation processes considered in our work. The former translates physics knowledge into mathematical equations that describe the underlying continuous degradation processes associated to a specific mechanism, e.g. wear, corrosion and cracking [10]; the latter approximates the development of continuous degradation by a process of transitions between a finite number of discrete states [11]. Recently, the authors have employed the piecewise-deterministic Markov process (PDMP) modeling framework to incorporate PBMs and MSMs and to treat the dependency of degradation processes [12]. In the present work, the authors introduce a set of PDMPs to incorporate also maintenance policies.

PBMs and MSMs are two widely used approaches, especially for highly reliable components, whose degradation/failure data are insufficient to build their lifetime distributions [12]. The effects of uncertain parameters in the MSMs have been considered in [13]. Global Sensitivity Analysis (GSA) has been employed to produce indices that assess the importance of the uncertain factors in the models, taking into account interactions among them. Such paper focuses on the importance indices of uncertain factors.

In this paper, we consider importance indices of components within multi-component systems taking into account the influence of multiple competing degradation processes, degradation dependency and maintenance tasks. GSA is not employed for such task, since it is not the uncertainty in the parameters that is considered. A literature review on component IMs is presented below, to position our contribution within the existing works. Component IMs were first introduced mathematically by Birnbaum [14] in 1969, in a binary setting (i.e. the system

and its components are either functioning or faulty). The Birnbaum IM (BIM) allows ranking components by looking at what happens to the system reliability when the reliabilities of the components are changed, one at a time. Afterwards, various IMs have been developed for binary components, including reliability achievement worth (RAW), reliability reduction worth (RRW), Fussel-Vesely and Barlow-Proschan IMs [15-17]. Other concepts of IMs have been proposed with focus to different aspects of the system, such as structure IMs, lifetime IMs, differential IMs and joint IMs [18].

For components whose description requires more than two states, e.g. to describe different degrees of functionalities or levels of degradation, definition of the component IMs have been extended in two directions: (1) metrics for components modeled by MSMs; (2) metrics for components modeled by continuous processes. For the first type, Armstrong [19] proposed IMs for multi-state systems (MSSs) with dual-mode failure components. For MSSs with multi-state components, Griffith [20] formalized the concept of system performance based on expected utility and generalized the BIM to evaluate the effect of component improvement on system performance. Wu and Chan [21] improved the Griffith IM by proposing a new utility importance of a state of a component to measure which component or which state of a certain component contributes the most to system performance. Si *et al.* [22] proposed the integrated IM, based on Griffith IM, to incorporate the probability distributions and transition rates of the component states, and the changes in system performance. Integrated IM can be used to evaluate how the transition of component states affects the system performance from unit time to different life stages, to system lifetime, and provide useful information for preventive actions (such as monitoring enhancement, construction improvement etc.) [23, 24]. The multi-state generalized forms of classically binary IMs have been proposed by Zio and Podofillini [25] and Levitin *et al.* [26]: these IMs quantify the importance of a multi-state component for achieving a given level of performance. Ramirez-Marquez and Coit [27] developed two types of composite IMs: (1) the general composite IMs considering only the possible component states; (2) the alternative composite IMs considering both the possible component states and the associated probabilities. For the second type, Gebraeel [28] proposed a prognostics-based ranking algorithm to rank the identical components based on their residual lives. Liu *et al.* [29] extended the BIM for components with multi-dimensional degradation processes under dynamic environments. Note that no IM has been developed for components whose (degradation) states are determined by both discrete and continuous processes, and are dependent upon other components, as it is often the case in practice [30].

To include dependency, Iyer [31] extended the Barlow-Proschan IM for components whose lifetimes are jointly absolutely continuous and possibly dependent, and Peng *et al.* [2] adapted the mean absolute deviation (MAD) IM (one of the alternative composite IMs) for statistically correlated (s-correlated) components subject to a one-dimension continuous degradation process; this enables to measure the expected absolute deviation in the reliability of a system with s-correlated degrading components, caused by different degrading performance levels of a particular component and the associated probabilities. To the knowledge of the authors, component IMs taking into account the dependency of multiple degradation processes within one component and among different components, with the inclusion of maintenance activities, have not been investigated in the literature (studies of IMs for repairable systems with *s*-independent components can be found in [24, 32]).

In this work, we extend the MAD to a more general setting of modeling by PDMP [33], to provide timely feedback on the criticality of a component with respect to the system reliability. The extension considers: (1) the dependency of multiple degradation processes within one component and different components; (2) discrete and continuous degradation processes; (3)

two types of maintenance tasks, condition-based preventive maintenance (PM) via periodic inspections and corrective maintenance (CM).Then, a method for the quantification of component IM is designed based on the finite-volume (FV) approach [34].

The rest of this paper is organized as follows. Section 2 presents the assumptions and degradation models under dependency and maintenance. Section 3 describes the proposed component IM. Section 4 introduces the proposed quantification method. Section 5 provides a numerical example referred to one subsystem of the residual heat removal system (RHRS) [35], to demonstrate the application of the proposed component IM and feasibility of the quantification method. Finally, Section 6 concludes the work.

2. MODELING DEGRDATION OF UNDER DEPENDENCY AND MAINTENANCE PDMP

2.1. General assumptions

- Consider a multi-component system, made of Q components coded in the vector $\boldsymbol{O} = \{O_1, O_2, \dots, O_Q\}$, each one with multiple degradation processes, possibly dependent. The degradation processes can be separated into two groups: (1) $\boldsymbol{L} = \{L_1, L_2, \dots, L_M\}$ modeled by M PBMs; (2) $\boldsymbol{K} = \{K_1, K_2, \dots, K_N\}$ modeled by N MSMs, where $L_m, m = 1, 2, \dots, M$ and $K_n, n = 1, 2, \dots, N$ are the indices of the degradation processes.
- The degradation state of a component $O_q \in \boldsymbol{O}, q = 1, 2, \dots, Q$, is determined by its degradation processes $\boldsymbol{D}_{O_q} \subseteq \boldsymbol{L} \cup \boldsymbol{K}$ and the component fails either when one of the degradation processes evolves beyond a threshold of failure in the continuous state stochastic process or reaches the discrete failure state in the multi-state stochastic transition process.
- A degradation process $L_m \in \boldsymbol{L}$ in the first group is described by d_{L_m} time-dependent continuous variables $\overrightarrow{X_{L_m}}(t) = \left(\overrightarrow{X_{L_m}^{\boldsymbol{D}}}(t), \overrightarrow{X_{L_m}^{\boldsymbol{P}}}(t)\right) \in \mathbb{R}^{d_{L_m}}$, whose evolutions are described by a set of first-order differential equations (physics equations) in terms of: (1) the non-decreasing degradation variables vector $\overrightarrow{X_{L_m}^{\boldsymbol{D}}}(t)$ (e.g. crack length) representing the component degradation condition; (2) the physical variables vector $\overrightarrow{X_{L_m}^{\boldsymbol{P}}}(t)$ (e.g. velocity) influencing $\overrightarrow{X_{L_m}^{\boldsymbol{D}}}(t)$ and vice versa. Due to degradation process L_m, the component fails when any degradation variable $x_{L_m}^i(t) \in \overrightarrow{X_{L_m}^{\boldsymbol{D}}}(t)$ exceeds its corresponding failure threshold denoted by $x_{L_m}^{i\,*}$. The set of failure states of the degradation variables $\overrightarrow{X_{L_m}}(t)$ is denoted by $\boldsymbol{\mathcal{F}}_{L_m}$.
- A degradation process $K_n \in \boldsymbol{K}$ in the second group is described by the state variable $Y_{K_n}(t)$, which takes values from a finite state set $\boldsymbol{S}_{K_n} = \{0_{K_n}, 1_{K_n}, \dots, d_{K_n}\}$, where '$d_{K_n}$' is the perfect functioning state and '0_{K_n}' is the complete failure state. All intermediate states are functioning or partially functioning. The evolution of the degradation process is characterized by the transition rates between states. The failure state set of the multi-state stochastic transition process of degradation $Y_{K_n}(t)$ is described by $\boldsymbol{\mathcal{F}}_{K_n} = \{0_{K_n}\}$.
- Dependencies between degradation processes may exist both within and between groups $\boldsymbol{L}$ and $\boldsymbol{K}$. The detailed formulations are given in eqs. (1-3).

- For degradation process $i \in \boldsymbol{L} \cup \boldsymbol{K}$, the inspection task I_i of PM is performed with fixed period T_i and brings the related component back to its initial state when i is found in the predefined state set $\boldsymbol{H}_i$.
- The component is restored to its initial state by CM, as soon as it fails.
- The inspection tasks and all maintenance actions are done instantaneously and without errors.

An illustration of two components O_1 and O_2 is shown in Fig. 1, where $\boldsymbol{D}_{O_1} = \{L_1\}$ and $\boldsymbol{D}_{O_2} = \{K_1\}$. PM is performed for L_1 if $\overrightarrow{X_{L_1}^{D}}(t)$ exceeds its threshold $x_{L_1}{}^{p}$ at the time of inspection and for K_1 if $Y_{K_1}(t)$ is in state 1 at the time of inspection.

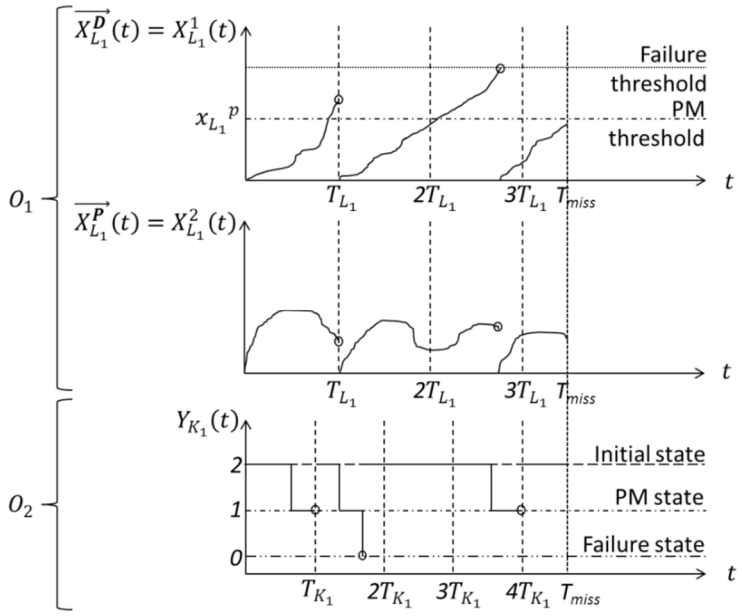

Fig. 1. An illustration of two components.

2.2. Degradation model of the system

The degradation state of the system is represented as

$$\vec{Z}(t) = \begin{pmatrix} \begin{pmatrix} \overrightarrow{X_{L_1}}(t) \\ \vdots \\ \overrightarrow{X_{L_M}}(t) \end{pmatrix} = \overrightarrow{X}(t) \\ \begin{pmatrix} Y_{K_1}(t) \\ \vdots \\ Y_{K_N}(t) \end{pmatrix} = \overrightarrow{Y}(t) \end{pmatrix} \in \boldsymbol{E} = \mathbb{R}^{d_L} \times \boldsymbol{S}, \forall t \geq 0 \quad (1)$$

where E is the space combining $\mathbb{R}^{d_L}$ ($d_{\boldsymbol{L}} = \sum_{m=1}^{M} d_{L_m}$) and $\boldsymbol{S}$ ($\boldsymbol{S} = \prod_{n=1}^{N} \boldsymbol{S}_{K_n}$).

A set of PDMPs $\overrightarrow{Z_k}(t), k = 1,2, \ldots$ is employed to model the system degradation processes, where a new PDMP is established once a maintenance task is performed. Let N_m denote the total number of maintenance tasks (PM and CM) the system has experienced till the mission time T_{miss}, then, $\overrightarrow{Z_k}(t), k = 1,2, \ldots, N_m$ is defined on $[T_m^{k-1}, T_m^k]$, where $T_m^k, k = 1,2, \ldots, N_m$

denotes the execution time of the *k*-th maintenance task and $T_m^0 = 0$. $\overrightarrow{Z_{N_m+1}}(t)$ is defined on $\left[T_m^{N_m}, T_{miss}\right]$. Fig. 2 shows this for the degradation processes in Fig. 1.

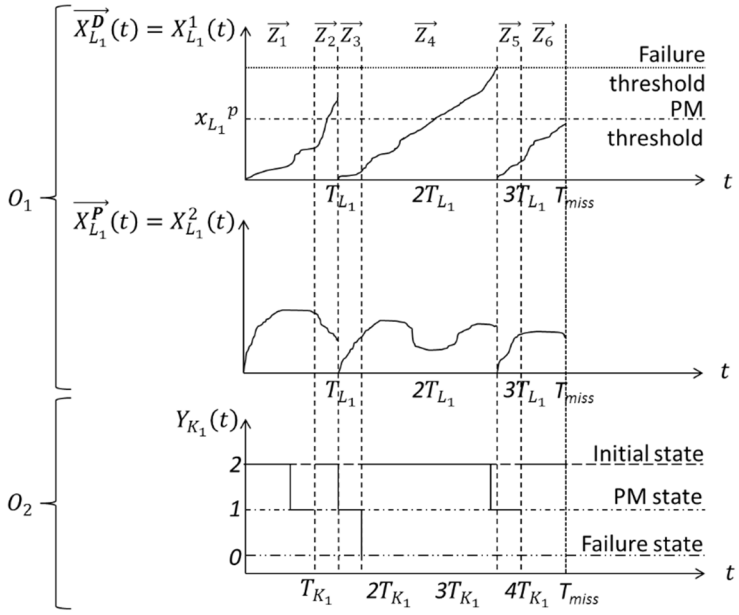

Fig. 2. An illustration of two components, modeled by PDMPs.

The evolution of the elements $\overrightarrow{Z_k}(t), k = 1,2, \dots, N_m + 1$, of the system state vector $\vec{Z}(t)$ involves (1) the stochastic transition process of $\vec{Y}(t)$ and (2) the deterministic progression of $\overrightarrow{X}(t)$, between successive transitions of $\vec{Y}(t)$, given $\vec{Y}(t)$. The first process is governed by the transition rates of $\vec{Y}(t)$:

$$\lim_{\Delta t \to 0} P\left(\vec{Y}(t + \Delta t) = \vec{j} \middle| \overrightarrow{Z_k}(t) = (\overrightarrow{X}(t), \vec{Y}(t) = \vec{\imath})^T, \boldsymbol{\theta_K}\right) = \lambda_{\vec{\imath}}\left(\vec{j} \middle| \overrightarrow{X}(t), \boldsymbol{\theta_K}\right)\Delta t, \forall\, \vec{\imath}, \vec{j} \in \boldsymbol{S}, \vec{\imath} \neq \vec{j} \quad (2)$$

where the parameter vector $\boldsymbol{\theta_K}$ represents environmental and operational factors influencing the degradation processes in $\boldsymbol{K}$, and $\lambda_{\vec{\imath}}\left(\vec{j} \middle| \overrightarrow{X}(t), \boldsymbol{\theta_K}\right)$ is the transition rate from state $\vec{\imath}$ to $\vec{j}$. The second evolution process is described by the deterministic physics equations as follows:

$$\dot{\vec{X}}(t) = \begin{pmatrix} \overrightarrow{\dot{X}_{L_1}}(t) \\ \vdots \\ \overrightarrow{\dot{X}_{L_M}}(t) \end{pmatrix} = \begin{pmatrix} \overrightarrow{f_{L_1}}\left(\overrightarrow{Z_k}(t), t \middle| \boldsymbol{\theta}_{L_1}\right) \\ \vdots \\ \overrightarrow{f_{L_M}}\left(\overrightarrow{Z_k}(t), t \middle| \boldsymbol{\theta}_{L_M}\right) \end{pmatrix} = \overrightarrow{f_{\boldsymbol{L}}}\left(\overrightarrow{Z_k}(t), t \middle| \boldsymbol{\theta_L} = \left(\boldsymbol{\theta}_{L_1}, \boldsymbol{\theta}_{L_2}, \dots, \boldsymbol{\theta}_{L_M}\right)\right) \quad (3)$$

where the parameter vector $\boldsymbol{\theta}_{L_m}, m = 1,2, \dots, M$ represents environmental and operational factors influencing the degradation processes in L_m. $\overrightarrow{Z_k}(T_m^{k-1})$ (the initial states of $\overrightarrow{Z_k}(t), k = 2, \dots, N_m + 1$) can be obtained according to $\overrightarrow{Z_{k-1}}(T_m^{k-1})$ and the (*k*-1)-th maintenance task. The degradation states of the system till T_{miss} can be represented by

$$\vec{Z}(t) = \sum_{k=1}^{N_m} \mathbf{1}_{[T_m^{k-1}, T_m^k[}(t) \cdot \overrightarrow{Z_k}(t) + \mathbf{1}_{\left[T_m^{N_m}, T_{miss}\right]}(t) \cdot \overrightarrow{Z_{N_m+1}}(t) \quad (4)$$

Since maintenance is performed instantaneously, the failure states of the system are infinitely approachable by $\vec{Z}(t)$, instead of being truly reached. We, then, use another stochastic process $\overrightarrow{Z'}(t)$, which can record the failure of the system as follows:

$$\overrightarrow{Z'}(t) = \mathbf{1}_{[0,T_m^1]}(t) \cdot \overrightarrow{Z_1}(t) + \sum_{k=2}^{N_m} \mathbf{1}_{]T_m^{k-1}, T_m^k]} \cdot \overrightarrow{Z_k}(t) + \mathbf{1}_{\left]T_m^{N_m}, T_{miss}\right]}(t) \cdot \overrightarrow{Z_{N_m+1}}(t) \quad (5)$$

Let $\boldsymbol{\mathcal{F}}$ denote the system failure state set: then, the system reliability at T_{miss} can be defined as follows:

$$R(T_{miss}) = P\left[\overrightarrow{Z'}(s) \notin \boldsymbol{\mathcal{F}}, \forall s \le T_{miss}\right] = P\left[\bigcap_{k=1}^{N_m}\left(\overrightarrow{Z_k}(T_m^k) \notin \boldsymbol{\mathcal{F}}\right) \cap \left(\overrightarrow{Z_{N_m+1}}(T_{miss}) \notin \boldsymbol{\mathcal{F}}\right)\right] \quad (6)$$

Since the component is restored to its initial state by corrective maintenance as soon as it fails, the failure states of the system can only be reached by $\overrightarrow{Z'}(t)$ at the execution time of the maintenance tasks $T_m^k, k = 1,2,\dots,N_m$ or at the mission time T_{miss}. Therefore, the event $\overrightarrow{Z'}(s) \notin \boldsymbol{\mathcal{F}}, \forall s \le T_{miss}$ can be represented by $\bigcap_{k=1}^{N_m}\left(\overrightarrow{Z_k}(T_m^k) \notin \boldsymbol{\mathcal{F}}\right) \cap \left(\overrightarrow{Z_{N_m+1}}(T_{miss}) \notin \boldsymbol{\mathcal{F}}\right)$.

3. COMPONENT IM

Ramirez-Marquez and Coit [27] proposed the MAD IM for MSSs with multi-state components, which evaluates the components criticality taking into account all the possible states and associated probabilities. Peng *et al.* [2] adapted it for binary systems with *s*-correlated components subject to one continuous degradation process.

For components whose (degradation) states are determined by both discrete and continuous processes, we propose an extension of MAD to provide timely feedbacks of the criticality of component O_q with multiple dependent competing degradation processes modeled by MSMs and PBMs, and giving consideration to PM and CM. The formulation is presented as follows:

$$CI_{O_q}(t) = E\left[\left|P\left(\overrightarrow{Z'}(s) \notin \boldsymbol{\mathcal{F}}, \forall s \le t | \overrightarrow{\boldsymbol{D}_{O_q}}(t)\right) - R(t)\right|\right] \quad (7)$$

where $\overrightarrow{\boldsymbol{D}_{O_q}}(t) = (\overrightarrow{X_{\boldsymbol{L}_p}}(t) = (\overrightarrow{X_{L_{p_1}}}(t), \dots, \overrightarrow{X_{L_{p_n}}}(t)), \overrightarrow{Y_{\boldsymbol{K}_q}}(t) = (Y_{K_{q_1}}(t), \dots, Y_{K_{qm}}(t)))$ and $\boldsymbol{D}_{O_q} = \{\boldsymbol{L}_p = \{L_{p_1}, \dots, L_{p_n}\}, \boldsymbol{K}_q = \{K_{q_1}, \dots, K_{q_m}\}\}$. It accounts for the expected absolute deviation in the system reliability caused by changes of all degradation processes of component O_q. Let $\mathbb{R}^{d_{L_p}} = \mathbb{R}^{\sum_{i=1}^{n} d_{L_{p_i}}}$ and $\boldsymbol{S}_{\boldsymbol{K}_q} = \prod_{i=1}^{m} \boldsymbol{S}_{K_{q_i}}$ denote the state space of $\overrightarrow{X_{\boldsymbol{L}_p}}(t)$ and $\overrightarrow{Y_{\boldsymbol{K}_q}}(t)$, respectively; eq. (7) can, then, be expressed as

$$CI_{O_q}(t) = \sum_{\overrightarrow{y_{\boldsymbol{K}_q}} \in \boldsymbol{S}_{\boldsymbol{K}_q}} \int_{\overrightarrow{x_{\boldsymbol{L}_p}} \in \mathbb{R}^{d_{\boldsymbol{L}_p}}} f_{\overrightarrow{\boldsymbol{D}_{O_q}}(t)}\left(d\overrightarrow{x_{\boldsymbol{L}_p}}, \overrightarrow{y_{\boldsymbol{K}_q}}\right)$$

$$\left|P(\overrightarrow{Z'}(s) \notin \boldsymbol{\mathcal{F}}, \forall s \le t | \overrightarrow{X_{\boldsymbol{L}_p}}(t) = \overrightarrow{x_{\boldsymbol{L}_p}}, \overrightarrow{Y_{\boldsymbol{K}_q}}(t) = \overrightarrow{y_{\boldsymbol{K}_q}}) - R(t)\right| \quad (8)$$

where $f_{\overrightarrow{\boldsymbol{D}_{O_q}}(t)}\left(d\overrightarrow{x_{\boldsymbol{L}_p}}, \overrightarrow{y_{\boldsymbol{K}_q}}\right)$ is the probability distribution of $\overrightarrow{\boldsymbol{D}_{O_q}}(t)$.

Let $N_m^t \ge 1$ denote the number of maintenance tasks that the system has experienced till t. According to eq. (6), we can obtain that:

$$R(T_{miss}) = P\left[\left(\bigcap_{k=1}^{N_m^t}\left(\overrightarrow{Z_k}(T_m^k) \notin \boldsymbol{\mathcal{F}}\right)\right) \cap \left(\overrightarrow{Z_{N_m^t+1}}(t) \notin \boldsymbol{\mathcal{F}}\right)\right] \quad (9)$$

and

$$P(\overrightarrow{Z'}(s) \notin \mathcal{F}, \forall s \le t | \overrightarrow{X_{\boldsymbol{L}_p}}(t) = \overrightarrow{x_{\boldsymbol{L}_p}}, \overrightarrow{Y_{\boldsymbol{K}_q}}(t) = \overrightarrow{y_{\boldsymbol{K}_q}}) =$$

$$\begin{cases} \frac{d\overrightarrow{x_{\boldsymbol{L}p}}}{f_{\overrightarrow{\boldsymbol{D}_{Oq}}(t)}\left(d\overrightarrow{x_{\boldsymbol{L}p}}, \overrightarrow{y_{\boldsymbol{K}q}}\right)} P\left[\left(\cap_{k=1}^{N_m^t}\left(\overrightarrow{Z_k}(T_m^k) \notin \mathcal{F}\right)\right) \cap \right. \\ \left. \left(\overrightarrow{Z^{\boldsymbol{D}_{Oq}}_{N_m^t+1}}\left(t | \overrightarrow{X_{\boldsymbol{L}_p}}(t) = \overrightarrow{x_{\boldsymbol{L}_p}}, \overrightarrow{Y_{\boldsymbol{K}_q}}(t) = \overrightarrow{y_{\boldsymbol{K}_q}}\right) \notin \mathcal{F}\right)\right], if\ f_{\overrightarrow{\boldsymbol{D}_{Oq}}(t)}\left(d\overrightarrow{x_{\boldsymbol{L}_p}}, \overrightarrow{y_{\boldsymbol{K}_q}}\right) \neq 0 \\ 0, if\ f_{\overrightarrow{\boldsymbol{D}_{Oq}}(t)}\left(d\overrightarrow{x_{\boldsymbol{L}_p}}, \overrightarrow{y_{\boldsymbol{K}_q}}\right) = 0 \end{cases} \quad (10)$$

where $\overrightarrow{Z^{D_{Oq}}_{N_m^t+1}}\left(t | \overrightarrow{X_{\boldsymbol{L}_p}}(t) = \overrightarrow{x_{\boldsymbol{L}_p}}, \overrightarrow{Y_{\boldsymbol{K}_q}}(t) = \overrightarrow{y_{\boldsymbol{K}_q}}\right) = (\overrightarrow{X_{L_1}}(t), \dots, \overrightarrow{X_{\boldsymbol{L}_p}}(t) = \overrightarrow{x_{\boldsymbol{L}_p}}, \dots, \overrightarrow{X_{L_M}}(t), Y_{K_1}(t), \dots, \overrightarrow{Y_{\boldsymbol{K}_q}}(t) = \overrightarrow{y_{\boldsymbol{K}_q}}, \dots, Y_{K_N}(t))^T$.

4. FV SCHEME FOR COMPONENT IM QUANTIFICATION

Let $p_t^{\overrightarrow{Z_k}}(d\overrightarrow{x}, \vec{\imath} \mid \boldsymbol{\theta} = \boldsymbol{\theta_L} \cup \boldsymbol{\theta_K}), \forall \overrightarrow{x} \in \mathbb{R}^{d_L}, \vec{\imath} \in \boldsymbol{S}$ denote the probability distribution of processes $\overrightarrow{Z_k}(t)$. Due to the complex behavior of the PDMP, the analytical solution for the probability distribution is difficult to obtain [36]. The FV approach developed in [34] can be used to obtain the approximated solution by discretizing the time space and the state space of the continuous variables, achieving accurate results within an admissible computing time, as shown in [37].

4.1. FV scheme for PDMP

4.1.1. Assumptions

This approach can be applied under the following assumptions:

- $\lambda_{\vec{\imath}}(\vec{\jmath}, \cdot\ | \boldsymbol{\theta_K}), \forall \vec{\imath}, \vec{\jmath} \in \boldsymbol{S}$ are continuous and bounded functions from $\mathbb{R}^{d_L}$ to $\mathbb{R}^+$.
- $\overrightarrow{f_{\boldsymbol{L}}^{\vec{\imath}}}(\cdot, \cdot | \boldsymbol{\theta_L}), \forall \vec{\imath} \in \boldsymbol{S}$ are continuous functions from $\mathbb{R}^{d_L} \times \mathbb{R}^+$ to $\mathbb{R}^{d_L}$ and locally Lipschitz continuous.
- $\overrightarrow{f_{\boldsymbol{L}}^{\vec{\imath}}}(\cdot, t | \boldsymbol{\theta_L}), \forall \vec{\imath} \in \boldsymbol{S}$ are sub-linear, i.e. there are some $V_1 > 0$ and $V_2 > 0$ such that
$$\forall \vec{x} \in \mathbb{R}^{d_L}, t \in \mathbb{R}^+ \left| \overrightarrow{f_{\boldsymbol{L}}^{\vec{\imath}}}(\vec{x}, t | \boldsymbol{\theta_L}) \right| \le V_1(\|\vec{x}\| + |t|) + V_2$$
- $div(\overrightarrow{f_{\boldsymbol{L}}^{\vec{\imath}}}(\cdot, \cdot | \boldsymbol{\theta_L})), \forall \vec{\imath} \in \boldsymbol{S}$ are almost everywhere bounded in absolute value by some real value $D > 0$ (independent of $\vec{\imath}$).

4.1.2. Solution approach

The time space $\mathbb{R}^+$is divided into small intervals $\mathbb{R}^+ = \cup_{n=0,1,2,\dots}[n\Delta t, (n+1)\Delta t[$ by setting the length of each interval $\Delta t > 0$ and the state space $\mathbb{R}^{d_L}$ of $\overrightarrow{X}(t)$ is divided into an admissible mesh $\mathcal{M}$ which satisfies that:

(13) $\cup_{A \in \mathcal{M}} A = \mathbb{R}^{d_L}$.

(14) $\forall A, B \in \mathcal{M},\ A \neq B \Rightarrow A \cap B = \emptyset$.

(15) $m_A = \int_A \overrightarrow{dx} > 0, \forall A \in \mathcal{M}$, where m_A is the volume of grid A.
(16) $sup_{A\in\mathcal{M}} diam(A) < +\infty$ where $diam(A) = sup_{\forall \vec{x},\vec{y}\in A}|\vec{x} - \vec{y}|$.

The numerical scheme aims at constructing an approximate value $\rho_t^{\overrightarrow{Z_k}}(\overrightarrow{x},\cdot\,|\boldsymbol{\theta})d\overrightarrow{x}$ for $p_t^{\overrightarrow{Z_k}}(d\overrightarrow{x},\cdot\,|\boldsymbol{\theta})$, such that $\rho_t^{\overrightarrow{Z_k}}(\overrightarrow{x},\cdot\,|\boldsymbol{\theta})$ is constant on each $A \times \{\vec{\imath}\} \times [n\Delta t, (n+1)\Delta t[, \forall A \in \mathcal{M}, \vec{\imath} \in \boldsymbol{S}, [n\Delta t, (n+1)\Delta t[\in [T_m^{k-1}, T_m^k]$:

$$\rho_t^{\overrightarrow{Z_k}}(\overrightarrow{x},\vec{\imath}|\boldsymbol{\theta}) = P_n^{\overrightarrow{Z_k}}(A,\vec{\imath}|\boldsymbol{\theta}), \forall \vec{\imath} \in \boldsymbol{S}, \vec{x} \in A, t \in [n\Delta t, (n+1)\Delta t[\tag{11}$$

$P_0^{\overrightarrow{Z_k}}(A,\vec{\imath}|\boldsymbol{\theta}), \forall \vec{\imath} \in \boldsymbol{S}, A \in \mathcal{M}$ is defined as follows:

$$P_0^{\overrightarrow{Z_k}}(A,\vec{\imath}|\boldsymbol{\theta}) = \int_A p_0^{\overrightarrow{Z_k}}(d\overrightarrow{x},\vec{\imath}|\boldsymbol{\theta})\,/m_A \tag{12}$$

Then, $P_{n+1}^{\overrightarrow{Z_k}}(A,\vec{\imath}\,|\,\boldsymbol{\theta}), \forall \vec{\imath} \in \boldsymbol{S}, A \in \mathcal{M}, n \in \mathbb{N}$ can be calculated considering the deterministic evaluation of $\overrightarrow{X}(t)$ and the stochastic evolution of $\overrightarrow{Y}(t)$ based on $P_n^{\overrightarrow{Z_k}}(\mathcal{M},\vec{\imath}|\boldsymbol{\theta})$ by the Chapman-Kolmogorov forward equation [38], as follows:

$$\begin{aligned} &P_{n+1}^{\overrightarrow{Z_k}}(A,\vec{\imath}|\boldsymbol{\theta}) \\ &= \frac{1}{1+\Delta t b_A^{\vec{\imath}}}\widehat{P_{n+1}^{\overrightarrow{Z_k}}}(A,\vec{\imath}|\boldsymbol{\theta}) + \Delta t \sum_{\vec{\jmath}\in\boldsymbol{S}} \frac{a_A^{\vec{\jmath}\vec{\imath}}}{1+\Delta t b_A^{\vec{\jmath}}}\widehat{P_{n+1}^{\overrightarrow{Z_k}}}(A,\vec{\jmath}|\boldsymbol{\theta}) \end{aligned} \tag{13}$$

where

$$a_A^{\vec{\jmath}\vec{\imath}} = \int_A \lambda_{\vec{\jmath}}(\vec{\imath},\vec{x}|\boldsymbol{\theta}_K)\overrightarrow{dx}/m_A\,, \forall \vec{\imath} \in \boldsymbol{S}, A \in \mathcal{M} \tag{14}$$

is the average transition rate from state $\vec{\jmath}$ to state $\vec{\imath}$ for grid A,

$$b_A^{\vec{\imath}} = \sum_{\vec{\jmath}\neq\vec{\imath}} a_A^{\vec{\imath}\vec{\jmath}}\,, \forall \vec{\imath} \in \boldsymbol{S}, A \in \mathcal{M} \tag{15}$$

is the average transition rate out of state $\vec{\imath}$ for grid A,

$$\widehat{P_{n+1}^{\overrightarrow{Z_k}}}(A,\vec{\imath}|\boldsymbol{\theta}) = \sum_{B\in\mathcal{M}} m_{BA}^{\vec{\imath}}\, P_n^{\overrightarrow{Z_k}}(B,\vec{\imath}|\boldsymbol{\theta})/m_A,\ \forall \vec{\imath} \in \boldsymbol{S}, A \in \mathcal{M} \tag{16}$$

is the approximate value of probability density function on $\{\vec{\imath}\} \times [(n+1)\Delta t, (n+2)\Delta t[\times A$ according to the deterministic evaluation of $\overrightarrow{X}(t)$,

$$m_{BA}^{\vec{\imath}} = \int_{\{\vec{y}\in B\,|\,\overrightarrow{g^{\vec{\imath}}}(\vec{y},\Delta t|\boldsymbol{\theta}_L)\in A\}} \overrightarrow{dy}\,, \forall \vec{\imath} \in \boldsymbol{S}, A, B \in \mathcal{M} \tag{17}$$

is the volume of the part of grid B which will enter grid A after time Δt according to the deterministic evaluation of $\overrightarrow{X}(t)$, where $\overrightarrow{g^{\vec{\imath}}}(\cdot,\cdot)$: $\mathbb{R}^{d_L} \times \mathbb{R} \to \mathbb{R}^{d_L}$ is the solution of

$$\frac{\partial}{\partial t}\overrightarrow{g^{\vec{\imath}}}(\vec{y},t|\boldsymbol{\theta}_L) = \overrightarrow{f_L^{\vec{\imath}}}\left(\overrightarrow{g^{\vec{\imath}}}(\vec{y},t|\boldsymbol{\theta}_L), t\middle|\,\boldsymbol{\theta}_L\right) \tag{18}$$

with

$$\overrightarrow{g^{\vec{\imath}}}(\vec{y},0|\boldsymbol{\theta}_L) = \vec{y} \tag{19}$$

$\overrightarrow{g^{\vec{\imath}}}(\vec{y},\Delta t|\boldsymbol{\theta}_L)$ gives the state of the deterministic behavior of $\overrightarrow{X}(t)$ after time Δt, starting from the state $\vec{y}$ while the processes $\vec{Y}(t)$ stay in state $\vec{\imath}$.

4.2. Quantification of component IM

Given the initial probability distribution $p_0^{\overrightarrow{Z_1}}(d\overrightarrow{x},\vec{\imath}|\boldsymbol{\theta})$ of the system, $P_0^{\overrightarrow{Z_1}}(A,\vec{\imath}|\boldsymbol{\theta}),\forall\vec{\imath}\in \boldsymbol{S},A\in\mathcal{M}$, can be obtained as:

$$P_0^{\overrightarrow{Z_1}}(A,\vec{\imath}|\boldsymbol{\theta})=\int_A p_0^{\overrightarrow{Z_1}}(d\overrightarrow{x},\vec{\imath}|\boldsymbol{\theta})\,/m_A \tag{20}$$

$P^{\overrightarrow{Z_1}}_{\lceil T_m^1/\Delta t\rceil}(A,\vec{\imath}|\boldsymbol{\theta}),\forall\vec{\imath}\in\boldsymbol{S},A\in\mathcal{M}$ can, then, be calculated through the FV scheme.

To calculate eq. (9) and $P[\left(\bigcap_{k=1}^{N_m^t}\left(\overrightarrow{Z_k}(T_m^k)\notin\mathcal{F}\right)\right)\cap(\overrightarrow{Z^{\boldsymbol{D}_{Oq}}_{N_m^t+1}}\left(t|\overrightarrow{X_{\boldsymbol{L}_p}}(t)=\overrightarrow{x_{\boldsymbol{L}_p}},\overrightarrow{Y_{\boldsymbol{K}_q}}(t)=\overrightarrow{y_{\boldsymbol{K}_q}}\right)\notin\mathcal{F})]$ in eq. (10), we are only interested in the situation that the system is functioning till t; thus, $P^{\overrightarrow{Z_k}}_{\lceil T_m^{k-1}/\Delta t\rceil}(A,\vec{\imath}|\boldsymbol{\theta}),\forall\vec{\imath}\in S,A\in\mathcal{M},k=2,3,\dots N_m^t+1$ is initiated as follows:

$$P^{\overrightarrow{Z_k}}_{\left\lceil\frac{T_m^{k-1}}{\Delta t}\right\rceil}(A,\vec{\imath}|\boldsymbol{\theta})=\begin{cases}P^{\overrightarrow{Z_{k-1}}}_{\left\lceil\frac{T_m^{k-1}}{\Delta t}\right\rceil}(A,\vec{\imath}|\boldsymbol{\theta})+\sum_{\left(A',\vec{\imath'}\right)\in\left\{\left(A^{k-1},\overrightarrow{\imath^{k-1}}\right)\right\}}P^{\overrightarrow{Z_{k-1}}}_{\left\lceil\frac{T_m^{k-1}}{\Delta t}\right\rceil}\left(A',\vec{\imath'}|\boldsymbol{\theta}\right),\\ \left(A',\vec{\imath'}\right)\notin\boldsymbol{\mathcal{F}}\\ if\ \left((A,\vec{\imath})\notin\boldsymbol{\mathcal{F}}\right)\ and\ \left(\nexists B\in\mathcal{M},\vec{\jmath}\in\boldsymbol{S}\colon(A,\vec{\imath})\in\{(B^{k-1},\overrightarrow{\jmath^{k-1}})\}\right)\\ 0,\\ if\ \left((A,\vec{\imath})\in\boldsymbol{\mathcal{F}}\right)\ or\ \left(\exists B\in\mathcal{M},\vec{\jmath}\in\boldsymbol{S}\colon(A,\vec{\imath})\in\{(B^{k-1},\overrightarrow{\jmath^{k-1}})\}\right)\end{cases} \tag{21}$$

where $\left\{\left(A^{k-1},\overrightarrow{\imath^{k-1}}\right)\right\},\forall\vec{\imath}\in\boldsymbol{S},A\in\mathcal{M}$, is the set containing all the states that step to the state $(A,\vec{\imath})$ caused by the $(k-1)$-th maintenance task. Then, we can obtain that

$$P\left[\left(\bigcap_{k=1}^{N_m^t}\left(\overrightarrow{Z_k}(T_m^k)\notin\boldsymbol{\mathcal{F}}\right)\right)\cap\left(\overrightarrow{Z_{N_m^t+1}}(t)\notin\boldsymbol{\mathcal{F}}\right)\right]=\sum_{(A,\vec{\imath})\notin\boldsymbol{\mathcal{F}}}m_A P^{\overrightarrow{Z_{N_m^t+1}}}_{\left\lceil\frac{t}{\Delta t}\right\rceil}(A,\vec{\imath}|\boldsymbol{\theta}) \tag{22}$$

$$P\left[\left(\bigcap_{k=1}^{N_m^t}\left(\overrightarrow{Z_k}(T_m^k)\notin\mathcal{F}\right)\right)\cap\left(\overrightarrow{Z^{\boldsymbol{D}_{Oq}}_{N_m^t+1}}\left(t|\overrightarrow{X_{\boldsymbol{L}_p}}(t)=\overrightarrow{x_{\boldsymbol{L}_p}},\overrightarrow{Y_{\boldsymbol{K}_q}}(t)=\overrightarrow{y_{\boldsymbol{K}_q}}\right)\notin\mathcal{F}\right)\right]=$$

$$\sum_{\substack{(A,\vec{\imath})\notin\boldsymbol{\mathcal{F}}\\ \left(\overrightarrow{x_{\boldsymbol{L}_p}},\overrightarrow{y_{\boldsymbol{K}_q}}\right)\subseteq(A,\vec{\imath})}}P^{\overrightarrow{Z_{N_m^t+1}}}_{\left\lceil\frac{t}{\Delta t}\right\rceil}(A,\vec{\imath}|\boldsymbol{\theta})\int_{A/\left(\overrightarrow{x_{\boldsymbol{L}_p}},\overrightarrow{y_{\boldsymbol{K}_q}}\right)}\overrightarrow{dx} \tag{23}$$

where $A/\left(\overrightarrow{x_{\boldsymbol{L}_p}},\overrightarrow{y_{\boldsymbol{K}_q}}\right)$ is the mesh by fixing $\overrightarrow{\boldsymbol{D}_{O_q}}(t)$ to $(\overrightarrow{x_{\boldsymbol{L}_p}},\overrightarrow{y_{\boldsymbol{K}_q}})$.

To calculate $f_{\overrightarrow{\boldsymbol{D}_{Oq}}(t)}\left(d\overrightarrow{x_{\boldsymbol{L}_p}},\overrightarrow{y_{\boldsymbol{K}_q}}\right)$ in eq. (8), (10), we are interested in the state of the system at t no matter whether the system is functioning till t or not; thus, $P^{\overrightarrow{Z_k}}_{\lceil T_m^{k-1}/\Delta t\rceil}(A,\vec{\imath}|\boldsymbol{\theta}),\forall\vec{\imath}\in\boldsymbol{S},A\in\mathcal{M},k=2,3,\dots N_m^t+1$ is initiated as follows:

$$P^{\overrightarrow{Z_k}}_{\left\lceil\frac{T_m^{k-1}}{\Delta t}\right\rceil}(A,\vec{\imath}|\boldsymbol{\theta})=\begin{cases}P^{\overrightarrow{Z_{k-1}}}_{\left\lceil\frac{T_m^{k-1}}{\Delta t}\right\rceil}(A,\vec{\imath}|\boldsymbol{\theta})+\sum_{\left(A',\vec{\imath'}\right)\in\left\{\left(A^{k-1},\overrightarrow{\imath^{k-1}}\right)\right\}}P^{\overrightarrow{Z_{k-1}}}_{\left\lceil\frac{T_m^{k-1}}{\Delta t}\right\rceil}\left(A',\vec{\imath'}|\boldsymbol{\theta}\right),\\ if\ \nexists B\in\mathcal{M},\vec{\jmath}\in\boldsymbol{S}\colon(A,\vec{\imath})\in\{(B^{k-1},\overrightarrow{\jmath^{k-1}})\}\\ 0,\\ if\ \exists B\in\mathcal{M},\vec{\jmath}\in\boldsymbol{S}\colon(A,\vec{\imath})\in\{(B^{k-1},\overrightarrow{\jmath^{k-1}})\}\end{cases} \tag{24}$$

We can obtain that

$$f_{\overrightarrow{\boldsymbol{D}_{O_q}}(t)}\left(d\overrightarrow{x_{\boldsymbol{L}_p}}, \overrightarrow{y_{\boldsymbol{K}_q}}\right) = d\overrightarrow{x_{\boldsymbol{L}_p}} \sum_{\substack{A\in\mathcal{M},\vec{\imath}\in\boldsymbol{S} \\ \left(\overrightarrow{x_{\boldsymbol{L}_p}},\overrightarrow{y_{\boldsymbol{K}_q}}\right)\subseteq(A,\vec{\imath})}} P^{\overrightarrow{Z_{N_m^t+1}}}_{\left\lfloor\frac{t}{\Delta t}\right\rfloor}(A,\vec{\imath}|\boldsymbol{\theta}) \int_{A/\left(\overrightarrow{x_{\boldsymbol{L}_p}},\overrightarrow{y_{\boldsymbol{K}_q}}\right)} \overrightarrow{dx} \quad (25)$$

$CI_{O_q}(t)$ can, then, be obtained by using eqs. (8)-(10), (20)-(25).

The pseudo-code for the quantification of component IM $CI_{O_q}(t)$ is presented as follows:

Set time t, length of each interval Δt and admissible mesh $\mathcal{M}$

Set the initial probability distribution $p_0^{\overrightarrow{Z_1}}(d\overrightarrow{x}, \vec{\imath}|\boldsymbol{\theta})$

Initialize the probability distribution of $\overrightarrow{Z_1}(0)$ by using eq. (20)

For $j = 1$ to N_m^t **do**

Calculate the probability distribution of $\overrightarrow{Z_J}(T_m^j)$ by using FV scheme

Calculate the initial probability distribution of $\overrightarrow{Z_{J+1}}(T_m^j)$ by using eq. (21)

End

Calculate the probability distribution of $\overrightarrow{Z_{N_m^t+1}}(t)$ by using FV scheme

Calculate the system reliability at time t by using eq. (22)

Calculate the conditional system reliability at time t by using eq. (23)

For $j = 1$ to N_m^t **do**

Calculate the probability distribution of $\overrightarrow{Z_J}(T_m^j)$ by using FV scheme

Calculate the initial probability distribution of $\overrightarrow{Z_{J+1}}(T_m^j)$ by using eq. (24)

End

Calculate the probability distribution of $\overrightarrow{Z_{N_m^t+1}}(t)$ by using FV scheme

Calculate the probability distribution of $\overrightarrow{\boldsymbol{D}_{O_q}}(t)$ by using eq. (25)

Calculate the component IM $CI_{O_q}(t)$ by using eq. (8)

□

5. ILLUSTRATIVE CASE

The system consists of a centrifugal pump and a pneumatic valve in series, and is a subsystem of the residual heat removal system (RHRS) of a nuclear power plant of Électricité de France (EDF). Given the series configuration, the failure of anyone of the two components can lead the subsystem to failure. A dependency in the degradation processes of the two components has been indicated by the experts: the pump vibrates due to degradation [39] which, in turn, leads the valve to vibrate, aggravating its own degradation processes [40].

5.1. Centrifugal pump

The pump is modeled by a MSM, modified from the one originally supplied by EDF upon discussion with the experts. It is a continuous-time homogeneous Markov chain as shown in

Fig. 3:

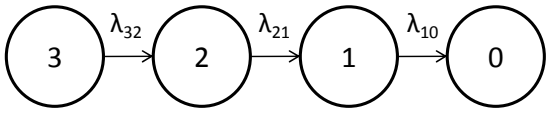

Fig. 3. Degradation process of the pump.

$S_p = \{0, 1, 2, 3\}$ denotes its degradation states set, where 3 is the perfect functioning state and 0 is the complete failure state. The parameters λ_{32}, λ_{21} and λ_{10} are the transition rates between the degradation states. Due to degradation, the pump vibrates when it reaches the degradation states 2 and 1. The intensity of the vibration of the pump on states 2 and 1 is evaluated as by the experts 'smooth' and 'rough', respectively.

5.2. Pneumatic valve

The simplified scheme of the pneumatic valve is shown in Fig. 4. It is a normally-closed, gas-actuated valve with a linear cylinder actuator.

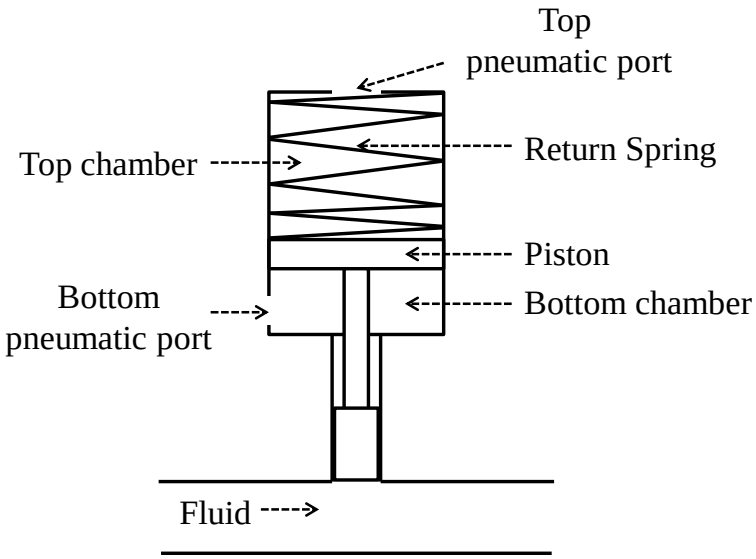

Fig. 4. Simplified scheme of the pneumatic valve [41].

The position of the piston is controlled by regulating the pressure of the pneumatic ports to fill or evacuate the top and bottom chambers. The degradation mechanism of the valve is considered as the external leak at the actuator connections to the bottom pneumatic port due to corrosion, and is modeled by a PBM. It is much more significant than the other degradation mechanisms according to the results shown in [41]. The valve is considered failed when the size of the external leak exceeds a predefined D_b^*. The PBM is used by EDF experts for degradation modeling, due to limited statistical degradation data on the valve behavior.

5.3. PDMP for the system

The degradation of the valve $\boldsymbol{L} = \{L_1\}$ is described by PBM and the degradation of the pump $\boldsymbol{K} = \{K_1\}$ is described by MSM. The degradation processes of the whole system are modeled by PDMP as follows:

$$\vec{Z}(t) = \begin{pmatrix} D_b(t) \\ Y_p(t) \end{pmatrix} \in \mathbb{R}^+ \times S_p \tag{26}$$

where $Y_p(t)$ denotes the degradation state of the pump at time t and $D_b(t)$ denotes the area of the leak hole at the bottom pneumatic port of the valve at time t. The space of the failure states of $\vec{Z}(t)$ is $\boldsymbol{\mathcal{F}} = [0, +\infty) \times \{\text{'0'}\} \cup [D_b^*, +\infty) \times \{1, 2, 3\}$. The development of the leak size is described by:

$$\dot{D}_b(t) = \omega_b(1 + \beta_{Y_p(t)}) \tag{27}$$

where ω_b is the original wear coefficient and where $\beta_{Y_p(t)}$ is the relative increment of the developing rate of the external leak caused by the vibration of the pump at the degradation state $Y_p = 2$ or 1. The parameter values related to the system degradation processes under accelerated aging conditions and to the maintenance tasks are presented in Table I. For confidentiality reasons, the values presented below are fictitious.

Table I Parameter values related to PDMP and the maintenance tasks

Parameter	Value
ω_b	1e-8 m^2/s
β_2	10%
β_1	20%
λ_{32}	3e-3 s-1
λ_{21}	3e-3 s-1
λ_{10}	3e-3 s-1
D_b^*	1.06e-5 m^2
T_{L_1}	1000 s
T_{K_1}	1000 s
H_{L_1}	[8e-6, D_b^*) m^2
H_{K_1}	{1, 2}

The system reliability at time t can be calculated as follows:

$$R(t) = P\left[(D_b(s) < D_b^*) \cap (Y_p(s) \neq 0), \forall s \leq t\right] \tag{28}$$

The component IMs for the valve and the pump are given in eq. (29) and eq. (30), respectively, as follows:

$$CI_V(t) = \int_{\mathbb{R}^+} f_{\overrightarrow{\boldsymbol{D}V}(t)}(x) \left| P[(D_b(s) < D_b^*) \cap (Y_p(s) \neq 0), \forall s \leq t \middle| D_b(t) = x)] - R(t) \right| dx \quad (29)$$

$$CI_P(t) = \sum_{i=0}^{3} P[Y_p(t) = i] \left| P[(D_b(s) < D_b^*) \cap (Y_p(s) \neq 0), \forall s \leq t \middle| Y_p(t) = i)] - R(t) \right| \quad (30)$$

Then, by using the proposed numerical method introduced in section 4, the values of the above equations can be calculated.

5.4. Results

The reliabilities of the whole system and the two components over a time horizon of T_{miss} =2000s, regarded as the mission time under accelerated conditions, are shown in Fig. 5. We can see from the figure that before around 870s (point A), the system reliability is basically determined by the pump reliability, since the valve is highly reliable. After that, the sharp decrease of the reliability of the valve due to degradation drives that of the system reliability, until the execution of the inspection tasks for the two components at 1000s. Because of the preventive maintenance, the failures of the system, the valve and the pump are mitigated.

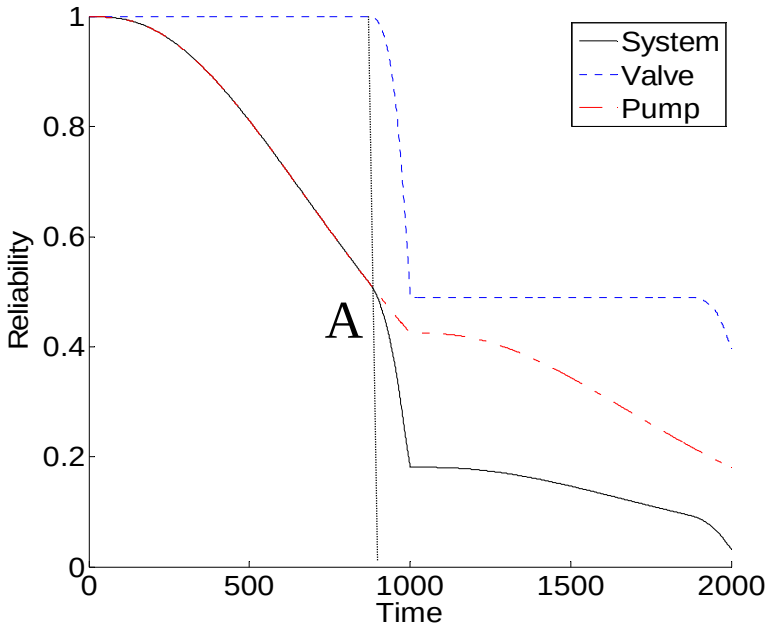

Fig. 5. The reliabilities of the system, the valve and the pump

The components IMs are shown in Fig. 6. Before around 400s (point B), the IMs of the two components are relatively close. Although the system reliability is dominated by the reliability of the pump, the probability of the pump at state 0 over the time horizon is limited to a very small value due to the corrective maintenance shown in Fig. 7, which can limit the component IM. After around 870s (point C), the pump IM experiences a sharp decrease while that of the valve experiences a sharp increase until 1000s, due to the evolution shown in Fig. 5. After the preventive maintenance is implemented, the difference between the components IMs begins to

reduce. Then, one can conclude that attention should be focused on the pump before 1000s and on the valve afterwards, to achieve higher levels of system reliability.

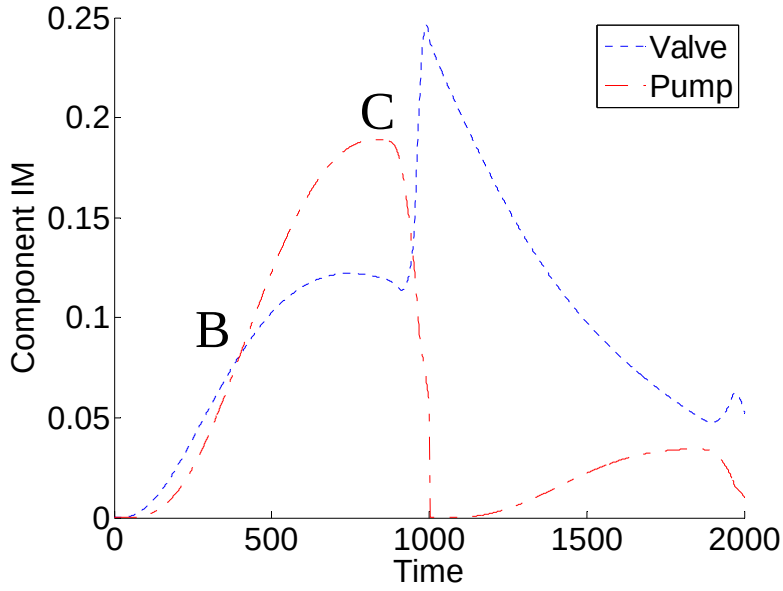

Fig. 6. The valve and pump IMs

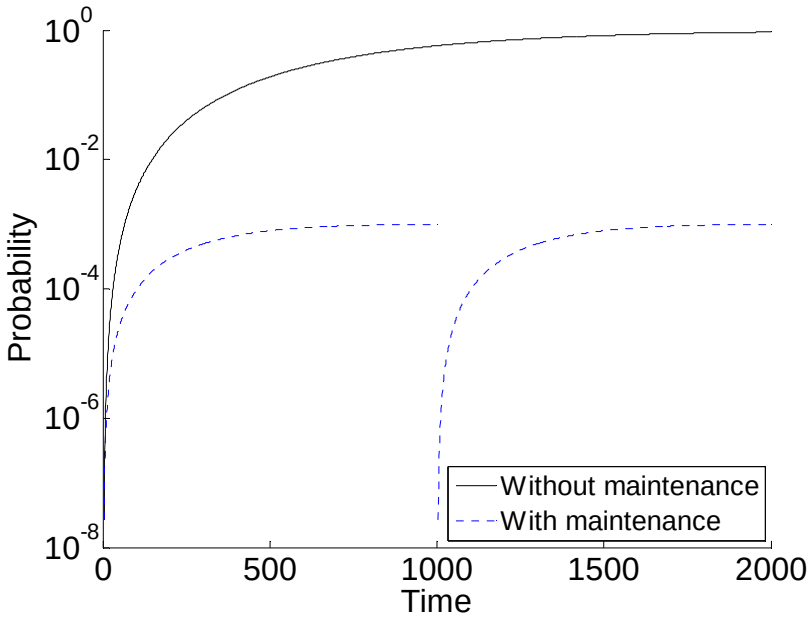

Fig. 7. The probability of the pump at state 0 (failure)

The reliabilities of the whole system and the two components over a time horizon of T_{miss} =2000s without maintenance are shown in Fig. 8. Before 1000s, the situations are the

same as with maintenance (Fig. 5). The sharp decrease of the reliability of the valve, then continues due to the lack of preventive maintenance, and the valve reaches failure after around 1060s, and the system fails too.

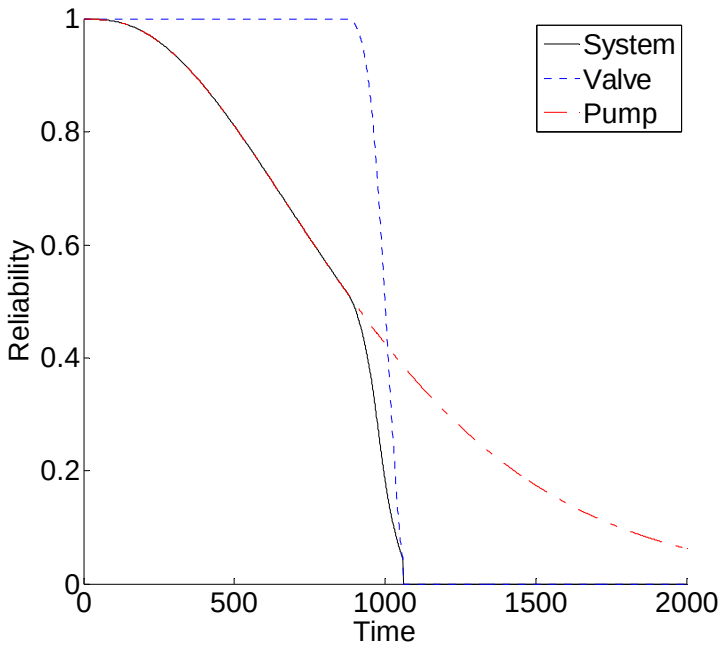

Fig. 8. The reliabilities of the system, valve and pump without maintenance

The related component IMs are shown in Fig. 9. From the figure, we can see that the criticality of the pump is higher than that of the valve most of the time until around 1015s (point E). Due to the absence of preventive maintenance, the system reliability quickly decreases to zero afterwards, which leads the components IMs to quickly decrease to zero. The gap between the two curves is due to the difference between the reliabilities of the two components, and reaches its maximum value at around 875s (point D), when the valve starts to contribute to the system failure.

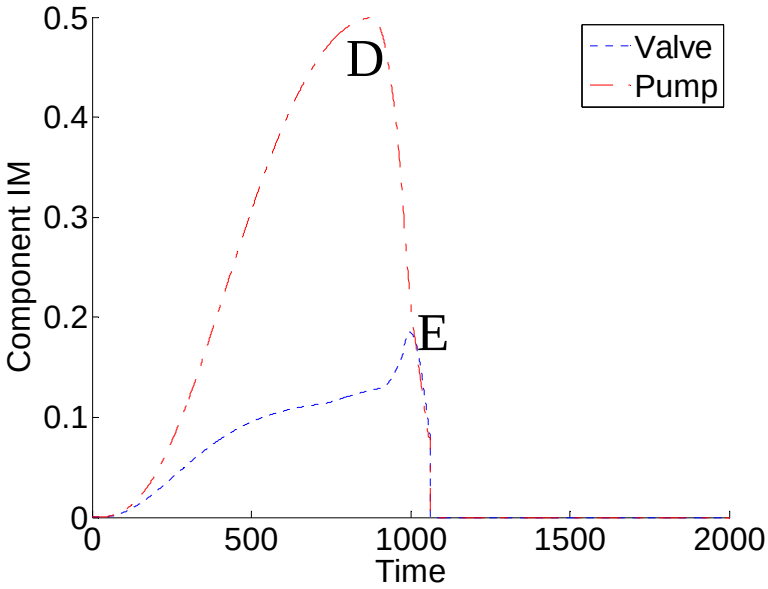

Fig. 9. The valve and pump IMs without maintenance

Finally, the reliabilities of the whole system and the two components over a time horizon of T_{miss} =2000s, without degradation dependency, are shown in Fig. 10. The system reliability is determined by the reliability of the pump since the valve is highly reliable. The IMs of the two components are shown in Fig. 11. The IM of the pump experiences a sudden change due to the preventive maintenance at 1000s, while that of the valve is always equal to zero.

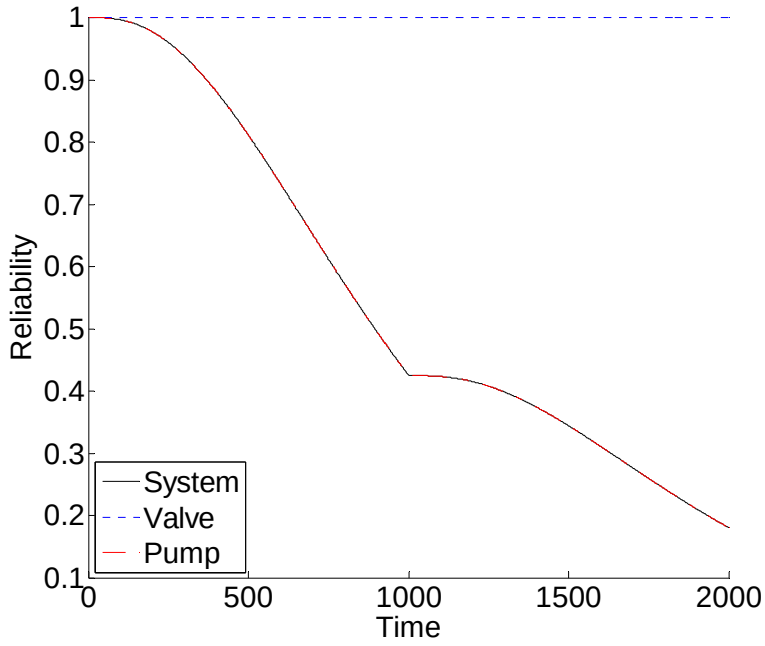

Fig. 10. The reliabilities of the system, the valve and the pump without degradation dependency

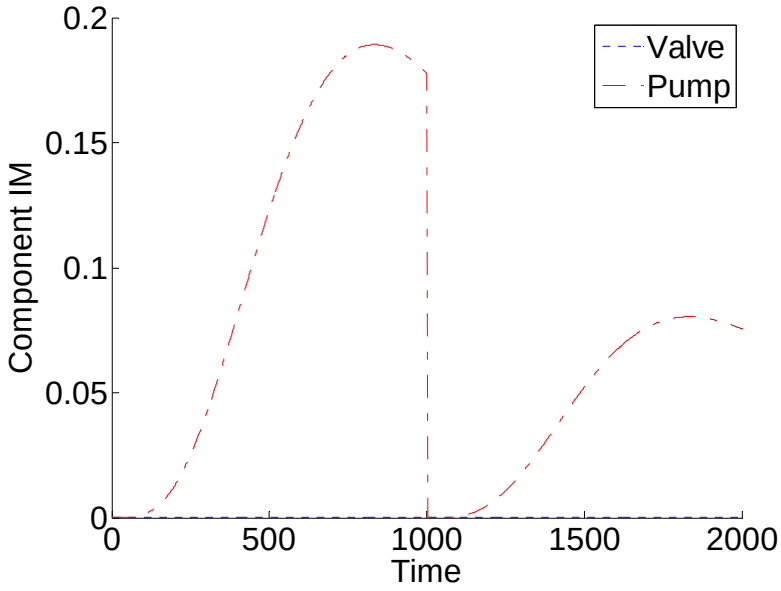

Fig. 11. The valve and pump IMs without degradation dependency

To investigate the impacts of the periods of the inspection tasks, the IMs of the two components with different inspection periods are shown in Fig. 12. We have tested two settings $T_{L_1} = T_{K_1} = 500s$ and $T_{L_1} = T_{K_1} = 250s$. From the figure, we can see that the IM of the valve is always equal to zero since it is highly reliable and that the increase of the inspection frequency can reduce the IM of the pump.

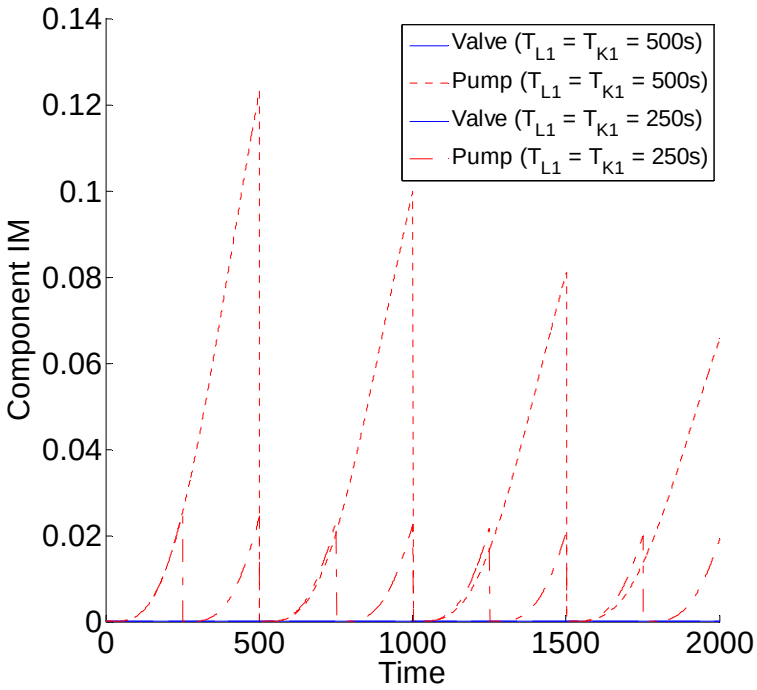

Fig. 12. The valve and pump IMs with different inspection periods

6. CONCLUSION

In this paper, we consider components with multiple competing degradation processes modeled by PBMs and MSMs. The PDMP modeling framework is employed to incorporate multiple dependent competing degradation processes and maintenance policies. To quantify the importance of different components within a system, MAD IM has been extended to accommodate components whose (degradation) states are determined by both discrete and continuous processes. The extended IM can provide timely feedbacks on the criticality of a component with respect to the system reliability. The degradation dependencies within one component and among different components, and two types of maintenance tasks (condition-based preventive maintenance by periodic inspections and corrective maintenance) have been taken into account. A quantification method based on the FV approach has been developed and illustrated in the application to a case study of a portion of an emergency system (the RHRS) from real-world nuclear power plants. The illustrative example shows that the extended IM can effectively estimate the criticality of different components under the conditions of interest.

As future work, it would be interesting to study how the sensitivity indices of the parameters of a component relate to the importance indices of that component, within a GSA framework.

REFERENCES

[1] W. Kuo and X. Zhu, "Some recent advances on importance measures in reliability," *Reliability, IEEE Transactions on,* vol. 61, pp. 344-360, 2012.

[2] H. Peng, D. W. Coit, and Q. Feng, "Component reliability criticality or importance measures for systems with degrading components," *Reliability, IEEE Transactions on,* vol. 61, pp. 4-12, 2012.

[3] Y. Wang and H. Pham, "Modeling the dependent competing risks with multiple degradation processes and random shock using time-varying copulas," *Reliability, IEEE Transactions on,* vol. 61, pp. 13-22, 2012.

[4] J. Lei, F. Qianmei, and D. W. Coit, "Reliability and Maintenance Modeling for Dependent Competing Failure Processes With Shifting Failure Thresholds," *Reliability, IEEE Transactions on,* vol. 61, pp. 932-948, 2012.

[5] N. Rasmekomen and A. K. Parlikad, "Maintenance Optimization for Asset Systems With Dependent Performance Degradation," *Reliability, IEEE Transactions on,* vol. 62, pp. 362-367, 2013.

[6] S. Albin and S. Chao, "Preventive replacement in systems with dependent components," *Reliability, IEEE Transactions on,* vol. 41, pp. 230-238, 1992.

[7] L. Jiang, Q. Feng, and D. W. Coit, "Reliability and maintenance modeling for dependent competing failure processes with shifting failure thresholds," *Reliability, IEEE Transactions on,* vol. 61, pp. 932-948, 2012.

[8] E. Keedy and Q. Feng, "A physics-of-failure based reliability and maintenance modeling framework for stent deployment and operation," *Reliability Engineering & System Safety,* vol. 103, pp. 94-101, 2012.

[9] A. Lisnianski and G. Levitin, *Multi-state system reliability: assessment, optimization and applications*: World scientific, 2003.

[10] M. Chookah, M. Nuhi, and M. Modarres, "A probabilistic physics-of-failure model for prognostic health management of structures subject to pitting and corrosion-fatigue," *Reliability Engineering & System Safety,* vol. 96, pp. 1601-1610, 2011.

[11] S. D. Unwin, P. P. Lowry, R. F. Layton, P. G. Heasler, and M. B. Toloczko, "Multi-state physics models of aging passive components in probabilistic risk assessment," in *International Topical Meeting on Probabilistic Safety Assessment and Analysis (PSA 2011)*, Wilmington, North Carolina, 2011, pp. 161-172.

[12] Y.-H. Lin, Y.-F. Li, and E. Zio, "Fuzzy Reliability Assessment of Systems with Multiple Dependent Competing Degradation Processes," *Fuzzy Systems, IEEE Transactions on (In press)*.

[13] C. M. Rocco and E. Zio, "Global sensitivity analysis in a Multi-state Physics Model of Component Degradation based on a hybrid State-Space Enrichment and Polynomial Chaos Expansion approach," *Reliability, IEEE Transactions on,* vol. 62, pp. 781-788.

[14] Z. W. Birnbaum, "On the importance of different components in a multicomponent system," *Multivariable analysis 2, New York: Academic Press,* pp. 581-592, 1969.

[15] W. Kuo and X. Zhu, "Relations and generalizations of importance measures in reliability," *Reliability, IEEE Transactions on,* vol. 61, pp. 659-674, 2012.

[16] R. E. Barlow and F. Proschan, "Importance of system components and fault tree events," *Stochastic Processes and their Applications,* vol. 3, pp. 153-173, 1975.

[17] D. Vasseur and M. Llory, "International survey on PSA figures of merit," *Reliability Engineering & System Safety,* vol. 66, pp. 261-274, 1999.

[18] W. Kuo and X. Zhu, *Importance measures in reliability, risk, and optimization: principles and applications*: John Wiley & Sons, 2012.

[19] M. J. Armstrong, "Reliability-importance and dual failure-mode components," *Reliability, IEEE Transactions on,* vol. 46, pp. 212-221, 1997.

[20] W. S. Griffith, "Multistate reliability models," *Journal of Applied Probability,* pp. 735-744, 1980.

[21] S. Wu and L.-Y. Chan, "Performance utility-analysis of multi-state systems," *Reliability, IEEE Transactions on,* vol. 52, pp. 14-21, 2003.

[22] S. Si, H. Dui, X. Zhao, S. Zhang, and S. Sun, "Integrated importance measure of component states based on loss of system performance," *Reliability, IEEE Transactions on,* vol. 61, pp. 192-202, 2012.

[23] S. Si, G. Levitin, H. Dui, and S. Sun, "Component state-based integrated importance measure for multi-state systems," *Reliability Engineering & System Safety,* vol. 116, pp. 75-83, 2013.

[24] H. Dui, S. Si, L. Cui, Z. Cai, and S. Sun, "Component Importance for Multi-State System Lifetimes With Renewal Functions," *Reliability, IEEE Transactions on,* vol. 63, pp. 105-117, 2014.

[25] E. Zio and L. Podofillini, "Monte Carlo simulation analysis of the effects of different system performance levels on the importance of multi-state components," *Reliability Engineering & System Safety,* vol. 82, pp. 63-73, 2003.

[26] G. Levitin, L. Podofillini, and E. Zio, "Generalised importance measures for multi-state elements based

on performance level restrictions," *Reliability Engineering & System Safety,* vol. 82, pp. 287-298, 2003.

[27] J. E. Ramirez-Marquez and D. W. Coit, "Composite importance measures for multi-state systems with multi-state components," *Reliability, IEEE Transactions on,* vol. 54, pp. 517-529, 2005.

[28] N. Gebraeel, "Prognostics-Based Identification of the Top-Units in a Fleet," *Automation Science and Engineering, IEEE Transactions on,* vol. 7, pp. 37-48, 2010.

[29] X. Liu, K. N. Al-Khalifa, E. A. Elsayed, D. W. Coit, and A. S. Hamouda, "Criticality measures for components with multi-dimensional degradation," *IIE Transactions,* 2013.

[30] S. Song, D. W. Coit, Q. Feng, and H. Peng, "Reliability Analysis for Multi-Component Systems Subject to Multiple Dependent Competing Failure Processes," 2014.

[31] S. Iyer, "The Barlow–Proschan importance and its generalizations with dependent components," *Stochastic processes and their applications,* vol. 42, pp. 353-359, 1992.

[32] B. Natvig, "Measures of component importance in nonrepairable and repairable multistate strongly coherent systems," *Methodology and Computing in Applied Probability,* vol. 13, pp. 523-547, 2011.

[33] C. Cocozza-Thivent, "Processus de renouvellement markovien, Processus de Markov déterministes par morceaux," *Online book available on the webpage: http://perso-math. univ-mlv. fr/users/cocozza. christiane/recherche-pageperso/PresentationRMetPDMP. html,* 2011.

[34] C. Cocozza-Thivent, R. Eymard, and S. Mercier, "A finite-volume scheme for dynamic reliability models," *IMA journal of numerical analysis,* vol. 26, pp. 446-471, 2006.

[35] R. Coudray and J. Mattei, "System reliability: An example of nuclear reactor system analysis," *Reliability Engineering,* vol. 7, pp. 89-121, 1984.

[36] M. Marseguerra and E. Zio, "Monte Carlo approach to PSA for dynamic process systems," *Reliability Engineering & System Safety,* vol. 52, pp. 227-241, 1996.

[37] R. Eymard and S. Mercier, "Comparison of numerical methods for the assessment of production availability of a hybrid system," *Reliability Engineering & System Safety,* vol. 93, pp. 168-177, 2008.

[38] M. H. Davis, *Markov models and optimization* vol. 49: CRC Press, 1993.

[39] S. Zhang, M. Hodkiewicz, L. Ma, and J. Mathew, "Machinery condition prognosis using multivariate analysis," in *Engineering Asset Management*: Springer, 2006, pp. 847-854.

[40] P. Moussou, S. Cambier, D. Lachene, S. Longarini, L. Paulhiac, and V. Villouvier, "Vibration investigation of a French PWR power plant piping system caused by cavitating butterfly valves," *ASME-PUBLICATIONS-PVP,* vol. 420, pp. 99-106, 2001.

[41] M. Daigle and K. Goebel, "A model-based prognostics approach applied to pneumatic valves," *International journal of prognostics and health management,* vol. 2, p. 008, 2011.

PAPER V: Y.-H. Lin, Y.-F. Li, E. Zio. A Framework for Modeling and Optimizing Maintenance in Systems Modeled by Piecewise-Deterministic Markov Processes Considering Epistemic Uncertainty. *Reliability, IEEE Transactions on*. (Under review)

A Framework for Modeling and Optimizing Maintenance in Systems Considering Epistemic Uncertainty and Degradation Dependency

Yan-Hui Lin[1], Yan-Fu Li[1], *Senior Member, IEEE* and Enrico Zio[1,2], *Senior Member, IEEE*

[1] Chair System Science and the Energy Challenge, Fondation Electricité de France (EDF), CentraleSupélec, Université Paris-Saclay, Grande Voie des Vignes, 92290 Chatenay-Malabry, France

[2]Politecnico di Milano, Italy

Abstract – This paper presents a modeling and optimization framework for the maintenance of systems under epistemic uncertainty. The degradation dependencies among different components and within one component are considered. The component degradation processes, the condition-based preventive maintenance and the corrective maintenance are described through a piecewise-deterministic Markov process modeling approach. Epistemic uncertainty, due to incomplete or imprecise knowledge about the degradation processes of the components, is treated by considering interval-valued parameters. This leads to the formulation of a multi-objective optimization problem whose objectives are the lower and upper bounds of the expected maintenance cost, and whose decision variables are the periods of inspections and the thresholds for preventive maintenance. A solution method to derive the optimal maintenance policy is proposed by combining finite-volume scheme for calculation, differential evolution and non-dominated sorting differential evolution for optimization. A case study pertaining to one subsystem of the residual heat removal system of a nuclear power plant is presented.

Index Terms – Maintenance optimization, epistemic uncertainty, degradation dependency, multi-objective optimization, piecewise-deterministic Markov process.

Acronyms

PBMs	Physics-based models
MSMs	Multi-state models
PDMP	Piecewise-deterministic Markov process
PM	Preventive maintenance
CM	Corrective maintenance
DE	Differential evolution
NSDE	Non-dominated sorting differential evolution
FV	Finite-volume
RHRS	Residual heat removal system

DMs	Decision makers

Notations

Q	Number of components in the system
$\boldsymbol{L}$	Group of degradation processes modeled by PBMs
$\boldsymbol{K}$	Group of degradation processes modeled by MSMs
$\boldsymbol{D}_{O_q}$	Degradation sate of component O_q
$\boldsymbol{X}_{L_m}(t)$	Time-dependent continuous variables of degradation process L_m
$\boldsymbol{X}_{L_m}^{\boldsymbol{D}}(t)$	Non-decreasing degradation variables vector
$\boldsymbol{X}_{L_m}^{\boldsymbol{P}}(t)$	Physical variables vector
$\boldsymbol{\mathcal{F}}_{L_m}$	Set of failure states of degradation process L_m
$Y_{K_n}(t)$	State variable of degradation process K_n
$\boldsymbol{S}_{K_n}$	Finite state set of degradation process K_n
$\boldsymbol{\mathcal{F}}_{K_n}$	Set of failure states of degradation process K_n
$\boldsymbol{\theta}_{\boldsymbol{K}}$	Environmental and operational factors in $\boldsymbol{K}$
$\lambda_i(j\|\boldsymbol{X}(t), \boldsymbol{\theta}_{\boldsymbol{K}})$	Transition rate from state i to j
$\boldsymbol{\theta}_{\boldsymbol{L}}$	Environmental and operational factors in $\boldsymbol{L}$
$\boldsymbol{f}_{\boldsymbol{L}}(\boldsymbol{Z}_k(t), t\|\boldsymbol{\theta}_{\boldsymbol{L}})$	Deterministic physics equations in $\boldsymbol{L}$
$\boldsymbol{Z}(t)$	Degradation state of the system
$\boldsymbol{\mathcal{F}}$	System failure state set
$\boldsymbol{H}_i$	Predefined state set of PM for degradation process i
T_i	Fixed period of PM for degradation process i
N_m	Number of maintenance tasks experienced by the system
T_{miss}	System mission time
T_m^k	Execution time of the *k*-th maintenance task
$\boldsymbol{Z}_k(t)$	Degradation state of the system defined on $[T_m^{k-1}, T_m^k]$
$C(t)$	Maintenance cost
C_{I_i}	Cost of the inspection task I_i
$C_P^{O_q}$	Cost of PM to component O_q
$N_P^{O_q}(t, \boldsymbol{H}, \boldsymbol{T} \mid \boldsymbol{\theta})$	Number of PM tasks to component O_q until time t
$N_D^{O_q}(t, \boldsymbol{H}, \boldsymbol{T} \mid \boldsymbol{\theta}, \boldsymbol{x}_{\boldsymbol{L}}^*)$	Number of CM tasks to component O_q until time t

C_F Penalty cost of experiencing a system failure

$N_F(t, \boldsymbol{H}, \boldsymbol{T} \mid \boldsymbol{\theta}, \boldsymbol{x}_L^*)$ Number of system failures until time until time t

$p_t^{\boldsymbol{Z}_k}(d\boldsymbol{z} \mid \boldsymbol{\theta})$ Probability distribution of $\boldsymbol{Z}_k(t)$

$\boldsymbol{z}_{O_q}$ Degradation state of the component O_q in $\boldsymbol{z}$

$\boldsymbol{H}_{O_q}$ State set for PM of the component O_q

$\boldsymbol{T}^{O_q}$ State set for PM of the component O_q

1. INTRODUCTION

Maintenance contributes to ensuring the safe and efficient operation of industrial systems [1]. The contribution to safety especially is in highly hazardous industries, such as the nuclear and aerospace ones. The interactions among components complicate the modeling for maintenance planning, which becomes a big challenge [2]. Thomas [3] has categorized these interactions into three groups: economic, structural and stochastic dependences. Economic dependence exists when the maintenance cost of several components is not equal to the sum of their individual maintenance costs. For example, Castanier *et al.* [4] have considered a condition-based maintenance policy for a two-unit deteriorating system, where the set-up cost of inspection is charged only once if the actions on the two components are combined. Van Dijkhuizen [5] has investigated the long-term grouping of preventive maintenance jobs in a multi-setup, multi-component production system where the set-up activities can be combined when several components are maintained at the same time. Structural dependence occurs if some working components need to be replaced or dismantled in order to execute the maintenance of the failed ones. For example, Dekker *et al.* [6] have studied the maintenance policy for asphalt roads where the number of maintenance services is limited by integrating neighboring segments into a homogeneous section which is completely repaired. Stochastic dependence, also referred to as probabilistic dependence, applies when the state of one component can affect those of other components or their failure rates. Failure interactions have been the most discussed cases for stochastic dependence [7] and imply that the failure of one component may lead to the failure of other components with certain probabilities, and/or influence their failure rates [8]. For example, Lai and Chen [9] have presented an economic periodic replacement model for a two-unit system where the failure of unit 1 can increase the failure rate of unit 2, while the failure of unit 2 induces unit 1 into instantaneous failure. Zequeira and Bérenguer [10] have studied the inspection policies for a two-component standby system, where the failure of one component can modify the conditional failure probability of the component still alive with probability p and do not modify it with probability $1-p$. Barros *et al.* [11], have optimized the maintenance policy for a two-unit parallel system where the failure of a component increases the failure rate of the surviving one.

In practice, the failure of industrial components is often the result of multiple and possibly competing mechanisms (e.g. friction-induced wear of the bearings and impeller wear caused by cavitation and erosion by the flow, can both lead to centrifugal pump failure [12]). For multi-component systems, the dependencies among these mechanisms within one component (e.g. the wear of rubbing surfaces influenced by the environmental stress shock within a micro-engine [13]), or/and among different components (e.g. the degradation of the pre-filtrations stations leading to a lower performance level of the sand filter in a water treatment plant [7])

need to be considered. Dependency among degradation mechanisms or processes has received less attention within the framework of maintenance modeling and optimization of multi-component systems, although they are of real concern in practice (e.g. the failure of a pump due to oxidation of contacts and bear wearing). Peng *et al.* [14] have developed a maintenance policy with periodic inspections when two dependent or correlated failure processes are considered. Jiang *et al.* [13] have further compared two preventive maintenance (PM) policies: age replacement policy and block replacement policy, combining immediate corrective replacement in consideration of shifting failure thresholds. Özekici [15] has considered interdependent aging processes between components due to continuous wear and shocks, and proposed an optimal periodic replacement policy. Rasmekomen and Parlikad [7] have considered degradation dependency in terms of output performance between one critical component and other parallel components based on aging processes, and the optimal age-based maintenance policy for this case was also studied. Yang *et al.* [16] have proposed a general statistical reliability model for repairable multi-component systems considering dependent competing risks, under a partially perfect repair assumption which considers that only the failed component, rather than the whole system, is replaced. Hong *et al.* [17] have used copulas to model degradation dependency among all the components of a system and obtained the optimal maintenance policy including condition-based PM with periodic inspections and instantaneous corrective maintenance (CM). Van Horenbeek and Pintelon [18] have proposed a dynamic predictive maintenance policy that minimizes the long-term mean maintenance cost per unit time while considering different component dependencies (i.e. economic, structural and stochastic dependence). Song *et al.* [19] have applied age replacement policy and inspection-based maintenance policy for systems whose components have *s*-dependent failure times, and the optimal replacement interval or inspection times are determined. Note that maintenance optimization for multi-component systems with multiple degradation processes within individual components has not been considered and only the pre-scheduled periods for inspection or maintenance are considered as the decision variables of the optimization problem.

To describe the component degradation mechanisms or processes, a number of models have been proposed in the field of reliability engineering. These models differ depending on the available information/data, and can be mainly classified into the following groups: statistical distributions (e.g. Bernstein distribution [20]), stochastic processes (e.g. Gamma process [21]), multi-state models (MSMs) (e.g. Markov model [22]) and physics-based models (PBMs) (e.g. physics model of the valve based on mass and energy balances [23]). Among the existing degradation models, physics-based models (PBMs) [24] and multi-state models (MSMs) [25] are two frequently used approaches, in the field of reliability engineering to describe the degradation of components, particularly when degradation/failure data are not sufficiently available to allow resorting to statistical or stochastic modeling, e.g. for highly reliable devices like those used in the nuclear and aerospace industries. Recently, a modeling approach employing a piecewise-deterministic Markov process (PDMP) has been proposed and developed in [26] to integrate PBMs and MSMs for dealing with the degradation dependencies among components and within one component.

An issue that arises in degradation modeling is epistemic uncertainty, due to the incomplete or imprecise knowledge of the degradation processes of the components, especially for the highly reliable ones. The values of the parameters of the physics equations (e.g. wear coefficients), influencing factors (e.g. temperatures and pressures) or transition rates between degradation states may be poorly known and inferred from the scarce data available and from elicited expert judgment [27]. This uncertainty must be reflected in the modeling and accounted for in the maintenance optimization that rests on it. Fuzzy sets have been employed to

mathematically represent epistemic uncertainty in some works [28-30] related to degradation modeling and maintenance. However, determining appropriate membership functions may be a difficult task in practice. In these cases, intervals can be used as a more general and less knowledge and information demanding representation of uncertainty than fuzzy sets [31].

To the knowledge of the authors, no study has considered epistemic uncertainty in maintenance modeling and optimization for multi-component systems with degradation dependency. In this paper, we do this by employing interval values to represent epistemic uncertainty in the parameters of the model. To derive the optimal maintenance policy, the maintenance cost is set as the objective function, which also takes an interval representation instead of a crisp value. Then, the objective is set as the interval-valued expected maintenance cost and its optimization is done within a bi-objective scheme considering lower and upper bounds values [32].

The main contribution of the paper is that it generalizes the existing maintenance models for multi-component systems by taking into account both degradation dependency among the components and epistemic uncertainty in the degradation models. More specific technical contributions are: for maintenance optimization: (1) the pre-scheduled period for inspection tasks and the thresholds for PM are considered as the decision variables in the optimization problem formulation; (2) a new optimization method integrating non-dominated sorting differential evolution (NSDE) [33], differential evolution (DE) [34] and finite-volume (FV) scheme for solving PDMP [35] is proposed to derive the optimal maintenance policy; for maintenance modeling: (1) epistemic uncertainty in the parameters of the model is taken into account by interval values; (2) the modeling approach previously proposed in [26] is extended by including condition-based PM with periodic inspections and CM.

The rest of the paper is structured as follows. Section 2 provides the assumptions and model descriptions. Section 3 presents the formulation of the maintenance optimization problem under uncertainty. Section 4 introduces the proposed solution approach for optimization. Section 5 demonstrates a case study on one subsystem of the residual heat removal system (RHRS) [36] of a nuclear power plant. Section 6 presents the numerical results and analysis. Section 7 concludes the work.

2. PROBLEM AND MODEL DESCRIPTION

2.1. Problem description

We consider a multi-component system made of Q components denoted by $O = \{O_1, O_2, \dots, O_Q\}$. Each component may be affected by multiple degradation mechanisms or processes, possibly dependent. The degradation processes can be separated into two groups: (1) $\boldsymbol{L} = \{L_1, L_2, \dots, L_M\}$ modeled by M PBMs; (2) $\boldsymbol{K} = \{K_1, K_2, \dots, K_N\}$ modeled by N MSMs, where $L_m, m = 1, 2, \dots, M$ and $K_n, n = 1, 2, \dots, N$ are the indexes of the degradation processes. The degradation state of a component $O_q \in \boldsymbol{O}, q = 1, 2, \dots, Q$, is determined by its degradation processes $\boldsymbol{D}_{O_q} \subseteq \boldsymbol{L} \cup \boldsymbol{K}$ and the component fails when one of its degradation processes becomes failure. A maintenance policy containing both CM and PM is considered.

2.2. Degradation models

In this section, PBMs, MSMs and PDMP modeling framework for systems considering degradation dependencies will be introduced, which are the basis of the problem and have been

proposed in [37].

2.2.1. PBMs

The following assumptions on PBMs are made [37]:

- A degradation process $\boldsymbol{X}_{L_m}(t), L_m \in \boldsymbol{L}$ in the first group, has d_{L_m} time-dependent continuous variables $\boldsymbol{X}_{L_m}(t) = \left(x_{L_m}^1(t), x_{L_m}^2(t), \dots, x_{L_m}^{d_{L_m}}(t)\right) \in \mathbb{R}^{d_{L_m}}$. A system of first-order differential equations (i.e. physics equations) $\dot{\boldsymbol{X}_{L_m}}(t) = \boldsymbol{f}_{L_m}\left(\boldsymbol{X}_{L_m}(t), t \mid \boldsymbol{\theta}_{L_m}\right)$, are used to characterize its evolution, where $\boldsymbol{\theta}_{L_m}$ are the parameters of the physics equations $\boldsymbol{f}_{L_m}$ (e.g. temperature and pressure). This assumption is made in [38] and widely used in practice [12, 23]. Note that higher-order differential equations can be converted into a system of a large number of first-order differential equations by introducing extra variables [39].
- $\boldsymbol{X}_{L_m}(t)$ can be divided into two groups of varaibles $\boldsymbol{X}_{L_m}(t) = (\boldsymbol{X}_{L_m}^{\boldsymbol{D}}(t), \boldsymbol{X}_{L_m}^{\boldsymbol{P}}(t))$: (1) $\boldsymbol{X}_{L_m}^{\boldsymbol{D}}(t)$ are the non-decreasing degradation variables describing the degradation process (e.g. leak area of the piston of the valve [23]), where $\boldsymbol{D}$ is the set of degradation variables indices; (2) $\boldsymbol{X}_{L_m}^{\boldsymbol{P}}(t)$ are the physical variables influencing $\boldsymbol{X}_{L_m}^{\boldsymbol{D}}(t)$ (e.g. velocity and force [12]), where $\boldsymbol{P}$ is the set of physical variable indices. For example, the friction-induced wear of the bearings is considered as one degradation process in [12]. It is represented by the increase in friction coefficients. The two friction coefficients associated with sliding and rolling friction are considered as the degradation variables. The rotational velocity of the pump is considered as the physical variable since it influences the increase in the coefficients of friction. The evolution of physical variables can be characterized by physics equations. If the variables can be modeled by physics equations and influence certain degradation variables, then, they are considered as physical variables. As long as one $x_{L_m}^i(t) \in \boldsymbol{X}_{L_m}^{\boldsymbol{D}}(t)$ reaches or exceeds its corresponding failure threshold $x_{L_m}^{i\ *}$, the generic degradation process L_m fails. Let $\boldsymbol{\mathcal{F}}_{L_m}$ denote the failure state set of L_m and $\boldsymbol{x}_{L_m}^*$ denote the set of all the failure thresholds of $\boldsymbol{X}_{L_m}^{\boldsymbol{D}}(t)$.

2.2.2. MSMs

The following assumptions on MSMs are made [37]:

- A degradation process, $Y_{K_n}(t), K_n \in K$ in the second group, takes values from a finite state set denoted by $S_{K_n} = \{0, 1, \dots, d_{K_n}\}$, where '$d_{K_n}$' is the perfect functioning state and '0' is the complete failure state. The transition rates $\lambda_i\left(j \mid \boldsymbol{\theta}_{K_n}\right), \forall\, i, j \in \boldsymbol{S}_{K_n}, i > j$ characterize the degradation transition probabilities from state i to state j, where $\boldsymbol{\theta}_{K_n}$ is the set of the environmental factors to K_n and the related parameters used in λ_i. We follow the assumption of Markov property which is widely used in practice to describe components degradation processes [25]. The transition rates between different degradation states are estimated from the degradation and/or failure data from historical field collection. Let $\boldsymbol{\mathcal{F}}_{K_n} = \{0\}$ denote the failure state set of K_n.

2.2.3. Degradation model of the system

The dependencies between degradation mechanisms or processes may exist within each group and between the two groups. The evolution trajectories of the continuous variables in the first group may be influenced by the degradation states of the second group. The transition times and transition directions of the degradation processes of the second group may depend on the degradation levels of the components in the first group [26]. PDMPs [40], which are a family of Markov processes involving deterministic evolution punctuated by random jumps, can be employed to model this type of dependency (the detailed formulations are shown in eqs. (2) and (3)). Let $\boldsymbol{X}(t) = \begin{pmatrix} \boldsymbol{X}_{L_1}(t) \\ \vdots \\ \boldsymbol{X}_{L_M}(t) \end{pmatrix}$ denote the degradation processes of the first group and $\boldsymbol{Y}(t) = \begin{pmatrix} Y_{K_1}(t) \\ \vdots \\ Y_{K_N}(t) \end{pmatrix}$ denote the degradation processes of the second group. The overall degradation process of the system is presented as

$$\boldsymbol{Z}(t) = \begin{pmatrix} \boldsymbol{X}(t) \\ \boldsymbol{Y}(t) \end{pmatrix} \in \boldsymbol{E} = \mathbb{R}^{d_L} \times \boldsymbol{S} \tag{1}$$

where $\boldsymbol{E}$ is a space combining $\mathbb{R}^{d_L}$ $(d_L = \sum_{m=1}^{M} d_{L_m})$ and $\boldsymbol{S} = \{0, 1, \dots, d_{\boldsymbol{S}}\}$ denotes the state set of process $\vec{Y}(t)$. The evolution of $\boldsymbol{Z}(t)$ has two parts: (1) the stochastic behavior of $\boldsymbol{Y}(t)$ and (2) the deterministic behavior of $\boldsymbol{X}(t)$ between two consecutive jumps of $\boldsymbol{Y}(t)$, given $\boldsymbol{Y}(t)$. The former is governed by the transition rates of $\boldsymbol{Y}(t)$, which depend on the states of the degradation processes in $\boldsymbol{X}(t)$ and also in $\boldsymbol{Y}(t)$, as follows:

$$\begin{aligned} &\lim_{\Delta t \to 0} P\left(\boldsymbol{Y}(t + \Delta t) = j \mid \boldsymbol{X}(t), \boldsymbol{Y}(t) = i, \boldsymbol{\theta_K} = \cup_{n=1}^{N} \boldsymbol{\theta}_{K_n}\right) / \Delta t \\ &= \lambda_i(j \mid \boldsymbol{X}(t), \boldsymbol{\theta_K}), \forall\, t \geq 0, i, j \in \boldsymbol{S}, i \neq j \end{aligned} \tag{2}$$

The latter is described by the deterministic physics, which depends on the states of the degradation processes in $\boldsymbol{Y}(t)$ and also in $\boldsymbol{X}(t)$, as follows:

$$\begin{aligned} \dot{\boldsymbol{X}}(t) &= \begin{pmatrix} \dot{\boldsymbol{X}}_{L_1}(t) \\ \vdots \\ \dot{\boldsymbol{X}}_{L_M}(t) \end{pmatrix} = \begin{pmatrix} \boldsymbol{f}_{L_1}^{\boldsymbol{Y}(t)}(\boldsymbol{X}(t), t \mid \boldsymbol{\theta}_{L_1}) \\ \vdots \\ \boldsymbol{f}_{L_M}^{\boldsymbol{Y}(t)}(\boldsymbol{X}(t), t \mid \boldsymbol{\theta}_{L_M}) \end{pmatrix} \\ &= \boldsymbol{f_L}^{\boldsymbol{Y}(t)}(\boldsymbol{X}(t), t \mid \boldsymbol{\theta_L} = \cup_{m=1}^{M} \boldsymbol{\theta}_{L_m}) \end{aligned} \tag{3}$$

Let $\boldsymbol{\mathcal{F}}$ denote the system failure state set, which depends on the structure of the system: then, the system reliability at mission time T_{miss} can be obtained as follows:

$$R(T_{miss}) = P[\boldsymbol{Z}(s) \notin \boldsymbol{\mathcal{F}}, \forall s \leq T_{miss}] \tag{4}$$

The system failure state set is dependent on system structure. To determine this set, reliability analysis tools such as fault tree [41] can be used to identify the combination of primary failure events leading to system failure.

2.3. Maintenance policy

The following assumptions are made based on actual maintenance activities performed in

industrial practice:

- The PM involves condition-based maintenance tasks, which recommend maintenance actions according to the information collected through condition inspections [42]. The inspection task $I_i, \forall\, i \in \boldsymbol{L} \cup \boldsymbol{K}$ related to one degradation process i is carried out with fixed period and a cost is associated with each inspection.
- If the state of one degradation process $i \in \boldsymbol{L} \cup \boldsymbol{K}$, reported by condition inspection, enters the predefined state set for PM denoted by $\boldsymbol{H}_i$, then the component containing this degradation process is restored to its initial state and a PM cost is incurred depending on the component type. Otherwise, no maintenance action is performed.
- Component failure can be detected immediately and the failed component is restored to its initial state by the CM [13], and a CM cost is incurred depending on the component type.
- The duration of inspection tasks is negligible and all maintenance actions are done instantaneously, compared with the lifetime of the components [14].

The degradation processes and the maintenance policy of an example system are shown in Fig 1, considering a mission time T_{miss}. It consists of two components O_1 and O_2. $\boldsymbol{D}_{O_1} = \{L_1\}$ and $\boldsymbol{D}_{O_2} = \{K_1\}$. T_{L_1} and T_{K_1} are the periods of the inspection tasks for I_{L_1} and I_{K_1}, respectively. For L_1, PM is carried out whenever its degradation variable $\boldsymbol{X}_{L_1}^{\boldsymbol{D}}(t)$ reaches or exceeds its PM threshold ${x_{L_1}}^{p}$ at the time of inspection. The physical variable $\boldsymbol{X}_{L_1}^{\boldsymbol{P}}(t)$ is also initialized immediately after PM is performed. For K_1, PM is carried out when it is in state '1' at the time of inspection.

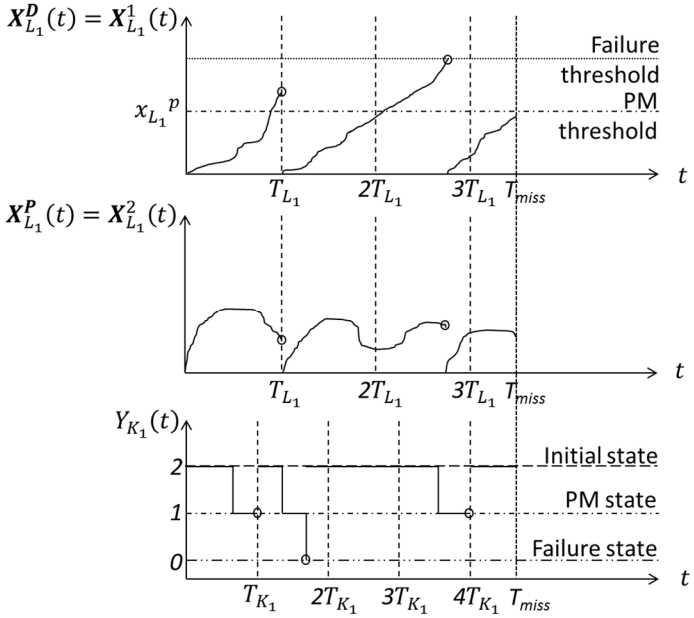

Fig. 1. An illustration of the degradation processes with maintenance policy, for an example system.

A CM is carried out instantaneously once any component fails and the failed component is restored to its initial state at the time of failure. Thus, the failure states of the degradation processes are infinitely approachable instead of being truly reached, because the maintenance tasks are assumed to be done instantaneously and $\boldsymbol{Z}(t)$ has a unique value from $\boldsymbol{E}$ at any time t.

To extend the PDMP to model the degradation processes and the maintenance policy, the difficulty is the discontinuity of $\boldsymbol{X}(t)$ due to the instantaneous change caused by the maintenance task. To solve this problem, we choose to divide the entire mission time into multiple intervals. In each interval, one new PDMP, $\boldsymbol{Z}_k(t), k = 1,2, \dots, N_m + 1$, is defined, where N_m is the number of maintenance tasks the system has experienced till the mission time. Let $T_m^k, k = 1,2, \dots, N_m$ denote the execution time of the k-th maintenance task, then $\boldsymbol{Z}_1(t)$ is defined on $[0, T_m^1]$, $\boldsymbol{Z}_{N_m+1}(t)$ is on $\left[T_m^{N_m}, T_{miss}\right]$ and $\boldsymbol{Z}_k(t), k = 2, \dots, N_m$ is on $[T_m^{k-1}, T_m^k]$, respectively. In this way, the failure states of the degradation processes can be reached by the process $\boldsymbol{Z}_k(t)$. The initial states $\boldsymbol{Z}_k(t), k = 2, \dots, N_m + 1$ are dependent on the maintenance task carried out at time T_m^{k-1} and $\boldsymbol{Z}_{k-1}(T_m^{k-1})$. Fig 2 shows this for the degradation processes in Fig 1.

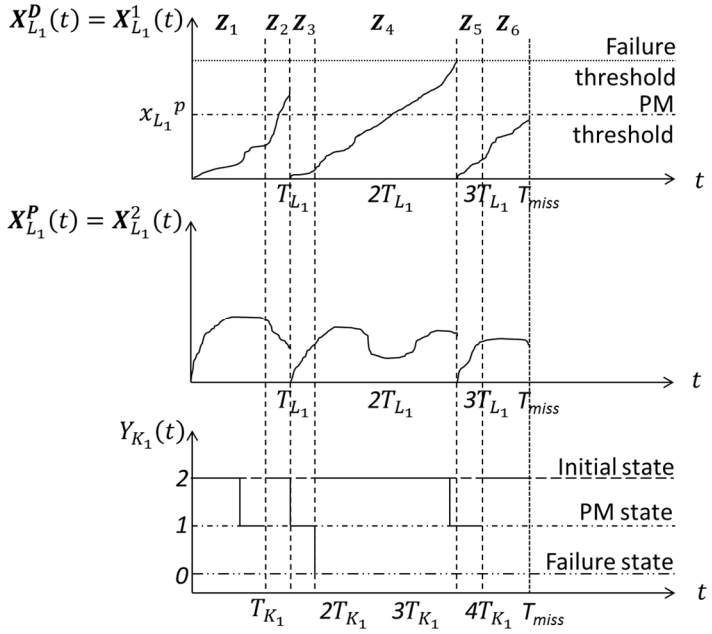

Fig. 2. An illustration of system maintenance, treated via PDMP.

This treatment is only for formulating the problem within the settings of PDMP and it does not impact the computational complexity. As we shall see later, we employ a FV scheme to solve the PDMP, which efficiently gives an approximate solution by discretizing the state space of the continuous variables and the time space of PDMP. The entire mission is, thus, divided into much smaller intervals to ensure the convergence of the approximated solution ($\Delta t \to 0$ and $|\mathcal{M}|/\Delta t \to 0$). The computational complexity depends on the number of small intervals defined in FV scheme, which has no relation with the number of multiple intervals defined in

the problem formulation.

In reality, the two major issues for the maintenance policy are to determine (1) the period $T_i, \forall\, i \in \boldsymbol{L} \cup \boldsymbol{K}$ for each inspection task I_i and (2) the state set for PM $\boldsymbol{H}_i, \forall\, i \in \boldsymbol{L} \cup \boldsymbol{K}$ for each degradation process i.

3. MAINTENANCE OPTIMIZATION UNDER UNCERTAINTY

3.1. Maintenance optimization criterion

In order to optimize the maintenance policy, the criterion considered is the expected maintenance cost over the system mission time. Let $C(t)$ denote the maintenance cost, $\boldsymbol{H} = \bigcup_{\forall\, i \in \boldsymbol{L} \cup \boldsymbol{K}} \boldsymbol{H}_i$ and $\boldsymbol{T} = \bigcup_{\forall\, i \in \boldsymbol{L} \cup \boldsymbol{K}} \boldsymbol{T}_i$, $\boldsymbol{\theta} = \boldsymbol{\theta}_{\boldsymbol{L}} \cup \boldsymbol{\theta}_{\boldsymbol{K}}$, $\boldsymbol{x}_{\boldsymbol{L}}^* = \bigcup_{m=1}^{M} \boldsymbol{x}_{L_m}^*$ for the system functioning until time t, we can write:

$$\mathbb{E}\big(C(t, \boldsymbol{H}, \boldsymbol{T} \mid \boldsymbol{\theta}, \boldsymbol{x}_{\boldsymbol{L}}^*)\big) = \sum_{i \in \boldsymbol{L} \cup \boldsymbol{K}} C_{I_i} \cdot \left\lfloor \frac{t}{T_i} \right\rfloor + \sum_{O_q \in \boldsymbol{O}} C_P^{O_q} \cdot \mathbb{E}(N_P^{O_q}(t, \boldsymbol{H}, \boldsymbol{T} \mid \boldsymbol{\theta}))$$
$$+ \sum_{O_q \in \boldsymbol{O}} C_D^{O_q} \cdot \mathbb{E}(N_D^{O_q}(t, \boldsymbol{H}, \boldsymbol{T} \mid \boldsymbol{\theta}, \boldsymbol{x}_{\boldsymbol{L}}^*)) + C_F \cdot \mathbb{E}(N_F(t, \boldsymbol{H}, \boldsymbol{T} \mid \boldsymbol{\theta}, \boldsymbol{x}_{\boldsymbol{L}}^*)) \quad (5)$$

where C_{I_i} is the cost of the inspection task I_i, $\left\lfloor \frac{t}{T_i} \right\rfloor$ is the number of times the inspection task I_i has been performed until time t, $C_P^{O_q}$ is the cost of PM to component O_q, $N_P^{O_q}(t, \boldsymbol{H}, \boldsymbol{T} \mid \boldsymbol{\theta})$ is the number of PM tasks to component O_q until time t, $N_D^{O_q}(t, \boldsymbol{H}, \boldsymbol{T} \mid \boldsymbol{\theta}, \boldsymbol{x}_{\boldsymbol{L}}^*)$ is the number of CM tasks to component O_q until time t, C_F is the penalty cost of experiencing a system failure and $N_F(t, \boldsymbol{H}, \boldsymbol{T} \mid \boldsymbol{\theta}, \boldsymbol{x}_{\boldsymbol{L}}^*)$ is the number of system failures until time t.

Let $p_t^{\boldsymbol{Z}_k}(d\boldsymbol{z} \mid \boldsymbol{\theta})$ denote the probability distribution of $\boldsymbol{Z}_k(t)$; we, then, obtain that

$$\mathbb{E}(N_P^{O_q}(t, \boldsymbol{H}, \boldsymbol{T} \mid \boldsymbol{\theta})) = \sum_{k \in \mathbb{N}^*} \sum_{T^i \in \boldsymbol{T}^{O_q}} \int_{\boldsymbol{z}_{O_q} \in \boldsymbol{H}_{O_q}} p_{T^i}^{\boldsymbol{Z}_k}(d\boldsymbol{z} \mid \boldsymbol{\theta}) \quad (6)$$

where $\boldsymbol{z}_{O_q}$ denotes the degradation state of the component O_q in $\boldsymbol{z}$, $\boldsymbol{H}_{O_q} = \bigcup_{i \in \boldsymbol{D}_{O_q}} \boldsymbol{H}_i$ denotes the state set for PM of the component O_q and $\boldsymbol{T}^{O_q}$ denotes the set of inspection time of the component O_q. The function $p_{T^i}^{\boldsymbol{Z}_k}(d\boldsymbol{z} \mid \boldsymbol{\theta})$ is the probability distribution of $\boldsymbol{Z}_k(t)$ at the inspection time $T^{\boldsymbol{i}}$,

$$\mathbb{E}(N_D^{O_q}(t, \boldsymbol{H}, \boldsymbol{T} \mid \boldsymbol{\theta}, \boldsymbol{x}_{\boldsymbol{L}}^*)) = \sum_{k \in \mathbb{N}^*} \int_0^t \int_{\boldsymbol{z}_{O_q} \in \boldsymbol{\mathcal{F}}_{O_q}} p_s^{\boldsymbol{Z}_k}(d\boldsymbol{z} \mid \boldsymbol{\theta}) ds \quad (7)$$

where $\boldsymbol{\mathcal{F}}_{O_q} = \bigcup_{i \in \boldsymbol{D}_{O_q}} \boldsymbol{\mathcal{F}}_i$ denotes the failure state set of the component O_q,

$$\mathbb{E}(N_F(t, \boldsymbol{H}, \boldsymbol{T} \mid \boldsymbol{\theta}, \boldsymbol{x}_{\boldsymbol{L}}^*)) = \sum_{k \in \mathbb{N}^*} \int_0^t \int_{\boldsymbol{z} \in \boldsymbol{\mathcal{F}}} p_s^{\boldsymbol{Z}_k}(d\boldsymbol{z} \mid \boldsymbol{\theta}) ds \quad (8)$$

3.2. Epistemic uncertainty

Due to the incomplete or imprecise knowledge about the degradation processes, epistemic uncertainty may exist:

- For PBMs: (1) the parameters (e.g. wear coefficient) and influencing factors (e.g. temperature and pressure) $\boldsymbol{\theta}_L$ may be poorly known and elicited from expert judgment [27]; (2) the failure thresholds $\boldsymbol{x}_{\boldsymbol{L}}^*$ may be uncertain due to imperfect information [43].

- For MSMs: (1) the state performances may be vaguely defined due to the imprecise discretization of the underlying continuous degradation processes [44]; (2) the transition rates between states may be difficult to estimate statistically due to insufficient data, especially for highly reliable components (e.g. valves and pumps in nuclear power plants, etc.) [45].

The experts in many cases can only confirm an interval of the possible minimum and maximum values of the uncertain transition rate. One practical way of dealing with epistemic uncertainty is to use intervals of values for the uncertain parameters [31]. In this respect, the following assumptions are made (a symbol with an underbar indicates the left limit of that interval, while a symbol with an overbar indicates the right limit of that interval):

- The value of $\forall \theta_i \in \boldsymbol{\theta}$, is represented by an interval $[\theta_i] = \left[\underline{\theta_i}, \overline{\theta_i}\right]$. Let $[\boldsymbol{\theta}] = \cup_{\theta_i \in \boldsymbol{\theta}} [\theta_i]$.
- The value of $\forall x_{L_m}^{i\ *} \in \boldsymbol{x}_{\boldsymbol{L_m}}^*, \forall\, L_m \in \boldsymbol{L}$, is represented by an interval $\left[x_{L_m}^{i\ *}\right] = \left[\underline{x_{L_m}^{i\ *}}, \overline{x_{L_m}^{i\ *}}\right]$. Let $\left[\boldsymbol{x}_{\boldsymbol{L_m}}^*\right] = \cup_{x_{L_m}^{i\ *} \in \boldsymbol{x}_{L_m}^*} \left[x_{L_m}^{i\ *}\right]$ and $[\boldsymbol{x}_{\boldsymbol{L}}^*] = \cup_{m=1}^{M} \left[\boldsymbol{x}_{L_m}^*\right]$.

$\mathbb{E}\left(C(t, \boldsymbol{H}, \boldsymbol{T} \mid \boldsymbol{\theta}, \boldsymbol{x}_{\boldsymbol{L}}^*)\right)$, then, is also an interval, denoted by

$$\left[\mathbb{E}\left(C(t, \boldsymbol{H}, \boldsymbol{T} \mid [\boldsymbol{\theta}], [\boldsymbol{x}_{\boldsymbol{L}}^*])\right)\right] =$$

$$\left[\min_{\substack{\boldsymbol{\theta} \in [\boldsymbol{\theta}] \\ \boldsymbol{x}_{\boldsymbol{L}}^* \in [\boldsymbol{x}_{\boldsymbol{L}}^*]}} \mathbb{E}\left(C(t, \boldsymbol{H}, \boldsymbol{T} \mid \boldsymbol{\theta}, \boldsymbol{x}_{\boldsymbol{L}}^*)\right), \max_{\substack{\boldsymbol{\theta} \in [\boldsymbol{\theta}] \\ \boldsymbol{x}_{\boldsymbol{L}}^* \in [\boldsymbol{x}_{\boldsymbol{L}}^*]}} \mathbb{E}\left(C(t, \boldsymbol{H}, \boldsymbol{T} \mid \boldsymbol{\theta}, \boldsymbol{x}_{\boldsymbol{L}}^*)\right)\right]$$

$$= \left[\underline{\mathbb{E}\left(C(t, \boldsymbol{H}, \boldsymbol{T} \mid [\boldsymbol{\theta}], [\boldsymbol{x}_{\boldsymbol{L}}^*])\right)}, \overline{\mathbb{E}\left(C(t, \boldsymbol{H}, \boldsymbol{T} \mid [\boldsymbol{\theta}], [\boldsymbol{x}_{\boldsymbol{L}}^*])\right)}\right] \quad (9)$$

3.3. Optimization problem

Based on the models presented above, the problem of maintenance optimization under uncertainty, on a mission time horizon T_{miss}, can be defined as:

$$\begin{aligned} &\text{Min } \left[\mathbb{E}\left(C(T_{miss}, \boldsymbol{H}, \boldsymbol{T} \mid [\boldsymbol{\theta}], [\boldsymbol{x}_{\boldsymbol{L}}^*])\right)\right] \\ &\text{Subject to } \boldsymbol{H}_i \subseteq W_i,\ \forall\, i \in \boldsymbol{L} \cup \boldsymbol{K} \\ &0 \le T_i \le T_{miss},\ \forall\, i \in \boldsymbol{L} \cup \boldsymbol{K} \end{aligned} \quad (10)$$

where $W_i = \begin{cases} \mathbb{R}^{d_i}, if & i \in \boldsymbol{L} \\ \boldsymbol{S}_i, if & i \in \boldsymbol{K} \end{cases}$.

For its solution, it can be reformulated as a multi-objective optimization problem:

$$\begin{aligned} &\text{Min } \underline{\mathbb{E}\left(C(T_{miss}, \boldsymbol{H}, \boldsymbol{T} \mid [\boldsymbol{\theta}], [\boldsymbol{x}_{\boldsymbol{L}}^*])\right)} \\ &\text{Min } \overline{\mathbb{E}\left(C(T_{miss}, \boldsymbol{H}, \boldsymbol{T} \mid [\boldsymbol{\theta}], [\boldsymbol{x}_{\boldsymbol{L}}^*])\right)} \\ &\text{Subject to } \boldsymbol{H}_i \subseteq W_i,\ \forall\, i \in \boldsymbol{L} \cup \boldsymbol{K} \\ &0 \le T_i \le T_{miss},\ \forall\, i \in \boldsymbol{L} \cup \boldsymbol{K} \end{aligned} \quad (11)$$

where $W_i = \begin{cases} \mathbb{R}^{d_i}, if \ \ i \in \boldsymbol{L} \\ \boldsymbol{S}_i, if \ \ \ i \in \boldsymbol{K} \end{cases}$.

This formulation optimizes the lower and upper bounds of interval simultaneously. Due to the limit of data, no probability distribution or membership function is assumed on the interval. The order relation between intervals which requires no information about distribution or membership function [32] (Definitions 3.1 and 3.3) can be used in this situation (let $A = [a_L, a_R]$ and $B = [b_L, b_R]$ denote two intervals, according to these definitions, $A \leq B \ iff \ a_L \leq b_L \ and \ a_R \leq b_R$). This leads to the definition of a multi-objective optimization problem with respect to the lower and upper bounds of the expected maintenance cost ($\underline{\mathbb{E}\big(C(T_{miss}, \boldsymbol{H}, \boldsymbol{T} \mid [\boldsymbol{\theta}], [\boldsymbol{x}_L^*])\big)}$ and $\overline{\mathbb{E}\big(C(T_{miss}, \boldsymbol{H}, \boldsymbol{T} \mid [\boldsymbol{\theta}], [\boldsymbol{x}_L^*])\big)}$). It also covers the minimax type of robust optimization based on worst-case analysis, which may generate conservative decisions under some situations [46]. Note that this order relation is a partial order so that the solutions of (11) obtained are Pareto optimal solutions.

Finding the Pareto optimal maintenance policy is a challenging problem, due to the complex behavior of the system involving the stochasticities of MSMs, time-dependent evolutions of PBMs and effects of the two types of maintenance.

4. SOLUTION APPROACH

In order to solve the multi-objective optimization problem defined in eq.(11), we employ (1) FV scheme to calculate $\mathbb{E}\big(C(T_{miss}, \boldsymbol{H}, \boldsymbol{T} \mid \boldsymbol{\theta}, \boldsymbol{x}_L^*)\big)$; (2) two DEs to compute the upper and lower bounds of the interval $\left[\mathbb{E}\big(C(T_{miss}, \boldsymbol{H}, \boldsymbol{T} \mid [\boldsymbol{\theta}], [\boldsymbol{x}_L^*])\big)\right]$, using the FV scheme for fitness evaluation; (3) NSDE to find the Pareto-optimal maintenance policy for $\boldsymbol{H}$ and $\boldsymbol{T}$, aiming at optimizing the interval produced by the two DEs. The meta-heuristic algorithm DE is chosen as the solution approach because 1) PDMP model is highly complex and non-linear and 2) DE is fit to optimizing continuous decision variables.

4.1. FV for solving PDMP

To obtain $\mathbb{E}\big(C(t, \boldsymbol{H}, \boldsymbol{T} \mid \boldsymbol{\theta}, \boldsymbol{x}_L^*)\big)$, $p_t^{\boldsymbol{Z}_k}(d\boldsymbol{z} = (d\boldsymbol{x}, i) \mid \boldsymbol{\theta})$ of PDMPs need to be calculated at first. Monte Carlo (MC) simulation methods can be used to solve it: however, the major shortcoming is the high computational burden. FV scheme is an alternative that can lead to results comparable to MC simulation, but in significantly shorter computing times [35]. FV scheme gives an approximate solution by discretizing the state space of the continuous variables and the time space of PDMP. Here, we employ an explicit FV scheme to PDMP, developed by Cocozza-Thivent *et al.* [35].

4.1.1. Assumptions

This approach can be applied under the following assumptions:

- The transition rates $\lambda_i(j \mid \cdot, \boldsymbol{\theta_K}), \forall i, j \in \boldsymbol{S}$ are continuous and bounded functions from $\mathbb{R}^{d_L}$ to $\mathbb{R}^+$.
- The physics equations ${\boldsymbol{f}_L}^i(\cdot, \cdot \mid \boldsymbol{\theta}_L), \forall i \in \boldsymbol{S}$ are continuous functions from $\mathbb{R}^{d_L} \times \mathbb{R}^+$ to $\mathbb{R}^{d_L}$ and locally Lipschitz continuous.

- The physics equations $\boldsymbol{f}_L{}^i(\cdot, t \mid \boldsymbol{\theta}_L,), \forall i \in \boldsymbol{S}$ are sub-linear, i.e. there are some $V_1 > 0$ and $V_2 > 0$ such that
$$\forall \boldsymbol{x} \in \mathbb{R}^{d_L}, t \in \mathbb{R}^+ \left|\boldsymbol{f}_L{}^i(\boldsymbol{x}, t \mid \boldsymbol{\theta}_L)\right| \leq V_1(\|\boldsymbol{x}\| + |t|) + V_2$$
- The functions $div(\boldsymbol{f}_L{}^i(\cdot,\cdot \mid \boldsymbol{\theta}_L)), \forall i \in \boldsymbol{S}$ are almost everywhere bounded in absolute value by some real value $D > 0$ (independent of i).

4.1.2. Solution approach

For the ease of notation, first we let $\boldsymbol{g}^i(\cdot,\cdot)$: $\mathbb{R}^{d_L} \times \mathbb{R} \to \mathbb{R}^{d_L}$ denote the solution of

$$\frac{\partial}{\partial t}\boldsymbol{g}^i(\boldsymbol{x}, t \mid \boldsymbol{\theta}_L) = \boldsymbol{f}_L{}^i\left(\boldsymbol{g}^i(\boldsymbol{x}, t \mid \boldsymbol{\theta}_L), t \,\middle|\, \boldsymbol{\theta}_L\right), \forall i \in \boldsymbol{S}, \boldsymbol{x} \in \mathbb{R}^{d_L}, t \in \mathbb{R} \tag{12}$$

with

$$\boldsymbol{g}^i(\boldsymbol{x}, 0 \mid \boldsymbol{\theta}_L) = \boldsymbol{x}, \forall i \in \boldsymbol{S}, \boldsymbol{x} \in \mathbb{R}^{d_L} \tag{13}$$

and $\boldsymbol{g}^i(\boldsymbol{x}, t \mid \boldsymbol{\theta}_L)$ is the result of the deterministic behavior of $\boldsymbol{X}(t)$ after time *t*, starting from the point $\boldsymbol{x}$ and while the processes $\boldsymbol{Y}(t)$ hold on state i.

The state space $\mathbb{R}^{d_L}$ of continuous variables $\boldsymbol{X}(t)$ is divided into an admissible mesh $\mathcal{M}$, which is a family of measurable subsets of $\mathbb{R}^{d_L}$ ($\mathcal{M}$ is a partition of $\mathbb{R}^{d_L}$) such that:

(17) $\bigcup_{A\in\mathcal{M}} A = \mathbb{R}^{d_L}$.

(18) $\forall A, B \in \mathcal{M},\ A \neq B \Rightarrow A \cap B = \emptyset$.

(19) $m_A = \int_A d\boldsymbol{x} > 0, \forall A \in \mathcal{M}$, where m_A is the volume of grid A.

(20) $sup_{A\in\mathcal{M}} diam(A) < +\infty$ where $diam(A) = sup_{\forall \boldsymbol{x},\boldsymbol{y}\in A}|\boldsymbol{x} - \boldsymbol{y}|$.

Additionally, the time space $\mathbb{R}^+$ is divided into small intervals $\mathbb{R}^+ = \bigcup_{n=0,1,2,\dots}[n\Delta t, (n+1)\Delta t[$, by setting the time step $\Delta t > 0$ (the length of each interval).

The numerical scheme aims at constructing an approximate value $\rho_t^{\boldsymbol{Z}_k}(\boldsymbol{x},\cdot \mid \boldsymbol{\theta})d\boldsymbol{x}$ for $p_t^{\boldsymbol{Z}_k}(d\boldsymbol{x},\cdot \mid \boldsymbol{\theta})$, such that $p_t^{\boldsymbol{Z}_k}(\boldsymbol{x},\cdot \mid \boldsymbol{\theta})$ is constant on each $A \times \{i\} \times [n\Delta t, (n+1)\Delta t[, \forall A \in \mathcal{M}, i \in \boldsymbol{S}, [n\Delta t, (n+1)\Delta t[\in [T_m^{k-1}, T_m^k]$:

$$p_t^{\boldsymbol{Z}_k}(\boldsymbol{x}, i \mid \boldsymbol{\theta}) = P_n^{\boldsymbol{Z}_k}(A, i \mid \boldsymbol{\theta}), \forall i \in \boldsymbol{S}, \boldsymbol{x} \in A, t \in [n\Delta t, (n+1)\Delta t[\tag{14}$$

$P_0^{\boldsymbol{Z}_k}(A, i \mid \boldsymbol{\theta}), \forall i \in \boldsymbol{S}, A \in \mathcal{M}$ is defined as follows:

$$P_0^{\boldsymbol{Z}_k}(A, i \mid \boldsymbol{\theta}) = \int_A p_0^{\boldsymbol{Z}_k}(d\boldsymbol{x}, i \mid \boldsymbol{\theta})\,/m_A \tag{15}$$

Then, $P_{n+1}^{\boldsymbol{Z}_k}(A, i \mid \boldsymbol{\theta}), \forall i \in \boldsymbol{S}, A \in \mathcal{M}, n \in \mathbb{N}$ can be calculated considering the deterministic evaluation of $\boldsymbol{X}(t)$ and the stochastic evolution of $\boldsymbol{Y}(t)$ based on $P_n^{\boldsymbol{Z}_k}(\mathcal{M}, i \mid \boldsymbol{\theta})$ by the Chapman-Kolmogorov forward equation, as follows:

$$P_{n+1}^{\boldsymbol{Z}_k}(A, i \mid \boldsymbol{\theta})$$
$$= \frac{1}{1+\Delta t b_A^i}\widehat{P_{n+1}^{\boldsymbol{Z}_k}}(A, i \mid \boldsymbol{\theta}) + \Delta t \sum_{j\in\boldsymbol{S}} \frac{a_A^{ji}}{1+\Delta t b_A^j}\widehat{P_{n+1}^{\boldsymbol{Z}_k}}(A, j \mid \boldsymbol{\theta}) \tag{16}$$

where

$$a_A^{ji} = \int_A \lambda_j(i, \boldsymbol{x} \mid \boldsymbol{\theta}_K)d\boldsymbol{x}/m_A\,, \forall i \in \boldsymbol{S}, A \in \mathcal{M} \tag{17}$$

is the average transition rate from state j to state i for grid A,

$$b_A^i = \sum_{j \neq i} a_A^{ij}, \forall i \in \boldsymbol{S}, A \in \mathcal{M} \tag{18}$$

is the average transition rate out of state i for grid A,

$$\widehat{P_{n+1}^{\boldsymbol{Z}_k}}(A, i \mid \boldsymbol{\theta}) = \sum_{B \in \mathcal{M}} m_{BA}^i P_n^{\boldsymbol{Z}_k}(B, i \mid \boldsymbol{\theta})/m_A, \ \forall i \in \boldsymbol{S}, A \in \mathcal{M} \tag{19}$$

is the approximate value of probability density function on $\{i\} \times [(n+1)\Delta t, (n+2)\Delta t[\times A$ according to the deterministic evaluation of $\boldsymbol{X}(t)$,

$$m_{BA}^i = \int_{\{\boldsymbol{y} \in B \mid \boldsymbol{g}^i(\boldsymbol{y}, \Delta t \mid \boldsymbol{\theta}_L) \in A\}} d\boldsymbol{y}, \forall i \in \boldsymbol{S}, A, B \in \mathcal{M} \tag{20}$$

is the volume of the part of grid B which will enter grid A after time Δt according to the deterministic evaluation of $\boldsymbol{X}(t)$.

The approximated solution $\rho_t^{\boldsymbol{Z}_k}(\boldsymbol{x}, \cdot \mid \boldsymbol{\theta})d\boldsymbol{x}$ weakly converges towards $p_t^{\boldsymbol{Z}_k}(d\boldsymbol{x}, \cdot \mid \boldsymbol{\theta})$ when $\Delta t \to 0$ and $|\mathcal{M}|/\Delta t \to 0$ where $|\mathcal{M}| = sup_{A \in \mathcal{M}} diam(A)$ [35]. $\mathbb{E}\big(C(T_{miss}, \boldsymbol{H}, \boldsymbol{T} \mid \boldsymbol{\theta}, \boldsymbol{x}_L^*)\big)$, then, can be obtained through eqs. (5)-(8).

4.2. DE approach

DE is a simple and efficient heuristic approach for single-objective global optimization, originally developed by Store and Price [34] for continuous problems. It often shows better performance than alternative optimization algorithms, e.g. genetic algorithms. The procedure of DE is briefly presented as follows:

Step 1: Initialize randomly the population P of $N_c \geq 4$ target individuals over the variables space.

Step 2: Generate the mutant individuals through the following mutation equation:

$$v_{i,G+1} = x_{r1,G} + F \cdot \big(x_{r2,G} - x_{r3,G}\big), \forall i \in \{1,2, \dots, N_c\} \tag{21}$$

where G is the current iteration number, $r_1, r_2, r_3 \in \{1,2, \dots, N_c\}$ are random indices satisfying $r_1 \neq r_2 \neq r_3 \neq i$ and $F \in [0, 2]$, determined by the user, is a constant factor controlling the amplification of $\big(x_{r2,G} - x_{r3,G}\big)$.

Step 3: Generate each trial individual through the following crossover equation:

$$u_{i,G+1}^j = \begin{cases} v_{i,G+1}^j, if \ (rand \leq CR) \ or \ j = irand(D) \\ x_{i,G}^j, if \ (rand > CR) \ and \ j \neq irand(D) \end{cases}, j = 1,2, \dots, D \tag{22}$$

where $u_{i,G+1}^j$, $v_{i,G+1}^j$ and $x_{i,G}^j$ are the j-th parameters of the vectors $u_{i,G+1}$, $v_{i,G+1}$ and $x_{i,G}$, respectively; $rand \in [0, 1]$ is a uniform random number; $CR \in [0, 1]$ is the crossover constant, determined by the user; D is the dimension of the individual vector; $irand(i)$ is a uniform discrete random number in the set $\{1,2, \dots, D\}$.

Step 4: Evaluate the target individual and its trial individual; select the best one as the target individual for the next generation.

Step 5: Go back to step 2, if the termination criterion is not met; otherwise, stop the algorithm.

The maximum iteration number (N_{max}), maximum fitness evaluation number (T_{max}) and minimum fitness error (eps) are typically employed individually or jointly as the termination criterion.

We use two DE algorithms (DE1 and DE2) using the FV scheme for the fitness function evaluation to obtain $\underline{\mathbb{E}\big(C(T_{miss}, \boldsymbol{H}, \boldsymbol{T} \mid [\boldsymbol{\theta}], [\boldsymbol{x}_L^*])\big)}$ and $\overline{\mathbb{E}\big(C(T_{miss}, \boldsymbol{H}, \boldsymbol{T} \mid [\boldsymbol{\theta}], [\boldsymbol{x}_L^*])\big)}$, respectively: DE1 selects the one with smallest value as the target individual for the next generation at step 4 whereas DE2 selects the one with largest value.

4.3. NSDE

For solving the multi-objective problem formulated in eq. (11), the non-dominated sorting mechanisms are incorporated into the single objective DE, similar to the work [33] where the non-dominated sorting mechanisms are combined with a modified binary DE (MBDE). For the details about this approach, please kindly refer to [33].

4.4. Integration of methods

These methods are integrated by using (1) FV scheme for the fitness evaluation in DE and (2) DE for the fitness evaluation in NSDE; the solution methods are integrated, for the first time, for maintenance optimization. The flowchart of the entire optimization methodology that integrates the methods mentioned above is shown in Fig. 3.

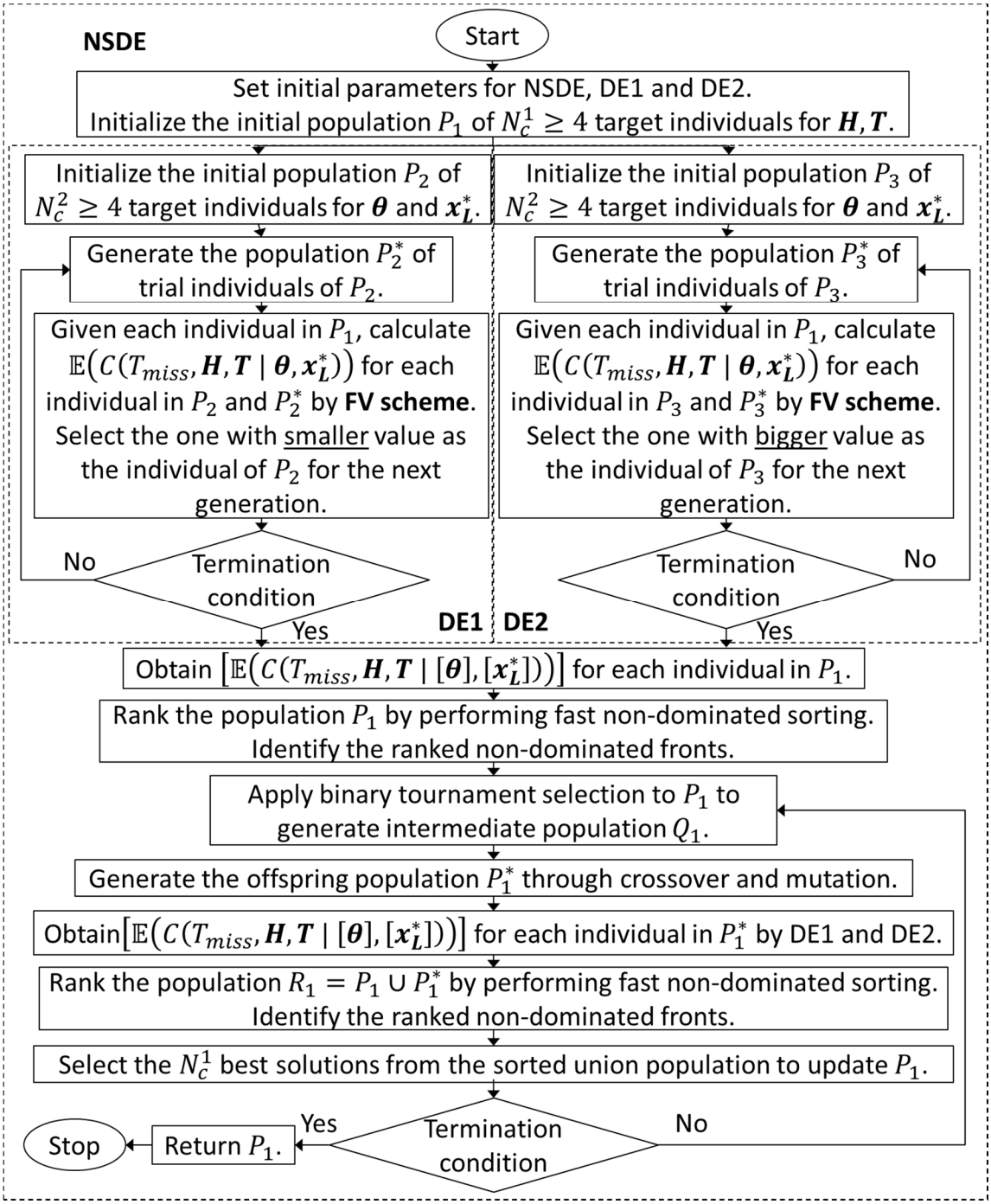

Fig. 3. Flowchart of the proposed optimization methodology.

In Fig. 3, N_c^1 is the size of the population P_1 of NSDE, which contains the target individuals for $\boldsymbol{H}$ and $\boldsymbol{T}$; N_c^2 and N_c^3 are respectively the sizes of population P_2 of DE1 and population P_3 of DE2, which contain the target individuals for $\boldsymbol{\theta}$; $P_i^*, i = 1, 2, 3$ is the population generated from P_i. The method starts with the random generation of N_c^1 individuals (i.e. candidate solutions) of $\boldsymbol{H}$ and $\boldsymbol{T}$ in the initial population P_1 in NSDE. Then, DE1 and DE2 are executed in parallel to calculate $\left[\mathbb{E}\left(C(T_{miss}, \boldsymbol{H}, \boldsymbol{T} \mid [\boldsymbol{\theta}], [\boldsymbol{x}_L^*])\right)\right]$ for each individual in P_1

as follows: (1) randomly generate N_c^2/N_c^3 individuals of $\boldsymbol{\theta}$ and $\boldsymbol{x_L^*}$, as the initial population P_2/P_3 in DE1/DE2; (2) generate the trial populations P_2^*/P_3^* for P_2/P_3 through mutation and crossover; (3) given the individual in P_1, use FV scheme to calculate $\mathbb{E}\left(C\left(T_{miss}, \boldsymbol{H}, \boldsymbol{T} \mid \boldsymbol{\theta}, \boldsymbol{x_L^*}\right)\right)$ for the paired individuals in P_2 and P_2^*/(P_3 and P_3^*), and select the one with smaller/bigger value as the individual of P_2/P_3 for the next generation; (4) go back to step (2), if the termination criterion is not met; otherwise, $\left[\mathbb{E}\left(C(T_{miss}, \boldsymbol{H}, \boldsymbol{T} \mid [\boldsymbol{\theta}], [\boldsymbol{x_L^*}])\right)\right]$ is obtained for each individual in P_1. Afterwards, the method returns to NSDE: (5) rank population P_1 by performing fast non-dominated sorting on $\left[\mathbb{E}\left(C(T_{miss}, \boldsymbol{H}, \boldsymbol{T} \mid [\boldsymbol{\theta}], [\boldsymbol{x_L^*}])\right)\right]$ and the ranked non-dominated fronts are, then, identified; (6) select the offspring population P_1^* based on the intermediate population Q_1, generated by crossover and mutation; (7) use DE1 and DE2 to obtain $\left[\mathbb{E}\left(C(T_{miss}, \boldsymbol{H}, \boldsymbol{T} \mid [\boldsymbol{\theta}], [\boldsymbol{x_L^*}])\right)\right]$ for each individual in P_1^*; (8) identify the ranked non-dominated fronts by performing fast non-dominated sorting on the population union $R_1 = P_1 \cup P_1^*$; (9) select the best N_c^1 solutions from the sorted union as the updated P_1; (10) go back to the step (6), if the termination criterion is not met; otherwise, the Pareto optimal maintenance policies are obtained.

5. ILLUSTRATIVE CASE

The illustrative case refers to one subsystem consisting of a centrifugal pump and a pneumatic valve in series, which is part of the residual heat removal system (RHRS) of a nuclear power plant. Given the series configuration, the subsystem is failed when one of the two components is failed. A degradation dependency between the two components has been considered upon discussion with experts of Électricité de France (EDF): the degradation of the pump will cause it to vibrate [47] which, in turn, will lead the valve to vibrate and therefore aggravate the degradation processes of the latter [48]. For confidentiality, the values of the model parameters and the costs of the maintenance policy presented below are altered so as to render them fictitious.

5.1. Centrifugal pump

The pump has one degradation process, related to the external leakage, which is modeled by a MSM modified from the one originally supplied by EDF. It is a continuous-time homogeneous Markov chain with constant transition rates as shown in Fig 4.

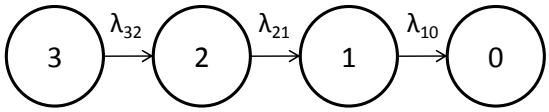

Fig. 4. Degradation process of the pump.

Let $Y_p(t)$ denote the degradation state of the pump at time t and $S_p = \{'0', '1', '2', '3'\}$ denote the degradation states set of the pump, where '3' is the perfect functioning state and '0' is the complete failure state. The pump is functioning until it reaches the state '0'. The pump can vibrate when it reaches the degradation states '2' and '1' due to degradation. The intensity of the vibration of the state '2' is assigned as 'smooth' and that of the state '1' is assigned as

'rough' by the experts. The parameters λ_{32}, λ_{21} and λ_{10} are the transition rates of the model of the degradation process.

5.2. Pneumatic valve

The pneumatic valve is a normally-closed, gas-actuated valve with a linear cylinder actuator. Its simplified scheme is shown in Fig 5.

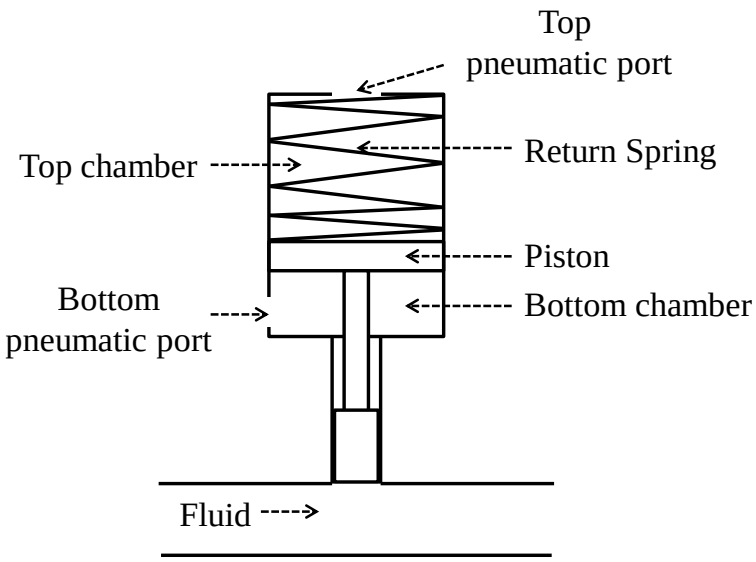

Fig. 5. Simplified scheme of the pneumatic valve [23].

By regulating the pressure of the pneumatic ports to fill or evacuate the top and bottom chambers, the position of the piston can be controlled. A return spring is linked with the piston to ensure the closure of the valve, when pressure is lost. The external leak at the actuator connections to the bottom pneumatic port due to corrosion and other environmental factors is chosen as the degradation mechanism of the valve, which is much more significant than the other degradation mechanisms according to the results shown in [23].

Let $D_b(t)$ denote the area of the leak hole at the bottom pneumatic port at time t, the development of the leak size is described by:

$$\dot{D_b}(t) = \omega_b(1 + \beta_{Y_p(t)}) \tag{23}$$

where ω_b is the original wear coefficient and where $\beta_{Y_p(t)}$ is the relative increment of the developing rate of the external leak at the bottom pneumatic port caused by the vibration of the pump at degradation state '2' or '1'.

The leak will lead the valve to be more difficult to open but easier to close. The threshold of the area of leak hole D_b^* is defined as the value above which ($D_b(t) > D_b^*$) the valve cannot reach the fully open position within the 15s time limit from the fully closed position, after an opening command is executed.

5.3. PDMP for the system under uncertainty

The degradation of the valve $\boldsymbol{L} = \{L_1\}$ is described by PBM and the degradation of the pump $\boldsymbol{K} = \{K_1\}$ is described by MSM. The degradation processes of the whole system are modeled by PDMP as follows:

$$\boldsymbol{Z}(t) = \begin{pmatrix} D_b(t) \\ Y_p(t) \end{pmatrix} \in \mathbb{R}^+ \times S_p \tag{24}$$

The space of the failure states of $\vec{Z}(t)$ is $\boldsymbol{\mathcal{F}} = [0, +\infty) \times \{\text{'0'}\} \cup [D_b^*, +\infty) \times \{\text{'1'}, \text{'2'}, \text{'3'}\}$. $\boldsymbol{\theta_L} = \{\omega_b\} \times \{\beta_2\} \times \{\beta_1\}, \boldsymbol{\theta_K} = \{\lambda_{32}\} \times \{\lambda_{21}\} \times \{\lambda_{10}\}$ and $\boldsymbol{x_L^*} = \{D_b^*\}$ are the uncertain parameters. As an example, a relative uncertainty of $\pm$10% of the original parameters values has been considered to assign their interval values. Their interval values are shown in Table I, under accelerated aging conditions.

Table I The interval values of the uncertain parameters in PDMP

Parameter	Interval value
ω_b	$[\omega_b] =$ [9e-9, 1.1e-8] m^2/s
β_2	$[\beta_2] =$ [9%, 11%]
β_1	$[\beta_1] =$ [18%, 22%]
λ_{32}	$[\lambda_{32}] =$ [2.7e-3, 3.3e-3] s-1
λ_{21}	$[\lambda_{21}] =$ [2.7e-3, 3.3e-3] s-1
λ_{10}	$[\lambda_{10}] =$ [2.7e-3, 3.3e-3] s-1
D_b^*	$[D_b^*] =$ [9.54e-6, 1.166e-5] m^2

The initial state of the system is assumed as follows:

$$\boldsymbol{Z}_0 = \begin{pmatrix} D_b(0) \\ Y_p(0) \end{pmatrix} = \begin{pmatrix} 0 \\ 3 \end{pmatrix} \tag{25}$$

which means that the two components are both in their perfect state. The initial probability distribution of the processes $(D_b(t), Y_p(t))_{t\geq 0}$, $p_0(d\boldsymbol{z} \mid \boldsymbol{\theta})$, hence, equals to $\delta_{\boldsymbol{Z}_0}(d\boldsymbol{z})$, where δ is the Dirac delta function.

5.4. Maintenance optimization

The problem of maintenance optimization under uncertainty on the horizon of the mission time T_{miss} can, then, be formulated as:

$$\text{Min } \underline{\mathbb{E}\big(C(T_{miss}, \boldsymbol{H}, \boldsymbol{T} \mid [\boldsymbol{\theta}], [\boldsymbol{x_L^*}])\big)}$$

$$\text{Min } \overline{\mathbb{E}\big(C(T_{miss}, \boldsymbol{H}, \boldsymbol{T} \mid [\boldsymbol{\theta}], [\boldsymbol{x_L^*}])\big)}$$

$$\text{Subject to } H_{L_1} \subseteq]0, \overline{D_b^*}[$$

$$\boldsymbol{H}_{K_1} \subseteq \{\text{'0'}, \text{'1'}, \text{'2'}, \text{'3'}\}$$
$$0 \leq T_i \leq T_{miss},\ \forall\, i \in \{L_1, K_1\} \tag{26}$$

The related costs affecting the maintenance policy are shown in Table II.

Table II The related costs of the maintenance policy

Task	Cost (k€)
Inspection of pump	2
PM of pump	5
CM of pump	10
Inspection of valve	2
PM of valve	5
CM of valve	10
Penalty	1000

6. RESULTS

At first, the proposed method has been run 150 generations to obtain the Pareto optimal maintenance policies, with the following parameter values: N_c^1 is set to 20; N_c^2 and N_c^3 are set to 10; T_{miss} is set to $1000\,s$ following the accelerated aging condition explained in our previous work [26]; CR is set to 0.7 for DE1 and DE2, and is set to 0.8 for NSDE; F is set to 0.5 for DE1 and DE2, and is set to 1 for NSDE. The values of N_c^1, N_c^2 and N_c^3 are chosen with respect to the computational complexity of the FV scheme and the limited computational resources. The parameters of DE1 and DE2 are determined after trials on different values. The parameters of NSDE are chosen similarly, except that the fitness functions (i.e. DE1 and DE2) are replaced by the computationally much cheaper surrogates $\mathbb{E}\left(C\left(T_{miss}, \boldsymbol{H}, \boldsymbol{T} \mid \overline{\boldsymbol{\theta}}, \underline{\boldsymbol{x}_L^*}\right)\right)$ and $\mathbb{E}\left(C\left(T_{miss}, \boldsymbol{H}, \boldsymbol{T} \mid \underline{\boldsymbol{\theta}}, \overline{\boldsymbol{x}_L^*}\right)\right)$, respectively. The reasons of using such surrogates are: 1) the system degradation speed reaches the maximum by taking $\overline{\boldsymbol{\theta}}, \underline{\boldsymbol{x}_L^*}$ and the minimum by taking $\underline{\boldsymbol{\theta}}, \overline{\boldsymbol{x}_L^*}$; 2) DE1 and DE2 are relatively time consuming.

All the experiments have been carried out by running the MATLAB algorithm on a PC with an Intel Core 2 Duo CPU at 1.97 GHz and a RAM of 1.95 GB. The average computation time for one generation of NSDE is about 3.23 hrs. The obtained Pareto front in the plane of the two objective functions, i.e. lower and upper bounds of the maintenance cost, is shown in Fig. 6.

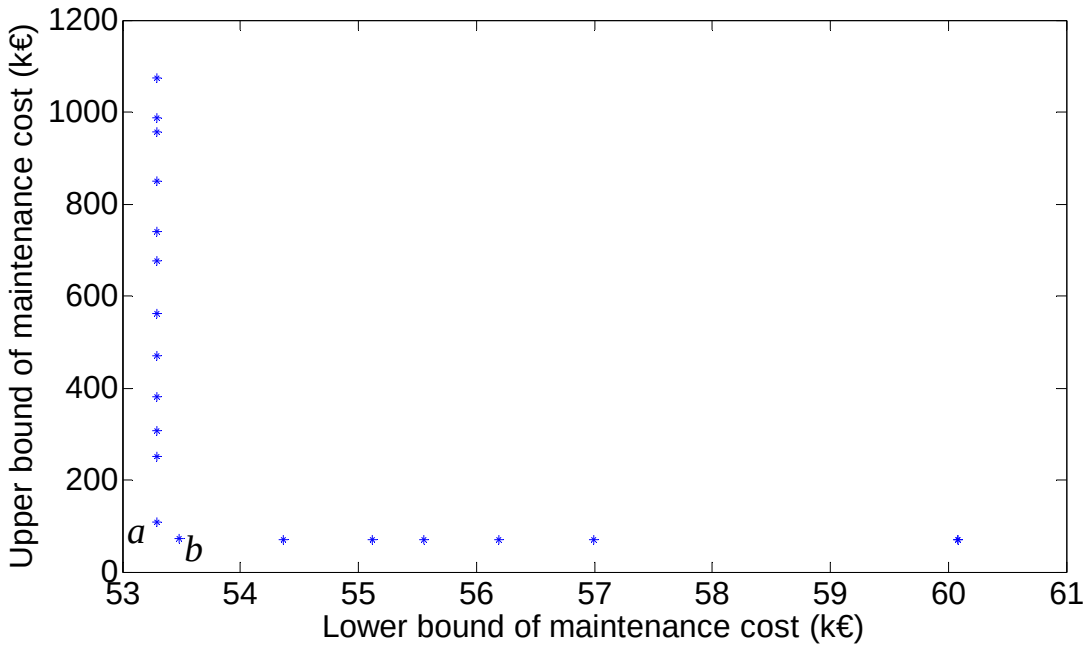

Fig. 6. The obtained Pareto front.

It is observed that the upper bounds cover a wide range whereas the lower bounds show much less variability. The solutions above a = (53.30, 108.45) k€ have big increments with respect to the upper bound, but they have nearly no difference in the lower bound compared with those of a. The solutions to the right of b = (53.49, 72.75) k€ show nearly no difference in the upper bound value, compared with that of b. The small differences between lower bounds are due to the fact that the failure of the components or of the system rarely occurs under these situations, so that the total cost is mainly composed of the PM costs and the inspections costs; on the contrary, the big differences between upper bounds are mainly due to the failures of components, which lead to the system failure and, thus, carry a high penalty cost. It also implies the fact that if the frequencies of inspections and PM exceed some value, then, the high penalty cost may be largely avoided. In practice, the solutions with very high upper bounds might not be appropriate for decision makers (DMs).

In case that the DMs intend to conduct a search within a certain budget, the method proposed is also capable of dealing with this situation. For instance, we can focus on the solutions within the region $[0, 100]$ k€ $\times$ $[0, 100]$ k€. The proposed method is run with the previous configurations plus a penalty of 100 k€ to be added to one objective of a solution, whenever the other objective exceeds 100 k€. The newly obtained Pareto front is shown in Fig. 7.

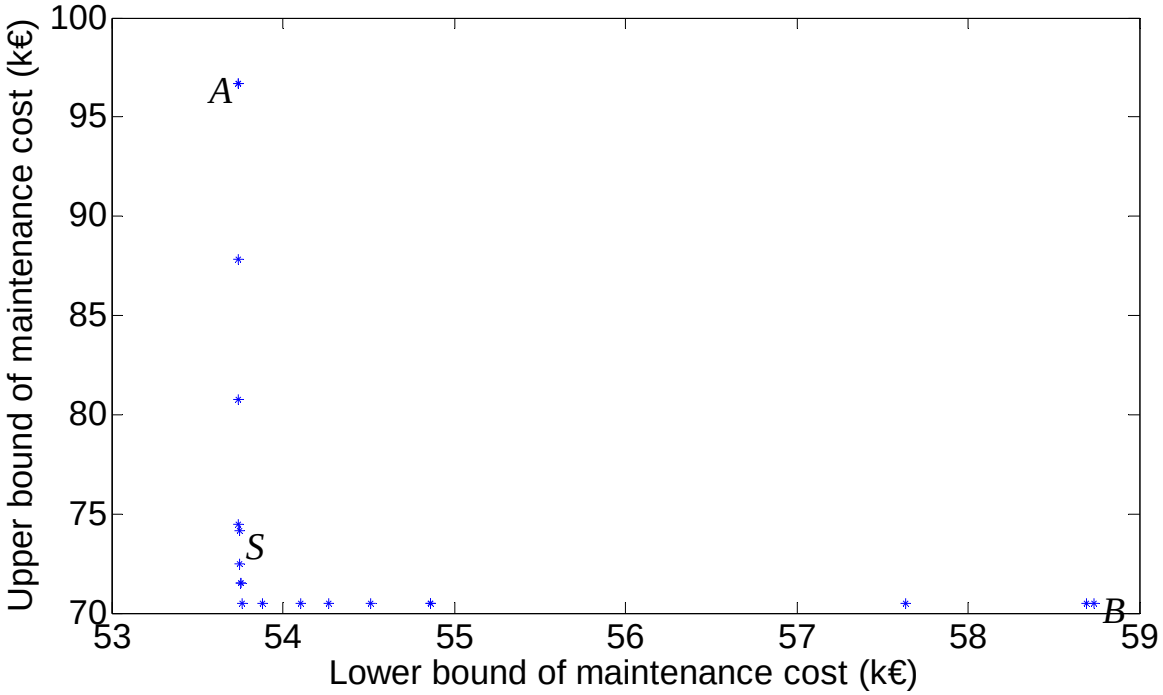

Fig. 7. The Pareto front obtained within the region $[0, 100]$ k€ $\times$ $[0, 100]$ k€.

Given the Pareto front, the DMs need eventually choose the maintenance policy according to their preferences since the solutions do not dominate each other. To simulate those common preferences of the DMs, we choose three solutions: *S*, the solution selected by the 'Min-Max' method, which selects the representative center of the Pareto front, and is among the most used ones [49]; *A* (corresponding to a selection by decision makers who are optimistic and pay more attention to the lower bound of the cost objective factor) and *B* (corresponding to a selection by decision makers who are conservative and pay more attention to the upper bound of the cost objective factor), the solutions with the minimum lower bound and minimum upper bound values, respectively. Solutions *A*, *B* and *S* represent three different preferences of the DMs. Detailed information on *S*, *A* and *B* is reported in Table III.

Table III Solutions *S*, *A* and *B*

Solution	*S*	*A*	*B*
Lower bound	53.74 k€	53.73 k€	58.69 k€
Upper bound	74.17 k€	96.69 k€	70.46 k€
T_{L_1}	773.47 s	808.55 s	563.00 s
T_{K_1}	66.77 s	66.77 s	66.77 s
H_{L_1}	[7.28 e-6, D_b^*) m^2	[7.66 e-6, D_b^*) m^2	[4.91 e-6, D_b^*) m^2
H_{K_1}	{'1', '2'}	{'1', '2'}	{'1', '2'}

The comparisons of the three solutions are done based on the illustrations in Fig. 8. It can be observed that *S* and *A* have nearly the same lower bound value, whereas *A* has a much higher upper bound. For the DMs, *S* might be more appropriate than *A* if the small difference 0.01 can be considered negligible. *S* and *A* both contain *B*: the DMs may choose *B* as the result of minimax robust optimization, whereas if they pay more attention to the lower bound, *A* can be the choice.

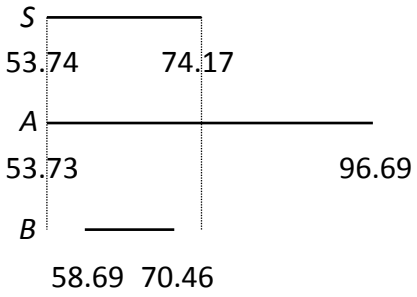

Fig. 8. The three selected solutions.

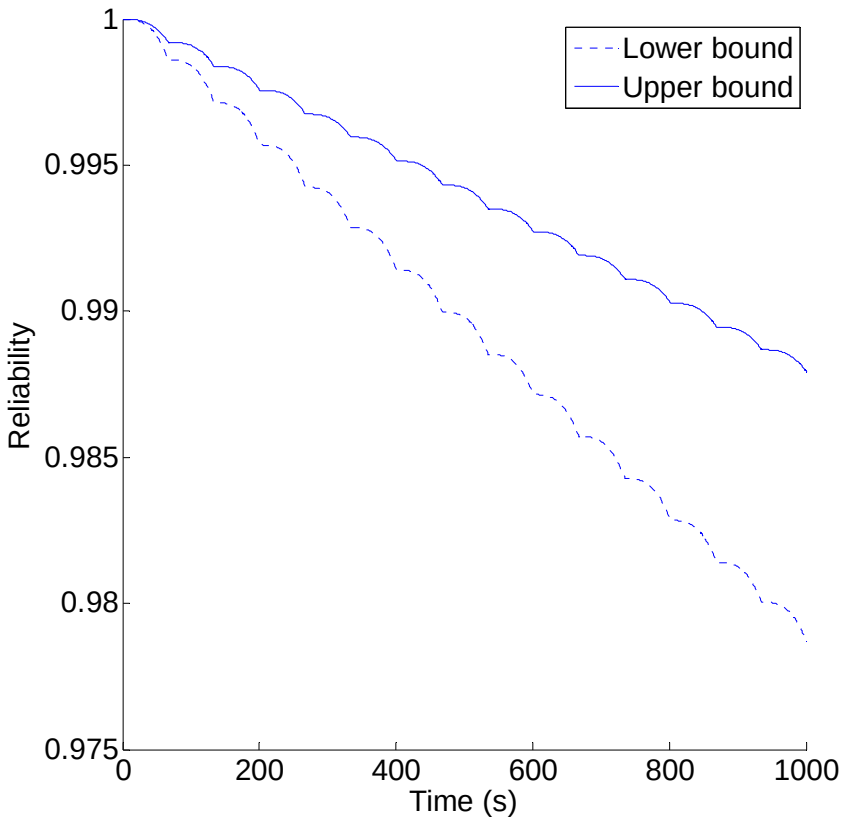

Fig. 9. The system reliability under the maintenace policy *S*.

Since the valve is highly reliable, the system reliability is basically determined by the pump reliability. The failures of the system are mitigated at each execution of the preventive maintenance.

To illustrate the convergence of the proposed method, the hypervolume indicator [50] with a point of reference defined as $(100, 100)$ and the generational distance [51] between the best Pareto fronts obtained at two consecutive generations, are used. Fig. 10 shows their trajectories during the evolution of NSDE without penalty. Fig. 11 shows the trajectories of NSDE with penalty. It is seen that NSDE generally converges after about 60 generations in both cases.

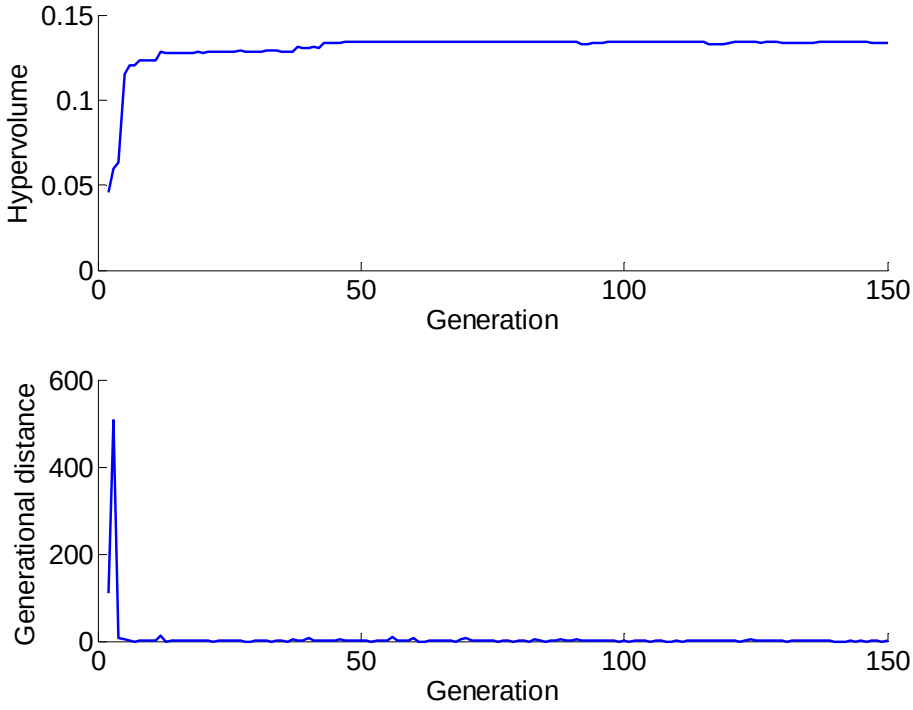

Fig. 10. The convergence plots for NSDE without penalty.

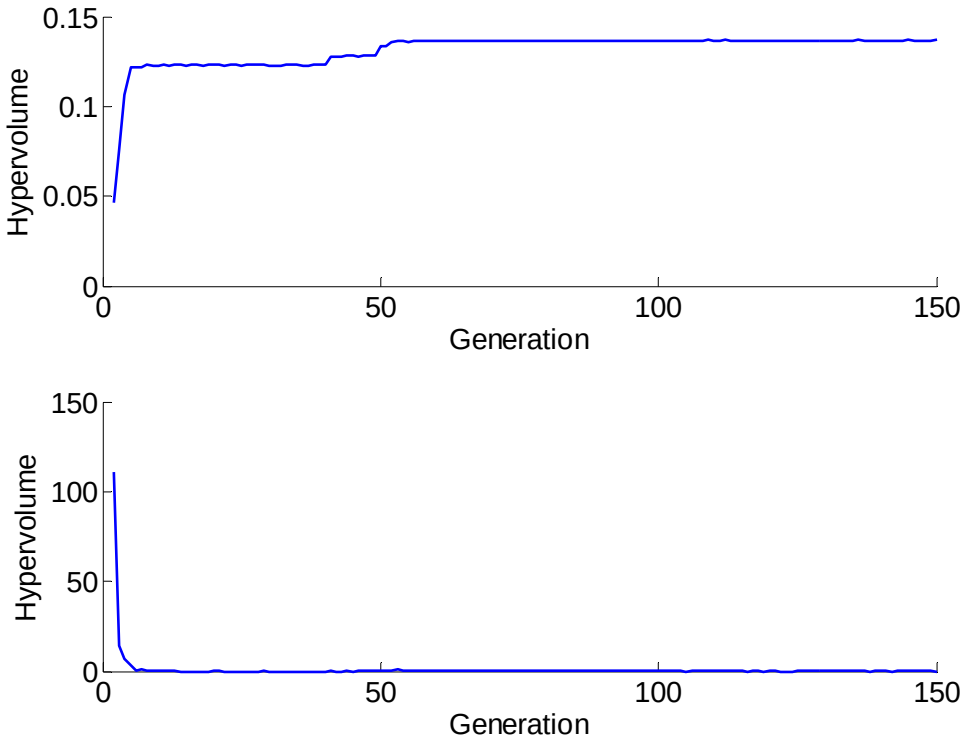

Fig. 11. The convergence plots for NSDE with penalty.

7. CONCLUSIONS AND FUTURE WORKS

In this work, we have considered the problem of maintenance modeling and optimization of multi-component systems, with degradation dependency and epistemic uncertainty. The component degradation processes, the condition-based PM and the CM are described through a PDMP modeling approach. Intervals are used to represent the uncertain parameters. Both the pre-scheduled periods for inspection tasks and the thresholds for PM are regarded as the decision variables in the maintenance optimization problem. Optimization is formulated in a multi-objective scheme aiming at minimizing the lower and upper bounds of the interval-valued maintenance cost. To derive the optimal maintenance policy, a solution method is proposed combing FV scheme, DE approach and NSDE approach. Results on a realistic case study show the feasibility of the procedure.

The main contribution of the paper is that it generalizes the existing maintenance models for multi-component systems by taking into account both degradation dependency among the components and epistemic uncertainty in the degradation models. As the future work, we plan to extend the proposed framework taking into account the economic and structural dependences between different components.

Limitations of the proposed solution approach lies in the computational burden and the memory requirements, when applied in high dimensional problems, due to the FV method which discretizes the state space of the continuous variables of PDMP. The computational expenses and memory requirement of the FV method increase almost linearly as the number of

meshes partitioning the state space increases, which is chosen by the users. For higher dimensional problems, we can limit the number of meshes to relieve computational burden. Note that in some cases the high dimensional problem can be decomposed into several low dimensional ones mutually independent on each other. Then, the FV schemes can be run on low dimensional problems in parallel. Besides, the computation time can be reduced via reducing the number of meshes set in FV schemes and the amount of memory required can be reduced via using sparse matrices. Improvement of these issues will be sought in future research.

Acknowledgement

The authors would like to thank Mrs. Dominique VASSEUR, Mr. Antoine DESPUJOLS and Mr. Emmanuel ARDILLON from the Department of Industrial Risk Management (MRI), Electricité de France R&D for their insightful comments. The work was supported by Electricité de France Contract No.8610-5910112096.

References

[1] G. Susto, A. Schirru, S. Pampuri, S. McLoone, and A. Beghi, "Machine Learning for Predictive Maintenance: a Multiple Classifiers Approach," *Industrial Informatics, IEEE Transactions on,* 2015.

[2] R. P. Nicolai and R. Dekker, *Optimal maintenance of multi-component systems: a review*: Springer, 2008.

[3] L. Thomas, "A survey of maintenance and replacement models for maintainability and reliability of multi-item systems," *Reliability Engineering,* vol. 16, pp. 297-309, 1986.

[4] B. Castanier, A. Grall, and C. Bérenguer, "A condition-based maintenance policy with non-periodic inspections for a two-unit series system," *Reliability Engineering & System Safety,* vol. 87, pp. 109-120, 2005.

[5] G. van Dijkhuizen, "Maintenance grouping in multi-step multi-component production systems," in *Maintenance, Modeling and Optimization*: Springer, 2000, pp. 283-306.

[6] R. Dekker, R. P. PLASMEIJER, and J. H. SWART, "Evaluation of a new maintenance concept for the preservation of highways," *IMA Journal of Management Mathematics,* vol. 9, pp. 109-156, 1998.

[7] N. Rasmekomen and A. K. Parlikad, "Maintenance Optimization for Asset Systems With Dependent Performance Degradation," *Reliability, IEEE Transactions on,* vol. 62, pp. 362-367, 2013.

[8] D. Murthy and D. Nguyen, "Study of a multi-component system with failure interaction," *European Journal of Operational Research,* vol. 21, pp. 330-338, 1985.

[9] M.-T. Lai and Y.-C. Chen, "Optimal periodic replacement policy for a two-unit system with failure rate interaction," *The international journal of advanced manufacturing technology,* vol. 29, pp. 367-371, 2006.

[10] R. I. Zequeira and C. Bérenguer, "On the inspection policy of a two-component parallel system with failure interaction," *Reliability Engineering & System Safety,* vol. 88, pp. 99-107, 2005.

[11] A. Barros, C. Berenguer, and A. Grall, "A maintenance policy for two-unit parallel systems based on imperfect monitoring information," *Reliability Engineering & System Safety,* vol. 91, pp. 131-136, 2006.

[12] M. Daigle and K. Goebel, "Multiple damage progression paths in model-based prognostics," in *Aerospace Conference, 2011 IEEE*, 2011, pp. 1-10.

[13] L. Jiang, Q. Feng, and D. W. Coit, "Reliability and maintenance modeling for dependent competing failure processes with shifting failure thresholds," *Reliability, IEEE Transactions on,* vol. 61, pp. 932-948, 2012.

[14] H. Peng, Q. Feng, and D. W. Coit, "Reliability and maintenance modeling for systems subject to multiple dependent competing failure processes," *IIE transactions,* vol. 43, pp. 12-22, 2010.

[15] S. Özekici, "Optimal periodic replacement of multicomponent reliability systems," *Operations Research,*

vol. 36, pp. 542-552, 1988.

[16] Q. Yang, N. Zhang, and Y. Hong, "Reliability analysis of repairable systems with dependent component failures under partially perfect repair," *Reliability, IEEE Transactions on,* vol. 62, pp. 490-498, 2013.

[17] H. Hong, W. Zhou, S. Zhang, and W. Ye, "Optimal condition-based maintenance decisions for systems with dependent stochastic degradation of components," *Reliability Engineering & System Safety,* vol. 121, pp. 276-288, 2014.

[18] A. Van Horenbeek and L. Pintelon, "A dynamic predictive maintenance policy for complex multi-component systems," *Reliability Engineering & System Safety,* vol. 120, pp. 39-50, 2013.

[19] S. Song, D. W. Coit, Q. Feng, and H. Peng, "Reliability analysis for multi-component systems subject to multiple dependent competing failure processes," *Reliability, IEEE Transactions on,* vol. 63, pp. 331-345, 2014.

[20] N. Gebraeel, A. Elwany, and J. Pan, "Residual life predictions in the absence of prior degradation knowledge," *Reliability, IEEE Transactions on,* vol. 58, pp. 106-117, 2009.

[21] J. Lawless and M. Crowder, "Covariates and random effects in a gamma process model with application to degradation and failure," *Lifetime Data Analysis,* vol. 10, pp. 213-227, 2004.

[22] M. J. Zuo, B. Liu, and D. Murthy, "Replacement–repair policy for multi-state deteriorating products under warranty," *European Journal of Operational Research,* vol. 123, pp. 519-530, 2000.

[23] M. Daigle and K. Goebel, "A model-based prognostics approach applied to pneumatic valves," *International journal of prognostics and health management,* vol. 2, p. 008, 2011.

[24] S. Reggiani, S. Poli, M. Denison, E. Gnani, A. Gnudi, G. Baccarani, S. Pendharkar, and R. Wise, "Physics-Based Analytical Model for HCS Degradation in STI-LDMOS Transistors," *Electron Devices, IEEE Transactions on,* vol. 58, pp. 3072-3080, 2011.

[25] M. Giorgio, M. Guida, and G. Pulcini, "An age-and state-dependent Markov model for degradation processes," *IIE Transactions,* vol. 43, pp. 621-632, 2011.

[26] Y.-H. Lin, Y. Li, and E. Zio, "Dynamic Reliability Models for Multiple Dependent Competing Degradation Processes," in *ESREL 2014*.

[27] M. Bazu, "A combined fuzzy-logic and physics-of-failure approach to reliability prediction," *Reliability, IEEE Transactions on,* vol. 44, pp. 237-242, 1995.

[28] P.-T. Chang, "Fuzzy strategic replacement analysis," *European Journal of Operational Research,* vol. 160, pp. 532-559, 2005.

[29] D. Singer, "A fuzzy set approach to fault tree and reliability analysis," *Fuzzy sets and systems,* vol. 34, pp. 145-155, 1990.

[30] O. Linda and M. Manic, "Uncertainty-robust design of interval type-2 fuzzy logic controller for delta parallel robot," *Industrial Informatics, IEEE Transactions on,* vol. 7, pp. 661-670, 2011.

[31] Z. Chaoyue, W. Jianhui, J. P. Watson, and G. Yongpei, "Multi-Stage Robust Unit Commitment Considering Wind and Demand Response Uncertainties," *Power Systems, IEEE Transactions on,* vol. 28, pp. 2708-2717, 2013.

[32] H. Ishibuchi and H. Tanaka, "Multiobjective programming in optimization of the interval objective function," *European Journal of Operational Research,* vol. 48, pp. 219-225, 1990.

[33] Y.-F. Li, G. Sansavini, and E. Zio, "Non-dominated sorting binary differential evolution for the multi-objective optimization of cascading failures protection in complex networks," *Reliability Engineering & System Safety,* vol. 111, pp. 195-205, 2013.

[34] R. Storn and K. Price, "Differential evolution–a simple and efficient heuristic for global optimization over continuous spaces," *Journal of global optimization,* vol. 11, pp. 341-359, 1997.

[35] C. Cocozza-Thivent, R. Eymard, and S. Mercier, "A finite-volume scheme for dynamic reliability models," *IMA journal of numerical analysis,* vol. 26, pp. 446-471, 2006.

[36] R. Coudray and J. Mattei, "System reliability: An example of nuclear reactor system analysis," *Reliability Engineering,* vol. 7, pp. 89-121, 1984.

[37] Y.-H. Lin, Y.-F. Li, and E. Zio, "Fuzzy Reliability Assessment of Systems with Multiple Dependent Competing Degradation Processes," *Fuzzy Systems, IEEE Transactions on,* 2014.

[38] A. Lorton, M. Fouladirad, and A. Grall, "A methodology for probabilistic model-based prognosis," *European Journal of Operational Research,* vol. 225, pp. 443-454, 2013.

[39] D. Zwillinger, *Handbook of differential equations*: Gulf Professional Publishing, 1998.

[40] C. Cocozza-Thivent, "Processus de renouvellement markovien, Processus de Markov déterministes par morceaux," *Online book available on the webpage: http://perso-math. univ-mlv. fr/users/cocozza.*

christiane/recherche-pageperso/PresentationRMetPDMP. html, 2011.

[41] W.-S. Lee, D. L. Grosh, F. A. Tillman, and C. H. Lie, "Fault Tree Analysis, Methods, and Applications ß A Review," *Reliability, IEEE Transactions on,* vol. 34, pp. 194-203, 1985.

[42] H. R. Golmakani, "Optimal age-based inspection scheme for condition-based maintenance using A* search algorithm," *International Journal of Production Research,* vol. 50, pp. 7068-7080, 2012.

[43] A. Usynin, J. W. Hines, and A. Urmanov, "Uncertain failure thresholds in cumulative damage models," in *Reliability and Maintainability Symposium, 2008. RAMS 2008. Annual*, 2008, pp. 334-340.

[44] Y. Liu, H.-Z. Huang, and G. Levitin, "Reliability and performance assessment for fuzzy multi-state elements," *Proceedings of the Institution of Mechanical Engineers, Part O: Journal of Risk and Reliability,* vol. 222, pp. 675-686, 2008.

[45] Y.-F. Li, E. Zio, and Y.-H. Lin, "A Multistate Physics Model of Component Degradation Based on Stochastic Petri Nets and Simulation," *Reliability, IEEE Transactions on,* vol. 61, pp. 921-931, 2012.

[46] D. Bertsimas and M. Sim, "The price of robustness," *Operations research,* vol. 52, pp. 35-53, 2004.

[47] S. Zhang, M. Hodkiewicz, L. Ma, and J. Mathew, "Machinery condition prognosis using multivariate analysis," in *Engineering asset management*: Springer, 2006, pp. 847-854.

[48] P. Moussou, S. Cambier, D. Lachene, S. Longarini, L. Paulhiac, and V. Villouvier, "Vibration investigation of a French PWR power plant piping system caused by cavitating butterfly valves," *ASME-PUBLICATIONS-PVP,* vol. 420, pp. 99-106, 2001.

[49] A. D. Belegundu and T. R. Chandrupatla, *Optimization concepts and applications in engineering*: Cambridge University Press, 2011.

[50] E. Zitzler, L. Thiele, M. Laumanns, C. M. Fonseca, and V. G. Da Fonseca, "Performance assessment of multiobjective optimizers: An analysis and review," *Evolutionary Computation, IEEE Transactions on,* vol. 7, pp. 117-132, 2003.

[51] D. A. Van Veldhuizen and G. B. Lamont, "On measuring multiobjective evolutionary algorithm performance," in *Evolutionary Computation, 2000. Proceedings of the 2000 Congress on*, 2000, pp. 204-211.

PAPER V: Y.-H. Lin, Y.-F. Li, E. Zio. A Framework for Modeling and Optimizing Maintenance in Systems Modeled by Piecewise-Deterministic Markov Processes Considering Epistemic Uncertainty. Reliability, IEEE Transactions on. (Under review)

PAPER VI: Y.-H. Lin, Y.-F. Li, E. Zio. Reliability Assessment of Systems Subject to Dependent Degradation Processes and Random Shock. *IIE Transactions*. (Under review)

Reliability Assessment of Systems Subject to Dependent Degradation Processes and Random Shocks

Abstract – System failures can be induced by internal degradation mechanisms or by external causes. In this paper, we consider the reliability of systems experiencing both degradation and random shock processes. The dependencies between degradation processes and random shocks, and among degradation processes are explicitly modelled. The degradation processes of system components are modeled by multi-state models (MSMs) and physics-based models (PBMs). The piecewise-deterministic Markov process modeling framework is employed to combine MSMs and PBMs, and for incorporating degradation and random shocks dependencies. The Monte Carlo simulation and finite-volume methods are used to compute the system reliability. A subsystem of a residual heat removal system in a nuclear power plant is considered as illustrative case.

Key Words – multi-state system, system reliability assessment, degradation, random shocks, dependency, piecewise-deterministic Markov process, Monte Carlo simulation, residual heat removal system.

Acronyms

PBMs	Physics-based models
MSMs	Multi-state models
PDMP	Piecewise-deterministic Markov process
MCS	Monte Carlo simulation
FV	Finite-volume
RHRS	Residual heat removal system

Notations

$\boldsymbol{K}$	Group of degradation processes modeled by MSMs
$\boldsymbol{L}$	Group of degradation processes modeled by PBMs
$\boldsymbol{S}_{K_n}$	Finite state set of degradation process K_n
$Y_{K_n}(t)$	State variable of degradation process K_n
$\lambda_i(j \mid \boldsymbol{\theta}_{K_n})$	Transition rate from state i to j
$\boldsymbol{\mathcal{F}}_{K_n}$	Set of failure states of degradation process K_n

$\boldsymbol{X}_{L_m}(t)$	Time-dependent continuous variables of degradation process L_m
$\boldsymbol{X}_{L_m}^{\boldsymbol{D}}(t)$	Non-decreasing degradation variables vector
$\boldsymbol{X}_{L_m}^{\boldsymbol{P}}(t)$	Physical variables vector
$\boldsymbol{\mathcal{F}}_{L_m}$	Set of failure states of degradation process L_m
$N(t)$	Number of random shocks occurred until time t
μ	Arrival rate of random shock process
$Y'_{K_n}(t)$	Degradation level of K_n considering random shocks
$\boldsymbol{\mathcal{F}}'_{K_n}$	Set of failure states of $Y'_{K_n}(t)$
W_i	Shock load of the i-th shock
D	Maximal material strength
$\boldsymbol{H}_i$	Instantaneous random increase caused by the i-th cumulative shock
$N^c(t)$	Number of cumulative shocks occurred until time t
$\boldsymbol{D}_{L_m}$	Degradation level of L_m considering random shocks
$\boldsymbol{Y}(t)$	Degradation state of the processes of set $\boldsymbol{K}$
$\boldsymbol{X}(t)$	Degradation state of the processes of set $\boldsymbol{L}$
$\boldsymbol{\theta}_{\boldsymbol{K}}$	Environmental and operational factors in $\boldsymbol{K}$
$\boldsymbol{\theta}_{\boldsymbol{L}}$	Environmental and operational factors in $\boldsymbol{L}$
$\boldsymbol{Z}(t)$	Degradation process of the system
$\boldsymbol{Y}'(t)$	Degradation state of the processes of set $\boldsymbol{K}$ considering random shocks
$\boldsymbol{X}'(t)$	Degradation state of the processes of set $\boldsymbol{L}$ considering random shocks
T_k	k-th jump time in $\boldsymbol{Y}'(t)$
$\boldsymbol{Z}_k = (\boldsymbol{X}'_k, \boldsymbol{Y}'_k)$	State of $\boldsymbol{Z}(t), \boldsymbol{X}'(t), \boldsymbol{Y}'(t)$ after k-th jump of $\boldsymbol{Y}'(t)$
$\boldsymbol{f}_{\boldsymbol{L}}^{\boldsymbol{Y}'(t)}(\boldsymbol{X}(t) \mid \boldsymbol{\theta}_{\boldsymbol{L}})$	Deterministic physics equations of $\boldsymbol{X}(t)$
$\lambda_{\boldsymbol{y}_i,\boldsymbol{y}_j}(\boldsymbol{x} \mid \boldsymbol{\theta}_{\boldsymbol{K}})$	Transition rate of $\boldsymbol{Y}'(t)$ from state $\boldsymbol{y}_i$ to $\boldsymbol{y}_j$
$N(\boldsymbol{i}, (d\boldsymbol{x}, \boldsymbol{y}_j), dt)$	Semi-Markov kernel of $\{\boldsymbol{Z}_n, T_n\}_{n\geq 0}$
$dF_{\boldsymbol{i}}(t)$	Probability distribution of holding time given $\boldsymbol{Z}_k = \boldsymbol{i}$

1. INTRODUCTION

System failures can be induced by internal degradation mechanisms (e.g. wear, fatigue and erosion) or by external causes (e.g. thermal and mechanical shocks) [1]. The interactions between these factors need to be considered under certain circumstances, e.g. when degradation processes and random shocks are *s*-dependent (e.g. single-event overloads with safe shock magnitudes can influence the fatigue crack growth of stents by causing instantaneous increase on the crack propagation [2]), or the degradation state of some components in one system can influence the degradation dynamics or the remaining useful life of the others (e.g. the degradation of the pre-filtration stations leading to a lower performance level of the sand filter in a water treatment plant [3]). Neglecting these aspects may result in overestimation of system reliability [4]. The evaluation of the system reliability over time can be an important and critical task. For example, the reliabilities of safety systems in nuclear power plants, such as reactor shutdown, emergency core cooling and other safety multi-component systems in nuclear industry, need to meet the requirements imposed by regulator to ensure their operational safety [5]. The instants when the requirements are not satisfied can be identified according to the reliability evaluation over time. Afterwards, the reliability improvement actions can be performed, such as maintenance, to avoid possible human and economic loss. In this paper, we investigate reliability assessment of multi-component systems subject to dependent degradation processes influenced by random shocks. The dependencies present challenging issues in system reliability modeling and assessment [6] (e.g. the micro-electromechanical systems which are complex design systems experiencing dependent component failure processes and multiple dependent competing failure processes for each component [7]).

In industrial systems, many critical components (e.g. valves and pumps in the nuclear and aerospace industries) are designed to be highly reliable, for which statistical degradation/failure data are often limited. In this case, multi-state models (MSMs) [8-10] and physics-based models (PBMs) [11-13] can be used to describe the evolution of degradation in components and systems. A MSM describes the degradation process in a discrete way, supported by material science knowledge [14] and/or available but limited degradation/failure historical data from field collection or degradation tests [9]. On the contrary, a PBM gives an integrated mechanistic description of the component life consistent with the underlying real degradation mechanisms under operating conditions [15], by using physics knowledge modeled by corresponding mathematical equations [11]. In practice, degradation models of different nature have to be applied depending on the available information of the degradation processes. Recently [16], the piecewise-deterministic Markov process (PDMP) modeling framework has been employed to incorporate PBMs and MSMs, and to treat the dependencies among degradation processes but without considering the influences of random shocks. On the other hand, random shocks can accelerate the degradation processes (e.g. internal thermal shocks and water hammers onto power plant components [17]).

The reliability of systems experiencing both degradation and random shocks is a problem that has been widely studied [4, 7, 14, 18-23]. The dependency among these processes leading to failure has posed some challenges to reliability modeling. A literature review is presented below, to position our contributions within the existing works. Previous research has focused on the dependency between one type of degradation processes (continuous or multi-state) and random shocks. For continuous degradation processes, Peng *et al.* [20] considered systems with one linear degradation path where shocks can bring additional abrupt degradation damage if the shock loads do not exceed the maximum strength of the material; multi-component systems subject to multiple linear degradation paths have been further considered by Song *et al.* [7]; Jiang *et al.* [19] considered changes in the maximal strength of the material when systems are deteriorating under different situations; Becker *et al.* [18] extended the theory of dynamic reliability to incorporate random changes of the degradation variables due to random shocks; Ye *et al.* [24] considered the destructive power of a shock depending not only on the shock's

magnitude but also on the state of the system; Wang *et al.* [25] considered two types of the effects of shocks: a sudden increase in the failure rate after a shock, and a direct random change in the degradation after the occurrence of a shock; Rafiee *et al.* [21] proposed reliability models for systems for which the degradation path has a changing degradation rate according to particular random shock patterns; Song *et al.* [22] studied random shocks with specific sizes or functions, which can selectively affect the degradation processes of one or more components (not necessarily all components) in one system. For multi-state degradation processes, Yang *et al*. [23] combined random shocks with Markov degradation models where shocks can lead the systems to further degraded states; Lin *et al*. [14] integrated random shocks into multi-state physics models of degradation processes where the influences of shocks are dependent on the current degradation condition; Ruiz-Castro [26] considered external shocks which could produce several effects; extreme failure, cumulative damage and when the damage reaches a threshold state, a non-repairable failure occurs, and changes in the internal performance of the device. Note that no work has considered systems with both continuous and multi-state degradation processes and subject to random shocks and few studies have explicitly considered both the dependencies between degradation processes and random shocks, and that among the degradation processes themselves. Wang and Pham [4] employed copulas to handle these two types of dependencies; however, sufficient degradation/failure data is required to determine the copula functions through statistical inference.

In this paper, we extend the PDMP modeling framework for system reliability assessment, considering not only the dependencies among degradation processes but also the impacts of random shocks. To the best knowledge of the authors, this is the first work investigating systems with both continuous and multi-state degradation processes, subject to random shocks and considering the dependencies between degradation processes and random shocks, and among degradation processes are considered. Since the analytical solution is difficult to obtain due to the complexity of the system being considered, we employ two numerical approaches to assess system reliability: the Monte Carlo (MC) simulation [27] and the finite-volume (FV) [28] methods.

The remainder of this article is organized as follows. Section 2 provides the assumptions and descriptions of the degradation processes and random shocks. Section 3 presents the extended model for systems with degradation and random shock processes, considering their dependencies. The proposed MC simulation and FV methods are presented in Section 4. Section 5 presents an illustrative an illustrative study taken from the real-world residual heat removal system (RHRS) operated by Électricité de France (EDF). It is one important subsystem consisting of a pneumatic valve and a centrifugal pump in series, and is widely used in a variety of domains for fluid delivery (from water supply to spacecraft fueling systems) [12, 29]. The RHRS is used for cooling the reactor during and following shutdown, contributing to safety by removing heat from the core and transferring it to the environment. Numerical results and analysis are presented in Section 6. Section 7 concludes the work.

2. ASSUMPTIONS AND MODEL DESCRIPTIONS

We consider a multi-component system. Each component may be affected by multiple degradation mechanisms or processes, possibly dependent. The degradation processes can be separated into two groups: (1) $\boldsymbol{K}$ consists of processes fit to be modeled by MSMs; (2) $\boldsymbol{L}$ consists of processes fit to be modeled by PBMs.

2.1. Degradation models

2.1.1. MSMs

We follow the assumptions on MSMs made in [16]:

- A degradation process, $Y_{K_n}(t), K_n \in \boldsymbol{K}$ of group (1), takes values from a finite state set denoted by $\boldsymbol{S}_{K_n} = \{0, 1, \dots, d\}$, where d is the perfect functioning state and 0 is the complete failure state. The component is functioning or partially functioning in the intermediate degradation states. The transition rates $\lambda_i(j \mid \boldsymbol{\theta}_{K_n}), \forall\, i, j \in \boldsymbol{S}_{K_n}, i > j$ characterize the degradation transition probabilities from state i to state j, where $\boldsymbol{\theta}_{K_n}$ represents the environmental factors relevant to K_n and the related parameters of λ_{K_n}. We follow the assumption of Markov property made in [9, 30, 31]. Markov processes are widely used in practice to describe components degradation processes. The transition rates between different degradation states are estimated from the degradation and/or failure data from historical field collection. The failure state set of the process K_n is denoted by $\boldsymbol{\mathcal{F}}_{K_n} = \{0\}$.

2.1.2. PBMs

We follow the assumptions on PBMs made in [16]:

- A degradation process $\boldsymbol{X}_{L_m}(t), L_m \in \boldsymbol{L}$ of group (2), has d_{L_m} time-dependent continuous variables, whose evolution is characterized by a system of first-order differential equations $\dot{\boldsymbol{X}}_{L_m}(t) = \boldsymbol{f}_{L_m}(\boldsymbol{X}_{L_m}(t), t \mid \boldsymbol{\theta}_{L_m})$, i.e. physics equations, where $\boldsymbol{\theta}_{L_m}$ represents the environmental factors influential to L_m (e.g. temperature and pressure) and the parameters used in $\boldsymbol{f}_{L_m}$. This assumption is made in [32] and widely used in practice [12, 29]. Note that higher-order differential equations can be converted into a system of first-order differential equations by introducing extra variables [33].
- $\boldsymbol{X}_{L_m}(t) = (\boldsymbol{X}^{\boldsymbol{D}}_{L_m}(t), \boldsymbol{X}^{\boldsymbol{P}}_{L_m}(t))$ contains: (1) the non-decreasing degradation variables $\boldsymbol{X}^{\boldsymbol{D}}_{L_m}(t)$ (e.g. leak area) describing the degradation process, where $\boldsymbol{D}$ is the set of degradation variables indices (the same assumption has been widely used in practical studies [2, 12, 29]); (2) the physical variables $\boldsymbol{X}^{\boldsymbol{P}}_{L_m}(t)$ (e.g. velocity and force), which influence $\boldsymbol{X}^{\boldsymbol{D}}_{L_m}(t)$, where $\boldsymbol{P}$ is the set of physical variable indices. The generic degradation process L_m reaches failure when one $x^i_{L_m}(t) \in \boldsymbol{X}^{\boldsymbol{D}}_{L_m}(t)$ reaches or exceeds its corresponding failure threshold denoted by $x^i_{L_m}{}^*$. The failure state set of the process L_m is denoted by $\boldsymbol{\mathcal{F}}_{L_m}$.

2.2. Random shocks

Random shocks can influence the degradation processes of the components. The following assumptions are made, similarly to various previous works [19-23].

- Random shocks occur in time according to a homogeneous Poisson process $\{N(t), t \geq 0\}$ with constant arrival rate μ (Fig. 1), where the random variable $N(t)$ denotes the number of random shocks occurred until time t.
- The damages of random shocks are divided into two types: extreme and cumulative.
- Extreme and cumulative shocks are mutually exclusive.
- Extreme shocks immediately lead the components to failure, whereas cumulative shocks gradually deteriorate the components.

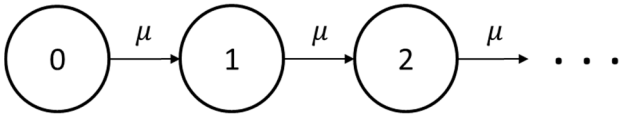

Fig. 1. Random shock process

3. DEPENDENT DEGRADATION PROCESSES AND RANDOM SHOCKS

3.1. Dependency between degradation processes and random shocks

Due to the different nature of PBMs and MSMs, the impacts of random shocks on the two groups of components are characterized in different ways.

3.1.1. Impacts on MSMs

In the generic degradation process $K_n \in \boldsymbol{K}$, random shocks can cause the process variable $Y_{K_n}(t)$ to step from state i to a further degraded state j with probability $p_{ij}, i > j$ [23], with p_{i0} denoting the probability that the random shock is extreme, i.e. leading to failure state 0 upon occurrence from state $Y_{K_n}(t) = i$. By combining the original degradation and the random shock processes, the resulting process $\boldsymbol{Y}'_{K_n}(t)$ is a homogeneous continuous-time Markov chain of the type depicted in Fig. 2. Each layer indicates one degradation state of $Y_{K_n}(t)$, and the numbers in each layer indicate the numbers of shocks experienced up to time t in the process K_n, denoted by k. The state of $\boldsymbol{Y}'_{K_n}(t)$ is, then, represented by pair $\left(Y_{K_n}(t), k\right)$. The transitions represented by solid lines are due to original degradation process, characterized by the original transition rates, which do not influence the value of k. The transitions represented by dotted lines are due to random shocks, which cause k to be increased by one. $\mu p_{ij}, i > j$ is the rate of occurrence of a shock which will cause the process stepping to the j-th layer from the i-th layer. Note that K_n fails whenever $Y_{K_n}(t)$ reaches the degradation state 0, no matter how many shocks it has experienced. Therefore, the space of the failure states of $\boldsymbol{Y}'_{K_n}(t)$ is denoted by $\boldsymbol{\mathcal{F}}'_{K_n} = \{(0, b), \forall b \in \mathbb{N}\}$. The state space of $\boldsymbol{Y}'_{K_n}(t)$ is denoted by $\boldsymbol{S}'_{K_n} = \left\{(a, b), \forall a \in \boldsymbol{S}_{K_n}, b \in \mathbb{N}\right\}$.

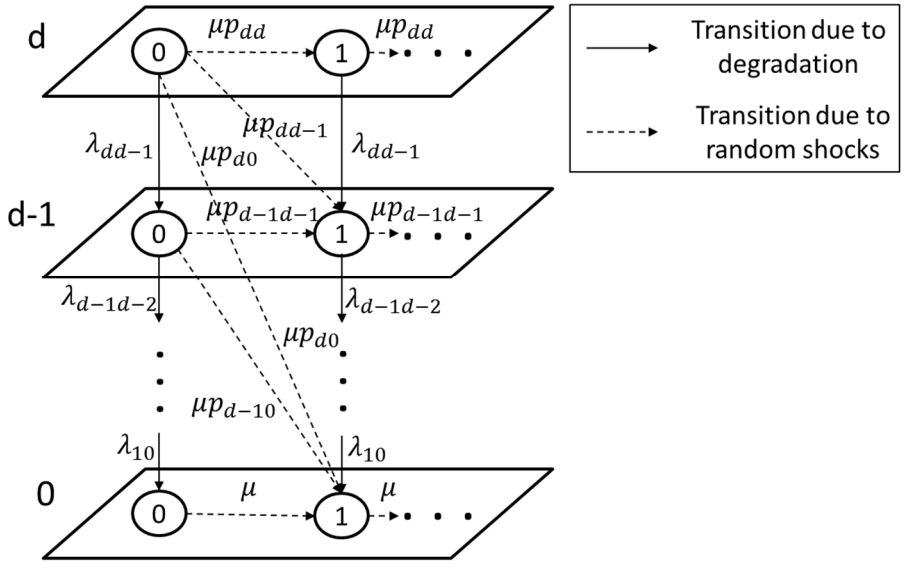

Fig. 2. Degradation process K_n and random shocks.

3.1.2. Impacts on PBMs

In the generic degradation process $L_m \in \boldsymbol{L}$, the i-th shock becomes extreme if the shock load W_i exceeds the maximal material strength D, otherwise, it can bring an instantaneous random increase $\boldsymbol{H}_i$ to $\boldsymbol{X}_{L_m}(t)$ [7]. The overall degradation level of L_m is expressed as

follows:

$$\boldsymbol{D}_{L_m}(t) = \begin{cases} \boldsymbol{X}_{L_m}(t) + \sum_{i=1}^{N^c(t)} \boldsymbol{H}_i, & if\ N'(t) \neq 0 \\ \boldsymbol{X}_{L_m}(t), & if\ N'(t) = 0 \end{cases} \quad (1)$$

where $N^c(t)$ is the number of cumulative shocks occurred in the developing L_m process before the extreme shock occurs until time t. The process L_m leads to failure if $\boldsymbol{D}_{L_m}(t)$ reaches the predefined failure state set $\boldsymbol{\mathcal{F}}_{L_m}$ or a shock with load larger than D occurs. An example of degradation process L_m considering random shocks is shown in Fig. 3, where W_i is the shock load of the i-th shock occurred at time t_i, $i = 1,2,3$. The center figure in Fig. 3 represents the evolution of the physical variable (e.g. velocity and force), which can influence the degradation variable (top figure) and may also be influenced by random shocks (bottom figure).

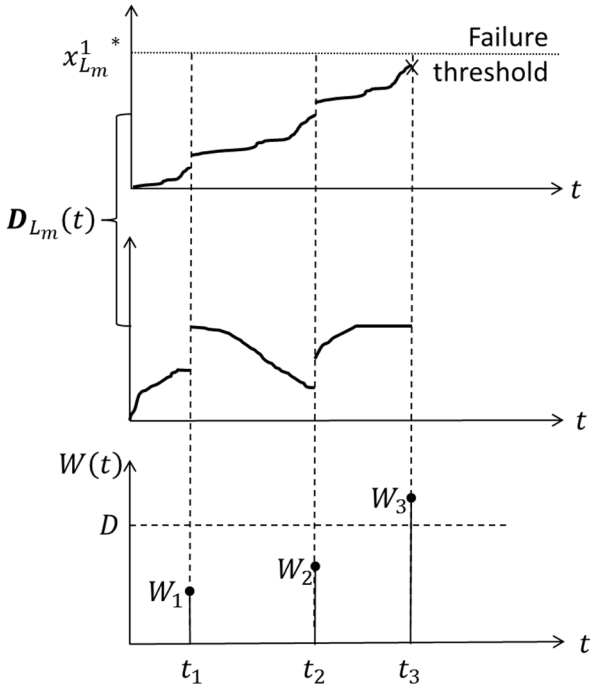

Fig. 3. An example of degradation process L_m with random shocks. Top Figure: degradation variable; Center Figure: physical variable; Bottom Figure: random shock process.

3.2. Dependency among degradation processes

Dependencies may exist among degradation processes within each group and between the two groups. The degradation states of the processes of set $\boldsymbol{K}$ may influence the evolution of the continuous variables of the degradation processes of set $\boldsymbol{L}$, and the degradation levels of the latter may influence the transition times and transition directions of the former (the detailed formulations are shown in eqs. (2) and (3)) [16].

Let $\boldsymbol{Y}(t) = (Y_{K_1}(t), \dots, Y_{K_N}(t)) \in \boldsymbol{S} = \{0, 1, \dots, d_{\boldsymbol{S}}\}$ and $\boldsymbol{X}(t) = \left(\boldsymbol{X}_{L_1}(t), \dots, \boldsymbol{X}_{L_M}(t)\right) \in \mathbb{R}^{d_L}$. The evolution of $\boldsymbol{Y}(t)$ is governed by the transition rates which depend on the states of the degradation processes in the first group $\boldsymbol{X}(t)$ and also in the second group $\boldsymbol{Y}(t)$, as follows:

$$\lim_{\Delta t \to 0} P\left(\boldsymbol{Y}(t + \Delta t) = \boldsymbol{j} \mid \boldsymbol{X}(t), \boldsymbol{Y}(t) = \boldsymbol{i}, \boldsymbol{\theta}_{\boldsymbol{K}} = \cup_{n=1}^{N} \boldsymbol{\theta}_{K_n}\right)/\Delta t = \lambda_{\boldsymbol{i}}(\boldsymbol{j} \mid \boldsymbol{X}(t), \boldsymbol{\theta}_{\boldsymbol{K}}), \forall\, t \geq 0, \boldsymbol{i}, \boldsymbol{j} \in \boldsymbol{S}, \boldsymbol{i} \neq \boldsymbol{j} \quad (2)$$

The evolution of $\boldsymbol{X}(t)$ is described by mathematical equations representing the underlying physics and depends on the states of the degradation processes in the second group $\boldsymbol{Y}(t)$ and also in the first group $\boldsymbol{X}(t)$, as follows:

$$\dot{\boldsymbol{X}}(t) = \left(\dot{\boldsymbol{X}}_{L_1}(t), \dots, \dot{\boldsymbol{X}}_{L_M}(t)\right) = \left(\boldsymbol{f}_{L_1}^{\boldsymbol{Y}(t)}(\boldsymbol{X}(t), t \mid \boldsymbol{\theta}_{L_1}), \dots, \boldsymbol{f}_{L_M}^{\boldsymbol{Y}(t)}(\boldsymbol{X}(t), t \mid \boldsymbol{\theta}_{L_M})\right) = \boldsymbol{f}_{\boldsymbol{L}}^{\boldsymbol{Y}(t)}(\boldsymbol{X}(t), t \mid \boldsymbol{\theta}_{\boldsymbol{L}} = \cup_{m=1}^{M} \boldsymbol{\theta}_{L_m}) \quad (3)$$

3.3. PDMPs for systems subject to degradation dependency and random shocks

Let $\boldsymbol{Z}(t)$denote the overall degradation process of the system:

$$\boldsymbol{Z}(t) = \left(\boldsymbol{X}'(t) = \left(\boldsymbol{D}_{L_1}(t), \dots, \boldsymbol{D}_{L_M}(t)\right), \boldsymbol{Y}'(t) = (\boldsymbol{Y}(t), N(t))\right) \in \boldsymbol{E} = \mathbb{R}^{d_L} \times \boldsymbol{S}' \quad (4)$$

where $\boldsymbol{E}$ is a space combining $\mathbb{R}^{d_L}$ and $\boldsymbol{S}' = \boldsymbol{S} \times \mathbb{N}$. Let $T_k, k \in \mathbb{N}$ denote the k-th jump time in $\boldsymbol{Y}'(t)$ and $\boldsymbol{Z}_k = \boldsymbol{Z}(T_k) = \left(\boldsymbol{X}'(T_k), \boldsymbol{Y}'(T_k)\right) = (\boldsymbol{X}'_k, \boldsymbol{Y}'_k)$. The evolution of $\boldsymbol{Z}(t)$ between two consecutive jumps of $\boldsymbol{Y}'(t)$, between which no shock occurs to the system and the degradation state does not change, can be written as follows:

$$\dot{\boldsymbol{Z}}(t) = (\dot{\boldsymbol{X}}'(t), \dot{\boldsymbol{Y}}'(t)) = \left(\boldsymbol{f}_{\boldsymbol{L}}^{\boldsymbol{Y}'(t)}(\boldsymbol{X}(t) \mid \boldsymbol{\theta}_{\boldsymbol{L}}), (\boldsymbol{0}, 0)\right), for\ t \in [T_k, T_{k+1}[\quad (5)$$

According to the definition in [34], $\boldsymbol{Z}(t)$ is a PDMP since (1) it can be written as $\boldsymbol{Z}(t) = \varphi(\boldsymbol{Z}_k, t - T_k), for\ t \in [T_k, T_{k+1}[$ and φ satisfies $\varphi(\boldsymbol{y}, t + s) = \varphi(\varphi(\boldsymbol{y}, t), s),\ \forall t, s \geq 0, \boldsymbol{y} \in \boldsymbol{E}$, and $t \to \varphi(\boldsymbol{y}, t), \forall t \geq 0, \boldsymbol{y} \in \boldsymbol{E}$ is right continuous with left limits and (2) $\{\boldsymbol{Z}_n, T_n\}_{n \geq 0}$is a Markov renewal process defined on the space $\boldsymbol{E} \times \mathbb{R}^+$. The probability that $\boldsymbol{Z}(t)$ will step to state $\boldsymbol{j}$ from state $\boldsymbol{Z}_k$ in the time interval $[T_k, T_k + t]$, given $\{\boldsymbol{Z}_i, T_i\}_{i \leq k}$ is as follows:

$$P[\boldsymbol{Z}_{k+1} = \boldsymbol{j}, T_{k+1} \in [T_k, T_k + t] \mid \{\boldsymbol{Z}_i,\ T_i\}_{i \leq k}] = P[\boldsymbol{Z}_{k+1} = \boldsymbol{j}, T_{k+1} \in [T_k, T_k + t] \mid \boldsymbol{Z}_k], \quad \forall k \in \mathbb{N}, \boldsymbol{j} \in \boldsymbol{E}, \boldsymbol{j} \neq \boldsymbol{Z}_k \quad (6)$$

$\{\boldsymbol{Z}_n, T_n\}_{n \geq 0}$ is characterized by the semi-Markov kernel $N\left(\boldsymbol{i} = (\boldsymbol{x}_i, \boldsymbol{y}_i), (d\boldsymbol{x}, \boldsymbol{y}_j), dt\right) = P\left[\boldsymbol{X}'_{k+1} \in [\boldsymbol{x}, \boldsymbol{x} + d\boldsymbol{x}], \boldsymbol{Y}'_{k+1} = \boldsymbol{y}_j, T_{k+1} - T_k \in [t, t + dt] \mid \boldsymbol{Z}_k = \boldsymbol{i}\right], \forall k \in \mathbb{N}, \boldsymbol{y}_i, \boldsymbol{y}_j \in \boldsymbol{S}', \boldsymbol{x}_i, d\boldsymbol{x} \in \mathbb{R}^{d_L}, d\boldsymbol{x} \to \boldsymbol{0}, dt \to 0$, which can be reformulated as follows:

$$N\left(\boldsymbol{i} = (\boldsymbol{x}_i, \boldsymbol{y}_i), (d\boldsymbol{x}, \boldsymbol{y}_j), dt\right) = P\left[\boldsymbol{X}'_{k+1} \in [\boldsymbol{x}, \boldsymbol{x} + d\boldsymbol{x}], \boldsymbol{Y}'_{k+1} = \boldsymbol{y}_j \mid T_{k+1} - T_k \in [t, t + dt], \boldsymbol{Z}_k = \boldsymbol{i}\right] \cdot P[T_{k+1} - T_k \in [t, t + dt] \mid \boldsymbol{Z}_k = \boldsymbol{i}] = Q\left(\varphi(\boldsymbol{i}, t), (d\boldsymbol{x}, \boldsymbol{y}_j)\right) dF_{\boldsymbol{i}}(t) \quad (7)$$

where $Q\left(\varphi(\boldsymbol{i}, t), (d\boldsymbol{x}, \boldsymbol{y}_j)\right)$ is the probability distribution of state $\boldsymbol{Z}_{k+1}$ given $T_{k+1} - T_k = t$ and $\boldsymbol{Z}_k = \boldsymbol{i}$ and $dF_{\boldsymbol{i}}(t)$ is the probability distribution of $T_{k+1} - T_k$ given $\boldsymbol{Z}_k = \boldsymbol{i}$. $Q\left(\varphi(\boldsymbol{i}, t), (d\boldsymbol{x}, \boldsymbol{y}_j)\right)$ can be reformulated as follows:

$$Q\left(\varphi(\boldsymbol{i} = (\boldsymbol{x}_i, \boldsymbol{y}_i), t), (d\boldsymbol{x}, \boldsymbol{y}_j)\right) = P\left[\boldsymbol{X}'_{k+1} \in [\boldsymbol{x}, \boldsymbol{x} + d\boldsymbol{x}], \boldsymbol{Y}'_{k+1} = \boldsymbol{y}_j \mid T_{k+1} - T_k \in [t, t + dt], \boldsymbol{Z}_k = \boldsymbol{i}\right] = P\left[\boldsymbol{X}'_{k+1} \in [\boldsymbol{x}, \boldsymbol{x} + d\boldsymbol{x}] \mid \boldsymbol{Y}'_{k+1} = \boldsymbol{y}_j, T_{k+1} - T_k \in [t, t + dt], \boldsymbol{Z}_k = \boldsymbol{i}\right] \cdot P\left[\boldsymbol{Y}'_{k+1} = \boldsymbol{y}_j \mid T_{k+1} - T_k \in [t, t + dt], \boldsymbol{Z}_k = \boldsymbol{i}\right] \quad (8)$$

Let $p_t(d\boldsymbol{z} = (d\boldsymbol{x}, \boldsymbol{y}_i))$ denote the probability distribution of $\boldsymbol{Z}(t)$, which obeys the Chapman-Kolmogorov equation [35] as follows:

$$\int_0^t \sum_{\boldsymbol{y}_i \in \boldsymbol{S}'} \int_{\mathbb{R}^{d_L}} \sum_{\boldsymbol{y}_j \in \boldsymbol{S}'} \lambda_{\boldsymbol{y}_i, \boldsymbol{y}_j}(\boldsymbol{x} \mid \boldsymbol{\theta}_{\boldsymbol{K}}) \left(\int_{\mathbb{R}^{d_L}} \psi(\boldsymbol{y}_j, y) \mu(\boldsymbol{y}_i, \boldsymbol{y}_j, \boldsymbol{x})(d\boldsymbol{y}) - \psi(\boldsymbol{y}_i, \boldsymbol{x})\right) p_s(d\boldsymbol{x}, \boldsymbol{y}_i) ds + \int_0^t \sum_{\boldsymbol{y}_i \in \boldsymbol{S}'} \int_{\mathbb{R}^{d_L}} \boldsymbol{f}_{\boldsymbol{L}}^{\boldsymbol{y}_i}(\boldsymbol{x} \mid \boldsymbol{\theta}_{\boldsymbol{L}}) div\left(\psi(\boldsymbol{y}_i, \boldsymbol{x})\right) p_s(d\boldsymbol{x}, \boldsymbol{y}_i) ds - \sum_{\boldsymbol{y}_i \in \boldsymbol{S}'} \int_{\mathbb{R}^{d_L}} \psi(\boldsymbol{y}_i, \boldsymbol{x})\, p_t(d\boldsymbol{x}, \boldsymbol{y}_i) + \sum_{\boldsymbol{y}'_i \in \boldsymbol{S}'} \int_{\mathbb{R}^{d_L}} \psi(\boldsymbol{y}_i, \boldsymbol{x})\, p_0(d\boldsymbol{x}, \boldsymbol{y}_i) = 0 \quad (9)$$

where $\lambda_{\boldsymbol{y}_i, \boldsymbol{y}_j}(\boldsymbol{x} \mid \boldsymbol{\theta}_{\boldsymbol{K}})$ is the transition rate of $\boldsymbol{Y}'(t)$ from state $\boldsymbol{y}_i$ to $\boldsymbol{y}_j$, $\psi(\cdot, \cdot)$ is any

continuously differentiable function from $\boldsymbol{S}' \times \mathbb{R}^{d_L}$ to $\mathbb{R}$ with a compact support and $\mu(\boldsymbol{y}_i, \boldsymbol{y}_j, \boldsymbol{x})(d\boldsymbol{y})$ is the probability of $\boldsymbol{X}'(t) \in [\boldsymbol{y}, \boldsymbol{y} + d\boldsymbol{y}]$ after jumping from $\boldsymbol{x}$ when $\boldsymbol{Y}'(t)$ steps to state $\boldsymbol{y}_j$ from state $\boldsymbol{y}_i$.

The reliability of the system at time t is defined as follows:

$$R(t) = P[\boldsymbol{Z}(s) \notin \boldsymbol{\mathcal{F}}, \forall s \leq t] = \int_{\boldsymbol{z} \notin \boldsymbol{\mathcal{F}}} p_t(d\boldsymbol{z}) \quad (10)$$

where $\boldsymbol{\mathcal{F}}$ is the space of the failure states of the system.

The parameters in the proposed model are mainly divided into three groups: (1) transition rates in multi-state models; (2) parameters in physics equations of physics-based models and (3) parameters charactering random shock processes. The values of the first group can be estimated, using degradation and/or failure data from historical field collection or degradation tests, through maximum likelihood estimation for complete or incomplete data [36, 37], it can also be estimated by domain experts using physics knowledge (e.g. the values of the transition rates in multi-state physics model [14]) are described by physics equations). For the second group, the laws of physics are used to build the equations describing the development of the underlying degradation mechanisms (e.g. fatigue, wear, corrosion, etc.) [12]. The related parameter values can be estimated through regression models using degradation and/or failure data. For example, the physics equations of the fatigue cracking of the seal are built according to Paris-Erdogan law in [38], which relates the stress intensity factor range to the crack growth under a fatigue stress regime. Their values are estimated through least squares regression methods by using data on crack length and cycles. The values of the third group can be estimated using related degradation and/or failure data obtained from historical field collection or shock tests [39] based on likelihood based inference or regression models [24]. For example, the Brown-Proschan model is employed to model wear and shock processes of tire treads in [24], the likelihood function can be derived based on cumulative hazard function and the parameter values are estimated through maximum likelihood estimation.

4. SYSTEM RELIABILITY ASSESSMENT UNDER DEPENDENT DEGRADATION AND RANDOM SHOCK PROCESSES

The analytical solution of $R(t)$ is difficult to obtain mainly due to the complex PDMPs used to model the dependent degradation and random shock processes [40]. Therefore, we consider the following two approximate methods: the MC simulation method [27] based on the semi-Markov kernel of $\{\boldsymbol{Z}_n, T_n\}_{n \geq 0}$ (eq. (7)) and the FV method [28] based on the Chapman-Kolmogorov equation (eq. (9)). They are two widely used approaches for solving PDMPs to evaluate reliability quantities. FV method approximates the probability density function of PDMPs by discretizing the state space of the continuous variables and the time space. It is a method that can lead to comparable results as MC simulation, using less computing time for low dimensional problems [41]. However, it is typically unsuited for high-dimensional problems or problems with complex equations describing the deterministic evolution. Besides, it is relatively more difficult to implement than MC simulation method.

4.1. MC simulation method

The MC simulation method to compute the system reliability at time t consists of replicating several times the life process of the system by repeatedly sampling its holding time and arrival state from the corresponding probability distributions. Each replication continues until the time of system evolution reaches t or until the system enters a state in the failure set $\boldsymbol{\mathcal{F}}$. The procedure of the MC simulation method is as follows:

Set N_{max} (the maximum number of replications) and $k = 0$ (index of replication)
Set $k' = 0$ (number of replications that end in a system failure state)
While $k < N_{max}$

Initialize the system by setting $\boldsymbol{Z} = (\boldsymbol{X}'(0), \boldsymbol{Y}'(0))$ (initial system state), and the time $T = 0$ (initial system time)
  Set $t' = 0$ (state holding time)
  While $T < t$
    Sample a t' by using the probability distribution $dF_{\boldsymbol{Z}}(t)$
    Sample an arrival state $\boldsymbol{y}$ for stochastic process $\boldsymbol{Y}'(t)$ and an arrival state $\boldsymbol{x}$ for process $\boldsymbol{X}'(t)$ by using eq. (8)
    Set $T = T + t'$
    If $T \leq t$
      Set $\boldsymbol{Z} = (\boldsymbol{x}, \boldsymbol{y})$
      If $\boldsymbol{Z} \in \boldsymbol{\mathcal{F}}$
        Set $k' = k' + 1$
        Break
      End if
    Else (when $T > t$)
      If $\varphi(\boldsymbol{Z}, t + t' - T) \in \boldsymbol{\mathcal{F}}$
        Set $k' = k' + 1$
        Break
      End if
    End if
  End While
  Set $k = k + 1$
End While □

The estimated system reliability at time t can be obtained by

$$\widehat{R_{MC}}(t) = 1 - k'/N_{max} \tag{11}$$

where *k*' represents the number of trials that end in the failure state of the system, and the sample variance [42] is:

$$var_{\widehat{R_{MC}}(t)} = \widehat{R_{MC}}(t)(1 - \widehat{R_{MC}}(t))/(N_{max} - 1) \tag{12}$$

MC simulation method is widely used in practice to evaluate system reliability [43]. It is based on the strong law of large numbers and the central limit theorem and provides an unbiased estimator. The error on the estimate can be controlled within a confidence interval built based on the sample variance given in eq. (12), which can guarantee the consistency of the estimate. The accuracy of MC simulation method increases as the number of replications increases. MC simulation method is more efficient to solve higher-dimensional problems, since the sample variance does not depend on the number of dimensions. There are certain techniques to improve the efficiency of MC simulation method (such as importance sampling, sequential MC, etc.) [43], which have to be designed according to the specific problems and have not been considered in our general reliability assessment framework.

4.2. FV method

The FV method is an alternative for the approximated solution of the system reliability, based on a discretization of the state space of the continuous variables and time space [41]. Here, we employ an explicit FV scheme developed by Cocozza-Thivent *et al.* [28]. The numerical scheme aims at constructing an approximate value $\rho_t(\boldsymbol{x}, \boldsymbol{y}_i)d\boldsymbol{x}$ for $p_t(d\boldsymbol{x}, \boldsymbol{y}_i)$. The estimated system reliability at time t, then, can be calculated as follows:

$$\widehat{R_{FV}}(t) = \int_{\boldsymbol{z} \notin \boldsymbol{\mathcal{F}}} \rho_t(\boldsymbol{z})d\boldsymbol{z} \tag{13}$$

See Appendix A for detailed descriptions of FV method. Due to the complexity of the Chapman-Kolmogorov equation (eq. (9)), there is no explicit expressions about the variance or uncertainty

associated with the estimation. However, the convergence of the method is proven in [28] under the condition that $\Delta t \to 0$ and $|\mathcal{M}|/\Delta t \to 0$ where $|\mathcal{M}|$ is the space step and Δt is the time step. The efficiency and the accuracy of the method have been shown through the numerical example in [28].

5. CASE STUDY

We consider a subsystem of a residual heat removal system (RHRS) in a nuclear power plant, which consists of a pneumatic valve and a centrifugal pump in series shown in Fig. 4.

For the degradation model of the pump, we consider a MSM modified from the one originally supplied by EDF [16], while for the valve we take the PBM proposed in [12].

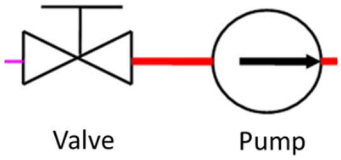

Fig. 4. Subsystem of RHRS, consisting of a centrifugal pump and a pneumatic valve.

5.1. Centrifugal pump

The degradation process of the pump is modeled by a four-state, continuous-time, homogeneous Markov chain as shown in Fig. 5.

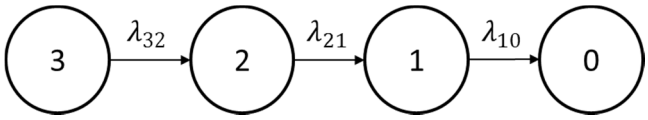

Fig. 5. Degradation process of the pump.

Among the four states of the pump, state 3 is the perfect functioning state and state 0 is the complete failure state. Let $Y_p(t)$ denote the degradation state of the pump at time t and $\boldsymbol{S}_p = \{3, 2, 1, 0\}$ denote the degradation states set. The pump is functioning until $Y_p(t) = 0$. The parameters λ_{32}, λ_{21} and λ_{10} are the transition rates between the degradation states, estimated from the available degradation and/or failure data. The pump vibrates when it reaches the degradation states 2 and 1; the intensity of the vibration of the pump on states 2 and 1 is evaluated by the experts as ‘smooth’ and ‘rough’, respectively. The set of the failure states of the pump is $\boldsymbol{\mathcal{F}}_p = \{0\}$.

5.2. Pneumatic valve

The simplified scheme of the pneumatic valve is shown in Fig. 6. The degradation of the valve is the external leak at the actuator connections to the bottom pneumatic port due to corrosion, and is modeled by a PBM due to limited statistical degradation data on the valve behavior. It is much more significant than the other degradation mechanisms according to the results shown in [12].

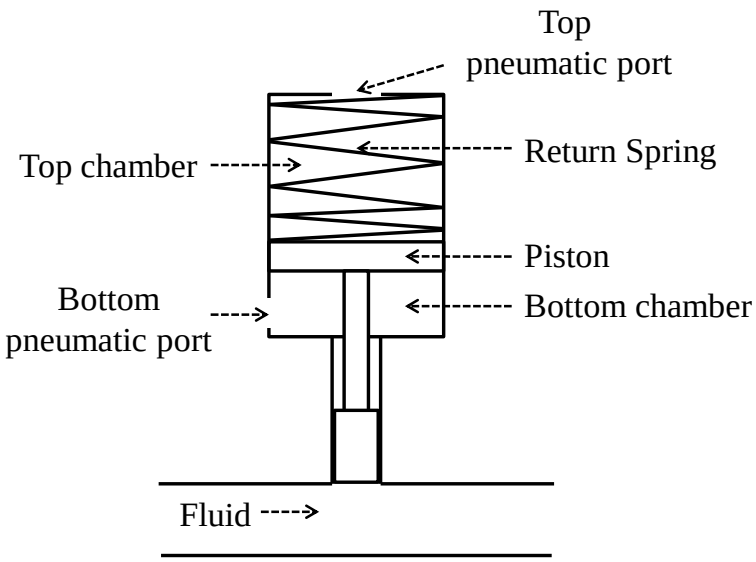

Fig. 6. Simplified scheme of the pneumatic valve [12].

Let $D_b(t)$ denote the area of the leak hole at the bottom pneumatic port of the valve at time t. The development of the leak size is described by $\dot{D}_b(t) = \omega_b$, where ω_b is the original wear coefficient. The valve is considered failed when the size of the external leak exceeds a predefined threshold D_b^*. The set of the failure states of the valve is $\boldsymbol{\mathcal{F}}_v = [D_b^*, +\infty)$.

5.3. Dependency between degradation processes

Dependency in the degradation processes of the two components has been indicated as a relevant problem by the experts of EDF: the pump vibrates due to degradation [44] which, in turn, leads the valve to vibrate, aggravating its own degradation processes [45]. The development of the leak size of the valve is, then, reformulated as follows [16]:

$$\dot{D}_b(t) = \omega_b(1 + \beta(Y_p(t))) \tag{14}$$

where $\beta(Y_p(t))$ is the function indicating the relative increment of the growth rate of the external leak caused by the vibration of the pump at the degradation state $Y_p(t)$.

5.4. Random shocks

According to the experts of EDF, random shocks like water hammers and internal thermal shocks [17] can worsen the degradation condition of both components of the subsystem considered or even immediately lead them to failures.

Random shocks can deteriorate the pump from its current state i to a degraded state j, as $p_{ij} = \frac{9\times(0.1)^{(i-j+1)}}{1-(0.1)^{(i+1)}}, i \geq j$, where p_{i0} denotes the probability of an extreme random shock leading the pump from state i directly to failure state 0. The formulation is taken from Yang *et al.*'s work [23], which satisfies that $\sum_{j=i}^{0} p_{ij} = 1$. By combining the degradation process of the pump with the random shock process, the resulting process takes the form shown in Fig. 7. The state of the process is represented by $Y(t) = \big(Y_p(t), m\big), m \in \mathbb{N}$, where m is the number of shocks experienced by the pump. The state space of the new process is denoted by $\boldsymbol{S} = \{(a, b), \forall a \in \boldsymbol{S}_p, b \in \mathbb{N}\}$ and the set of failure states of the pump is $\boldsymbol{\mathcal{F}}_{\boldsymbol{p}}' = \{(0, b), \forall b \in \mathbb{N}\}$.

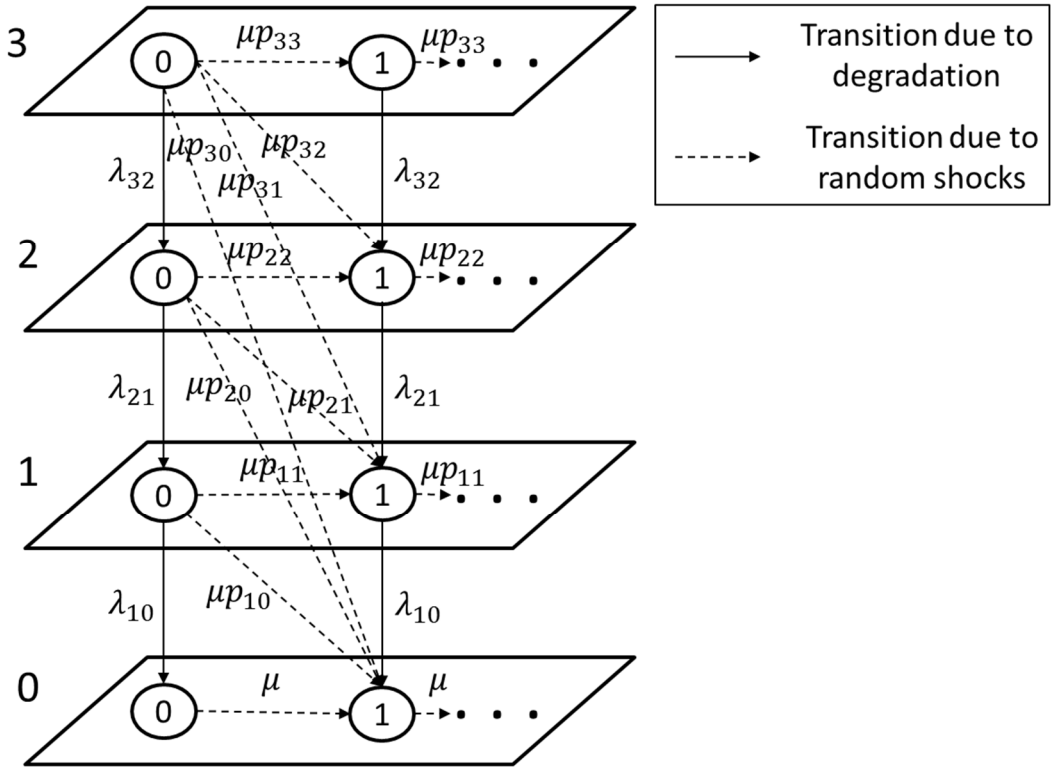

Fig. 7. Degradation and random shock processes of the pump.

For the valve, the i-th shock becomes extreme if the shock load W_i exceeds the maximal material strength D, otherwise, it can bring an instantaneous random increase H_i to the total external leak size [7]. W_i and H_i are assumed to be i.i.d. random variables following folded normal distributions [46], $W_i = |a|$ and $H_i = |b|$, where $a \sim N(\mu_h, \sigma_h^2)$ and $b \sim N(\mu_w, \sigma_w^2)$.

5.5. PDMP for the system considering dependency

An illustration of the composite degradation process of the valve considering random shocks and the degradation state of the pump is shown in Fig. 8, where the system experienced a random shock at time t_i, with the shock load W_i, $i = 1,3,4$. The first two shocks cause instantaneous random increases on $D(t)$, the last shock lead the valve to failure. The vibration of the pump accelerates the degradation process of the valve at times t_2 and t_3, when the pump stepped to a further degraded state.

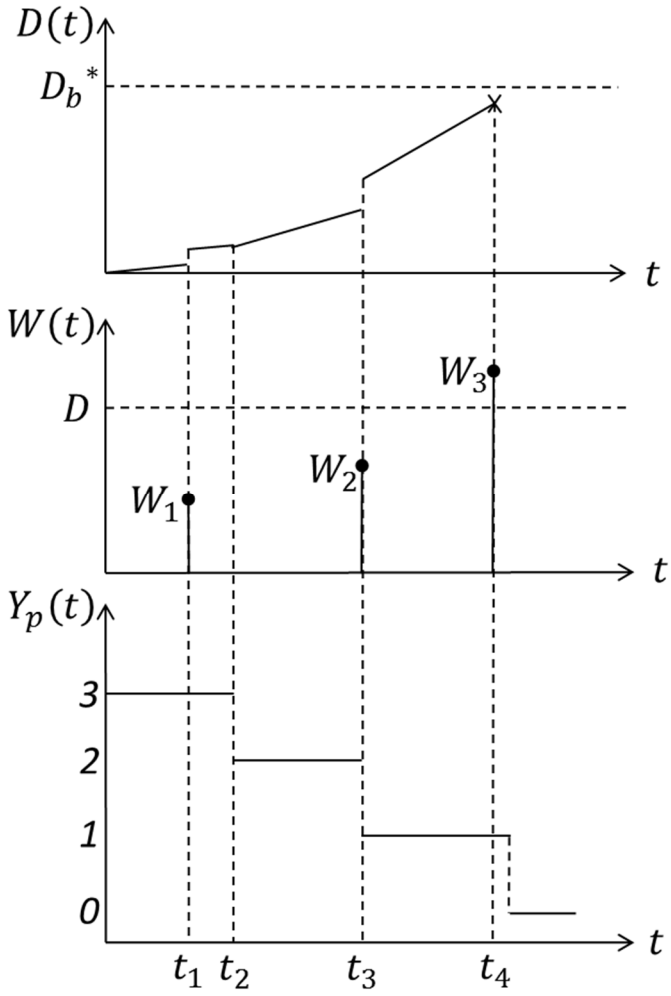

Fig. 8. An illustration of the degradation of the valve considering random shocks and the degradation state of the pump. Top Figure: degradation process of the valve; Center Figure: random shock processes; Bottom Figure: degradation process of the pump.

The degradation processes of the whole system can be represented by:

$$\boldsymbol{Z}(t) = (D(t), Y(t)) \in \mathbb{R}^+ \times \boldsymbol{S} = \boldsymbol{E} \tag{15}$$

Let $T_k, k \in \mathbb{N}$ denote the k-th jump time in $Y(t)$ and $\boldsymbol{Z}_k = (D_k, Y_k) = \boldsymbol{Z}(T_k)$. The evolution of $\boldsymbol{Z}(t)$ between two consecutive jumps of $Y(t)$, between which no shock occurs to the system and the degradation state of the pump does not change, can be written as follows:

$$\begin{aligned} \dot{\boldsymbol{Z}}(t) &= (\dot{D}(t), \dot{Y}(t)) \\ &= (\omega_b(1 + \beta(Y_p(t))), (0,0)) \\ &= (\nu(Y(t)), (0,0)), for\ t \in [T_k, T_{k+1}[\end{aligned} \tag{16}$$

where $\nu(\cdot)$ is used to denote the corresponding equation.

By integrating eq. (25), we can obtain that:

$$\begin{aligned} \boldsymbol{Z}(t) &= (D_k + (t - T_k)\omega_b(1 + \beta(Y_p(T_k))), Y_k) \\ &= (\varphi_1(\boldsymbol{Z}_k, t - T_k), Y_k), for\ t \in [T_k, T_{k+1}[\\ &= \varphi(\boldsymbol{Z}_k, t - T_k), for\ t \in [T_k, T_{k+1}[\end{aligned} \tag{17}$$

where $\varphi_1(\cdot)$ and $\varphi(\cdot)$ are used to denote the corresponding equations.

Let $p_t(dx, \boldsymbol{y}_i)$ denote the probability distribution of $\boldsymbol{Z}(t)$. Given the series logic configuration of the system considered, the system fails when one of the two components fails; the reliability of the system at time t is, then, defined as follows:

$$R(t) = P[\boldsymbol{Z}(s) \notin \boldsymbol{\mathcal{F}}, \forall s \leq t] = \int_{x \notin \boldsymbol{\mathcal{F}}_v} \sum_{\boldsymbol{y}_i \notin \boldsymbol{\mathcal{F}}'_p} p_t(dx, \boldsymbol{y}_i) \quad (18)$$

where $\boldsymbol{\mathcal{F}} = \mathbb{R}^+ \times \boldsymbol{\mathcal{F}}'_p \cup \boldsymbol{\mathcal{F}}_v \times \boldsymbol{S}$ is the set of the failure states of the system.

The parameter values related to the system degradation processes and random shocks under accelerated aging conditions are presented in Table I. The first eight parameter values related to the degradation processes are taken from [16], the values of μ_w, σ_w and D are taken from [20] and those of μ, μ_h and σ_h are assumed arbitrarily. The parameter values are set upon the discussion with the experts from EDF.

Table I Parameter values

Parameter	Value
λ_{32}	3e-3 /s
λ_{21}	3e-3 /s
λ_{10}	3e-3 /s
ω_b	1e-8 m^2/s
$\beta(3)$	0
$\beta(2)$	10%
$\beta(1)$	20%
$\beta(0)$	0
D_b^*	1.06e-5 m^2
μ	5e-3 /s
μ_w	1.2 Gpa
σ_w	0.2 Gpa
D	1.5 Gpa.
μ_h	1e-7 m^2
σ_h	2e-8 m^2

6. NUMERICAL RESULTS AND ANALYSIS

The MC simulation and the FV methods are employed to estimate the system reliability. All the experiments are carried out in MATLAB on a PC with an Intel Core 2 Duo CPU at 3.06 GHz and a RAM of 3.07 GB. MC simulations with 10^3, 10^4 and 10^5 replications (named MC1, MC2 and MC3, respectively) are applied over a time horizon of $T_{miss} = 1000\ s$ for the system reliability estimation. System holding time, arrival state for stochastic process $Y(t)$ and arrival state for process $D(t)$ can be sampled by using the probability distribution eq. (28), the probability mass function eq. (30) and the probability distribution eq. (31), respectively. See Appendix B for detailed descriptions of these equations.

The results are shown in Fig. 9. It is seen that the MC simulation method requires a number of replications to achieve the desired level of accuracy. The average computation times of MC1, MC2 and MC3 are 0.21 s, 2.17 s and 21.77 s, respectively.

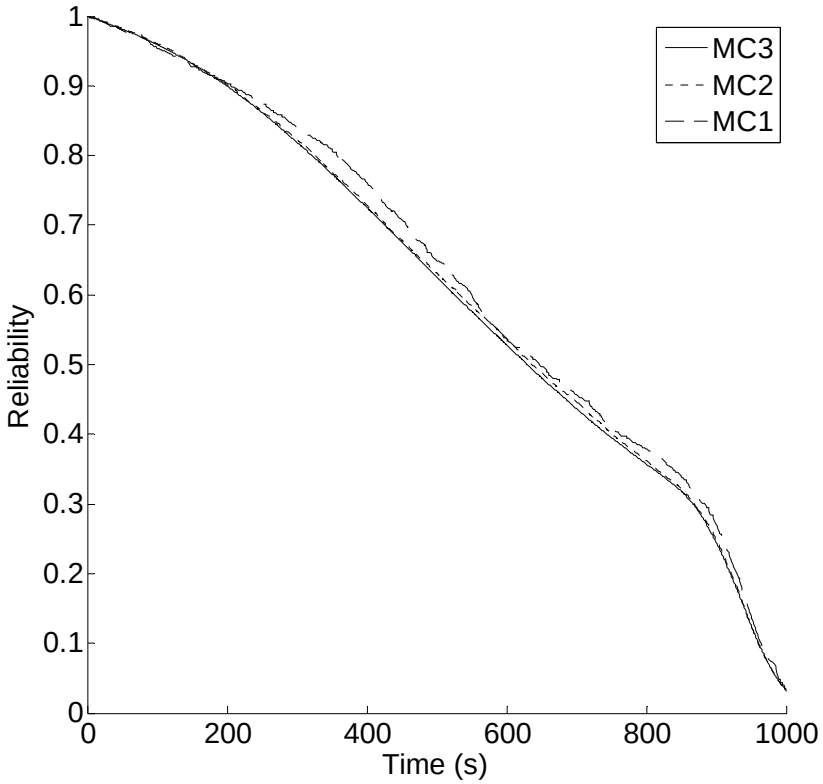

Fig. 9. System reliability estimated by MC1, MC2 and MC3.

For the FV method, the state space $\mathbb{R}^+$ of $D(t)$ has been divided into an admissible mesh $\mathcal{M} = \cup_{m=0,1,2,\dots} [m\Delta x, (m+1)\Delta x[$ and the time space $\mathbb{R}^+$ has been divided into small intervals $\mathbb{R}^+ = \cup_{n=0,1,2,\dots} [n\Delta t, (n+1)\Delta t[$. See Appendix C for the application of FV method.

The system reliability estimated by the FV method, is shown in Fig. 10 with the following different parameter settings: (1) FV1: $\Delta x = 5e-9, \Delta t = 0.5$; (2) FV2: $\Delta x = 1.5e-8, \Delta t = 1.5$ and (3) FV3: $\Delta x = 4.5e-8, \Delta t = 4.5$. The accuracy of the FV scheme increases as the space step Δx and the time step Δt are reduced. The average computation times of FV1, FV2 and FV3 are 0.19 s, 1.93 s and 26.39 s, respectively.

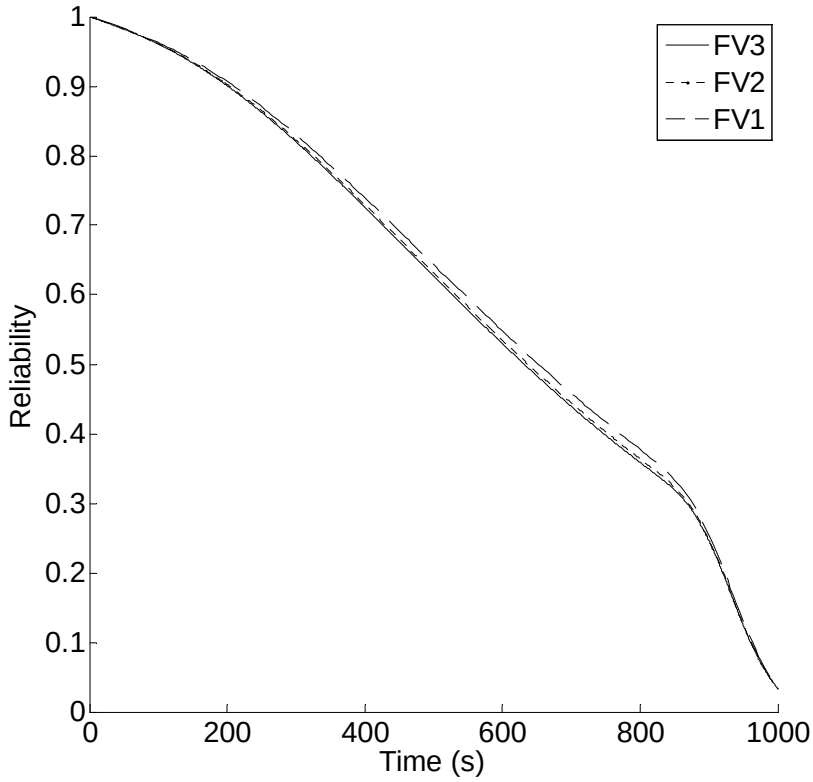

Fig. 10. System reliability estimated by FV1, FV2 and FV3.

The quantitative comparison of the most accurate results obtained by MC3 with those obtained by FV3 is shown in Table II. The sample variances associated with system reliability values estimated by MC3 are less than 2.5e-6 according to eq. (12), which means the results are sufficiently consistent and accurate. The quantitative comparison of results obtained by MC3 and FV3 shown in Table II is only used to show that FV scheme can achieve comparable results to the MC simulation method (relative error less than 0.9%) in the illustrative case. Note that FV3 gives deterministic results since the values of Δx and Δt do not change, which guarantees the accuracy and consistency of the quantitative comparison. To provide more information, we have added Fig. 11 to compare the results obtained by MC3 with that obtained by FV3 over the time horizon. For this case study, the computational expense of the two methods is similar.

Table II Quantitative comparison of the results obtained by MC3 and FV3

Method / Time	MC3	FV3	Relative error
100s	0.9611	0.9607	0.0438%
200s	0.9021	0.9011	0.1162%
300s	0.8230	0.8205	0.3027%
400s	0.7285	0.7263	0.2974%
500s	0.6284	0.6271	0.2109%
600s	0.5312	0.5300	0.2394%
700s	0.4395	0.4397	0.0365%
800s	0.3576	0.3591	0.4157%

900s	0.2467	0.2459	0.3204%
1000s	0.0335	0.0332	0.8955%

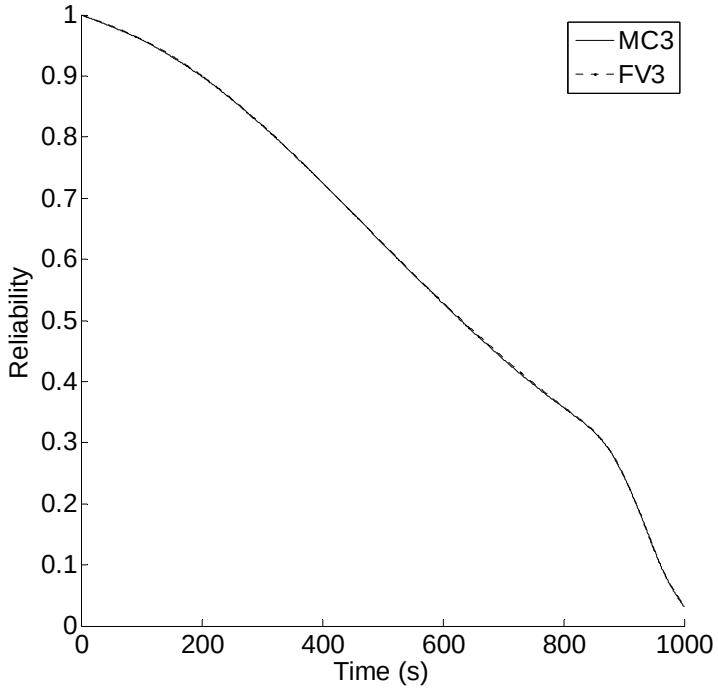

Fig. 11. Comparison of the results obtained by MC3 and FV3.

The reliability values of the valve, the pump and the system with/without random shocks, obtained by MC3, are shown in Fig. 12. The numerical comparisons on the reliability of the system, the valve and the pump with/without random shocks at the final time of 1000 s are presented in Table III.

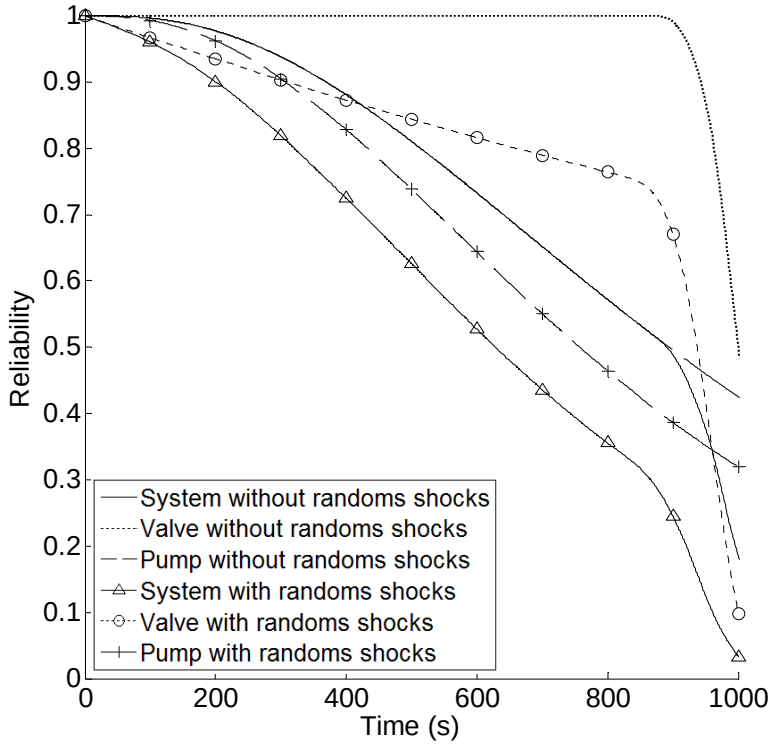

Fig. 12. The reliability of the system, the valve and the pump with/without random shocks.

When random shocks are ignored, the system reliability is basically determined by the pump before around 870 s, since the valve is highly reliable. After that, the sharp decrease of the valve reliability due to degradation leads to the same behavior in the system reliability. When random shocks are considered, the system reliability is determined by both the pump reliability and the valve reliability from the beginning until around 850 s, since the valve is no longer as highly reliable as before. Then, the valve reliability decreases sharply due to the joint effects of random shocks and degradation, and this drives also the sharp decrease of the system reliability. We can see from the results that neglecting random shocks can result in an underestimation of the reliability of the system and of the components.

Table III Comparison of reliability with/without random shocks at 1000 s

	Reliability without random shocks	Reliability with random shocks	Relative change
System	0.18	0.033	81.67%
Valve	0.50	0.099	80.20%
Pump	0.43	0.32	25.58%

Following one assumption of our work (i.e. limited historical data), epistemic uncertainty can arise due to the incomplete or imprecise knowledge about the degradation processes and the governing parameters of the pump and the valve, which has been considered in [16] by describing the degradation model parameters as intervals (or fuzzy numbers). In the revised manuscript, we follow the settings in [16] where a relative deviation of ±10% to the original parameters values has been considered for λ_{32}, λ_{21}, λ_{10}, ω_b, $\beta(3)$, $\beta(2)$, $\beta(1)$ and $\beta(0)$ upon the discussions with the domain experts from EDF. The lower and upper bounds of system reliability under uncertainty, and the original values without uncertainty obtained by

MC3 are shown in Fig. 13. The lower bound of system reliability with uncertainty decreases more sharply after around 790 s, earlier than that without uncertainty. It is seen that the system fails after around 964 s, because at that time the valve is completely failed. The upper bound of system reliability with uncertainty does not experience a rapid decrease because the valve is mostly functioning over the time horizon.

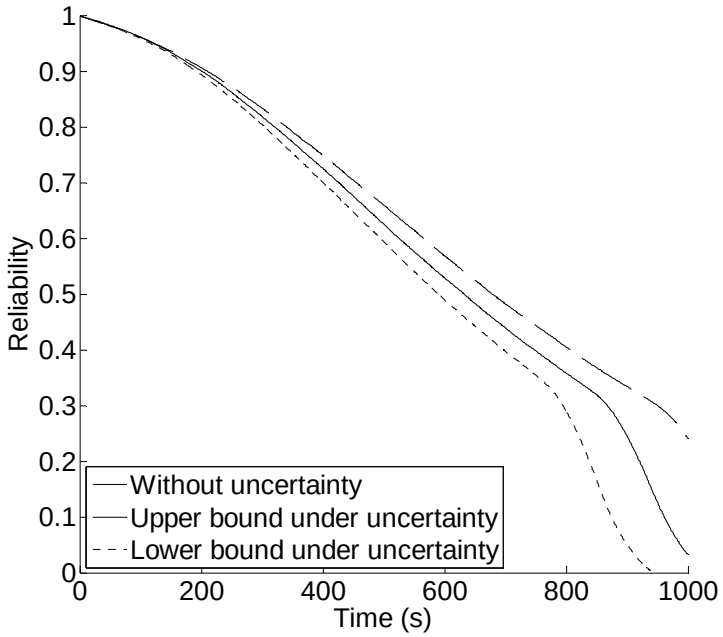

Fig. 13. The lower and upper bounds of system reliability with uncertainty, and the original values without uncertainty obtained by MC3.

7. CONCLUSIONS

In this paper, we presented reliability models for systems experiencing both degradation processes and random shocks. The degradation processes involve both continuous and multi-state processes, which are modeled by MSMs and PBMs, respectively. The dependencies between degradation processes and random shocks and among degradation processes are addressed by PDMP modeling. The procedures of the MC simulation and FV methods to solve the model are developed. A subsystem of a RHRS in a nuclear power plant, which consists of a pneumatic valve and a centrifugal pump, is considered as the illustrative example to demonstrate the effectiveness and modeling capabilities of the proposed framework. As original contribution and differently from our previous work [16], this work is first in considering system reliability under both continuous and multi-state degradation processes, random shocks and their dependencies.

As future work, we will include maintenance in the model and derive optimal maintenance policies under the conditions considered.

Acknowledgement

The authors would like to thank Mrs. Dominique VASSEUR, Mr. Antoine DESPUJOLS and Mr. Emmanuel ARDILLON from the Department Industrial Risks Management (MRI), Electricité de France R&D for their insightful comments. The work was supported by Electricité de France Contract No.8610-5910112096.

References

[1] L. Jiang, Q. Feng, and D. W. Coit, "Modeling zoned shock effects on stochastic degradation in dependent failure processes," *IIE Transactions,* vol. 47, pp. 460-470, 2015.

[2] E. Keedy and Q. Feng, "Reliability analysis and customized preventive maintenance policies for stents with stochastic dependent competing risk processes," *Reliability, IEEE Transactions on,* vol. 62, pp. 887-897, 2013.

[3] N. Rasmekomen and A. K. Parlikad, "Maintenance optimization for asset systems with dependent performance degradation," *Reliability, IEEE Transactions on,* vol. 62, pp. 362-367, 2013.

[4] Y. Wang and H. Pham, "Modeling the dependent competing risks with multiple degradation processes and random shock using time-varying copulas," *Reliability, IEEE Transactions on,* vol. 61, pp. 13-22, 2012.

[5] M. Marseguerra, E. Zio, and L. Podofillini, "A multiobjective genetic algorithm approach to the optimization of the technical specifications of a nuclear safety system," *Reliability Engineering & System Safety,* vol. 84, pp. 87-99, 2004.

[6] A. Schöttl, "A reliability model of a system with dependent components," *IEEE transactions on reliability,* vol. 45, pp. 267-271, 1996.

[7] S. Song, D. W. Coit, Q. Feng, and H. Peng, "Reliability analysis for multi-component systems subject to multiple dependent competing failure processes," *Reliability, IEEE Transactions on,* vol. 63, pp. 331-345, 2014.

[8] M. Black, A. Brint, and J. Brailsford, "A semi-Markov approach for modelling asset deterioration," *Journal of the Operational Research Society,* vol. 56, pp. 1241-1249, 2005.

[9] M. Giorgio, M. Guida, and G. Pulcini, "An age-and state-dependent Markov model for degradation processes," *IIE Transactions,* vol. 43, pp. 621-632, 2011.

[10] R. Moghaddass and M. J. Zuo, "Multistate degradation and supervised estimation methods for a condition-monitored device," *IIE Transactions,* vol. 46, pp. 131-148, 2014.

[11] M. Chookah, M. Nuhi, and M. Modarres, "A probabilistic physics-of-failure model for prognostic health management of structures subject to pitting and corrosion-fatigue," *Reliability Engineering & System Safety,* vol. 96, pp. 1601-1610, 2011.

[12] M. J. Daigle and K. Goebel, "A model-based prognostics approach applied to pneumatic valves," *International Journal of Prognostics and Health Management* vol. 2, pp. 84-99, 2011.

[13] W. Wang, Z. Shen, and V. Dinavahi, "Physics-Based Device-Level Power Electronic Circuit Hardware Emulation on FPGA," *Industrial Informatics, IEEE Transactions on,* vol. 10, pp. 2166-2179, 2014.

[14] Y.-H. Lin, Y.-F. Li, and E. Zio, "Integrating Random Shocks Into Multi-State Physics Models of Degradation Processes for Component Reliability Assessment," *Reliability, IEEE Transactions on,* vol. 64, pp. 154-166, 2015.

[15] X. Hu, R. Xiong, and B. Egardt, "Model-based dynamic power assessment of lithium-ion batteries considering different operating conditions," *Industrial Informatics, IEEE Transactions on,* vol. 10, pp. 1948-1959, 2014.

[16] Y.-H. Lin, Y.-F. Li, and E. Zio, "Fuzzy Reliability Assessment of Systems with Multiple Dependent Competing Degradation Processes," *Fuzzy Systems, IEEE Transactions on,* 2014.

[17] J. Salonen, P. Auerkari, O. Lehtinen, and M. Pihkakoski, "Experience on in-service damage in power plant components," *Engineering Failure Analysis,* vol. 14, pp. 970-977, 2007.

[18] G. Becker, L. Camarinopoulos, and D. Kabranis, "Dynamic reliability under random shocks," *Reliability Engineering & System Safety,* vol. 77, pp. 239-251, 2002.

[19] L. Jiang, Q. Feng, and D. W. Coit, "Reliability and maintenance modeling for dependent competing failure processes with shifting failure thresholds," *Reliability, IEEE Transactions on,* vol. 61, pp. 932-948, 2012.

[20] H. Peng, Q. Feng, and D. W. Coit, "Reliability and maintenance modeling for systems subject to multiple dependent competing failure processes," *IIE transactions,* vol. 43, pp. 12-22, 2010.

[21] K. Rafiee, Q. Feng, and D. W. Coit, "Reliability modeling for dependent competing failure processes with changing degradation rate," *IIE Transactions,* vol. 46, pp. 483-496, 2014.

[22] S. Song, D. W. Coit, and Q. Feng, "Reliability for systems of degrading components with distinct component shock sets," *Reliability Engineering & System Safety,* vol. 132, pp. 115-124, 2014.

[23] W. S. Yang, D. E. Lim, and K. C. Chae, "Maintenance of multi-state production systems deteriorated by random shocks and production," *Journal of Systems Science and Systems Engineering,* vol. 20, pp. 110-118, 2011.

[24] Z. S. Ye, L. C. Tang, and H. Y. Xu, "A distribution-based systems reliability model under extreme shocks and natural degradation," *Reliability, IEEE Transactions on,* vol. 60, pp. 246-256, 2011.

[25] Z. Wang, H.-Z. Huang, Y. Li, and N.-C. Xiao, "An approach to reliability assessment under degradation and shock process," *Reliability, IEEE Transactions on,* vol. 60, pp. 852-863, 2011.
[26] J. E. Ruiz-Castro, "Markov counting and reward processes for analysing the performance of a complex system subject to random inspections," *Reliability Engineering & System Safety,* vol. 145, pp. 155-168, 2016.
[27] M. Marseguerra and E. Zio, "Monte Carlo approach to PSA for dynamic process systems," *Reliability Engineering & System Safety,* vol. 52, pp. 227-241, 1996.
[28] C. Cocozza-Thivent, R. Eymard, and S. Mercier, "A finite-volume scheme for dynamic reliability models," *IMA journal of numerical analysis,* vol. 26, pp. 446-471, 2006.
[29] M. J. Daigle and K. Goebel, "Model-based prognostics with concurrent damage progression processes," *Systems, Man, and Cybernetics: Systems, IEEE Transactions on,* vol. 43, pp. 535-546, 2013.
[30] R. H. Yeh, "Optimal inspection and replacement policies for multi-state deteriorating systems," *European Journal of Operational Research,* vol. 96, pp. 248-259, 1997.
[31] M. J. Zuo, B. Liu, and D. Murthy, "Replacement–repair policy for multi-state deteriorating products under warranty," *European Journal of Operational Research,* vol. 123, pp. 519-530, 2000.
[32] A. Lorton, M. Fouladirad, and A. Grall, "A methodology for probabilistic model-based prognosis," *European Journal of Operational Research,* vol. 225, pp. 443-454, 2013.
[33] D. Zwillinger, *Handbook of differential equations*: Gulf Professional Publishing, 1998.
[34] C. Cocozza-Thivent, "Processus de renouvellement markovien, Processus de Markov déterministes par morceaux," *Online book available on the webpage: http://perso-math.univ-mlv.fr/users/cocozza.christiane/recherche-page-perso/PresentationRMetPDMP.html,* 2011.
[35] M. H. Davis, *Markov Models & Optimization* vol. 49: CRC Press, 1993.
[36] A. Lisnianski, I. Frenkel, and Y. Ding, "Statistical Analysis of Reliability Data for Multi-state Systems," *Multi-state System Reliability Analysis and Optimization for Engineers and Industrial Managers,* pp. 117-142, 2010.
[37] E. Ogurtsova, "Estimating transition rates for multistate models from panel data and repeated cross-sections," *University of Groningen,* 2014.
[38] M. Newby, "Estimation of Paris-Erdogan law parameters and the influence of environmental factors on crack growth," *International journal of fatigue,* vol. 13, pp. 291-301, 1991.
[39] H. A. Chan and P. J. Englert, *Accelerated stress testing handbook: Guide for achieving quality products*: Wiley-IEEE Press, 2001.
[40] P.-E. Labeau, "A Monte Carlo estimation of the marginal distributions in a problem of probabilistic dynamics," *Reliability Engineering & System Safety,* vol. 52, pp. 65-75, 1996.
[41] R. Eymard and S. Mercier, "Comparison of numerical methods for the assessment of production availability of a hybrid system," *Reliability Engineering & System Safety,* vol. 93, pp. 168-177, 2008.
[42] E. Lewis and F. Böhm, "Monte Carlo simulation of Markov unreliability models," *Nuclear engineering and design,* vol. 77, pp. 49-62, 1984.
[43] E. Zio, *The Monte Carlo simulation method for system reliability and risk analysis*: Springer, 2013.
[44] S. Zhang, M. Hodkiewicz, L. Ma, and J. Mathew, "Machinery condition prognosis using multivariate analysis," in *Engineering asset management*: Springer, 2006, pp. 847-854.
[45] P. Moussou, S. Cambier, D. Lachene, S. Longarini, L. Paulhiac, and V. Villouvier, "Vibration investigation of a French PWR power plant piping system caused by cavitating butterfly valves," *ASME-PUBLICATIONS-PVP,* vol. 420, pp. 99-106, 2001.
[46] F. Leone, L. Nelson, and R. Nottingham, "The folded normal distribution," *Technometrics,* vol. 3, pp. 543-550, 1961.

Appendix A: FV method

Assumptions

The FV method for determining the approximated solution of the system reliability can be developed under the following assumptions [28]:

- The transition rates $\lambda_{\boldsymbol{y}_i,\boldsymbol{y}_j}(\cdot \mid \boldsymbol{\theta_K})$, $\forall \boldsymbol{y}_i, \boldsymbol{y}_j \in \boldsymbol{S'}$ are continuous and bounded functions from $\mathbb{R}^{d_L}$ to $\mathbb{R}^+$.
- The physics equations $\boldsymbol{f_L}^{\boldsymbol{y}_i}(\cdot \mid \boldsymbol{\theta_L}), \forall \boldsymbol{y}_j \in \boldsymbol{S'}$ are continuous functions from $\mathbb{R}^{d_L}$ to $\mathbb{R}^{d_L}$ and locally Lipschitz continuous.
- The physics equations $\boldsymbol{f_L}^{\boldsymbol{y}_i}(\cdot \mid \boldsymbol{\theta_L}), \forall \boldsymbol{y}_i \in \boldsymbol{S'}$ are sub-linear, i.e. there are some $V_1 > 0$ and $V_2 > 0$ such that
$$\forall \boldsymbol{x} \in \mathbb{R}^{d_L}, t \in \mathbb{R}^+ | \boldsymbol{f_L}^{\boldsymbol{y}_i}(\boldsymbol{x} \mid \boldsymbol{\theta_L})| \leq V_1 \|\boldsymbol{x}\| + V_2$$
- The functions $div(\boldsymbol{f_L}^{\boldsymbol{y}_i}(\cdot \mid \boldsymbol{\theta_L})), \forall \boldsymbol{y}_i \in \boldsymbol{S'}$ are almost everywhere bounded in absolute value by some real value $D > 0$ (independent of $\boldsymbol{y}_i$).
- If $\phi(\cdot)$ is a continuous and bounded function from $\mathbb{R}^{d_L}$ to $\mathbb{R}$, then, $\boldsymbol{x} \to \int \phi(\vec{y}) \mu(\boldsymbol{y}_i, \boldsymbol{y}_j, \boldsymbol{x})(d\boldsymbol{y})$ is continuous from $\mathbb{R}^{d_L}$ to $\mathbb{R}$.

Solution approach

For ease of notation, we let $\boldsymbol{g}^{\boldsymbol{y}_i}(\cdot, \cdot \mid \boldsymbol{\theta_L})$: $\mathbb{R}^{d_L} \times \mathbb{R} \to \mathbb{R}^{d_L}$ denote the solution of

$$\frac{\partial}{\partial t} \boldsymbol{g}^{\boldsymbol{y}_i}(\boldsymbol{x}, t \mid \boldsymbol{\theta_L}) = \boldsymbol{f_L}^{\boldsymbol{y}_i}(\boldsymbol{g}^{\boldsymbol{y}_i}(\boldsymbol{x}, t \mid \boldsymbol{\theta_L}) \mid \boldsymbol{\theta_L}), \forall \boldsymbol{y}_i \in \boldsymbol{S'}, \boldsymbol{x} \in \mathbb{R}^{d_L}, t \in \mathbb{R} \quad (19)$$

with

$$\boldsymbol{g}^{\boldsymbol{y}_i}(\boldsymbol{x}, 0 \mid \boldsymbol{\theta_L}) = \boldsymbol{x}, \forall \boldsymbol{y}_i \in \boldsymbol{S'}, \boldsymbol{x} \in \mathbb{R}^{\mathrm{d_L}} \quad (20)$$

and $\boldsymbol{g}^{\boldsymbol{y}_i}(\boldsymbol{x}, t \mid \boldsymbol{\theta_L})$ being the result of the deterministic behavior of $\boldsymbol{X}(t)$ after time *t*, starting from the point $\boldsymbol{x}$ while the processes $\boldsymbol{Y'}(t)$ hold on state $\boldsymbol{y}_i$.

The state space $\mathbb{R}^{d_L}$ of continuous variables $\boldsymbol{X'}(t)$ is divided into an admissible mesh $\mathcal{M}$, which is a family of measurable subsets of $\mathbb{R}^{d_L}$, i.e., $\mathcal{M}$ is a partition of $\mathbb{R}^{d_L}$ such that:

(21) $\bigcup_{A \in \mathcal{M}} A = \mathbb{R}^{d_L}$.

(22) $\forall A, B \in \mathcal{M},\ A \neq B \Rightarrow A \cap B = \emptyset$.

(23) $m_A = \int_A d\boldsymbol{x} > 0, \forall A \in \mathcal{M}$, where m_A is the volume of grid A.

(24) $sup_{A \in \mathcal{M}} diam(A) < +\infty$ where $diam(A) = sup_{\forall \boldsymbol{x}, \boldsymbol{y} \in A} |\boldsymbol{x} - \boldsymbol{y}|$.

Additionally, the time space $\mathbb{R}^+$is divided into small intervals $\mathbb{R}^+ = \bigcup_{n=0,1,2,\ldots} [n\Delta t, (n+1)\Delta t[$ by setting the time step $\Delta t > 0$ (the length of each interval).

The numerical scheme aims at constructing an approximate value $\rho_t(\boldsymbol{x}, \cdot)d\boldsymbol{x}$ for $p_t(d\boldsymbol{x}, \cdot)$, such that $\rho_t(\boldsymbol{x}, \cdot)$ is constant on each $[n\Delta t, (n+1)\Delta t[\times A \times \{\boldsymbol{y}_i\}, \forall A \in \mathcal{M}, \boldsymbol{y}_i \in \boldsymbol{S'}$:

$$\rho_t(\boldsymbol{x}, \boldsymbol{y}_i) = P_n(A, \boldsymbol{y}_i), \forall \boldsymbol{y}_i \in \boldsymbol{S'}, \boldsymbol{x} \in A, t \in [n\Delta t, (n+1)\Delta t[\quad (21)$$

$P_0(A, \boldsymbol{y}_i), \forall \boldsymbol{y}_i \in \boldsymbol{S'}, A \in \mathcal{M}$ is defined as follows:

$$P_0(A, \boldsymbol{y}_i) = \int_A p_0(d\boldsymbol{x}, \boldsymbol{y}_i) / m_A \quad (22)$$

Then, $P_{n+1}(A, \boldsymbol{y}_i)$ can be calculated considering the deterministic evaluation of $\boldsymbol{X}(t)$ and the stochastic evolution of $\boldsymbol{Y'}(t)$ based on $P_n(\mathcal{M}, \boldsymbol{y}_i)$ by the Chapman-Kolmogorov forward equation, as follows:

$$P_{n+1}(A, \boldsymbol{y}_i) = \frac{1}{1+\Delta t b_A^{\boldsymbol{y}_i}} \widehat{P_{n+1}}(A, \boldsymbol{y}_i) + \Delta t \sum_{B \in \mathcal{M}} \sum_{\boldsymbol{y}_j \in \boldsymbol{S'}} \frac{a_{B,A}^{\boldsymbol{y}_j, \boldsymbol{y}_i}}{1+\Delta t b_A^{\boldsymbol{y}_j}} \widehat{P_{n+1}}(B, \boldsymbol{y}_j) \quad (23)$$

where

$$a_{B,A}^{\boldsymbol{y}_j, \boldsymbol{y}_i} = \int_A \lambda_{\boldsymbol{y}_j, \boldsymbol{y}_i}(\boldsymbol{x} \mid \boldsymbol{\theta_K}) \int_B \mu(\boldsymbol{y}_j, \boldsymbol{y}_i, \boldsymbol{x})(d\boldsymbol{y}) \boldsymbol{x} / m_A \quad (24)$$

is the average transition rate from state $\boldsymbol{y}_j$ and grid B to state $\boldsymbol{y}_i$ and grid A,

$$b_A^{\boldsymbol{y}_i} = \int_A \sum_{\boldsymbol{y}_j \in \boldsymbol{S'}} \lambda_{\boldsymbol{y}_i, \boldsymbol{y}_j}(\boldsymbol{x} \mid \boldsymbol{\theta_K}) d\boldsymbol{x} / m_A \quad (25)$$

is the average transition rate out of state $\boldsymbol{y}_i$ for grid A,

$$\widehat{P_{n+1}}(A, \boldsymbol{y}_i) = \sum_{B \in \mathcal{M}} m_{BA}^{\boldsymbol{y}_i} P_n(B, \boldsymbol{y}_i) / m_A \quad (26)$$

is the approximate value of probability density function on $[(n+1)\Delta t, (n+2)\Delta t[\times A \times \{\boldsymbol{y}_i\}$

according to the deterministic evolution of $\boldsymbol{X}(t)$,

$$m_{BA}^{\boldsymbol{y}_i} = \int_{\{\boldsymbol{y}\in B \mid \boldsymbol{g}^{\boldsymbol{y}_i}(\boldsymbol{y},\Delta t \mid \boldsymbol{\theta_L})\in A\}} d\boldsymbol{y} \tag{27}$$

is the volume of the part of grid B which will enter grid A after time Δt, according to the deterministic evolution of $\boldsymbol{X}(t)$.

The approximated solution $\rho_t(\boldsymbol{x},\cdot)d\boldsymbol{x}$ weakly converges towards $p_t(d\boldsymbol{x},\cdot)$ when $\Delta t \to 0$ and $|\mathcal{M}|/\Delta t \to 0$ where $|\mathcal{M}| = sup_{A\in\mathcal{M}} diam(A)$.

Appendix B: Equations for MC simulation method in case study

The semi-Markov kernel of $\{\boldsymbol{Z}_n, T_n\}_{n\geq 0}$ is $N\big(\boldsymbol{i}=(x,\boldsymbol{y}_i),(dx,\boldsymbol{y}_j),dt\big) = Q(\varphi(\boldsymbol{i},t),(dx,\boldsymbol{y}_j))\ \ dF_{\boldsymbol{i}}(t), \forall k\in\mathbb{N}, \boldsymbol{y}_i,\boldsymbol{y}_j\in\boldsymbol{S}, x\in\mathbb{R}^+, dx\to 0, dt\to 0$. According to the degradation models of the system, we can obtain that:

$$dF_{\boldsymbol{i}=(x,\boldsymbol{y}_i)}(t) = \lambda_{\boldsymbol{y}_i} e^{-\lambda_{\boldsymbol{y}_i} t} dt \tag{28}$$

where $\lambda_{\boldsymbol{y}_i}$ is the sum of the outgoing transition rates of $Y(t)$ from state $\boldsymbol{y}_i$, and

$$\begin{aligned} &Q(\varphi(\boldsymbol{i},t),(dx,\boldsymbol{y}_i)) \\ &= P\big[D_{k+1}\in[x,x+dx] \mid Y_{k+1}=\boldsymbol{y}_j, T_{k+1}-T_k\in[t,t+dt], \boldsymbol{Z}_k=\boldsymbol{i}\big] \\ &\cdot P\big[Y_{k+1}=\boldsymbol{y}_j \mid T_{k+1}-T_k\in[t,t+dt], \boldsymbol{Z}_k=\boldsymbol{i}\big] \end{aligned} \tag{29}$$

where

$$\begin{aligned} &P\big[Y_{k+1}=\boldsymbol{y}_j \mid T_{k+1}-T_k\in[t,t+dt], \boldsymbol{Z}_k=\boldsymbol{i}\big] \\ &= P\big[Y_{k+1}=\boldsymbol{y}_j \mid Y_k=\boldsymbol{y}_i\big] \\ &= \frac{\lambda_{y_i,y_j}}{\lambda_{y_i}} \end{aligned} \tag{30}$$

where $\lambda_{\boldsymbol{y}_i,\boldsymbol{y}_j}$ is the transition rate of $Y(t)$ from state $\boldsymbol{y}_i$ to state $\boldsymbol{y}_j$, and

$$\begin{aligned} &P\big[D_{k+1}\in[x,x+dx] \mid Y_{k+1}=\boldsymbol{y}_j, T_{k+1}-T_k\in[t,t+dt], \boldsymbol{Z}_k=\boldsymbol{i}\big] \\ &= \begin{cases} P\big[\varphi_1(\boldsymbol{i},t)+H(T_k+t)\in[x,x+dx]\big], \\ if\ transition\ from\ \boldsymbol{y}_i\ to\ \boldsymbol{y}_j\ is\ due\ to\ random\ shock \\ \delta_{\varphi_1(\boldsymbol{i},t)}(dx), \\ if\ transition\ from\ \boldsymbol{y}_i\ to\ \boldsymbol{y}_j\ is\ due\ to\ degradation \end{cases} \end{aligned} \tag{31}$$

where $H(T_k+t)$ is the instantaneous random increase caused by shock at time T_k+t, δ is the Dirac delta function and

$$\begin{aligned} &P\big[\varphi_1(\boldsymbol{i},t)+H(T_k+t)\in[x,x+dx]\big] \\ &= \begin{cases} \Phi\big(\frac{D-\mu_w}{\sigma_w}\big)\cdot\frac{1}{\sigma_h}\phi\big(\frac{x-\varphi_1(\boldsymbol{i},t)-\mu_h}{\sigma_h}\big)\big)dx, \\ if\ x < D_b^* \\ \big(1-\Phi\big(\frac{D-\mu_w}{\sigma_w}\big)\big)\cdot\delta_{\varphi_1(\boldsymbol{i},t)+D_b^*}(dx) + \Phi\big(\frac{D-\mu_w}{\sigma_w}\big)\cdot\frac{1}{\sigma_h}\phi\big(\frac{x-\varphi_1(\boldsymbol{i},t)-\mu_h}{\sigma_h}\big)\big)dx, \\ if\ x \geq D_b^* \end{cases} \end{aligned} \tag{32}$$

where $\Phi(\cdot)$ and $\phi(\cdot)$ are the cumulative distribution function and the probability density function of a folded normal distribution related to the standard normal distribution, respectively. Here, since an extreme shock can directly lead the valve to failure, we assume each extreme shock increase the total external leak size by D_b^* to formulate the problem within the settings of PDMP. Note that this assumption will not change the reliability of the valve.

Appendix C: Application of FV method in case study

The probability distribution of $\boldsymbol{Z}(t)$, $p_t(dx,\boldsymbol{y}_i)$, obeys the Chapman-Kolmogorov

equation [35] as follows:

$$\int_0^t \sum_{\boldsymbol{y}_i \in \boldsymbol{S}} \int_{\mathbb{R}^+} \sum_{\boldsymbol{y}_j \in \boldsymbol{S}} \lambda_{\boldsymbol{y}_i,\boldsymbol{y}_j} \left(\int_{\mathbb{R}^+} \psi(\boldsymbol{y}_j, y) \mu(\boldsymbol{y}_i, \boldsymbol{y}_j, x)(dy) - \psi(\boldsymbol{y}_i, x) \right) p_s(dx, \boldsymbol{y}_i) ds + \int_0^t \sum_{\boldsymbol{y}_i \in \boldsymbol{S}} \int_{\mathbb{R}^+} v(\boldsymbol{y}_i) div\left(\psi(\boldsymbol{y}_i, x)\right) p_s(dx, \boldsymbol{y}_i) ds - \sum_{\boldsymbol{y}_i \in \boldsymbol{S}} \int_{\mathbb{R}^+} \psi(\boldsymbol{y}_i, x)\, p_t(dx, \boldsymbol{y}_i) + \sum_{\boldsymbol{y}_i \in \boldsymbol{S}} \int_{\mathbb{R}^+} \psi(\boldsymbol{y}_i, x)\, p_0(dx, \boldsymbol{y}_i) = 0 \quad (33)$$

where $\psi(\cdot,\cdot)$ is any continuously differentiable function from $\boldsymbol{S} \times \mathbb{R}^+$ to $\mathbb{R}$ with a compact support and $\mu(\boldsymbol{y}_i, \boldsymbol{y}_j, x)(dy)$ is the probability of $D(t) \in [y, y + dy]$ after jumping from x when $Y(t)$ steps to state $\boldsymbol{y}_j$ from state $\boldsymbol{y}_i$ as follows:

$$\mu(\boldsymbol{y}_i, \boldsymbol{y}_j, x)(dy) = \begin{cases} \Phi\left(\frac{D-\mu_w}{\sigma_w}\right) \cdot \frac{1}{\sigma_h} \phi\left(\frac{y-x-\mu_h}{\sigma_h}\right) dy, \\ if\ transition\ from\ \boldsymbol{y}_i\ to\ \boldsymbol{y}_j\ is\ due\ to\ random\ shock\ and\ y < D_b^* \\ \left(1 - \Phi\left(\frac{D-\mu_w}{\sigma_w}\right)\right) \cdot \delta_{x+D_b^*}(dy) + \Phi\left(\frac{D-\mu_w}{\sigma_w}\right) \cdot \frac{1}{\sigma_h} \phi\left(\frac{y-x-\mu_h}{\sigma_h}\right) dy \\ if\ transition\ from\ \boldsymbol{y}_i\ to\ \boldsymbol{y}_j\ is\ due\ to\ random\ shock\ and\ y \geq D_b^* \\ \delta_x(dy), \\ if\ transition\ from\ \boldsymbol{y}_i\ to\ \boldsymbol{y}_j\ is\ due\ to\ degradation \end{cases} \quad (34)$$

$P_0(m, \boldsymbol{y}_i)$ is defined as follows:

$$P_0(m, \boldsymbol{y}_i) = \int_{m\Delta x}^{(m+1)\Delta x} p_0(dx, \boldsymbol{y}_i) / \Delta x \quad (35)$$

where $p_0(dx, \boldsymbol{y}_i) = \delta_0(dx) \cdot \mathbf{1}_{\{\boldsymbol{y}_i = (3,0)\}}$. Then, $P_{n+1}(m, \boldsymbol{y}_i)$, $n \in \mathbb{N}$ can be calculated considering the deterministic evolution of $D(t)$ and the stochastic evolution of $Y(t)$ based on $P_n(\cdot,\ \cdot)$ by the Chapman-Kolmogorov forward equation, as follows:

$$P_{n+1}(m, \boldsymbol{y}_i) = \frac{1}{1 + \Delta t \lambda_{\boldsymbol{y}_i}} \widehat{P_{n+1}}(m, \boldsymbol{y}_i) + \Delta t \sum_{m' \in \mathbb{N}} \sum_{\boldsymbol{y}_j \in \boldsymbol{S}} \frac{a_{m',m}^{\boldsymbol{y}_j,\boldsymbol{y}_i}}{1 + \Delta t \lambda_{\boldsymbol{y}_j}} \widehat{P_{n+1}}(m', \boldsymbol{y}_j) \quad (36)$$

where

$$a_{m',m}^{\boldsymbol{y}_j,\boldsymbol{y}_i} = \lambda_{\boldsymbol{y}_j,\boldsymbol{y}_i} \int_{m'\Delta x}^{(m'+1)\Delta x} \int_{m\Delta x}^{(m+1)\Delta x} \mu(\boldsymbol{y}_j, \boldsymbol{y}_i, x)(dy) dx / \Delta x \quad (37)$$

is the average transition rate from state $\boldsymbol{y}_j$ and grid $[m'\Delta x, (m'+1)\Delta x[$ to state $\boldsymbol{y}_i$ and grid $[m\Delta x, (m+1)\Delta x[$,

$$\widehat{P_{n+1}}(m, \boldsymbol{y}_i) = \sum_{m' \in \mathbb{N}} v_{m',m}^{\boldsymbol{y}_i} P_n(m', \boldsymbol{y}_i) / \Delta x \quad (38)$$

is the approximate value of probability density function on $[m\Delta x, (m+1)\Delta x[\times \{\boldsymbol{y}_i\}$ according to the deterministic evolution of $D(t)$ between jumps of $Y(t)$ and

$$v_{m',m}^{\boldsymbol{y}_i} = \int_{\{x \in [m'\Delta x, (m'+1)\Delta x[\ |\ (\varphi_1((x,\boldsymbol{y}_i), \Delta t) \in [m\Delta x, (m+1)\Delta x[\}} dx \quad (39)$$

is the volume of the part of grid $[m'\Delta x, (m'+1)\Delta x[$ which will enter grid $[m\Delta x, (m+1)\Delta x[$ after time Δt according to the deterministic evaluation of $D(t)$.

PAPER VII: Y.-H. Lin, Y.-F. Li, E. Zio. A Reliability Assessment Framework for Systems with Multiple Dependent Competing Degradation Processes. *Systems, Man, and Cybernetics: Systems, IEEE Transactions on*. (Accepted)

A Reliability Assessment Framework for Systems with Degradation Dependency by Combining Binary Decision Diagrams and Monte Carlo simulation

Yan-Hui Lin[1], Yan-Fu Li[1] senior member IEEE, Enrico Zio[1,2] senior member IEEE

[1] *Chair on Systems Science and the Energetic Challenge, Fondation EDF, at Ecole Centrale Paris- Supelec, France*

[2]*Politecnico di Milano, Italy*

Abstract – Components are often subject to multiple competing degradation processes. This paper presents a reliability assessment framework for multi-component systems whose component degradation processes are modeled by multi-state and physics-based models with limited statistical degradation/failure data. The piecewise-deterministic Markov process modeling approach is employed to treat dependencies between the degradation processes within one component or/and among components. A computational method combining binary decision diagrams (BDDs) and Monte Carlo simulation (MCS) is developed to solve the model. A BDD is used to encode the fault tree of the system and obtain all the paths leading to system failure or operation. MCS is used to generate random realizations of the model and compute the system reliability. A case study is presented, with reference to one branch of the residual heat removal system (RHRS) of a nuclear power plant.

Key Words – System reliability analysis, Degradation dependency, Piecewise-deterministic Markov process, Binary decision diagrams, Monte Carlo simulation.

Acronyms

PBMs	Physics-based models
MSMs	Multi-state models
FTA	Fault tree analysis
CCFs	Common cause failures
BDDs	Binary decision diagrams
MCS	Monte Carlo simulation
RHRS	Residual heat removal system
WDFLM	Weighting depth-first left-most
DFLM	Depth-first left-most

ite if-then-else

Notations

C	Number of components in the system
L	Group of degradation processes modeled by PBMs
K	Group of degradation processes modeled by MSMs
$\boldsymbol{D}_{Oc}$	Degradation state of component O_c
$\overrightarrow{X_{L_m}}(t)$	Time-dependent continuous variables of degradation process L_m
$\overrightarrow{X_{L_m}^D}(t)$	Non-decreasing degradation variables vector
$\overrightarrow{X_{L_m}^P}(t)$	Physical variables vector
$\mathcal{F}_{L_m}$	Set of failure states of degradation process L_m
$Y_{K_n}(t)$	State variable of degradation process K_n
S_{K_n}	Finite state set of degradation process K_n
$\mathcal{F}_{K_n}$	Set of failure states of degradation process K_n
$\vec{Z}(t)$	Degradation state of the system
θ_K	Environmental and operational factors in K
$\lambda_i(j \mid \boldsymbol{\theta}_{K_n})$	Transition rate from state i to j
θ_L	Environmental and operational factors in L
$\overrightarrow{f_{L_m}}(\overrightarrow{X_{L_m}}(t), t \mid \boldsymbol{\theta}_{L_m})$	Physics equations of degradation process L_m
$\overrightarrow{Z_{p,q}}(t)$	Stochastic process of one group of interdependent degradation processes
$N\left(\vec{\imath}, \overrightarrow{dz}, ds \mid \boldsymbol{\theta}_{K_q}\right)$	Semi-Markov kernel

1. INTRODUCTION

Most components undergo degradation processes before failure. A number of degradation models have been proposed in the field of reliability engineering based on the available information/data, which can be mainly classified into the following groups: statistical distributions (e.g. Bernstein distribution [1]), stochastic processes (e.g. Gamma process [2]),

multi-state models (MSMs) (e.g. semi-Markov model [3]) and physics-based models (PBMs) (e.g. probabilistic superposition model [4]). Among the existing degradation models, PBMs [5-7] and MSMs [8-10] can be used to describe the evolution of degradation in structures, systems and components, for which statistical degradation/failure data are insufficient, e.g. the highly reliable devices in the nuclear and aerospace industries. A PBM gives an integrated mechanistic description of the component life consistent with the underlying real degradation mechanisms (e.g. wear, corrosion, fatigue, etc.) by using physics knowledge and equations [4], whereas a MSM describes the degradation process in a discrete way, supported by material science knowledge, degradation and/or failure data from historical field collection or degradation tests [11, 12].

In reality, components/systems are often subject to multiple competing degradation processes. The dependencies among these processes within one component (e.g. the wear of rubbing surfaces influenced by the environmental stress shock within a micro-engine [13]), or/and among different components (e.g. the degradation of the pre-filtrations stations leading to a lower performance level of the sand filter in a water treatment plant [14]) need to be considered. Components can be dependent due to functional dependence, where the failure of a trigger component causes other components to become inaccessible or unusable [15, 16]. Competing failure propagation and failure isolation effects have been studied in [17, 18], where a failure not only causes outage to the component from which the failure originates, but also propagates through all other system components causing the entire system failure and failure isolation occurs when the failure of one component causes other components within the same system to become isolated from the system.

Recently, the authors have employed the piecewise-deterministic Markov process (PDMP) modeling framework to integrate PBMs and MSMs for treating the dependencies among degradation processes [19] for a system with a small number of components, where the whole system is modeled by one PDMP. For systems of larger size, the high dimension of its PDMP can lead to very heavy computational burdens, because solving the PDMP of a small system is already time consuming due to the combinatorial nature of MSMs and the need to simulate the trajectory between any two system states [19]. In addition, the dependencies may only exist within certain groups of components and leave different groups being independent [20], and the causes to systems failure are not easy to be identified.

Fault tree analysis (FTA) [21] is typically used to identify the combinations of events leading to system failure and compute its probability by using minimal cut sets found from the fault tree structure. For real systems, this can be computationally intensive, when the tree structure is large and, especially, if it contains repeated basic events [22]. In addition, all basic events are usually assumed statistically independent.

Common cause failures (CCFs) of components have been considered in [23-25]: implicit and explicit methods have been developed to evaluate the system reliability. In binary-state systems, components failures with dependent propagation effects have been studied in [26], within a dynamic FTA framework. The statistical dependence of component states across different phases of phased-mission systems has been treated by using multiple-valued decision diagrams to encode fault trees in [27, 28].

On the contrary, the dependencies of the degradation processes leading to failure of different components need to be considered which render certain basic events under different gates being dependent. To the knowledge of the authors, there is no published research work to tackle this problem, of practical reference [29].

To take into account such dependencies at a relatively low computational cost for systems

of larger size, a system reliability assessment method is proposed combining binary decision diagrams (BDDs) [30] and Monte Carlo simulation (MCS) [31]. Instead of modeling the degradation of the whole system by one PDMP as in [19], the proposed method can identify the groups of components being dependent and decompose the original PDMP into a group of smaller ones which are independent from each other and easier to be solved. Besides, the states of these PDMPs leading to the systems failure can be easily obtained. Firstly, a fault tree is transformed to a BDD from which all paths leading to the system failure or operation can be efficiently obtained. BDDs [30] are directed acyclic graphs, encoding Shannon's decomposition of a formula, and have been implemented in many domains; they possess the feature of sharing equivalent subgraphs and hence can reduce the computational time and memory requirements [32]. An algorithm based on BDD has been developed for reliability analysis of phased-mission systems with multimode failures in [33] to improve the efficiency and reduce the computational complexity. BDD has also been employed for network reliability and sensitivity analysis in [34]. Secondly, MCS is used to estimate the probability of each path to compute the system reliability taking into account the dependencies between basic events, since analytically solving the PDMPs is difficult, if not impossible, due to the large size and complex behavior of the system [35].

The rest of this paper is organized as follows. Section 2 provides the assumptions and model descriptions. The proposed reliability assessment method is presented in Section 3. Section 4 presents one case study on one branch of a residual heat removal system (RHRS) of a nuclear power plant. Section 5 concludes the work.

2. ASSUMPTIONS AND MODEL DESCRIPTION

2.1 General assumptions

We consider a multi-component system, made of C components denoted by $\boldsymbol{O} = \{O_1, O_2, \dots, O_C\}$.

The following assumptions are made:

- The fault tree of the system is available and contains Q basic events denoted by $\boldsymbol{e} = \{e_1, e_2, \dots, e_Q\}$ which include the failures of components and other events such as erroneous operation caused by human errors. The component-failure type of events are determined by their underlying degradation processes.
- Each component may be affected by multiple degradation processes, possibly dependent. The degradation processes can be separated into two groups: (1) $\boldsymbol{L} = \{L_1, L_2, \dots, L_M\}$ modeled by M PBMs; (2) $\boldsymbol{K} = \{K_1, K_2, \dots, K_N\}$ modeled by N MSMs, where $L_m, m = 1, 2, \dots, M$ and $K_n, n = 1, 2, \dots, N$ are the indexes of the degradation processes. The degradation state of a component $O_c \in \boldsymbol{O}, c = 1, 2, \dots, C$, is determined by its degradation processes $\boldsymbol{D}_{O_c} \subseteq \boldsymbol{L} \cup \boldsymbol{K}$ and the component fails when its degradation processes enter its failure state space (see the two bullets below for its definition).
- A degradation process $L_m \in \boldsymbol{L}$ in the first group is described by d_{L_m} time-dependent continuous variables $\overrightarrow{X_{L_m}}(t) = \left(\overrightarrow{X_{L_m}^{\boldsymbol{D}}}(t), \overrightarrow{X_{L_m}^{\boldsymbol{P}}}(t)\right) \in \mathbb{R}^{d_{L_m}}$ in terms of: (1) the non-decreasing degradation variables vector $\overrightarrow{\mathrm{X}_{L_m}^{\boldsymbol{D}}}(\mathrm{t})$ (e.g. crack length) representing the component degradation condition; (2) the physical variables $\overrightarrow{X_{L_m}^{\boldsymbol{P}}}(t)$ (e.g. velocity)

influencing $\overrightarrow{X_{L_m}^{D}}(t)$ and vice versa. d_{L_m} is the number of non-decreasing degradation variables and physical variables for a degradation process L_m. Their evolution is characterized by a system of first-order differential equations $\overrightarrow{\dot{X}_{L_m}}(t) = \overrightarrow{f_{L_m}}\left(\overrightarrow{X_{L_m}}(t), t \mid \boldsymbol{\theta}_{L_m}\right)$, i.e. physics equations, where $\boldsymbol{\theta}_{L_m}$ represents the environmental factors to L_m (e.g. temperature and pressure) and the parameters used in $\overrightarrow{f_{L_m}}$. The evolution of physical variables can be characterized by physics equations. The environmental factors are the parameters of the physics equations and their evolution is not characterized by physics equations. If any environmental or operational factor is modeled by physics equations and influencing the degradation variables, then, it is considered as one physical variable. L_m fails when one $x_{L_m}^{i}(t) \in \overrightarrow{X_{L_m}^{D}}(t)$ reaches or exceeds its corresponding failure threshold denoted by ${x_{L_m}^{i}}^{*}$. The failure state set of L_m is denoted by $\boldsymbol{\mathcal{F}}_{L_m}$. An example of L_1 is shown in Fig. 1.

- A degradation process $K_n \in \boldsymbol{K}$ in the second group is described by the state variable $Y_{K_n}(t)$, which takes values from a finite state set $\boldsymbol{S}_{K_n} = \{0_{K_n}, 1_{K_n}, \dots, d_{K_n}\}$, where '$d_{K_n}$' is the perfect functioning state and '0_{K_n}' is the complete failure state. All intermediate states are functioning or partially functioning. The transition rates $\lambda_i\left(j \mid \boldsymbol{\theta}_{K_n}\right), \forall\, i, j \in \boldsymbol{S}_{K_n}, i > j$ characterize the degradation transition probabilities from state i to state j, where $\boldsymbol{\theta}_{K_n}$ represents the environmental factors to K_n and the related coefficients of λ_{K_n}. The failure state set of K_n is denoted by $\boldsymbol{\mathcal{F}}_{K_n} = \{0_{K_n}\}$. An example of K_1 is shown in Fig. 2.

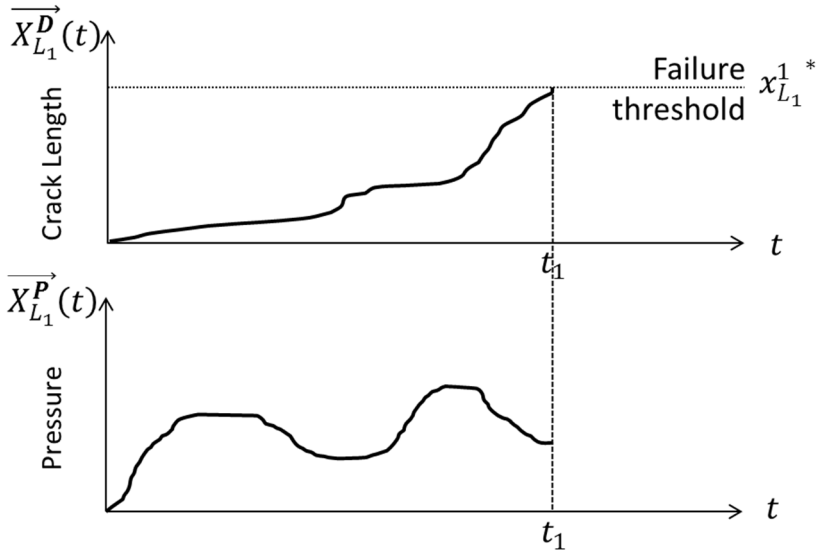

Fig. 1. An illustration of L_1.

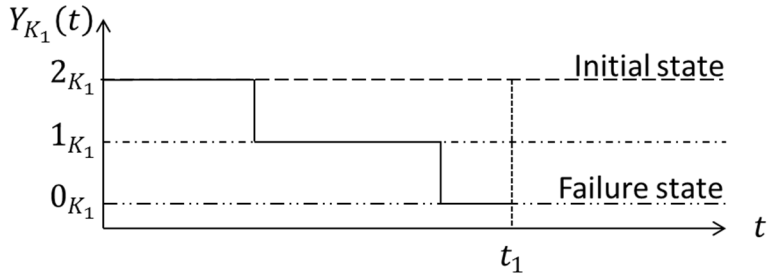

Fig. 2. An illustration of K_1.

Dependencies between degradation processes may exist both within and across groups $\boldsymbol{L}$ and $\boldsymbol{K}$. The degradation levels of the components in the first group may influence the transition times and transition directions of the degradation processes of the second group and the degradation states of the second group may influence the evolution trajectories of the continuous variables in the first group [19]. PDMPs are employed to model this dependency, the detailed formulations are shown in eqs. (1) and (2).

2.2 PDMPs for dependent degradation processes

Let us consider one group of interdependent degradation processes $\boldsymbol{L}_p = \{L_{p_1}, \dots, L_{p_n}\}$ and $\boldsymbol{K}_q = \{K_{q_1}, \dots, K_{q_m}\}$, which have no dependencies with the other degradation processes. Their degradation states are represented by

$$\overrightarrow{Z_{p,q}}(t) = \begin{pmatrix} \begin{pmatrix} \overrightarrow{X_{L_{p_1}}}(t) \\ \vdots \\ \overrightarrow{X_{L_{p_n}}}(t) \end{pmatrix} = \overrightarrow{X_p}(t) \\ \begin{pmatrix} Y_{q_1}(t) \\ \vdots \\ Y_{q_m}(t) \end{pmatrix} = \overrightarrow{Y_q}(t) \end{pmatrix} \in \boldsymbol{E}_{p,q} = \mathbb{R}^{d_{\boldsymbol{L}p}} \times \boldsymbol{S}_{\boldsymbol{K}_q}, \forall t \geq 0 \tag{1}$$

where $\boldsymbol{E}_{p,q}$ is the space combining $\mathbb{R}^{d_{\boldsymbol{L}p}}$ ($d_{\boldsymbol{L}_p} = \sum_{k=1}^{n} d_{L_{p_k}}$) and $\boldsymbol{S}_{\boldsymbol{K}_q} = \{0, 1, \dots, d_{\boldsymbol{K}_q}\}$ denotes the state set of process $\overrightarrow{Y_q}(t)$.

The evolution of the vector of degradation states $\overrightarrow{Z_{p,q}}(t)$ involves (1) the stochastic transition process of $\overrightarrow{Y_q}(t)$ and (2) the deterministic progression of $\overrightarrow{X_p}(t)$, between successive transitions of $\overrightarrow{Y_q}(t)$, given $\overrightarrow{Y_q}(t)$. The first process is governed by the transition rates of $\overrightarrow{Y_q}(t)$, which depend on the degradation levels of the components in the first group, as follows::

$$\begin{aligned} &\lim_{\Delta t \to 0} P\left(\overrightarrow{Y_q}(t + \Delta t) = \vec{j} \middle| \overrightarrow{Z_{p,q}}(t) = (\overrightarrow{X_p}(t), \overrightarrow{Y_q}(t) = \vec{\imath})^T, \boldsymbol{\theta}_{\boldsymbol{K}_q}\right) \\ &= \lambda_{\vec{\imath}}^{q}\left(\vec{j} | \overrightarrow{X_p}(t), \boldsymbol{\theta}_{\boldsymbol{K}_q}\right) \Delta t, \forall\, \vec{\imath}, \vec{j} \in \boldsymbol{S}_{\boldsymbol{K}_q}, \vec{\imath} \neq \vec{j} \end{aligned} \tag{2}$$

where the parameter vector $\boldsymbol{\theta}_{\boldsymbol{K}_q}$ represents environmental and operational factors influencing the degradation processes in $\boldsymbol{K}_q$. The second evolution process is described by the deterministic physics equations which depend on the degradation states of the second group as follows:

$$\overrightarrow{\dot{X}_p}(t) = \begin{pmatrix} \overrightarrow{\dot{X}_{L_{p_1}}}(t) \\ \vdots \\ \overrightarrow{\dot{X}_{L_{p_n}}}(t) \end{pmatrix} = \begin{pmatrix} \overrightarrow{f_{L_{p_1}}}\left(\overrightarrow{Z_{p,q}}(t), t \middle| \boldsymbol{\theta}_{L_{p_1}}\right) \\ \vdots \\ \overrightarrow{f_{L_{p_n}}}\left(\overrightarrow{Z_{p,q}}(t), t \middle| \boldsymbol{\theta}_{L_{p_n}}\right) \end{pmatrix}$$
$$= \overrightarrow{f_{L_p}}\left(\overrightarrow{Z_{p,q}}(t), t \middle| \boldsymbol{\theta}_{\boldsymbol{L}_p} = \left(\boldsymbol{\theta}_{L_{p_1}}, \dots, \boldsymbol{\theta}_{L_{p_n}}\right)\right) \quad (3)$$

where the parameter vector $\boldsymbol{\theta}_{L_{p_k}}, k = 1,2, \dots, n$ represents environmental and operational factors influencing the degradation processes in L_{p_k}. It should be noted that the evolution of one degradation process in $\overrightarrow{Z_{p,q}}(t)$ depends on the states of all the degradation processes in $\overrightarrow{Z_{p,q}}(t)$.

3. METHODOLOGY

In this section, a computational method combining BDDs and MCS is proposed.

3.1 Binary decision diagrams

A BDD is a directed acyclic graph encoding Shannon's decomposition of a formula. A BDD has two terminal vertices labeled 1 and 0 to indicate the failure and operation of the system, respectively. Each non-terminal vertex is labeled with a variable and has two outgoing edges: 1-edge and 0-edge which indicate the occurrence and non-occurrence of the corresponding basic event, respectively.

A BDD is employed to encode the fault tree of the system according to the given ordering of the indicator variable X_i used to denote the occurrence or non-occurrence of the basic event i ($X_i = 1$ indicating the occurrence of the basic event i and $X_i = 0$ indicating the opposite). The size of the BDD largely depends on the given ordering and the problem of finding the global optimal ordering is an intractable task [36, 37]. Several ordering heuristics have been developed, whose performances may vary on different problems. In this work, we employ the weighting depth-first left-most (WDFLM) ordering technique proposed in [38], which leads to satisfactory results according to the tests in [39, 40]. WDFLM first assigns weight 1 to each basic event. Then, it traverses the fault tree bottom-up to calculate the weight of each gate by adding the weights of all its inputs, i.e. gates and basic events. Fig. 3 shows an example of a fault tree where the weights of the gates are obtained through WDFLM.

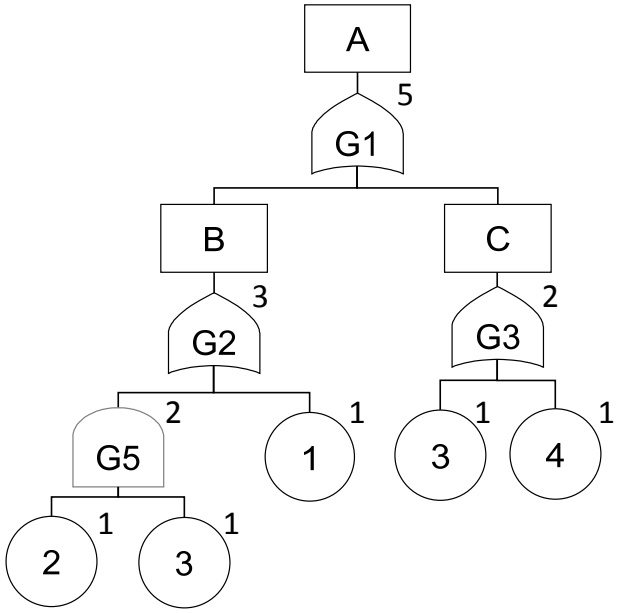

Fig. 3. An illustration of fault tree labeled with weights.

Then, the inputs of a gate are rearranged in the order of increasing weights as shown in Fig. 4.

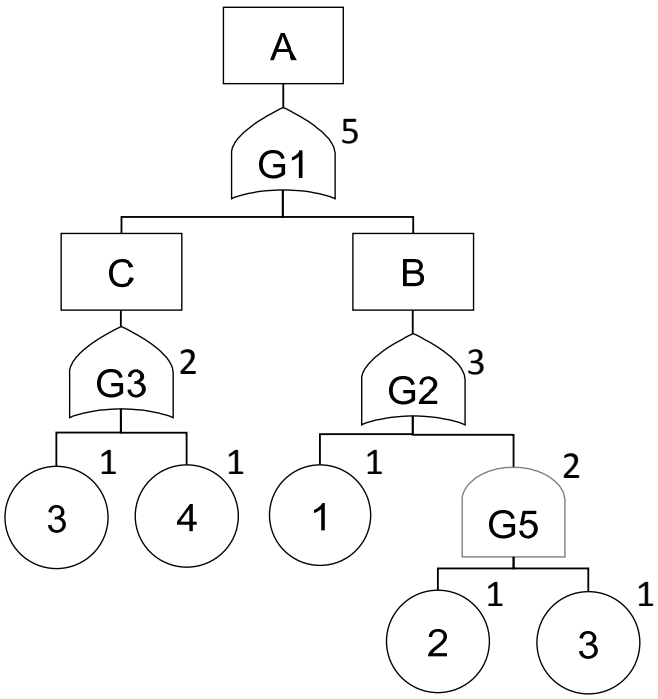

Fig. 4. An illustration of fault tree with rearranged inputs of gates.

Finally, the depth-first left-most (DFLM) ordering technique [41] is applied to the fault tree

to get the variable ordering. In this technique, the basic events are placed in the ordered list as soon as they are encountered during the DFLM traversal of the fault tree. Let $<$ be a total ordering of variables, for the fault tree in Fig. 3 it is $X_3 < X_4 < X_1 < X_2$.

Based on the variable ordering, the related BDD can be constructed using the bottom-up procedure. Firstly, all basic events $i, i \in \boldsymbol{e}$ are associated with the if-then-else (ite) structure [42] $ite(X_i, 1, 0)$, where $ite(X_i, f_1, f_2) = (X_i \wedge f_1) \vee (\neg X_i \wedge f_2)$, which means if the basic event i occurs then consider function f_1 else consider function f_2. Then, work from the bottom to the top of the fault tree and obtain the ite structure for each gate by using the following principle: let us consider two variables $X_a < X_b$ and four functions f_1, f_2, f_3, f_4, let $<>$ be any logic operation AND or OR, then:

$$ite(X_a, f_1, f_2) <> ite(X_a, f_3, f_4) = ite(X_a, f_1 <> f_3, f_2 <> f_4) \quad (4)$$

and

$$ite(X_a, f_1, f_2) <> ite(X_b, f_3, f_4) = ite\big(X_a, f_1 <> ite(X_b, f_3, f_4), f_2 <> ite(X_b, f_3, f_4)\big) \quad (5)$$

The ite structure of the top event of the fault tree in Fig. 3 can be obtained as $\mathrm{ite}(\mathrm{X_3}, 1, \mathrm{ite}(\mathrm{X_4}, 1, \mathrm{ite}(\mathrm{X_1}, 1, 0)))$. The associated BDD shown in Fig. 5 can be constructed by breaking down each ite structure into its left and right branches, and eliminating the vertexes that are not useful (a vertex is not useful when its two outgoing edges point to the same vertex or it is equivalent to another vertex) [43].

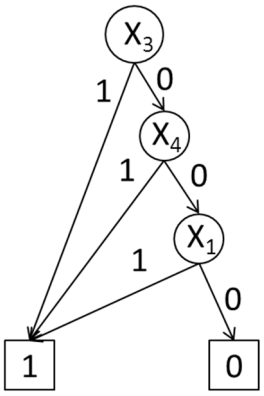

Fig. 5. BDD for fault tree in Fig. 3.

Finally, all the paths leading to system failure can be obtained as $(1)X_3 = 1, (2)X_3 = 0, X_4 = 1, (3)X_3 = 0, X_4 = 0, X_1 = 1$ and the path leading to system operation is $X_3 = 0, X_4 = 0, X_1 = 0$. The exact system reliability is equal to the sum of the probability of occurrence of the paths leading to system operation or $1 -$ the sum of the probability of occurrence of the paths leading to system failure.

3.2 MCS for PDMPs

To derive the probability of occurrence of one path, all the PDMPs containing the variables involved in that path need to be solved. Since the PDMPs are independent from each other, the product of the probabilities of PDMPs being in the states indicated by the path equals the

probability of occurrence of that path. Analytically solving the PDMPs is a difficult task, whereas MCS is well suited.

We develop a MCS algorithm for solving the PDMPs. It consists of sampling the transition time and the arrival state for the MSMs and, then, calculating the behavior of the PBMs within the transition times using the physics equation.

Refer to one PDMP presented in Section 2.2. Let $\overrightarrow{Z_{p,q}^k} = \overrightarrow{Z_{p,q}}(T^k) = \begin{pmatrix} \overrightarrow{X_p}(T^k) \\ \overrightarrow{Y_q^k} \end{pmatrix} \in \boldsymbol{E}_{p,q}, k \in \mathbb{N}$, where $\overrightarrow{Y_q^k} \in S_{K_q}, k \in \mathbb{N}$ denotes the state of $\overrightarrow{Y_q}(t)$ after k transitions from the beginning (a transition occurs as long as any one of the elements in $\overrightarrow{Y_q}(t)$ changes its state) and T^k denotes the time of arrival at state $\overrightarrow{Y_q^k}$. Then, $\left\{\overrightarrow{Z_{p,q}^k}, T^k\right\}_{k\geq 0}$ is a Markov renewal process defined on the space $\boldsymbol{E}_{p,q} \times \mathbb{R}^+$ [44]. We can obtain that

$$P\left[\overrightarrow{Z_{p,q}^{n+1}} \in B, T^{n+1} \in [T^n, T^n + \Delta t] | \overrightarrow{Z_{p,q}^n} = \vec{\imath}, \boldsymbol{\theta}_{K_q}\right] = \iint\limits_{B*[0,\Delta t]} N\left(\vec{\imath}, \overrightarrow{dz}, ds | \boldsymbol{\theta}_{K_q}\right) \quad \forall\, n \geq 0, \Delta t \geq 0, \vec{\imath} \in \boldsymbol{E}_{p,q}, B \in \varepsilon \tag{6}$$

where ε is a σ-algebra of $\boldsymbol{E}_{p,q}$ and $N\left(\vec{\imath}, \overrightarrow{dz}, ds | \boldsymbol{\theta}_{K_q}\right)$ is a semi-Markov kernel on $\boldsymbol{E}_{p,q}$, which verifies that $\iint_{\boldsymbol{E}_{p,q}*[0,\Delta\, t]} N\left(\vec{\imath}, \overrightarrow{dz}, ds | \boldsymbol{\theta}_{K_q}\right) \leq 1, \forall\, \Delta t \geq 0, \vec{\imath} \in \boldsymbol{E}_{p,q}$. It can be further developed as:

$$N\left(\vec{\imath}, \overrightarrow{dz}, ds | \boldsymbol{\theta}_{K_q}\right) = dF_{\vec{\imath}}\left(s | \boldsymbol{\theta}_{K_q}\right) \beta\left(\vec{\imath}, \overrightarrow{dz} | s, \boldsymbol{\theta}_{K_q}\right) \tag{7}$$

where

$$dF_{\vec{\imath}}\left(s | \boldsymbol{\theta}_{K_q}\right) \tag{8}$$

is the probability density function of $T^{n+1} - T^n$ given $\overrightarrow{Z_{p,q}^n} = \vec{\imath}$ and

$$\beta\left(\vec{\imath}, \overrightarrow{dz} | s, \boldsymbol{\theta}_{K_q}\right) \tag{9}$$

is the conditional probability of state $\overrightarrow{Z_{p,q}^{n+1}}$ given $T^{n+1} - T^n = s$.

The simulation procedure consists of sampling the transition time from (8) and the arrival state from (9) for $\overrightarrow{Y_q}(t)$, then, calculating $\overrightarrow{X_p}(t)$ within the transition times, by using the physics equation eq. (3) until the time of system evolution reaches a certain mission time T_{miss}.

To calculate the probability of occurrence of one path (let $\overrightarrow{\boldsymbol{Z}_{p,q}^*}$ indicate the state space, which contains all the states of $\overrightarrow{Z_{p,q}}(t)$ that are consistent with the state of the path), the procedure of the MCS is presented as follows.

Set N_{max} (the maximum number of replications) and $k = 0$ (index of replication)

Set $k' = 0$ (number of trials that end in the state indicated by the path)

While $k < N_{max}$

Initialize the system by setting $\overrightarrow{Z'_{p,q}}(0) = \begin{pmatrix} \overrightarrow{X_p}(0) \\ \overrightarrow{Y'_q} \end{pmatrix}$ (initial state), and the time $T = 0$ (initial system time)

Set $t' = 0$ (state holding time)

While $T \leq T_{miss}$

Sample a t' by using (8)

Sample an arrival state $\overrightarrow{Y''_q}$ for stochastic process $\overrightarrow{Y_q}(t)$ from all the possible states by using (9)

Calculate $\overrightarrow{X_p}(s), \forall s \in [T, T + t']$ by using eq. (3)

Set $\overrightarrow{Z'_{p,q}}(s) = \begin{pmatrix} \overrightarrow{X_p}(s) \\ \overrightarrow{Y'_q} \end{pmatrix}, \forall s \in [T, T + t'[$

Set $T = T + t'$, $\overrightarrow{Z'_{p,q}}(T) = \begin{pmatrix} \overrightarrow{X_p}(T) \\ \overrightarrow{Y''_q} \end{pmatrix}$ and $\overrightarrow{Y'_q} = \overrightarrow{Y''_q}$

End While

If $\overrightarrow{Z'_{p,q}}(T_{miss}) \in \overrightarrow{\boldsymbol{Z}^*_{p,q}}$

Set $k' = k' + 1$

End if

Set $k = k + 1$

End While □

The estimated probability of occurrence of one path at time T_{miss} can be obtained by

$$\hat{P}(T_{miss}) = 1 - k'/N_{max} \tag{10}$$

with the sample variance [45] as follows:

$$var_{\hat{P}(T_{miss})} = \hat{P}(T_{miss})(1 - \hat{P}(T_{miss}))/(N_{max} - 1) \tag{11}$$

3.3 Flowchart of the proposed method

The flowchart of the whole proposed computational method combining BDDs and MCS is shown in Fig. 6.

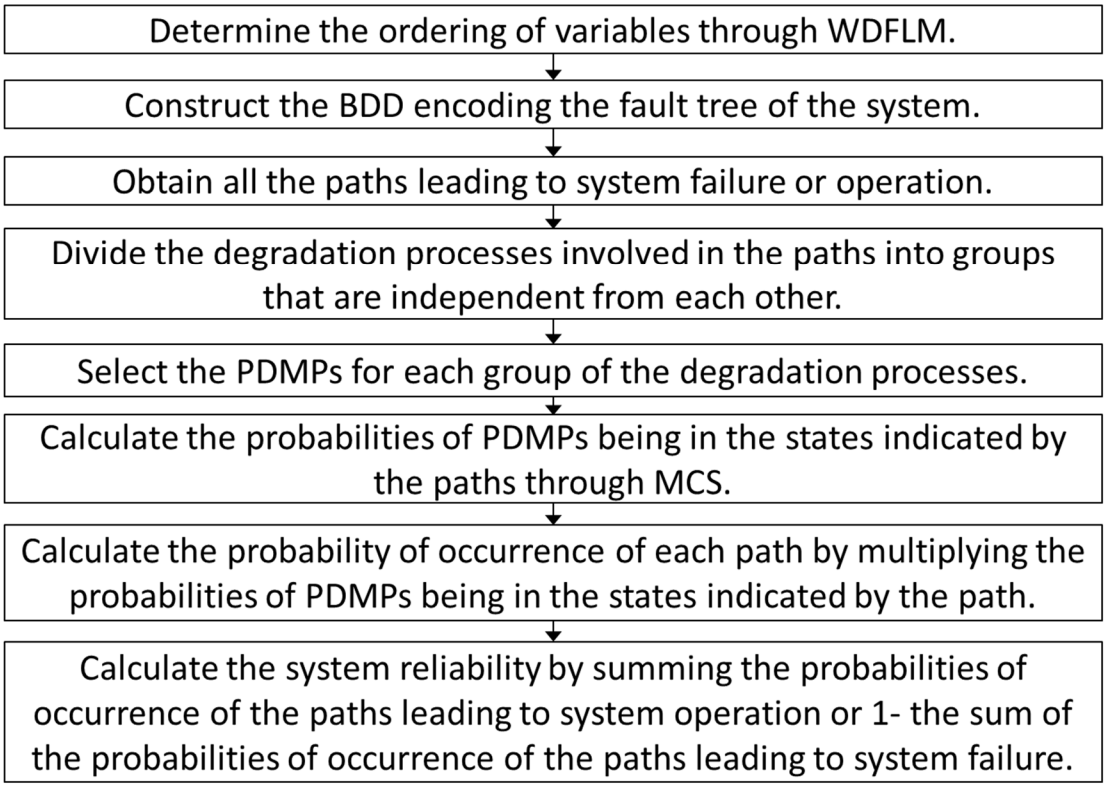

Fig. 6. The flowchart of the computational method.

4. CASE STUDY

The illustrative case refers to one branch of the RHRS [46] of a nuclear power plant shown in Fig. 7. The fault tree is shown in Fig. 8. The definitions of the basic events are presented in Table I.

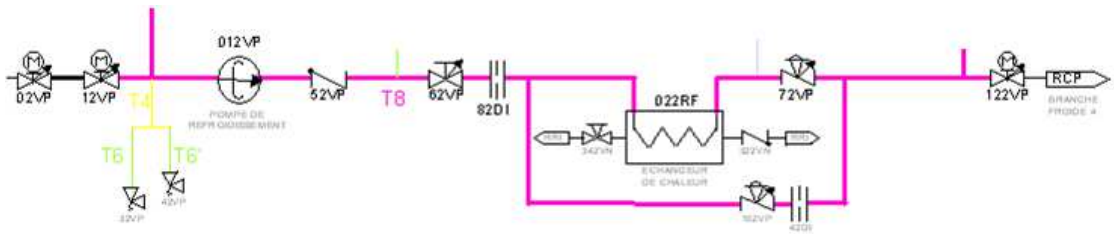

Fig. 7. The diagram of one branch of the RHRS.

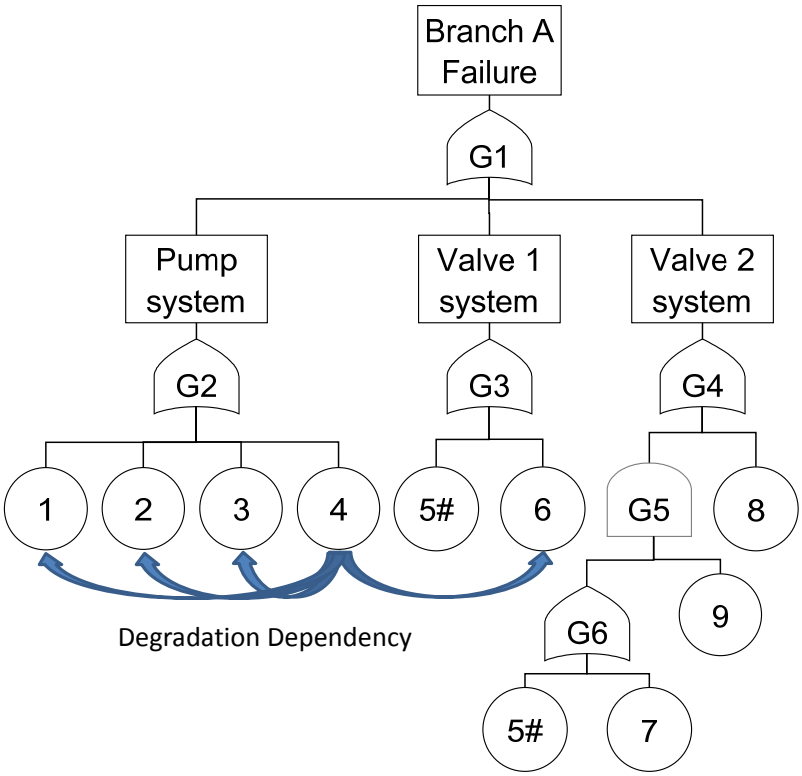

Fig. 8. The fault tree of one branch of the RHRS.

Table I Definitions of the basic events

Basic event	Definition
1	Failure of the circuit breaker
2	Failure of the motor
3	Failure of the pump contactor
4	Failure of the pump
5#	Closure due to human error
6	Failure of the valve
7	Failure of the diaphragm
8	Failure of the pneumatic valve VP1
9	Failure of the pneumatic valve VP2

By knowledge and experience of the field experts, the degradation dependency is described as follows: the degradation of the pump can lead it to vibrate [47], which will, in turn, cause the vibration of the other neighboring components (e.g. the valve) and therefore aggravate the degradation process of the latters [48]. The dependency exists between basic events 1,2,3,4 and 6, as indicated in Fig. 6.

The component degradation models provided by the expert colleagues of Electricité de France are presented below. Some degradation processes are modeled by PBMs if their degradation data is unavailable and, thus, the physics equations have to be used, whereas the others are modeled by MSMs supported by the degradation and/or failure data from historical field collection.

The circuit breaker, motor and pump contactor each have one degradation process modeled by MSMs K_1, K_2 and K_3 respectively, as shown in Fig. 9.

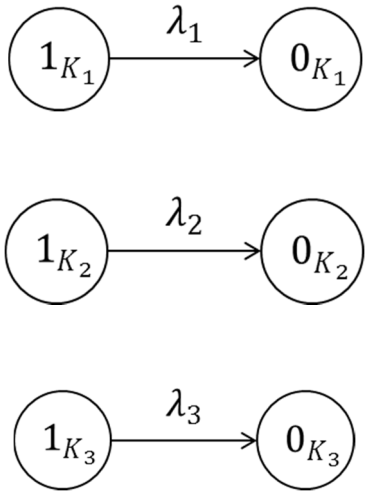

Fig. 9. The representation of the degradation processes of the circuit breaker, motor and pump contactor.

The pump has two degradation processes modeled by MSMs K_4 and K_5, as shown in Fig. 10. K_4 relates to the failure on demand and K_5 relates to the external leakage which can cause the pump to vibrate when $Y_{K_5}(t)$ reaches the state 1_{K_5}.

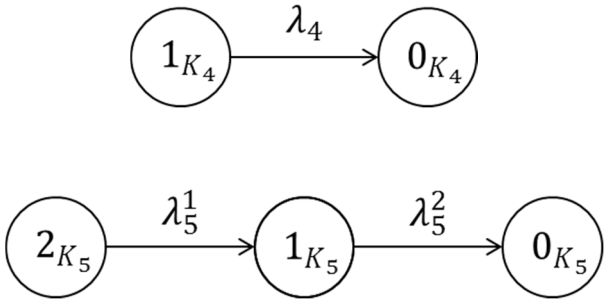

Fig. 10. The representation of the degradation processes of the pump.

Closure due to human error follows one MSM K_6, as shown in Fig. 11.

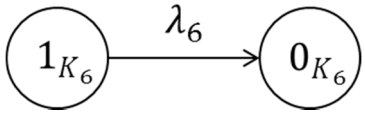

Fig. 11. The process of closure due to human error.

The valve has one degradation process modeled by one PBM L_1 related to the crack propagation due to manufacturing defects. L_1 is based on a deterministic crack growth model, which follows Paris–Erdogan law [49]. For the phase of crack propagation, the threshold is defined as the number of cycles calculated as follows,

$$N_c = \frac{1/(\frac{m}{2}-1)*(1/a_0^{\left(\frac{m}{2}-1\right)}-1/a_c^{\left(\frac{m}{2}-1\right)})}{C(f(R)_{Max}Y_{Max}\sqrt{\pi}\Delta\sigma_{Max})^m} \tag{12}$$

where the definition of the parameters can be found in [50]. The valve fails when the number of solicitation exceeds N_c. The equivalent number of solicitations executed per year is assumed to be constant and equal to d_c.

The diaphragm has one degradation process modeled by one PBM L_2 related to the cavitation erosion mechanism, which can cause the thickness loss. The threshold is defined as the thickness required to ensure pressure resistance, which is calculated as follows,

$$t_m = PD_0/2(S + yP) \tag{13}$$

where P is the estimated pressure for RHRS, D_0 is the outside diameter of the pipe, y is a coefficient and S is the allowable stress in the pipe. The diaphragm fails when the thickness loss exceeds t_m. The annual loss of thickness is assumed to be constant and equal to d_m.

The pneumatic valves VP1 and VP2 each have one degradation process modeled by MSMs K_7 and K_8 respectively, as shown in Fig. 12.

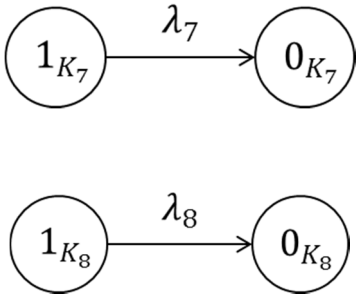

Fig. 12. The representation of the degradation processes of the pneumatic valves.

K_5 has impacts on K_1, K_2, K_3, K_4 and L_1. When $Y_{K_5}(t)$ reaches the state 1_{K_5} the transition rates of K_1, K_2, K_3 and K_4 will increase to λ_1', λ_2', λ_3' and λ_4', respectively, and d_c in L_1 will change to $d_c{}'$. All the parameter values in the degradation models are presented in Table II. For confidentiality, we use artificially scaled values; they are set in a way to simulate the system under accelerated aging conditions.

Table II Parameter values

Parameter	Value
λ_1	6.65e-8 /h
λ_2	1.8e-6 /h
λ_3	4.4e-7 /h
λ_4	1.3e-5 /h
λ_5^1	4.7e-5 /h
λ_5^2	1.3e-5 /h
λ_6	1.5e-5 /h
λ_7	1.95e-8 /h
λ_8	1.95e-8 /h
m	4 S.U.
a_0	3.6 mm
a_c	9.3 mm
C	1.8e-12 S.U.
$f(R)_{Max}$	2 S.U.
Y_{Max}	1.18 S.U.
$\Delta\sigma_{Max}$	0 MPa
d_c	10 /yr
P	41 b
D_0	273 mm

S	101 Mpa
y	0.4 S.U.
d_m	7 mm /yr
λ_1'	9.31e-8 /h
λ_2'	2.52e-6 /h
λ_3'	6.16e-7 /h
λ_4'	1.82e-5 /h
$d_c{}'$	15 /yr

Applying the WDFLM ordering heuristic [38], the variable ordering obtained is $X_{5\#} < X_6 < X_1 < X_2 < X_3 < X_4 < X_8 < X_9 < X_7$. The corresponding BDD is shown in Fig. 13. There are two paths leading to system operation: (1) $X_{5\#} = 0, X_6 = 0, X_1 = 0, X_2 = 0, X_3 = 0, X_4 = 0, X_8 = 0, X_9 = 0$ and (2) $X_{5\#} = 0, X_6 = 0, X_1 = 0, X_2 = 0, X_3 = 0, X_4 = 0, X_8 = 0, X_9 = 1, X_7 = 0$.

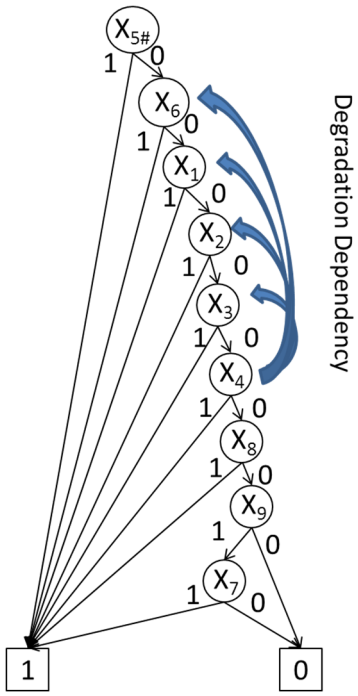

Fig. 13. The BDD corresponding to the fault tree shown in fig. 8.

The degradation processes are divided into five groups: $\{K_6\}, \{L_2\}, \{K_7\}, \{K_8\}$ and

$\{K_1, K_2, K_3, K_4, K_5, L_1\}$. Each of the first four groups has only one degradation model. The PDMP related to the last group is presented as follows,

$$\overrightarrow{Z_{1,5}}(t) = \begin{pmatrix} N(t) \\ Y_{K_1}(t) \\ Y_{K_2}(t) \\ Y_{K_3}(t) \\ Y_{K_4}(t) \\ Y_{K_5}(t) \end{pmatrix} \in \boldsymbol{E}_{1,5} = \mathbb{R} \times \prod_{q=1}^{5} \boldsymbol{S}_{\boldsymbol{K}_q}, \forall t \geq 0 \quad (14)$$

where $N(t)$ denotes the number of solicitations applied till t, $\dot{N}(t) = \begin{cases} d_c, if\ Y_{K_5}(t) = 2_{K_5} \\ d_c{}', if\ Y_{K_5}(t) = 1_{K_5} \end{cases}$ and $Y_{K_q}(t), q = 1,2, \ldots, 5$ are characterized by the related transition rates.

MCS over a time horizon of 8 years has been run 10^6 times to solve the PDMPs and, then, estimate the probability of occurrence of each path. The numerical experiments are carried out in MATLAB on a PC with an Intel Core 2 Duo CPU at 3.06 GHz and a RAM of 3.07 GB. The estimated system reliability with and without dependency throughout the time horizon, under accelerated conditions, is shown in Fig. 14. The average computation time is 34.3 s. We can see from the Figure that neglecting dependency can lead to overestimation of the system reliability. The system reliability with dependency has experienced one rapid decrease after around 6.2 year (point A), which is due to the valve failure in some simulation trials caused by the vibration of the pump. This sharp decrease in system reliability relates to the sharp increase in the system failure time density function, as shown in Fig. 15.

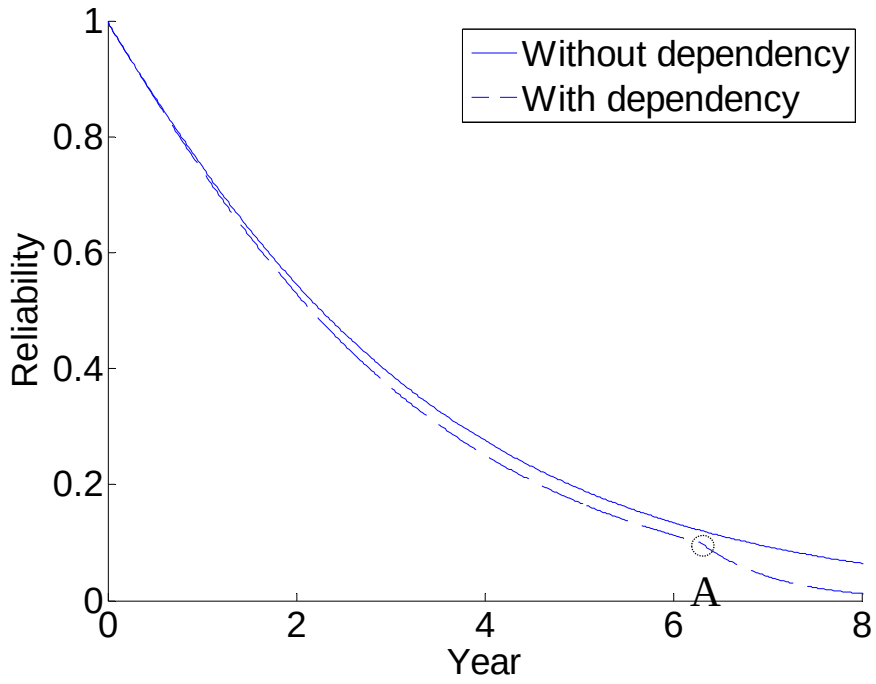

Fig. 14. The estimated system reliability with/without dependency.

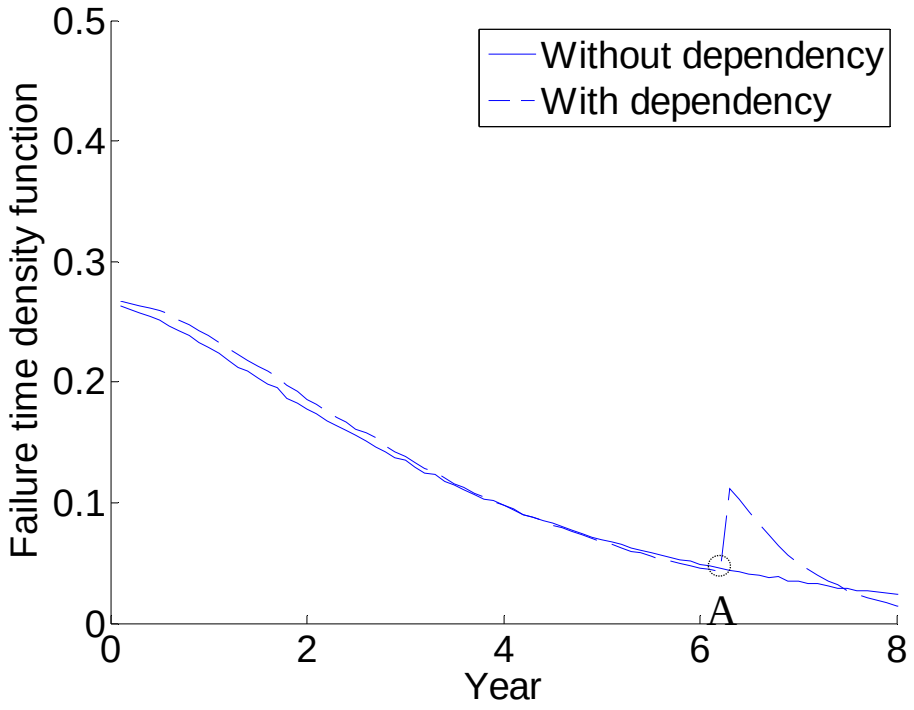

Fig. 15. The system failure time density function with/without dependency.

5. CONCLUSION

In this paper, we have proposed a framework for the reliability assessment of systems whose components have dependent competing degradation processes. The modeling framework rests on MSMs and PBMs, and the PDMP modeling approach is employed to treat dependencies between the degradation processes within one component or/and among components. The numerical solution involves the translation of the system fault tree into a BDD, and the estimation of the probabilities of the paths of events occurrences by MCS. The case study demonstrates the relevance of degradation process dependencies for the system reliability.

It is interesting to include failure isolation as future research in our proposed model. Failure detection and isolation can be used to mitigate degradation dependency by performing corresponding maintenance tasks or failure isolation actions.

Acknowledgement

The authors would like to thank Mrs. Dominique VASSEUR, Mr. Antoine DESPUJOLS and Mr. Emmanuel ARDILLON from the Department Industrial Risks Management (MRI), Electricité de France R&D for their insightful comments. The work was supported by Electricité de France Contract No.8610-5910112096.

References

[1] N. Gebraeel, A. Elwany, and J. Pan, "Residual life predictions in the absence of prior degradation knowledge," *Reliability, IEEE Transactions on,* vol. 58, pp. 106-117, 2009.

[2] J. Lawless and M. Crowder, "Covariates and random effects in a gamma process model with application to degradation and failure," *Lifetime Data Analysis,* vol. 10, pp. 213-227, 2004.

[3] M. Black, A. Brint, and J. Brailsford, "A semi-Markov approach for modelling asset deterioration," *Journal of the Operational Research Society,* vol. 56, pp. 1241-1249, 2005.

[4] M. Chookah, M. Nuhi, and M. Modarres, "A probabilistic physics-of-failure model for prognostic health management of structures subject to pitting and corrosion-fatigue," *Reliability Engineering & System Safety,* vol. 96, pp. 1601-1610, 2011.

[5] M. Daigle and K. Goebel, "A model-based prognostics approach applied to pneumatic valves," *International journal of prognostics and health management,* vol. 2, p. 008, 2011.

[6] S. Reggiani, S. Poli, M. Denison, E. Gnani, A. Gnudi, G. Baccarani, S. Pendharkar, and R. Wise, "Physics-Based Analytical Model for HCS Degradation in STI-LDMOS Transistors," *Electron Devices, IEEE Transactions on,* vol. 58, pp. 3072-3080, 2011.

[7] E. Keedy and Q. Feng, "A physics-of-failure based reliability and maintenance modeling framework for stent deployment and operation," *Reliability Engineering & System Safety,* vol. 103, pp. 94-101, 2012.

[8] R. Moghaddass and M. J. Zuo, "Multistate degradation and supervised estimation methods for a condition-monitored device," *IIE Transactions,* vol. 46, pp. 131-148, 2014.

[9] A. Lisnianski and G. Levitin, *Multi-state system reliability: assessment, optimization and applications*: World scientific, 2003.

[10] W. Li and H. Pham, "Reliability modeling of multi-state degraded systems with multi-competing failures and random shocks," *Reliability, IEEE Transactions on,* vol. 54, pp. 297-303, 2005.

[11] M. Giorgio, M. Guida, and G. Pulcini, "An age-and state-dependent Markov model for degradation processes," *IIE Transactions,* vol. 43, pp. 621-632, 2011.

[12] Y.-F. Li, E. Zio, and Y.-H. Lin, "A multistate physics model of component degradation based on stochastic Petri nets and simulation," *Reliability, IEEE Transactions on,* vol. 61, pp. 921-931, 2012.

[13] L. Jiang, Q. Feng, and D. W. Coit, "Reliability and maintenance modeling for dependent competing failure processes with shifting failure thresholds," *Reliability, IEEE Transactions on,* vol. 61, pp. 932-948, 2012.

[14] N. Rasmekomen and A. K. Parlikad, "Maintenance Optimization for Asset Systems With Dependent Performance Degradation," *Reliability, IEEE Transactions on,* vol. 62, pp. 362-367, 2013.

[15] L. Xing, C. Wang, and G. Levitin, "Competing failure analysis in non-repairable binary systems subject to functional dependence," *Proceedings of the Institution of Mechanical Engineers, Part O: Journal of Risk and Reliability,* vol. 226, pp. 406-416, 2012.

[16] C. Wang, L. Xing, and G. Levitin, "Competing failure analysis in phased-mission systems with functional dependence in one of phases," *Reliability Engineering & System Safety,* vol. 108, pp. 90-99, 2012.

[17] L. Xing and G. Levitin, "Combinatorial analysis of systems with competing failures subject to failure isolation and propagation effects," *Reliability Engineering & System Safety,* vol. 95, pp. 1210-1215, 2010.

[18] C. Wang, L. Xing, and G. Levitin, "Reliability analysis of multi-trigger binary systems subject to competing failures," *Reliability Engineering & System Safety,* vol. 111, pp. 9-17, 2013.

[19] Y.-H. Lin, Y. Li, and E. Zio, "Dynamic Reliability Models for Multiple Dependent Competing Degradation Processes," in *ESREL 2014*.

[20] S. Song, D. W. Coit, and Q. Feng, "Reliability for systems of degrading components with distinct component shock sets," *Reliability Engineering & System Safety,* vol. 132, pp. 115-124, 2014.

[21] W.-S. Lee, D. L. Grosh, F. A. Tillman, and C. H. Lie, "Fault Tree Analysis, Methods, and Applications ∂ A Review," *Reliability, IEEE Transactions on,* vol. 34, pp. 194-203, 1985.

[22] R. M. Sinnamon and J. Andrews, "New approaches to evaluating fault trees," *Reliability Engineering & System Safety,* vol. 58, pp. 89-96, 1997.

[23] C. Wang, L. Xing, and G. Levitin, "Explicit and implicit methods for probabilistic common-cause failure analysis," *Reliability Engineering & System Safety,* vol. 131, pp. 175-184, 2014.

[24] J. K. Vaurio, "An implicit method for incorporating common-cause failures in system analysis," *Reliability, IEEE Transactions on,* vol. 47, pp. 173-180, 1998.

[25] J. K. Vaurio, "Treatment of general dependencies in system fault-tree and risk analysis," *Reliability, IEEE Transactions on,* vol. 51, pp. 278-287, 2002.

[26] L. Xing, G. Levitin, C. Wang, and Y. Dai, "Reliability of systems subject to failures with dependent propagation effect," *Systems, Man, and Cybernetics: Systems, IEEE Transactions on,* vol. 43, pp. 277-290, 2013.

[27] Y. Mo, L. Xing, and S. V. Amari, "A Multiple-Valued Decision Diagram Based Method for Efficient Reliability Analysis of Non-Repairable Phased-Mission Systems," *Reliability, IEEE Transactions on,* vol. 63, pp. 320-330, 2014.

[28] Y. Mo, L. Xing, and J. B. Dugan, "MDD-Based Method for Efficient Analysis on Phased-Mission Systems With Multimode Failures," *Systems, Man, and Cybernetics: Systems, IEEE Transactions on,* vol. 44, pp. 757-769, 2014.

[29] S. Song, D. W. Coit, Q. Feng, and H. Peng, "Reliability Analysis for Multi-Component Systems Subject to Multiple Dependent Competing Failure Processes," *Reliability, IEEE Transactions on,* vol. 63, pp. 331-345, 2014.

[30] R. E. Bryant, "Graph-based algorithms for boolean function manipulation," *Computers, IEEE Transactions on,* vol. 100, pp. 677-691, 1986.

[31] E. Zio, *The Monte Carlo simulation method for system reliability and risk analysis*: Springer, 2013.

[32] A. Rauzy, "New algorithms for fault trees analysis," *Reliability Engineering & System Safety,* vol. 40, pp. 203-211, 1993.

[33] Z. Tang and J. B. Dugan, "BDD-based reliability analysis of phased-mission systems with multimode failures," *Reliability, IEEE Transactions on,* vol. 55, pp. 350-360, 2006.

[34] L. Xing, "An efficient binary-decision-diagram-based approach for network reliability and sensitivity analysis," *Systems, Man and Cybernetics, Part A: Systems and Humans, IEEE Transactions on,* vol. 38, pp. 105-115, 2008.

[35] M. Marseguerra and E. Zio, "Monte Carlo approach to PSA for dynamic process systems," *Reliability Engineering & System Safety,* vol. 52, pp. 227-241, 1996.

[36] B. Bollig and I. Wegener, "Improving the variable ordering of OBDDs is NP-complete," *Computers, IEEE Transactions on,* vol. 45, pp. 993-1002, 1996.

[37] S. J. Friedman and K. J. Supowit, "Finding the optimal variable ordering for binary decision diagrams," in *Proceedings of the 24th ACM/IEEE Design Automation Conference*, 1987, pp. 348-356.

[38] S.-i. Minato, N. Ishiura, and S. Yajima, "Shared binary decision diagram with attributed edges for efficient Boolean function manipulation," in *Design Automation Conference, 1990. Proceedings., 27th ACM/IEEE*, 1990, pp. 52-57.

[39] M. Bouissou, F. Bruyere, and A. Rauzy, "BDD based fault-tree processing: A comparison of variable ordering heuristics," in *Proceedings of European Safety and Reliability Association Conference, ESREL'97*, 1997.

[40] Y. Mo, F. Zhong, H. Liu, Q. Yang, and G. Cui, "Efficient Ordering Heuristics in Binary Decision Diagram–based Fault Tree Analysis," *Quality and Reliability Engineering International,* vol. 29, pp. 307-315, 2013.

[41] R. Tarjan, "Depth-first search and linear graph algorithms," *SIAM journal on computing,* vol. 1, pp. 146-160, 1972.

[42] K. S. Brace, R. L. Rudell, and R. E. Bryant, "Efficient implementation of a BDD package," in *Proceedings of the 27th ACM/IEEE design automation conference*, 1991, pp. 40-45.

[43] N. Limnios, *Fault trees* vol. 675: John Wiley & Sons, 2010.

[44] C. Cocozza-Thivent, "Processus de renouvellement markovien, Processus de Markov déterministes par morceaux," *Online book available on the webpage: http://perso-math. univ-mlv. fr/users/cocozza. christiane/recherche-pageperso/PresentationRMetPDMP. html,* 2011.

[45] E. Lewis and F. Böhm, "Monte Carlo simulation of Markov unreliability models," *Nuclear Engineering and Design,* vol. 77, pp. 49-62, 1984.

[46] R. Coudray and J. Mattei, "System reliability: An example of nuclear reactor system analysis," *Reliability Engineering,* vol. 7, pp. 89-121, 1984.

[47] S. Zhang, M. Hodkiewicz, L. Ma, and J. Mathew, "Machinery condition prognosis using multivariate analysis," in *Engineering asset management*: Springer, 2006, pp. 847-854.

[48] P. Moussou, S. Cambier, D. Lachene, S. Longarini, L. Paulhiac, and V. Villouvier, "Vibration investigation of a French PWR power plant piping system caused by cavitating butterfly valves," *ASME-PUBLICATIONS-PVP,* vol. 420, pp. 99-106, 2001.

[49] P. Paris and F. Erdogan, "A critical analysis of crack propagation laws," *Journal of Fluids Engineering,* vol. 85, pp. 528-533, 1963.

[50] S. Marie, S. Chapuliot, Y. Kayser, M. Lacire, B. Drubay, B. Barthelet, P. Le Delliou, V. Rougier, C. Naudin,

and P. Gilles, "French RSE-M and RCC-MR code appendices for flaw analysis: Presentation of the fracture parameters calculation—Part III: Cracked pipes," *International Journal of Pressure Vessels and Piping,* vol. 84, pp. 614-658, 2007.